VETERINARY REPRODUCTIVE IMMUNOLOGY

EDITED BY: Juan G. Maldonado-Estrada, Fuller Warren Bazer and Dariusz Jan Skarzynski

PUBLISHED IN: Frontiers in Veterinary Science

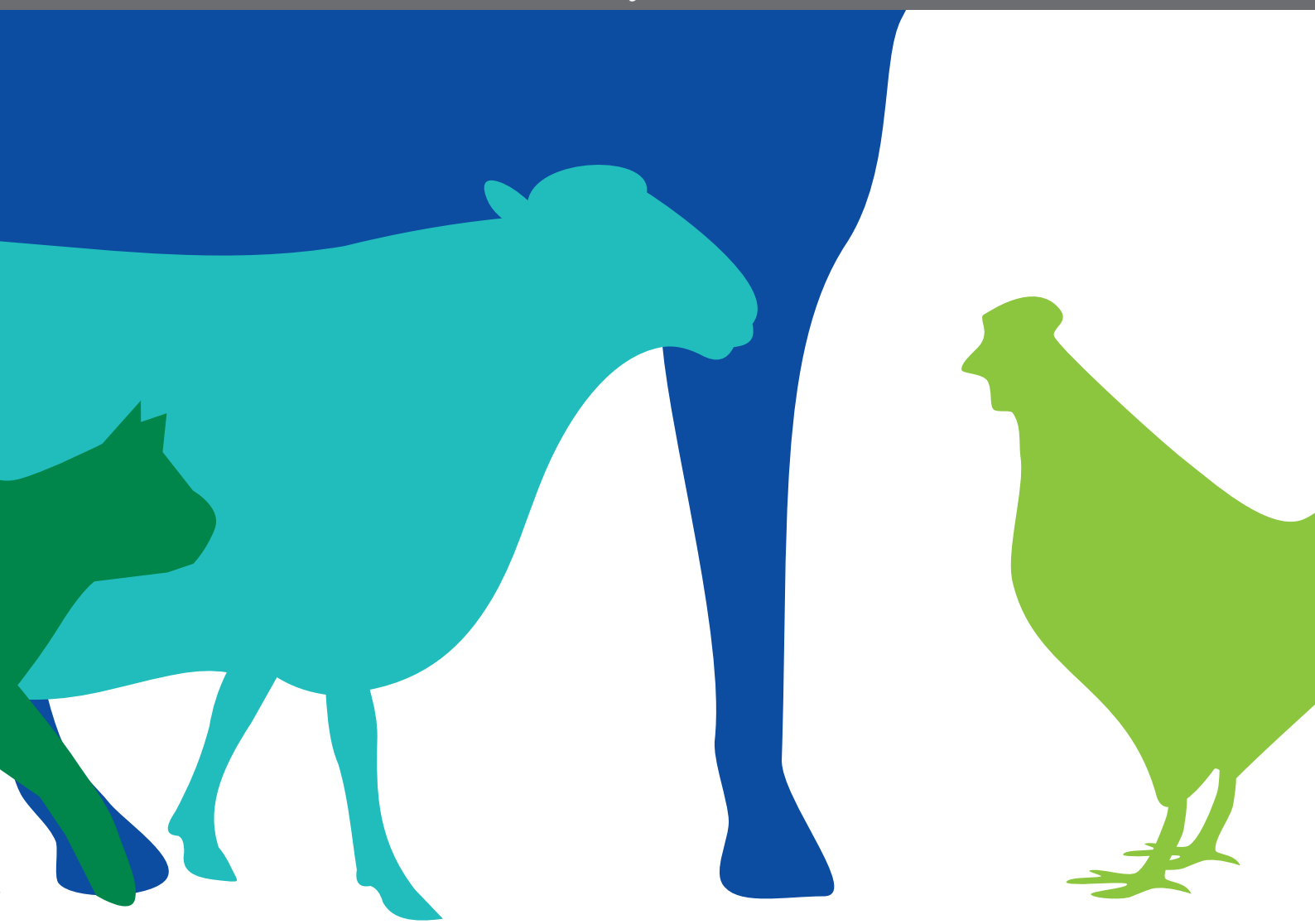

frontiers Research Topics

ISSN 1664-8714
ISBN 978-2-88974-392-6
DOI 10.3389/978-2-88974-392-6

About Frontiers

Frontiers is more than just an open-access publisher of scholarly articles: it is a pioneering approach to the world of academia, radically improving the way scholarly research is managed. The grand vision of Frontiers is a world where all people have an equal opportunity to seek, share and generate knowledge. Frontiers provides immediate and permanent online open access to all its publications, but this alone is not enough to realize our grand goals.

Frontiers Journal Series

The Frontiers Journal Series is a multi-tier and interdisciplinary set of open-access, online journals, promising a paradigm shift from the current review, selection and dissemination processes in academic publishing. All Frontiers journals are driven by researchers for researchers; therefore, they constitute a service to the scholarly community. At the same time, the Frontiers Journal Series operates on a revolutionary invention, the tiered publishing system, initially addressing specific communities of scholars, and gradually climbing up to broader public understanding, thus serving the interests of the lay society, too.

Dedication to Quality

Each Frontiers article is a landmark of the highest quality, thanks to genuinely collaborative interactions between authors and review editors, who include some of the world's best academicians. Research must be certified by peers before entering a stream of knowledge that may eventually reach the public - and shape society; therefore, Frontiers only applies the most rigorous and unbiased reviews.
Frontiers revolutionizes research publishing by freely delivering the most outstanding research, evaluated with no bias from both the academic and social point of view. By applying the most advanced information technologies, Frontiers is catapulting scholarly publishing into a new generation.

What are Frontiers Research Topics?

Frontiers Research Topics are very popular trademarks of the Frontiers Journals Series: they are collections of at least ten articles, all centered on a particular subject. With their unique mix of varied contributions from Original Research to Review Articles, Frontiers Research Topics unify the most influential researchers, the latest key findings and historical advances in a hot research area! Find out more on how to host your own Frontiers Research Topic or contribute to one as an author by contacting the Frontiers Editorial Office: frontiersin.org/about/contact

VETERINARY REPRODUCTIVE IMMUNOLOGY

Topic Editors:
Juan G. Maldonado-Estrada, University of Antioquia, Colombia
Fuller Warren Bazer, Texas A&M University, United States
Dariusz Jan Skarzynski, Institute of Animal Reproduction and Food Research (PAS), Poland

Citation: Maldonado-Estrada, J. G., Bazer, F. W., Skarzynski, D. J., eds. (2022). Veterinary Reproductive Immunology. Lausanne: Frontiers Media SA.
doi: 10.3389/978-2-88974-392-6

Table of Contents

05 ***Editorial: Veterinary Reproductive Immunology***
Dariusz J. Skarzynski, Fuller W. Bazer and Juan G. Maldonado-Estrada

10 ***The Inhibition of Cathepsin G on Endometrial Explants With Endometrosis in the Mare***
Ana Amaral, Carina Fernandes, Sofia Morazzo, Maria Rosa Rebordão, Anna Szóstek-Mioduchowska, Karolina Lukasik, Barbara Gawronska-Kozak, Luís Telo da Gama, Dariusz Jan Skarzynski and Graça Ferreira-Dias

21 ***Pre- and Post-partum Concentrations of Interleukin 1α, Interleukin 8, and α1-Acid Glycoprotein in Vaginal Fornix and Endometrium of Dairy Cows With Clinical Cervicitis***
Darío A. Vallejo-Timarán, Ali Bazzazan, Mariela Segura, Nelson E. Prieto-Cárdenas and Rejean C. Lefebvre

32 ***Selected Uterine Immune Events Associated With the Establishment of Pregnancy in the Dog***
Miguel Tavares Pereira, Renata Nowaczyk, Rita Payan-Carreira, Sonia Miranda, Selim Aslan, Duygu Kaya and Mariusz P. Kowalewski

48 ***Expression of Caspases in the Pig Endometrium Throughout the Estrous Cycle and at the Maternal-Conceptus Interface During Pregnancy and Regulation by Steroid Hormones and Cytokines***
Wonchul Jung, Inkyu Yoo, Jisoo Han, Minjeong Kim, Soohyung Lee, Yugeong Cheon, Minsun Hong, Bo-Young Jeon and Hakhyun Ka

61 ***Messenger RNA Expression of Selected Factors at Different Sites of the Bovine Endometrium Associated With Uterine Health***
Harald Pothmann, Paula Flick, Alexander Tichy, Christoph Gabler and Marc Drillich

68 ***Differential Signals From TNFα-Treated and Untreated Embryos in Uterine Tissues and Splenic CD4+ T Lymphocytes During Preimplantation Pregnancy in Mice***
Katarzyna Buska-Mach, Anna Ewa Kedzierska, Adam Lepczynski, Agnieszka Herosimczyk, Małgorzata Ozgo, Pawel Karpinski, Agnieszka Gomulkiewicz, Daria Lorek, Anna Slawek, Piotr Dziegiel and Anna Chelmonska-Soyta

84 ***Insights Into Extracellular Vesicle/Exosome and miRNA Mediated Bi-Directional Communication During Porcine Pregnancy***
Mallikarjun Bidarimath, Harshavardhan Lingegowda, Jessica E. Miller, Madhuri Koti and Chandrakant Tayade

97 ***Three-Dimensional Live Imaging of Bovine Preimplantation Embryos: A New Method for IVF Embryo Evaluation***
Yasumitsu Masuda, Ryo Hasebe, Yasushi Kuromi, Masayoshi Kobayashi, Kanako Urataki, Mitsugu Hishinuma, Tetsuya Ohbayashi and Ryo Nishimura

114 ***Short Term Safety, Immunogenicity, and Reproductive Effects of Combined Vaccination With Anti-GnRH (Gonacon) and Rabies Vaccines in Female Feral Cats***
Shiri Novak, Boris Yakobson, Shir Sorek, Liat Morgan, Smadar Tal, Ran Nivy, Roni King, Lauren Jaebker, Douglas C. Eckery and Tal Raz

131 *Integrating miRNA and mRNA Profiling to Assess the Potential miRNA–mRNA Modules Linked With Testicular Immune Homeostasis in Sheep*
Taotao Li, Xia Wang, Ruirui Luo, Xuejiao An, Yong Zhang, Xingxu Zhao and Youji Ma

145 *Inhibition of the C-X-C Motif Chemokine 12 (CXCL12) and Its Receptor CXCR4 Reduces Utero-Placental Expression of the VEGF System and Increases Utero-Placental Autophagy*
Ryan L. Ashley, Cheyenne L. Runyan, Marlie M. Maestas, Elisa Trigo and Gail Silver

frontiers in Veterinary Science

EDITORIAL
published: 10 January 2022
doi: 10.3389/fvets.2021.823169

Editorial: Veterinary Reproductive Immunology

Dariusz J. Skarzynski[1], *Fuller W. Bazer*[2] *and Juan G. Maldonado-Estrada*[3]*

[1] *Department of Reproductive Immunology and Pathology, Institute of Animal Reproduction and Food Research, Polish Academy of Science, Olsztyn, Poland,* [2] *Department of Animal Science, Texas A&M University, College Station, TX, United States,* [3] *OHVRI Research Group, Escuela de Medicina Veterinaria, Universidad de Antioquia, Medellín, Colombia*

Keywords: domestic animals, endometrium, fetal allograft, innate immune cells, Medawar paradox, pregnancy loss, reproductive immunology, T-regulatory cells

Editorial on the Research Topic

Veterinary Reproductive Immunology

FROM MEDAWAR'S PARADOX TO NEUROIMMUNOENDOCRINE, METABOLIC AND ENVIRONMENTAL INTEGRATION

The field of Reproductive Immunology has evolved from the paradigms of transplantation immunology to an integrated concept of interactions between the endocrine, immune, nervous, and reproductive systems as critical components of the physiology of reproduction. The origin of reproductive immunology was the Medawar paradox when he proposed several theories explaining failure of the mother to reject the fetal allograft in an epoch when the rules of Major Histocompatibility Complex and its compromise in transplantation immunology were defined. From an orthodox immunologist's perspective, it is hard to fully understand the mechanisms underlying maternal-fetal tolerance in mammalian reproduction. Medawar's theories were tested experimentally by several scientists, whose results are considered fundamental to the origin of reproductive immunology. Although Medawar' paradox is considered the inflection point for the origin of reproductive immunology (1, 2), Billington (3) stated that Mechnikov and Landsteiner were the pioneers of reproductive immunology with their discoveries of expression of phagocytic cells and Fc receptors in placentae that are responsible for uptake of placental antibodies in women during gestation. Also, there was the discovery of hemolytic anemia in the rhesus monkey and its treatment with counteracting antibodies, respectively (3). Since the first hypotheses proposed by Medawar on the possible mechanisms of non-rejection of the fetal allografts, to the pioneering studies in rodents and in women undertaken by Beer, Billingham, Scott, and Yang on maternal-fetal tolerance in the 60's (3), pioneers in reproductive immunology have paved the way for current research in reproductive immunology of human and other mammals.

Regarding the compromise of MHC antigens in reproduction, Billington reported that fetal size was greater when female mice produced fetuses from a strain different from their own (4). In this paper, Billington cited early work highlighting the importance of fetal antigens and cells in establishing maternal-fetal tolerance in mice, rats, cattle, and humans. In that epoch, the first report on circulating syncytiotrophoblast fragments in human pregnancy and their possible relationship to maternal tolerance to the fetal allograft (5) provided further evidence of for a relationship to pathologies such as preeclampsia (6).

Several pieces of evidence support the role of fetal MHC antigens in successful pregnancies, depending on the species and stage of gestation (7–12). The presence of maternal cells in the fetal circulation and fetal cells and cell-free DNA trafficking into the maternal circulation was reported for humans [(13–15), and reviewed in (16)], mice (17–19), and domestic animal species (20–22). The trafficking of cells between the mother and the fetus is a crucial component of the interaction

Edited and reviewed by:
Ahmed Tibary,
Washington State University,
United States

***Correspondence:**
Juan G. Maldonado-Estrada
juan.maldonado@udea.edu.co

Specialty section:
This article was submitted to Animal Reproduction - Theriogenology, a section of the journal Frontiers in Veterinary Science

Received: *26 November 2021*
Accepted: *06 December 2021*
Published: *10 January 2022*

Citation:
Skarzynski DJ, Bazer FW and Maldonado-Estrada JG (2022) Editorial: Veterinary Reproductive Immunology. Front. Vet. Sci. 8:823169. doi: 10.3389/fvets.2021.823169

between maternal and fetal immune cells (13, 23–25), highlighting the importance of maternal cells in "educating" the fetal immune system for the antigenic environment it will face in postnatal life [(26), reviewed in (27, 28)]. The presence of maternal immune cells at the maternal-fetal interface is accepted as a critical component of the physiology of gestation (29) and in pathological conditions such as hypertensive disorders of pregnancy, including preeclampsia (30–32).

Several authors proposed that fetal cells bearing MHC antigens and other circulating fetal antigens could act as conventional triggers of the maternal cellular immune responses resulting in rejection of the fetal allograft and maternally induced runt disease in the offspring (33, 34). Accordingly, the work of led by Clark and Chaouat with the CBA2/DBA model in the 1980s (35–37) provided evidence of immune-mediated fetal resorption. This model helped test several hypotheses on the compromise of stressful conditions in the physiopathology of immune-mediated pregnancy loss.

In the late 1970s and early 1980s, research by Martal et al. (38, 39) and Bazer and Roberts group on ovine and bovine trophoblast interferons established the molecular basis of maternal recognition of pregnancy in ruminants (40–42) and triggered an exciting field of research in the maternal-fetal dialogue between the endometrium, the corpus luteum, and the hypothalamic-hypophyseal axis.

The work led by Anne Croy showed the essential role that the trophoblast layer of the placenta plays in maintaining interspecies pregnancies (43). Furthermore, Croy's team (44) and Moffett's group (45, 46) provided evidence for the importance of uterine Natural Killer cells, dendritic cells (47), and innate uterine lymphoid cells [reviewed in (48)] for successful pregnancies in mice and humans, highlighting the importance of innate immune cells in the physiology of gestation. Besides, the works by Antczak and Allen on the compromise of the maternal immune response in the developing chorionic girdles in equine placentation in the early 80's (49, 50) provided evidence for the importance of cells of the adaptive immune system in successful placental development and fetal growth in mares.

The proposal of an immunotropic hypothesis (51) elicited new and exciting concepts to the field of reproductive immunology [(52, 53), reviewed in (54, 55)] and elicited controversy (56–58) on the importance of the adaptive immune system in gestation maintenance. The initial concept of a Th1/Th2 balance required for successful gestation further evolved toward the concept of a balance between regulatory T cells (T-reg) (59) and T-reg/Th17 cells being critical for successful pregnancies (60, 61).

From the beginning of the twenty-first century, several studies by Skarzynski's group provided evidence for a neuro-immuno-endocrine interaction between the endometrium and corpus luteum in cattle (62–67) and horses (68, 69) and the role epithelial cells play in the maternal-fetal dialogue (70). Concomitantly, there were results from Bazer's group on the compromise of several modulators in the maternal-fetal dialogue in sheep (71–75) add critical evidence regarding the function of the reproductive system as an integrated system in which neuro-immune-endocrine and metabolic cues are integrated for successful reproduction (or failure if loss of homeostasis). Other research groups around the world provided additional evidence for the importance of cellular and humoral immune components and processes in the physiology of pregnancy (54, 76–79). Failure in several processes were implicated in immune-mediated embryonic and fetal losses during the course of gestation [reviewed in (80)].

In this special edition on Veterinary Reproductive Immunology, several papers contributed to increasing our understanding of neuro-immune-endocrine interactions related to physiological and pathological conditions of gestation. The papers provide novel results related to anti-GnRH vaccines in cats, the establishment of pregnancy in dogs, processes related to endometrial function in cattle, horses, and pigs, and pre-implantation signaling in mice. Further, the papers included address state-of-the-art protocols in molecular biology, providing readers, scientists, and clinicians with advanced concepts on reproductive immunology. The discussion is still open, as mentioned by Billington (3), who proposed that reproductive immunology would continuously provide scientific information and controversy (3), as it is an essential aspect of research and discovery in the field of animal reproduction. New research areas, including glycan expression at the maternal-fetal interface in the placenta of several animal species and humans, are becoming more prominent in reproductive immunology. However, there are still a lack of comprehensive theories integrating the contributions of findings from studies in glycobiology into concepts related to successful mammalian reproduction. Even though there is abundant scientific evidence for the essential roles that signals from immune, endocrine, nervous, epithelial, stromal, and trophoblast cells produce to intercommunicate the endocrine, immune, neural, and reproductive tissues, no explicit theories exist to fully explain the way these systems function and contribute to maintaining the physiology of gestation or why, when the system is altered, there are losses of gestations. For these reasons, in the future, we will seek momentum in research whereby the scientific community will provide an integrated view on the homeostasis required for successful reproduction, including integration of immunology, genomics, proteomics, glycomics, and environmental influences in mammalian reproduction.

AUTHOR CONTRIBUTIONS

DS discussed and corrected the final version of the manuscript. All authors contributed to the article and approved the submitted version.

FUNDING

This work was supported by Etrategia de Sostebibilidad de Grupos, CODI, Universidad de Antioquia to JM-E and internal grant of IARFR PAS No 5/FBW/2021 supports to DS. FB was also supported by Grant Arginine and secreted phosphoprotein 1 mediate cell signaling to enhance conceptus development and survival from the National Institute of Food and Agriculture

(NIFA) as Competitive Grant no. 2016-67015-24958 from the USDA National Institute of Food and Agriculture and Roles of fructose and glucose in growth and development of ovine and porcine conceptuses, Competitive Grant No. 2018-67015-28093.

ACKNOWLEDGMENTS

The authors thank to their corresponding institutions for financial support of their research and academic activities.

REFERENCES

1. Medawar PB. Some immunological and endocrinological problems were raised by the evolution of viviparity in vertebrates. *Symp Soc Exp Biol.* (1953) 7:320–38.
2. Rendell V, Bath NM, Brennan TV. Medawar's paradox and immune mechanisms of fetomaternal tolerance. *OBM Transplant.* (2020) 4:26. doi: 10.21926/obm.transplant.2001104
3. Billington WD. Origins and evolution of reproductive immunology: a personal perspective. *J Reprod Immunol.* (2015) 108:2–5. doi: 10.1016/j.jri.2014.10.003
4. Billington WD. Influence of immunological dissimilarity of mother and foetus on size of placenta in mice. *Nature.* (1964) 202:317–8. doi: 10.1038/202317a0
5. Billingham RE. Transplantation immunity and the maternal-fetal relation. *N Engl J Med.* (1964) 270:720–5. doi: 10.1056/NEJM196404022701406
6. Redman CW, Sargent IL. Microparticles and immunomodulation in pregnancy and preeclampsia. *J Reprod Immunol.* (2007) 76:61–7. doi: 10.1016/j.jri.2007.03.008
7. Wells M, Hsi BL, Faulk WP. Class I antigens of the major histocompatibility complex on cytotrophoblast of the human placental basal plate. *Am J Reprod Immunol.* (1984) 6:167–74. doi: 10.1111/j.1600-0897.1984.tb00132.x
8. Billington WD, Burrows FJ. The rat placenta expresses paternal class I major histocompatibility antigens. *J Reprod Immunol.* (1986) 9:155–60. doi: 10.1016/0165-0378(86)90008-2
9. Crump A, Donaldson WL, Miller J, Kydd JH, Allen WR, Antczak DF. Expression of major histocompatibility complex (MHC) antigens on horse trophoblast. *J Reprod Fertil Suppl.* (1987) 35:379–88.
10. Hunt JS, Fishback JL, Andrews GK, Wood GW. Expression of class I HLA genes by trophoblast cells. Analysis by *in situ* hybridization. *J Immunol.* (1988) 140:1293–99.
11. Redline RW, Lu CY. Localization of fetal major histocompatibility complex antigens and maternal leukocytes in murine placenta. Implications for maternal-fetal immunological relationship. *Lab Invest.* (1989) 61:27–36.
12. Donaldson WL, Zhang CH, Oriol JG, Antczak DF. Invasive equine trophoblast expresses conventional class I major histocompatibility complex antigens. *Development.* (1990) 110:63–71.
13. Herzenberg LA, Bianchi DW, Schröder J, Cann HM, Iverson GM. Fetal cells in the blood of pregnant women: detection and enrichment by fluorescence-activated cell sorting. *Proc Natl Acad Sci USA.* (1979) 76:1453–5. doi: 10.1073/pnas.76.3.1453
14. Lo YM, Lo ES, Watson N, Noakes L, Sargent IL, Thilaganathan B, et al. Two-way cell traffic between mother and fetus: biologic and clinical implications. *Blood.* (1996) 88:4390–5.
15. Adams Waldorf KM, Gammill HS, Lucas J, Aydelotte TM, Leisenring WM, Lambert NC, et al. Dynamic changes in fetal microchimerism in maternal peripheral blood mononuclear cells, CD4+ and CD8+ cells in normal pregnancy. *Placenta.* (2010) 31:589–94. doi: 10.1016/j.placenta.2010.04.013
16. Bianchi DW, Khosrotehrani K, Way SS, MacKenzie TC, Bajema I, O'Donoghue K. Forever connected: the lifelong biological consequences of fetomaternal and maternofetal microchimerism. *Clin Chem.* (2021) 67:351–62. doi: 10.1093/clinchem/hvaa304
17. Khosrotehrani K, Wataganara T, Bianchi DW, Johnson KL. Fetal cell-free DNA circulates in the plasma of pregnant mice: relevance for animal models of fetomaternal trafficking. *Hum Reprod.* (2004) 19:2460–4. doi: 10.1093/humrep/deh445
18. Vernochet C, Caucheteux SM, Kanellopoulos-Langevin C. Bi-directional cell trafficking between mother and fetus in mouse placenta. *Placenta.* (2007) 28:639–49. doi: 10.1016/j.placenta.2006.10.006
19. Zeng XX, Tan KH, Yeo A, Sasajala P, Tan X, Xiao ZC, et al. Pregnancy-associated progenitor cells differentiate and mature into neurons in the maternal brain. *Stem Cells Dev.* (2010) 19:1819–30. doi: 10.1089/scd.2010.0046
20. McConico A, Butters K, Lien K, Knudsen B, Wu X, Platt JL, et al. In utero cell transfer between porcine littermates. *Reprod Fertil Dev.* (2011) 23:297–302. doi: 10.1071/RD10165
21. Gash KK, Yang M, Fan Z, Regouski M, Rutigliano HM, Polejaeva IA. Assessment of microchimerism following somatic cell nuclear transfer and natural pregnancies in goats. *J Anim Sci.* (2019) 97:3786–94. doi: 10.1093/jas/skz248
22. Brown JA, Niland ES, Pierce NL, Taylor JB. Validation of fetal microchimerism after pregnancy in the ovine using qPCR. *Transl Anim Sci.* (2021) 5:txab100. doi: 10.1093/tas/txab100
23. Piotrowski P, Croy BA. Maternal cells are widely distributed in murine fetuses in utero. *Biol Reprod.* (1996) 54:1103–10. doi: 10.1095/biolreprod54.5.1103
24. Bonney EA, Matzinger P. The maternal immune system's interaction with circulating fetal cells. *J Immunol.* (1997) 158:40–7.
25. Marleau AM, Greenwood JD, Wei Q, Singh B, Croy BA. Chimerism of murine fetal bone marrow by maternal cells occurs in late gestation and persists into adulthood. *Lab Invest.* (2003) 83:673–81. doi: 10.1097/01.lab.0000067500.85003.32
26. Khosrotehrani K, Johnson KL, Guégan S, Stroh H, Bianchi DW. Natural history of fetal cell microchimerism during and following murine pregnancy. *J Reprod Immunol.* (2005) 66:1–12. doi: 10.1016/j.jri.2005.02.001
27. Stelzer IA, Thiele K, Solano ME. Maternal microchimerism: lessons learned from murine models. *J Reprod Immunol.* (2015) 108:12–25. doi: 10.1016/j.jri.2014.12.007
28. Stelzer IA, Urbschat C, Schepanski S, Thiele K, Triviai I, Wieczorek A, et al. Vertically transferred maternal immune cells promote neonatal immunity against early life infections. *Nat Commun.* (2021) 12:4706. doi: 10.1038/s41467-021-24719-z
29. Craven CM, Ward K. Syncytiotrophoblastic fragments in first-trimester decidual veins: evidence of placental perfusion by the maternal circulation early in pregnancy. *Am J Obstet Gynecol.* (1999) 181:455–9. doi: 10.1016/s0002-9378(99)70578-8
30. Huppertz B, Kingdom J, Caniggia I, Desoye G, Black S, Korr H, et al. Hypoxia favours necrotic versus apoptotic shedding of placental syncytiotrophoblast into the maternal circulation. *Placenta.* (2003) 24:181–90. doi: 10.1053/plac.2002.0903
31. Wei J, Blenkiron C, Tsai P, James JL, Chen Q, Stone PR, et al. Placental trophoblast debris mediated feto-maternal signalling via small RNA delivery: implications for preeclampsia. *Sci Rep.* (2017) 7:14681. doi: 10.1038/s41598-017-14180-8
32. Carrasco-Wong I, Aguilera-Olguín M, Escalona-Rivano R, Chiarello DI, Barragán-Zúñiga LJ, Sosa-Macías M, et al. Syncytiotrophoblast stress in early onset preeclampsia: the issues perpetuating the syndrome. *Placenta.* (2021) 113:57–66. doi: 10.1016/j.placenta.2021.05.002
33. Beer AE, Billingham RE, Yang SL. Maternally induced transplantation immunity, tolerance, and runt disease in rats. *J Exp Med.* (1972) 135:808–26. doi: 10.1084/jem.135.4.808
34. Beer AE, Billingham RE. Maternally acquired runt disease. *Science.* (1973) 179:240–3. doi: 10.1126/science.179.4070.240
35. Clark DA, Croy BA, Rossant J, Chaouat G. Immune presensitization and local intrauterine defences as determinants of success or failure of murine interspecies pregnancies. *J Reprod Fertil.* (1986) 77:633–43. doi: 10.1530/jrf.0.0770633
36. Clark DA, Chaouat G, Guenet JL, Kiger N. Local active suppression and successful vaccination against spontaneous abortion in CBA/J mice. *J Reprod Immunol.* (1987) 10:79–85. doi: 10.1016/0165-0378(87)90052-0

37. Chaouat G, Menu E, Clark DA, Dy M, Minkowski M, Wegmann TG. Control of fetal survival in CBA x DBA/2 mice by lymphokine therapy. *J Reprod Fertil.* (1990) 89:447–58. doi: 10.1530/jrf.0.0890447
38. Martal J, Lacroix MC, Loudes C, Saunier M, Wintenberger-Torrès S. Trophoblastin, an antiluteolytic protein present in early pregnancy in sheep. *J Reprod Fertil.* (1979) 56:63–73. doi: 10.1530/jrf.0.0560063
39. Charpigny G, Reinaud P, Huet JC, Guillomot M, Charlier M, Pernollet JC, et al. High homology between a trophoblastic protein (trophoblastin) isolated from ovine embryo and alpha-interferons. *FEBS Lett.* (1988) 228:12–16. doi: 10.1016/0014-5793(88)80574-x
40. Godkin JD, Bazer FW, Moffatt J, Sessions F, Roberts RM. Purification and properties of a major, low molecular weight protein released by the trophoblast of sheep blastocysts at day 13-21. *J Reprod Fertil.* (1982) 65:141–50. doi: 10.1530/jrf.0.0650141
41. Godkin JD, Bazer FW, Roberts RM. Ovine trophoblast protein 1, an early secreted blastocyst protein, binds specifically to uterine endometrium and affects protein synthesis. *Endocrinology.* (1984) 114:120–30. doi: 10.1210/endo-114-1-120
42. Helmer SD, Hansen PJ, Anthony RV, Thatcher WW, Bazer FW, Roberts RM. Identification of bovine trophoblast protein-1, a secretory protein immunologically related to ovine trophoblast protein-1. *J Reprod Fertil.* (1987) 79:83–91. doi: 10.1530/jrf.0.0790083
43. Croy BA, Rossant J, Clark DA. Histological and immunological studies of post implantation death of *Mus caroli* embryos in the *Mus musculus* uterus. *J Reprod Immunol.* (1982) 4:277–93. doi: 10.1016/0165-0378(82)90003-1
44. Croy BA, Gambel P, Rossant J, Wegmann TG. Characterization of murine decidual natural killer (NK) cells and their relevance to the success of pregnancy. *Cell Immunol.* (1985) 93:315–26. doi: 10.1016/0008-8749(85)90137-6
45. Trundley A, Moffett A. Human uterine leukocytes and pregnancy. *Tissue Antigens.* (2004) 63:1–12. doi: 10.1111/j.1399-0039.2004.00170.x
46. Moffett A, Loke C. Immunology of placentation in eutherian mammals. *Nat Rev Immunol.* (2006) 6:584–94. doi: 10.1038/nri1897
47. Gardner L, Moffett A. Dendritic cells in the human decidua. *Biol Reprod.* (2003) 69:1438–46. doi: 10.1095/biolreprod.103.017574
48. Huhn O, Zhao X, Esposito L, Moffett A, Colucci F, Sharkey AM. How do uterine natural killer and innate lymphoid cells contribute to successful pregnancy? *Front Immunol.* (2021) 12:607669. doi: 10.3389/fimmu.2021.607669
49. Antczak DF, Allen WR. Invasive trophoblast in the genus Equus. *Ann Immunol.* (1984) 135D:325–31. doi: 10.1016/s0769-2625(84)81201-5
50. Allen WR, Skidmore JA, Stewart F, Antczak DF. Effects of fetal genotype and uterine environment on placental development in equids. *J Reprod Fertil.* (1993) 98:55–60. doi: 10.1530/jrf.0.0980055
51. Wegmann TG, Lin H, Guilbert L, Mosmann TR. Bidirectional cytokine interactions in the maternal-fetal relationship: is successful pregnancy a TH2 phenomenon? *Immunol Today.* (1993) 14:353–6. doi: 10.1016/0167-5699(93)90235-D
52. Oliveira LJ, Mansouri-Attia N, Fahey AG, Browne J, Forde N, Roche JF, et al. Characterization of the Th profile of the bovine endometrium during the oestrous cycle and early pregnancy. *PLoS ONE.* (2013) 8:e75571. doi: 10.1371/journal.pone.0075571
53. Ealy AD, Speckhart SL, Wooldridge LK. Cytokines that serve as embryokines in cattle. *Animals.* (2021) 11:2313. doi: 10.3390/ani11082313
54. Piccinni MP, Raghupathy R, Saito S, Szekeres-Bartho J. Cytokines, hormones and cellular regulatory mechanisms favoring successful reproduction. *Front Immunol.* (2021) 12:717808.
55. Wang P, Jiang G, Ju W, Cai Y, Wang J, Wu F. Influence of Bushen Tiaochong cycle therapy on Th1/Th2 deviation, sex hormone level, and pregnancy outcome of alloimmune recurrent spontaneous abortion. *Evid Based Complement Alternat Med.* (2021) 2021:8624414. doi: 10.1155/2021/8624414
56. Billington WD. Species diversity in the immunogenetic relationship between mother and fetus: is trophoblast insusceptibility to immunological destruction the only essential common feature for the maintenance of allogeneic pregnancy? *Exp Clin Immunogenet.* (1993) 10:73–84.
57. Chaouat G. The Th1/Th2 paradigm: still important in pregnancy? *Semin Immunopathol.* (2007) 29:95–113. doi: 10.1007/s00281-007-0069-0
58. Chaouat G. Inflammation, NK cells and implantation: friend and foe (the good, the bad and the ugly?): replacing placental viviparity in an evolutionary perspective. *J Reprod Immunol.* (2013) 97:2–13. doi: 10.1016/j.jri.2012.10.009
59. Maeda Y, Ohtsuka H, Tomioka M, Oikawa M. Effect of progesterone on Th1/Th2/Th17 and regulatory T cell-related genes in peripheral blood mononuclear cells during pregnancy in cows. *Vet Res Commun.* (2013) 37:43–9. doi: 10.1007/s11259-012-9545-7
60. Huang N, Chi H, Qiao J. Role of regulatory T cells in regulating fetal-maternal immune tolerance in healthy pregnancies and reproductive diseases. *Front Immunol.* (2020) 11:1023. doi: 10.3389/fimmu.2020.01023
61. Tsuda S, Nakashima A, Morita K, Shima T, Yoneda S, Kishi H, et al. The role of decidual regulatory T cells in the induction and maintenance of fetal antigen-specific tolerance: imbalance between regulatory and cytotoxic T cells in pregnancy complications. *Hum Immunol.* (2021) 82:346–52. doi: 10.1016/j.humimm.2021.01.019
62. Miyamoto Y, Skarzynski DJ, Okuda K. Is tumor necrosis factor alpha a trigger for the initiation of endometrial prostaglandin F(2alpha) release at luteolysis in cattle? *Biol Reprod.* (2000) 62:1109–15. doi: 10.1095/biolreprod62.5.1109
63. Murakami S, Miyamoto Y, Skarzynski DJ, Okuda K. Effects of tumor necrosis factor-alpha on secretion of prostaglandins E2 and F2alpha in bovine endometrium throughout the estrous cycle. *Theriogenology.* (2001) 55:1667–78. doi: 10.1016/s0093-691x(01)00511-8
64. Okuda K, Kasahara Y, Murakami S, Takahashi H, Woclawek-Potocka I, Skarzynski DJ. Interferon-tau blocks the stimulatory effect of tumor necrosis factor-alpha on prostaglandin F2alpha synthesis by bovine endometrial stromal cells. *Biol Reprod.* (2004) 70:191–7. doi: 10.1095/biolreprod.103.019083
65. Nishimura R, Bowolaksono A, Acosta TJ, Murakami S, Piotrowska K, Skarzynski DJ, et al. Possible role of interleukin-1 in the regulation of bovine corpus luteum throughout the luteal phase. *Biol Reprod.* (2004) 71:1688–93. doi: 10.1095/biolreprod.104.032151
66. Skarzynski DJ, Piotrowska KK, Bah MM, Korzekwa A, Woclawek-Potocka I, Sawai K, et al. Effects of exogenous tumour necrosis factor-alpha on the secretory function of the bovine reproductive tract depend on tumour necrosis factor-alpha concentrations. *Reprod Domest Anim.* (2009) 44:371–9. doi: 10.1111/j.1439-0531.2007.01016.x
67. Duong HT, Piotrowska-Tomala KK, Acosta TJ, Bah MM, Sinderewicz E, Majewska M, et al. Effects of cortisol on pregnancy rate and corpus luteum function in heifers: an *in vivo* study. *J Reprod Dev.* (2012) 58:223–30. doi: 10.1262/jrd.11-122t
68. Galvão A, Skarzynski DJ, Szóstek A, Silva E, Tramontano A, Mollo A, et al. Cytokines tumor necrosis factor-α and interferon-γ participate in modulation of the equine corpus luteum as autocrine and paracrine factors. *J Reprod Immunol.* (2012) 93:28–37. doi: 10.1016/j.jri.2011.11.002
69. Rebordão MR, Amaral A, Fernandes C, Silva E, Lukasik K, Szóstek-Mioduchowska A, et al. Enzymes present in neutrophil extracellular traps may stimulate the fibrogenic PGF2α pathway in the mare endometrium. *Animals.* (2021) 11:2615. doi: 10.3390/ani11092615
70. Okuda K, Sakumoto R, Okamoto N, Acosta TJ, Abe H, Okada H, et al. Cellular localization of genes and proteins for tumor necrosis factor-α (TNF), TNF receptor types I and II in bovine endometrium. *Mol Cell Endocrinol.* (2010) 330:41–8. doi: 10.1016/j.mce.2010.07.025
71. Choi Y, Johnson GA, Spencer TE, Bazer FW. Pregnancy and interferon tau regulate major histocompatibility complex class I and beta2-microglobulin expression in the ovine uterus. *Biol Reprod.* (2003) 68:1703–10. doi: 10.1095/biolreprod.102.012708
72. Wang X, Frank JW, Xu J, Dunlap KA, Satterfield MC, Burghardt RC, et al. Functional role of arginine during the peri-implantation period of pregnancy. II. Consequences of loss of function of nitric oxide synthase NOS3 mRNA in ovine conceptus trophectoderm. *Biol Reprod.* (2014) 91:59. doi: 10.1095/biolreprod.114.121202
73. Lenis YY, Johnson GA, Wang X, Tang WW, Dunlap KA, Satterfield MC, et al. Functional roles of ornithine decarboxylase and arginine decarboxylase during the peri-implantation period of pregnancy in sheep. *J Anim Sci Biotechnol.* (2018) 9:10. doi: 10.1186/s40104-017-0225-x

74. Halloran KM, Stenhouse C, Wu G, Bazer FW. Arginine, agmatine, and polyamines: key regulators of conceptus development in mammals. *Adv Exp Med. Biol.* (2021) 1332:1385–105. doi: 10.1007/978-3-030-74180-8_6
75. Hoskins EC, Halloran KM, Stenhouse C, Moses RM, Dunlap KA, Satterfield MC, et al. Pre-implantation exogenous progesterone and pregnancy in sheep: I. polyamines, nutrient transport, and progestamedins. *J Anim Sci Biotechnol.* (2021) 12:39. doi: 10.1186/s40104-021-00554-6
76. Co EC, Gormley M, Kapidzic M, Rosen DB, Scott MA, Stolp HA, et al. Maternal decidual macrophages inhibit NK cell killing of invasive cytotrophoblasts during human pregnancy. *Biol Reprod.* (2013) 88:155. doi: 10.1095/biolreprod.112.099465
77. Fu B, Wei H. Decidual natural killer cells and the immune microenvironment at the maternal-fetal interface. *Sci China Life Sci.* (2016) 59:1224–31. doi: 10.1007/s11427-016-0337-1
78. Alok A, Karande AA. The role of glycodelin as an immune-modulating agent at the feto-maternal interface. *J Reprod Immunol.* (2009) 83:124–7. doi: 10.1016/j.jri.2009.06.261
79. Jena SR, Nayak J, Kumar S, Kar S, Dixit A, Samanta L. Paternal contributors in recurrent pregnancy loss: cues from comparative proteome profiling of seminal extracellular vesicles. *Mol Reprod Dev.* (2021) 88:96–112. doi: 10.1002/mrd.23445
80. Xu L, Li Y, Sang Y, Li DJ, Du M. Crosstalk between trophoblasts and decidual immune cells: the cornerstone of maternal-fetal immunotolerance. *Front Immunol.* (2021) 12:642392. doi: 10.3389/fimmu.2021.642392

Conflict of Interest: The authors declare that the research was conducted in the absence of any commercial or financial relationships that could be construed as a potential conflict of interest.

frontiers in Veterinary Science

ORIGINAL RESEARCH
published: 30 October 2020
doi: 10.3389/fvets.2020.582211

The Inhibition of Cathepsin G on Endometrial Explants With Endometrosis in the Mare

*Ana Amaral[1], Carina Fernandes[1], Sofia Morazzo[1], Maria Rosa Rebordão[1,2], Anna Szóstek-Mioduchowska[3], Karolina Lukasik[3], Barbara Gawronska-Kozak[3], Luís Telo da Gama[1], Dariusz Jan Skarzynski[3] and Graça Ferreira-Dias[1]**

[1] Department Morfologia e Função, Faculdade de Medicina Veterinária, CIISA—Centro de Investigação Interdisciplinar em Sanidade Animal, Universidade de Lisboa, Lisboa, Portugal, [2] Polytechnic of Coimbra, Coimbra Agriculture School, Coimbra, Portugal, [3] Institute of Animal Reproduction and Food Research, Polish Academy of Science, Olsztyn, Poland

OPEN ACCESS

Edited by:
Natali Krekeler,
The University of Melbourne, Australia

Reviewed by:
Carolina Paula Bianchi,
National University of Central Buenos Aires, Argentina
Maria Alejandra Stornelli,
National University of La Plata, Argentina

***Correspondence:**
Graça Ferreira-Dias
gmlfdias@fmv.ulisboa.pt

Specialty section:
This article was submitted to Animal Reproduction - Theriogenology, a section of the journal Frontiers in Veterinary Science

Received: 10 July 2020
Accepted: 24 September 2020
Published: 30 October 2020

Citation:
Amaral A, Fernandes C, Morazzo S, Rebordão MR, Szóstek-Mioduchowska A, Lukasik K, Gawronska-Kozak B, Telo da Gama L, Skarzynski DJ and Ferreira-Dias G (2020) The Inhibition of Cathepsin G on Endometrial Explants With Endometrosis in the Mare. Front. Vet. Sci. 7:582211. doi: 10.3389/fvets.2020.582211

Although proteases found in neutrophil extracellular traps (NETs) have antimicrobial properties, they also stimulate collagen type 1 (COL1) production by the mare endometrium, contributing for the development of endometrosis. Cathepsin G (CAT), a protease present in NETs, is inhibited by specific inhibitors, such as cathepsin G inhibitor I (INH; β-keto-phosphonic acid). Matrix metallopeptidases (MMPs) are proteases involved in the equilibrium of the extracellular matrix. The objective of this study was to investigate the effect of CAT and INH (a selective CAT inhibitor) on the expression of MMP-2 and MMP-9 and on gelatinolytic activity. In addition, the putative inhibitory effect of INH on CAT-induced COL1 production in mare endometrium was assessed. Endometrial explants retrieved from mares in follicular phase or midluteal phase were treated for 24 or 48 h with CAT, inhibitor alone, or both treatments. In explants, transcripts (quantitative polymerase chain reaction) of *COL1A2*, *MMP2*, and *MMP9*, as well as the relative abundance of COL1 protein (Western blot), and activity of MMP-2 and MMP-9 (zymography) were evaluated. The protease CAT induced COL1 expression in explants, at both estrous cycle phases and treatment times. The inhibitory effect of INH was observed on *COL1A2* transcripts in follicular phase at 24-h treatment, and in midluteal phase at 48 h ($P < 0.05$), and on the relative abundance of COL protein in follicular phase and midluteal phase explants, at 48 h ($P < 0.001$). Our study suggests that MMP-2 might also be involved in an earlier response to CAT, and MMP-9 in a later response, mainly in the follicular phase. While the use of INH reduced CAT-induced COL1 endometrial expression, MMPs might be involved in the fibrogenic response to CAT. Therefore, in mare endometrium, the use of INH may be a future potential therapeutic means to reduce CAT-induced COL1 formation and to hamper endometrosis establishment.

Keywords: endometrosis, cathepsin G, cathepsin G inhibitor, fibrosis, metallopeptidases

INTRODUCTION

In the endometrium, the innate and adaptive immune mechanisms, which rely on a complex network of key components (mainly growth factors/cytokines, immune cells, and epithelial and stromal cells), modulate integrated interactions between the endocrine system and the immune system. As such, they regulate uterine physiological function and provide protection against pathogens (1–3). Disruption of those immune-endocrine mediated mechanisms may lead to endometrial dysfunction and ultimately to fibrogenesis and infertility (2, 3).

A transient breeding-induced endometritis is a normal process to remove bacteria and the excess of spermatozoa from the uterus, causing an increase of neutrophils influx to the uterine lumen, which in turn increases the uterine inflammatory reaction (4–6). If the inflammation becomes chronic, the persistent influx of neutrophils toward the endometrium prompts to chronic degenerative alterations, ending in endometrosis (endometrial fibrosis) (7). However, impaired uterine clearance (6), repeated endometritis (8), and aging and multiple pregnancies (9) have been described as triggering factors of equine endometrosis. Equine endometrial fibrosis is a progressive and irreversible severe fibrotic disorder in the endometrium (7, 10, 11), causing subfertility/infertility. At the initial stage of endometrosis, fibroblasts differentiate into myofibroblasts responsible for the synthesis of collagen fibers and extracellular matrix deposition, ultimately leading to endometrial periglandular fibrosis (7, 12). Thus, these histological changes are the culprit of a decrease in pregnancy rates in the mare (10, 13).

The presence of bacteria or semen in the equine endometrium (14–16) induces neutrophil migration from blood to the uterus to fight the infection. These neutrophils release proteins and components from the nucleus that form "neutrophil extracellular traps" (NETs) extracellularly (14, 16, 17). Proteases present in NETs, namely, cathepsin G (CAT), elastase (ELA), or myeloperoxidase (MPO), possess strong antimicrobial properties, aiding on killing bacteria in the extracellular environment. However, their persistence may lead to chronic inflammation and degenerative changes in equine endometrium (18). Increased collagen type 1 (COL1) in mare endometrial explants challenged with NET components has been described previously (18–20).

Cathepsin G participates to a greater extent to inflammation and fibrosis establishment in chronic obstructive pulmonary disease (COPD) in humans (21). Also, CAT action was associated with aortic stenosis remodeling and fibrosis (22), renal fibrosis after ischemia (23) glomerulonephritis and renal failure (24), lung cystic fibrosis [(25), reviewed by (26), (27)], and fibrotic Dupuytren disease in humans (28). Cathepsin G inhibitor I (β-keto-phosphonic acid; INH) is a small non-peptide molecule that in a selective, potent, and reversible manner inhibits CAT. This inhibitor could be used for the treatment of COPD and asthma in humans (21, 29, 30). Additionally, INH exhibits an anti-inflammatory action in rats with glycogen-induced peritonitis and lipopolysaccharide-induced inflammation of the airways (29) and in airway inflammatory diseases dependent on CAT in animal models (30).

Matrix metallopeptidases (MMPs) are involved in extracellular matrix balance and in endometrial tissue remodeling (31). These enzymes have the capability to degrade extracellular matrix structural components, such as collagen (32). In the equine endometrium, during bacterial and breeding-induced acute endometritis, MMP-2 and MMP-9 are engaged in the inflammatory reaction and COL modification (33). But, if an alteration in the regulation of these MMPs or a prolonged exposure to inflammation occurs, it leads to deposition of COL and subsequent establishment of endometrial fibrosis (33). In our recent *in vitro* studies on equine endometrium, MMP expression was affected by mediators of inflammation, such as interleukins, transforming growth factor β1 (TGFβ1), and prostaglandins (PGs) (12, 34, 35); differs among stages of endometrosis (35); and might be implicated in fibrotic response to ELA (20).

It has been known that ELA and CAT proteases released by neutrophils are capable of destroying the extracellular matrix, stimulating leukocyte migration, and inducing tissue remodeling (29, 36). Our previous *in vitro* studies reported them as being also associated with endometrial fibrosis establishment (18–20). In fact, ELA, CAT, and MPO appear to act as profibrotic factors in mare endometrosis (18). The inhibition of ELA using sivelestat sodium salt, a specific ELA inhibitor, provoked a downregulation of *COL1A2* mRNA transcription (18, 20). Among proteases present in NETs, the one that shows the predominant proteolytic activity is ELA. Nevertheless, when ELA was immune depleted from NETs derived from healthy human neutrophils, the remaining activity was attributed to CAT (37). Moreover, in the pathophysiology of COPD in humans, CAT seems to play a particularly important role (29). These findings justify the recent development of diagnostic tests that use CAT as a COPD marker (38). Thus, the importance of studying inhibitors of proteases present in NETs, such as CAT, is imperative for the development of putative therapeutic measures for the control of fibrosis.

Because CAT (present in NETs) and MMPs appear to be involved in the development of equine endometrosis (18, 20), we have decided to investigate potential putative ways of fighting this condition by impairing fibrosis formation. We hypothesized that by inhibiting CAT using a specific inhibitor (β-keto-phosphonic acid), it would be possible to reduce the COL1 output and thus hinder the profibrotic response to CAT in equine endometrial explants. Therefore, the objective of this *in vitro* study was to investigate the INH inhibitory action on the relative abundance of CAT-induced COL1 protein in explants of mare endometrium. In addition, the influence of CAT and INH on MMP-2 and MMP-9 expression and gelatinolytic activity was assessed.

MATERIALS AND METHODS

Animals

From April to September, at an abattoir in Poland (Rawicz), uteri and jugular venous blood were randomly retrieved postmortem

from cyclic mares destined for meat production, according to the European (European Food Safety Authority, AHAW/04-027) legislation. Mares' average age was 12 years. The official veterinary inspection certified that those mares were healthy, and their meat was safe for human consumption. Estrous cycle phase of each mare was determined based on ovarian and uterine features and on progesterone plasma concentration, as previously described (18, 39). Thus, mares, which presented a follicle >35-mm diameter, absence of an active corpus luteum, and plasma progesterone concentration <1 ng/mL, were classified as being in the follicular phase. In contrast, the existence of a well-developed corpus luteum associated with the presence of follicles with a diameter between 15 and 20 mm and plasma progesterone concentration >6 ng/mL were the grounds for considering those mares in the midluteal phase. For the present study, follicular phase ($n = 8$) and midluteal phase ($n = 7$) endometria were used. After collection, jugular venous blood in ethylenediaminetetraacetic acid tubes and uteri were transported on ice to the laboratory. The uteri were placed in ice-cold Dulbecco modified Eagle medium (DMEM) F-12 Ham medium (D/F medium; 1:1 (vol/vol); D-2960; Sigma–Aldrich, St. Louis, MO, USA), supplemented with antibiotics, such as penicillin (100 IU/mL; P3032; Sigma–Aldrich) and streptomycin (100 μg/mL; S9137; Sigma–Aldrich), and an antimycotic drug, amphotericin (2 μg /mL; A2942; Sigma–Aldrich). All the mares' uteri used were examined for the absence of endometritis, both macroscopically and microscopically. The macroscopic examination enabled the visualization of increased mucus production or altered endometrial surface color in the presence of endometritis. The microscopic evaluation of the eventual presence of bacteria and/or neutrophils in the endometrium was accomplished by collecting the cells with a sterile swab, rolled on a glass slide, and colored with Diff-Quick stain (18, 40). Endometritis was the grounds for discarding the uteri. To perform the histological and endometrial classification (41), two fresh endometrial samples (around 0.5-cm width by 2-cm length), immediately after collection, from each uterus were immersed in 4% buffered paraformaldehyde. Changes in mare endometrium were assessed as described by Kenney and Doig (41). Regarding the amount of endometrial inflammation and/or fibrosis, endometria were classified as I, IIA, IIB, or III categories, according to Kenney and Doig (41). Slight to scattered inflammation (endometritis) or mild fibrosis (endometrosis) or mild lymphatic lacunae can be found in Kenney and Doig's category IIA. In category IIB, there might be moderate inflammation, but mostly moderate fibrosis that can be multifocal or diffuse, or moderate lymphatic lacunae (41, 42), although, in this study, only endometria with mild to moderate fibrotic lesions (IIA or IIB category) were used, avoiding endometria with inflammation (endometritis). Besides, no category III endometria were used to exclude possible variations due to increased endometrial fibrotic lesions.

In vitro Endometrial Explant Culture

Strips (around 0.5-cm width by 2- to 3-cm length) of endometrium from the ipsilateral horn to the active ovary were detached from the myometrium after the uterus was washed in phosphate-buffered saline (PBS) with streptomycin (100 μg /mL; S9137; Sigma–Aldrich) and penicillin (100 IU/mL; P3032; Sigma–Aldrich) added.

For explant culture experiments, strips of endometrium were put in ice-cold PBS supplemented with antibiotics (as above) in a Petri dish. Then, the endometrium strips were washed with PBS supplemented with antibiotics and endometrial explants, cut, and blotted with filter paper. The explants, weighing from 20 to 30 mg each, were placed in a single well of a sterile 24-well cell culture plate (Eppendorf, #0030 722.116) with 1 mL of DMEM culture medium with bovine serum albumin (0.1% wt/vol; 735078; Roche Diagnostics, Mannheim, Germany), streptomycin (100 μg/mL; S9137; Sigma–Aldrich), penicillin (100 IU/mL; P3032; Sigma–Aldrich), and amphotericin (2 μg/mL; A2942; Sigma–Aldrich). The endometrial explants were preincubated at 38°C, in a 5% CO_2 humidified atmosphere (Biosafe Eco-Integra Biosciences, Chur, Switzerland), for 1 h, and submitted to 150 rpm gentle shaking, as described previously (18). Afterward, culture medium was replaced, and equine endometrial explants were treated for 24 or 48 h, as follows: (i) vehicle (negative control)—culture medium alone; (ii) CAT (1 μg/mL; A6942, Applichem GmbH, Germany); (iii) cathepsin G inhibitor I (INH; 1 μg/mL; β-keto-phosphonic acid; $C_{36}H_{33}N_2O_6P$, sc-221399; Santa Cruz Biotechnology, USA); and (iv) CAT (1 μg/mL) + INH (1 μg/mL). Each treatment was performed in quadruplicate. The INH was added after 1 h of preincubation, at the time of culture medium replacement, to allow time for the inhibitor to bind. Protease CAT was added 1 h later. In studies undergoing a total of 48 h, after 24-h treatment, 1 μg/mL of IHN was added once again to the culture medium, because in the pretrial its inhibitory effect remained for only 24 h and waned at 48-h treatment. At the end of each treatment time, explants were collected and placed in RNAlater (R901, Sigma–Aldrich), while conditioned media were collected and stored at −80°C. In a previous study, as a positive control for COL expression, endometrial tissue response to a fibrotic stimulus was assessed by adding TGFβ1 (a profibrotic cytokine) to tissue culture medium (20). To assess viability, the explants were also incubated with oxytocin (OXT), as described before (20).

As shown by our previous work, when dose assessment was determined (18), the use of 1 μg/mL of CAT proved to induce the expression of fibrotic marker, TGFβ1. A dose–response pilot experiment was performed to assess the most suitable concentration of INH, based in other previous *in vitro* studies (43). The INH was tested using 0.01, 0.1, 1, 10, and 100 μg/mL, and the optimal concentration that inhibited *COL1A2* transcription was 1 μg/mL (data not shown).

Assessment of Endometrial Explants Viability

The assessment of endometrial explant viability was based on lactate dehydrogenase (LDH) activity as described before (20) and on OXT-induced $PGF_{2\alpha}$ secretion in conditioned culture medium. The $PGF_{2\alpha}$ secretion was determined by using an enzyme immunoassay kit (ADI-901-069, Enzo), according to the manufacturer's instructions.

Quantitative Real-Time Polymerase Chain Reaction

Total RNA from equine endometrial treated explants was extracted using TRI Reagent® (T9424; Sigma–Aldrich), as indicated by the manufacturer. After, RNA quantification and quality evaluation were performed, as described previously (20). Specific primers for the reference gene ribosomal protein L32 (*RPL32*) and for *COL1A2, MMP2,* and *MMP9* are presented in **Table 1**. The reference gene *RPL32* was the most stable internal control, already determined in a previous study (20, 44). All the reactions for target and reference genes were performed in duplicate, on a 96 well plate (4306737; Applied Biosystems) and run in a StepOnePlus™ Real-Time PCR System (Applied Biosystems, Warrington, UK). To confirm specificity, the polymerase chain reaction (PCR) products were run on a 2.5% agarose gel, and relative mRNA data were quantified using the quantitative PCR miner algorithm. Briefly, the average of the cyclic threshold (Cq) and the primer efficiency level (E) for each sample were related using the following equation: [1/(1þE)Cq]. Afterward, the expression levels of the target genes were normalized against the reference gene (45).

Western Blot Analysis

Protein relative abundance of COL1 was determined by Western blot technique using a non-staining total protein loading control as previously described (20, 46). The membranes were incubated overnight, at 4°C with the primary antibody against COL1 (1:1,000 diluted; 20121; Novotec, Lyon, France), as previously defined (18). The secondary antibody used was horseradish peroxidase–conjugated anti-rabbit (1:20,000; P0448; DakoCytomation, Carpinteria, CA, USA) incubated at room temperature for 1.5 h. Visualization of the relative abundance of COL1 protein was accomplished by luminol enhanced chemiluminescence (Super Signal West Pico, 34077; Thermo Scientific, Waltham, MA, USA). For band normalization in each membrane, and to allow band comparison between membranes, a standard sample of a blend of endometrial explants (30 μg) was loaded in a single lane, in all gels. Image acquisition and band normalization were performed, as described (20, 47).

TABLE 1 | Primers used in quantitative PCR.

Gene (accession number)	Sequence 5′-3′	Amplicon
COL1A2 (XM_001492939.3)	Forward: CAAGGGCATTAGGGGACACA	196
	Reverse: ACCCACACTTCCATCGCTTC	
MMP2 (XM_001493281.2)	Forward: TCCCACTTTGATGACGACGA	115
	Reverse: TTGCCGTTGAAGAGGAAAGG	
MMP9 (NM_001111302.1)	Forward: GCGGTAAGGTGCTGCTGTTC	177
	Reverse: GAAGCGGTCCTGGGAGAAGT	
RPL32 (XM_001492042.6)	Forward: AGCCATCTACTCGGCGTCA	144
	Reverse: GTCAATGCCTCTGGGTTTCC	

COL1A2, collagen type 1 α2; MMP2, matrix metallopeptidase 2; MMP9, matrix metallopeptidase 9; RPL32, ribosomal protein L32.

Zymography

The activity of MMP-2 and MMP-9 on gelatin gel was assessed by zymography, through a non-staining total protein loading control, as previously described (20, 48, 49). Gels and samples of culture medium supernatant were handled, as referred by Amaral et al. (20). In all gels, molecular weight determination was made using recombinant human MMP-2 protein, CF (902-MP-010; R&D Systems, Minneapolis, USA) and recombinant human MMP-9 Western Blot Standard Protein (WBC018; R&D Systems). In order to normalize and compare gels, a standard sample (40 μg) of mixed culture medium was also loaded. The images detection and MMPs gelatinolytic activity were determined as already reported (20). Briefly, using Image Lab 6.0 (Bio-Rad) software, the lanes were detected in a non-staining total protein gel image, and the bands corresponding to MMP-2 and MMP-9 activity were detected on the Coomassie staining image. The normalization factor and volume of target protein were calculated by the software, and then the values were adjusted for variation in the protein load.

Statistical Analysis

The variables assessed in this study were *COL1A2*, *MMP2*, and *MMP9* transcription; COL1 protein relative abundance; and gelatinolytic activity of both proactive and active forms of MMP-2 and MMP-9. The Kolmogorov–Smirnov test in Proc Univariate function of SAS v. 9.4 (SAS Institute Inc.) and visual examination were used to check data normality. The square root and logarithmic transformations were achieved because some of the variables did not show a normal distribution, and the best transformation method was chosen. At first, the response variables were analyzed by PROC GLM of SAS, as a function of the different treatments: combination of the use of CAT, use of INH, estrous cycle phase, and incubation time, in a total of 16 treatment combinations. Using the PDIFF option of PROC GLM, the least square means of the treatments combinations were compared, and the results were considered significant as $P < 0.05$. For data plotting, the means were back transformed to the original scale. Afterward, the two-, three-, and four-way interactions of the treatment combinations were also performed. In **Figures 1**, **2**, the results of relative abundance of COL1 protein and *COL1A2*, *MMP2*, and *MMP9* transcripts are depicted as median with interquartile range. In **Figure 3**, gelatinolytic activity data for MMP-2 and MMP-9 are shown as least square means ± SEM. The graphs presented were built using GraphPad PRISM.

RESULTS

Long-Term Viability of Explants From Equine Endometrium

As shown before by Amaral et al. (20), *COL1A2* transcription and protein relative abundance of COL1 were upregulated in response to TGFβ1 treatment. About viability data, no difference was found in LDH activity between 1- and 24-h treatment times,

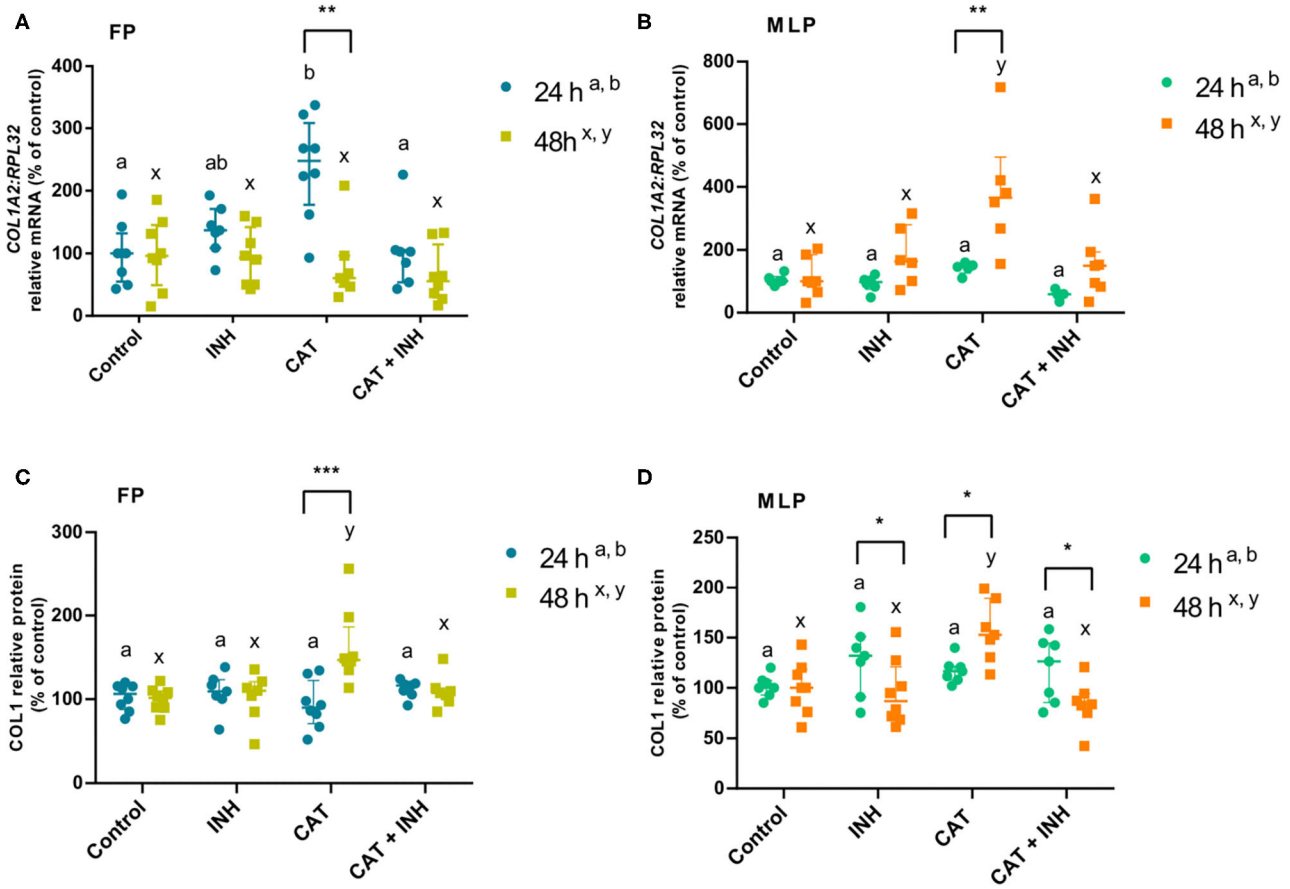

FIGURE 1 | Relative collagen type 1 (*COL1A2*) mRNA transcription **(A,B)** and protein (COL1) relative abundance **(C,D)** in follicular phase (FP) and midluteal phase (MLP) mare endometrial explants treated for 24 or 48 h with culture medium alone (control), cathepsin G inhibitor I (INH: 1 μg/mL), cathepsin G (CAT: 1 μg/mL), or CAT (1 μg/mL) + INH (1 μg/mL). Data are shown as median with interquartile range. Results were considered significant at $P < 0.05$. Different superscript letters indicate significant differences between treatments within each treatment time (a,b: 24 h; x,y: 48 h). Asterisks indicate statistical differences between times of treatment for the same treatment (*$P < 0.05$, **$P < 0.01$, ***$P < 0.001$).

but a slight decrease was shown at 48 h, regardless of estrous cycle phase. Besides, mare endometrial tissues treated with OXT augmented $PGF_{2\alpha}$ secretion at both estrous cycle phases and treatment times (**Supplementary Table 1**).

The Effect of INH on CAT-Induced COL1

Supplementary Table 2 lists the interactions among treatments, time of treatment, and estrous cycle phase. The differences between estrous cycle phases (follicular phase vs. midluteal phase) within each treatment and treatment times are presented in **Supplementary Table 3**.

The treatment with CAT elevated *COL1A2* transcripts in follicular phase endometrial explants at 24 h ($P < 0.01$; **Figure 1A**) and in midluteal phase tissue at 48 h ($P < 0.0001$; **Figure 1B**) relative to the respective control group. Nevertheless, the combination of CAT and INH downregulated *COL1A2* transcripts compared to the corresponding CAT-treated groups (follicular phase 24 h: $P < 0.01$; midluteal phase 48 h: $P < 0.001$; **Figures 1A,B**). In midluteal phase, at 48 h, the transcription also increased in CAT-treated explants regarding INH-treated group ($P < 0.001$; **Figure 1B**).

In CAT-treated tissues, COL1 protein relative abundance increased in the longest period of treatment both in follicular phase ($P < 0.01$; **Figure 1C**) and midluteal phase explants ($P < 0.001$; **Figure 1D**, **Supplementary Figure 1**) relative to the control group. The association of CAT and INH reduced protein relative abundance after 48-h treatment both in follicular phase ($P < 0.01$; **Figure 1C**) and midluteal phase explants ($P < 0.001$; **Figure 1D**, **Supplementary Figure 1**) compared to the respective CAT-treated groups. Explants treated with CAT also elevated COL protein relative abundance at 48 h, both in follicular phase ($P < 0.01$; **Figure 1C**), and in midluteal phase endometria ($P < 0.001$; **Figure 1D**, **Supplementary Figure 1**), when compared to the respective INH-treated group.

At 24 h, in follicular phase, in the CAT-treated group, *COL1A2* mRNA transcription was higher when compared to 48 h (**Figure 1A**), although the protein relative abundance was higher at 48 h (**Figure 1C**). But, in midluteal phase tissues, CAT treatment upregulated *COL1A2* transcripts (**Figure 1B**) and

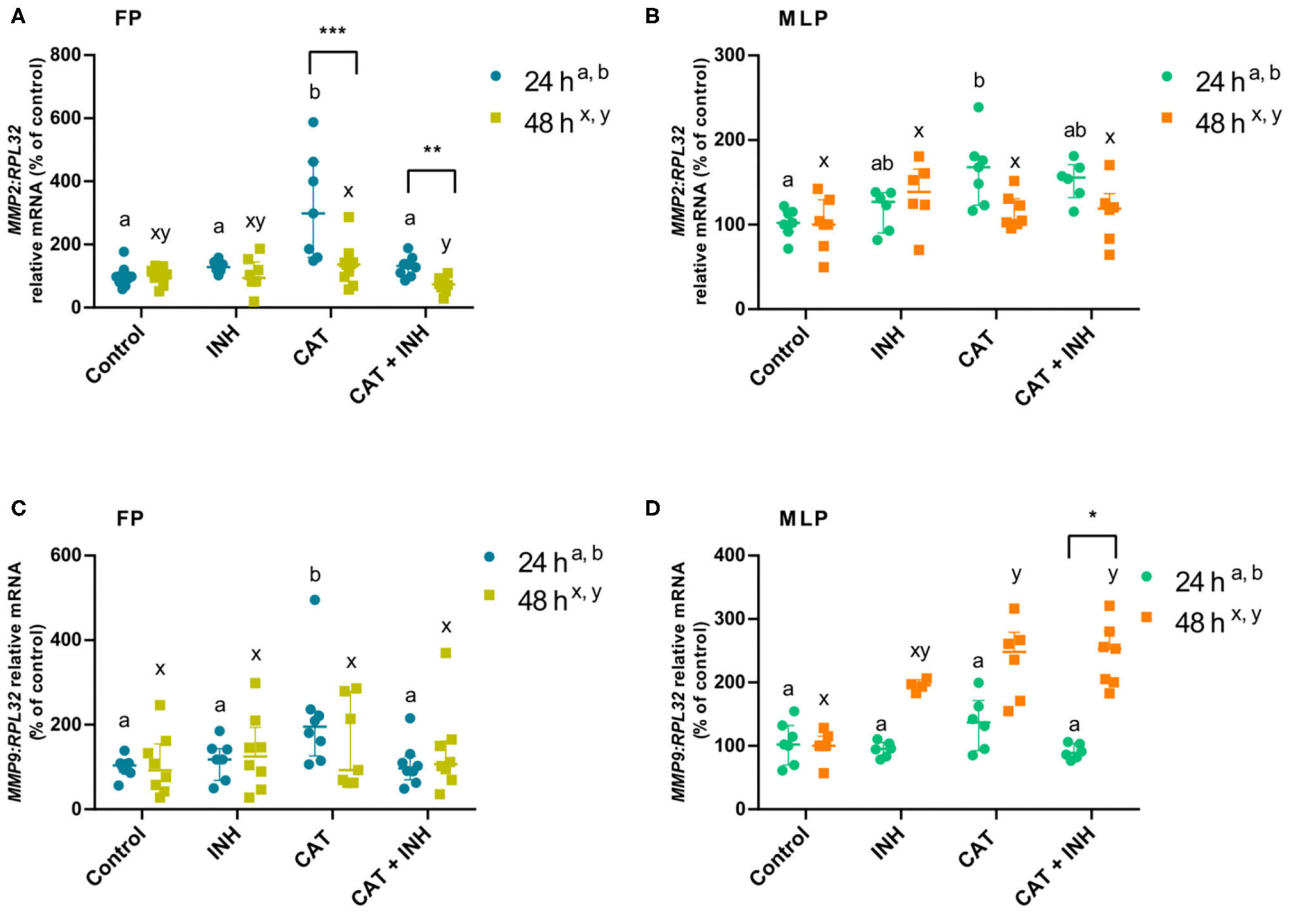

FIGURE 2 | Relative mRNA transcription of *MMP2* **(A,B)** and *MMP9* **(C,D)** in follicular phase (FP) and midluteal phase (MLP) mare endometrial explants treated for 24 or 48 h with culture medium alone (control), cathepsin G inhibitor I (INH: 1 μg/mL), cathepsin G (CAT: 1 μg/mL), or CAT (1 μg/mL) + INH (1 μg/mL). Data are shown as median with interquartile range. Results were considered significant at $P < 0.05$. Different superscript letters indicate significant differences between treatments within each treatment time (a,b: 24 h; x,y: 48 h). Asterisks indicate statistical differences between times of treatment for the same treatment (*$P < 0.05$, **$P < 0.01$, ***$P < 0.001$).

COL1 protein relative abundance (**Figure 1D**) at 48 h when compared to 24 h. Also, in midluteal phase at 48 h, the COL1 protein relative abundance was reduced in INH-treated and CAT+INH–treated groups when compared to 24-h treatment (**Figure 1D**, **Supplementary Figure 1**).

Evaluation of CAT and INH Effect on MMP Expression

The *MMP2* transcript levels increased in CAT-treated explants in follicular phase at 24 h compared to its respective control group ($P < 0.001$) and INH group ($P < 0.05$; **Figure 2A**). But, when those explants were submitted to the combination of CAT and INH, there was a reduction in *MMP2* mRNA, comparing to the respective CAT-treated tissues ($P < 0.01$; **Figure 2A**). In the same estrous cycle phase, but after 48-h treatment, CAT+INH treatment reduced *MMP2* transcripts in relation to the CAT-treated group ($P < 0.01$; **Figure 2A**), which was not increased when compared to control. In midluteal phase explants, at 24 h, CAT treatment augmented *MMP2* mRNA when related to the respective control ($P < 0.05$; **Figure 2B**).

In the follicular phase, at 24 h, the CAT treatment was able to increase *MMP9* mRNA levels in endometrial explants with respect to the respective control group ($P < 0.01$; **Figure 2C**) and INH-treated group ($P < 0.05$; **Figure 2C**). However, the CAT+INH–treated explants reduced *MMP9* transcripts compared to the CAT-treated group ($P < 0.05$; **Figure 2C**). At 48 h, midluteal phase endometrium treated with CAT upregulated *MMP9* transcription ($P < 0.05$), which further increased with CAT+INH treatment ($P < 0.01$; **Figure 2D**) compared to the non-treated group.

In follicular phase, the treatments of CAT and CAT+INH increased *MMP2* transcripts at 24 h in comparison to 48 h (**Figure 2A**). In contrast, in midluteal phase endometrium, in explants treated for 48 h, the combination of CAT and INH augmented *MMP9* transcripts with respect to 24-h treatment ($P < 0.05$; **Figure 2D**).

The analysis of the proform of MMP-2 gelatinolytic activity has shown that INH-treated and CAT-treated groups decreased its activity in follicular phase at 24 h ($P < 0.05$; **Figure 3A**, **Supplementary Figure 1**). Nevertheless, in follicular phase

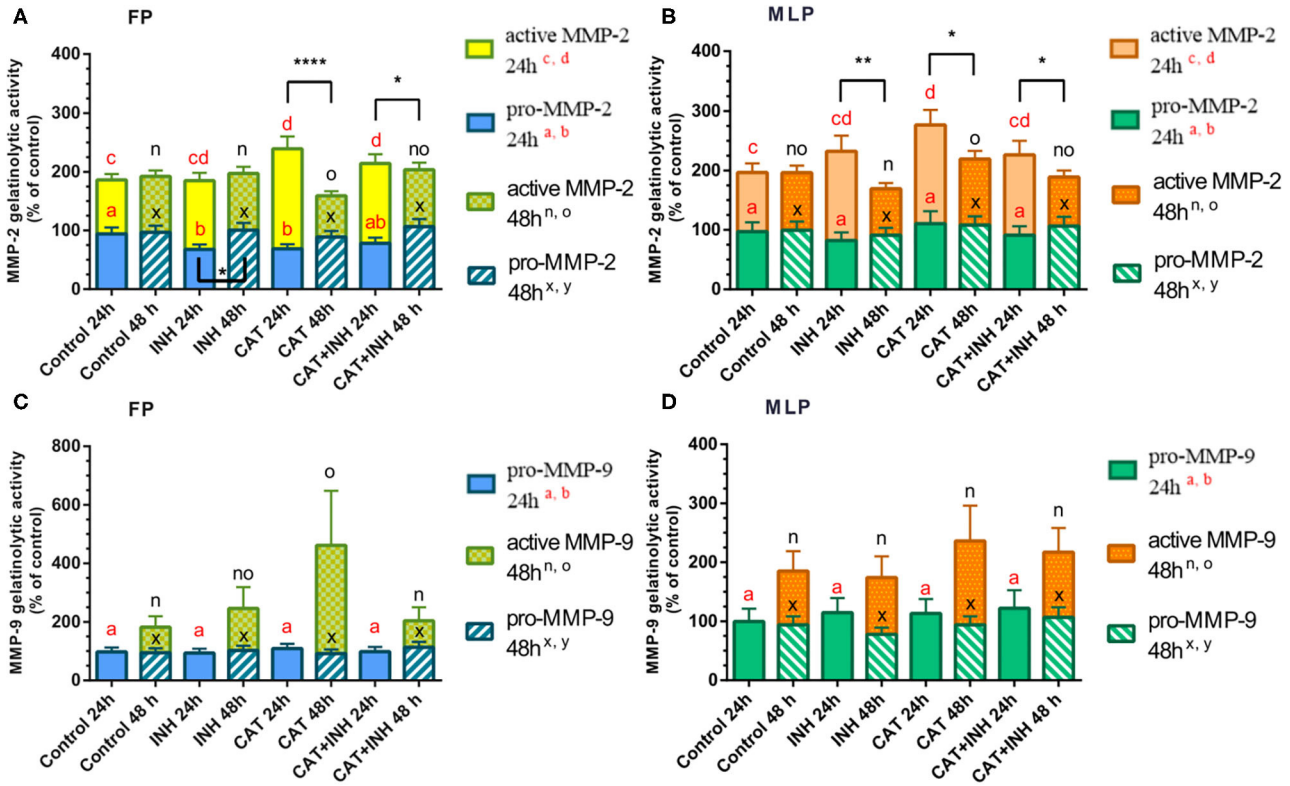

FIGURE 3 | Relative gelatinolytic activities of MMP-2 **(A,B)** and MMP-9 **(C,D)** in follicular phase (FP) and midluteal phase (MLP) mare endometrial explants treated for 24 or 48 h with culture medium alone (control), cathepsin G inhibitor I (INH: 1 μg/mL), cathepsin G (CAT: 1 μg/mL) or CAT (1 μg/mL) + INH (1 μg/mL). All values are expressed as percentage of change from control (non-treated tissues). Bars represent least square means ± SEM, and results were considered significant at $P < 0.05$. Different superscript letters indicate significant differences between treatments within each treatment time. Asterisks indicate statistical differences between different treatment times for the same treatment and for the same form of MMP (*$P < 0.05$, **$P < 0.01$, ****$P < 0.0001$).

endometrial explants treated for 24 h with CAT and combination of CAT+INH, the gelatinolytic activity of MMP-2 active form was upregulated with respect to the control group ($P < 0.001$ and $P < 0.05$, respectively; **Figure 3A**, **Supplementary Figure 1**). The active MMP-2 gelatinolytic activity was augmented in midluteal phase tissues treated for 24 h with CAT compared to the control group ($P < 0.05$; **Figure 3B**). At 48 h, in midluteal phase, CAT treatment increased active MMP-2 gelatinolytic activity comparing to INH-treated group ($P < 0.05$; **Figure 3B**, **Supplementary Figure 1**).

The gelatinolytic activity of MMP-9 active form was detected in both estrous cycle phases, but only at 48-h treatment (**Figures 3C,D**). In follicular phase explants, treated with CAT, the active MMP-9 gelatinolytic activity increased comparing to the control group ($P < 0.05$; **Figure 3C**) and was reduced in CAT+INH–treated tissues, in comparison to the respective group treated with CAT ($P < 0.05$; **Figure 3C**, **Supplementary Figure 1**).

The gelatinolytic activity of pro–MMP-2 enzyme in the INH-treated group was downregulated at 24 h in follicular phase explants (**Figure 3A**, **Supplementary Figure 1**). The stimulatory effect of CAT was higher in follicular phase at 24 h than at 48 h on active MMP-2 gelatinolytic activity (**Figure 3A**), and the combination of CAT and INH reduced the gelatinolytic activity at 48 h comparing to 24-h treatment (**Figure 3A**, **Supplementary Figure 1**). In midluteal phase endometrium, all treatments upregulated the active gelatinolytic activity of MMP-2 at 24 h, compared to 48 h (**Figure 3B**, **Supplementary Figure 1**).

DISCUSSION

In the present study, CAT induced COL1 expression in explants of mare endometrium, at follicular phase and midluteal phase in a time-dependent manner. The *COL1A2* mRNA results show that CAT acts as a profibrotic protease, mainly in follicular phase, as a response to a shorter stimulus, and in midluteal phase as a response to a longer stimulus. During the follicular phase, endogenous estrogen thickens the uterine wall and increases uterine muscular tone and vascularization. The cervix is relaxed and opens (50). The endometrial glands also proliferate, and the lamina propria becomes highly edematous (10). The mare endometrium is more prone to inflammation and more reactive at estrus, which might explain why the explants obtained at the follicular phase, under the influence of estrogens, were reactive to CAT after a short time of stimulation. Moreover, a longer time of CAT exposition was needed to increase expression of COL1

at the protein level. The COL1 protein relative abundance was increased by CAT only at 48 h in both estrous cycle phases.

One of the aims of this study was to evaluate if by inhibiting CAT using a specific inhibitor (IHN) it would be possible to reduce CAT-induced COL1 relative abundance in equine endometrium. This inhibitor blocks the increase of monocyte chemoattractant protein 1 and tumor necrosis factor α, both linked to airway hyperactivity (29), and blocks neutrophilia (51). We showed in our study that the inhibitory effects of IHN were detected in the longest treatment time, corresponding to the increased COL1 relative abundance induced by CAT treatment. To the best of our knowledge, this is the first study describing that by inhibiting CAT, it is possible to reduce COL1 relative abundance in equine endometrium *in vitro*. Therefore, we suggest that this treatment could be a possible approach to prevent the formation of endometrosis. In fact, INH offers a promising therapeutic strategy in chronic inflammatory conditions, such as asthma or COPD (26). Future *in vivo* studies are crucial to test this hypothesis. Currently, despite the therapies proposed to treat equine endometrosis, there is no routinely available effective treatment (42, 52). Several therapeutic approaches, as mechanical curettage or intrauterine application of chemical agents (kerosene, dimethyl sulfoxide, isotonic salt) or mesenchymal stem cells, have been studied (53–55). Nevertheless, they caused rather short-term beneficial effects and/or did not improve pregnancy rates (53–55). Thus, the need for evaluating the *in vivo* efficacy of INH in the treatment of equine endometrosis associated with NETs is imperative. Indeed, our findings may be the grounds for further *in vivo* trials for INH testing.

Fibrosis is the result of a disruption in the balance of the extracellular matrix, with increased synthesis and deposition of extracellular matrix components and decreased degradation of those products (56). The MMPs have been considered as being part of the highly regulated systems that control this extracellular matrix turnover (57). An increase in the active form of MMP-2 has been reported in mare endometrosis (58), although other works showed no changes in MMP-2 or MMP-9 expression between normal and fibrotic equine endometrium (59). Another study done by Centeno et al. (60) found that *MMP2* transcription was upregulated in endometrial fibrosis. Moreover, we have recently reported an upregulation of MMP-2 and MMP-9 levels in mare endometrial tissue with mild to moderate lesions, as well as an increase of MMP-9 levels in fibroblasts and epithelial cells challenged by TGFβ1 (35). In other tissues, CAT has previously been capable to activate pro–MMP-2 in human tumor cell invasion (61) and together with MMP-9 may enhance TGFβ signaling in a tumor murine model (62). The inconsistency between MMP expression found in normal and fibrotic equine endometrium may be explained by the fact that fibrotic changes, as in other tissues (e.g., lungs) (63), are diffuse. The collected tissue may not always reflect the entire condition of the fibrotic organ and thus might not fully address the cellular and spatial heterogeneity of fibrosis. Additionally, because endometria at different stages of fibrosis were obtained postmortem from different mares, it was not feasible to evaluate the evolution of the fibrogenic process individually. This may have affected the results and thus could also explain the inconsistent pattern found. However, despite these limitations, also observed in other tissues, understanding of the molecular pathways and the expression of various factors involved in equine endometrosis is rather important, by unraveling changes associated with this pathological condition.

In our study, the gelatinolytic activity of MMP-2 active form in endometrial explants increased in response to CAT treatment after the shortest treatment time (24 h), at both estrous cycle phases. Nevertheless, this profibrotic effect of CAT was diminished with INH addition in follicular phase tissue treated for 24 h. Apparently, MMP-2 appears to be involved in an immediate response, perturbing extracellular matrix balance. So, MMP-2 can mediate an acute response to a CAT-induced inflammation, regardless of the estrous cycle phase.

In follicular phase endometrial explants, the gelatinolytic activity of MMP-9 active form increased with CAT treatment and was inhibited by INH at 48 h. This suggests MMP-9 involvement, especially in follicular phase equine endometrium, remodeling the fibrogenic response to a prolonged exposition to CAT.

Elevated levels of MMPs in the endometrium may also indicate a cellular response to an altered extracellular matrix balance, as part of the normal regulation of MMP expression. In fact, the main role attributed to MMPs is their action on the turnover and degradation of extracellular matrix substrates. Regulation of MMPs activity takes place at the stages of gene transcription, protein production, activation of proenzymes, and inhibition of the active enzymes by tissue inhibitor of matrix metallopeptidases or α2-macroglobulin (64). Many of these factors can contribute to the differences found between gene transcription, proenzyme, and active form of MMP-2 and MMP-9. In addition, MMP-9 may be regulated by ovarian steroids, which can explain why this enzyme activity differed according to various estrous cycle phases (65). Many mechanisms are involved in the response to CAT profibrotic stimulus, and more studies are necessary to unravel the role of MMPs, either in healthy or fibrotic endometrium.

CONCLUSIONS

Even though our previous (18, 20) and present results suggest that ELA and CAT are profibrotic factors and are involved in equine endometrial fibrosis establishment, the study of other causes, including the role of other proteases found in NETs, is vital to fully understand the mechanisms of endometrosis pathogenesis. The use of a selective CAT inhibitor was effective on the reduction of COL1 expression. Therefore, these novel data may contribute to the development of a new prophylactic or therapeutic approach for endometrosis. Although the use of a broad-spectrum protease inhibitor or specific selective inhibitors combined may be needed to obtain a strong and more effective inhibitory effect. MMP-2 might be involved in an earlier response to CAT, independent of estrous cycle phase, and MMP-9 in a later response, mainly in the follicular phase.

DATA AVAILABILITY STATEMENT

The raw data supporting the conclusions of this article will be made available by the authors, without undue reservation.

AUTHOR CONTRIBUTIONS

GF-D and DS: conceptualization, resources, data curation, visualization, supervision, project administration, and funding acquisition. AA, CF, SM, MR, AS-M, KL, and BG-K: methodology. AA, CF, and LT: formal analysis. AA, CF, MR, SM, AS-M, and KL: investigation. AA: writing—original draft preparation. GF-D, DS, AS-M, MR, BG-K, and LT: writing—review and editing. All authors have read and agreed to the published version of the manuscript.

FUNDING

The research was supported by Fundação para a Ciência e Tecnologia (FCT) research grants (UIDP/CVT/00276/2020 and PTDC/CVT-REP/4202/2014) and by a grant from the National Science Centre, Poland (project no. 2019/35/D/NZ9/02989). GF-D, DS, AS-M, and CF were supported by the bilateral Polish–Portugal research project under the agreement of NAWA project (No. PPN/BIL/2018/1/00250/U/0001). AA was awarded a Doctoral fellowship from Fundação para a Ciência e Tecnologia (SFRH/BD/101058/2014).

ACKNOWLEDGMENTS

The authors wish to acknowledge Maria do Rosário Luís and Katarzyna Jankowska for histology preparations, and Pedro Pinto-Bravo, Paula Brito, and Agnieszka Baclawska for laboratory assistance.

SUPPLEMENTARY MATERIAL

The Supplementary Material for this article can be found online at: https://www.frontiersin.org/articles/10.3389/fvets.2020.582211/full#supplementary-material

REFERENCES

1. Skarzynski DJ, Szostek-Mioduchowska AZ, Rebordão MR, Moza Jalali B, Piotrowska-Tomala KK, Leciejewska N, et al. Neutrophils, monocytes and other immune components in the equine endometrium: friends or foes? *Theriogenology*. (2020) 150:150–7. doi: 10.1016/j.theriogenology.2020.01.018
2. Hickey DK, Patel MV, Fahey JV, Wira CR. Innate and adaptive immunity at mucosal surfaces of the female reproductive tract: stratification and integration of immune protection against the transmission of sexually transmitted infections. *J Reprod Immunol.* (2011) 88:185–94. doi: 10.1016/j.jri.2011.01.005
3. Sheldon IM, Owens S-E, Turner ML. Innate immunity and the sensing of infection, damage and danger in the female genital tract. *J Reprod Immunol.* (2017) 119:67–73. doi: 10.1016/j.jri.2016.07.002
4. Katila T. Onset and duration of uterine inflammatory response of mares after insemination with fresh semen. *Biol Reprod.* (1995) 52:515–7. doi: 10.1093/biolreprod/52.monograph_series1.515
5. Troedsson MHT. Breeding-induced endometritis in mares. *Vet Clin N Am-Equine.* (2006) 22:705–12. doi: 10.1016/j.cveq.2006.07.003
6. Leblanc M, Causey R. Clinical and subclinical endometritis in the mare: both threats to fertility. *Reprod Domest Anim.* (2009) 44:10–22. doi: 10.1111/j.1439-0531.2009.01485.x
7. Hoffmann C, Ellenberger C, Mattos Rc, Aupperle H, Dhein S, Stief B, et al. The equine endometrosis: new insights into the pathogenesis. *Anim Reprod Sci.* (2009) 111:261–78. doi: 10.1016/j.anireprosci.2008.03.019
8. Doig PA, Mcknight JD, Miller RB. The use of endometrial biopsy in the infertile mare. *Can Vet J*. (1981) 22:72–6.
9. Ricketts Sw, Alonso S. The effect of age and parity on the development of equine chronic endometrial disease. *Equine Vet J.* (1991) 23:189–92. doi: 10.1111/j.2042-3306.1991.tb02752.x
10. Kenney RM. Cyclic and pathologic changes of the mare endometrium as detected by biopsy, with a note on early embryonic death. *J Am Vet Med Assoc*. (1978) 172:241–62.
11. Kenney RM. The aetiology, diagnosis, and classification of chronic degenerative endometritis. In: Hughes JP, Editor. *Workshop on Equine Endometritis*. Newmarket: Equine Vet J (1992). p. 186
12. Szóstek-Mioduchowska AZ, Baclawska A, Rebordão MR, Ferreira-Dias G, Skarzynski DJ. Prostaglandins effect on matrix metallopeptidases and collagen in mare endometrial fibroblasts. *Theriogenology*. (2020) 153:74–84. doi: 10.1016/j.theriogenology.2020.04.040
13. Liepina E, Antane V. Endometrial histological changes and pregnancy rates in mares impaired cervical drainage. In: *Proceedings of 29th International Scientific Conference Animals*. Jelgava, Latvia: Health Food Hygiene (2010). p. 73–8.
14. Alghamdi AS, Foster DN. Seminal dnase frees spermatozoa entangled in neutrophil extracellular traps. *Biol Reprod.* (2005) 73:1174–81. doi: 10.1095/biolreprod.105.045666
15. Alghamdi AS, Lovaas BJ, Bird SL, Lamb GC, Rendahl AK, Taube PC, et al. Species-specific interaction of seminal plasma on sperm–neutrophil binding. *Anim Reprod Sci*. (2009) 114:331–44. doi: 10.1016/j.anireprosci.2008.10.015
16. Rebordão Mr, Carneiro C, Alexandre-Pires G, Brito P, Pereira C, Nunes T, et al. Neutrophil extracellular traps formation by bacteria causing endometritis in the Mare. *J Reprod Immunol.* (2014) 106:41–9. doi: 10.1016/j.jri.2014.08.003
17. Brinkmann V. Neutrophil extracellular traps kill bacteria. *Science.* (2004) 303:1532–5. doi: 10.1126/science.1092385
18. Rebordão Mr, Amaral A, Lukasik K, Szóstek-Mioduchowska A, Pinto-Bravo P, Galvão A, et al. Constituents of neutrophil extracellular traps induce *in vitro* collagen formation in mare endometrium. *Theriogenology.* (2018) 113:8–18. doi: 10.1016/j.theriogenology.2018.02.001
19. Amaral A, Fernandes C, Lukasik K, Szóstek-Mioduchowska A, Baclawska A, Rebordão MR, et al. Elastase inhibition affects collagen transcription and prostaglandin secretion in mare endometrium during the estrous cycle. *Reprod Dom Anim.* (2018) 53:66–9. doi: 10.1111/rda.13258
20. Amaral A, Fernandes C, Rebordão Mr, Szóstek-Mioduchowska A, Lukasik K, Gawronska-Kozak B, et al. The *in vitro* inhibitory effect of sivelestat on elastase induced collagen and metallopeptidase expression in equine endometrium. *Animals*. (2020) 10:863. doi: 10.3390/ani10050863
21. Brehm A, Geraghty P, Campos M, Garcia-Arcos I, Dabo Aj, Gaffney A, et al. Cathepsin G Degradation of phospholipid transfer protein (Pltp) augments pulmonary inflammation. *Faseb J.* (2014) 28:2318–31. doi: 10.1096/fj.13-246843
22. Helske S, Syväranta S, Kupari M, Lappalainen J, Laine M, Lommi J, et al. Possible role for mast cell-derived cathepsin G in the adverse remodelling of stenotic aortic valves. *Eur Heart J.* (2006) 27:1495–504. doi: 10.1093/eurheartj/ehi706
23. Shimoda N, Fukazawa N, Nonomura K, Fairchild Rl. Cathepsin G is required for sustained inflammation and tissue injury after reperfusion of ischemic kidneys. *Am J Pathol*. (2007) 170:930–40. doi: 10.2353/ajpath.2007.060486

24. Cohen-Mazor M, Mazor R, Kristal B, Sela S. Elastase and cathepsin G from primed leukocytes cleave vascular endothelial cadherin in hemodialysis patients. *Biomed Res Int.* (2014) 2014:459640. doi: 10.1155/2014/459640
25. Sedor J, Hogue L, Akers K, Boslaugh S, Schreiber J, Ferkol T. Cathepsin-G interferes with clearance of pseudomonas aeruginosa from mouse lungs. *Pediatr Res.* (2007) 61:26–31. doi: 10.1203/01.pdr.0000250043.90468.c2
26. Kosikowska P, Lesner A. Inhibitors of cathepsin G: a patent review (2005 to present). *Expert Opin Ther Pat.* (2013) 23:1611–24. doi: 10.1517/13543776.2013.835397
27. Twigg Ms, Brockbank S, Lowry P, Fitzgerald Sp, Taggart C, Weldon S. The role of serine proteases and antiproteases in the cystic fibrosis lung. *Mediat Inflamm.* (2015) 2015:293053. doi: 10.1155/2015/293053
28. Tan K, Brasch Hd, Van Schaijik B, Armstrong Jr, Marsh Rw, Davis Pf, et al. Expression and localization of cathepsins B, D, and G in dupuytren's disease. *Plast Reconstr Surg.* (2018) 6:E1686. doi: 10.1097/GOX.0000000000001686
29. De Garavilla L, Greco MN, Sukumar N, Chen ZW, Pineda AO, Mathews FS, et al. A novel, potent dual inhibitor of the leukocyte proteases cathepsin G and chymase: molecular mechanisms and anti-inflammatory activity *in vivo*. *J Biol Chem.* (2005) 280:18001–7. doi: 10.1074/jbc.M501302200
30. Maryanoff Be, De Garavilla L, Greco Mn, Haertlein Bj, Wells Gi, Andrade-Gordon P, et al. Dual inhibition of cathepsin G and chymase is effective in animal models of pulmonary inflammation. *Am J Respir Crit Care Med.* (2010) 181:247–53. doi: 10.1164/rccm.200904-0627OC
31. Wang X, Khalil RA. Matrix metalloproteinases, vascular remodeling, and vascular disease. *Adv Pharmacol.* (2018) 81:241–330. doi: 10.1016/bs.apha.2017.08.002
32. Salamonsen L. Tissue injury and repair in the female human reproductive tract. *Reproduction.* (2003) 125:301–11. doi: 10.1530/reprod/125.3.301
33. Oddsdóttir C, Riley SC, Leask R, Edwards DR, Elaine D, Watson Ed. Activities of matrix metalloproteinases-9 and−2 in uterine fluid during induced equine endometritis. *Pferdeheilkunde.* (2008) 24:70–3. doi: 10.21836/PEM20080114
34. Szóstek-Mioduchowska AZ, Baclawska A, Okuda K, Skarzynski DJ. Effect of proinflammatory cytokines on endometrial collagen and metallopeptidase expression during the course of equine endometrosis. *Cytokine.* (2019) 123:154767. doi: 10.1016/j.cyto.2019.154767
35. Szóstek-Mioduchowska A, Słowińska M, Pacewicz J, Skarzynski Dj, Okuda K. matrix metallopeptidase expression and modulation by transforming growth factor-B1 in equine endometrosis. *Sci Rep.* (2020) 10:1119. doi: 10.1038/s41598-020-58109-0
36. Owen CA, Campbell EJ. The cell biology of leukocyte-mediated proteolysis. *J Leukoc Biol.* (1999) 65:137–50. doi: 10.1002/jlb.65.2.137
37. O'donoghue AJ, Jin Y, Knudsen GM, Perera NC, Jenne DE, Murphy JE, et al. Global substrate profiling of proteases in human neutrophil extracellular traps reveals consensus motif predominantly contributed by elastase. *PLoS ONE.* (2013) 8:E75141. doi: 10.1371/journal.pone.0075141
38. Gudmann NS, Manon-Jensen T, Sand JMB, Diefenbach C, Sun S, Danielsen A, et al. Lung tissue destruction by proteinase 3 and cathepsin G mediated elastin degradation is elevated in chronic obstructive pulmonary disease. *Biochem Biophys Res Commun.* (2018) 503:1284–90. doi: 10.1016/j.bbrc.2018.07.038
39. Roberto Da Costa RP, Serrão PM, Monteiro S, Pessa P, Silva JR, Ferreira-Dias G. Caspase-3-mediated apoptosis and cell proliferation in the equine endometrium during the oestrous cycle. *Reprod Ferti. Dev.* (2007) 19:925. doi: 10.1071/RD06159
40. Rebordão Mr, Amaral A, Lukasik K, Szóstek-Mioduchowska A, Pinto-Bravo P, Galvão A, et al. Impairment of the antifibrotic prostaglandin E2 pathway may influence neutrophil extracellular traps–induced fibrosis in the mare endometrium. *Domest Anim Endocrinol.* (2019) 67:1–10. doi: 10.1016/j.domaniend.2018.10.004
41. Kenney RM, Doig PA. Equine endometrial biopsy. In: Morrow DA, Editor. *Current Therapy In Theriogenology 2: Diagnosis, Treatment, And Prevention Of Reproductive Diseases In Small And Large Animals*. Philadelphia, PA: Saunders WB (1986). p. 723–9.
42. Schöniger S, Schoon H-A. The healthy and diseased equine endometrium: a review of morphological features and molecular analyses. *Animals.* (2020) 10:625. doi: 10.3390/ani10040625
43. Reich M, Lesner A, Łegowska A, Sieńczyk M, Oleksyszyn J, Boehm Bo, Burster T. application of specific cell permeable cathepsin g inhibitors resulted in reduced antigen processing in primary dendritic cells. *Mol Immunol.* (2009) 46:2994–9. doi: 10.1016/j.molimm.2009.06.017
44. Dheda K, Huggett JF, Bustin SA, Johnson MA, Rook G, Zumla A. Validation of housekeeping genes for normalizing RNA expression in real-time PCR. *Biotechniques.* (2004) 37:112–9. doi: 10.2144/04371RR03
45. Zhao S, Fernald RD. Comprehensive algorithm for quantitative real-time polymerase chain reaction. *J Comput Biol.* (2005) 12:1047–64. doi: 10.1089/cmb.2005.12.1047
46. Ladner Cl, Yang J, Turner RJ, Edwards RA. Visible fluorescent detection of proteins in polyacrylamide gels without staining. *Anal Biochem.* (2004) 326:13–20. doi: 10.1016/j.ab.2003.10.047
47. Posch A, Kohn J, Oh K, Hammond M, Liu N. V3 stain-free workflow for a practical, convenient, and reliable total protein loading control in western blotting. *Jove.* (2013) 82:50948. doi: 10.3791/50948
48. Manuel JA, Gawronska-Kozak B. Matrix metalloproteinase 9 (Mmp-9) is upregulated during scarless wound healing in athymic nude mice. *Matrix Biol.* (2006) 25:505–14. doi: 10.1016/j.matbio.2006.07.008
49. Raykin J, Snider E, Bheri S, Mulvihill J, Ethier CR. A modified gelatin zymography technique incorporating total protein normalization. *Anal Biochem.* (2017) 521:8–10. doi: 10.1016/j.ab.2017.01.003
50. Aurich C. Reproductive cycles of horses. *Anim Reprod Sci.* (2011) 124:220–8. doi: 10.1016/j.anireprosci.2011.02.005
51. Abraham WM. Modeling of asthma, copd and cystic fibrosis in sheep. *Pulm Pharmacol Ther.* (2008) 21:743–54. doi: 10.1016/j.pupt.2008.01.010
52. Buczkowska J, Kozdrowski R, Nowak M, Ra A, Mrowiec J. Endometrosis—significance for horse reproduction, pathogenesis, diagnosis, and proposed therapeutic methods. *Pol J Vet Sci.* (2014) 17:547–54. doi: 10.2478/pjvs-2014-0083
53. Ley WB, Bowen JM, Sponenberg DP, Lessard PN. Dimethyl sulfoxide intrauterine therapy in the mare: effects upon endometrial histological features and biopsy classification. *Theriogenology.* (1989) 32:263–76. doi: 10.1016/0093-691X(89)90317-8
54. Keller A, Neves AP, Appuerle H, Steiger K, Garbade P, Schoon Ha, et al. Repetitive experimental bacterial infections do not affect the degree of uterine degeneration in the mare. *Anim Reprod Sci.* (2006) 94:276–9. doi: 10.1016/j.anireprosci.2006.04.012
55. Mambelli Li, Mattos Rc, Winter Ghz, Madeiro Ds, Morais Bp, Malschitzky E, et al. Changes in expression pattern of selected endometrial proteins following mesenchymal stem cells infusion in mares with endometrosis. *PLoS ONE.* (2014) 9:e97889. doi: 10.1371/journal.pone.0097889
56. Harvey A, Montezano AC, Lopes RA, Rios F, Touyz RM. Vascular fibrosis in aging and hypertension: molecular mechanisms and clinical implications. *Can J Cardiol.* (2016) 32:659–68. doi: 10.1016/j.cjca.2016.02.070
57. Vandooren J, Van Den Steen Pe, Opdenakker G. Biochemistry and molecular biology of gelatinase B or matrix metalloproteinase-9 (Mmp-9): the next decade. *Crit Rev Biochem Mol Biol.* (2013) 48:222–72. doi: 10.3109/10409238.2013.770819
58. Walter I, Handler J, Miller I, Aurich C. Matrix metalloproteinase 2 (Mmp-2) and tissue transglutaminase (Tg 2) are expressed in periglandular fibrosis in horse mares with endometrosis. *Histol Histopathol.* (2005) 20:1105–13.
59. Aresu L, Benali S, Giannuzzi D, Mantovani R, Castagnaro M, Falomo ME. The role of inflammation and matrix metalloproteinases in equine endometriosis. *J Vet Sci.* (2012) 13:171. doi: 10.4142/jvs.2012.13.2.171
60. Centeno LAM, Bastos HBA, Bueno VLC, Trentin JM, Fiorenza MF, Fiala-Rechsteiner S, et al. Gene expression of Mmp-1, Mmp-2 And TNF-α in the endometrium of mares with different degrees of fibrosis. *J Equine Vet Sci.* (2018) 66:143–4. doi: 10.1016/j.jevs.2018.05.182
61. Shamamian P, Schwartz Jd, Pocock Bjz, Monea S, Whiting D, Marcus Sg, et al. Activation of progelatinase A (Mmp-2) by neutrophil elastase, cathepsin G, and proteinase-3: a role for inflammatory cells in tumor invasion and angiogenesis. *J Cell Physiol.* (2001) 189:197–206. doi: 10.1002/jcp.10014

62. Wilson TJ, Nannuru KC, Singh RK. Cathepsin G-mediated activation of pro-matrix metalloproteinase 9 at the tumor-bone interface promotes transforming growth factor- signaling and bone destruction. *Mol Cancer Res.* (2009) 7:1224–33. doi: 10.1158/1541-7786.MCR-09-0028
63. Vukmirovic M, Kaminski N. Impact of transcriptomics on our understanding of pulmonary fibrosis. *Front Med.* (2018) 5:87. doi: 10.3389/fmed.2018.00087
64. Sternlicht Md, Werb Z. How matrix metalloproteinases regulate cell behavior. *Annu Rev Cell Dev Biol.* (2001) 17:463–516. doi: 10.1146/annurev.cellbio.17.1.463
65. Nothnick W. Regulation of uterine matrix metalloproteinase-9 and the role of micrornas. *Semin Reprod Med.* (2008) 26:494–9. doi: 10.1055/s-0028-1096129

Conflict of Interest: The authors declare that the research was conducted in the absence of any commercial or financial relationships that could be construed as a potential conflict of interest.

frontiers in Veterinary Science

ORIGINAL RESEARCH
published: 02 February 2021
doi: 10.3389/fvets.2020.605773

Pre- and Post-partum Concentrations of Interleukin 1α, Interleukin 8, and α1-Acid Glycoprotein in Vaginal Fornix and Endometrium of Dairy Cows With Clinical Cervicitis

Darío A. Vallejo-Timarán[1], Ali Bazzazan[2], Mariela Segura[2], Nelson E. Prieto-Cárdenas[3] and Rejean C. Lefebvre[3]*

[1] One Health and Veterinary, Innovative Research and Development (OHVRI) Research Group, School of Veterinary Medicine, University of Antioquia, Medellín, Colombia, [2] Department of Biomedicine, Faculty of Veterinary Medicine, University of Montreal, Saint-Hyacinthe, QC, Canada, [3] Department of Clinical Sciences, Faculty of Veterinary Medicine, University of Montreal, Saint-Hyacinthe, QC, Canada

OPEN ACCESS

Edited by:
Dariusz Jan Skarzynski, Institute of Animal Reproduction and Food Research (PAN), Poland

Reviewed by:
Takeshi Osawa, University of Miyazaki, Japan
Iain M. Sheldon, Swansea University, United Kingdom
Slawomir Zdunczyk, University of Warmia and Mazury in Olsztyn, Poland

***Correspondence:**
Darío A. Vallejo-Timarán
dario.vallejo@uam.edu.co;
dantonio.vallejo@udea.edu.co

Specialty section:
This article was submitted to Animal Reproduction - Theriogenology, a section of the journal Frontiers in Veterinary Science

Received: *13 September 2020*
Accepted: *31 December 2020*
Published: *02 February 2021*

Citation:
Vallejo-Timarán DA, Bazzazan A, Segura M, Prieto-Cárdenas NE and Lefebvre RC (2021) Pre- and Post-partum Concentrations of Interleukin 1α, Interleukin 8, and α1-Acid Glycoprotein in Vaginal Fornix and Endometrium of Dairy Cows With Clinical Cervicitis. Front. Vet. Sci. 7:605773. doi: 10.3389/fvets.2020.605773

Innate immunity is the principal sensor responsible of the local immune response to control mucosal bacterial contamination of the reproductive tract after parturition, triggering a pro-inflammatory process in the mucosa of the uterus, the vaginal and the cervix. However, knowledge about the inflammation process and outcome of the cervix in dairy cows is scarce even though it plays an important anatomic and functional role between the vagina and the uterus. The objective of the present study was to describe the cellular and humoral local innate immune response during clinical cervicitis (CC) in the uterus and vaginal fornix in pre- and post-partum periods of dairy cows. A retrospective descriptive study was performed involving 26 animals, characterized as clinical cervicitis cows ($n = 19$) and healthy cows ($n = 7$). Blood and mucus of the different compartments of the genital tract were sampled and records of the cows' genital exam were performed four times: −1 w (day −7 ± 2, prepartum), +1 w (day +7 ± 4), +3 w (day +21 ± 4) and +5 w (day +35 ± 4) postpartum. Clinical cervicitis was defined as cows exhibiting a cervix grade−2 and healthy cows were defined as a cow clinically normal with a grade-0 cervix at time +5 w. Blood white cell count, vaginal fornix and endometrial neutrophils percentage, and the concentrations of interleukin 1α (IL1), interleukin 8 (IL8), and α1-acid glycoprotein (AGP) in mucus were determined. The results showed that 23% of the cows were categorized as CC at time +5 w. Cases of CC with purulent vaginal discharge or subclinical endometritis shown the highest cytokine production. At +3 w, IL1, IL8, and AGP concentrations in the uterus and the fornix were significantly higher in CC than healthy cows (CH). In conclusion, the 3-week postpartum is a critical point to evaluate cytokines and acute phase proteins; where IL1 and IL8 variation kept a direct relation with neutrophils numbers and function. The presence of AGP in the endometrium infer a homeostatic proinflammatory protective balance effect, modulating the local uterine innate immune response during peripartum.

Keywords: innate immunity, vaginal fornix, cervicitis, endometritis, inflammation, dairy cow, postpartum, uterine diseases

INTRODUCTION

Most parturient cows (90%) experience bacterial contamination of the uterine cavity and endometrial damages that trigger an active inflammatory response to clear the infection and repair the tissues, respectively (1, 2). However, the innate immune response does not always control uterine bacterial imbalances; therefore, causing a prolonged genital tract inflammation and a delay of the uterine involution indulging a postpartum uterine disease (3–6). The incidence of postpartum uterine disease (PUD) is high in dairy cows worldwide and includes clinical (metritis, endometritis) and non-clinically conditions such as subclinical endometritis (7) affecting the overall animal fertility.

The diagnosis of PUD is limited by the lack of clarity regarding the case criteria, difficulties associated with the diagnosis of subclinical conditions, and variable sensitivity and specificity of the different diagnostic tests in relation to the absence of direct visual assessment of the endometrium (8, 9). The discrepancies between clinical findings and the diagnostic test could be explained by the presence of an inflammatory process in tissues other than the endometrium like the cervix uteri and the vagina (10). The cytological evidence of cervical inflammation was reported in 19% of sub-fertile cows (11). Previous studies reported that 60.8 and 45% of dairy cows had clinical cervicitis and cytological cervicitis, respectively, between 42 and 50 days postpartum (10, 12). However, knowledge of inflammation or infection of the cervix and the subsequent influence on reproduction in dairy cows is limited.

The capacity of the uterus to resolve a genital tract infection depends on its ability to detect and respond to microbial ligands (1, 13). Innate immunity is the principal sensor responsible for immune response to control bacterial contamination of the uterus after parturition. The pathogen-associated molecular patterns (PAMPs) present in bacteria are quickly detected by the pattern recognition receptors (PRRs) in the host cells. The engage between PAMPs and PRRs such as Toll-Like Receptor (TLRs) initiate a signaling cascade resulting in the synthesis and production of pro-inflammatory cytokines such as Tumor Necrosis Factor alpha (TNF-α), interleukins (IL-1-α, IL-6) and chemokines (IL-8) (14, 15). For example, the chemokine IL8 is produced mainly by activated macrophages in response to bacterial PAMPs directing the upregulation of adhesion molecules to enhance neutrophil recruitment to the inflammatory area (13, 16). As a result, uterine inflammation is characterized by the significant presence polymorphonuclear leukocyte infiltration (Neutrophils) as well (14).

The lack of a complete genital examination in postpartum dairy cows without appreciation of the molecular immunological mechanisms underlying changes at the cellular or systemic level could explain the limited understanding of the general process involved in PUD (17). Therefore, the aim of the present study was to describe the innate immune response in the uterus (Ut) and vaginal fornix (Fx) in the pre- and post-partum periods of dairy cows with clinical cervicitis.

MATERIALS AND METHODS

Study Population and Sampling

A retrospective descriptive study (**Figure 1**) was performed involving 26 animals defined as, clinical cervicitis cows ($n = 19$) and healthy cows ($n = 7$). Cows were selected from a database of a previous sampling in which 85 dairy cows (purposively selected) were followed and sampled [blood and vaginal fornix (Fx) and uterine mucus (Ut)] during the pre- and postpartum period. For the present study, clinical data of the database and the stored blood and mucus samples were used. Blood samples were collected from the coccygeal vein of the tail head and placed in a tube with an anticoagulant, immediately placed on ice and transported to the laboratory within ∼3 h. After 30 min at room temperature and gentle agitation, the complete hematology analysis was carried out with a VetScan HM5 hematology analyzer (Abaxis Global Diagnostics, Union City, CA, USA). The mucus and smears samples for cytokines and neutrophils percentage assessments were performed with the cytobrush technique (18). A sterile cytobrush (CytoSoft, Camarillo, CA, USA) was screwed onto a stainless steel rod (65 cm long × 4 mm diameter) within a stainless steel tube. The apparatus was inserted into a hard protective plastic sheath (IMV Technologies, L'Aigle, France) before insertion into a second protective sheath (30 cm long Sani-Shield Rod Protector, Agtech, Manhattan, NY, USA). The doubled sheathed instrument was used to collect cellular material of mucosa of vaginal fornix and endometrium using the sterile cytobrush. A cervical sample brush and uterine sample brush were collected into a sterile tube with 1 ml of phosphate buffered saline (PBS) and stored frozen at −80°C and used in the present study to determine the immune response.

The cows came from three commercial dairy herds in Québec (Canada) that were housed in a tie-stall barn and milked twice daily. The rolling herd average for milk production was 9,000 kg. Cows were fed a total mixed ration of corn and hay silage to meet the nutrient requirements of dairy cows recommended by the National Research Council (19). Farms were visited weekly by the same veterinarians and all cows were vaccinated at 40 and 26 days before parturition against E. coli (2 ml IM, J-VAC®, Boehringer Ingelheim, Burlington, Ontario, Canada, L7L 5H4) and between 10 and 30 days postpartum against IBR, BVD type 1, BVD type 2, PI3, and BRSV (2 ml IM, Bovi-shield GOLD5® FPTM 5 L5, Zoetis, Kirkland, Québec, Canada, H9H 4M7). In addition, all pregnant cows were injected with Se (5.0 ml, D-60 before calving, MU-SE, Intervet, Merk, Kirkland, Québec, Canada, H9H 4M7).

The database includes records of cow's clinical exam performed four times: −1 w (day −7 ± 2, prepartum), +1 w (day +7 ± 4), +3 w (day +21 ± 4) and +5 w (day +35 ± 4) postpartum (**Figure 1**). Data collection included clinical data associated with reproductive assessment (vaginoscopy, transrectal exams, purulent vaginal discharge, cervix characteristics, uterine horn symmetry, and ovarian structures), cytological exams (neutrophil count in the fornix of the vagina and in the uterus) and blood samples (white blood cell count).

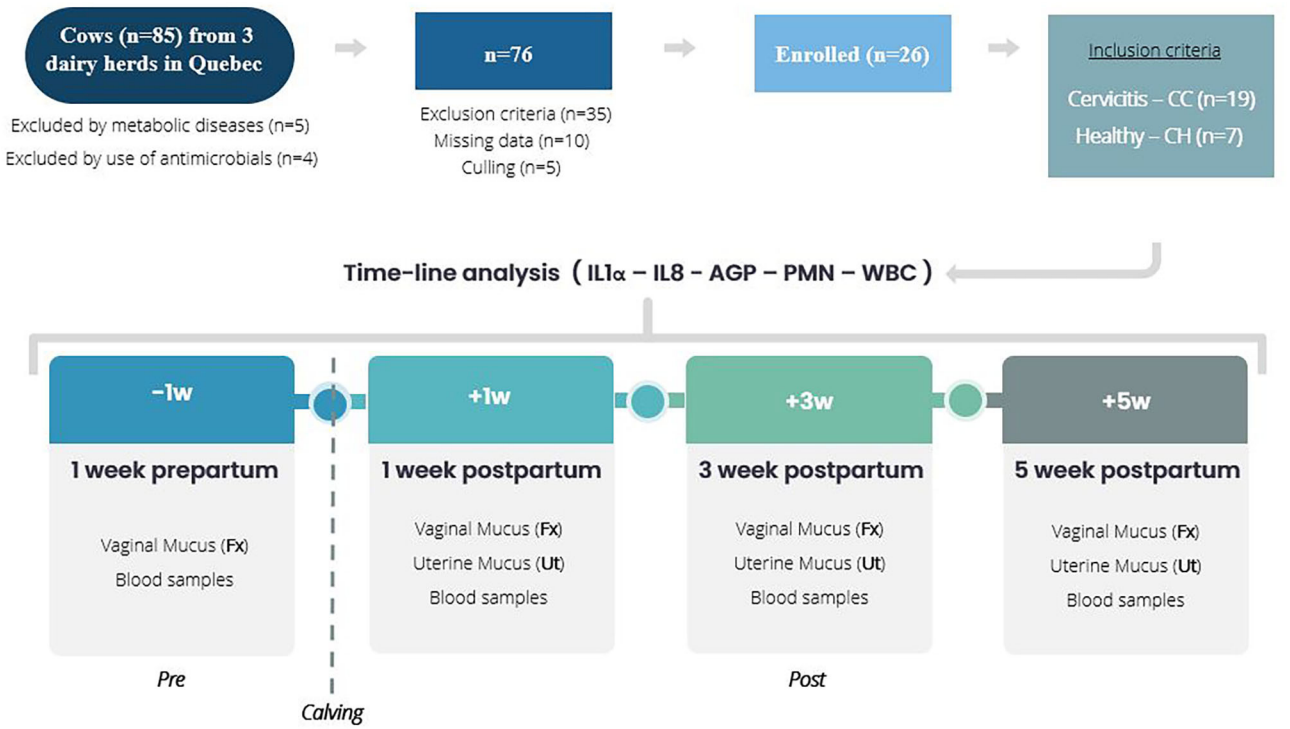

FIGURE 1 | Study design. Timeline analysis of innate immune responses of clinical cervicitis in pre- and post-partum dairy cows ($n = 26$) from three dairy herds in Quebec in 2016. A retrospective study involving database and stored blood and mucus (vaginal fornix, Fx – uterine, Ut) sampling of 26 dairy cows from three commercial dairy herds in Quebec. Cows diagnosed with clinical cervicitis ($n = 19$) and healthy ($n = 7$) were involved in a time-course analysis from 1 week before calving to 5 weeks after calving to establish variations for white blood cell count (WBC), uterine PMN percentage, and vaginal fornix and uterine mucus cytokines (IL1 – IL8 – AGP).

Case Definition

For the animal selection, postpartum disorders were defined. Clinical metritis was characterized as abnormally enlarged uterus and purulent uterine discharge within the first 21 days postpartum without systemic clinical sings (20). At 5 weeks postpartum, clinical endometritis (CE) was defined as a cow exhibiting purulent vaginal discharge – PVD (20) or subclinical endometritis (SE) in cows with a proportion of neutrophils exceeding 5% on endometrial cytology in absence of PVD and anomalies on transrectal examination (9). On vaginoscopy, cervix was classified as GRADE 0 (Normal) without abnormality; GRADE 1 (normal) with the second cervical fold swollen without redness and prolapsing through the first ring, and GRADE 2 (Clinical Cervicitis, CC) with the second fold swollen and red prolapsing through the first ring without PVD (10).

Exclusion Criteria and Animal Selection

Based on reproductive assessment records, as exclusion criteria, animals were rejected of the database because of: (1) systemic illness or clinical conditions other of the reproductive tract (2) calving disorders (dystocia, twins, fetal membranes retention) and (3) animals that in the final reproductive exam (+5 w), exhibited endometritis (clinical or subclinical) without clinical evidence of clinical cervicitis. Clinical cervicitis (CC) criteria in this research was considered when, posterior to applying the exclusion criterion, the cervix had reddening of the supra-vaginal portion of the cervix with edema and prolapse of the second cervical fold (cervix grade−2 at the 5-week examination). Healthy cows (CH) were defined as a cow clinically normal with a cervix grade-0 or grade-1 at the 5 w and, without postpartum disorders during all the follow-up period (−1 w +1 w; +3 w; +5 w postpartum).

From the data ($n = 85$), animals were rejected because of culling ($n = 5$), use of antimicrobials ($n = 4$), metabolic disease ($n = 5$), missing data ($n = 10$), and exclusion criteria ($n = 35$). Finally, 26 cows were enrolled in the study: 19 met the case definition criteria for cervicitis and seven met the criterion defined for healthy cows (**Figure 1**).

Measurement of Cytokine Concentration in Vaginal and Uterine Samples

The concentrations of interleukin 1α (IL1), interleukin 8 (IL8), and α1-acid glycoprotein (AGP) were determined by using commercial kits (GENORISE SCIENTIFIC, INC. Philadelphia, USA): Bovine IL-1α ELISA Kit Nori® (minimum detection range 3–200 pg/ml, assay sensitivity 1 pg/ml, intra-assay CV 6%, inter-assay CV 9%); Bovine IL-8 ELISA Kit Nori® (minimum detection range 12–800 pg/ml, assay sensitivity 2 pg/ml, intra-assay CV 6%, inter-assay CV 9%) and; Bovine AGP ELISA

Kit Nori® (minimum detection range 2.5–160 ng/ml, assay sensitivity 0.5 ng/ml, intra-assay CV 5%, inter-assay CV 9%). All procedures were performed according to the guidelines provided by the manufacturers. Briefly, centrifugation of the content of stored tubes (cytobrush with cervical or uterine mucus in 1 ml PBS) was performed to collect the supernatant of uterine mucus and vaginal fornix mucus before to be added to 96-well microplates and incubated for 1 h at room temperature. After aspiration and washing (with 300 µL of Assay Buffer, three times), 100 µL of the working dilution of Detection Antibody (diluted in Regent Diluent) were added to each well and incubated for 1 h. The plates were washed and then incubated with 100 µL of the working dilution of HRP conjugate solutions for 20 min at room temperature, washed again, and then incubated with 100 µL of the substrate solution for 5 min. Finally, 50 µL of the Stop Solution were added. The optical density of each well was then measured at 450 nm in Microplate Spectrophotometer (SpectraMax® Plus 384 Absorbance Plate Reader, USA). A standard curve for each ELISA Kit was constructed by plotting the mean absorbance for each standard on the y-axis against the concentration on the x-axis to calculate the R^2 coefficient.

Data Analysis

Categorical variables included in the analysis were time of examination (−1, +1, +3, +5 w weeks postpartum), sample origin (Vaginal fornix – Uterus) and clinical profile [healthy (CH), clinical cervicitis (CC), clinical cervicitis + purulent vaginal discharge (CC + PVD), clinical cervicitis + subclinical endometritis (CC + SE)]. Continuous variables were concentrations of IL1, IL8, and AGP, the proportion of polymorphonuclear neutrophils (PMN) in the vaginal fornix and the uterus (percentage of PMN in a 300-cell count), and the white blood cell count (WBC).

Continuous variables were assessed for normal distribution using histogram with Gaussian distribution graph and Shapiro-Wilk test. A nonparametric test (Mann-Whitney) was used to estimate a difference in the concentrations of IL1, IL8, AGP into the comparisons groups: (1) CC – CH; (2) Ut – Fx and (3) (−1 w) – (+1 w) – (+3 w) – (+5 w). When a significant difference was found, the power to detect a difference (with a 95% confidence interval) was calculated considering the number of cows per group (cervicitis – Healthy) and the mean and standard error of the mean (for IL1, IL8, AGP) found in each comparisons group.

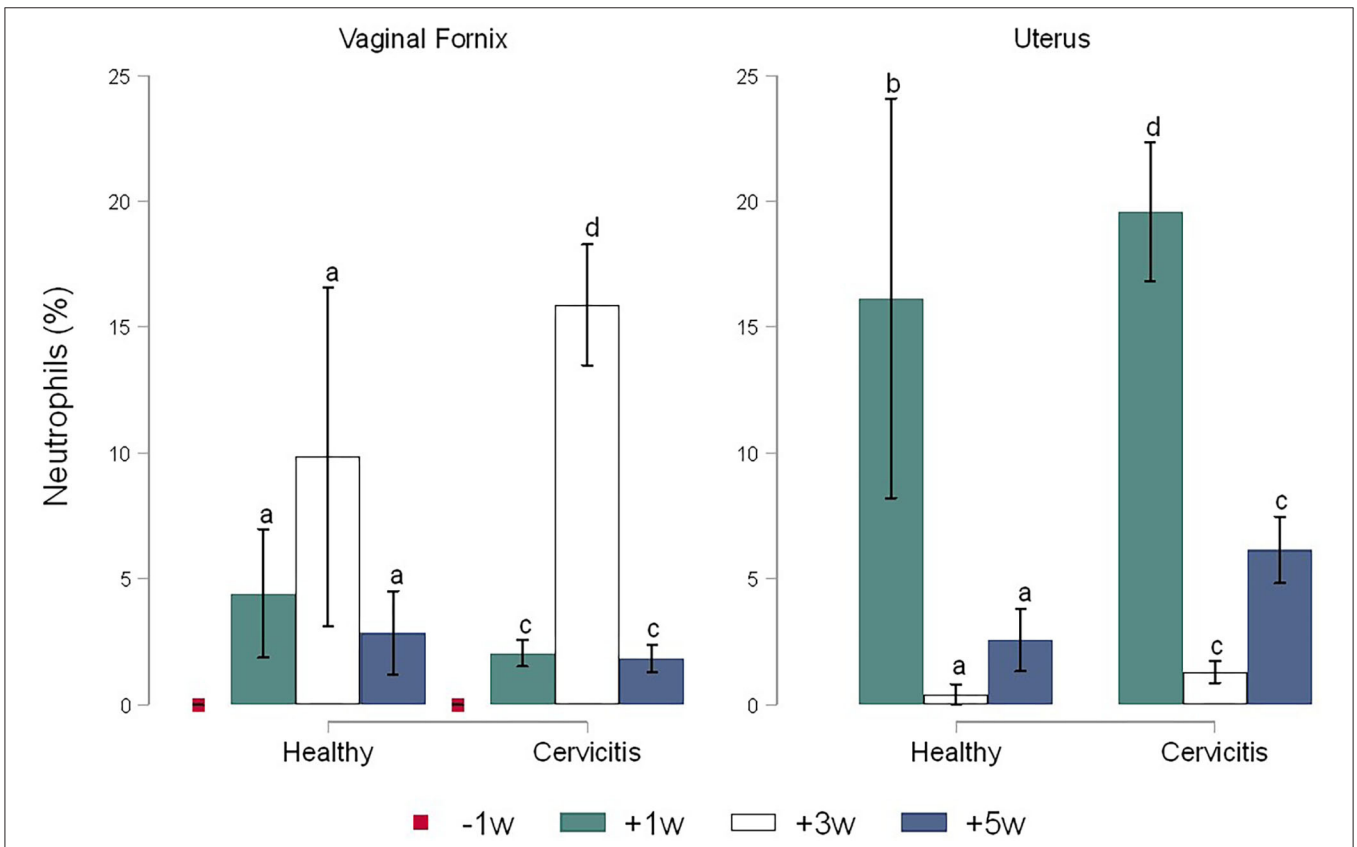

FIGURE 2 | Time-course variations in the pre-and post-partum percentage of neutrophils in the vaginal fornix and uterine mucus of cows ($n = 26$) defined as clinical cervicitis cows ($n = 19$) and healthy cows ($n = 7$) from three dairy herds in Quebec in 2016. Time-course variations (weeks −1 w +1 w +3 w +5 w) of neutrophils percentage, time-course differences are indicated with superscript a-b (for healthy cows), and c-d (for clinical cervicitis cows). Means without a common superscript differed ($P < 0.05$).

The statistical differences found were reported only when the power was ≥70%.

All analyses were conducted in Stata® Statistical Software (Release 15. College Station, TX: Stata Corp LP).

RESULTS

Clinical Characteristics of Cervicitis

This research showed that 23% of the cows ($n = 19$) at +5 w were categorized as cervicitis. In addition, some cases of CC appeared with purulent vaginal discharge – CC + PVD ($n = 4$) or subclinical endometritis – CC+SE ($n = 9$).

Percentage of PMN in the Mucus of the Vaginal Fornix and the Uterus

The percentage of PMN in the vaginal fornix of CC cows changed during the sampling time pre- and post-partum respectively. On time +3 w, PMN in the vaginal fornix of CC cows were 15.89% ($P = 0.001$), 13.84% ($P = 0.005$) and 14.05% ($P = 0.004$) higher than at −1, +1, and +5 w respectively. There were not significant differences between CH and CC animals at −1 w however, there were significant differences between CH and CC animals ($p < 0.05$) at +1, +3, and +5 w respectively. In CC cows, the PMN% was the highest at +3 w and the lowest at +1 and +5 w. In uterine mucus, cows with CC showed a significant difference ($p < 0.05$) in the PMN% in all the sampling times with the highest percentage at +1 w. However, there was no difference between CC/CH (**Figure 2**).

Cytokine Variations by Examination Time, Case/Control, and Sample Origin

The calculate R^2 coefficient for IL1, IL8, and AGP were 0.75, 0.86, and 0.98 respectively. No significant differences were found for cytokines by sampling times. Comparison between CC and CH cows showed statistical differences only for time +3 w where the concentrations of IL1 in Fx (1.05 ± 0.01 pg/ml) and in Ut (0.065 ± 0.01 pg/ml) of CC cows were significantly higher ($P = 0.005$) than in the Fx (0.038 ± 0.019 pg/ml) and in the Ut (0.035 ± 0.016 pg/ml) of CH cows (**Figure 3**). In addition, the concentrations of IL8 in CC cows were more elevated than CH cows in both the Fx (0.73 ± 0.14 pg/ml vs. 0.27 ± 0.14 pg/ml, $P = 0.043$) and uterine (0.60 ± 0.11 pg/ml vs. 0.32 ± 0.16 pg/ml, $P = 0.040$) at +3 w respectively (**Figure 4**). The concentration of AGP in Fx (**Figure 5**) for CC was 2.76 ng/ml higher than CH ($P = 0.0018$) at +3 w. Comparison between Fx and Ut for CC cows at +3 w showed that IL1 and AGP concentrations in Fx were 0.003 ng/ml

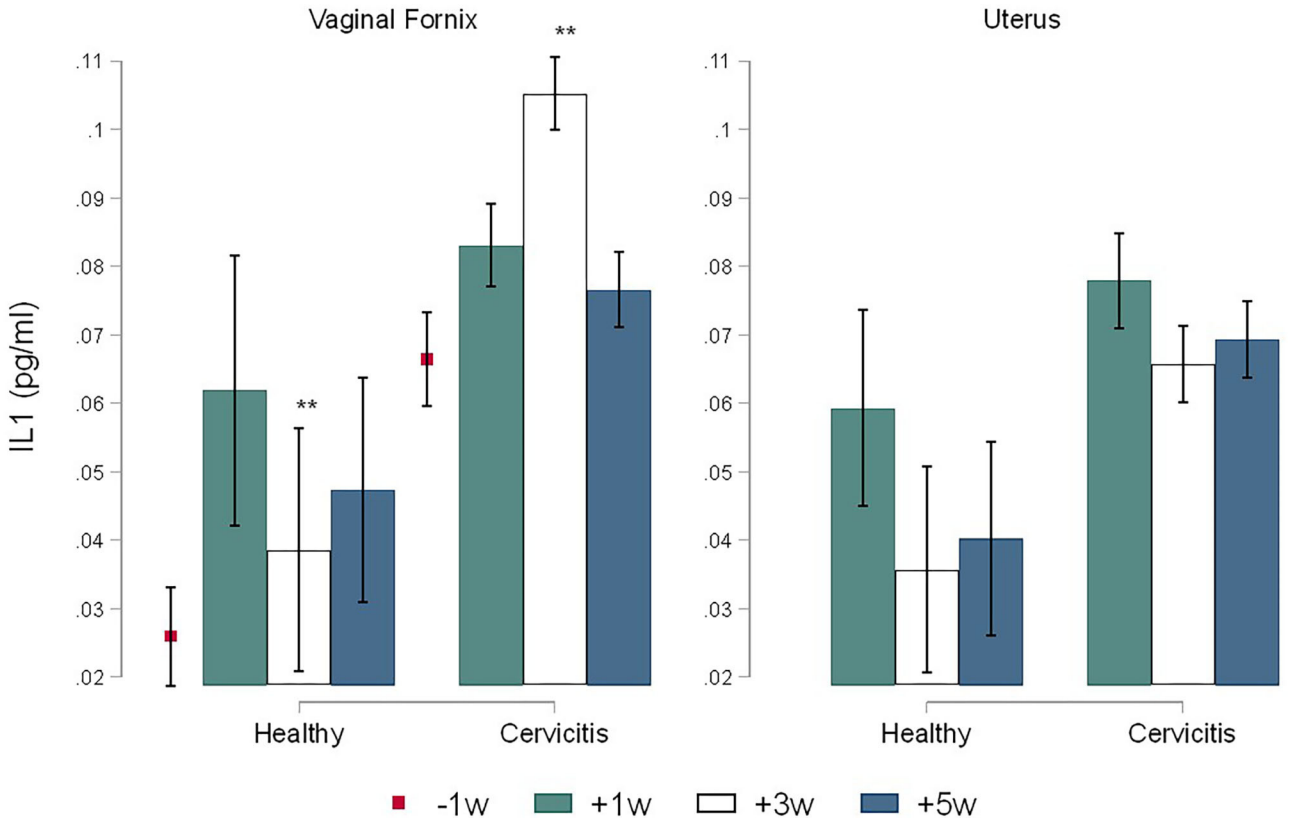

FIGURE 3 | Time-course variations (Mean ± SEM) in pre and post-partum concentrations of IL1 IL8 in the vaginal fornix and uterine mucus of cows ($n = 26$) defined as clinical cervicitis cows ($n = 19$) and healthy cows ($n = 7$) from three dairy herds in Quebec in 2016. Time-course variations (weeks −1 w +1 w +3 w +5 w) of Interleukin 1α (pg/ml) concentrations (Mean ± SEM). An asterisk indicates a significant difference at $p \leq 0.05$ (*) or $p \leq 0.01$ (**) for the Mann-Whitney Test (Ha: clinical cervicitis cows ≠ healthy cows).

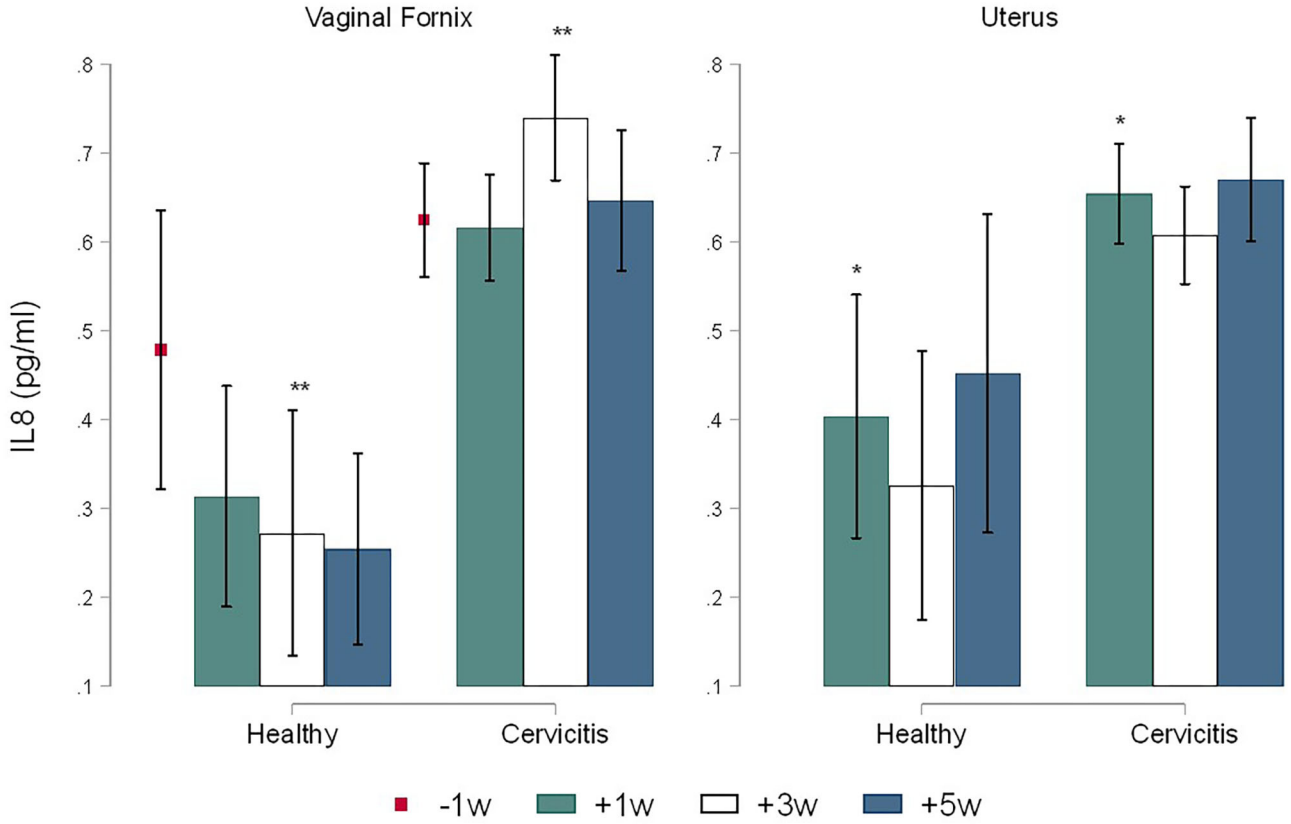

FIGURE 4 | Time-course variations (Mean ± SEM) in pre and post-partum concentrations of IL8 in the vaginal fornix and uterine mucus of cows ($n = 26$) defined as clinical cervicitis cows ($n = 19$) and healthy cows ($n = 7$) from three dairy herds in Quebec in 2016. Time-course variations (weeks −1 w +1 w +3 w +5 w) of α1-acid glycoprotein (pg/ml) concentrations (Mean ± SEM). An asterisk indicates a significant difference at $p \leq 0.05$ (*) or $p \leq 0.01$ (**) for the Mann-Whitney Test (Ha: clinical cervicitis cows ≠ healthy cows).

($P = 0.018$) and 1.93 ng/ml ($P = 0.002$) higher respectively than in the Ut samples. No significant difference was found between Fx and Ut concentrations of IL1, IL8 and AGP in CH cows at time +3 w ($p > 0.05$).

Cytokine Variations by Clinical Characteristics of Cervicitis

Cases of cervicitis (CC) diagnosed at +5 w occurred concurrently with other uterine disorders (**Table 1**). At the time −1 w, Fx IL1 was higher in cows with CC+SE compared with CH cows ($P = 0.016$). At the time +3 w, Fx IL1 and IL8 concentrations were higher for CC+SE cows compared with CH cows ($P < 0.05$). At the time +5 w, Fx IL8 and AGP were higher for CC + SE cows compared with CH cows ($P < 0.05$). In uterine samples, at time +3 w: (a) Ut IL1 was higher in cows with CC + SE compared with CC + PVD cows ($P = 0.08$); (b) Ut AGP was higher for CC + SE cows compared with CC + PVD cows ($P = 0.028$).

White Blood Cell Count (WBC), Variations by Examination Time and Case/Control

For monocytes (Mon), neutrophils (PMN) eosinophils (Eos), and basophils (Bas), there were no significant differences ($p > 0.05$) between CC cows and healthy cows (CH). At the time +1 w, WBC was higher compared to −1, +3, and +5 w (**Figure 6**).

DISCUSSION

Innate immunity plays an important role in keeping postpartum reproductive tract microflora balance; where the cervix acts as an anatomical barrier protecting the uterus from external pathogens producing cervical mucus (12, 21, 22). During postpartum, puerperal physiological modifications occurring in the reproductive tract, changes in the local microflora and arisen of potential pathogens, and physical traumas associated with calving or obstetrical manipulations may trigger cervical inflammation. In the present study, clinical cervicitis was diagnosed in 23% of the cows examined at 5 weeks postpartum showing a red, edematous, and prolapsed cervical fold. Moreover, some cases were accompanied by purulent vaginal discharge or subclinical endometritis. The authors measured an increase of neutrophils in the reproductive tract (uterus and fornix), a major production of pro-inflammatory cytokines (IL-1) and chemokines (IL-8), and the recruitment of circulating neutrophils and monocytes meaning that postpartum cervicitis

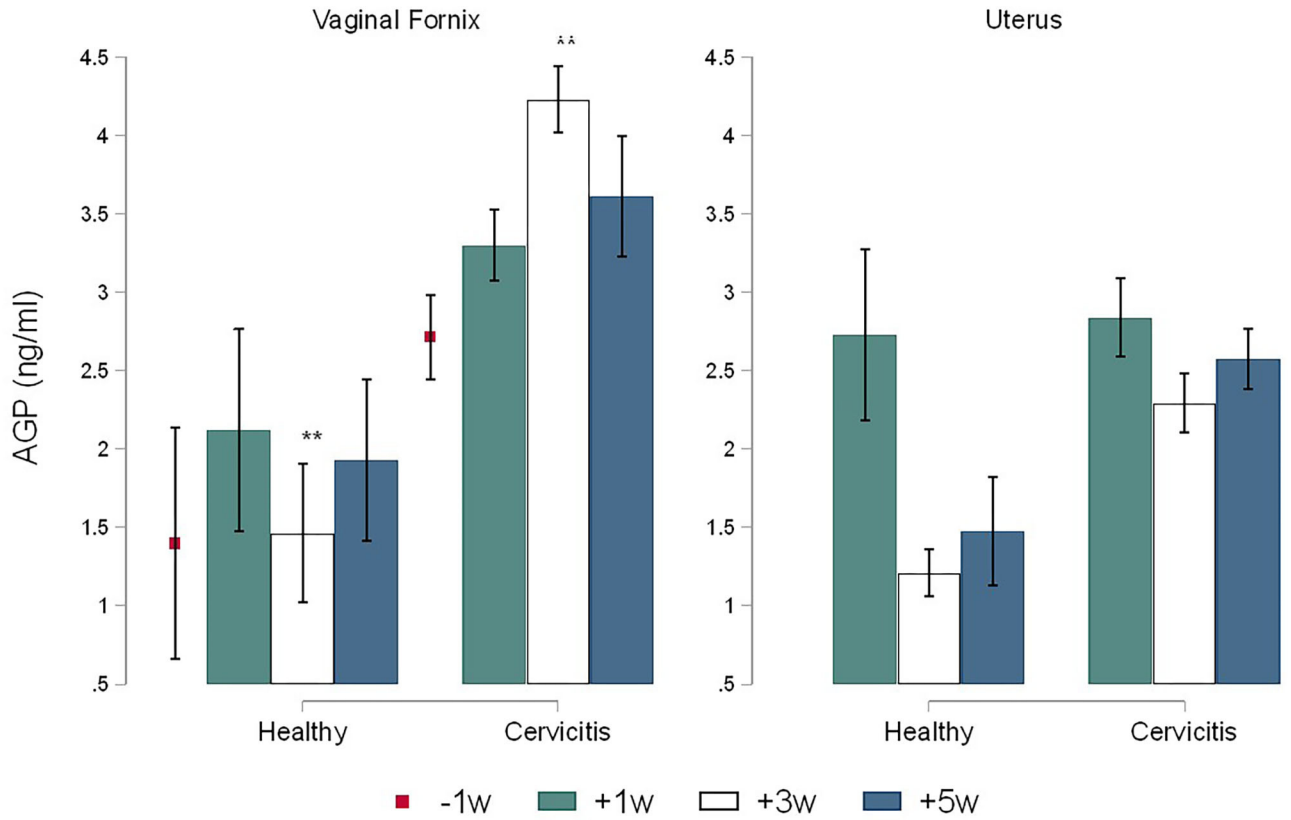

FIGURE 5 | Time-course variations (Mean ± SEM) in pre-and post-partum concentrations of AGP in the vaginal fornix and uterine mucus of cows ($n = 26$) defined as clinical cervicitis cows ($n = 19$) and healthy cows ($n = 7$) from three dairy herds in Quebec in 2016. Time-course variations (weeks −1 w +1 w +3 w +5 w) of α1-acid glycoprotein (ng/ml) concentrations (Mean ± SEM). An asterisk indicates a significant difference at $p \leq 0.05$ (*) or $p \leq 0.01$ (**) for the Mann-Whitney Test (Ha: clinical cervicitis cows ≠ healthy cows).

is a process initially controlled by innate immunity. In addition, cervicitis was accompanied by uterine inflammation (clinical and subclinical endometritis) in 41% ($n = 13$) of the cases. Interaction between clinical endometritis, subclinical endometritis, and cervicitis is not well-characterized. However, even with a clear physical partition of the reproductive tract and a well-defined histologic definition of each organ in cows one can hypothesize that the process of clearance of the reproductive tract inflammation in postpartum cows may proceed from the upper (uterus) to the lower organs (cervix). More studies are needed to understand the process of inflammation and the interaction between the different compartments of the reproductive tract of the cow in a postpartum situation.

The current research describes the innate immune response in the uterus and the vaginal fornix, and the variations occurring during the pre- and postpartum periods (−1, +1, +3, +5 w) in cows with clinical cervicitis. The concentrations of IL-1, IL8, and AGP in the Fx mucus of CC cows increased from −1 to +3 w reaching the highest concentration at +3 weeks followed by a decrease at +5 w. However, the concentrations of cytokines and the chemokine stayed high during the whole postpartum period (+1 to +5 w) in CC cows. The present results correlate with the increase of the bacterial community in the vagina most likely coming from the environment in the weeks after calving (20, 23). The postpartum period is characterized by calving-associated physical barriers relaxation including an open cervix and a negative pressure created by repeated uterine contraction and relaxation. As a result, there is an enhancement of bacterial contamination in bovine uteri and vagina after calving, initially by Gram-negative bacteria follow by Gram-positive bacteria decreasing the levels of neutrophils and cytokines (2). Therefore, inflammatory cytokines are expressed in the vaginal and uterine mucosa in a time-related manner during the postpartum period with a significant increase around 3 weeks after calving (24). As partitioning of the reproductive tract is reestablished with closure of the cervix and bacteria trapped in the reproductive tract, the innate immune response may persist longer in CC cows comparatively to CH cows where bacterial clearance is more prompt.

In the current research, the results of CC cows show an increased concentration of AGP in relation to IL1 and IL8 in Fx. The α1-acid alpha glycoprotein AGP is an Acute Phase Protein normally expressed by the liver and usually found in blood, however extrahepatic expression of bovine AGP has

TABLE 1 | Mean ± SEM for AGP, IL1, and IL8 in vaginal fornix and uterine mucus of pre-and post-partum cows ($n = 26$) defined as healthy, clinical cervicitis, and clinical cervicitis plus additional uterine disease conditions.

Week	Sample	Disease	IL1 (pg/ml)	IL8 (pg/ml)	AGP (ng/ml)
			M ± SEM	M ± SEM	M ± SEM
−1 w	Fx	CH	0.02 ± 0.00	0.47 ± 0.16	1.39 ± 0.79
		CC	0.06 ± 0.02	0.55 ± 0.18	2.51 ± 0.72
		CC + PVD	0.03 ± 0.01	0.39 ± 0.13	1.82 ± 0.54
		CC + SE	0.12 ± 0.03[a]	1.24 ± 0.37	5.02 ± 1.8
+1 w	Fx	CH	0.06 ± 0.02	0.31 ± 0.13	2.11 ± 0.69
		CC	0.07 ± 0.02	0.53 ± 0.21	3.38 ± 0.65
		CC + PVD	0.07 ± 0.01	0.50 ± 0.15	3.22 ± 0.88
		CC + SE	0.10 ± 0.02	0.98 ± 0.33	3.33 ± 0.77
	Ut	CH	0.05 ± 0.01	0.40 ± 0.14	2.73 ± 0.58
		CC	0.06 ± 0.02	0.48 ± 0.18	2.32 ± 0.87
		CC + PVD	0.06 ± 0.01	0.54 ± 0.10	2.63 ± 0.73
		CC + SE	0.12 ± 0.04	1.16 ± 0.34	4.05 ± 1.40
+3 w	Fx	CH	0.03 ± 0.01	0.27 ± 0.14	1.46 ± 0.48
		CC	0.09 ± 0.01	0.58 ± 0.21	3.19 ± 0.31
		CC + PVD	0.09 ± 0.01	0.55 ± 0.16	4.64 ± 0.77
		CC + SE	0.13 ± 0.03[a]	1.37 ± 0.39[a]	4.85 ± 0.95
	Ut	CH	0.03 ± 0.01	0.32 ± 0.16	1.21 ± 0.16
		CC	0.05 ± 0.02	0.52 ± 0.16	1.83 ± 0.63
		CC + PVD	0.05 ± 0.01	0.45 ± 0.13	1.85 ± 0.50
		CC + SE	0.11 ± 0.01[b]	1.08 ± 0.31	3.96 ± 0.74[b]
+5 w	Fx	CH	0.04 ± 0.01	0.25 ± 0.11	1.93 ± 0.55
		CC	0.07 ± 0.02	0.48 ± 0.21	2.37 ± 0.64
		CC + PVD	0.06 ± 0.01	0.41 ± 0.14	2.70 ± 0.52
		CC + SE	0.10 ± 0.02	1.40 ± 0.52[a]	7.5 ± 3.00[a]
	Ut	CH	0.04 ± 0.01	0.45 ± 0.19	1.47 ± 0.37
		CC	0.07 ± 0.01	0.55 ± 0.23	2.16 ± 0.54
		CC + PVD	0.04 ± 0.01	0.47 ± 0.14	2.37 ± 0.54
		CC + SE	0.11 ± 0.02	1.27 ± 0.38	3.64 ± 1.23

Time-course variations (weeks −1 w +1 w +3 w +5 w) of Interleukin 1α (pg/ml), Interleukin 8 (pg/ml) and α1-acid glycoprotein (ng/ml) concentrations (Mean ± SEM) in vaginal fornix (Fx) and uterine mucus (Ut) of cows with cervicitis CC, cervicitis plus purulent vaginal discharge (CC + PVD), cervicitis plus subclinical endometritis (CC + SE), and healthy CH.

[a] *Indicate a significative difference Mann-Whitney Test $p \leq 0.05$ (compared with CH cows).*

[b] *Indicate significative difference Mann-Whitney Test $p \leq 0.05$ (compared with CC + PVD cows).*

been reported in tissues like uteri and ovaries (25–29). The protein AGP possesses an immunomodulatory activity and it is believed to play an important role in the regulation of local inflammation by reducing the tissue damages caused by excessive activation of the complement. It modulates apoptosis in bovine monocytes and the degranulation of neutrophils involved in the fine-tuning of neutrophil activity during the inflammation (27, 28, 30, 31). In the study, AGP concentrations (**Figure 5**) increased during cervicitis, mainly at +3 w ($p < 0.05$) however, when cervicitis and subclinical endometritis were both present AGP concentration in Fx was higher at 5 w ($p < 0.05$) (**Table 1**). The present results agree with previous work that demonstrated a higher level of plasma AGP in cows developing uterine infection in comparison with cows without endometritis (32). AGP can modulate locally the uterine innate immune response in different cases such as normal uterine involution, cervicitis or endometritis without the presence of a systemic inflammatory process. In cows, AGP is contained in neutrophil granules and released when activated. More specifically, the highly glycosylated AGP is syntheses in myelocytes, stored, and released in secondary granules by activated neutrophils representing a fine-tuning of the neutrophil's function (Down-regulatory effect) reducing the damages caused by an excess of inflammatory response (28, 31, 33). In vaginal samples of CH, similar concentrations of AGP (**Figure 5**) were found during the pre- and the postpartum period in concordance with the changes in neutrophils (**Figure 2**) indicating some endogenous homeostatic role. The present results infer that endometrial and vaginal production of AGP has an important role in neutrophil function in both in healthy and infected cows. However, there is scarce information related with the role of AGP in postpartum uterine disease in dairy cows and, a potential use of acute phase proteins as predictor of postpartum uterine infections in dairy cows have been reported (34), therefore more research is needed.

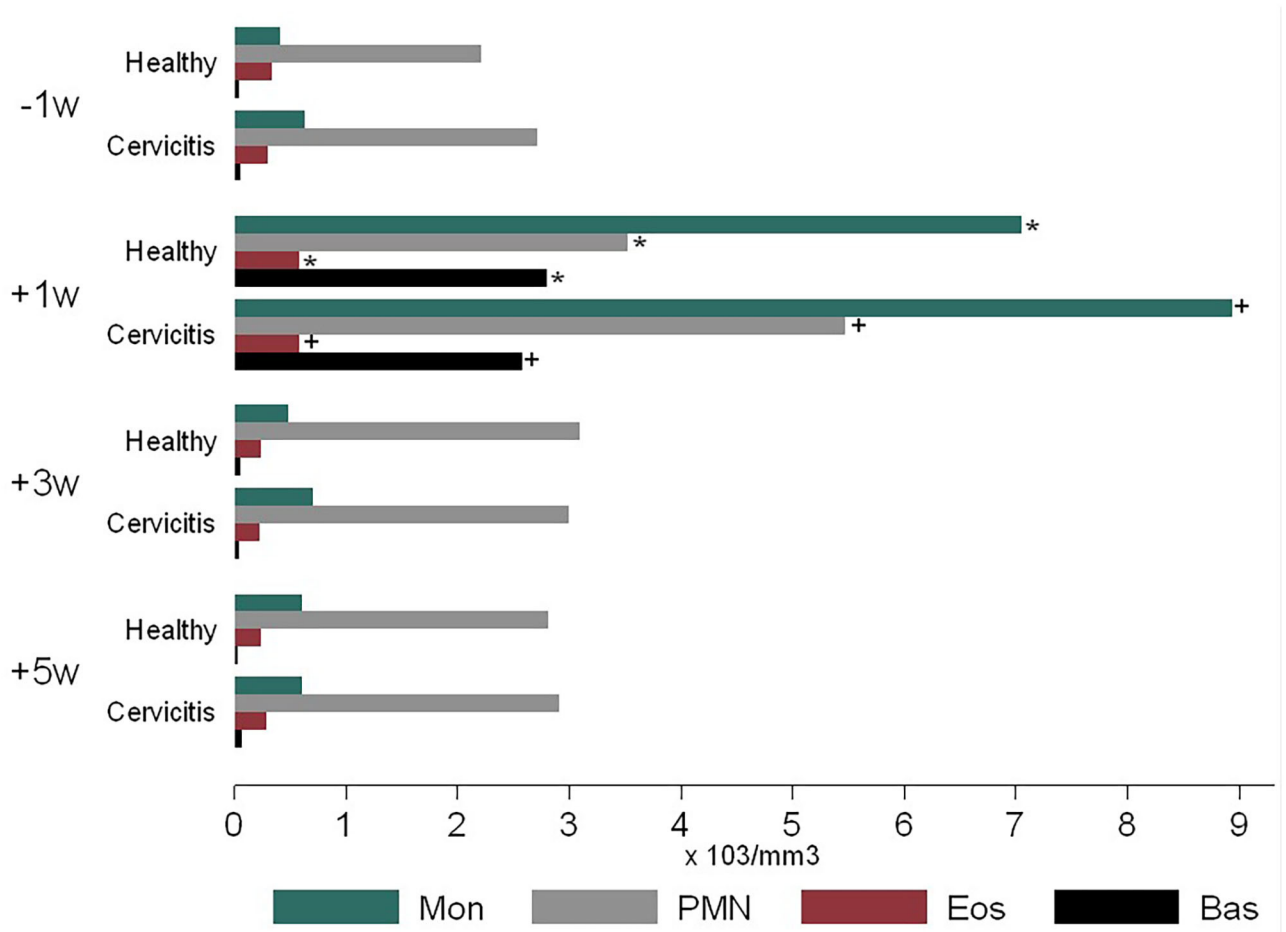

FIGURE 6 | Time-course variations in pre-and post-partum white blood cell count of cows ($n = 26$) defined as clinical cervicitis cows ($n = 19$) and healthy cows ($n = 7$) from three dairy herds in Quebec in 2016. Time-course variations (weeks −1 w +1 w +3 w +5 w) of blood cell count (×103 mm^3) for monocytes (Mo), Neutrophils (Neu), Eosinophils (Eos), Basophiles (Bas). Body mark (*) indicates a significative difference in CH cows at $p \leq 0.05$ for sample time comparison (weeks −1 w +1 w +3 w +5 w). Body mark (+) indicates a significative difference in CC cows at $p \leq 0.05$ for sample time comparison (weeks −1 w +1 w +3 w +5 w).

The parturition period requires extensive remodeling of the cervix before parturition (cervical softening and ripening) for the transformation of the cervix from a closed rigid structure to one that opens for birth (35, 36). At −1 w, a high blood neutrophil count, an increased concentration of IL-8, and a detectable IL1 and AGP concentrations were measured in CC and CH cows. The present results agree with the increase in expression of IL-8 enabling the influx of neutrophils in the cervical tissue that excretes the matrix metalloproteinase which contributes to the softening of the cervix (37, 38). Moreover, parturition is associated with the local accumulation of IL8, which acts synergistically with PGE2 to attract polymorphonuclear neutrophils. Hence, activation of placental leukocyte population releases proteolytic enzymes that degrade the caruncles, thus facilitating fetal membrane separation and advancing the progression of labor (37, 39). Therefore, fetal membrane separation is directly linked to inflammatory changes in the uteroplacental interface. The current results from −1 w prepartum to +1 w postpartum might explain the link between the increase of uterine IL-8, the blood monocytes levels, and the endometrial concentrations of neutrophils. Increased apoptosis, caruncular degradation, and IL-8 production around parturition trigger a massive influx of neutrophil and mononuclear cells into the uterus and the cervix that expel their placenta normally (39). The prepartum increased IL8 concentration found in the present research could be related to cervical ripening before parturition which is a physiological pro-inflammatory process influenced by regulatory cytokines.

In the first week postpartum, the current research found an increase in uterine neutrophils percentage, blood neutrophils and monocytes levels (**Figures 2–6**). This is an expected finding considering that tissue macrophages release IL1 and IL8 acting as a pro-inflammatory and chemo-attracting process coordinating the recruitment of neutrophils to the site of infection enhancing an inflammatory repairing response. The increase of blood monocytes at +1 w (**Figure 6**) may result in more differentiation of monocyte in macrophages in the reproductive tissues for a better clearance of pathogens and a more effective control

of inflammation (15, 40). The abundance of monocyte around parturition reflects the participation of macrophages in the recognition and phagocytosis of cells undergoing apoptosis and capture of bacterial lipopolysaccharides (41). The present results agree with the important role of the expression of pro-inflammatory cytokines and chemokines for calving; where IL1 and IL8 concentrations were at least 8-fold higher in the cervix at parturition than during the gestation (38).

In conclusion, the present study describes cytokines and AGP modulation of the local innate immune response in cows with cervicitis during the postpartum period. The clinical findings of the present study allow diagnosing the presence of a regulated proinflammatory process in the external section of the cervix with certain reliability. The prolapse of the second cervical fold could be related to an inflammatory process in the inner part of the cervix also (clinical cervicitis). The 3 w postpartum was found to be a critical point showing significative increase in the concentration for all markers of inflammation studied. Variations of IL1 and IL8 during the time course of the study were associated with the neutrophils function and most likely part of a normal homeostatic process. These cytokines concentrations were higher in cows with clinical cervicitis than healthy cows. With a proinflammatory protective effect, IL1, IL8 and AGP can modulate locally the uterine innate immune response involving neutrophils in normal uterine involution and in cases of cervicitis or endometritis without the presence of a systemic inflammatory process. Cervicitis can occur in the concomitance of other recognized postpartum uterine clinical conditions (clinical - subclinical endometritis) potentially reducing fertility. As a limitation of the study, we found concentrations for IL1 and IL8 below of the detection range reported for the kit, this is related to the type of sample used [brush with cervical mucus sample and brush with uterine mucus sample collected in a sterile tube with 1 ml of phosphate-buffered saline (PBS) and stored frozen at −80°C]. The kits were selected based on the manufacturer's recommendations for the type of sample. Nevertheless, considering that studies on this topic are scarce, and have different disease definitions, research methods, and limitations (small number of observations, retrospective data, the absence of a sample size calculation, discrepancies between range detection reported for the kits and IL concentrations), further information is needed to understand better the impact of cervicitis on postpartum uterine disease and fertility.

DATA AVAILABILITY STATEMENT

The raw data supporting the conclusions of this article will be made available by the authors, without undue reservation.

ETHICS STATEMENT

This research was performed in compliance with the experimental practices and standards approved by the animal care committee of the University of Montreal (247-29-227).

AUTHOR CONTRIBUTIONS

DV-T and RL conceived and designed the study and analyzed the data and performed the statistical analysis. AB, NP-C, and RL collected clinical data and mucus and blood samples. DV-T conducted the cytokine assays. DV-T, AB, MS, and RL organized and interpreted the database. DV-T, MS, and RL wrote and revised the manuscript. All authors contributed to the article and approved the submitted version.

FUNDING

This project was supported by the Department of Clinical Sciences, Faculty of Veterinary Medicine, University of Montreal, Canada, and the Inter-American Institute for co-operation on agriculture IICA - Delegation in Canada Scholarship RIAP 2019 (Research and Internship Assistance Program Canada) Acta NRC/CA-008.

ACKNOWLEDGMENTS

We acknowledge Beatrice Despres for technical support.

REFERENCES

1. Sheldon IM, Dobson H. Postpartum uterine health in cattle. *Anim Reprod Sci*. (2004) 82–3:295–306. doi: 10.1016/j.anireprosci.2004.04.006
2. Dadarwal D, Palmer C, Griebel P. Mucosal immunity of the postpartum bovine genital tract. *Theriogenology*. (2017) 104:62–71. doi: 10.1016/j.theriogenology.2017.08.010
3. Carneiro LC, Cronin JG, Sheldon IM. Mechanisms linking bacterial infections of the bovine endometrium to disease and infertility. *Reprod Biol*. (2016) 16:1–7. doi: 10.1016/j.repbio.2015.12.002
4. Herath S, Lilly ST, Fischer DP, Williams EJ, Dobson H, Bryant CE, et al. Bacterial lipopolysaccharide induces an endocrine switch from prostaglandin F2α to prostaglandin E2 in bovine endometrium. *Endocrinology*. (2009) 150:1912–20. doi: 10.1210/en.2008-1379
5. Herath S, Williams EJ, Lilly ST, Gilbert RO, Dobson H, Bryant CE, et al. Ovarian follicular cells have innate immune capabilities that modulate their endocrine function. *Reproduction*. (2007) 134:683–93. doi: 10.1530/REP-07-0229
6. Williams EJ. Drivers of post-partum uterine disease in dairy cattle. *Reprod Domest Anim*. (2013) 48:53–8. doi: 10.1111/rda.12205
7. Sheldon IM, Cronin J, Goetze L, Donofrio G, Schuberth H-J. Defining postpartum uterine disease and the mechanisms of infection and immunity in the female reproductive tract in cattle1. *Biol Reprod*. (2009) 81:1025–32. doi: 10.1095/biolreprod.109.077370
8. Dubuc J, Duffield TF, Leslie KE, Walton JS, LeBlanc SJ. Definitions and diagnosis of postpartum endometritis in dairy cows. *J Dairy Sci*. (2010) 93:5225–33. doi: 10.3168/jds.2010-3428
9. Wagener K, Gabler C, Drillich M. A review of the ongoing discussion about definition, diagnosis and pathomechanism of subclinical endometritis in dairy cows. *Theriogenology*. (2017) 94:21–30. doi: 10.1016/j.theriogenology.2017.02.005
10. Hartmann D, Rohkohl J, Merbach S, Heilkenbrinker T, Klindworth HP, Schoon HA, et al. Prevalence of cervicitis in dairy cows and its effect on reproduction. *Theriogenology*. (2016) 85:247–53. doi: 10.1016/j.theriogenology.2015.09.029
11. Sylte MJ, Corbeil LB, Inzana TJ. Haemophilus somnus. *Microbiology*. (2001) 69:1650–60. doi: 10.1128/IAI.69.3.1650-1660.2001

12. Deguillaume L, Geffré A, Desquilbet L, Dizien A, Thoumire S, Vornière C, et al. Effect of endocervical inflammation on days to conception in dairy cows. *J Dairy Sci*. (2012) 95:1776–83. doi: 10.3168/jds.2011-4602
13. Chapwanya A, Meade KG, Foley C, Narciandi F, Evans ACO, Doherty ML, et al. The postpartum endometrial inflammatory response: a normal physiological event with potential implications for bovine fertility. *Reprod Fertil Dev*. (2012) 24:1028–39. doi: 10.1071/RD11153
14. Adnane M, Chapwanya A, Kaidi R, Meade KG, O'Farrelly C. Profiling inflammatory biomarkers in cervico-vaginal mucus (CVM) postpartum: potential early indicators of bovine clinical endometritis? *Theriogenology*. (2017) 103:117–22. doi: 10.1016/j.theriogenology.2017.07.039
15. Singh J, Murray RD, Mshelia G, Woldehiwet Z. The immune status of the bovine uterus during the peripartum period. *Vet J*. (2008) 175:301–9. doi: 10.1016/j.tvjl.2007.02.003
16. Fischer C, Drillich M, Odau S, Heuwieser W, Einspanier R, Gabler C. Selected pro-inflammatory factor transcripts in bovine endometrial epithelial cells are regulated during the oestrous cycle and elevated in case of subclinical or clinical endometritis. *Reprod Fertil Dev*. (2010) 22:818–29. doi: 10.1071/RD09120
17. Chapwanya A, Meade KG, Doherty ML, Callanan JJ, Mee JF, O'Farrelly C. Histopathological and molecular evaluation of Holstein-Friesian cows postpartum: toward an improved understanding of uterine innate immunity. *Theriogenology*. (2009) 71:1396–407. doi: 10.1016/j.theriogenology.2009.01.006
18. Kasimanickam R, Duffield TF, Foster RA, Gartley CJ, Leslie KE, Walton JS, et al. Endometrial cytology and ultrasonography for the detection of subclinical endometritis in postpartum dairy cows. *Theriogenology*. (2004) 62:9–23. doi: 10.1016/j.theriogenology.2003.03.001
19. National Research Council. *Nutrient Requirements of Dairy Cattle*. 7th revised ed. Washington, DC: The National Academies Press (2001).
20. Sheldon IM, Williams EJ, Miller ANA, Nash DM, Herath S. Uterine diseases in cattle after parturition. *Vet J*. (2008) 176:115–21. doi: 10.1016/j.tvjl.2007.12.031
21. Eurell JA, Frapier BL. *Wiley: Dellmann's Textbook of Veterinary Histology*. 6th ed. Iowa City, IA: Blackwell Pub (2006).
22. Dhaliwal GS, Murray RD, Woldehiwet Z. Some aspects of immunology of the bovine uterus related to treatments for endometritis. *Anim Reprod Sci*. (2001) 67:135–52. doi: 10.1016/S0378-4320(01)00124-5
23. Jeon SJ, Vieira-Neto A, Gobikrushanth M, Daetz R, Mingoti RD, Parize ACB, et al. Uterine microbiota progression from calving until establishment of metritis in dairy cows. *Appl Environ Microbiol*. (2015) 81:6324–32. doi: 10.1128/AEM.01753-15
24. Gabler C, Fischer C, Drillich M, Einspanier R, Heuwieser W. Time-dependent mRNA expression of selected pro-inflammatory factors in the endometrium of primiparous cows postpartum. *Reprod Biol Endocrinol*. (2010) 8:1–9. doi: 10.1186/1477-7827-8-152
25. Fournier T, Medjoubi NN, Porquet D. Alpha-1-acid glycoprotein. *Biochim Biophys Acta*. (2000) 1482:157–71. doi: 10.1016/S0167-4838(00)00153-9
26. Lecchi C, Avallone G, Giurovich M, Roccabianca P, Ceciliani F. Extra hepatic expression of the acute phase protein alpha 1-acid glycoprotein in normal bovine tissues. *Vet J*. (2009) 180:256–8. doi: 10.1016/j.tvjl.2007.12.027
27. Rahman MM, Lecchi C, Sauerwein H, Mielenz M, Häußler S, Restelli L, et al. Expression of α1-acid glycoprotein and lipopolysaccharide binding protein in visceral and subcutaneous adipose tissue of dairy cattle. *Vet J*. (2015) 203:223–7. doi: 10.1016/j.tvjl.2014.12.001
28. Rahman MM, Miranda-Ribera A, Lecchi C, Bronzo V, Sartorelli P, Franciosi F, et al. Alpha1-acid glycoprotein is contained in bovine neutrophil granules and released after activation. *Vet Immunol Immunopathol*. (2008) 125:71–81. doi: 10.1016/j.vetimm.2008.05.010
29. Lecchi C, Scarafoni A, Bronzo V, Martino PA, Cavallini A, Sartorelli P, et al. α1-Acid glycoprotein modulates phagocytosis and killing of *Escherichia coli* by bovine polymorphonuclear leucocytes and monocytes. *Vet J*. (2013) 196:47–51. doi: 10.1016/j.tvjl.2012.07.022
30. Ceciliani F, Pocacqua V, Miranda-Ribera A, Bronzo V, Lecchi C, Sartorelli P. α1-Acid glycoprotein modulates apoptosis in bovine monocytes. *Vet Immunol Immunopathol*. (2007) 116:145–52. doi: 10.1016/j.vetimm.2007.01.006
31. Miranda-Ribera A, Lecchi C, Bronzo V, Scaccabarozzi L, Sartorelli P, Franciosi F, et al. Down-regulatory effect of alpha1-acid glycoprotein on bovine neutrophil degranulation. *Comp Immunol Microbiol Infect Dis*. (2010) 33:291–306. doi: 10.1016/j.cimid.2008.10.009
32. Cairoli F, Battocchio M, Veronesi MC, Brambilla D, Conserva F, Eberini I, et al. Serum protein pattern during cow pregnancy: Acute-phase proteins increase in the peripartum period. *Electrophoresis*. (2006) 27:1617–25. doi: 10.1002/elps.200500742
33. Theilgaard-Mönch K, Jacobsen LC, Rasmussen T, Niemann CU, Udby L, Borup R, et al. Highly glycosylated α1-acid glycoprotein is synthesized in myelocytes, stored in secondary granules, and released by activated neutrophils. *J Leukoc Biol*. (2005) 78:462–70. doi: 10.1189/jlb.0105042
34. Manimaran A, Kumaresan A, Jeyakumar S, Mohanty TK, Sejian V, Kumar N, et al. Potential of acute phase proteins as predictor of postpartum uterine infections during transition period and its regulatory mechanism in dairy cattle. *Vet World*. (2016) 9:91–100. doi: 10.14202/vetworld.2016.91-100
35. Mahendroo M. Cervical remodeling in term and preterm birth: Insights from an animal model. *Reproduction*. (2012) 143:429–38. doi: 10.1530/REP-11-0466
36. Timmons B, Akins M, Mahendroo M. Cervical remodeling during pregnancy and parturition. *Trends Endocrinol Metab*. (2010) 21:353–61. doi: 10.1016/j.tem.2010.01.011
37. Van Engelen E, Taverne MAM, Everts ME, van der Weijden GC, Doornenbal A, Breeveld Dwarkasing VNA. Cervical diameter in relation to uterine and cervical EMG activity in early postpartum dairy cows with retained placentas after PGF2alpha induced calving. *Theriogenology*. (2007) 68:213–22. doi: 10.1016/j.theriogenology.2007.04.054
38. Van Engelen E, De Groot MW, Breeveld-Dwarkasing VNA, Everts ME, Van Der Weyden GC, Taverne MAM, et al. Cervical ripening and parturition in cows are driven by a cascade of pro-inflammatory cytokines. *Reprod Domest Anim*. (2009) 44:834–41. doi: 10.1111/j.1439-0531.2008.01096.x
39. Attupuram NM, Kumaresan A, Narayanan K, Kumar H. Cellular and molecular mechanisms involved in placental separation in the bovine: a review. *Mol Reprod Dev*. (2016) 83:287–97. doi: 10.1002/mrd.22635
40. Sheldon IM, Cronin JG, Bromfield JJ. Tolerance and innate immunity shape the development of postpartum uterine disease and the impact of endometritis in dairy cattle. *Annu Rev Anim Biosci*. (2018) 7:361–84. doi: 10.1146/annurev-animal-020518-115227
41. Streyl D, Kenngott R, Herbach N, Wanke R, Blum H, Sinowatz F, et al. Gene expression profiling of bovine peripartal placentomes: detection of molecular pathways potentially involved in the release of foetal membranes. *Reproduction*. (2012) 143:85–105. doi: 10.1530/REP-11-0204

Conflict of Interest: The authors declare that the research was conducted in the absence of any commercial or financial relationships that could be construed as a potential conflict of interest.

frontiers in Veterinary Science

ORIGINAL RESEARCH
published: 09 February 2021
doi: 10.3389/fvets.2020.625921

Selected Uterine Immune Events Associated With the Establishment of Pregnancy in the Dog

Miguel Tavares Pereira[1†], Renata Nowaczyk[2†], Rita Payan-Carreira[3], Sonia Miranda[4], Selim Aslan[5], Duygu Kaya[6] and Mariusz P. Kowalewski[1]*

[1] Institute of Veterinary Anatomy, Vetsuisse Faculty, University of Zurich (UZH), Zurich, Switzerland, [2] Division of Histology and Embryology, Department of Biostructure and Animal Physiology, Faculty of Veterinary Medicine, Wroclaw University of Environmental and Life Sciences, Wroclaw, Poland, [3] Mediterranean Institute for Agriculture, Environment (MED) and Department of Veterinary Medicine, University of Évora, Évora, Portugal, [4] Animal and Veterinary Research Center (CECAV), University of Trás-os-Montes and Alto Douro, Vila Real, Portugal, [5] Department of Obstetrics and Gynecology, Faculty of Veterinary Medicine, Near East University, Nicosia, Cyprus, [6] Department of Obstetrics and Gynecology, Faculty of Veterinary Medicine, Kafkas University, Kars, Turkey

OPEN ACCESS

Edited by:
Dariusz Jan Skarzynski, Institute of Animal Reproduction and Food Research (PAN), Poland

Reviewed by:
Roman Dabrowski, University of Life Sciences of Lublin, Poland
Sudson Sirivaidyapong, Chulalongkorn University, Thailand

***Correspondence:**
Mariusz P. Kowalewski
kowalewskipl@yahoo.de;
kowalewski@vetanat.uzh.ch

[†] These authors have contributed equally to this work

Specialty section:
This article was submitted to Animal Reproduction - Theriogenology, a section of the journal Frontiers in Veterinary Science

Received: 04 November 2020
Accepted: 07 December 2020
Published: 09 February 2021

Citation:
Tavares Pereira M, Nowaczyk R, Payan-Carreira R, Miranda S, Aslan S, Kaya D and Kowalewski MP (2021) Selected Uterine Immune Events Associated With the Establishment of Pregnancy in the Dog. Front. Vet. Sci. 7:625921. doi: 10.3389/fvets.2020.625921

In the dog, implantation takes place at approximately 17 days of embryonal life and, while exposed to relatively high circulating progesterone concentrations, embryos presence is required for the formation of decidua. Furthermore, a balance between pro- and anti-inflammatory responses in conceptus-maternal communication is crucial for the onset of pregnancy. Strikingly, the understanding of such immune mechanisms in canine reproduction is still elusive. Here, canine uterine samples from pre-implantation (day 10–12, E+) and corresponding non-pregnant controls (E–), implantation (day 17, Imp) and post-implantation (day 18–25, Post-Imp) stages of pregnancy were used to investigate the expression and localization of several immune-related factors. The most important findings indicate increased availability of *CD4*, *MHCII*, *NCR1*, *IDO1*, *AIF1*, *CD25*, *CCR7*, and *IL6* in response to embryo presence (E+), while *FoxP3* and *CCL3* were more abundant in E– samples. Implantation was characterized by upregulated levels of *FoxP3*, *IL12a*, *ENG*, and *CDH1*, whereas *CD4*, *CCR7*, *IL8*, and *-10* were less represented. Following implantation, decreased transcript levels of *TNFR1*, *MHCII*, *NCR1*, *TLR4*, *CD206*, *FoxP3,* and *IL12a* were observed concomitantly with the highest expression of *IL6* and *IL1β*. MHCII, CD86, CD206, CD163, TNFα, IDO1, and AIF1 were immunolocalized in macrophages, CD4 and Nkp46 in lymphocytes, and some signals of IDO1, AIF1, and TNF-receptors could also be identified in endothelial cells and/or uterine glands. Cumulatively, new insights regarding uterine immunity in the peri-implantation period are provided, with apparent moderated pro-inflammatory signals prevailing during pre-implantation, while implantation and early trophoblast invasion appear to be associated with immunomodulatory and rather anti-inflammatory conditions.

Keywords: dog (*Canis lupus familiaris*), immune system, uterus, early pregnancy, embryo-maternal communication

INTRODUCTION

The uterine mucosal immune system plays an important role during maternal recognition and establishment of pregnancy. This is accomplished by maintaining a balance between the defense against pathogens and the tolerance toward the allogeneic sperm and semiallogeneic embryo, adapting thereby to different pregnancy-associated events (e.g., implantation, placentation, parturition) and contributing to tissue remodeling (1–3). This balance relies on the complex population of resident immune cells, composed of, e.g., macrophages, natural killer (NK) cells, B and T lymphocytes, regulated by local and systemic signaling, including endocrine insults (1, 2, 4, 5), and changing during the progression of pregnancy. This, i.e., regards the polarization of uterine macrophages. Thus, as shown e.g., in humans, pre-implantation is marked by a predominant presence of M1 (pro-inflammatory) macrophages, transitioning to a mixed, M1/M2, population during trophoblast attachment and a predominant presence of M2 macrophages following placentation [reviewed in (6)]. While the role of all of the different immune cell populations in the uterus is not fully understood, some, like the NK are crucial in the onset of pregnancy. In the human and mouse uterus they are required for the formation of highly invasive (hemochorial) deciduate placenta [reviewed in (7, 8)]. NK cells are the most prevalent immune cell population in the uterus in these species and are involved in the regulation of trophoblast invasion, playing key roles in the remodeling of spiral arterioles during the formation of decidual tissue [reviewed in (8)]. However, despite presenting a deciduate endotheliochorial placenta, no such mechanisms are known for the dog, nor has the composition of the immune system been thoroughly studied in this species.

Furthermore, translational research from other species to the dog is limited by the canine species-specific decidualization mechanisms as a part of the peculiar reproductive physiology. Thus, lacking an active luteolytic event, non-pregnant bitches present a physiological pseudopregnancy that lasts frequently longer than pregnancy, with luteal P4 circulating levels similar to those observed in pregnant animals [reviewed in (9)]. Additionally, canine oocytes require oviductal maturation to reach fertilization competence, while implantation and development of a decidual endotheliochorial placenta start around days 17–18 after fertilization (10–12). Despite the high P4 levels observed during this period, no spontaneous decidualization can be observed in non-pregnant bitches, as the presence of the implanting blastocyst is needed to induce the differentiation of maternal stromal cells into decidual cells [reviewed in (13)]. Nevertheless, while the presence of an embryo-derived antiluteolytic signal is not needed in this species, cross-talk between the embryo and maternal tissue is still required for the establishment of pregnancy. Indeed, the presence of free-floating blastocysts has been associated with changes in the uterine transcriptome indicating modulation of, e.g., extracellular matrix components and immune system-related factors (14–16).

However, with regard to the involvement of the immune system in the establishment of pregnancy, available information for the dog pales in contrast to what is known for other species with a deciduate placenta. Canine early pregnancy is associated with increased circulating levels of acute phase and heat shock proteins that, due to their high sensitivity to the health status of the animal, have limited use as markers of pregnancy [reviewed in (13)]. As for embryo-induced changes, earlier qualitative analyses of the pre-implantation uterine immune milieu in pregnant and pseudopregnant bitches described differences in the presence of factors like CD4, CD8, INFγ, TNFα, and some interleukins (17, 18). In a later study from our group, the presence of free-floating embryos was associated with the predicted activation of signaling pathways involving IL1, IL10, toll-like receptor (TLR) and NFκB, and increased expression of chemokines and other immune regulators (14). As for the period of implantation and placentation, the available information is limited to the observed increased availability of leukemia inhibitory factor (LIF) and macrophage colony-stimulating (MCS) factor in placentation sites, in contrast with early pregnancy (17, 19). Furthermore, while immunohistochemical description of $CD3^+$ T lymphocytes, macrophages and B lymphocytes is available for non-pregnant bitches (20), nothing is known regarding the uterine immune population of pregnant animals.

Consequently, while the immune system plays an important role in the onset of pregnancy, there is only scarce information available for the dog. To address this knowledge gap, the aim of this study was to characterize factors constituting the uterine immune milieu during the early stages of canine pregnancy, i.e., during the free-floating embryo stage (pre-implantation), at the time of implantation (day 17) and during placental formation (post-implantation). We investigated the expression and/or localization of twenty four different immune factors that serve as markers of different immune cells subsets and/or are involved in immune regulation. In addition, gene expression of six factors involved in tissue growth and remodeling was also evaluated.

MATERIALS AND METHODS

Tissue Collection and Preservation

Uterine- and utero-placental samples from 27 ($n = 27$) healthy, mixed breed bitches aged 2–8 years old were allotted to the present work. All samples had been used before and details on animal manipulation and determination of pregnancy status were described in (14, 21–23). Briefly, animals were monitored for the onset of spontaneous ovulation by vaginal cytology and progesterone (P4) measurements. Health condition of the animals was evaluated by routine clinical examination. P4 levels were determined by radioimmunoassay, as previously described (24). Ovulation was considered to have occurred when circulating levels of P4 exceeded 5 ng/ml, and bitches were mated 2–3 days later (time needed for oocyte maturation and completion of the first meiotic division). Day of mating was considered day 0 of pregnancy. Samples were collected by ovariohysterectomy at different pregnancy stages: pre-implantation (days 8–12, before embryo apposition), at the day of implantation (Imp, day 17, $n = 5$) and during early placentation (post-implantation stage, Post-Imp, days 18–25, $n = 5$). During pre-implantation, early

pregnancy was confirmed by uterine flushing and recovery of embryos (E+, $n = 9$). Animals in which no embryo was recovered between days 8–12 were considered not pregnant (E-, $n = 8$). Following surgery, retrieved uterine samples (including all histological layers) were immediately trimmed of connective tissues and washed in cold PBS. From Imp and Post-Imp groups, implantation/placentation sites were collected (the Post-Imp stage included the early utero-placental formation). For RNA analysis, samples were immersed in RNAlater (Ambion Biotechnology GmbH, Wiesbaden, Germany) for 24 h at 4°C and then stored at −80°C until used for RNA isolation. For histological analysis, samples were fixed for 24 h in 10% neutral phosphate-buffered formalin, washed with PBS, dehydrated in a graded ethanol series and embedded in the paraffin equivalent HistoComp (Vogel, Giessen, Germany).

Animal experiments were carried out in accordance with animal welfare legislation and were approved by the responsible ethics committee of the Justus-Liebig University Giessen, Germany (permits no. II 25.3-19c20-15c GI 18/14 and VIG3-19c-20/15 GI 18,14), and of the University of Ankara, Turkey (permits no. Ankara 2006/06 and 2008-25-124). Samples from day 17 of pregnancy were collected at the "Hospital Veterinário do Baixo Vouga", Portugal, after informed consent of the owners (22).

Total RNA Isolation, High Capacity Reverse Transcription, Pre-amplification of cDNA, and Semi-quantitative Real-Time TaqMan PCR (qPCR)

Total RNA was isolated using the TRIzol reagent (Invitrogen, Carlsbad, CA, USA) following the manufacturer's instructions and concentration and purity were assessed with a NanoDrop 2000C spectrophotometer (ThermoFisher scientific AG Reinach, Switzerland). The elimination of possible genomic DNA contamination was performed using the RQ1 RNA-free DNase Kit (Promega, Dübendorf, Switzerland) following the instructions provided by the manufacturer. Reverse transcription (RT) and pre-amplification of cDNA were performed by applying the High Capacity cDNA Reverse Transcription Kit (Applied Biosystems by ThermoFisher Scientific, Foster City, CA, USA), using 10 ng total RNA as starting material. Next, the TaqMan PreAmp Master Mix Kit (Applied Biosystems) was applied following the supplier's protocols and as previously described (25). Briefly, all used predesigned commercially available TaqMan systems (obtained from Applied Biosystems) and self-designed primers and 6-carboxyfluorescein (6-FAM) and 6-carboxytetramethylrhodamine (TAMRA) labeled probes (ordered from Microsynth AG, Balgach, Switzerland), were pooled. Afterwards, cDNA from each sample was mixed with PreAmp Master Mix and pooled TaqMan assays and samples were amplified in an Eppendorf Mastercycler (Vaudax-Eppendorf AG, Basel, Switzerland). A complete list of the predesigned TaqMan systems and self-designed primers and 6-FAM and TAMRA probes used is presented in **Table 1**.

The expression of the 29 selected target genes was investigated by real-time TaqMan PCR. The construction of self-designed primers and probes was based on published coding sequences (CDS). For genes where only predicted CDS were available (i.e., CD206 and NCR1), products were commercially sequenced (Microsynth) to confirm the specificity of amplicons. Efficiency values of PCR reactions were validated to ensure approximately 100% as previously described (25, 26). The protocols used for sample preparation and semi-quantitative real-time TaqMan PCR were published previously (25–27). TaqMan PCR was run with FastStart Universal Probe Master (ROX, Roche Diagnostics AG, Switzerland) and 5 µl pre-amplified cDNA. Reactions were run in duplicate in an automated ABI PRISM 7500 Sequence Detection System (Applied Biosystems). Autoclaved water and minus-RT controls were used instead of cDNA as negative controls, and relative quantification of gene expression was performed with the comparative Ct method (ΔΔCt), as previously described (26, 27). Values were calibrated to average expression in E– samples and normalized with the expression of reference genes. In preliminary experiments, the expression of three potential reference genes (*GAPDH, β-ACTIN* and *CYCLOPHILIN*) was evaluated in all used samples and their stability values were calculated using the online tool RefFinder (28). *β-ACTIN* and *GAPDH* were selected as more stable than *CYCLOPHILIN* and used as reference genes for ΔΔCt evaluation.

Immunohistochemical Staining

Immunohistochemical (IHC) detection of 12 protein targets for which commercial canine cross-reacting antibodies were available (listed in **Table 2**) was performed using the standard indirect immunoperoxidase method, following our previously described protocol for canine tissues (27, 29). Briefly, formalin-fixed and paraffin-embedded tissue samples were cut in 2–3 µm thick sections, mounted on microscope slides (SuperFrost; Menzel-Glaeser, Braunschweig, Germany), deparaffinized and rehydrated. Slides were then heated in 10 mM citrate buffer (pH 6.0) in a microwave oven for antigen retrieval and endogenous peroxidase activity was quenched with 0.3% hydrogen peroxide diluted in methanol. Non-specific binding sites were blocked with 10% horse or goat serum (depending on the secondary antibody used), and samples were incubated overnight at +4°C. Dilutions of the selected primary antibodies are described in **Table 2**. Samples were then incubated with biotin-labeled secondary antibodies (horse anti-goat IgG BA-9500, goat anti-rabbit IgG BA1000 or horse anti-mouse IgG BA-2000, all purchased from Vector Laboratories Inc., Burlingame, CA, USA), diluted 1:100 in immunohistochemistry buffer (0.8 mM Na_2HPO_4, 1.47 mM KH_2PO4, 2.68 mM KCl, and 137 mM NaCl, containing 0.3% Triton X; pH 7.2–7.4), followed by the avidin-peroxidase Vectastain ABC kit (Vector Laboratories Inc.). Peroxidase activity was detected using a liquid DAB + substrate kit (Dako Schweiz AG, Baar, Switzerland). Contrast staining was performed with hematoxylin and slides were mounted with Histokit (Assistant, Osterode, Germany). Evaluation of primary antibodies specificity was performed by replacing the primary antibody with a non-immune IgG from the same species and at the same concentration (isotype control, rabbit IgG I-1000, goat IgG I-5000, and mouse IgG I-2000, all from Vector Laboratories Inc.). Slides were evaluated

TABLE 1 | List of gene symbols, corresponding gene names, and TaqMan systems used for semi-quantitative real time qPCR.

Gene	Name	Accession numbers	Primer sequence		Product length (bp)
MHCII	Major histocompatibility complex II	NM_001011723.1	Forward	5′-GGA GAG CCC AAC ATC CTC ATC-3′	90
			Reverse	5′-GGT GAC AGG GTT TCC ATT TCG-3′	
			TaqMan probe	5′-TCG ACA AGT TCT CCC CAC C-3′	
CD206/MCR1	Cluster of differentiation 206/mannose receptor C-Type 1	XM_005617091.3	Forward	5′-GGC AGG AAG ATT GTG TCG TCA T-3′	108
			Reverse	5′-TGG GCT GGG TTT GAG ATT TC-3′	
			TaqMan probe	5′-TGG GCA GAT CGA GCC TGC GAG-3′	
NCR1	Natural cytotoxicity triggering receptor 1	NM_001284448.1	Forward	5′-CTG GGA TCA CAC TGC CCA TAA T-3′	103
			Reverse	5′-CCT CTT CCT GCA AAG CCA GTA-3′	
			TaqMan probe	5′-CTT TCC TGG TCC TGA TGG CCC TCA-3′	
IL1β	Interleukin 1 beta	NM_001037971.1	Forward	5′-TGC CAA GAC CTG AAC CAC AGT-3′	97
			Reverse	5′-CTG ACA CGA AAT GCC TCA GAC T-3′	
			TaqMan probe	5′-CAT CCA GTT GCA AGT CTC CCA CCA GC-3′	
IL6	Interleukin 6	AF275796.1	Forward	5′-AAA GAG CAA GGT AAA GAA TCA GGA TG-3′	124
			Reverse	5′-GCA GGA TGA GGT GAA TTG TG-3′	
			TaqMan probe	5′-ACT CCT GAC CCA ACC ACA GAC GCC A-3′	
IL8/CXCL8	Interleukin 8/ C-X-C motif chemokine ligand 8	NM_001003200.1	Forward	5′-CCA CAC CTT TCC ATC CCA AA-3′	114
			Reverse	5′-CCA GGC ACA CCT CAT TTC CA-3′	
			TaqMan probe	5′-CTG AGA GTG ATT GAC AGT GGC CCA CAT TGT-3′	
TNFα	Tumor necrosis factor alpha	NM_001003244	Forward	5′-TGC CCT TCC ACC CAT GTG-3′	96
			Reverse	5′-AGG GCT CTT GAT GGC AGA GA-3′	
			TaqMan probe	5′-CCC ACA CCA TCA GCC GCT TCG-3′	
TNFR1	Tumor necrosis factor receptor 1	XM_849381	Forward	5′-TGT GTG GCT GCA GGA AGA AC-3′	114
			Reverse	5′-GCT TCT CTT GGC AGG AGA TCT-3′	
			TaqMan probe	5′-ACT CCA CCC TCT GCC TCA ATG GCA-3′	
TNFR2	Tumor necrosis factor receptor 2	XM_005617982	Forward	5′-CCA GCA GAG CGA GTA CTT CGA-3′	95
			Reverse	5′-TCG AGG TCT TGG TGC AGA AGA-3′	
			TaqMan probe	5′-CAT GTG TCC CCC TGG CTC CCA C-3′	
IDO1	Indolamin 2,3-dioxygenase 1	XM_532793.5	Forward	5′-TGA TGG CCT TAG TGG ACA CAA G-3′	116
			Reverse	5′-TCT GTG GCA AGA CTT TTC GA-3′	
			TaqMan probe	5′-CAG CGC CTT GCA CGT CTG GC-3′	
AIF1	Allograft inflammatory factor 1	XM_532072.5	Forward	5′-CGA ATG CTG GAG AAA CTT GGT-3′	107
			Reverse	5′-TGA GAA AGT CAG AGT AGC TGAAGG T-3′	
			TaqMan probe	5′-TCC CCA AGA CCC ATC TGG AGC TCA A-3′	
GAPDH	Glyceraldehyde-3-phosphate dehydrogenase	AB028142.1	Forward	5′-GCT GCC AAA TAT GAC GAC ATC A-3′	75
			Reverse	5′-GTA GCC CAG GAT GCC TTT GAG-3′	
			TaqMan probe	5′-TCC CTC CGA TGC CTG CTT CAC TAC CTT-3′	
CD163	Cluster of differentiation 163		Pre-designed assay from Applied Biosystems, Prod.No. Cf02627321_m1		
CD4	Cluster of differentiation 4		Pre-designed assay from Applied Biosystems, Prod.No. Cf02627842_m1		
CD8	Cluster of differentiation 8		Pre-designed assay from Applied Biosystems, Prod.No. Cf02627888_m1		
CD25/IL2Ra	Cluster of differentiation 25/interleukin 2 receptor alpha		Pre-designed assay from Applied Biosystems, Prod.No. Cf02623133_m1		
FoxP3	Forkhead Box P3		Pre-designed assay from Applied Biosystems, Prod.No. Cf02741703_m1		
IL10	Interleukin 10		Pre-designed assay from Applied Biosystems, Prod.No. Cf02624264_m1		
IL12a	Interleukin 12		Pre-designed assay from Applied Biosystems, Prod.No. Cf02628398_m1		
TGFβ	Transforming growth factor 1 beta		Pre-designed assay from Applied Biosystems, Prod.No. Cf02623324_m1		
CCL3	C-C motif chemokine ligand 3		Pre-designed assay from Applied Biosystems, Prod.No. Cf02671956_m1		
CCL13	C-C motif chemokine ligand 13		Pre-designed assay from Applied Biosystems, Prod.No. Cf02622470_mH		
CCR7	C-C motif chemokine receptor 7		Pre-designed assay from Applied Biosystems, Prod.No. Cf02654980_m1		
TLR4	Toll-like receptor 4		Pre-designed assay from Applied Biosystems, Prod.No. Cf02622203_g1		
IGF1	Insulin-like growth factor 1		Pre-designed assay from Applied Biosystems, Prod.No. Cf02627846_m1		

(Continued)

TABLE 1 | Continued

Gene	Name	Primer sequence
IGF2	Insulin-like growth factor 2	Pre-designed assay from Applied Biosystems, Prod.No. Cf02647136_m1
ENG	Endoglin	Pre-designed assay from Applied Biosystems, Prod.No. Cf02658400_m1
CDH1	Cadherin-1/epithelial cadherin (E-cadherin)	Pre-designed assay from Applied Biosystems, Prod.No. Cf02624268_m1
ECM2	Extracellular matrix protein 2	Pre-designed assay from Applied Biosystems, Prod.No. Cf02641132_m1
MMP2	Matrix metalloperoteinase 2	Pre-designed assay from Applied Biosystems, Prod.No. Cf02741675_m1
β-ACTIN	Beta-actin	Pre-designed assay from Applied Biosystems, Prod.No. Cf03023880_g1
PPIA/Cyclophilin	Peptidylprolyl isomerase A	Pre-designed assay from Applied Biosystems, Prod.No. Cf03986523_gH

TABLE 2 | List of antibodies and corresponding dilutions used in immunohistochemical staining.

Target protein	Product reference and manufacturer	Dilution
MHCII	ORB101661 (Biorbyt, Cambridge, UK)	1:200
CD86	ORB49101 (Biorbyt, Cambridge, UK)	1:400
Nkp46	ORB157934 (Biorbyt, Cambridge, UK)	1:400
CD4	AB125711 (Abcam, Cambridge, UK)	1:400
CD8	AB101500 (Abcam, Cambridge, UK)	1:100
TNFα	AB6671 (Abcam, Cambridge, UK)	1:200
TNFR1	AB19139 (Abcam, Cambridge, UK)	1:200
TNFR2	AB15563 (Abcam, Cambridge, UK)	1:200
IDO1	LS-C174759 (LSBio, Seattle, WA, USA)	1:50
AIF1	LS-B2403 (LSBio, Seattle, WA, USA)	1:400
CD206	SC-376108 (Santa Cruz Biotecnology Inc., Santa Cruz, CA, USA)	1:400
CD163	DB045 (DB Biotech, Kosice, SK)	1:400

TABLE 3 | Surface markers selected for identification of macrophage and lymphocyte subsets.

Macrophage phenotype	Selected markers
M1	↑MHCII, CD86, CD4
M2a	CD206
M2b	↓MHCII, CD86
M2c	CD163
T lymphocyte subpopulation	**Selected markers**
Tc (cytotoxic)	CD8
Th (helper)	CD4, CD25
Treg (regulatory)	CD4, CD25, FoxP3
NK (natural killer)	Nkp46 (NCR1)

Selection of investigated markers was performed based on current literature (6, 32, 33, 36-40). (↑ = high expression, ↓ = low expression).

qualitatively using a Leica DMRXE light microscope with a Leica DFC425 camera (Leica Microsystems, Wetzlar, Germany). Identification of macrophages and lymphocytes was performed by observing positive staining against specific factors, in some cases following staining of consecutive slides, and morphological characterization of cells following descriptions available in the literature (30, 31).

Statistical Analysis

Statistical evaluation of real-time TaqMan PCR was performed using the software GraphPad 2.06 (GraphPad Software Inc, San Diego, CA, USA). To evaluate the differences between the analyzed groups (i.e., in response to the presence or absence of embryos in the pre-implantation period, and between pre-implantation, implantation, and post-implantation stages) parametric one-way analysis of variance (ANOVA) followed by Tukey-Kramer multiple comparisons post-test were applied. Furthermore, the comparison between CD4 and CD8 expression in each experimental group was performed with an unpaired two-tailed Student's *t*-test. Numerical results for relative gene expression are presented as mean ± standard error of the mean (SEM). $P < 0.05$ was considered statistically significant.

RESULTS

With the aim of characterizing the presence and localization of several subsets of macrophages and lymphocytes in the early pregnant canine uterus, several relevant immune system markers, described in **Table 3**, were evaluated. Furthermore, the expression of several cytokines, immune regulators, and factors involved in tissue growth and remodeling was also assessed. The expression of the 29 target genes was detectable in samples from all experimental groups, although the transcript abundance of some of them at specific stages (indicated in Figures) was low and, sometimes, below detection limits. Among these were *FoxP3* and *IL12a* in samples from the Post-Imp stage (**Figures 1H**, **3E**, respectively) and *CCL13* on the day of implantation (day 17, **Figure 3K**). In addition, specific staining was obtained with all tested antibodies in all evaluated samples.

Detection of Macrophages and Lymphocytes Markers

To investigate the presence of different macrophage phenotypes in the canine uterus during the establishment of pregnancy, the expression of *MHCII*, *CD206*, and *CD163* was evaluated. Pregnancy status (E+ vs. E–) and/or stage, significantly affected the expression of transcripts encoding for *MHCII* ($P < 0.01$) and *CD206* ($P < 0.0001$), but no significant changes were

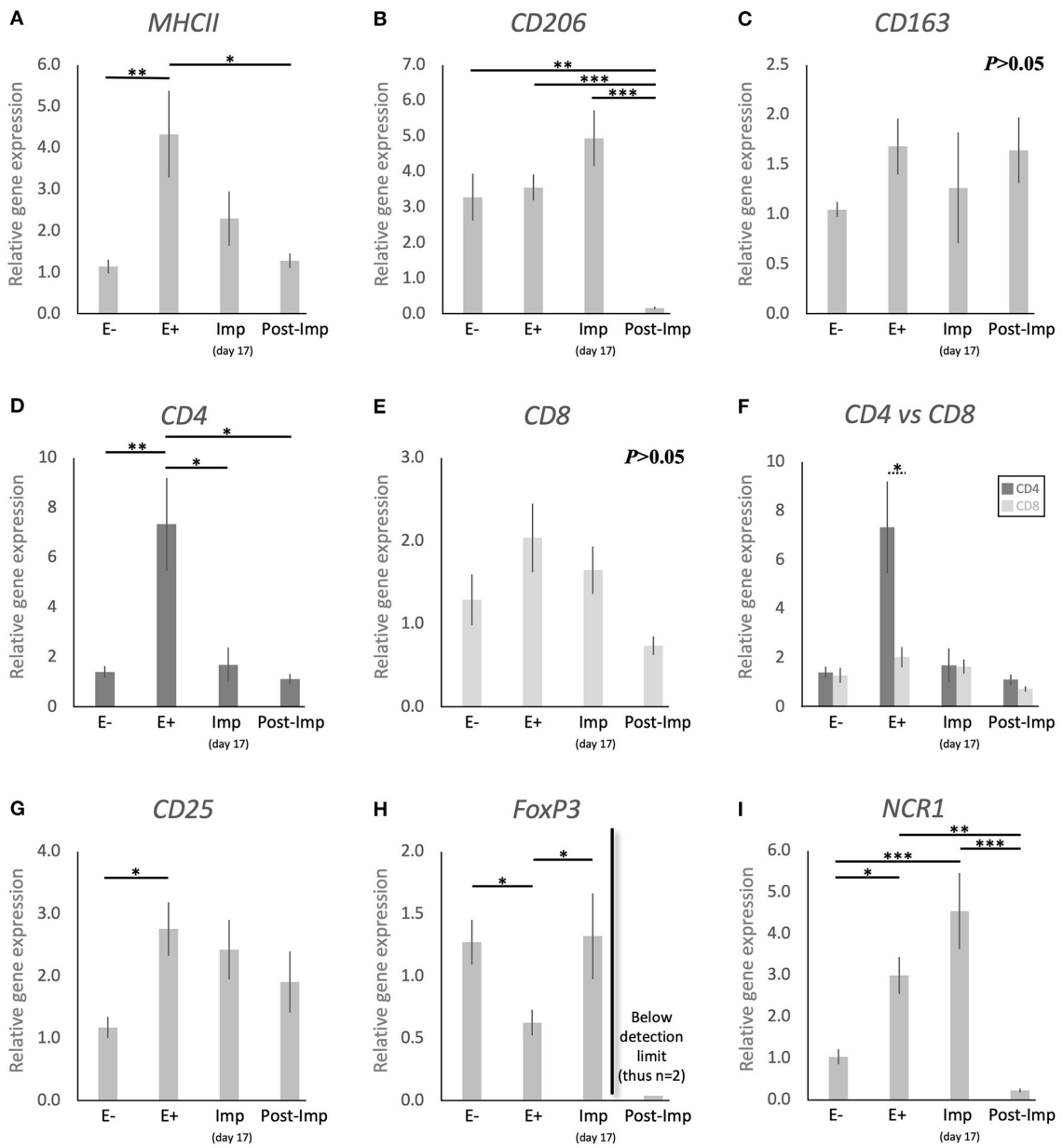

FIGURE 1 | Relative gene expression of selected immune cell markers in the canine early pregnant uterus. Relative gene expression as determined by semi-quantitative real time (TaqMan) PCR (mean ± SEM). **(A–E,G–I)** One-way ANOVA was applied to test the effects of time (pregnancy stage) on gene expression revealing: $P = 0.005$ for *MHCII*, $P < 0.0001$ for CD206, $P = 0.2$ for CD163, $P = 0.0032$ for *CD4*, $P = 0.06$ for *CD8*, $P = 0.02$ for *CD25*, $P = 0.01$ for *FoxP3* and $P < 0.0001$ for *NCR1*. In the case of $P < 0.05$, the analysis was followed by a Tukey-Kramer multiple comparisons post-test. **(F)** Comparison of relative gene expression between CD4 and CD8 was evaluated by applying Student's unpaired two-tailed *t*-test at each investigated stage. Bars with asterisks differ at: $^{*}P < 0.05$, $^{**}P < 0.01$, $^{***}P < 0.001$.

observed in the expression of *CD163* ($P > 0.05$, **Figure 1C**). The presence of embryos in the early pregnant uterus prior to implantation (E+) was associated with a higher expression of MHCII, in contrast to its non-pregnant counterparts (E–, $P < 0.01$, **Figure 1A**). This was not the case for *CD206*, for which the presence of embryos had no effect on the transcript levels (**Figure 1B**). However, considering the progression of pregnancy, the expression of *MHCII* and *CD206* was the lowest post-implantation (Post-Imp) when compared with E+ for *MHCII* ($P < 0.05$, **Figure 1A**) or all previous stages for *CD206* ($P < 0.001$, **Figure 1B**).

The different subsets of T lymphocytes were assessed by evaluating the uterine availability of transcripts encoding for *CD4*, *CD8*, *CD25*, *FoxP3*, and *NCR1* (that encodes for NKp46).

Significant changes in the expression of *CD4* ($P < 0.01$), *CD25* ($P < 0.05$), *FoxP3* ($P < 0.01$), and *NCR1* ($P < 0.0001$) were observed in relation to the presence/absence of pregnancy and/or its stage, while *CD8* did not differ significantly ($P > 0.05$) across all analyzed groups (**Figure 1**). In the early pre-implantation period (days 8–12, E+), the presence of an embryo was associated with increased expression of *CD4* ($P < 0.01$, **Figure 1D**), *CD25* ($P < 0.05$, **Figure 1G**), and *NCR1* ($P < 0.05$, **Figure 1I**), compared with E- samples, while *FoxP3* was downregulated ($P < 0.01$, **Figure 1H**). Regarding pregnancy stage, *CD4* expression was also the highest during pre-implantation (E+), in contrast with the later stages, i.e., Imp and Post-Imp, when its uterine expression was significantly suppressed ($P < 0.05$, **Figure 1D**). In addition, *CD4* expression at the E+ stage was significantly higher than *CD8* ($P < 0.05$, **Figure 1F**). As for *FoxP3*, although the presence of embryos had a suppressive effect on its expression, its expression increased during Imp ($P < 0.05$, **Figure 1H**). Interestingly, following implantation the levels of *FoxP3* mRNA were significantly suppressed and fell below detection limits in most of the samples (**Figure 1H**). Similarly, the expression of *NCR1* decreased significantly after implantation (Post-Imp), compared with E+ and Imp ($P < 0.01$ and $P < 0.001$, respectively, **Figure 1F**).

To further evaluate the immune infiltrate in the canine uterus during the peri-implantation period, the immunolocalization of factors selected as markers of different immune cell subsets was also evaluated by IHC. Regarding factors expressed by macrophages, some MHCII positive cells were observed in the superficial layer of the endometrium of pregnant animals during the pre-implantation stage (**Figure 2A**), with a similar localization pattern observed for CD86 (**Figure 2B**). Likewise, CD206-positive signals were observed in macrophages mainly localized in superficial endometrial layers during pre-implantation (E+, **Figure 2C**). However, their localization appeared to change in subsequent stages of pregnancy, as cells expressing CD206 could be found scattered throughout the different layers of the endometrium and around deep uterine glands during implantation (**Figure 2D**) and in Post-Imp samples (**Figure 2E**). Isolated CD206-positive cells could also be identified in the myometrium in the different pregnancy stages (represented on **Figure 2E**). As for CD163, sporadic positive cells were observed in the superficial layer of the endometrium in pre-implantation (E+, **Figure 2F**) and Imp (**Figure 2G**) samples, while single cells identified as macrophages were present in the deep layers of the endometrium during post-implantation (**Figure 2H**). The differentiation between CD4-positive lymphocytes (MHCII-negative) and macrophages (MHCII-positive) was based on cell morphology and staining of consecutive slides against CD4 and MHCII (**Figures 2I,J**). CD4-positive lymphocytes were observed within the connective tissue in the superficial layer during the pre-implantation stage (**Figures 2I,K**). Additionally, scarce cells staining positive to CD8 could also be found in the same region of the endometrium (**Figure 2L**). At the time of implantation, lymphocytes expressing CD4 were mainly localized in the superficial layer of the endometrium (**Figure 2M**, top panel), with some being localized within blood vessels (**Figure 2M**, bottom panel). Moreover, staining against NKp46 was observed in numerous cells localized mainly at the surface layer of the endometrium and around blood vessels in pre-implantation (E+) and Imp samples (**Figures 2N,O**). However, during the post-implantation stage, NK cells were observed not only around superficial uterine glands (**Figure 2P**, left panel), but also around deep uterine glands (**Figure 2P**, right panel).

Cytokines and Other Immune Regulators

To further characterize the immune milieu during the early stages of canine pregnancy, the expression of different cytokines was evaluated, including members of the TGF and TNF families, chemokines, and their receptors (**Figure 3**). The presence of the embryo and/or establishment of pregnancy were related to changes in the expression of *IL1β* ($P < 0.0001$), *IL6* ($P < 0.0001$), *IL8* ($P < 0.0001$), *IL10* ($P < 0.01$), *IL12a* ($P < 0.05$), *TNFR1* ($P < 0.05$), *CCL3* ($P < 0.01$), and *CCR7* ($P < 0.01$). In contrast, *TGFβ* (**Figure 3F**), *TNFα* (**Figure 3G**), and *TNFR1* (**Figure 3I**) were not significantly affected ($P > 0.05$) by time in any of the analyzed groups. Furthermore, although no significant changes in the expression of *CCL13* were observed between the E–, E+, and Post-Imp groups ($P > 0.05$), its expression was apparently strongly suppressed at the time of implantation, being below detection limits in several samples (**Figure 3K**). The exposure of the uterus to embryos (E+) was associated with increased expression of *IL6* ($P < 0.05$, **Figure 3B**) and *CCR7* ($P < 0.05$, **Figure 3L**), when compared with E– samples, while the availability of *CCL3* transcripts was significantly lower in E+ ($P < 0.05$) and Post-Imp samples ($P < 0.01$, **Figure 3J**). Implantation was associated with the highest availability of *IL12a* ($P < 0.01$, **Figure 3E**), whereas its abundance was severely affected in the Post-Imp stage as it could not be detected in several samples (**Figure 3E**). This was different from what was observed for *IL1β* and *IL6* transcripts. Their strongly increased expression was observed during early placentation compared with the Imp stage ($P < 0.001$, **Figures 3A,B**, respectively). In contrast, early pregnancy was characterized by diminishing *IL8* levels, decreasing continuously following the onset of pregnancy, during implantation (Imp) and early placental development (Post-Imp) ($P < 0.01$, **Figure 3C**). Similar effects were observed for *IL10*, which was significantly reduced following the attachment of embryos and Post-Imp ($P < 0.05$, **Figure 3D**). Finally, *TNFR1* was downregulated during the progression of early pregnancy, being significantly lower in Post-Imp ($P < 0.05$, **Figure 3H**) compared with pre-implantation (E+) samples. As for *CCR7*, following its upregulated levels induced by embryo presence, its uterine levels were significantly suppressed during implantation ($P < 0.05$, **Figure 3L**).

In addition to cytokines, the presence of other factors involved in the uterine response to early pregnancy was assessed (*TLR4*, *IDO1*, and *AIF1*, **Figures 4A–C**). Stage- or embryo-dependent effects were observed in all three factors: $P < 0.01$ for *TLR4*, and $P < 0.05$ for *IDO1* and *AIF1*. The mRNA availability of *TLR4* decreased dramatically and was the lowest post-implantation, when compared with all earlier stages ($P < 0.05$, **Figure 4A**). In contrast, *IDO1* and *AIF1* responded positively to the presence of free-floating embryos ($P < 0.05$, **Figures 4B,C**); their expression

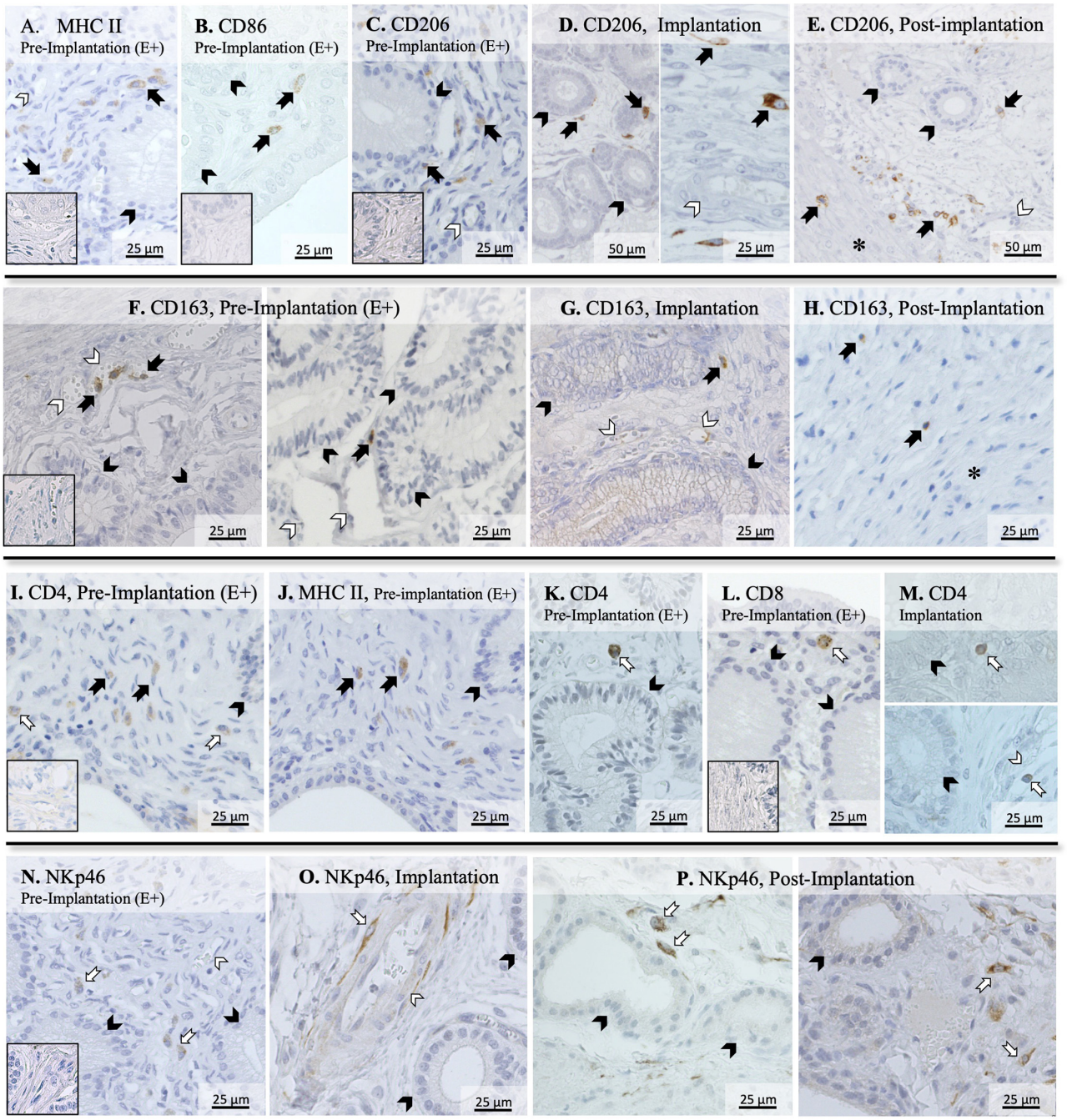

FIGURE 2 | Immunolocalization of selected markers of macrophages and lymphocytes in the canine uterus. Immunohistochemical detection of MHCII, CD86, CD206, CD163, CD4, CD8, and NKp46 (encoded by *NCR1*) at selected stages during early pregnancy. MHCII **(A)** and CD86 **(B)** were localized in individual macrophages distributed in the superficial layer of the endometrium during pre-implantation. **(C–E)** CD206 signals were observed in macrophages localized in the superficial layer of the endometrium during pre-implantation, around uterine glands **(C)**. At the time of implantation, CD206-positive macrophages were present around uterine glands **(D**, left panel**)**, and scattered in the endometrium during implantation **(D**, right panel**)**, and post-implantation period **(E)**. Isolated cells could also be identified in the myometrium in Post-Imp samples **(E)**. **(F–H)** CD163 was expressed by macrophages detected in the superficial layer of the endometrium during pre-implantation **(F)** and implantation **(G)**. At post-implantation, single CD163-positive macrophages were localized in deep layers of the endometrium, close to the myometrium **(H)**. To differentiate CD4-expressing macrophages ($MHCII^{+}$) and lymphocytes ($MHCII^{-}$), consecutive slides were stained against CD4 **(I)** and MHCII **(J)**. Both CD4 **(K)** and CD8-positive lymphocytes **(L)** were localized in the superficial layer of the endometrium during pre-implantation. During implantation **(M)**, individual $CD4^{+}$ lymphocytes were identified in endometrial superficial layer (top panel) and within blood vessels (bottom panel). Nkp46 (NK cells) were localized in the superficial layer of the endometrium **(N)** and around blood vessels **(O)** during pre-implantation and implantation stages. In samples from post-implantation stage **(P)**, NK cells were identified around superficial (left panel) and deep uterine glands (right panel). (solid arrow = macrophages; open arrow = lymphocytes; closed arrowhead = uterine gland; open arrowhead = blood vessel; asterisk = myometrium). No staining was observed in the isotype controls [inset in **(A–C,F,I,L,N)**].

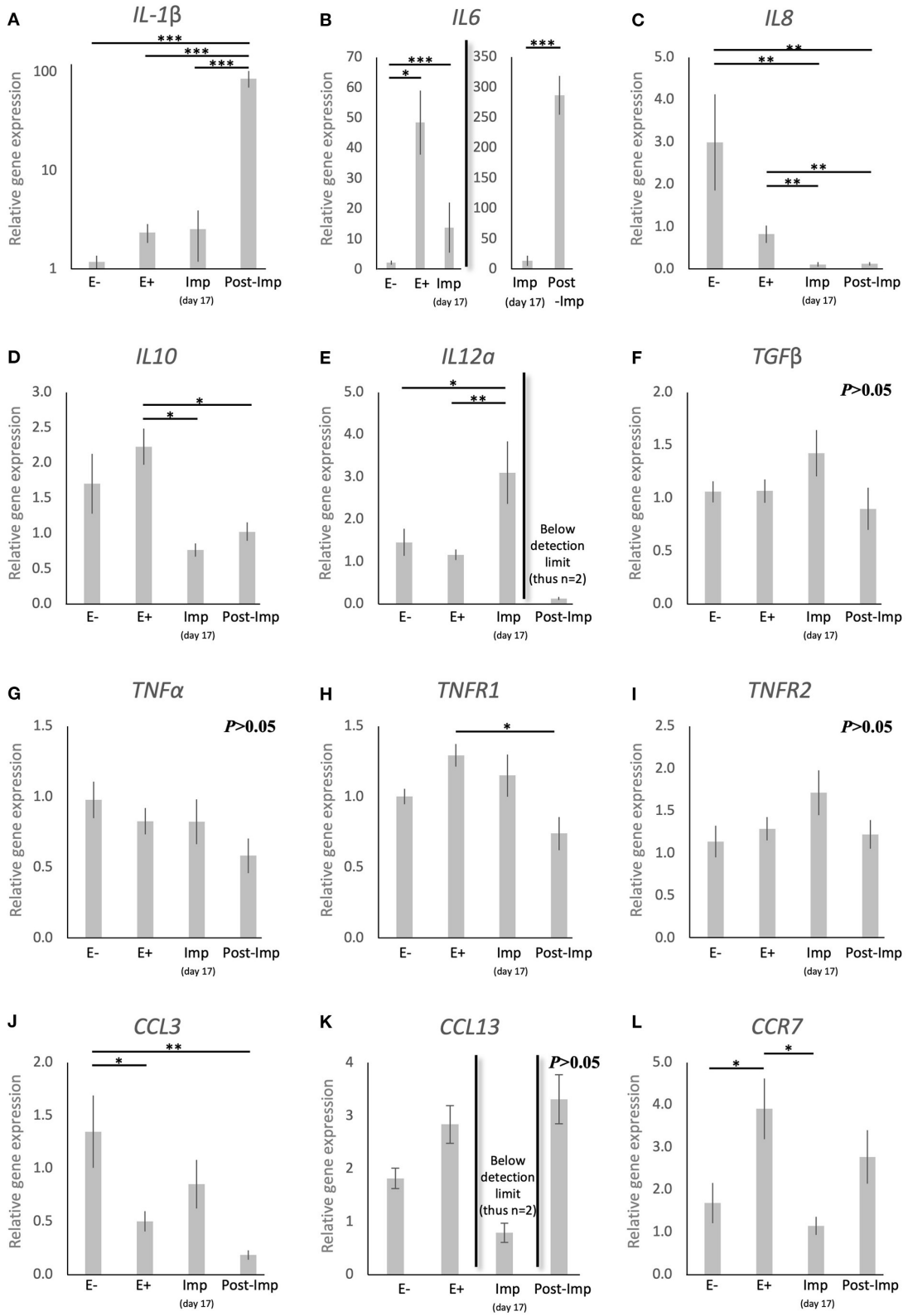

FIGURE 3 | Relative gene expression of selected cytokines in the canine uterus. **(A–L)** Relative gene expression as determined by semi-quantitative real time (TaqMan) PCR (mean ± SEM). One-way ANOVA was applied, revealing: $P < 0.0001$ for *IL1β*, $P < 0.0001$ for *IL6*, $P < 0.0001$ for *IL8*, $P = 0.01$ for *IL10*, $P = 0.02$ for *IL12a*, $P = 0.16$ for *TGFβ*, $P = 0.19$ for *TNFα*, $P = 0.02$ for *TNFR1*, $P = 0.19$ for *TNFR2*, $P = 0.006$ for *CCL3*, $P = 0.083$ for *CCL13* and $P = 0.01$ for *CCR7*. In the case of $P < 0.05$, this was followed by a Tukey-Kramer multiple comparisons post-test. Bars with asterisks differ at: $^{*}P < 0.05$, $^{**}P < 0.01$, $^{***}P < 0.001$.

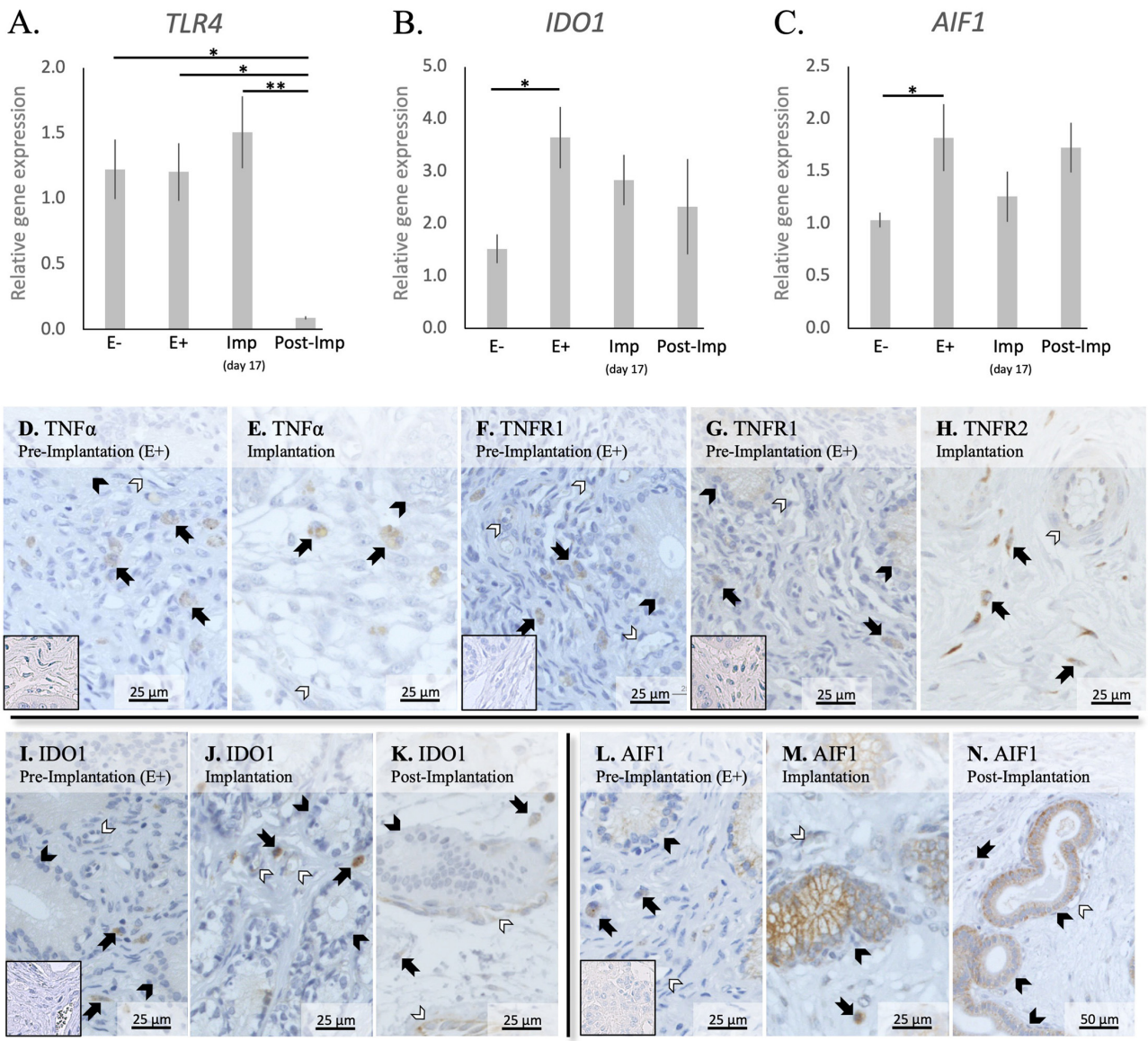

FIGURE 4 | Relative gene expression and localization of TLR4, IDO1 and AIF1 in the canine uterus. **(A–C)** Relative gene expression as determined by semi-quantitative real time (TaqMan) PCR (mean ± SEM). One-way ANOVA was applied to test the variation among the investigated groups, revealing: $P = 0.0033$ for *TLR4*, $P = 0.03$ for *IDO1*, and $P = 0.04$ for *AIF1*. In the case of $P < 0.05$, this was followed by Tukey-Kramer multiple comparisons post-test. Bars with asterisks differ at: $^{*}P < 0.05$, $^{**}P < 0.01$. **(D–M)** Immunohistochemical localization of members of the TNF-system, IDO1, and AIF1 in the canine uterus at selected stages of early pregnancy. Signals of TNFα were present in macrophages during the pre-implantation **(D)** and implantation **(E)** periods. Similarly, both TNFR1 **(F)** and TNFR2 **(G,H)** were present in macrophages. In addition, weaker signals for both receptors were also observed in epithelial cells of uterine glands during pre-implantation **(F,G)** and in endothelial cells **(F,H)**. Positive signals of IDO1 were detected in macrophages between superficial glands during pre-implantation **(I)** and were also detected in endothelial cells at the time of implantation **(J)**. At post implantation, weaker signals were observed in macrophages localized in deep endometrium layers, as well as in endothelial cells **(K)**. AIF1 positive signals were identified in macrophages close to superficial uterine glands in pre-implantation **(L)** and implantation **(M)** stages, while at post-implantation they were localized in the deep layer of the endometrium **(N)**. Some weak signals were also observed in uterine glands at the pre-implantation period **(L)**, while apparently stronger signals were observed in the same glands at implantation **(M)** and post-implantation **(N)**. Weak positive signals were also detected in endothelial cells **(M, N)** (solid arrow = macrophages; closed arrowhead = uterine gland; open arrowhead = blood vessel). No staining is observed in the isotype controls [inset in **(D,F,G,I,L)**].

was, however, not further affected during the establishment of early pregnancy ($P > 0.05$).

The localization of different factors involved in immune regulation, i.e., members from the TNF-system, IDO1 and AIF1, was further evaluated (**Figures 4D–N**). TNFα-positive signals were observed in cells identified as macrophages in the superficial layer of the endometrium in pre-implantation (E+) and Imp samples (**Figures 4D,E**), with some rare cells being localized in the myometrium (not shown). As for its receptors, positive signals for TNFR1 could be identified in immune cells localized

around superficial glands, with weaker signals also being visible in endothelial cells and glandular epithelial cells (**Figure 4F**). Regarding TNFR2, immune cells also presented positive signals in E+ and Imp samples (**Figures 4G,H**). However, only at the time of implantation could positive staining of the endothelium be observed (**Figure 4H**). Positive signals of IDO1 could be found during the pre-implantation phase in macrophages localized close to the luminal surface of the endometrium (**Figure 4I**). At the time of implantation, additional signals for IDO1 were present in some single cells localized within the myometrium (not shown) as well as, to a lesser extent, in endothelial cells (**Figure 4J**). Despite a similar localization pattern in Post-Imp samples, with IDO1 signals being present in macrophages and endothelial cells, positive signals appeared to be weaker at this stage and macrophages were mainly localized around deep uterine glands (**Figure 4K**) and within the connective tissue of the myometrium (not shown). As for AIF1, positive signals during pre-implantation were observed in macrophages localized close to superficial uterine glands and in the epithelial cells of these glands (**Figure 4L**). At the time of implantation, positive signals in glandular epithelium appeared stronger than in pre-implantation (**Figure 4M**). In addition, a low number of positively stained macrophages was still observed around the superficial glands and some weaker signals were detected in endothelial cells (**Figure 4M**). Finally, in Post-Imp samples, weak signals were observed in macrophages around deep glands (**Figure 4N**), with positive staining also detected in the epithelium of these deep glands and in endothelial cells (**Figure 4N**).

IGFs and Markers of Tissue Remodeling

The uterine expression of selected factors acting as growth factors or involved in tissue remodeling was evaluated (**Figure 5**). Time-dependent effects were observed in the expression of *IGF1* ($P < 0.001$), *IGF2* ($P < 0.01$), *ENG* ($P < 0.0001$), *CDH1* ($P < 0.001$), *ECM2* ($P < 0.0001$), and *MMP2* ($P < 0.05$). These were related predominantly to the stages of pregnancy as none of these factors were significantly modulated in response to the presence or absence of an embryo between days 8–12 (E– vs. E+). Interestingly, following the significant induction of *ENG* and *CDH1* in response to embryo attachment (E+ vs. Imp, $P < 0.05$ and $P < 0.001$, respectively; **Figures 5C,D**), the expression of all factors was significantly reduced after initiation of invasion and placentation (Post-Imp) ($P < 0.05$, **Figures 5A–F**).

DISCUSSION

Considering the importance of the immune system in conceptus-maternal communication during the establishment of pregnancy, highlighted in several species, the lack of knowledge regarding the dog is striking. This relates not only to the characterization of local immune signaling, but also to the absence of information regarding the immune cell population present in the uterus during pregnancy. Here, by investigating the expression and/or localization of selected markers in the dog uterus, we aimed to determine the presence of different subsets of macrophages and T lymphocytes known to play a role in the establishment of pregnancy in other species. The evaluation of the expression of different cytokines and growth factors was aimed at further characterization of the uterine immune milieu, addressing the functional dynamics between the implanting conceptus and maternal structures.

The differentiation between subsets of macrophages and lymphocytes presents several challenges, with different phenotypes expressing similar surface markers. Thus, the selection of a range of factors, as presented in **Table 3**, is required for such differentiation. Macrophages can polarize into M1 (classical activation, involved in the pro-inflammatory Th1 response) and M2 (alternative activation) phenotypes, with the latter presenting M2a (involved in the Th2 immune response), M2b (involved in pro-inflammatory responses and immune regulation), or M2c (tissue repair/remodeling) characteristics (6, 32–35). Both CD86 and MHCII are expressed in M1 and M2b macrophages, although the latter have a lower expression of MHCII (32, 33). Thus, while the evaluation of CD86 gene expression would not have been useful in validating the presence of each of these two different phenotypes, the immunohistochemical detection of MHCII allowed their differentiation. Furthermore, the expression of CD206 and CD163 was also investigated targeting the evaluation of macrophages with M2a and M2c functions (32). With regard to lymphocytes, the expression of CD8 by cytotoxic T cells is widely recognized, while NK cells can be identified by their production of NKp46 (encoded by NCR1) (36). Furthermore, both activated helper (Th) and regulatory (Treg) T cells phenotypes express CD4 and CD25 (37–40). Thus, the detection of FoxP3, a specific marker of Treg cells, was further required for differentiation among these cell populations (40). The evaluation of several immune factors that can be associated with different immune cell subsets (e.g., the expression of TLR4 and CCR7 by M1 macrophages) further substantiated the present analysis.

In agreement with previous findings (14, 17, 18), the presence of the embryo was associated with the modulation of the uterine immune milieu during the pre-implantation period (E+). Among the factors evaluated, the expression of *MHCII*, *CD4*, *CD25,* and *NCR1* was upregulated, while lower expression of *FoxP3* was observed. MHCII, which is essential for antigen recognition by T cells, is expressed in a wide variety of antigen presenting cells, including macrophages, monocytes, and dendritic cells. Its expression in other endometrial cells, like epithelial and stromal cells, has been reported in some species, e.g., in humans and rodents (41, 42), but in the present study positive signals were restricted to macrophages localized within the endometrial stroma. Interestingly, these MHCII-positive signals were colocalized with the cellular distribution of CD86-positive cells, suggesting that the increased expression of *MHCII* in the pre-implantation period, in contrast to E- and Post-Imp, appears to be associated with an increased infiltration of macrophages with M1 characteristics. As for lymphocytes, the increased expression of *NCR1*, a specific marker of NK cells, suggests an increased infiltration of these cells in response to the presence of the embryos. The potential importance of NK cells during early pregnancy will be addressed below.

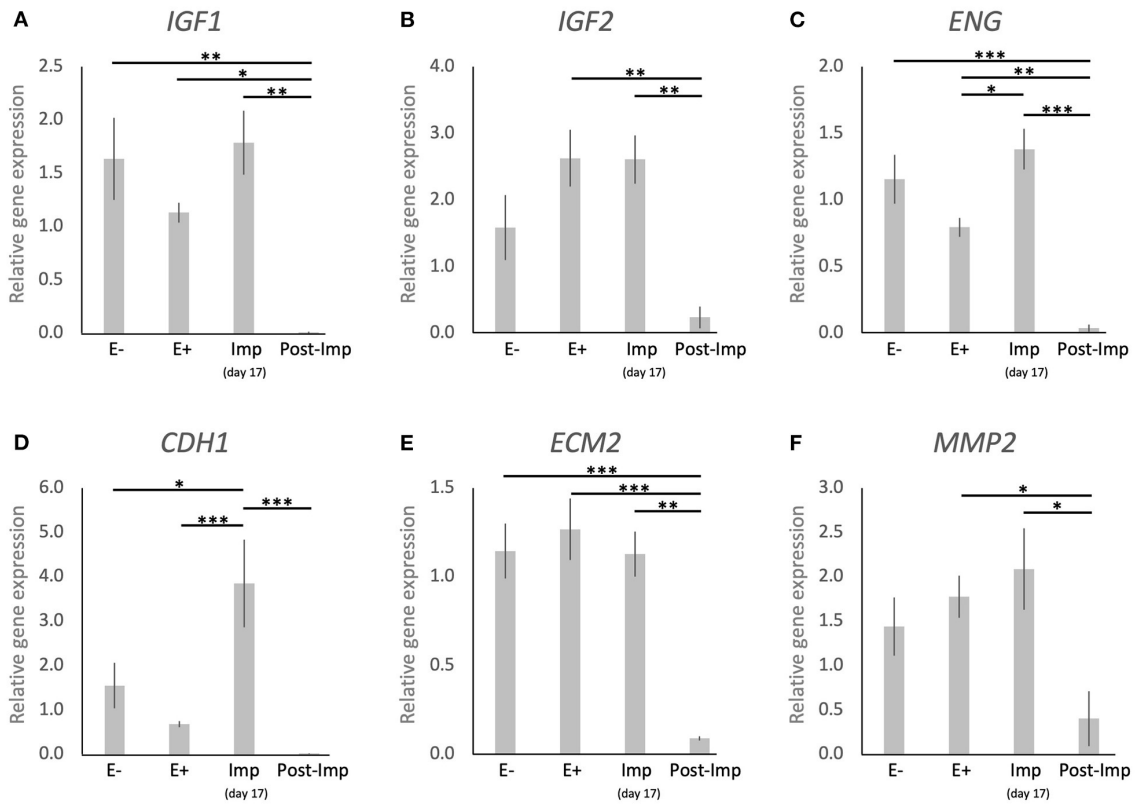

FIGURE 5 | Relative gene expression of selected factors involved in tissue remodeling in the canine uterus. **(A–F)** Relative gene expression as determined by semi-quantitative real time (TaqMan) PCR (mean ± SEM). One-way ANOVA was applied, revealing: $P = 0.0007$ for *IGF1*, $P = 0.0032$ for *IGF2*, $P < 0.0001$ for *ENG*, $P = 0.0002$ for *CDH1*, $P < 0.0001$ for *ECM2*, $P = 0.0174$ for *MM2*. In the case of $P < 0.05$, this was followed by a Tukey-Kramer multiple comparisons post-test. Bars with asterisks differ at: $^{*}P < 0.05$, $^{**}P < 0.01$, $^{***}P < 0.001$.

Furthermore, the increased availability of *CD4* and *CD25*, accompanied by a decreased expression of *FoxP3*, a specific marker of Treg cells (40), appears to indicate an increased presence of Th cells in the uterus prior to implantation. This was further supported by the significantly higher expression of *CD4* than of the cytotoxic *CD8* (43). Even though the discrimination between Th subpopulations was not performed in the present work, the apparently concomitantly increased abundance of M1 and NK cell markers in the pre-implantation period suggests the presence of a dominant Th1 immunity in response to embryo presence. Pre-implantation was also marked by increased expression of the anti-inflammatory *IL10* and a decreased expression of the chemoattractant *CCL3*. Adding to our observation of a lower expression of *CD8* than *CD4*, this might be related to the presence of local immunomodulatory signals involved in the immunotolerance toward the embryo. Moreover, the canine embryo could be also involved in modulating the uterine immune response through the expression of factors like prostaglandin synthase 2 (PTGS2/COX2), PGE2 synthase (PTGES), and IGFs, as shown previously (15). In particular, PGE2 appears to be of importance for modulating the uterine immune milieu by being associated with suppression of cytotoxic activities of local immune cells [reviewed in (44)]. Furthermore, uterine-derived signals might also be involved in this immunomodulatory process. As also shown in our previous study, both *IDO1* and *AIF1* were upregulated in response to embryo presence (14). IDO1 plays a crucial role in prevention of immune-driven fetal rejection in the mouse (45). By controlling tryptophan degradation, this enzyme regulates leukocyte activation and is involved in a plethora of immunomodulatory mechanisms, i.e., decreasing NK cells cytotoxic activity, promoting Treg cell activation while inhibiting the functions of other T cell subsets and promoting the conversion of M1 macrophages to the M2 phenotype (46–49). In contrast, the role of AIF1 in the uterus is still poorly understood, but it has been associated not only with immunomodulatory processes, but also with proliferative and vascular mechanisms in several systems (50–53). Thus, IDO1 and AIF1 might be involved in the modulation of immune response in the pre-implantation period. In addition to both factors being localized in macrophages, IDO1 positive signals were also present in the endometrial endothelium during implantation and AIF1 expression was observed in epithelial glandular cells. Based on this, the modulation of the inflammatory signaling observed in the pre-implantation period appears to involve different uterine cell populations.

In contrast with the pre-implantation period, *MHCII* and *TLR4* were strongly downregulated during early placentation. Similarly, *CCR7* together with *CD4* were suppressed toward implantation and early placentation, cumulatively suggesting a decrease in M1 activity. This decrease in M1 activity following the establishment of pregnancy appears to reflect the situation described previously for other species, like the human and cow, where a shift between M1 and M2 activity is observed following placentation (6, 54). In humans, the decrease in M1 activity appears to be crucial for the maintenance of pregnancy, as the imbalance in the M1/M2 macrophage population is associated with an inadequate remodeling of uterine vascularization and spontaneous abortion [reviewed in (6, 38)]. Following this line, in the dog, implantation and, thus, early decidualization, was also marked by upregulated expression of *FoxP3*. This suggests an increased activity of the immunosuppressive Treg cells, even more strongly implying the functional transition from a proinflammatory to a modulatory immune reaction to embryo presence, attachment, and the ongoing morpho-functional remodeling of the uterus. While the full understanding of the role of Treg in the uterus is still missing, a decreased number of these cells is associated with recurrent abortions and preeclampsia in humans, and their depletion in mice leads to pregnancy loss (38, 39, 55). Thus, the presence of immunosuppressive Treg cells appears to be crucial in embryo-maternal contact and could also apply to canine reproduction. With regard to the regulation of this immune population, PGE2 increases the expression of FoxP3 in human peripheral CD4+CD25+ mononuclear cells (56). Thus, by expressing PTGES (15), the implanting canine embryo might be responsible for a local increase of PGE2 that could be involved in this increased presence of Treg cells. Furthermore, IL12a is described as being upregulated in actively suppressing Treg cells (57, 58), while IL6 can inhibit Treg cell activity and FoxP3 expression (59). Thus, considering that *IL12a* presented its highest expression during implantation, while *IL6* was downregulated, it appears plausible that these interleukins might be involved in the regulation of Treg cell presence in the uterus at the time of implantation. Furthermore, besides modulating Treg activity, IL12a is also involved in the activation of NK cells (60, 61). As mentioned elsewhere, these cells play a key role in the development of the decidua in humans and mice, mainly by modulating blood vessel development (7, 8). Following the increased expression of *NCR1* observed here in the pre-implantation and implantation periods, there appears to be an increased number of NK cells in the uterus during the establishment of canine pregnancy. Furthermore, the localization of NK cells close to uterine blood vessels in the superficial layer of the endometrium during pre-implantation and implantation might also suggest the involvement of this population in the modulation of uterine vascularization and decidualization as described in other species presenting decidua (7, 8). However, this hypothesis still needs to be verified for the dog.

Regarding the factors involved in uterine remodeling, *ENG* and *CDH1* became upregulated at the time of implantation compared with their expression in the pre-implantation uterus. ENG acts as a TGFβ receptor and, in the murine uterus, is associated with uterine receptivity for the implanting embryo (62). CDH1, that encodes for E-cadherin, is an important factor in cell adhesion and is involved in the functional modulation of endometrial morphology and implantation in several species [reviewed in (63)]. Thus, the increased expression of these factors implies their involvement in the canine implantation process.

Finally, the post-implantation period was marked by decreased availability of markers of M1 (*MHCII*, *TLR4*) and M2a (*CD206*, *IL10*) macrophages, T cells (*CD4*), NK cells (*NCR1*), and an apparent decrease of the marker of Treg cells *FoxP3*, in addition to other cytokines (*IL8*, *IL12a*, *TNFR1*). Although the quantification of immune cells in the uterus was not within the scope of the present work, these expression patterns suggest a decreased immune activity in the uterus during this period, despite the significantly increased expression of the pro-inflammatory *IL1β*. We found it interesting that the localization of CD206, CD163, and NKp46 positive cells was predominantly associated with the superficial uterine compartments during pre-implantation, contrasting with their increased presence in deeper endometrial layers following early placentation, i.e., during the post-implantation stage. It appears that not only the composition of the uterine immune population is affected with the progression of pregnancy, but also its localization in the uterus appears to change. These effects imply the presence of immunosuppressive signals possibly required to allow the invasion of the trophoblast during the placentation process. Furthermore, the expression of growth factors (*IGF1*, *IGF2*) and markers of tissue remodeling (*ENG*, *CDH1*, *ECM2,* and *MMP2)* was decreased during the post-implantation stage, at the time where the development of the placenta is accompanied by significant tissue remodeling. Nevertheless, considering that the samples analyzed in this study were derived from implantation sites, the decreased expression of factors involved in tissue growth and remodeling might actually reflect the proteolytic activity of the trophoblast over the endometrium during invasion.

Conclusions

The evaluation of several immune cell-specific markers and other immune factors provided new insights into the uterine immunological status and possible functional dynamics during the early stages of canine gestation (summarized in **Figure 6**). The presence of the embryo clearly modulated the uterine milieu, inducing a controlled pro-inflammatory signaling in the pre-implantation period. This early stage appears to be under the influence of Th cells, that prevail over cytotoxic lymphocytes, accompanied by an increased presence of macrophages with proinflammatory M1 characteristics. Furthermore, the increased presence of NK cells during the pre-implantation and implantation periods suggests the involvement of this population in endometrial remodeling. Interestingly, Treg cells appear to have an important role at the time of implantation, probably being involved in the suppression of immune responses toward the invading embryo. To which extent the immune system-derived factors contribute to the concomitantly occurring

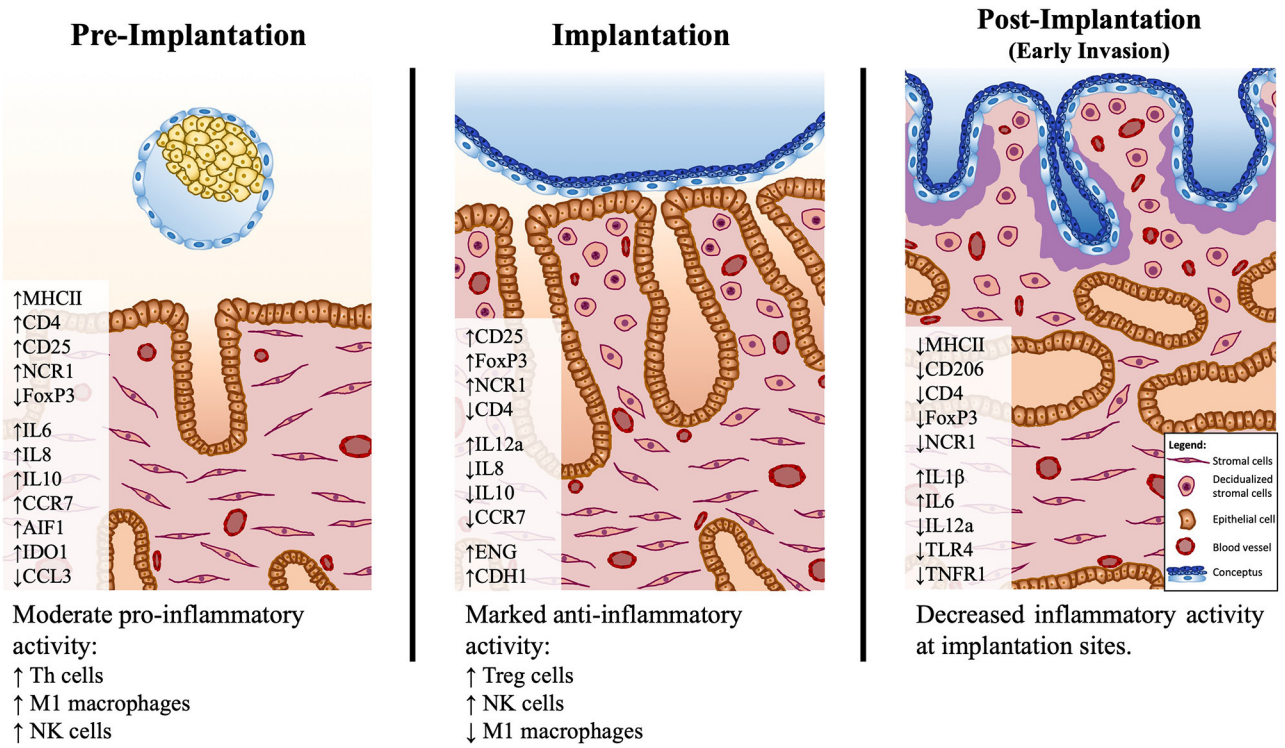

FIGURE 6 | Schematic presentation of the proposed model of immune system–mediated events in the canine uterus during establishment of pregnancy. Arrows (↑ and ↓) indicate increased or decreased expression, respectively, of different selected factors during establishment of pregnancy: pre-implantation (days 10–12), implantation (day 17 of embryonal life), and post-implantation (day 25 of pregnancy). The presence of the free-floating embryo during pre-implantation is associated with increased inflammatory activity, marked by upregulated expression of markers of M1 macrophages (*MHCII*) and Th lymphocytes (*CD4*, *CD25*). This reaction appears to be moderated by the increased expression of immunomodulatory factors like *IDO1*, *AIF1*, and *IL10*. There is a shift in the immune milieu at the time of implantation, with decreased transcripts of *MHCII* and increased transcripts of Treg markers (*FoxP3*). Both pre-implantation and implantation stages show increased expression of the NK cell marker *NCR1*. During implantation, concomitantly, the first morphological signs of decidualization are observed in subepithelial endometrial layers. The contribution of the immune system-derived factors to the decidualization process needs further clarification. In the post-implantation period, the expression of several factors investigated is decreased at the implantation sites, indicating a decreased local immune activity in response to embryo invasion.

canine-specific decidualization, remains to be investigated. Post-implantation proteolytic activity of the early invading trophoblast at implantation sites appears to be associated with locally decreased immune activity accompanied by lowered expression of IGFs and factors involved in tissue remodeling. In the modulation of immune responses, local factors like IDO1 and AIF1, derived from different uterine cellular components, and embryo-derived factors like PGE2 might be involved. Still to be considered is the species-specific uterine exposure to high circulating P4 levels. The immunosuppressive properties of P4 have been described in several mammals, including humans and rodents [reviewed in (64)]. Thus, the potential role of P4 in modulating local uterine immune responses in the dog appears plausible and should be taken into consideration in future research. Finally, the increased presence of NK and Treg cells in the pre-implantation and/or implantation stages implies similarities between the canine uterine immune milieu and the situation observed in humans and rodents [reviewed in (7, 8, 39)]. In fact, in our previous microarray paper, a higher correlation of embryo-induced effects in the uterus was observed between the dog and humans than with other domestic mammals (14). Such similarities appear to be further linked to the preparation of the uterus for the formation of the decidua and, possibly, also for the placentation. However, despite sharing the common reproductive goals of avoiding embryo rejection and successful implantation, and taking into account the restricted (shallow) invasion of the trophoblast during the formation of the canine endotheliochorial placenta, there may be species-specific regulatory features related to the local immune response in the dog.

DATA AVAILABILITY STATEMENT

The raw data supporting the conclusions of this article will be made available by the authors, without undue reservation.

ETHICS STATEMENT

The animal study was reviewed and approved by Justus-Liebig University Giessen, Germany (permits no. II 25.3-19c20-15c GI 18/14 and VIG3-19c-20/15 GI 18,14); University of Ankara, Turkey (permits no. Ankara 2006/06 and 2008-25-124).

Written informed consent was obtained from the owners for the participation of their animals in this study.

AUTHOR CONTRIBUTIONS

MTP and RN were involved in developing the concept of the present study, experimental design, generating data, analysis and interpretation of data, and drafting of the manuscript. RP-C, SM, SA, and DK were involved in the collection of tissue material, knowledge transfer, critical discussion and interpretation of data, and revision of the manuscript. MPK designed and supervised the project, and was involved in interpretation of the data, and drafting and revision of the manuscript. All authors read and approved the final manuscript.

FUNDING

The present work was supported by the Swiss National Science Foundation (SNSF) research grant number 31003A_182481.

ACKNOWLEDGMENTS

Authors were thankful to Dr. Sharon Mortimer for the careful editing of the manuscript. The technical expertise and contributions of Elisabeth Högger and Ricardo Fernandez Rubia are greatly appreciated. Part of the laboratory work was performed using the logistics at the Center for Clinical Studies, Vetsuisse Faculty, University of Zurich.

REFERENCES

1. Rodriguez Garcia M, Patel MV, Shen Z, Fahey JV, Biswas N, Mestecky J, et al. Mucosal Immunity in the Human Female Reproductive Tract. *Mucosal Immunol*. (2015) 2:2097–124. doi: 10.1016/B978-0-12-415847-4.00108-7
2. Turner ML, Healey GD, Sheldon IM. Immunity and inflammation in the uterus. *Reprod. Domest Anim*. (2012) 47(Suppl. 4):402–9. doi: 10.1111/j.1439-0531.2012.02104.x
3. Mold JE, McCune JM. Immunological tolerance during fetal development: from mouse to man. *Adv. Immunol*. (2012) 115:73–111. doi: 10.1016/B978-0-12-394299-9.00003-5
4. Robertson SA. Control of the immunological environment of the uterus. *Rev. Reprod*. (2000) 5:164–74. doi: 10.1530/revreprod/5.3.164
5. Bulmer JN, Longfellow M, Ritson A. Leukocytes and resident blood cells in endometrium. *Ann. N. Y. Acad. Sci*. (1991) 622:57–68. doi: 10.1111/j.1749-6632.1991.tb37850.x
6. Brown MB, von Chamier M, Allam AB, Reyes L. M1/M2 macrophage polarity in normal and complicated pregnancy. *Front. Immunol*. (2014) 5:606. doi: 10.3389/fimmu.2014.00606
7. Erlebacher A. Immunology of the maternal-fetal interface. *Annu. Rev. Immunol*. (2013) 31:387–411. doi: 10.1146/annurev-immunol-032712-100003
8. Gaynor LM, Colucci F. Uterine natural killer cells: functional distinctions and influence on pregnancy in humans and mice. *Front. Immunol*. (2017) 8:467. doi: 10.3389/fimmu.2017.00467
9. Kowalewski MP, Gram A, Kautz E, Graubner FR. The dog: nonconformist, not only in maternal recognition signaling. *Adv. Anat. Embryol. Cell Biol*. (2015) 216:215–37. doi: 10.1007/978-3-319-15856-3_11
10. Amoroso EC. Placentation. In: Parkes AS, editor. *Marshall's Physiology of Reproduction*. London: Longmans Greens and Co (1952).
11. Kehrer A. Zur Entwicklung und Ausbildung des Chorions der Placenta zonaria bei Katze, Hund und Fuchs. *Z. Anat. Entwicklungsgeschich*. (1973) 143:25–42. doi: 10.1007/BF00519908
12. Concannon PW, McCann JP, Temple M. Biology and endocrinology of ovulation, pregnancy and parturition in the dog. *J. Reprod. Fertil. Suppl*. (1989) 39:3–25.
13. Kowalewski MP, Tavares Pereira M, Kazemian A. Canine conceptus-maternal communication during maintenance and termination of pregnancy, including the role of species-specific decidualization. *Theriogenology*. (2020) 150:329–38. doi: 10.1016/j.theriogenology.2020.01.082
14. Graubner FR, Gram A, Kautz E, Bauersachs S, Aslan S, Agaoglu AR, et al. Uterine responses to early pre-attachment embryos in the domestic dog and comparisons with other domestic animal species. *Biol. Reprod*. (2017) 97:197–216. doi: 10.1093/biolre/iox063
15. Kautz E, Gram A, Aslan S, Ay SS, Selcuk M, Kanca H, et al. Expression of genes involved in the embryo-maternal interaction in the early-pregnant canine uterus. *Reproduction*. (2014) 147:703–17. doi: 10.1530/REP-13-0648
16. Schafer-Somi S, Sabitzer S, Klein D, Reinbacher E, Kanca H, Beceriklisoy HB, et al. Vascular endothelial (VEGF) and epithelial growth factor (EGF) as well as platelet-activating factor (PAF) and receptors are expressed in the early pregnant canine uterus. *Reprod. Domest. Anim*. (2013) 48:20–6. doi: 10.1111/j.1439-0531.2012.02019.x
17. Beceriklisoy HB, Schafer-Somi S, Kucukaslan I, Agaoglu R, Gultiken N, Ay SS, et al. Cytokines, growth factors and prostaglandin synthesis in the uterus of pregnant and non-pregnant bitches: the features of placental sites. *Reprod. Domest. Anim*. (2009) 44(Suppl 2):115–9. doi: 10.1111/j.1439-0531.2009.01443.x
18. Schafer-Somi S, Beceriklisoy HB, Budik S, Kanca H, Aksoy OA, Polat B, et al. Expression of genes in the canine pre-implantation uterus and embryo: implications for an active role of the embryo before and during invasion. *Reprod. Domest. Anim*. (2008) 43:656–63. doi: 10.1111/j.1439-0531.2007.00966.x
19. Schafer-Somi S, Klein D, Beceriklisoy HB, Sabitzer S, Ay SS, Agaoglu AR, et al. Uterine progesterone receptor and leukaemia inhibitory factor mRNA expression in canine pregnancy. *Reprod. Domest. Anim*. (2009) 44(Suppl. 2):109–14. doi: 10.1111/j.1439-0531.2009.01390.x
20. Pires MA, Payan-Carreira R. Resident macrophages and lymphocytes in the canine endometrium. *Reprod. Domest. Anim*. (2015) 50:740–9. doi: 10.1111/rda.12567
21. Kowalewski MP, Beceriklisoy HB, Pfarrer C, Aslan S, Kindahl H, Kucukaslan I, et al. Canine placenta: a source of prepartal prostaglandins during normal and antiprogestin-induced parturition. *Reproduction*. (2010) 139:655–64. doi: 10.1530/REP-09-0140
22. Graubner FR, Reichler IM, Rahman NA, Payan-Carreira R, Boos A, Kowalewski MP. Decidualization of the canine uterus: from early until late gestational *in vivo* morphological observations, and functional characterization of immortalized canine uterine stromal cell lines. *Reprod. Domest. Anim*. (2017) 52(Suppl 2):137–47. doi: 10.1111/rda.12849
23. Kowalewski MP, Beceriklisoy HB, Aslan S, Agaoglu AR, Hoffmann B. Time related changes in luteal prostaglandin synthesis and steroidogenic capacity during pregnancy, normal and antiprogestin induced luteolysis in the bitch. *Anim. Reprod. Sci*. (2009) 116:129-38. doi: 10.1016/j.anireprosci.2008.12.011
24. Hoffmann B, Kyrein HJ, Ender ML. An efficient procedure for the determination of progesterone by radioimmunoassay applied to bovine peripheral plasma. *Horm. Res*. (1973) 4:302–10. doi: 10.1159/000178317
25. Tavares Pereira M, Gram A, Nowaczyk RM, Boos A, Hoffmann B, Janowski T, et al. Prostaglandin-mediated effects in early canine corpus luteum: *in vivo* effects on vascular and immune factors. *Reprod. Biol*. (2019) 10:100–11. doi: 10.1016/j.repbio.2019.02.001
26. Kowalewski MP, Meyer A, Hoffmann B, Aslan S, Boos A. Expression and functional implications of peroxisome proliferator-activated receptor gamma (PPARgamma) in canine reproductive tissues during normal pregnancy and parturition and at antiprogestin induced abortion. *Theriogenology*. (2011) 75:877–86. doi: 10.1016/j.theriogenology.2010.10.030
27. Kowalewski MP, Schuler G, Taubert A, Engel E, Hoffmann B. Expression of cyclooxygenase 1 and 2 in the canine corpus luteum during diestrus. *Theriogenology*. (2006) 66:1423–30. doi: 10.1016/j.theriogenology.2006.01.039

28. Xie F, Xiao P, Chen D, Xu L, Zhang B. miRDeepFinder: a miRNA analysis tool for deep sequencing of plant small RNAs. *Plant Mol. Biol.* (2012) 80:75–84. doi: 10.1007/s11103-012-9885-2
29. Gram A, Fox B, Buchler U, Boos A, Hoffmann B, Kowalewski MP. Canine placental prostaglandin E2 synthase: expression, localization, and biological functions in providing substrates for prepartum PGF2alpha synthesis. *Biol. Reprod.* (2014) 91:154. doi: 10.1095/biolreprod.114.122929
30. Ross M, Pawlina W. *Histology, A Text and Atlas with Correlated Cell and Molecular Biology*. 6th ed. Philadelphia, PA: Lippincott Williams & Wilkins (2011).
31. Liebich H. *Funktionelle Histologie der Haussäugetiere und Vögel, Lehrbuch und Farbatlas für Studium und Praxis*. 5th ed. Stuttgart: Schattauer (2009). doi: 10.1055/b-005-148994
32. Roszer T. Understanding the mysterious M2 macrophage through activation markers and effector mechanisms. *Mediators Inflamm*. (2015) 2015:816460. doi: 10.1155/2015/816460
33. Mantovani A, Sica A, Sozzani S, Allavena P, Vecchi A, Locati M. The chemokine system in diverse forms of macrophage activation and polarization. *Trends Immunol.* (2004) 25:677–86. doi: 10.1016/j.it.2004.09.015
34. Mantovani A, Sozzani S, Locati M, Allavena P, Sica A. Macrophage polarization: tumor-associated macrophages as a paradigm for polarized M2 mononuclear phagocytes. *Trends Immunol.* (2002) 23:549–555. doi: 10.1016/S1471-4906(02)02302-5
35. Mills CD, Kincaid K, Alt JM, Heilman MJ, Hill AM. M-1/M-2 macrophages and the Th1/Th2 paradigm. *J. Immunol.* (2000) 164:6166–73. doi: 10.4049/jimmunol.164.12.6166
36. Montaldo E, Del Zotto G, Della Chiesa M, Mingari MC, Moretta A, De Maria A, et al. Human NK cell receptors/markers: a tool to analyze NK cell development, subsets and function. *Cytometry A*. (2013) 83:702–13. doi: 10.1002/cyto.a.22302
37. Nancy P, Erlebacher A. T cell behavior at the maternal-fetal interface. *Int. J. Dev. Biol.* (2014) 58:189-98. doi: 10.1387/ijdb.140054ae
38. Ruocco MG, Chaouat G, Florez L, Bensussan A, Klatzmann D. Regulatory T-cells in pregnancy: historical perspective, state of the art, and burning questions. *Front. Immunol.* (2014) 5:389. doi: 10.3389/fimmu.2014.00389
39. Aluvihare VR, Kallikourdis M, Betz AG. Regulatory T cells mediate maternal tolerance to the fetus. *Nat. Immunol.* (2004) 5:266–71. doi: 10.1038/ni1037
40. Hori S, Nomura T, Sakaguchi S. Control of regulatory T cell development by the transcription factor Foxp3. *Science*. (2003) 299:1057–61. doi: 10.1126/science.1079490
41. Wallace PK, Yeaman GR, Johnson K, Collins JE, Guyre PM, Wira CR. MHC class II expression and antigen presentation by human endometrial cells. *J. Steroid Biochem. Mol. Biol.* (2001) 76:203–11. doi: 10.1016/S0960-0760(00)00149-7
42. Wira CR, Rossol RM. Antigen-presenting cells in the female reproductive tract: influence of the estrous cycle on antigen presentation by uterine epithelial and stromal cells. *Endocrinology*. (1995) 136:4526–34. doi: 10.1210/endo.136.10.7664673
43. Zhang N, Bevan MJ. CD8(+) T cells: foot soldiers of the immune system. *Immunity*. (2011) 35:161–8. doi: 10.1016/j.immuni.2011.07.010
44. Kalinski P. Regulation of immune responses by prostaglandin E2. *J. Immunol.* (2012) 188:21–8. doi: 10.4049/jimmunol.1101029
45. Mellor AL, Munn DH. Tryptophan catabolism prevents maternal T cells from activating lethal anti-fetal immune responses. *J. Reprod. Immunol.* (2001) 52:5–13. doi: 10.1016/S0165-0378(01)00118-8
46. Munn DH, Shafizadeh E, Attwood JT, Bondarev I, Pashine A, Mellor AL. Inhibition of T cell proliferation by macrophage tryptophan catabolism. *J. Exp. Med.* (1999) 189:1363–72. doi: 10.1084/jem.189.9.1363
47. Croxatto D, Vacca P, Canegallo F, Conte R, Venturini PL, Moretta L, et al. Stromal cells from human decidua exert a strong inhibitory effect on NK cell function and dendritic cell differentiation. *PLoS ONE*. (2014) 9:e89006. doi: 10.1371/journal.pone.0089006
48. Wang XF, Wang HS, Wang H, Zhang F, Wang KF, Guo Q, et al. The role of indoleamine 2,3-dioxygenase (IDO) in immune tolerance: focus on macrophage polarization of THP-1 cells. *Cell Immunol.* (2014) 289:42–8. doi: 10.1016/j.cellimm.2014.02.005
49. Munn DH, Zhou M, Attwood JT, Bondarev I, Conway SJM, Brown C, et al. Prevention of allogeneic fetal rejection by tryptophan catabolism. *Science*. (1998) 281:1191–3. doi: 10.1126/science.281.5380.1191
50. Shimada S, Iwabuchi K, Watano K, Shimizu H, Yamada HM, Minakami H, Onoe K. Expression of allograft inflammatory factor-1 in mouse uterus and poly (I:C)-induced fetal resorption. *Am. J. Reprod. Immunol.* (2003) 50:104–12. doi: 10.1034/j.1600-0897.2003.00060.x
51. Tian Y, Jain S, Kelemen SE, Autieri MV. AIF-1 expression regulates endothelial cell activation, signal transduction, and vasculogenesis. *Am. J. Physiol. Cell Physiol.* (2009) 296:C256–66. doi: 10.1152/ajpcell.00325.2008
52. Jia J, Cai Y, Wang R, Zhao Y-F. Overexpression of allograft inflammatory factor-1 promotes the proliferation and migration of human endothelial cells (HUV-EC-C) probably by up-regulation of basic fibroblast growth factor. *Pediatr. Res.* (2010) 67:29–34. doi: 10.1203/PDR.0b013e3181bf572b
53. Zhao YY, Yan DJ, Chen ZW. Role of AIF-1 in the regulation of inflammatory activation and diverse disease processes. *Cell Immunol.* (2013) 284:75–83. doi: 10.1016/j.cellimm.2013.07.008
54. Oliveira LJ, McClellan S, Hansen PJ. Differentiation of the endometrial macrophage during pregnancy in the cow. *PLoS ONE*. (2010) 5:e13213. doi: 10.1371/journal.pone.0013213
55. Sasaki Y, Darmochwal-Kolarz D, Suzuki D, Sakai M, Ito M, Shima T, et al. Proportion of peripheral blood and decidual CD4(+) CD25(bright) regulatory T cells in pre-eclampsia. *Clin. Exp. Immunol.* (2007) 149:139–45. doi: 10.1111/j.1365-2249.2007.03397.x
56. Mahic M, Yaqub S, Johansson CC, Tasken K, Aandahl EM. FOXP3+CD4+CD25+ adaptive regulatory T cells express cyclooxygenase-2 and suppress effector T cells by a prostaglandin E2-dependent mechanism. *J. Immunol.* (2006) 177:246–54. doi: 10.4049/jimmunol.177.1.246
57. Shen H, Wang C, Fan E, Li Y, Zhang W, Zhang L. Upregulation of interleukin-35 subunits in regulatory T cells in a murine model of allergic rhinitis. *ORL J. Otorhinolaryngol. Relat. Spec.* (2014) 76:237–47. doi: 10.1159/000369141
58. Shevach EM. Mechanisms of foxp3+ T regulatory cell-mediated suppression. *Immunity*. (2009) 30:636–45. doi: 10.1016/j.immuni.2009.04.010
59. Kimura A, Kishimoto T. IL-6: regulator of Treg/Th17 balance. *Eur. J. Immunol.* (2010) 40:1830–5. doi: 10.1002/eji.201040391
60. Kobayashi M, Fitz L, Ryan M, Hewick RM, Clark SC, Chan S, et al. Identification and purification of natural killer cell stimulatory factor (NKSF), a cytokine with multiple biologic effects on human lymphocytes. *J. Exp. Med.* (1989) 170:827–45. doi: 10.1084/jem.170.3.827
61. Zhao J, Zhao J, Perlman S. Differential effects of IL-12 on Tregs and non-Treg T cells: roles of IFN-gamma, IL-2 and IL-2R. *PLoS ONE*. (2012) 7:e46241. doi: 10.1371/journal.pone.0046241
62. Basanna S, Chadchan SB, Kumar V, Maurya VK, Soni UK, Jha RK. Endoglin (CD105) coordinates the process of endometrial receptivity for embryo implantation. *Mol. Cell Endocrinol.* (2016) 425:69–83. doi: 10.1016/j.mce.2016.01.014
63. McEwan M, Lins RJ, Munro SK, Vincent ZL, Ponnampalam AP, Mitchell MD. Cytokine regulation during the formation of the fetal-maternal interface: focus on cell-cell adhesion and remodelling of the extra-cellular matrix. *Cytokine Growth Factor Rev.* (2009) 20:241–9. doi: 10.1016/j.cytogfr.2009.05.004
64. Shah NM, Lai PF, Imami N, Johnson MR. Progesterone-related immune modulation of pregnancy and labor. *Front. Endocrinol.* (2019) 10:198. doi: 10.3389/fendo.2019.00198

Conflict of Interest: The authors declare that the research was conducted in the absence of any commercial or financial relationships that could be construed as a potential conflict of interest.

frontiers in Veterinary Science

ORIGINAL RESEARCH
published: 12 February 2021
doi: 10.3389/fvets.2021.641916

Expression of Caspases in the Pig Endometrium Throughout the Estrous Cycle and at the Maternal-Conceptus Interface During Pregnancy and Regulation by Steroid Hormones and Cytokines

*Wonchul Jung[1], Inkyu Yoo[1], Jisoo Han[1], Minjeong Kim[1], Soohyung Lee[1], Yugeong Cheon[1], Minsun Hong[1], Bo-Young Jeon[2] and Hakhyun Ka[1]**

[1] Department of Biological Science and Technology, Yonsei University, Wonju, South Korea, [2] Department of Biomedical Laboratory Science, Yonsei University, Wonju, South Korea

OPEN ACCESS

Edited by:
Dariusz Jan Skarzynski,
Institute of Animal Reproduction and Food Research (PAS), Poland

Reviewed by:
Beenu Moza Jalali,
Institute of Animal Reproduction and Food Research (PAS), Poland
Agnieszka Blitek,
Institute of Animal Reproduction and Food Research of PAS, Poland

***Correspondence:**
Hakhyun Ka
hka@yonsei.ac.kr

Specialty section:
This article was submitted to Animal Reproduction - Theriogenology, a section of the journal Frontiers in Veterinary Science

Received: 15 December 2020
Accepted: 25 January 2021
Published: 12 February 2021

Citation:
Jung W, Yoo I, Han J, Kim M, Lee S, Cheon Y, Hong M, Jeon B-Y and Ka H (2021) Expression of Caspases in the Pig Endometrium Throughout the Estrous Cycle and at the Maternal-Conceptus Interface During Pregnancy and Regulation by Steroid Hormones and Cytokines. Front. Vet. Sci. 8:641916. doi: 10.3389/fvets.2021.641916

Caspases, a family of cysteine protease enzymes, are a critical component of apoptotic cell death, but they are also involved in cellular differentiation. The expression of caspases during apoptotic processes in reproductive tissues has been shown in some species; however, the expression and regulation of caspases in the endometrium and placental tissues of pigs has not been fully understood. Therefore, we determined the expression of caspases *CASP3*, *CASP6*, *CASP7*, *CASP8*, *CASP9*, and *CASP10* in the endometrium throughout the estrous cycle and pregnancy. During the estrous cycle, the expression of all caspases and during pregnancy, the expression of *CASP3*, *CASP6*, and *CASP7* in the endometrium changed in a stage-specific manner. Conceptus and chorioallantoic tissues also expressed caspases during pregnancy. CASP3, cleaved-CASP3, and CASP7 proteins were localized to endometrial cells, with increased levels in luminal and glandular epithelial cells during early pregnancy, whereas apoptotic cells in the endometrium were limited to some scattered stromal cells with increased numbers on Day 15 of pregnancy. In endometrial explant cultures, the expression of some caspases was affected by steroid hormones (estradiol-17β and/or progesterone), and the cytokines interleukin-1β and interferon-γ induced the expression of *CASP3* and *CASP7*, respectively. These results indicate that caspases are dynamically expressed in the endometrium throughout the estrous cycle and at the maternal-conceptus interface during pregnancy in response to steroid hormones and conceptus signals. Thus, caspase action could be important in regulating endometrial and placental function and epithelial cell function during the implantation period in pigs.

Keywords: pig, endometrium, apoptosis, caspase, differentiation

INTRODUCTION

The structure and function of the uterus changes significantly during the reproductive cycle and pregnancy in mammalian species. The degree of change in the endometrium during the cycle varies by species, with the most dramatic changes found in humans and non-human primates, which form a hemochorial type placenta (1–3). In pigs, which form a true epitheliochorial type placenta, the endometrium also undergoes morphological and functional change during the estrous cycle and pregnancy (4). During the estrous cycle in pigs, endometrial change is affected mainly by the ovarian steroid hormones estrogen and progesterone (5, 6), and during early pregnancy, it is driven by conceptus-derived signals, including estrogen and the cytokines interleukin-1β (IL1B), interferon-δ (IFND), and interferon-γ (IFNG), in addition to ovarian steroid hormones (4, 7, 8).

Apoptosis, a programmed cell death, plays a critical role in a variety of physiological processes in multicellular organisms. For example, it maintains functional tissue homeostasis by eliminating unwanted or dysfunctional cells (9, 10). Apoptosis occurs in the endometrium during the estrous cycle and pregnancy to regulate endometrial homeostasis (11, 12). In the human endometrium, apoptotic cell death is observed in endometrial epithelial and stromal cells, with a higher apoptotic rate in the late secretory to early proliferative phases than in the late proliferative to mid-secretory phases of the menstrual cycle (13). In pigs, cells undergoing apoptosis are detected mainly in endometrial stroma during the estrous cycle and early pregnancy and in luminal epithelial cells at the proestrus phase of the estrous cycle, but apoptotic cell death does not occur as dramatically in pigs as it does in primates during the reproductive cycle (14).

Apoptotic cell death is induced by intrinsic and extrinsic pathways. The intrinsic pathway is mediated by various intracellular stress and mitochondrial factors, whereas the extrinsic pathway is triggered by extracellular death signals, such as tumor necrosis factor (TNF) superfamily members: TNF-α, Fas ligand (FASLG), and TNF-related apoptosis-inducing ligand (TRAIL, also known as TNFSF10) (15, 16). The two pathways result in the activation of caspases, which are cytoplasmic cysteine protease enzymes, to induce apoptotic cell death. Caspases play essential roles in apoptosis and inflammation and are divided into two groups, initiator caspases (CASP8, CASP9, and CASP10) and executioner caspases (CASP3, CASP6, and CASP7) (9, 17, 18). Once the executioner caspases are activated by the initiator caspases, they recognize the aspartic residue of various intracellular target proteins and cleave them to cause apoptotic cell death. In that way, caspases are used as a representative marker for cells in which apoptosis has occurred. However, the apoptotic signaling pathway that activates caspases also plays an important role in the differentiation of various cell types, such as immune cells, trophoblasts, spermatocytes, epithelial cells, and stem cells (19, 20). It has been suggested that caspase activation is locally regulated during cellular remodeling without causing apoptotic cell death and that transient caspase activity is used for cell fate determination (10, 21).

Although endometrial changes during the estrous cycle and pregnancy involve the apoptotic process and the function of caspases is essential during apoptotic cell death and cellular differentiation, the pattern of caspase expression in the endometrium during the estrous cycle and pregnancy is not fully understood in pigs. We hypothesized that caspases are expressed in the endometrium during the estrous cycle and at the maternal-conceptus interface during pregnancy to regulate apoptosis and cellular differentiation. Therefore, we determined in pigs (1) the expression of caspases (*CASP3*, *CASP6*, *CASP7*, *CASP8*, *CASP9*, and *CASP10*) in the endometrium during the estrous cycle and pregnancy, conceptus tissues during early pregnancy, and chorioallantoic tissues during mid- to late pregnancy; (2) the localization of caspases and apoptotic cells in the endometrium; and (3) the regulation of caspase expression by the steroid hormones estrogen and progesterone and by the cytokines IL1B and IFNG in endometrial tissues.

MATERIALS AND METHODS

Animals and Tissue Preparation

All experimental procedures involving animals were conducted in accordance with the Guide for the Care and Use of Research Animals in Teaching and Research and approved by the Institutional Animal Care and Use Committee of Yonsei University and the National Institute of Animal Science. Sexually mature Landrace and Yorkshire crossbred female gilts of similar age (6–8 months) and weight (100–120 kg) were assigned randomly to either cyclic or pregnant status, as described previously (22). Gilts assigned to the pregnant uterus status group were artificially inseminated with fresh boar semen at the onset of estrus (Day 0) and 12 h later. The reproductive tracts of the gilts were obtained immediately after slaughter on Days 0, 3, 6, 9, 12, 15, or 18 of the estrous cycle or Days 10, 12, 15, 30, 60, 90, or 114 of pregnancy ($n = 3$–6/day/status). Pregnancy was confirmed by the presence of apparently normal filamentous conceptuses in uterine flushings on Days 10, 12, and 15 and the presence of embryos and placenta on later days of pregnancy. Conceptus tissues were obtained from uterine flushings on Days 12 and 15 of pregnancy. Uterine flushings were obtained by introducing and recovering 25 ml of phosphate-buffered saline (PBS; pH 7.4) into each uterine horn. Chorioallantoic tissues were obtained on Days 30, 60, 90, and 114 of pregnancy ($n = 3$–4/day). Endometrial tissues from prepubertal gilts ($n = 8$; approximately 6 months of age) that had not undergone the estrous cycle, with no corpus luteum formed, were obtained from a local slaughterhouse. Endometrium, dissected free of myometrium, was collected from the middle portion of each uterine horn, snap-frozen in liquid nitrogen, and stored at −80°C prior to RNA extraction. For immunohistochemistry, cross-sections of the endometrium were fixed in 4% paraformaldehyde in PBS (pH 7.4) for 24 h and then embedded in paraffin as previously described (23).

Explant Cultures

To determine the effects of steroid hormones, IL1B, and IFNG on the expression of caspase mRNA in the endometrium, endometrial tissue was dissected from the myometrium and placed into warm phenol red-free Dulbecco's modified Eagle's medium/F-12 (DMEM/F-12) (Sigma) containing penicillin G

(100 IU/ml) and streptomycin (0.1 mg/ml), as described previously (23–25) with some modifications. The endometrium was minced with scalpel blades into small pieces (2–3 mm^3), and 500 mg were placed into T25 flasks with serum-free modified DMEM/F-12 containing 10 μg/ml insulin (Sigma), 10 ng/ml transferrin (Sigma), and 10 ng/ml hydrocortisone (Sigma). To analyze the effect of steroid hormones on the expression of caspases, endometrial explants from immature gilts, immediately after mincing, were cultured with rocking in the presence of increasing doses of estradiol-17β (E_2; 0, 5, 50, or 500 pg/ml; Sigma) or progesterone (P_4; 0, 0.3, 3, or 30 ng/ml; Sigma) for 24 h in an atmosphere of 5% CO_2 in air at 37°C. The doses were chosen to encompass the full concentration range of physiological levels of E_2 and P_4 in the endometrium during the estrous cycle and pregnancy (8). To analyze the effect of IL1B on *CASP3* and the effect of IFNG on *CASP7* expression, endometrial explant tissues from Day 12 of the estrous cycle were treated with E_2 (10 ng/ml), P_4 (30 ng/ml), and increasing doses of IL1B (0, 1, 10, and 100 ng/ml; Sigma) or IFNG (0, 1, 10, and 100 ng/ml; R&D Systems, Minneapolis, MN, USA) at 37°C for 24 h. To determine the effect of the steroid hormones on the expression of *CASP3* during the implantation period, endometrial explant tissues from Day 12 of the estrous cycle were treated with ethanol (control), E_2 (10 ng/ml; Sigma, USA), P_4 (30 ng/ml; Sigma, USA), P_4+E_2, P_4+E_2+ICI182,780 (ICI; an estrogen receptor antagonist; 200 ng/ml; Tocris Bioscience, Ellisville, MO, USA), or P_4+E_2+RU486 (RU; a progesterone receptor antagonist; 30 ng/ml; Sigma, USA) for 24 h. The explant tissues were then harvested, and total RNA was extracted for a real-time RT-PCR analysis to determine the expression levels of caspase mRNA. These experiments were conducted using endometrium from three gilts on Day 12 of the estrous cycle in triplicate and eight immature gilts.

Total RNA Extraction, Reverse Transcription-Polymerase Chain Reaction (RT-PCR), and Cloning of Porcine Caspase cDNA

Total RNA was extracted from endometrial and conceptus tissues using TRIzol reagent (Invitrogen, Carlsbad, CA, USA) according to the manufacturer's recommendations, as described previously (22). The quantity of RNA was assessed spectrophotometrically, and RNA integrity was validated following electrophoresis in 1% agarose gel. Four micrograms of total RNA from endometrial, conceptus, and chorioallantoic tissues were treated with DNase I (Promega, Madison, WI, USA) and reverse transcribed using SuperScript II Reverse Transcriptase (Invitrogen) to obtain cDNA. The cDNA templates were then diluted at a 1:4 ratio with sterile water and amplified by PCR using Taq polymerase (Takara Bio, Shiga, Japan) and specific primers based on porcine caspase mRNA sequences. The PCR conditions, sequences of primer pairs for caspases, and expected product sizes are listed in **Supplementary Table 1**. The PCR products were separated on 2% agarose gel and visualized by ethidium bromide staining. The identity of each amplified PCR product was verified by sequence analysis after cloning into the pCRII vector (Invitrogen).

Quantitative Real-Time RT-PCR

To analyze the levels of caspase expression in the endometrial and chorioallantoic tissues, real-time RT-PCR was performed using an Applied Biosystems StepOnePlus System (Applied Biosystems, Foster City, CA, USA) with the SYBR Green method, as described previously (22). Complementary DNA was synthesized from 4 μg of total RNA isolated from different uterine endometrial and chorioallantoic tissues, and the newly synthesized cDNA (total volume of 21 μl) was diluted 1:4 with sterile water and used for PCR. Power SYBR Green PCR Master Mix (Applied Biosystems) was used for the PCR reactions. The final reaction volume of 20 μl contained 2 μl of cDNA, 10 μl of 2× Master mix, 2 μl of each primer, and 4 μl of distilled H_2O. The annealing temperature and number of cycles for PCR were the same for all products obtained. The results are reported as expression relative to that detected on Day 0 of the estrous cycle, that on Day 30 of pregnancy in chorioallantoic tissues, or that in control explant tissues after normalization of the transcript amount to the geometric mean of endogenous porcine ribosomal protein L7 (*RPL7*) and ubiquitin B (*UBB*), and TATA binding protein (*TBP*) controls, all using the $2^{-\Delta\Delta CT}$ method as previously described (26).

Immunohistochemical Analysis

To identify the type(s) of porcine endometrial cells expressing CASP3, cleaved-CASP3, CASP7, poly (ADP-ribose) polymerase (PARP1), an enzyme that is cleaved during apoptosis and used as a hallmark for apoptosis (27), and cleaved-PARP1, sections were immunostained. Sections (5 μm thick) were deparaffinized and rehydrated in an alcohol gradient. Tissue sections were boiled in citrate buffer (pH 6.0) for 10 min. Then, they were washed with PBST (PBS with 0.1% Tween-20) three times, and a peroxidase block was performed with 0.5% (v/v) H_2O_2 in methanol for 30 min. Tissue sections were then blocked with 10% normal goat serum for 30 min at room temperature. Rabbit polyclonal anti-CASP3 antibody (5 μg/ml; Cell Signaling, Danvers, MA, USA), rabbit polyclonal anti-cleaved-CASP3 antibody (5 μg/ml; Cell Signaling), mouse monoclonal anti-CASP7 antibody (5 μg/ml; Enzo Life Sciences, Farmingdale, NY, USA), rabbit polyclonal anti-PARP1 antibody (1 μg/ml; Santa Cruz Biotechnology, Santa Cruz, CA, USA), or rabbit monoclonal anti-cleaved-PARP1 antibody (1 μg/ml; GeneTex, Irvine, CA, USA) were added and incubated overnight at 4°C in a humidified chamber. For each tissue tested, purified normal rabbit IgG or mouse IgG was substituted for the primary antibody as a negative control. Tissue sections were washed with PBST three times. Biotinylated goat anti-rabbit or anti-mouse secondary antibody (1 μg/ml; Vector Laboratories, Burlingame, CA, USA) was added and incubated for 1 h at room temperature. Following washes with PBST, a streptavidin peroxidase conjugate (Invitrogen) was added to the tissue sections, which were then incubated for 10 min at room temperature. The sections were washed with PBST, and aminoethyl carbazole substrate (Invitrogen) was added to the tissue sections, which were then incubated for 10 min at room temperature. The tissue sections were washed in water, counterstained with Mayer's hematoxylin, and coverslipped. Images were captured using an Eclipse TE2000-U microscope

(Nikon, Seoul, Korea) and processed with Adobe Photoshop CS6 software (Adobe Systems, Seattle, WA, USA).

TUNEL Assay and Immunofluorescence

Apoptotic cells in endometrial tissue sections were analyzed using the terminal deoxynucleotidyl transferase-mediated dUTP nick end labeling (TUNEL) assay with an In Situ Cell Death Detection Kit (Roche Diagnostics, Mannheim, Germany) used according to the manufacturer's recommendations, as described previously (28). Endometrial tissue sections (5 μm thick) were deparaffinized and rehydrated in an alcohol gradient. The sections were then boiled with 0.1 M citrate buffer (pH 6.0) for 3 min, cooled at room temperature for 10 min, and then washed three times in PBS. For a positive control for TUNEL staining, the sections were treated with DNase I (3 U/ml; Promega) in 50 mM Tris-HCl (pH 7.5), 10 mM $MgCl_2$, and 1 mg/ml bovine serum albumin (BSA; Bovogen Biologicals, Melbourne, Australia) for 10 min at room temperature and then washed with PBS. Tissue sections were then blocked with 0.1 M Tris-HCl (pH 7.5) containing 3% (w/v) BSA and 20% (v/v) normal bovine serum for 30 min at room temperature. The TUNEL reaction was performed according to the kit instructions. After the TUNEL reactions, tissue sections were washed with PBS. The tissue sections were counterstained with 4',6-diamidino-2-phenylindole (DAPI), and fluorescence images were captured using an Eclipse TE2000-U microscope (Nikon, Seoul, Korea) with Adobe Photoshop CS6 software (Adobe Systems, Seattle, WA, USA).

Statistical Analysis

Data from real-time RT-PCR for caspase expression were subjected to ANOVA using the general linear models procedures in SAS (Cary, NC, USA). As sources of variation, the model included day, pregnancy status (cyclic or pregnant, Days 12 and 15 post-estrus), and their interactions to evaluate steady-state levels of caspase mRNA. Data from real-time RT-PCR performed to assess the effects of day of the estrous cycle (Days 0, 3, 6, 9, 12, 15, and 18) and pregnancy (Days 10, 12, 15, 30, 60, 90, and 114) and the effects of day of pregnancy (Days 30, 60, 90, and 114) on chorioallantoic tissues were analyzed using a least squares regression analysis. The effects of E_2, P_4, IL1B, and IFNG doses on explant cultures were analyzed by one-way ANOVA followed by Tukey's post-test. Data from real-time RT-PCR to assess the effects of steroid hormones and their receptor antagonists on explant culture were analyzed by preplanned orthogonal contrasts (control vs. E_2; control vs. P_4; P_4 vs. P_4+E_2; P_4+E_2 vs. P_4+E_2+ICI; and P_4+E_2 vs. P_4+E_2+RU). Data are presented as means with standard error of the mean. A P-value <0.05 was considered significant, and P-values 0.05–0.10 were considered to indicate a trend toward significance.

RESULTS

Expression of Caspase mRNA in the Endometrium During the Estrous Cycle and Pregnancy

In real-time RT-PCR analyses, we found that *CASP3*, *CASP6*, *CASP7*, *CASP8*, *CASP9*, and *CASP10* mRNA was expressed in the endometrium during the estrous cycle and pregnancy (**Figure 1**). During the estrous cycle, the steady-state levels of *CASP3* (quadratic, $P = 0.0572$), *CASP6* (quadratic, $P < 0.01$), *CASP7* (linear, $P < 0.05$), *CASP8* (quadratic, $P < 0.01$), and *CASP10* (quadratic, $P < 0.05$) mRNA changed, with the highest levels of *CASP3*, *CASP6*, *CASP7*, and *CASP8* in the proestrus phase and that of *CASP10* in the proestrus to metestrus phase. On Days 12 and 15 post-estrus, the expression of *CASP3* was affected by day ($P < 0.05$), status ($P < 0.01$), and the day x status interaction ($P < 0.05$). The expression of *CASP6* was affected by the day x status interaction ($P < 0.05$), that of *CASP7* was affected by day ($P < 0.05$), that of *CASP8* was affected by status ($P < 0.01$), and that of *CASP9* was affected by day ($P < 0.01$). The expression of *CASP10* was not affected by day, status, or the day x status interaction. During pregnancy, the steady-state levels of *CASP3* (linear, $P = 0.0526$), *CASP6* (cubic, $P = 0.073$), *CASP7* (linear, $P < 0.05$), and *CASP10* (quadratic, $P < 0.05$), but not *CASP8* or *CASP9* mRNA, changed with the highest levels on Day 12 for *CASP3*, on Day 15 for *CASP7*, and Day 60 for *CASP6* and *CASP10*.

Expression of Caspase mRNA in Conceptuses During Early Pregnancy and Chorioallantoic Tissues in Later Stages of Pregnancy

In RT-PCR analysis using cDNAs from conceptuses from Days 12 and 15 of pregnancy, we found that *CASP3*, *CASP6*, *CASP7*, *CASP8*, and *CASP10* mRNA but not *CASP9* mRNA in conceptuses from both days of early pregnancy (**Figure 2A**). These caspases were also detectable in endometrial tissues from same days. In addition, we performed real-time RT-PCR analyses to determine whether the expression of *CASP3*, *CASP6*, *CASP7*, *CASP8*, *CASP9*, and *CASP10* mRNA changed in chorioallantoic tissues during pregnancy. The abundance of *CASP3*, *CASP6*, *CASP7*, *CASP8*, *CASP9*, and *CASP10* mRNA in chorioallantoic tissues changed, with the highest levels on Day 30 for *CASP3* and at term for *CASP6*, *CASP7*, *CASP8*, *CASP9*, and *CASP10* (linear effect of day for *CASP6*, *CASP7*, *CASP8*, *CASP9*, and *CASP10*, $P < 0.01$; quadratic effect of day for *CASP3*, $P < 0.01$) (**Figure 2B**).

Localization of CASP3, Cleaved-CASP3, and CASP7 Proteins in the Endometrium on Days 12 and 15 Post-estrus

Having determined that *CASP3*, *CASP6*, *CASP7*, *CASP8*, *CASP9*, and *CASP10* mRNA was present in the endometrium during the estrous cycle and pregnancy and in conceptuses and chorioallantoic tissues during pregnancy and that the expression of *CASP3* and *CASP7* mRNA was highest during early pregnancy, we next determined the cellular localization of the CASP3, cleaved-CASP3 (an active form), and CASP7 proteins in the endometrium on Days 12 and 15 post-estrus using immunohistochemistry (**Figure 3**). CASP3 proteins were mainly detected in endometrial luminal (LE) and glandular epithelial (GE) cells and in scattered stromal cells, with stronger signal intensity on Days 12 and 15 of pregnancy than during the estrous cycle, and they were localized subcellularly to both the cytoplasm

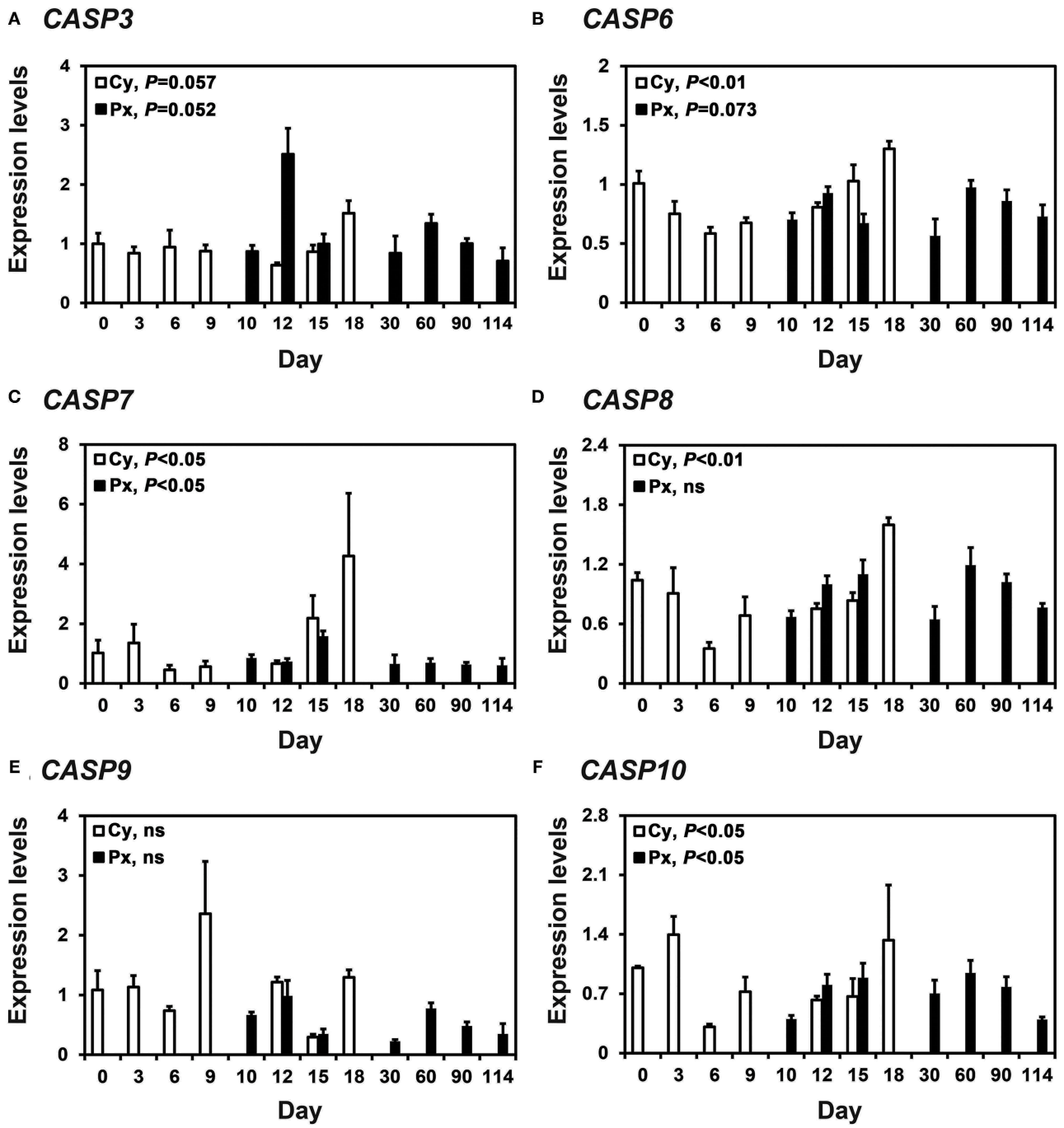

FIGURE 1 | Expression of *CASP3* **(A)**, *CASP6* **(B)**, *CASP7* **(C)**, *CASP8* **(D)**, *CASP9* **(E)**, and *CASP10* **(F)** mRNA in the endometrium during the estrous cycle and pregnancy in pigs. Endometrial tissue samples from cyclic (Cy) and pregnant (Px) gilts were analyzed by real-time RT-PCR, and data are reported as the expression relative to that detected on Day 0 of the estrous cycle after normalization to the transcript amount of the endogenous *RPL7*, *UBB*, and *TBP* mRNAs. Data are presented as the mean with standard error. Statistical significances for the effect of day during the estrous cycle and pregnancy are indicated; ns, not significant.

and the nucleus (**Figure 3A**). The active form of CASP3, cleaved-CASP3 protein, was localized primarily to the nucleus of LE cells and some stromal cells in the endometrium on Days 12 and 15 of pregnancy (**Figure 3B**). Both CASP3 and cleaved-CASP3 proteins were detected in the small intestine used as a positive control. CASP7 protein was localized to the cytoplasm of LE and stromal cells in the endometrium, but only on Day 15 of pregnancy (**Figure 3C**). Trophectoderm cells in conceptuses were also positive for CASP7 protein on Day 15 of pregnancy (**Figure 3C**). CASP7 protein was detected in the lymph node used

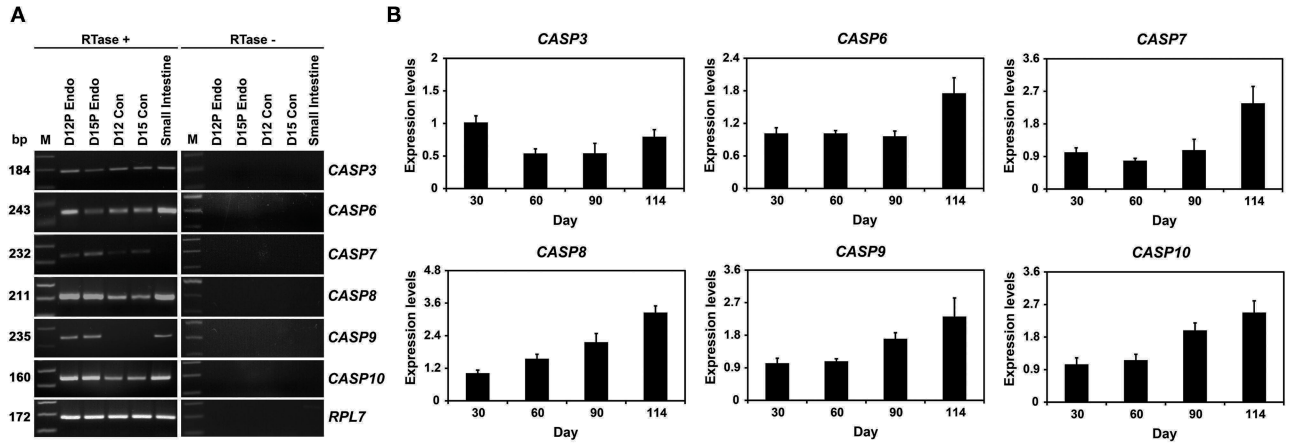

FIGURE 2 | Expression of *CASP3*, *CASP6*, *CASP7*, *CASP8*, *CASP9*, and *CASP10* by conceptuses from Days 12 and 15 of pregnancy **(A)** and chorioallantoic tissues during mid- to late pregnancy **(B)**. **(A)** RT-PCR analyses of *CASP3*, *CASP6*, *CASP7*, *CASP8*, *CASP9*, and *CASP10* mRNA in conceptuses on Days 12 and 15 of pregnancy were performed using total RNA preparations. *RPL7* was used as a positive control. RTase ±, with (+) or without (–) reverse transcriptase; M, molecular marker; D12 Endo, endometrium on day 12 of pregnancy; D12 Con, Day 12 conceptus; D15 Con, Day 15 conceptus. **(B)**. Real-time RT-PCR analyses of the expression of *CASP3*, *CASP6*, *CASP7*, *CASP8*, *CASP9*, and *CASP10* mRNA in chorioallantoic tissues on Days 30, 60, 90, and 114 of pregnancy. Data are reported as expression relative to that detected on Day 30 of pregnancy after normalization to the transcript amount of the endogenous *RPL7*, *UBB*, and *TBP* mRNAs control, and data are presented as means with standard errors.

as a positive control. Immunohistochemistry for cleaved-CASP7 was not done due to the lack of an appropriate antibody to detect porcine cleaved-CASP7 protein.

TUNEL Staining and PARP Cleavage Analysis for *in situ* Apoptotic Cell Death in the Endometrium During the Estrous Cycle and Pregnancy

Because CASP3 and CASP7 proteins were localized to endometrial epithelial and stromal cells during the estrous cycle and pregnancy, we determined whether cells expressing CASP3 and CASP7 were undergoing apoptotic cell death. Because apoptotic cells undergo DNA degradation and PARP1, an enzyme involved in DNA repair, is cleaved by caspases (29), we performed the TUNEL assay and immunostaining of PARP1 and cleaved-PARP1 in endometrial tissues from pregnant pigs. We found that apoptotic cells in the endometrium during pregnancy were predominantly in stromal cells, not in epithelial cells, with many apoptotic cells found on Day 15 of pregnancy and very few cells found during the later stages of pregnancy (**Figure 4A**). PARP1 protein was localized to most cell types in the endometrium on Days 12 and 15 of the estrous cycle and pregnancy (**Figure 4B**), but cleaved-PARP1, a marker for apoptotic cells, was localized primarily to stromal cells on Day 15 of pregnancy (**Figure 4C**). The PARP1 and cleaved-PARP1 proteins were also detected in the ovary used as a positive control.

Effects of the Steroid Hormones E_2 and P_4 on Caspase Expression in Endometrial Tissue of Prepubertal Gilts

Because the expression of caspases changed during the estrous cycle and because E_2 from the ovary and P_4 from the corpus luteum regulate the expression of many endometrial genes during the cycle (4, 8), we hypothesized that E_2 and P_4 might affect the expression of caspases in the endometrium. Therefore, we obtained endometrial tissues from immature gilts, which had not been exposed to cyclical ovarian hormones, and treated them with increasing doses of E_2 or P_4. We found that the expression of *CASP7* mRNA was decreased by E_2 (0 vs. 500 pg/ml, $P < 0.05$), but the expression of *CASP3*, *CASP6*, *CASP8*, *CASP9*, and *CASP10* mRNA was unaffected by E_2 (**Figure 5**). The expression of *CASP7* (0 vs. 30 ng/ml, $P < 0.05$), *CASP8* (0 vs. 3 ng/ml and 0 vs. 30 ng/ml, $P < 0.01$), and *CASP10* (0 vs. 3 ng/ml, $P < 0.01$; 0 vs. 30 ng/ml, $P < 0.05$), but not *CASP3*, *CASP6*, and *CASP9*, was affected by P_4 treatment (**Figure 6**).

Effects of IL1B and Steroid Hormones on *CASP3* and the Effect of IFNG on *CASP7* Expression in Endometrial Tissues

Because the expression of *CASP3* and *CASP7* was highest on Days 12 and 15 of pregnancy, respectively, and porcine conceptuses secrete estrogen and IL1B2 into the uterine lumen on Day 12 and IFND and IFNG on Day 15 (4, 8), we assumed that the expression of *CASP3* on Day 12 could be affected by estrogen and IL1B and that of *CASP7* on Day 15 of pregnancy could be affected by IFNG. We treated endometrial explant tissues from Day 12 of the estrous cycle with increasing doses of IL1B and steroid hormones and found that IL1B induces the expression of *CASP3* (0 vs. 1 ng/ml, $P < 0.05$; **Figure 7A**), but steroid hormones and their receptor antagonists do not affect the expression of *CASP3* (**Figure 7B**). When increasing doses of IFNG were administered, the IFNG induced the expression of *CASP7* (0 vs. 10 pg/ml, 0 vs. 100 pg/ml; $P < 0.01$) (**Figure 7C**).

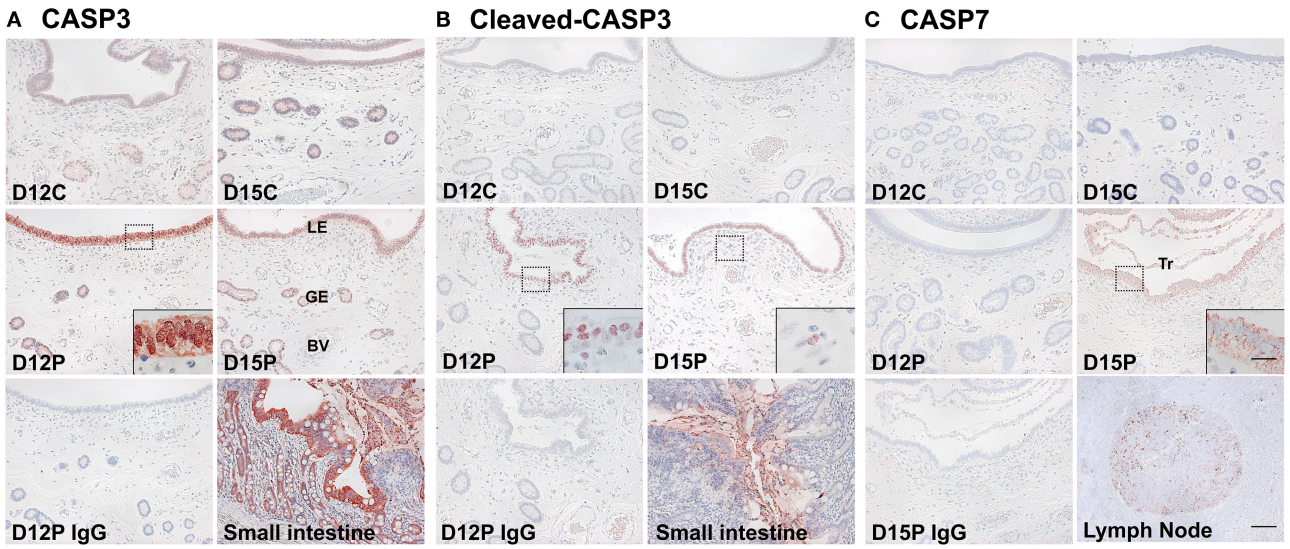

FIGURE 3 | Immunohistochemical localization of CASP3 **(A)**, cleaved-CASP3 **(B)**, and CASP7 **(C)** proteins in the endometrium on Days 12 and 15 post-estrus. Representative uterine sections from Days 12 or 15 of pregnancy immunostained with normal IgG are shown as negative controls, and tissue sections from the small intestine and lymph node serve as positive controls for CASP3, cleaved-CASP3, and CASP7 immunostaining. D, Day; C, estrous cycle; P, pregnancy; LE, luminal epithelium; GE, glandular epithelium; BV, blood vessel; Tr, trophectoderm. Bars = 100 μm and 20 μm in insets.

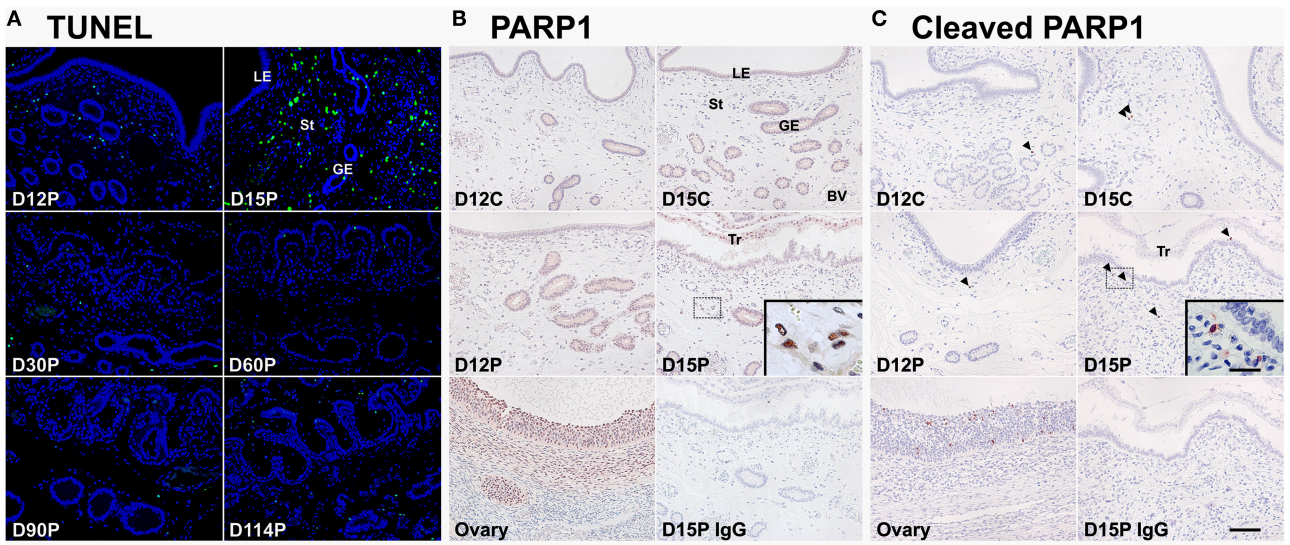

FIGURE 4 | TUNEL staining **(A)** and immunohistochemical localization of PARP1 **(B)** and cleaved-PARP1 **(C)** proteins for *in situ* apoptotic cell death in the endometrium during the estrous cycle and pregnancy. Cells undergoing apoptosis in the endometrium during pregnancy were localized using the TUNEL assay (green), and tissue morphology is shown by DAPI staining. Representative uterine sections from Day 15 of pregnancy immunostained with normal IgG are shown as negative control and tissue sections from the ovary serve as positive controls for PARP1 and cleaved-PARP1 immunostaining. D, day; P, pregnancy; LE, luminal epithelium; GE, glandular epithelium; St, stroma; BV, blood vessel; Tr, trophectoderm. Arrowheads indicate cleaved-PARP1-positive cells. Bar = 100 μm and 20 μm in inset.

DISCUSSION

The significant findings of this study in pigs were: (1) caspases *CASP3*, *CASP6*, *CASP7*, *CASP8*, *CASP9*, and *CASP10* were expressed in the endometrium during the estrous cycle and pregnancy in a stage- and pregnancy status–specific manner; (2) conceptuses on Days 12 and 15 of pregnancy and chorioallantoic tissues from Day 30 of pregnancy to term expressed caspases, except *CASP9*, on Days 12 and 15 of pregnancy; (3) CASP3, cleaved-CASP3, and CASP7 proteins were localized to endometrial cells, with increased signal intensity in LE and GE cells during early pregnancy; (4) apoptotic cells in

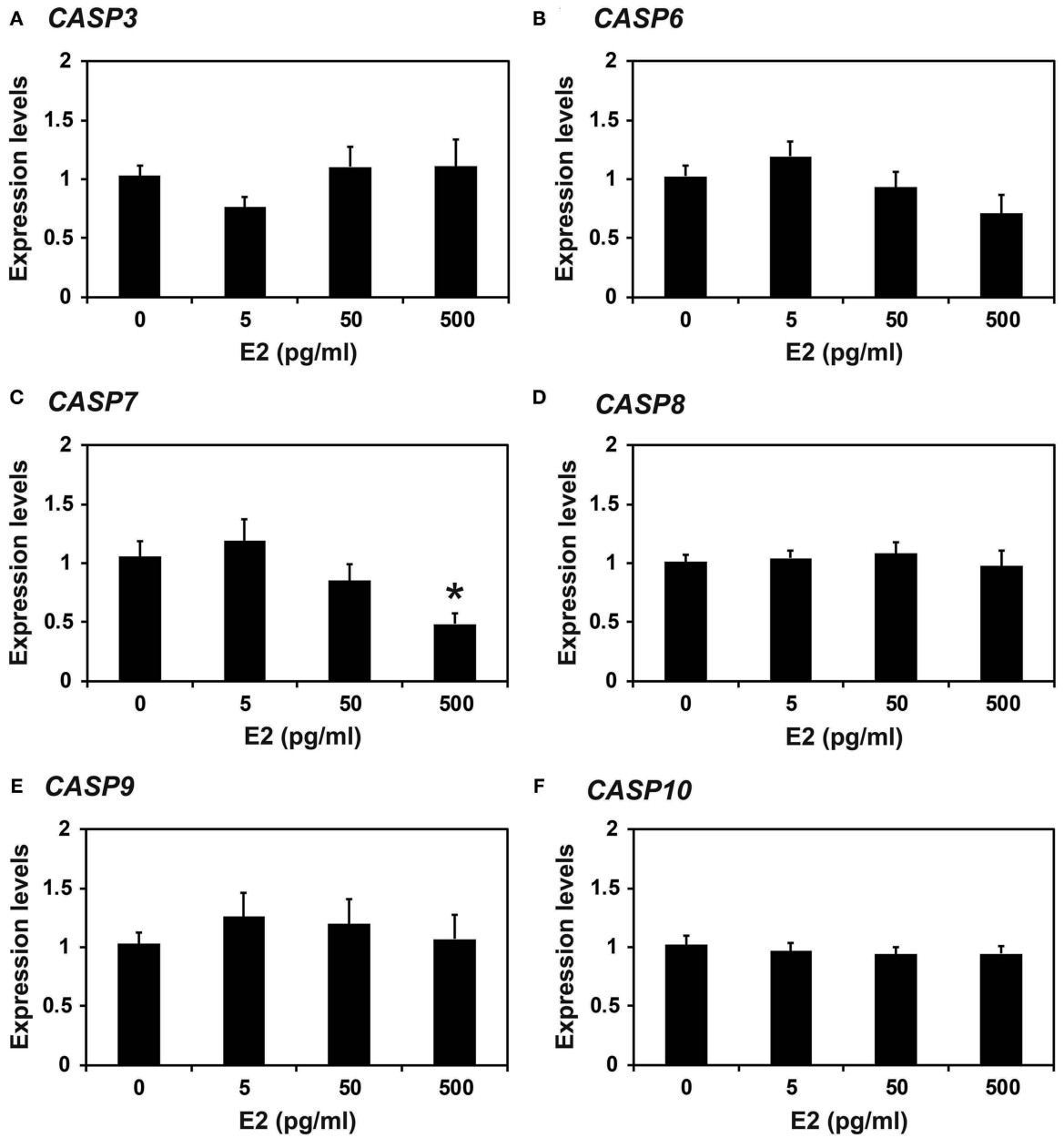

FIGURE 5 | Effect of estradiol on *CASP3* **(A)**, *CASP6* **(B)**, *CASP7* **(C)**, *CASP8* **(D)**, *CASP9* **(E)**, and *CASP10* **(F)** mRNA in endometrial explant cultures. Endometrial explants from immature gilts were cultured at 37°C in DMEM/F-12 with increasing doses of estradiol-17β (E_2; 0, 5, 50, and 500 pg/ml) for 24 h. Experiments were performed with endometria from eight gilts. The abundance of mRNA, determined by real-time RT-PCR, is relative to that of *CASP3*, *CASP6*, *CASP7*, *CASP8*, *CASP9*, and *CASP10* mRNA in the control group of endometrial explants (0 pg/ml E_2) after normalization to the transcript amount of *RPL7*, *UBB*, and *TBP* mRNAs. Data are presented as the mean with standard error. The asterisk denotes statistically significant difference when values were compared with the control group: $^*P < 0.05$.

the endometrium were localized to some scattered stromal cells, with increased numbers on Day 15 of pregnancy; (5) E_2 and P_4 affected the expression of some caspases in endometrial tissues; and (6) IL1B and IFNG upregulated the expression of *CASP3* and *CASP7*, respectively, in endometrial explant tissues.

Caspases are essential mediators of apoptosis and play an important role in a variety of biological processes (9, 10, 17). Two groups of caspases, initiator caspases and executioner caspases, are activated during the pathway to apoptotic activation. Caspases are expressed in the endometrium during the reproductive cycle and pregnancy and that they mediate apoptotic cell death in various species (2, 30, 31). However, the expression of all initiator and executioner caspases in the endometrium throughout the estrous/menstrual cycle and at the maternal-conceptus interface during pregnancy has not been fully studied in any species. The results of this study indicate the

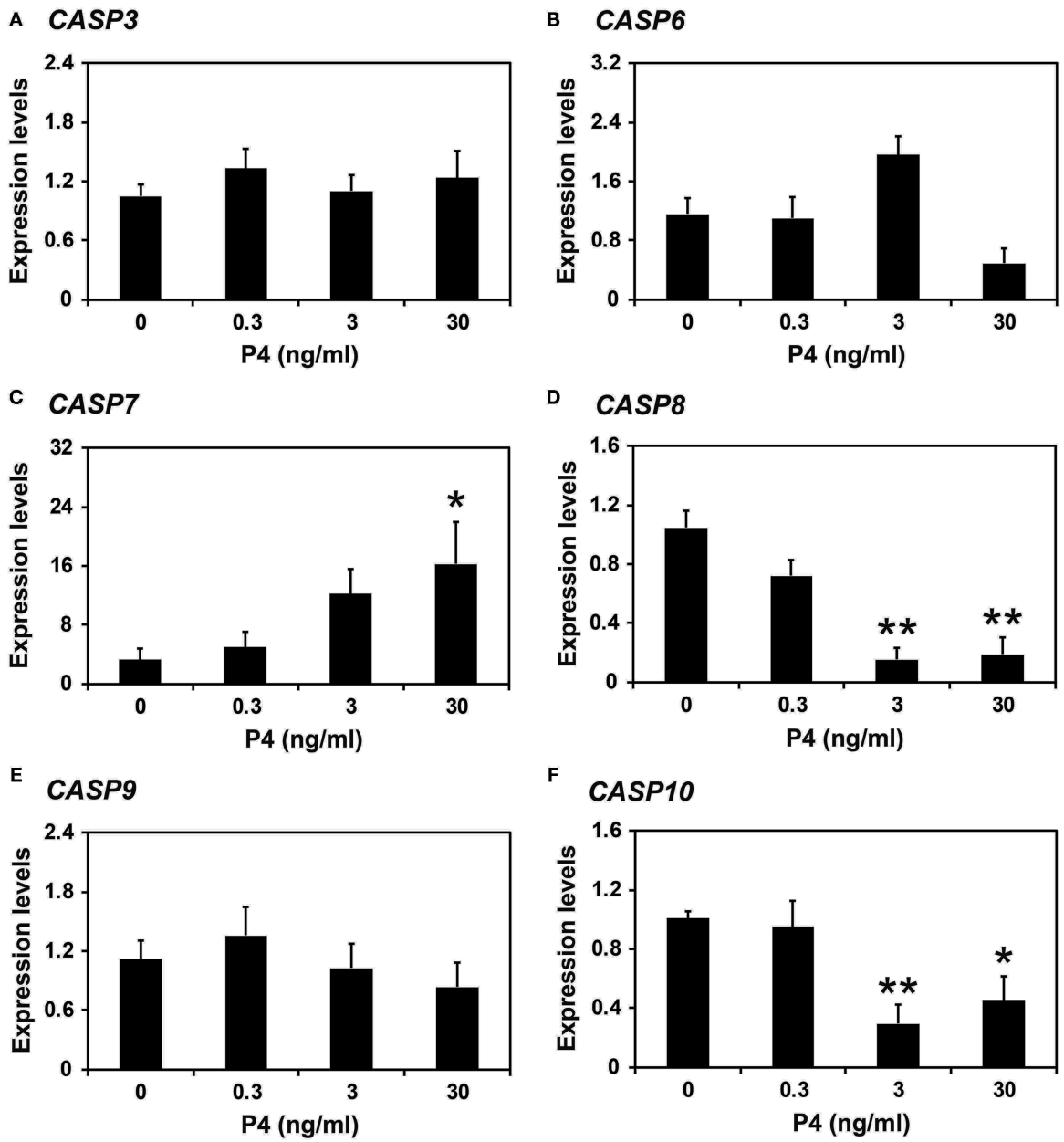

FIGURE 6 | Effect of progesterone on *CASP3* **(A)**, *CASP6* **(B)**, *CASP7* **(C)**, *CASP8* **(D)**, *CASP9* **(E)**, and *CASP10* **(F)** mRNA in endometrial explant cultures. Endometrial explants from immature gilts were cultured at 37°C in DMEM/F-12 with increasing doses of progesterone (P_4; 0, 0.3, 3, and 30 ng/ml) for 24 h. Experiments were performed with endometria from eight gilts. The abundance of mRNA, determined by real-time RT-PCR, is relative to that of *CASP3*, *CASP6*, *CASP7*, *CASP8*, *CASP9*, and *CASP10* mRNA in the control group of endometrial explants (0 ng/ml P_4) after normalization to the transcript amount of *RPL7*, *UBB*, and *TBP* mRNAs. Data are presented as the mean with standard error. The asterisks denote statistically significant differences when values were compared with the control group: $^*P < 0.05$; $^{**}P < 0.01$.

variable expression of the initiator and executioner caspases in the endometrium during the estrous cycle and pregnancy and in conceptus/chorioallantoic tissues throughout pregnancy in pigs.

During the estrous cycle, the expression of caspases *CASP3*, *CASP6*, *CASP7*, *CASP8*, and *CASP10* changed with the stage of the cycle, with the highest levels in the proestrus phase for *CASP3*, *CASP6*, and *CASP7* and in the proestrus to metestrus phase for *CASP8* and *CASP10*. These data indicate that the expression of caspases is dynamically regulated in the endometrium during the estrous cycle and may be related to cyclic remodeling of this tissue in pigs. The incidence of apoptotic cell death in LE cells was previously shown by TUNEL assay to be highest in the estrus phase in pigs (14), suggesting that caspases expressed in the proestrus phase could cause apoptotic cell death in

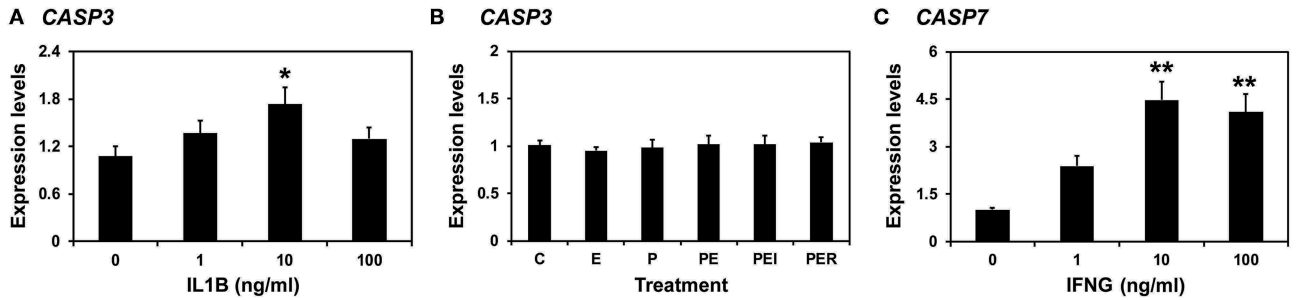

FIGURE 7 | Effects of IL1B **(A)** and steroid hormones **(B)** on the expression of *CASP3* and the effect of IFNG on *CASP7* **(C)** in endometrial explant cultures. Endometrial explants from gilts on Day 12 of the estrous cycle were cultured **(A)** with increasing doses of IL1B (0, 1, 10, and 100 ng/ml) in the presence of with E_2 (estradiol-17β; 10 ng/ml) and P_4 (progesterone; 30 ng/ml), **(B)** with steroid hormones [control (C), E_2 (E), P_4 (P), E_2 + P_4 (PE), E_2+P_4+ICI (I, an estrogen receptor antagonist) (PEI), or E_2+P_4+RU (R; a progesterone receptor antagonist) (PER)], or **(C)** with increasing doses of IFNG (0, 1, 10, and 100 ng/ml) in the presence of with E_2 (10 ng/ml) and P_4 (30 ng/ml). The abundance of mRNA expression, determined by real-time RT-PCR analyses, was relative to that for *CASP3* and *CASP7* mRNA in the control group of endometrial explants after normalization to the transcript amounts of *RPL7*, *UBB*, and *TBP* mRNAs. Data are presented as means with standard error. These treatments were performed in triplicate using tissues obtained from each of three gilts. The asterisks denote statistically significant differences when values were compared with the control group: $^*P < 0.05$; $^{**}P < 0.01$.

the endometrium in the estrus phase. In bovine endometrium, *CASP3* expression does not change during the estrous cycle, but active forms of CASP3 proteins increase at the follicular and early luteal phases compared with the mid- to late luteal phase (2). Furthermore, *CASP8* expression in the bovine endometrium increases toward the follicular phase from the luteal phase (31). Thus, it seems that the endometrial expression of some caspases increases in pigs and cows as the cycle moves toward the estrus phase.

The pattern of caspase expression in the endometrium during the estrous cycle led us to postulate that the expression of caspases and the activation of apoptotic signaling could be related to cyclical changes in the endometrium triggered by the actions of steroid hormones from the ovary. In this study, we found that P_4 decreased the expression of *CASP8* and *CASP10* in endometrial explant tissues. Because the endometrial expression of *CASP8* and *CASP10* was low at the diestrus phase and high at the proestrus to metestrus phase of the estrous cycle, it is likely that P_4 causes the decreased levels of *CASP8* and *CASP10* expression in the endometrium at the diestrus phase of the cycle in pigs. However, P_4 increased the expression of *CASP7*, whereas E_2 decreased the expression of *CASP7* in endometrial explant tissues, even though the endometrial expression of *CASP7* was high in the proestrus phase of the cycle, when plasma levels of P_4 and E_2 decrease and increase, respectively (8). These data indicate that the regulation of *CASP7* expression in the endometrium during the estrous cycle is much more complex than can be explained by the simple action of P_4 and E_2 and thus needs further analysis.

Although the levels of caspase expression during pregnancy have not been much studied in any species, it has been shown that the levels of active Casp3 protein in the rat endometrium are highest at mid-pregnancy (30). In this study, the endometrial expression of caspases *CASP3*, *CASP6*, *CASP7*, and *CASP10* during pregnancy changed, with the highest levels occurring during early pregnancy for *CASP3* and *CASP7* and during mid-pregnancy for *CASP6* and *CASP10*, suggesting that the expression of caspases is pregnancy stage–specific and varies with the type of caspase. In particular, we observed that the expression of *CASP3* and *CASP7* was highest on Days 12 and 15 of pregnancy, respectively, which is the period when conceptuses interact with the endometrium for implantation (4, 7, 8). Because the implanting porcine conceptus secretes estrogen and IL1B on Day 12 of pregnancy and type I and II IFNs, IFND and IFNG, around Day 15 of pregnancy (4, 8), we postulated that estrogen and/or IL1B might be responsible for inducing *CASP3* expression in the endometrium on Day 12 and that IFNG might be responsible for inducing *CASP7* expression on Day 15 of pregnancy. Indeed, our results performed using endometrial explant culture revealed increased expression of CASP3 in response to IL1B but not E_2, whereas CASP7 expression was stimulated by IFNG. These data indicate that the expression of *CASP3* and *CASP7* in the endometrium during early pregnancy in pigs is induced by conceptus-derived IL1B and IFNG, respectively.

Because CASP3 and CASP7 are well-known executioner caspases during apoptosis (9, 17), we determined which cell type(s) expressed CASP3 and CASP7 proteins in the endometrium during early pregnancy and whether the cells expressing CASP3 and CASP7 were undergoing apoptotic cell death. Our results show that CASP3 and active CASP3 proteins were predominantly localized to LE and stromal cells on Days 12 and 15 of pregnancy and that the CASP7 protein was primarily localized to LE cells on Day 15 of pregnancy. Interestingly, however, results from the TUNEL assay and cleaved-PARP1 staining show that only stromal cells in the endometrium, not epithelial cells, were undergoing apoptosis during early pregnancy. These data suggest that CASP3 and CASP7 might not be involved in endometrial epithelial apoptosis during early pregnancy in pigs.

Executioner caspases CASP3, CASP6, and CASP7 play critical roles in both apoptotic cell death and cell differentiation

in various cell types, such as keratinocytes, muscle cells, neurons, and stem cells (18). Also, the initiator caspase CASP8, which is expressed by cytotrophoblast cells, is involved in the differentiation of cytotrophoblast cells into the syncytiotrophoblast layer in human placental villi (32–34). Thus, the increased endometrial expression of CASP3 and CASP7 in response to conceptus-derived signals at the time of conceptus implantation could be expected to act on epithelial cell differentiation instead of activating apoptosis. Indeed, at the time of implantation LE cells of the porcine endometrium show various aspects of differentiated cellular characteristics: changed morphology (35–37), increased production of secretory proteins, including fibroblast growth factor 7 (38) and secreted phosphoprotein 1 (39), and increased expression of immunity-related molecules, including interferon α/β receptor 1 and 2 (40), interferon gamma receptor 1 and 2 (25), cysteine-X-cysteine motif chemokine ligand 12 (41), TNF superfamily 10 (28), and cytotoxic T-lymphocyte-associated protein 4 (Yoo and Ka, unpublished data). The expression of most of those molecules in endometrial epithelial cells is induced by conceptus signals, estrogen, IL1B, or IFNG, and those molecules play important roles in conceptus implantation. Thus, it is likely that CASP3 and CASP7 are also involved in activating the differentiation process of endometrial LE cells in response to conceptus-derived signals. However, the nature of the differentiated cellular characteristics mediated by CASP3 and CASP7 in endometrial LE cells still needs further study.

Our results also show that caspases were expressed in conceptus tissues during early pregnancy and in chorioallantoic tissues during mid- to late pregnancy. In particular, the levels of *CASP6*, *CASP7*, *CASP8*, *CASP9*, and *CASP10* expression in chorioallantoic tissues increased as the pregnancy came to term. However, as determined by TUNEL assay in this study, apoptotic cells were barely detectable in chorioallantoic tissues during pregnancy. It has been shown that CASP3 proteins levels in porcine placental tissue are higher on Day 30 than on Days 60, 80, and 90 of pregnancy, what coincides with the expression pattern of *CASP3* mRNA in this study (42). In ovine placentas, CASP3 and CASP9 proteins increase toward term, and the levels of active CASP3 and CASP9 are increased in placentas with intrauterine growth restriction pregnancy compared with normal pregnancy (43). In bovine placental tissues obtained at parturition, CASP3 and CASP8 mRNA and proteins are expressed (44), and CASP8 and CASP10 are expressed in human placental villi at term (33, 45). Thus, the expression of caspases in placental tissues is common among mammalian species and increases toward term. In addition, because accumulated evidence shows that apoptotic cell death increases in the placenta when pregnancy complications occur, such as intrauterine growth restriction, preeclampsia and preterm premature rupture of membranes in humans (46, 47), and in placental tissues derived from somatic cell nuclear transfer–cloned embryos in pigs (48), it is likely that caspases are important in regulating placental function and are activated in situations of inappropriate placental development during pregnancy.

CONCLUSION

In conclusion, the results of this study in pigs show that caspases are expressed in the endometrium, with differential expression patterns throughout the estrous cycle and pregnancy, and in the conceptus and chorioallantoic tissues during pregnancy; CASP3 and CASP7 are localized primarily to endometrial epithelial cells during early pregnancy; the steroid hormones E_2 and P_4 regulate the expression of caspases in endometrial tissues; and IL1B and IFNG induce the expression of *CASP3* and *CASP7*, respectively, in endometrial tissues. These results suggest that caspases dynamically expressed in the endometrium and at the maternal-conceptus interface could play important roles in the establishment and maintenance of pregnancy in pigs by regulating apoptosis and epithelial differentiation.

DATA AVAILABILITY STATEMENT

The original contributions presented in the study are included in the article/**Supplementary Material**, further inquiries can be directed to the corresponding author/s.

ETHICS STATEMENT

The animal study was reviewed and approved by Institutional Animal Care and Use Committee of Yonsei University.

AUTHOR CONTRIBUTIONS

WJ, MH, B-YJ, and HK: conceptualization, methodology. IY, JH, MK, SL, and YC: investigation. WJ, IY, and HK: data analysis, writing—original draft preparation. MH and B-YJ: writing—reviewing and editing. HK: supervision, funding acquisition. All authors contributed to the article and approved the submitted version.

FUNDING

This work was supported by The National Research Foundation Grant funded by the Korean Government (#2019R1A2C1004670), Republic of Korea.

SUPPLEMENTARY MATERIAL

The Supplementary Material for this article can be found online at: https://www.frontiersin.org/articles/10.3389/fvets.2021.641916/full#supplementary-material

REFERENCES

1. Reynolds LP, Borowicz PP, Vonnahme KA, Johnson ML, Grazul-Bilska AT, Wallace JM, et al. Animal models of placental angiogenesis. *Placenta.* (2005) 26:689–708. doi: 10.1016/j.placenta.2004.11.010
2. Arai M, Yoshioka S, Tasaki Y, Okuda K. Remodeling of bovine endometrium throughout the estrous cycle. *Anim Reprod Sci.* (2013) 142:1–9. doi: 10.1016/j.anireprosci.2013.08.003
3. Bazer FW. Pregnancy recognition signaling mechanisms in ruminants and pigs. *J Anim Sci Biotechnol.* (2013) 4:23. doi: 10.1186/2049-1891-4-23
4. Bazer FW, Johnson GA. Pig blastocyst-uterine interactions. *Differentiation.* (2014) 87:52–65. doi: 10.1016/j.diff.2013.11.005
5. Oberleithner H, Riethmuller C, Ludwig T, Shahin V, Stock C, Schwab A, et al. Differential action of steroid hormones on human endothelium. *J Cell Sci.* (2006). 119(Pt 9):1926–32. doi: 10.1242/jcs.02886
6. Annie L, Gurusubramanian G, Roy VK. Estrogen and progesterone dependent expression of visfatin/NAMPT regulates proliferation and apoptosis in mice uterus during estrous cycle. *J Steroid Biochem Mol Biol.* (2019) 185:225–36. doi: 10.1016/j.jsbmb.2018.09.010
7. Geisert RD, Whyte JJ, Meyer AE, Mathew DJ, Juarez MR, Lucy MC, et al. Rapid conceptus elongation in the pig: an interleukin 1 beta 2 and estrogen-regulated phenomenon. *Mol Reprod Dev.* (2017) 84:760–74. doi: 10.1002/mrd.22813
8. Ka H, Seo H, Choi Y, Yoo I, Han J. Endometrial response to conceptus-derived estrogen and interleukin-1beta at the time of implantation in pigs. *J Anim Sci Biotechnol.* (2018) 9:44. doi: 10.1186/s40104-018-0259-8
9. Crawford ED, Wells JA. Caspase substrates and cellular remodeling. *Annu Rev Biochem.* (2011) 80:1055–87. doi: 10.1146/annurev-biochem-061809-121639
10. Nakajima YI, Kuranaga E. Caspase-dependent non-apoptotic processes in development. *Cell Death Differ.* (2017) 24:1422–30. doi: 10.1038/cdd.2017.36
11. Song J, Rutherford T, Naftolin F, Brown S, Mor G. Hormonal regulation of apoptosis and the Fas and Fas ligand system in human endometrial cells. *Mol Hum Reprod.* (2002) 8:447–55. doi: 10.1093/molehr/8.5.447
12. Joswig A, Gabriel HD, Kibschull M, Winterhager E. Apoptosis in uterine epithelium and decidua in response to implantation: evidence for two different pathways. *Reprod Biol Endocrinol.* (2003) 1:44. doi: 10.1186/1477-7827-1-44
13. Kokawa K, Shikone T, Nakano R. Apoptosis in the human uterine endometrium during the menstrual cycle. *J Clin Endocrinol Metab.* (1996) 81:4144–7. doi: 10.1210/jcem.81.11.8923873
14. Okano A, Ogawa H, Takahashi H, Geshi M. Apoptosis in the porcine uterine endometrium during the estrous cycle, early pregnancy and post partum. *J Reprod Dev.* (2007) 53:923–30. doi: 10.1262/jrd.18139
15. Fluhr H, Wenig H, Spratte J, Heidrich S, Ehrhardt J, Zygmunt M. Non-apoptotic Fas-induced regulation of cytokines in undifferentiated and decidualized human endometrial stromal cells depends on caspase-activity. *Mol Hum Reprod.* (2011) 17:127–34. doi: 10.1093/molehr/gaq082
16. Spratte J, Princk H, Schutz F, Rom J, Zygmunt M, Fluhr H. Stimulation of chemokines in human endometrial stromal cells by tumor necrosis factor-alpha and interferon-gamma is similar under apoptotic and non-apoptotic conditions. *Arch Gynecol Obstet.* (2018) 297:505–12. doi: 10.1007/s00404-017-4586-3
17. Riedl SJ, Shi Y. Molecular mechanisms of caspase regulation during apoptosis. *Nat Rev Mol Cell Biol.* (2004) 5:897–907. doi: 10.1038/nrm1496
18. Shalini S, Dorstyn L, Dawar S, Kumar S. Old, new and emerging functions of caspases. *Cell Death Differ.* (2015) 22:526–39. doi: 10.1038/cdd.2014.216
19. Levy R, Nelson DM. To be, or not to be, that is the question. *Apoptosis in human trophoblast Placenta.* (2000) 21:1–13. doi: 10.1053/plac.1999.0450
20. Yi CH, Yuan J. The Jekyll and Hyde functions of caspases. *Dev Cell.* (2009) 16:21–34. doi: 10.1016/j.devcel.2008.12.012
21. Solier S, Fontenay M, Vainchenker W, Droin N, Solary E. Non-apoptotic functions of caspases in myeloid cell differentiation. *Cell Death Differ.* (2017) 24:1337–47. doi: 10.1038/cdd.2017.19
22. Lee S, Yoo I, Han J, Ka H. Antimicrobial peptides cathelicidin, PMAP23, and PMAP37: Expression in the endometrium throughout the estrous cycle and at the maternal-conceptus interface during pregnancy and regulation by steroid hormones and calcitriol in pigs. *Theriogenology.* (2021) 160:1–9. doi: 10.1016/j.theriogenology.2020.10.034
23. Seo H, Kim M, Choi Y, Lee CK, Ka H. Analysis of lysophosphatidic acid (LPA) receptor and LPA-induced endometrial prostaglandin-endoperoxide synthase 2 expression in the porcine uterus. *Endocrinology.* (2008) 149:6166–75. doi: 10.1210/en.2008-0354
24. Han J, Yoo I, Lee S, Jung W, Kim HJ, Hyun SH, et al. Atypical chemokine receptors 1, 2, 3 and 4: Expression and regulation in the endometrium during the estrous cycle and pregnancy and with somatic cell nucleus transfer-cloned embryos in pigs. *Theriogenology.* (2019) 129:121–9. doi: 10.1016/j.theriogenology.2019.02.021
25. Yoo I, Seo H, Choi Y, Jang H, Han J, Lee S, et al. Analysis of interferon-gamma receptor IFNGR1 and IFNGR2 expression and regulation at the maternal-conceptus interface and the role of interferon-gamma on endometrial expression of interferon signaling molecules during early pregnancy in pigs. *Mol Reprod Dev.* (2019) 86:1993–2004. doi: 10.1002/mrd.23287
26. Livak KJ, Schmittgen TD. Analysis of relative gene expression data using real-time quantitative PCR and the 2(-Delta Delta C(T)) method. *Methods.* (2001) 25:402–8. doi: 10.1006/meth.2001.1262
27. Germain M, Affar EB, D'Amours D, Dixit VM, Salvesen GS, Poirier GG. Cleavage of automodified poly(ADP-ribose) polymerase during apoptosis. Evidence for involvement of caspase-7. *J Biol Chem.* (1999) 274:28379–84. doi: 10.1074/jbc.274.40.28379
28. Yoo I, Kye YC, Han J, Kim M, Lee S, Jung W, et al. Uterine epithelial expression of the tumor necrosis factor superfamily: a strategy for immune privilege during pregnancy in a true epitheliochorial placentation species. *Biol Reprod.* (2020) 102:828–42. doi: 10.1093/biolre/ioz233
29. Soldani C, Scovassi AI. Poly(ADP-ribose) polymerase-1 cleavage during apoptosis: an update. *Apoptosis.* (2002) 7:321–8. doi: 10.1023/a:1016119328968
30. Shooner C, Caron PL, Frechette-Frigon G, Leblanc V, Dery MC, Asselin E. TGF-beta expression during rat pregnancy and activity on decidual cell survival. *Reprod Biol Endocrinol.* (2005) 3:20. doi: 10.1186/1477-7827-3-20
31. Groebner AE, Schulke K, Unterseer S, Reichenbach HD, Reichenbach M, Buttner M, et al. Enhanced proapoptotic gene expression of XAF1, CASP8 and TNFSF10 in the bovine endometrium during early pregnancy is not correlated with augmented apoptosis. *Placenta.* (2010) 31:168–77. doi: 10.1016/j.placenta.2009.12.017
32. Black S, Kadyrov M, Kaufmann P, Ugele B, Emans N, Huppertz B. Syncytial fusion of human trophoblast depends on caspase 8. *Cell Death Differ.* (2004) 11:90–8. doi: 10.1038/sj.cdd.4401307
33. Ka H, Hunt JS. FLICE-inhibitory protein: expression in early and late gestation human placentas. *Placenta.* (2006) 27:626–34. doi: 10.1016/j.placenta.2005.08.004
34. Longtine MS, Chen B, Odibo AO, Zhong Y, Nelson DM. Caspase-mediated apoptosis of trophoblasts in term human placental villi is restricted to cytotrophoblasts and absent from the multinucleated syncytiotrophoblast. *Reproduction.* (2012) 143:107–21. doi: 10.1530/REP-11-0340
35. Stroband HW, Taverne N, Langenfeld K, Barends PM. The ultrastructure of the uterine epithelium of the pig during the estrous cycle and early pregnancy. *Cell Tissue Res.* (1986) 246:81–9. doi: 10.1007/BF00219003
36. Cencic A, Guillomot M, Koren S, La Bonnardiere C. Trophoblastic interferons: do they modulate uterine cellular markers at the time of conceptus attachment in the pig? *Placenta.* (2003) 24:862–9. doi: 10.1016/s0143-4004(03)00135-8
37. Jalali BM, Lukasik K, Witek K, Baclawska A, Skarzynski DJ. Changes in the expression and distribution of junction and polarity proteins in the porcine endometrium during early pregnancy period. *Theriogenology.* (2020) 142:196–206. doi: 10.1016/j.theriogenology.2019.09.041
38. Ka H, Jaeger LA, Johnson GA, Spencer TE, Bazer FW. Keratinocyte growth factor is up-regulated by estrogen in the porcine uterine endometrium and functions in trophectoderm cell proliferation and differentiation. *Endocrinology.* (2001) 142:2303–10. doi: 10.1210/endo.142.6.8194
39. Garlow JE, Ka H, Johnson GA, Burghardt RC, Jaeger LA, Bazer FW. Analysis of osteopontin at the maternal-placental interface in pigs. *Biol Reprod.* (2002) 66:718–25. doi: 10.1095/biolreprod66.3.718
40. Jang H, Choi Y, Yoo I, Han J, Kim M, Ka H. Characterization of interferon alpha and beta receptor IFNAR1 and IFNAR2 expression and regulation in the uterine endometrium during the estrous cycle and pregnancy in pigs. *Theriogenology.* (2017) 88:166–73. doi: 10.1016/j.theriogenology.2016.09.025

41. Han J, Jeong W, Gu MJ, Yoo I, Yun CH, Kim J, et al. Cysteine-X-cysteine motif chemokine ligand 12 and its receptor CXCR4: expression, regulation, and possible function at the maternal-conceptus interface during early pregnancy in pigs. *Biol Reprod*. (2018). doi: 10.1093/biolre/ioy147
42. Sanchis EG, Cristofolini AL, Fiorimanti MR, Barbeito CG, Merkis CI. Apoptosis and cell proliferation in porcine placental vascularization. *Anim Reprod Sci.* (2017) 184:20–8. doi: 10.1016/j.anireprosci.2017.06.009
43. Monson T, Wright T, Galan HL, Reynolds PR, Arroyo JA. Caspase dependent and independent mechanisms of apoptosis across gestation in a sheep model of placental insufficiency and intrauterine growth restriction. *Apoptosis.* (2017) 22:710–8. doi: 10.1007/s10495-017-1343-9
44. Kamemori Y, Wakamiya K, Nishimura R, Hosaka Y, Ohtani S, Okuda K. Expressions of apoptosis-regulating factors in bovine retained placenta. *Placenta.* (2011) 32:20–6. doi: 10.1016/j.placenta.2010.10.016
45. Dubova EA, Pavlov KA, Aleksandrova NV, Baev OR, Shchyogolev AI, Sukhikh GT. Caspase expression in placental terminal villi in spontaneous and induced pregnancy. *Bull Exp Biol Med.* (2014) 158:92–6. doi: 10.1007/s10517-014-2700-0
46. Tanir HM, Sener T, Artan S, Kaytaz B, Sahin-Mutlu F, Ozen ME. Programmed cell death (apoptosis) in placentas from normal pregnancy and pregnancy complicated by term (t) and preterm (p) premature rupture of membranes (PROM). *Arch Gynecol Obstet*. (2005) 273:98–103. doi: 10.1007/s00404-005-0028-8
47. Longtine MS, Chen B, Odibo AO, Zhong Y, Nelson DM. Villous trophoblast apoptosis is elevated and restricted to cytotrophoblasts in pregnancies complicated by preeclampsia, IUGR, or preeclampsia with IUGR. *Placenta.* (2012) 33:352–9. doi: 10.1016/j.placenta.2012.01.017
48. Chae JI, Cho SK, Seo JW, Yoon TS, Lee KS, Kim JH, et al. Proteomic analysis of the extraembryonic tissue from cloned porcine embryos. *Mol Cell Proteomics.* (2006) 5:1559–66. doi: 10.1074/mcp.M500427-MCP200

Conflict of Interest: The authors declare that the research was conducted in the absence of any commercial or financial relationships that could be construed as a potential conflict of interest.

frontiers in Veterinary Science

BRIEF RESEARCH REPORT
published: 05 March 2021
doi: 10.3389/fvets.2021.649758

Messenger RNA Expression of Selected Factors at Different Sites of the Bovine Endometrium Associated With Uterine Health

Harald Pothmann[1]*, *Paula Flick*[1,2], *Alexander Tichy*[3], *Christoph Gabler*[2] and *Marc Drillich*[1]

[1] Clinical Unit for Herd Health Management in Ruminants, University Clinic for Ruminants, Vetmeduni Vienna, Vienna, Austria,
[2] Department of Veterinary Medicine, Institute of Veterinary Biochemistry, Freie Universität Berlin, Berlin, Germany,
[3] Department of Scientific Biomedicine, Platform of Bioinformatics and Biostatistics, Vetmeduni Vienna, Vienna, Austria

Recent studies have elucidated the role of several pro-inflammatory factors as mediators of inflammatory processes in the bovine endometrium. Only few studies, however, have analyzed samples collected from different regions of the uterus of the same animal. In this study, we tested the hypothesis that on a molecular level, clinical endometritis is characterized by inflammatory responses spread over the entire endometrium. Furthermore, we assume that subclinical endometritis is described by an inflammation of local regions of the uterus. Therefore, the objective of this study was to assess the mRNA expression of uterus-associated pro-inflammatory factors at five pre-defined endometrial sites, i.e., *corpus uteri*, left horn base, left horn tip, right horn base, and right horn tip, in cows with clinical and subclinical endometritis and in healthy controls. We analyzed the mRNA expression of interleukin 1 alpha, interleukin 1 beta, C-X-C motif chemokine ligand 8, prostaglandin-endoperoxide synthase 2, protein tyrosine phosphatase receptor type C, carcinoembryonic antigen related cell adhesion molecule 1, and mucin 4 and 16. Based on vaginoscopy and endometrial cytology ($\geq$ 5% polymorphonuclear neutrophils) between 28 to 34 days in milk, 18 Simmental cows were categorized in clinical endometritis group ($n = 7$), subclinical endometritis group ($n = 4$), and healthy group ($n = 7$). In general, the analyses revealed a great variation of mRNA expression between sites and animals. Differences were found between different uterine health statuses, but the variation between the sampling sites within the groups was not significant ($P > 0.05$). This indicates that inflammatory processes at the end of the postpartum period can be regarded as multi-focal or spread throughout the uterus independent from the uterine health status.

Keywords: mRNA, pro-inflammatory factors, uterine health, endometrium, cows

OPEN ACCESS

Edited by:
Dariusz Jan Skarzynski, Institute of Animal Reproduction and Food Research (PAS), Poland

Reviewed by:
Kieran G. Meade, University College Dublin, Ireland
Wojciech Barański, University of Warmia and Mazury in Olsztyn, Poland

***Correspondence:**
Harald Pothmann
harald.pothmann@vetmeduni.ac.at

Specialty section:
This article was submitted to Animal Reproduction - Theriogenology, a section of the journal Frontiers in Veterinary Science

Received: *05 January 2021*
Accepted: *12 February 2021*
Published: *05 March 2021*

Citation:
Pothmann H, Flick P, Tichy A, Gabler C and Drillich M (2021) Messenger RNA Expression of Selected Factors at Different Sites of the Bovine Endometrium Associated With Uterine Health. Front. Vet. Sci. 8:649758. doi: 10.3389/fvets.2021.649758

INTRODUCTION

Postpartum (pp) uterine disorders, such as metritis, clinical endometritis (CE), and subclinical endometritis (SE), have negative short- and long-term impact on bovine fertility (1–3). Bacterial infections provoke the release of pro-inflammatory factors, such as prostaglandins and cytokines, e.g., interleukin 1A (*IL1A*), interleukin 1 B (*IL1B*), and C-X-C motif chemokine ligand 8 (*CXCL8*)

(4–6). These chemoattractants play a central role in the innate immune response to regulate the migration of immune cells, e.g., polymorphonuclear neutrophils (PMN), which accomplish phagocytosis in the uterine tissue (7). Detailed information about the physiological function of pro-inflammatory factors involved in inflammatory processes was recently reviewed by Pascottini et al. (8).

The cytobrush (CB) technique was reported as a reliable and accurate method for endometrial sampling and the diagnosis of SE by determining the proportion of PMN in the smears (9–11). It has been discussed whether a single sample is representative for the entire endometrium and affects the accuracy of the diagnosis of SE [reviewed by (12, 13)]. The CB technique can also be used to evaluate the mRNA expression in the endometrial samples. An increased mRNA expression of cytokines was found in cows with SE and CE compared with healthy controls (14, 15). Repeated sampling of the same cows showed no or only few intra-cow variations of the mRNA expression of selected factors (16, 17).

The aim of the present study was to assess mRNA pattern of transcripts involved in physiological and pathological processes, obtained from different endometrial sites *in vivo* in cows with different uterine health status. In this study, we tested the hypothesis that on a molecular level, clinical endometritis is characterized by inflammatory responses spread over the entire endometrium. Furthermore, we assume that subclinical endometritis is characterized by an inflammation of local regions of the uterus. As additional comparison group, we included healthy control cows.

MATERIALS AND METHODS

Study Design

This study was approved by the institutional ethics committee and the national authority according to §8 of Law for Animal Experiments, Tierversuchsgesetz-TVG (BMWFW-68.205/0156-WF/II/3b/2014) and performed at the research farm VetFarm Kremesberg, University of Veterinary Medicine Vienna, Austria.

The herd comprised ∼80 lactating dairy cows, housed in free stall barns with cubicles. Eighteen Simmental cows (14 multipara, four primipara, no history of Cesarean section or dystocia) were enrolled. All cows were examined between day 28 to 34 pp by transrectal palpation and vaginoscopy, followed by uterine CB sampling at five pre-defined sites. Cows with purulent or mucopurulent vaginal discharge were defined as affected with CE (18). Subclinical endometritis was characterized by the absence of vaginal discharge, but with $\geq$ 5% PMN in one of the five endometrial smears (19). The absence of vaginal discharge and a proportion of $<$ 5% PMN in the cytological samples defined the healthy control (HC) cows.

Endometrial Sampling

Five endometrial samples were collected by CB technique from each cow in the same order of sampling, as described (13). In brief, the CB (Gynobrush, Heinz Herenz, Hamburg, Germany) was inserted through a metal tube (50 cm in length, 6 mm inner diameter) and forwarded under manual control to the sites in the following order: (i) *corpus uteri* (CU), (ii) base of the left horn (LHB), (iii) tip of the left horn (LHT), (iv) base of the right horn (RHB), and (v) tip of the right horn (RHT). After retraction, the CB was rolled onto a microscope slide and thereafter stored in tubes at −80°C for RNA analysis. The slides were dried, fixed, stained (Hemacolor Merck, Darmstadt, Germany) and examined under a microscope by using X 400 magnification (Olympus CX21, Olympus, Tokyo, Japan). The percentage of PMN was determined by counting 300 endometrial cells and PMN in total (11).

Total RNA Extraction, Reverse Transcription, and Real-Time PCR

After thawing the CB, total RNA was extracted using RNeasy Plus Mini Kit (Qiagen, Hilden, Germany) according to the manufacturer's instructions. Quantification of total RNA was performed by spectrophotometry (NanoDrop ND-1000 Peqlab Biotechnology, Erlangen, Germany) at 260 nm. Quality and integrity of the isolated total RNA was assessed using the Bioanalyzer 2100 and the Agilent RNA 6000 Nano Kit (both Agilent Technologies, Waldbronn, Germany). The RNA integrity number of the isolated RNA was greater 8.0 and the OD 260/280 $>$ 2.0. Possible genomic DNA contaminations were removed by using DNase. Reverse transcription to generate DNA was performed as described (16). In brief, single stranded cDNA was generated from 100 ng total RNA per sample with the addition of 200 U RevertAid Reverse Transcriptase and 2.5 μM random hexamer primers (both Thermo Scientific, Schwerte, Germany) in a total volume of 60 μl. To confirm the absence of any genomic DNA or contaminations, samples without reverse transcriptase were prepared as negative controls. The generated DNA served as template for real-time PCR to quantify mRNA of the selected factors in the endometrial cells. Gene transcripts, primer sequences and further parameter used for real-time PCR are listed in **Supplementary Table 1**.

Real-time PCR was conducted using the Rotor-Gene 3000 (Corbett Research, Mortlake, Australia), as described (16). In brief, amplification of 1 μl cDNA per sample was carried out in the presence of 0.4 μM of each primer (forward and reverse) and 5 μl 2 × SensiMix SYBR Low-ROX (Bioline, Luckenwalde, Germany) in a total reaction volume of 10 μl. Denaturation at 95°C for 10 min was followed by a three-step amplification in 45 cycles: denaturation at 95°C for 15 s, annealing for 20 s (**Supplementary Table 1**), and extension at 72°C for 30 s. Subsequently, a melting curve program (50–99°C) with continuous fluorescence measurement confirmed specific amplification.

Quantification of mRNA was performed with dilution series and comparison with standards amplified simultaneously. Messenger RNA expression of each sample was normalized with the succinate dehydrogenase complex flavoprotein subunit A (*SDHA*) and glyceraldehyde-3-phosphate dehydrogenase (*GAPDH*) real-time PCR data. Calculation of mRNA expression of protein tyrosine phosphatase receptor type C (*PTPRC*; formerly known as *CD45*) and carcinoembryonic antigen related cell adhesion molecule 1 (*CEACAM1*; formerly known as CD66a), prostaglandin-endoperoxide synthase 2 (*PTGS2*), *IL1A*,

IL1B, C-X-C motif chemokine ligand 8 (C-X-C motif) ligand 8 (*CXCL8*; formerly known as *IL8*), and mucins (*MUC*) MUC4 and *MUC16* was performed using Rotor-Gene 6.1 software.

Statistical Analysis

Statistical analyses were performed with SPSS Statistics version 23.0 (IBM, New York, USA). Data was tested for normality with Kolmogorov-Smirnov test. For each sample, normalized mRNA expression for the selected factors at the five pre-defined endometrial sites was calculated. Median, interquartile range (IQR), mean and standard deviation (SD) of normalized mRNA expression were calculated to describe the variation within cows with different uterine health status. At the level of endometrial sites, the variance of normalized mRNA expression, determined as the coefficient of variation (CV: quotient of SD and mean) was calculated. The normally distributed data was analyzed by ANOVA using the CV as dependent variable and HC, SE, and CE as factors to compare with. Scheffe test was conducted for *post hoc* multiple comparisons. Normalized mRNA expression of selected transcripts on cow-level, categorized according to uterine health status, was shown in box plots and compared by Kruskal-Wallis test and pairwise by Mann-Whitney-*U* test. The level of significance was set at $P < 0.05$.

RESULTS

Seven cows were diagnosed with CE, four with SE, and seven were regarded as healthy (HC). Descriptive statistics and statistical analyses of mRNA expression at the five different endometrial sites related to uterine health (CE, SE, HC) are presented in **Tables 1**–**3**. Proportion of normalized mRNA expression of selected pro-inflammatory factors from cows with different uterine health status (SE, CE, and HC) and significant differences are shown in **Figure 1**.

Endometrial mRNA Expression at the Five Sampling Sites

Comparing the median mRNA expression at the five pre-defined sites resulted in no differences within cows with SE, CE, and HC cows (Kruskal-Wallis test: $P > 0.05$, **Tables 1**–**3**). Overall, the high IQR indicated a great variation of mRNA expression at all different endometrial sites, in particular in cows with CE (**Tables 1**–**3**). Moreover, the CV of mRNA expression at the five endometrial sites was high and revealed no differences between the groups CE, SE, and HC (**Table 4**).

Endometrial mRNA Expression Related to Uterine Health Status

Median mRNA expression of *IL1A*, *IL1B*, and *CXCL8* was increased in cows with SE and CE compared with HC cows, whereas *MUC16* mRNA expression was only increased in SE cows compared with HC cows ($P < 0.05$; **Figure 1**). Expression of *IL1A*, *IL1B,* and *CXCL8* mRNA in SE was 27-, 17-, and 30-fold higher than in HC cows. Expression of *MUC16* mRNA was 2.6-fold higher in SE compared with HC cows. No differences of median mRNA expression between groups were found for *PTPRC*, *CEACAM1*, *PTGS2*, and *MUC4* ($P > 0.05$).

TABLE 1 | Median, interquartile range (IQR), mean, and standard deviation (SD) of normalized mRNA expression for different pro-inflammatory factors and mucins in the endometrium at the *corpus uteri* (CU), the base of the left horn (LHB), the tip of the left horn (LHT), the base of the right horn (RHB) and the tip of the right horn (RHT) collected from seven cows with clinical endometritis (CE) on day 28 to 34 postpartum.

CE cows ($n = 7$)		Endometrial sites				
Factor		**LHT**	**RHT**	**RHB**	**LHB**	**CU**
PTGS2	Median (IQR)	1.6 (50.1)	0.5 (209.6)	1.6 (331.6)	3.2 (21.9)	1.1 (16.6)
	Mean (SD)	177.8 (437.9)	84.0 (178.3)	132.9 (265.0)	111.4 (281.7)	205.4 (535.2)
PTPRC	Median (IQR)	0.7 (2.5)	1.0 (0.8)	1.5 (5.8)	0.6 (1.7)	0.6 (1.7)
	Mean (SD)	1.5 (1.5)	0.6 (1.5)	2.8 (3.9)	1.1 (1.2)	1.7 (2.6)
CEACAM1	Median (IQR)	3.3 (2.8)	2.5 (9.7)	1.5 (9.4)	1.2 (4.2)	1.6 (6.1)
	Mean (SD)	2.6 (5.0)	4.5 (6.5)	4.7 (6.3)	5.5 (10.8)	5.1 (8.9)
Il1A	Median (IQR)	659.9 (2,237)	608.5 (26,878)	1,815 (19,737)	228.4 (3,865)	1,841 (5,871)
	Mean (SD)	36,761 (95,367)	10,872 (23,531)	8,296 (15,950)	13,039 (31,750)	26,511 (65,930)
Il1B	Median (IQR)	0.8 (86.3)	0.3 (147.9)	1.1 (36.0)	0.5 (40.1)	0.6 (98.8)
	Mean (SD)	242.0 (578.9)	59.2 (89.9)	14.7 (25.3)	13.8 (22.7)	182.9 (440.3)
CXCL8	Median (IQR)	1.6 (377.5)	0.8 (283.0)	1.1 (171.9)	2.0 (59.6)	0.7 (6.3)
	Mean (SD)	476.2 (1,034)	113.4 (214.3)	69.1 (147.8)	34.7 (65.3)	590.0 (1,557)
MUC4	Median (IQR)	41.6 (107.8)	27.4 (279.0)	35.5 (52.5)	3.3 (101.5)	47.6 (138.7)
	Mean (SD)	54.4 (50.1)	118.0 (180.2)	29.6 (26.9)	36.5 (55.6)	122.0 (203.7)
MUC16	Median (IQR)	2.3 (2.5)	1.5(2.7)	0.8 (7.9)	0.9 (2.1)	3.2 (2.8)
	Mean (SD)	2.3 (1.6)	1.7 (1.6)	3.8(5.6)	1.8 (1.7)	2.5 (1.3)

PTGS2, prostaglandin-endoperoxide synthase 2; PTPRC, protein tyrosine phosphatase receptor type C; CEACAM1, carcinoembryonic antigen related cell adhesion molecule 1; IL1A, interleukin 1 alpha; IL1B, interleukin 1 beta; CXCL8, C-X-C motif chemokine ligand 8; MUC4, mucin 4; MUC16, mucin 16.

TABLE 2 | Median, interquartile range (IQR), mean, and standard deviation (SD) of normalized mRNA expression for different pro-inflammatory factors and mucins in the endometrium at the *corpus uteri* (CU), the base of the left horn (LHB), the tip of the left horn (LHT), the base of the right horn (RHB) and the tip of the right horn (RHT) collected from four cows with subclinical endometritis (SE) on day 28 to 34 postpartum.

SE cows ($n = 4$)		Endometrial sites				
Factor		**LHT**	**RHT**	**RHB**	**LHB**	**CU**
PTGS2	Median (IQR)	19.2 (141.0)	3.9 (3.4)	25.2 (56.8)	80.2 (554.0)	27.3 (417.9)
	Mean (SD)	56.0 (85.9)	4.0 (1.8)	28.7 (30.0)	212.9 (326.0)	149.4 (262.6)
PTPRC	Median (IQR)	0.6 (1.9)	2.1 (3.4)	0.4 (1.8)	0.7 (0.4)	0.9 (1.9)
	Mean (SD)	1.2 (1.2)	2.1 (1.8)	1.0 (1.1)	0.7 (0.2)	1.1 (1.0)
CEACAM1	Median (IQR)	3.3 (16.4)	2.8 (8.1)	0.5 (16.2)	3.6 (24.7)	2.3 (21.0)
	Mean (SD)	6.9 (9.5)	3.9 (4.4)	5.7 (10.6)	9.7 (14.8)	7.9 (12.9)
Il1A	Median (IQR)	826.0 (6,414)	1.8 (5.3)	12.8 (4,446)	7.9 (14,777)	34.6 (17,190)
	Mean (SD)	2,415 (3,808)	2.4 (2.9)	1,489 (2,959)	4,928 (9,846)	5,748 (11,444)
Il1B	Median (IQR)	1.6 (.2)	0.3 (1.6)	1.3 (4.1)	1.8 (8.2)	5.9 (20.0)
	Mean (SD)	3.3(4.7)	0.6 (0.9)	2.0 (2.2)	3.5 (4.7)	9.4 (11.1)
CXCL8	Median (IQR)	3.2 (28.6)	2.5 (56.7)	4.0 (31.0)	15.8 (27.7)	6.2 (524.1)
	Mean (SD)	11.3 (17.9)	20.2 (36.8)	12.2 (19.0)	15.1 (15.6)	177.6 (346.3)
MUC4	Median (IQR)	6.1 (43.2)	98.0 (243.9)	9.6 (70.3)	12.4 (60.2)	9.2 (631.1)
	Mean (SD)	17.1 (25.8)	114.7 (134.0)	26.8 (41.6)	24.9 (34.4)	213.7 (415.0)
MUC16	Median (IQR)	2.8 (3.5)	1.2 (1.6)	2.4 (5.4)	3.3 (1.8)	2.4 (2.2)
	Mean (SD)	3.0 (1.8)	1.3 (0.9)	3.5 (3.1)	3.5 (0.9)	2.5 (1.1)

PTGS2, prostaglandin-endoperoxide synthase 2; PTPRC, protein tyrosine phosphatase receptor type C; CEACAM1, carcinoembryonic antigen related cell adhesion molecule 1; IL1A, interleukin 1 alpha; IL1B, interleukin 1 beta; CXCL8, C-X-C motif chemokine ligand 8; MUC4, mucin 4; MUC16, mucin 16.

TABLE 3 | Median, interquartile range (IQR), mean, and standard deviation (SD) of normalized mRNA expression for different pro-inflammatory factors and mucins in the endometrium at the *corpus uteri* (CU), the base of the left horn (LHB), the tip of the left horn (LHT), the base of the right horn (RHB) and the tip of the right horn (RHT) collected from seven healthy cows (HC) on day 28 to 34 postpartum.

HC cows ($n = 7$)		Endometrial sites				
Factor		**LHT**	**RHT**	**RHB**	**LHB**	**CU**
PTGS2	Median (IQR)	6.1 (10.2)	3.1 (5.3)	7.0 (8.1)	9.2 (22.2)	4.6 (17.2)
	Mean (SD)	33.3 (76.0)	3.6 (3.4)	7.2 (8.1)	39.1 (78.0)	17.7 (29.9)
PTPRC	Median (IQR)	0.5 (0.8)	0.6 (1.4)	0.5 (0.2)	0.6 (0.5)	0.5 (0.4)
	Mean (SD)	0.8 (0.6)	0.9 (0.6)	0.5 (0.5)	0.7 (0.8)	0.3 (0.5)
CEACAM1	Median (IQR)	4.0 (11.8)	2.5 (4.2)	2.7 (13.6)	3.1 (35.8)	4.1 (10.0)
	Mean (SD)	5.7 (6.4)	4.0 (5.0)	6.5 (9.0)	13.7 (17.3)	6.0 (5.4)
Il1A	Median (IQR)	0.01 (1.9)	0.4 (22.4)	5.6 (206.4)	0.3 (203.3)	0.2 (0.6)
	Mean (SD)	258.8 (683.8)	64.8 (160.4)	410.5 (946.9)	98.6 (185.3)	26.9 (70.6)
Il1B	Median (IQR)	0.1 (0.2)	0.1 (0.6)	0.1 (0.2)	0.1 (0.2)	0.01 (0.1)
	Mean (SD)	0.2 (0.2)	0.4 (0.6)	0.1 (0.2)	0.1 (0.1)	0.1 (0.1)
CXCL8	Median (IQR)	0.1 (0.2)	0.01 (0.8)	0.1 (0.2)	0.1 (0.2)	0.1 (0.2)
	Mean (SD)	0.2 (0.3)	0.7 (1.3)	0.6 (1.3)	0.2 (0.3)	0.1 (0.2)
MUC4	Median (IQR)	6.5 (23.4)	11.2 (130.0)	1.2 (30.8)	15.0 (21.5)	6.6 (20.2)
	Mean (SD)	19.2 (30.4)	68.1 (90.1)	31.9 (66.3)	18.2 (25.0)	24.8 (49.3)
MUC16	Median (IQR)	1.0 (5.7)	0.9 (2.3)	0.8 (1.3)	0.9 (3.5)	2.8 (4.6)
	Mean (SD)	2.3 (2.8)	1.3 (1.2)	1.3 (1.7)	1.7 (2.1)	2.2 (2.4)

PTGS2, prostaglandin-endoperoxide synthase 2; PTPRC, protein tyrosine phosphatase receptor type C; CEACAM1, carcinoembryonic antigen related cell adhesion molecule 1; IL1A, interleukin 1 alpha; IL1B, interleukin 1 beta; CXCL8, C-X-C motif chemokine ligand 8; MUC4, mucin 4; MUC16, mucin 16.

DISCUSSION

In the course of an inflammatory process, cells of the immune system synthesize a broad range of pro-inflammatory factors. The mRNA expression of certain cytokines and glycoproteins are dependent on the health status of the bovine endometrium, the stage of the estrus cycle and anatomical sections of the uterus (15–17). This study aimed to provide new information

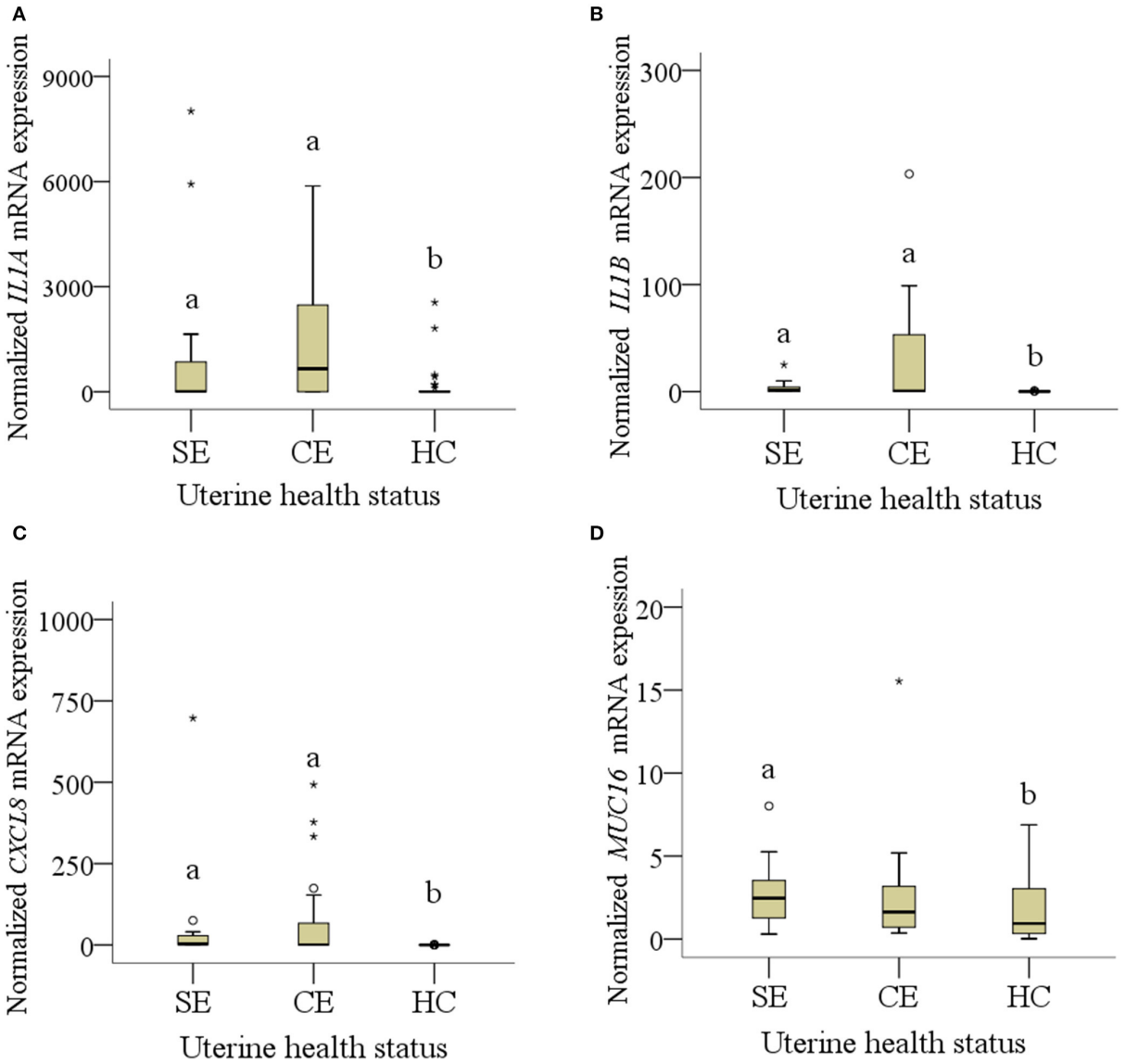

FIGURE 1 | (A–D): mRNA expression of normalized **(A)** *IL1A*, **(B)** *IL1B*, **(C)** *CXCL8* and **(D)** *MUC16* collected from four cows (20 samples) with subclinical endometritis (SE), seven cows (31 samples*) with clinical endometritis (CE) and seven (35 samples) healthy cows (HE). In CE, four samples were missing because of failed cytobrush sampling. Only diagrams showing significant results of pro-inflammatory factors and mucins are presented. Different letters indicate significant differences between groups: a:b < 0.05. The circle mean outliers and asterisks mean extreme outliers (values).

about the inflammatory response at different sites of the uterus and for cows with different uterine health status at the end of the postpartum period, i.e., when the regeneration of the epithelium is supposed to be completed. Our hypothesis was that on a molecular level, clinical endometritis is characterized by inflammatory responses spread over the entire endometrium, whereas subclinical endometritis is described by an inflammation of local regions of the uterus. The results of the multi-site comparison between the mRNA expressions of the selected transcripts, however, did not support our hypothesis since the variation of mRNA expression was independent from uterine health status. In this study, we analyzed a limited number of factors. Our selection was based on previous studies and represented factors associated with uterine disorders. In further research, the inflammatory response on molecular level should be investigated including more transcripts, additional signs of uterine inflammation as well as cow-specific factors, such as stage of lactation, parity, and the previously pregnant and non-pregnant uterine horns.

The mRNA expression at different uterine sites has hardly been investigated. Gabler et al. (16) reported first information showing no region-dependent mRNA expression for different PGE synthases and ILs comparing the *corpus uteri*, the ipsilateral, and contralateral horn from uterine tissues collected

TABLE 4 | Oneway ANOVA of the coefficient of variation (CV) for the normalized mRNA expression of selected transcripts in five pre-defined endometrial sites obtained from seven cows with clinical endometritis (CE), four with subclinical endometritis (SE), and seven healthy control cows (HC) on days 28 to 34 postpartum.

Factor	Group	Mean	SD	SEM	CI lower bound	CI upper bound	*P*
PTGS2	CE	1.2	0.6	0.2	0.659	1.827	0.26
	SE	0.94	0.2	0.1	0.693	1.192	
	HC	0.7	0.4	0.1	0.417	1.109	
PTPRC	CE	0.8	0.5	0.2	0.372	1.197	0.83
	SE	0.8	0.4	0.2	0.107	1.452	
	HC	0.6	0.2	0.1	0.431	0.867	
CEACAM1	CE	0.7	0.3	0.1	0.454	1.042	0.73
	SE	0.6	0.2	0.1	0.263	0.972	
	HC	0.7	0.2	0.1	0.475	0.937	
IL1A	CE	1.1	0.6	0.2	0.552	1.670	0.82
	SE	1.4	0.7	0.3	0.339	2.413	
	HC	1.3	0.7	0.3	0.676	1.932	
IL1B	CE	1.2	0.41	0.1	0.802	1.503	0.75
	SE	1.2	0.7	0.4	0.105	2.373	
	HC	1.0	0.4	0.1	0.676	1.378	
CXCL8	CE	1.3	0.4	0.2	0.929	1.752	0.60
	SE	1.3	0.5	0.21	0.487	2.045	
	HC	1.1	0.4	0.2	0.703	1.439	
MUC4	CE	0.8	0.6	0.2	0.295	1.339	0.40
	SE	1.1	0.3	0.2	0.568	1.661	
	HC	0.7	0.5	0.2	0.220	1.162	
MUC16	CE	0.6	0.3	0.1	0.339	0.877	0.94
	SE	0.6	0.2	0.1	0.280	0.842	
	HC	0.6	0.2	0.1	0.426	0.739	

Mean, standard deviation (SD), and standard error of the mean (SEM) of CV. Lower and upper bound of confidence interval (CI) and P-value of multiple comparison (Scheffe test). PTGS2, prostaglandin-endoperoxide synthase 2; PTPRC, protein tyrosine phosphatase receptor type C; CEACAM1, carcinoembryonic antigen related cell adhesion molecule 1; IL1A, interleukin 1 alpha; IL1B, interleukin 1 beta; CXCL8, C-X-C motif chemokine ligand 8; MUC4, mucin 4; MUC16, mucin 16.

at the abattoir. Bauersachs et al. (17) identified a couple of genes with lower expression in the *corpus uteri* of healthy heifers after slaughtering, but the majority of transcripts were similar expressed across the uterine horns. In our study, mRNA expression was not different, but overall, the results indicate a high variation of mRNA expression of selected factors at the five different sites. Interleukin 1 beta is contributing to inflammatory processes by stimulating the production of *CXCL5* and by activating vascular endothelial cells to promote migration of neutrophils (20, 21). C-X-C motif chemokine ligand 8 is responsible for recruitment of PMN (22), which may explain the higher abundance in endometric cows.

In agreement with other studies (15, 23, 24), the mRNA expression of *IL1A*, *IL1B*, and *CXCL8* was increased in cows showing signs of CE and SE compared with healthy control cows. These results indicate the immune-modulating response of *IL*s to infections. In the present study, the mRNA expression of *MUC16* was more abundant in SE compared with healthy cows. In contrast, Wagener et al. (25) found higher *MUC16* mRNA expression in the follicular phase of subfertile and healthy cows. Mucins are protective glycoproteins for epithelial tissues against bacterial invasion (26), therefore, an upregulation in endometric cows with SE can be expected.

This study provides some new aspects of inflammatory reactions in the bovine endometrium on a molecular level and contributes to our understanding of uterine pathologies. In addition, multi-site sampling and analysis of pro-inflammatory factors may be used to improve or validate the diagnosis of endometritis.

DATA AVAILABILITY STATEMENT

The raw data supporting the conclusions of this article will be made available by the authors, without undue reservation.

ETHICS STATEMENT

The animal study was reviewed and approved by Ethik- und Tierschutzkommission, University of Veterinary Medicine, Vienna, Austria. Written informed consent was obtained from the owners for the participation of their animals in this study.

AUTHOR CONTRIBUTIONS

HP: first author, contributed in sampling and writing the manuscript. PF: Contributed in laboratory work. AT: mastermind

of statistical analyses, contributed to Materials and Methods. CG: supervisor of laboratory work, contributed to study design and Materials and Methods. MD: last author, mastermind of study design, supervising the manuscript. All authors contributed to the article and approved the submitted version.

ACKNOWLEDGMENTS

The authors like to acknowledge the support of the farm manager, the veterinarians, and the employees of the VetFarm Kremesberg, as well as Christoph Holder, Institute for Veterinary Biochemistry, Freie Universität Berlin.

SUPPLEMENTARY MATERIAL

The Supplementary Material for this article can be found online at: https://www.frontiersin.org/articles/10.3389/fvets.2021.649758/full#supplementary-material

Supplementary Table 1 | Gene transcript, primer sequences and annealing temperature used for real-time PCR with subsequently resulting amplicon length.

REFERENCES

1. Cheong SH, Nydam DV, Galvão KN, Crosier BM, Gilbert RO. Cow-level and herd-level risk factors for subclinical endometritis in lactating Holstein cows. *J Dairy Sci.* (2011) 94:762–70. doi: 10.3168/jds.2010-3439
2. Dubuc J, Duffield TF, Leslie KE, Walton JS, LeBlanc SJ. Effects of postpartum uterine diseases on milk production and culling in dairy cows. *J Dairy Sci.* (2011) 94:1339–46. doi: 10.3168/jds.2010-3758
3. Gilbert RO, Shin ST, Guard CL, Erb HN, Frajblat M. Prevalence of endometritis and its effects on reproductive performance of dairy cows. *Theriogenology.* (2005) 64:1879–88. doi: 10.1016/j.theriogenology.2005.04.022
4. Bergqvist A, Bruse C, Carlberg M, Carlström K. Interleukin 1β, interleukin-6, and tumor necrosis factor-α in endometriotic tissue and in endometrium. *Fertil Steril.* (2001) 75:489–95. doi: 10.1016/S0015-0282(00)01752-0
5. Romagnani P, Lasagni L, Annunziato F, Serio M, Romagnani S. CXC chemokines: the regulatory link between inflammation and angiogenesis. *Trends Immunol.* (2004) 25:201–9. doi: 10.1016/j.it.2004.02.006
6. LeBlanc SJ. Interactions of metabolism, inflammation, and reproductive tract health in the postpartum period in dairy cattle. *Reprod Domest Anim.* (2012) 47:18–30. doi: 10.1111/j.1439-0531.2012.02109.x
7. Cai TQ, Weston PG, Lund LA, Brodie B, McKenna DJ, Wagner WC. Association between neutrophil functions and periparturient disorders in cows. *Am J Vet Res.* (1994) 55:934–43.
8. Pascottini OB, LeBlanc SJ. Modulation of immune function in the bovine uterus peripartum. *Theriogenology.* (2020) 150:193–200. doi: 10.1016/j.theriogenology.2020.01.042
9. Kasimanickam R, Duffield TF, Foster RA, Gartley CJ, Leslie KE, Walton, et al. S. et al. A comparison of the cytobrush and uterine lavage techniques to evaluate endometrial cytology in clinically normal postpartum dairy cows. *Canadian Vet J.* (2005) 46:255–9.
10. Barlund CS, Carruthers TD, Waldner CL, Palmer CW. A comparison of diagnostic techniques for postpartum endometritis in dairy cattle. *Theriogenology.* (2008) 69:714–23. doi: 10.1016/j.theriogenology.2007.12.005
11. Melcher Y, Prunner I, Drillich M. Degree of variation and reproducibility of different methods for the diagnosis of subclinical endometritis. *Theriogenology.* (2014) 82:57–63. doi: 10.1016/j.theriogenology.2014.03.003
12. De Boer MW, LeBlanc SJ, Dubuc J, Meier S, Heuwieser W, Arlt, et al. et al. Invited review: systematic review of diagnostic tests for reproductive-tract infection and inflammation in dairy cows. *J Dairy Sci.* (2014) 97:3983–99. doi: 10.3168/jds.2013-7450
13. Pothmann H, Müller J, Pothmann I, Tichy A, Drillich M. Reproducibility of endometrial cytology using cytobrush technique and agreement for the diagnosis of subclinical endometritis between five predefined endometrial sites. *Reprod Domest Anima.* (2018) 54:350–7. doi: 10.1111/rda.13367
14. Gabler C, Fischer C, Drillich M, Einspanier R, Heuwieser W. Time-dependent mRNA expression of selected pro-inflammatory factors in the endometrium of primiparous cows postpartum. *Reprod Biol Endocrin.* (2010) 8:152. doi: 10.1186/1477-7827-8-152
15. Peter S, Michel G, Hahn A, Ibrahim M, Lubke-Becker A, Jung, et al. Puerperal influence of bovine uterine health status on the mRNA expression of pro-inflammatory factors. *J Physiol Pharmacol.* (2015) 66:449–62.
16. Gabler C, Drillich M, Fischer C, Holder C, Heuwieser W, Einspanier R. Endometrial expression of selected transcripts involved in prostaglandin synthesis in cows with endometritis. *Theriogenology.* (2009) 71:993–1004. doi: 10.1016/j.theriogenology.2008.11.009
17. Bauersachs S, Ulbrich SE, Gross K, Schmidt SEM, Meyer HHD, Einspanier, et al. et al. Gene expression profiling of bovine endometrium during the oestrous cycle: Detection of molecular pathways involved in functional changes. *J Mol Endocrinol.* (2005) 34:889–908. doi: 10.1677/jme.1.01799
18. Sheldon IM, Lewis GS, LeBlanc JS, Gilbert RO. Defining postpartum uterine disease in cattle. *Theriogenology.* (2006) 65:1516–30. doi: 10.1016/j.theriogenology.2005.08.021
19. Madoz LV, Giuliodori MJ, Jaureguiberry M, Plöntzke J, Drillich M, de la Sota RL. The relationship between endometrial cytology during estrous cycle and cutoff points for the diagnosis of subclinical endometritis in grazing dairy cows. *J Dairy Sci.* (2013) 96:4333–9. doi: 10.3168/jds.2012-6269
20. Dinarello CA. The IL-1 family and inflammatory diseases. *Clin Exp Rheumatol.* (2002) 20:1–3.
21. Williams MA, Cave CM, Quaid G, Solomkin JS. Chemokine regulation of neutrophil function in surgical inflammation. *Arch Surg.* (1999) 134:1360–6. doi: 10.1001/archsurg.134.12.1360
22. Hoc RC, Schraufstätter IU, Cochrane CG. *In vivo*, *in vitro*, and molecular aspects of interleukin-8 and the interleukin-8 receptors. *Lab Clin Med.* (1996) 128:134–45. doi: 10.1016/S0022-2143(96)90005-0
23. Fischer C, Drillich M, Odau S, Heuwieser W, Einspanier R, Gabler C. Selected pro-inflammatory factor transcripts in bovine endometrial epithelial cells are regulated during the oestrous cycle and elevated in case of subclinical or clinical endometritis. *Reprod Fert Develop.* (2010) 22:818–29. doi: 10.1071/RD09120
24. Galvão KN, Santos NR, Galvão JS, Gilbert RO. Association between endometritis and endometrial cytokine expression in postpartum Holstein cows. *Theriogenology.* (2011) 76:290–9. doi: 10.1016/j.theriogenology.2011.02.006
25. Wagener K, Pothmann H, Prunner I, Peter S, Erber R, Aurich, et al. Endometrial mRNA expression of selected pro-inflammatory factors and mucins in repeat breeder cows with and without subclinical endometritis. *Theriogenology.* (2017) 90:237–44. doi: 10.1016/j.theriogenology.2016.12.013
26. Pluta K, McGettigan PA, Reid CJ, Browne JA, Irwin JA, Tharmalingam, et al. Molecular aspects of mucin biosynthesis and mucus formation in the bovine cervix during the periestrous period. *Physiol Genomics.* (2012) 44:1165–78. doi: 10.1152/physiolgenomics.00088.2012

Conflict of Interest: The authors declare that the research was conducted in the absence of any commercial or financial relationships that could be construed as a potential conflict of interest.

frontiers in Veterinary Science

ORIGINAL RESEARCH
published: 08 March 2021
doi: 10.3389/fvets.2021.641553

Differential Signals From TNFα-Treated and Untreated Embryos in Uterine Tissues and Splenic CD4$^+$ T Lymphocytes During Preimplantation Pregnancy in Mice

*Katarzyna Buska-Mach[1], Anna Ewa Kedzierska[1], Adam Lepczynski[2], Agnieszka Herosimczyk[2], Małgorzata Ozgo[2], Pawel Karpinski[1,3], Agnieszka Gomulkiewicz[4], Daria Lorek[1], Anna Slawek[1], Piotr Dziegiel[4] and Anna Chelmonska-Soyta[1,5]**

[1] Hirszfeld Institute of Immunology and Experimental Therapy, Polish Academy of Sciences, Wrocław, Poland, [2] Department of Physiology, Cytobiology and Proteomics, West Pomeranian University of Technology, Szczecin, Poland, [3] Department of Genetics, Wroclaw Medical University, Wrocław, Poland, [4] Department of Human Morphology and Embryology, Wroclaw Medical University, Wrocław, Poland, [5] The Faculty of Veterinary Medicine, Wroclaw University of Environmental and Life Sciences, Wrocław, Poland

OPEN ACCESS

Edited by:
Dariusz Jan Skarzynski,
Institute of Animal Reproduction and Food Research (PAS), Poland

Reviewed by:
Juan G. Maldonado-Estrada,
University of Antioquia, Colombia
Deqiang Miao,
Washington State University, United States
Stefan Cikos,
Institute of Animal Physiology (SAS), Slovakia

***Correspondence:**
Anna Chelmonska-Soyta
anna.soyta@upwr.edu.pl

Specialty section:
This article was submitted to Animal Reproduction - Theriogenology, a section of the journal Frontiers in Veterinary Science

Received: 14 December 2020
Accepted: 12 February 2021
Published: 08 March 2021

Citation:
Buska-Mach K, Kedzierska AE, Lepczynski A, Herosimczyk A, Ozgo M, Karpinski P, Gomulkiewicz A, Lorek D, Slawek A, Dziegiel P and Chelmonska-Soyta A (2021) Differential Signals From TNFα-Treated and Untreated Embryos in Uterine Tissues and Splenic CD4$^+$ T Lymphocytes During Preimplantation Pregnancy in Mice. Front. Vet. Sci. 8:641553. doi: 10.3389/fvets.2021.641553

The main aim of this study was to examine if a female mouse body in preimplantation pregnancy can distinguish between embryos of normal and impaired biological quality in the local and peripheral compartments. Normal (control group) and TNFα (tumor necrosis factor-α)-treated embryos (experimental group) at the morula stage were non-surgically transferred into the uteri of CD-1 strain [Crl:CD1(Icr)] female murine recipients. Twenty-four hours after the embryo transfer, females were euthanised, and uteri and spleens were dissected. In uterine tissues (local compartment), we assessed the expression of 84 genes comprising nine signal transduction pathways, using a modified RT² Profiler PCR Array. In the spleen (peripheral compartment), we determined the proteome of splenic CD4$^+$ lymphocytes using 2D protein electrophoresis with subsequent protein identification by mass spectrometry. Sample clustering and differential gene expression analyses within individual signal transduction pathways revealed differential expression of genes in the uteri of females after transplantation of normal vs. TNFα-treated embryos. The most affected signal transduction cascade was the NFKB (Nuclear factor NF-kappa-B) pathway, where 87.5% of the examined genes were significantly differentially expressed. Proteomic analysis of splenic CD4$^+$ T lymphocytes revealed significant differential expression of 8 out of 132 protein spots. Identified proteins were classified as proteins influenced by cell stress, proteins engaged in the regulation of cytoskeleton stabilization and cell motility, and proteins having immunomodulatory function. These results support the hypothesis that even before embryo implantation, the body of pregnant female mice can sense the biological quality of an embryo both at the local and peripheral level.

Keywords: embryo, TNF, uterus, pregnancy, CD4 lymphocytes, preimplantation, proteome, T cells

INTRODUCTION

The maternal recognition of the embryo is essential during implantation for the establishment of pregnancy and its maintenance. During the preimplantation period of the pregnancy paracrine signaling is the main way of interaction between the mother and the embryo. At this time, the uterine mucosa is strongly influenced by steroid hormones, which change the secretory activity of the endometrium and ensures optimal development of the embryo (1–3). On the other hand, the presence of an embryo in the uterus itself modulates the metabolism of endometrial tissue by influencing the expression of genes involved primarily in tissue remodeling and immunological processes (3). The presence of the embryo in the uterus before implantation is also signaled outside the tissues of the reproductive system. This process is particularly marked in cells of the immune system (4, 5). Additionally, recent work by Behura et al. (6) showed that the expression of genes of the receptors and their ligands in uterine and brain tissues at the preimplantation period of pregnancy is related. The mechanism of signal transmission from the uterus to the brain remains unknown. On the other hand, the neural connections of the sympathetic and parasympathetic systems and the sensory fibers with immune cells at the periphery indicate that signal transmission between distant compartments of the body may be guided by neurochemical conduction (7). The functional significance of these links needs further investigation. Nevertheless, it can be assumed that the early embryo-uterine-immune and nervous system interaction underlie the fundamental mechanisms of pregnancy maintenance, including fetal immune tolerance (4, 8), and also still not the well-recognized mechanism of brain control of early pregnancy.

During the pre-implantation phase not only embryo recognition takes place. It is a moment of critical decisions that are being made by a pregnant female: continuation of gestation or its rejection. In humans, pregnancy rejection could be expressed by the incidence of early embryo death and pregnancy loss and is estimated to constitute ∼30% of known pregnancies (9). A similar phenomenon is observed in pigs and cattle, where approximately 30% of early pregnancies are lost (10, 11). This high embryo death rate before implantation signifies the result of an intensive embryo selection process. This process is dependent on mutual interactions between the mother and embryo, and its dysfunction leads to the survival of unwanted embryos with low biological competence. In turn, this situation results in an increased abortion rate in more advanced stages of pregnancy (12). Therefore, proper assessment of the biological competence of an embryo by the pregnant female is critical for avoiding an unnecessary energy investment and maternal stress associated with pregnancy failure. The preimplantation embryos manifest their presence both in local and peripheral compartments of the immune system. Our previous work has shown that locally, in the uterus, the presence of the embryo before implantation selectively affects the murine gene expression regulated by signal transduction pathways. In the majority of signaling pathways in pregnant female mice compared to females in pseudopregnancy down-regulation of the uterine gene expression was observed (13). Our results are similar to those reported by other authors, who have shown that normal pregnancies modulate gene expression in the endometrium before the trophoblastic invasion (14–20). It is worth noting that gene expression of some signaling pathways in horses, pigs, and cattle, mainly those induced by interferons, is conservative, which indicates common mechanisms of pregnancy recognition in mammals (21). Existing studies have revealed that *in vitro* cultured human decidual cells can distinguish the biological quality of embryos (12). Therefore, it is suggested that human decidua may act as a natural biosensor of the developmental potential of pregnancy. Although an early foeto–maternal dialogue in the uterus is well-documented, the recognition and response of the maternal peripheral immune system to the presence of fetal antigens remains unknown. It is still debated whether maternal peripheral leukocytes' awareness of conceptus antigens is an important event for the establishment of a pregnancy-related immune alteration. Nevertheless, peripheral Th1/Th2 switch during pregnancy and diminished frequency of transgenic T lymphocytes specific for male H-Y antigens in pregnant females with male fetuses indicate pregnancy-induced immunomodulation (22). This observation points to the ability of lymphocytes to recognize pregnancy-related antigens at the periphery. Moreover, in BALB/c females mated with transgenic males that express a green fluorescent protein (GFP) the presence of GFP DNA was confirmed in the spleen, blood, and some maternal organs beginning on 0.5 days *post coitum* (dpc). GFP expression was under the control of the β-actin promoter (homozygous, C57BL/6 background). This observation is another evidence, which confirms the presence of paternal antigens in maternal tissues during early pregnancy (23) and suggests the possibility of their immune recognition. Besides, our previous work showed that splenic antigen-presenting cells (APCs) change their costimulatory phenotype in preimplantation pregnancy (24, 25). Also, we revealed that the presence of a preimplantation embryo changes the proteome of splenic T $CD4^+$ lymphocytes in pregnant female mice compared to pseudopregnant mice (26). These examples support the hypothesis that the maternal peripheral immune system recognizes early pregnancy and is able to adjust its immunophenotype to a new semi-allogeneic antigen challenge. On the other hand, in the preimplantation period of abortion-prone pregnancy (CBA/J♀xDBA/2J♂), significant differences in the frequency of female splenic regulatory T lymphocytes are observed in comparison to normal pregnancies (27). This finding suggests that the process of development of peripheral immune tolerance is different during the early stages of normal and compromised pregnancy.

Here, we studied the expression of genes related to uterine pathways of signal transduction and protein expression in peripheral lymphocytes in female recipients of normal and TNFα-treated embryos. TNFα has adverse effects on early embryonic development. It induces stable phosphatidylserine redistribution in the plasma membrane of embryos. Phosphatidylserine redistribution is believed to be an early signal in the process of apoptosis. It also significantly increases the incidence of apoptotic cells in blastocyst (28). However,

TNFα-treated embryos continued their development to the stage of the hatched blastocyst. What is important is that after the transfer into recipient mice, TNFα pre-treated blastocysts got implanted at approximately the same rate as control embryos did (28). Nevertheless, the rate of resorption among fetuses after exposure to this cytokine increased significantly (28, 29). Therefore, TNFα-treated embryos can be described as developmentally compromised, yet implantation-competent.

Taking into consideration all the aforementioned mechanisms of early recognition of preimplantation pregnancy, we wondered whether TNFα-treated embryos with a compromised developmental potential may signal their presence differently from normal embryos under *ex vivo* conditions both in the local and peripheral compartment. For this purpose, we screened the expression of uterine genes involved in signal transduction pathways (local compartment) and protein expression in splenic lymphocytes (peripheral compartment) in female recipients of normal or TNFα-treated embryos.

MATERIALS AND METHODS

Animals

Outbred CD-1 [Crl:CD1(Icr)] mice purchased from Charles River Laboratories (Sulzfeld, Germany) were housed under specific pathogen-free (SPF) conditions on a dark–light cycle 12:12. All surgical procedures were performed under isoflurane anesthesia and meloxicam analgesia. Every effort was made to minimize the animals' suffering. All the animal experiments were approved by the Local Ethics Committee for Experiments on Animals at the Hirszfeld Institute of Immunology and Experimental Therapy in Wroclaw (approval No. 41/2010).

We studied two groups of femal mice ($n = 10$ in each group): after non-surgical transfer of normal embryos (NE) or TNFα-treated embryos (TNE).

Female Embryo Donors and Collection of Embryos

Embryo donors were 4–6 weeks old super ovulated female mice. Superovulation was induced by two intraperitoneal injections. First- 5 IU of pregnant mare serum gonadotropin (Folligon, Intervet, Poland) and 46 h later 5 IU of human chorionic gonadotropin (Chorulon, Intervet, Poland). Six hours after the last injection, females were mated with males (of previously confirmed fertility). The day when the vaginal plug was observed was designated as 0 dpc (days *post coitum*). At 1 day of pregnancy, the embryo donor mice were euthanised, and the uteri with oviducts and ovaries were dissected. The oviducts and uteri were checked for the presence of embryos by uterine flushings under microscopic examination on a heating table. Embryos were collected into 400 μL of warm embryo-manipulation medium M2 (Sigma, Poland). From one superovulated female mouse, on average 32 ± 9 embryos were flushed. A layout of the entire experiment is presented in **Figure 1**.

Embryo Culture and TNFα Treatment

On the day of collection (1 dpc), morphologically normal embryos (2-cell stage embryos) were pooled from 2 to 3 female donors and randomly distributed into two groups: normal (control) embryos and TNFα-treated embryos. Each drop of the medium contained 8–10 embryos. Collected embryos from the first group were then cultured at 37°C in 30 μL microdrops of the M16 medium (Sigma, Poland) under mineral oil in the atmosphere containing 5% of CO_2, whereas embryos from the second group were cultured in drops with the addition of 50 ng/ml mouse recombinant TNFα (Sigma Poland). Embryos from both the experimental and control group were used in the experiments on developmental progress, phosphatidylserine expression, and embryo transfer.

Developmental Progress Assessment of Normal and TNFα-Treated Embryos

Collected embryos (1 dpc) of both groups were cultured as indicated above and inspected under a stereoscopic microscope at 1, and 3 dpc. The numbers of 2-cell embryos (arrested), 3–5-cell embryos, and >5-cell embryos (morula) were determined at each examination. Then morulae were selected and washed 10 times in fresh constitutive changes of M2 medium drops, transferred to a fresh M16 medium, and then observed for two consecutive days, i.e., 3 and 4 dpc. The numbers of morulae, blastocysts, and hatched blastocysts were determined on each day of observations.

Phosphatidylserine Expression in TNFα-Treated Embryos

Collected embryos (1 dpc) of both groups were cultured up to the morula stage as indicated in section Embryo Culture and TNFα Treatment. Randomly selected morulae from both groups of embryos ($n = 10$) were stained with annexin V and propidium iodide (Annexin-V-FLUOS Staining Kit, Roche Diagnostics, Poland) to confirm the expression of phosphatidylserine as an early sign of apoptosis induction in blastomeres in embryos (28, 30). Briefly, the embryos were transferred to freshly prepared and preheated microdrops of PBS supplemented with Ca^{2+} Mg^{2+}, supplemented with bovine serum albumin (BSA; Sigma, Poland). The embryos were washed three times, each time in a fresh microdrop of PBS (100 μL). Afterward, they were stained at room temperature for 10 min with the Annexin-V-FLUOS (Sigma, Poland) solution reagent with the addition of propidium iodide (20 μL of working-strength solution). After that, the embryos were washed in 10 μL microdrops of fresh PBS with Ca^{2+} Mg^{2+}. Before the evaluation under a fluorescence microscope (Leica), the embryos were transferred into microdrops of fresh PBS with the addition of an anti-fade solution (Sigma, Poland). The observations were performed immediately after completed staining.

Female Embryo Recipients and Embryo Transfer

Prior to the transfer of embryos, the oestrous cycle of 6- to 8-week-old recipient females was controlled by Cytocolor staining (MerckMilipore) of vaginal smears. The females in the proestrus phase (before an oestrous phase, in which ovulation takes place) were mated with vasectomised males to induce

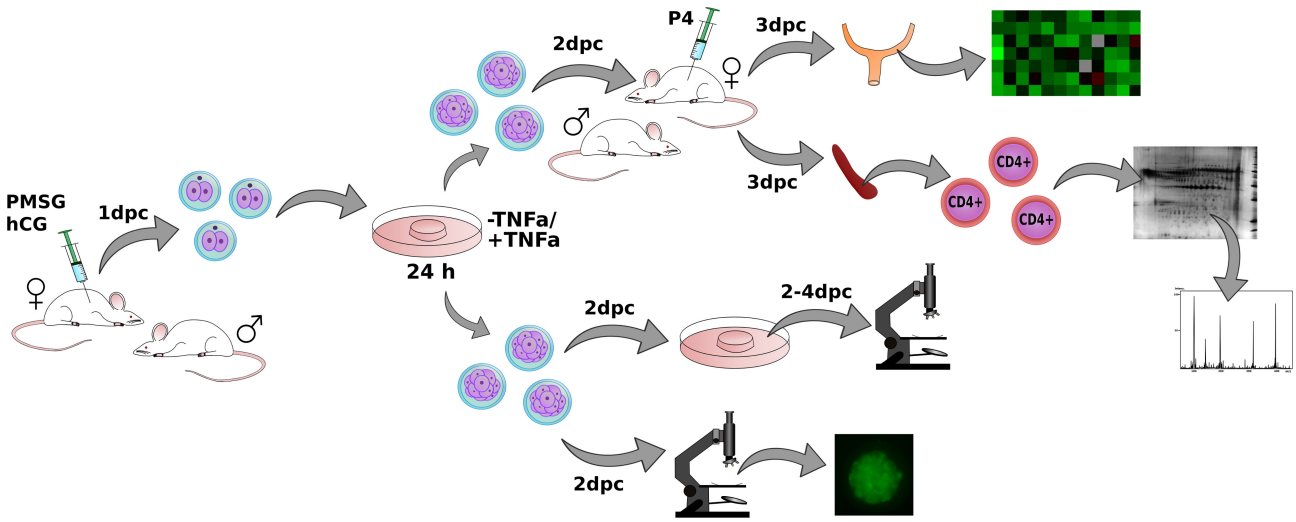

FIGURE 1 | The layout of the entire experiment. Female mouse donors were superovulated by PMSG (Pregnant Mare Serum Gonadotropin) and hCG (human Choriogonadotropin) injections and mated with fertile males. Embryos were collected at the 1st day *post-coitum* (dpc) and cultured for the next 24 h in the presence or without TNFα. Embryos were transferred into progesterone-treated and mated with vasectomized males, female recipients. Uteri and spleens from recipient females were dissected. Gene expression and proteome of $CD4^+$ lymphocytes were examined in obtained tissues. A separate group of embryos was examined *in vitro* for checking the developmental progress and phosphatidylserine expression.

pseudopregnancy (3). The successful mating was confirmed by the presence of the vaginal plug and was designated as day 0 of pseudopregnancy. At 0 and 1 dpc, the recipient females were treated with a subcutaneous supply of progesterone P4 (Sigma, Poland) at a dose of 0.2 mg per 100 µl per animal to reduce uterine contractions and to prevent the expulsion of transferred material (31).

Embryos from the control and experimental group designated for transfer were cultured for 24 h, i.e., until 2 dpc as indicated in section Embryo Culture and TNFα Treatment. Then, they were carefully washed 10 times in a sequence of fresh warm M2 medium drops. Only morulae with the best morphological score (evenly sized blastomeres with a smooth profile) were selected and subdivided into groups of embryos designated for transfer to female recipient mice. In total 400 embryos (200 in each group) were transferred into recipient females.

At 2 dpc of pseudopregnancy, non-surgical embryo transfer of normal embryos or TNFα-treated embryos was performed using an NSET® Device (ParaTechs, USA). The procedure was performed on females without anesthesia, by inserting the catheter into one of the uterine horns (through the vagina) and with the expulsion of 20 embryos (in 1.8 µl of medium M16) per mouse, according to the manufacturer's instructions. To restrict stressful conditions connected with handling and catheter insertion, overall manipulation time not exceeded 10–20 s. The whole procedure was performed in silence without the presence of bystanders.

At 24 h after the embryo transfer, at 3 dpc, the female recipients were euthanised, and spleens and uteri were dissected. The uteri were analyzed for the presence of embryos (successful transfer confirmation) by uterine flushings under microscopic examination. For further investigation only pregnant (embryo containing) whole uterine horns were preserved. The dissected spleens were preserved for subsequent isolation of $CD4^+$ T cells. Dissected uteri were cut and sampled randomly for subsequent RNA isolation and gene expression experiments.

RNA Isolation and cDNA Synthesis

Collected uterine horns were homogenized and total RNA was isolated as previously described (13). Isolated total RNA was purified using the RNeasy Mini Kit (Qiagen, USA) with an additional step of DNase digestion (DNase I, Qiagen, USA). The resulting RNA (from each group) was combined into three pools consisting of RNA samples from 3, 3, and 4 uteri, respectively. Total RNA (∼1 µg from each uterus) was transcribed to cDNA with the use of RT^2 First Strand Kit (Qiagen, USA). Obtained cDNA was further used for the uterine preimplantation transcriptome investigation.

Real-Time PCR

Real-time PCR was carried out using the SensiFAST SYBR Hi-ROX Kit (Bioline Ltd., Blirt, Poland) and an ABI StepOnePlus Thermal Cycler System (Applied Biosystems) as previously described (13). In brief, custom RT^2 Profiler PCR Arrays (SABioscience, USA) used for real-time PCR ($n = 3$ for each group) were designed as previously explained (13). Each array allowed us to identify most relevant genes belonging to 9 signaling pathways: the NFKB pathway, TGFB pathway, P53 pathway, Mitogenic pathway, NOTCH pathway, LDL pathway, WNT pathway, Hedgehog pathway, and JAK–STAT pathway (**Table 1**). Array used for these experiments, enables analysis of the expression of 84 downstream genes responsive to activation or inhibition of signal transduction pathway. Each array included primers for target genes and a panel of reference genes.

TABLE 1 | The list of 84 analyzed genes (divided into nine signaling pathways) and their relative expression levels in groups TNE and NE as measured by a real-time PCR array.

Gene symbol	GeneBank	Gene description	$2^{-\Delta Ct}$ TNE group	Standard deviation TNE	$2^{-\Delta Ct}$ NE group	Standard deviation NE	Fold change $2^{-\Delta Ct}$ TNE/$2^{-\Delta Ct}$ NE
NFKB pathway							
Birc3	NM_007464	Baculoviral IAP repeat-containing 3	**0.0053**	**1.72E-05**	***0.0103***	**0.00009**	**0.51**
Cxcl1	NM_008176	Chemokine (C-X-C motif) ligand 1	**0.0002**	**1.31E-05**	***0.0011***	**0.00014**	**0.18**
Icam1	NM_010493	Intercellular adhesion molecule 1	0.0079	0.000961	0.0088	0.00389	0.9
Il2	NM_008366	Interleukin 2	0.0000	2.1E-08	0.0000	0.00001	0
Myd88	NM_010851	Myeloid differentiation primary response gene 88	**0.0023**	***0.000201***	**0.0013**	**0.00024**	**1.77**
Nfkbia	NM_010907	Nuclear factor of kappa light polypeptide gene enhancer in B cells inhibitor, α	**0.0334**	**0.000166**	**0.0481**	**0.00213**	**0.69**
Nos2	NM_010927	Nitric oxide synthase 2, inducible	**0.0027**	**5.69E-05**	***0.0011***	**0.00002**	**2.45**
Stat1	NM_009283	Signal transducer and activator of transcription 1, transcript variant 2	**0.0134**	**0.000453**	**0.00353**	**0.0187**	**3.8**
Vcam1	NM_011693	Vascular cell adhesion molecule 1	**0.0011**	**3.81E-05**	**0.0021**	**0.00010**	**0.52**
TGFB pathway							
Atf4	NM_009716	Activating transcription factor 4	0.0309	0.00083	0.0586	0.01619	0.53
Cdkn1a	NM_007669	Cyclin-dependent kinase inhibitor 1A (P21), transcript variant 1	0.0013	0.000137	0.0016	0.00012	0.81
Cdkn1b	NM_009875	Cyclin-dependent kinase inhibitor 1B	0.0235	0.001351	0.0199	0.00044	1.18
Cdkn2a	NM_009877	Cyclin-dependent kinase inhibitor 2A, transcript variant 1	0.0002	2.43E-05	0.0004	0.00015	0.5
Cdkn2b	NM_007670	Cyclin-dependent kinase inhibitor 2B (p15, inhibits CDK4)	0.0010	0.00018	0.0010	0.00007	1
Id1	NM_010495	Inhibitor of DNA binding 1	0.0226	0.003536	0.0274	0.00110	0.82
Id2	NM_010496	Inhibitor of DNA binding 2	0.0440	0.000839	0.0457	0.00370	0.96
Myc	NM_010849	Myelocytomatosis oncogene, transcript variant 1	0.0226	0.000277	0.0331	0.01068	0.68
Sox4	NM_009238	SRY (sex determining region Y)-box 4	**0.0014**	**7.33E-05**	**0.0009**	**0.00014**	**1.56**
P53 pathway							
Bax	NM_007527	BCL2-associated X protein	0.0145	0.001641	0.0173	0.00006	0.84
Cdkn1a	NM_007669	Cyclin-dependent kinase inhibitor 1A (P21). transcript variant 1	0.0013	0.000137	0.0016	0.00012	0.81
Egfr	NM_007912	Epidermal growth factor receptor. transcript variant 2	0.0019	0.000246	0.0246	0.01164	0.08
Fas	NM_007987	Fas (TNF receptor superfamily member 6)	0.0057	0.001815	0.0075	0.00453	0.76
Gadd45a	NM_007836	Growth arrest and DNA-damage-inducible 45 alpha	0.0097	0.001188	0.0085	0.00021	1.14
Pcna	NM_011045	Proliferating cell nuclear antygen	0.0511	0.000501	0.0539	0.00594	0.95
Rb1	NM_009029	Retinoblastoma 1	0.0051	0.000255	0.0054	0.00035	0.94
Tnf	NM_013693	Tumor necrosis factor	0.0002	8.15E-05	0.0005	0.00031	0.4
Trp53	NM_011640	Transformation related protein 53, transcript variant 1	**0.0073**	**6.79E-05**	**0.0089**	**0.00002**	**0.82**
Mdm2	NM_010786	Transformed mouse 3T3 cell double minute 2, transcript variant 1	**0.0135**	**0.000672**	**0.0171**	**0.00004**	**0,79**
Igfbp3	NM_008343	Insulin-like growth factor binding protein 3	0.1362	0.057531	0.0606	0.00524	2.25
Atf2	NM_009715	Activating transcription factor 2, transcript variant 2	0.0199	0.002011	0.0217	0.00132	0.92
Bax	NM_007527	BCL2-associated X protein	0.0145	0.001641	0.0173	0.00006	0.84
MITOGENIC pathway							
Egr1	NM_007913	Early growth response 1	0.0171	0.000259	0.0246	0.01164	0.7
Egfr	NM_007912	Epidermal growth factor receptor, transcript variant 2	0.0019	0.000246	0.0017	0.00001	1.12
Fos	NM_010234	FBJ osteosarcoma oncogene	0.0057	0.001815	0.0075	0.00453	0.76
Jun	NM_010591	Jun proto-oncogene	0.0188	0.000799	0.0231	0.00711	0.81
Nab2	NM_008668	Ngfi-A binding protein 2, transcript variant 1	0.0004	0.00019	0.0006	0.00012	0.67
Map3k1	NM_011945	Mitogen-activated protein kinase kinase kinase 1	0.0033	2.92E-05	0.0044	0.00062	0.75
Map3k2	NM_011946	Mitogen-activated protein kinase kinase kinase 2	0.0100	0.00062	0.0132	0.00179	0.76
Mapk1	NM_011949	Mitogen-activated protein kinase 1, transcript variant 1	0.0425	0.003356	0.0436	0.00033	0.97
Mapk3	NM_011952	Mitogen-activated protein kinase 3	0.0281	0.001653	0.0271	0.00196	1.04
Map2k1	NM_008927	Mitogen-activated protein kinase kinase 1	0.0111	0.001117	0.0099	0.00150	1.12

(Continued)

TABLE 1 | Continued

Gene symbol	GeneBank	Gene description	$2^{-\Delta Ct}$ TNE group	Standard deviation TNE	$2^{-\Delta Ct}$ NE group	Standard deviation NE	Fold change $2^{-\Delta Ct}$ TNE/$2^{-\Delta Ct}$ NE
Map2k2	NM_023138	Mitogen-activated protein kinase kinase 2	0.0016	9.83E-05	0.0021	0.00047	0.76
Atf2	NM_009715	Activating transcription factor 2, transcript variant 2	0.0199	0.002011	0.0217	0.00132	0.92
Trp53	NM_011640	Transformation related protein 53, transcript variant 1	**0.0073**	**6.79E-05**	**0.0089**	**0.00002**	**0.82**
NOTCH pathway							
Ccnd1	NM_007631	Cyclin D1	0.0201	0.002465	0.0342	0.01177	0.59
Cd44	NM_009851	CD44 antigen, transcript variant 1	0.0285	0.00288	0.0413	0.01007	0.69
Hes1	NM_008235	Hairy and enhancer of split 1 (Drosophila)	0.0071	0.000701	0.0152	0.00414	0.47
Hes5	NM_010419	Hairy and enhancer of split 5 (Drosophila)	0.0004	6.81E-06	0.0003	0.00014	1.33
Hey1	NM_010423	Hairy/enhancer-of-split related with YRPW motif 1	0.0018	1.92E-05	0.0016	0.00013	1.13
Hey2	NM_013904	Hairy/enhancer-of-split related with YRPW motif 2	0.0008	1.21E-05	0.0008	0.00013	1
Id1	NM_010495	Inhibitor of DNA binding 1	0.0226	0.003536	0.0274	0.00110	0.82
Jag1	NM_013822	Jagged 1	0.0110	0.001173	0.0142	0.00150	0.77
Il2ra	NM_008367	Interleukin 2 receptor, alpha chain	0.0004	4.78E-06	0.0004	0.00008	1
Notch1	NM_008714	Notch 1	0.0043	0.000661	0.0039	0.00112	1.1
Ppard	NM_011145.3	Peroxisome proliferator activated receptor delta	0.0018	0.000179	0.0017	0.00017	1.06
Pparg	NM_011146	Peroxisome proliferator activated receptor gamma, transcript variant 2	**0.0006**	**3.34E-05**	**0.0007**	0.00002	0.86
LDL patway							
Ccl2	NM_011333	Chemokine (C-C motif) ligand 2	0.0028	0.000353	0.0131	0.00875	0.21
Csf1	NM_001113529	Colony stimulating factor 1	0.0030	0.000419	0.0055	0.00278	0.55
Csf2	NM_009969	Colony stimulating factor 2 (granulocyte-macrophage)	0.0002	2.41E-05	0.0003	0.00000	0.67
Sele	NM_011345	Selectin, endothelial cell	0.0009	2.45E-05	0.0009	0.00009	1
Selp	NM_011347	Selectin, platelet	0.0031	5.59E-05	0.0032	0.00056	0.97
Vcam1	NM_011693	Vascular cell adhesion molecule 1	**0.0011**	**3.81E-05**	**0.0021**	**0.00010**	**0.52**
WNT patway							
Axin2	NM_015732	Axin2	0.0066	0.000882	0.0082	0.00153	0.8
Birc5	NM_009689	Baculoviral IAP repeat-containing 5, transcript variant1	0.0190	0.000796	0.0136	0.00227	1.4
Ccnd1	NM_007631	Cyclin D1	0.0201	0.002465	0.0342	0.01177	0.59
Ccnd2	NM_009829	Cyclin D2	0.0133	0.000735	0.0160	0.00200	0.83
Cdh1	NM_009864	Cadherin 1	0.0100	0.000315	0.0110	0.00368	0.91
Jun	NM_010591	Jun proto-oncogene	0.0188	0.000799	0.0231	0.00711	0.81
Lef1	NM_010703	Lymphoid enhancer binding factor 1, transcript variant 1	0.0090	0.000215	0.0075	0.00225	1.2
Myc	NM_010849	Myelocytomatosis oncogene, transcript variant 1	0.0226	0.000277	0.0331	0.01068	0.68
Pparg	NM_011146	Peroxisome proliferator activated receptor gamma, transcript variant 2	**0.0006**	**3.34E-05**	**0.0007**	**0.00002**	**0.86**
Tcf7	NM_009331	Transcription factor 7, T cell specific	0.0065	0.000102	0.0075	0.00083	0.87
Vegfa	NM_009505	Vascular endothelial growth factor A, transcript variant 2	**0.0138**	**2.42E-06**	**0.0191**	**0.00146**	**0.72**
Wisp1	NM_018865	WNT1 inducible signaling pathway protein 1	**0.0028**	**0.000233**	**0.0039**	**0.00016**	**0.72**
HEDGEHOG pathway							
Bcl2	NM_009741	B cell leukemia/lymphoma 2, transcript variant 1	0.0095	4.77E-06	0.0100	0.00192	0.95
Bmp2	NM_007553	BZne morphogenetic protein 2	0.0008	0.000125	0.0012	0.00032	0.67
Bmp4	NM_007554	Bone morphogenetic protein 4	0.0047	6.82E-05	0.0068	0.00176	0.69
Foxa2	NM_010446	Forkhead box A2, transcript variant 2	0.0008	3.07E-05	0.0007	0.00027	1.14
Hhip	NM_020259	Hedgehog-interacting protein	0.0017	0.000204	0.0016	0.00049	1.06
Ptch1	NM_008957	Patched homolog 1	0.0076	0.000214	0.0071	0.00056	1.07
Wnt2	NM_023653	Wingless-type MMTV integration site family, member 2	0.0002	4.67E-06	0.0003	0.00001	0.67
Wnt5a	NM_009524	Wingless-type MMTV integration site family, member 5A, transcript variant 1	**0.0246**	**0.002775**	**0.0337**	**0.00140**	**0.73**
Wnt6	NM_009526	Wingless-type MMTV integration site family, member 6	0.0005	0.000164	0.0006	0.00002	0.83

(Continued)

TABLE 1 | Continued

Gene symbol	GeneBank	Gene description	$2^{-\Delta Ct}$ TNE group	Standard deviation TNE	$2^{-\Delta Ct}$ NE group	Standard deviation NE	Fold change $2^{-\Delta Ct}$ TNE/$2^{-\Delta Ct}$ NE
JAK/STAT pathway							
Cxcl9	NM_008599	Chemokine (C-X-C motif) ligand 9	**0.0001**	**6.72E-05**	**0.0006**	**0.00025**	**0.17**
Ccnd1	NM_007631	Cyclin D1	0.0201	0.002465	0.0342	0.01177	0.59
Gata3	NM_008091	GATA binding protein 3	0.0010	1.48E-06	0.0010	0.00012	1
Il4ra	NM_001008700	Interleukin 4 receptor, Ralpha	0.0082	0.000112	0.0055	0.00146	1.49
Irf1	NM_008390	Interferon regulatory factor 1. transcript variant 1	0.0123	0.000843	0.0149	0.00041	0.83
Mmp10	NM_019471	Matrix metallopeptidase 10	0.0123	0.000843	0.0005	0.00021	24.6
Nos2	NM_010927	Nitric oxide synthase 2, inducible	**0.0027**	**5.69E-05**	**0.0011**	**0.00002**	**2.45**
Socs3	NM_007707	Suppressor of cytokine signaling 3	0.0063	0.000131	0.0046	0.00127	1.37
Crucial to implantation genes							
Hoxa10	NM_008263	Homeobox A10. transcript variant 1	0.1223	0.00938	0.1143	0.02479	1.07
Lif	NM_008501	Leukemia inhibitory factor, transcript variant 1	0.0015	0.000563	0.0008	0.00041	1.88
Ptgs2	NM_011198	Prostaglandin-endoperoxide synthase 2	0.0005	9.42E-05	0.0019	9.12E-05	0.25

Statistically significant differences (Student's t-test, n = 3) in gene expression are boldfaced; $p < 0.05$.

The panel consisted of 5 genes: glyceraldehyde 3-phosphate dehydrogenase (*Gapdh*), glucuronidase β (*Gusb*), hypoxanthine guanine phosphoribosyl transferase (*Hprt*), heat shock protein α family class B member 1 (*Hsp90ab1*), and beta actin (*Actb*). *Actb* was automatically designated to normalize PCR Array data according to manufacturer instructions and due to the most stable expression, as its threshold cycle (C_t) value did not differ by more than a factor of 0.5 between the arrays (data not shown). The transcriptome obtained in the experimental group was compared to that of the control group. Changes in the threshold cycle (ΔC_t) values were calculated for each gene by subtracting the mean threshold cycle (C_t) of the *Actb* reference gene from the threshold cycle value of a gene in question. The normalized quantity of transcripts was calculated as $2^{-\Delta Ct}$.

Unsupervised Clustering of RT-PCR Data

Unsupervised hierarchical clustering has been performed using ΔC_t as an input. The decision on the optimal number of sample clusters was made based on consensus partitioning implemented in the "cola" Bioconductor package. Partitioning was performed by use of hierarchical clustering. We tested a range of clusters (K) from 2 to 5 across increasing variable subsets (from "10" to "70" in 10 steps) with 20 repeats and random resampling of 80% of samples. Optimal K has been deduced based on inspection of plots generated by the "cola" package including PAC score, Shilouette score, Rand and Jaccard indexes.

$CD4^+$ T-Cell Isolation and Separation

A single-cell suspension of splenocytes was obtained by immediately squeezing the collected spleen through the cell strainer into an ammonium chloride solution (8.3 g/L) enabling erythrocyte lysis. Splenocytes were sorted using the EasySep™ Mouse $CD4^+$ T Cell Isolation Kit (StemCell™ Technologies). Flow-cytometric analysis involving staining with a fluorescein isothiocyanate (FITC)-conjugated anti-mouse CD4 antibody (eBioscience) confirmed the purity of the isolated cells. The average purity was 88.0% ± 5.01 of $CD4^+$ cells among all the isolated lymphocytes. The average concentration of isolated cells was $(3.5 \pm 2.45) \times 10^6$/ml [$(1.0–9.5) \times 10^6$ cells/ml per sorting]. Isolated $CD4^+$ cells were then separated for membrane lysis and protein separation by 2-dimensional electrophoresis (2-DE).

2-DE and Imaging

Sample preparation for 2-DE analysis was performed using the same procedure as previously described (26). Due to low protein content, 7 μg of each sample (two replicates of each individual) was used for the 2-DE separation. The isoelectric focusing (IEF) was carried out on 7 cm IPG strips with nonlinear pH interval 4–7 (Bio-Rad, USA) with the aid of the Protean® IEF Cell (Bio-Rad, USA) using the rapid protocol for the 7 cm strip (3,000 V, 50 μA, 15,000 Vh). Once separated by IEF, the strips were further incubated in the basal equilibration buffer (6 M urea, 0.5 M Tris/HCl pH 6.8, 2% w/v SDS, 30% w/v glycerol) with an addition of 1% (w/v) of dithiothreitol for 15 min. Next, the strips were placed in the same basal buffer with an addition of 2.5% (w/v) of iodoacetamide for another 20 min. After the equilibration process. The proteins covered with negatively charged SDS molecules were separated using SDS-PAGE on the 12% polyacrylamide gels using Protean Plus™ Dodeca Cell™ electrophoretic chamber (Bio-Rad, USA) at 100 V for 120 min at room temperature. Subsequently, gels with resolved proteins were visualized with silver stain according to Chevallet et al. (32). Gel images were digitalized using GS-800™ Calibrated Densitometer (Bio-Rad, USA). Then, protein spots expression patterns on digital images representing both control and experimental conditions were analyzed using PDQuest v. 8.0.1 Advanced (Bio-Rad, USA). The proteins spots that appeared on at least four gels representing the replicate group were further processed. The gel matching was performed on the basis of the master image protein spots distribution pattern. Normalized spots volumes were taken for the quantitative

analysis of the protein spots abundance. The experimental and intragroup variability was assessed as a coefficient of variation (CV%). The significance level (*P*-values below or equal to 0.05 were assumed to indicate significance) was used to select differentially expressed protein spots. The differences between the control and experimental groups were expressed as arithmetic mean and on that basis, fold change ratio was calculated. The molecular weights of protein spots were calculated against the Precision Plus Protein™ Standard Plugs (Bio-Rad, USA) mass ruler. Experimental *pI*s were calculated on the basis of pH gradient distribution of the IPG strips. The qualitative gels served as a source of protein spots harvested for protein identification. For this purpose, pooled protein samples (∼70 μg of lymphocyte total protein) were separated in 2 replicates. Protein spots detection was performed using colloidal Coomassie stain according to the methodology described by Pink et al. (33).

Mass Spectrometry

Significantly altered spots were manually excised from the preparative 2-D gels, destained and trypsin digested according to the protocol previously described by Chełmońska-Soyta et al. (15). The obtained peptide mixtures were then extracted from the gel pieces with 100% acetonitrile (ACN). Next, the equal volumes (1:1 μl) of peptide mixtures and CHCA matrix solution (5 mg/ml α-cyano-4-hydroxy-cinnamic acid, 0.1% v/v trifluoroacetic acid in 50% v/v ACN) were deposited on the targets of MALDI-MSP AnchorChip™ 600/96 plate (Bruker Daltonics, Germany). External calibration within the peptides mass range between 700 and 3,200 Da was performed using peptide mass standard II (Bruker Daltonics, Germany). Mass spectra acquisition was carried out in the positive ionization with reflection mode using Microflex™ MALDI TOF mass spectrometer (Bruker Daltonics, Germany). Peptide mass lists were compared with *in silico* protein digestion data deposited in the protein sequence databases (NCBI and Uniprot) using MASCOT search engine. The following query criteria were applied: cysteine modification, methionine oxidation, 150 ppm peptide mass tolerance, one trypsin missed cleavage site. Probabilistic scoring algorithm was used to assess the significance of protein identification followed by the minimal 20% of sequence coverage value. Determination of subcellular protein distribution was analyzed using Euk-mPLoc 2.0 (http://www.csbio.sjtu.edu.cn/bioinf/euk-multi-2/).

Statistical Analysis

Statistical analysis was carried out in the R program. Shapiro test was used to assess the shape of the data distribution. The Mann–Whitney test (non-parametric), Student's *t*-test, or χ^2 test (embryo developmental assessment) was performed based on the shape of the data distribution. Data with *P*-values below 0.05 were considered significant.

RESULTS

Embryo Development Assessment

The culture of collected embryos up to the morula stage in the presence of TNFα revealed no significant differences (χ^2 test, $p > 0.05$) in the development rate in comparison to untreated embryos (**Table 2**). To check the developmental competency of *in vitro*–obtained morulae, the embryos were examined at consecutive time points until the stage of the hatched blastocyst (4 dpc). The developmental rates of washed morulae were similar between the two groups of embryos (**Table 3**).

Phosphatidylserine Expression

As in our previous experiments (30), we confirmed the expression of phosphatidylserine using FITC-labeled Annexin V in all the examined TNFα-treated embryos, whereas it was not detectable in embryos of the control group. We did not observe PI staining in nuclei of examined embryos. In several TNFα-treated embryos, expression of phosphatidylserine was observed in single blastomeres; however, in most of the examined embryos, a uniform pattern of staining was recorded (**Figure 2**).

Real-Time PCR

Real-time PCR analysis resulted in significantly altered ($p < 0.05$) expression of 16 genes. The expression of 3 of these genes was up-regulated and the remaining 13 were down-regulated in the TNE group compared to the NE group. **Table 1** presents differentially expressed genes assigned to the nine selected pathways. All the statistically significant down-regulated genes belonged to eight out of nine investigated pathways [NFKB, WNT, Janus kinase (JAK)/Signal Transducer and Activator of Transcription (STAT), protein 53 (P53), HEDGEHOG, NOTCH, low-density lipoprotein (LDL), and MITOGENIC] with 43.8 and 18.7% belonging to NFKB and WNT pathways, respectively. Taking into consideration the number of significantly altered, i.e., down- and up-regulated genes in each pathway as compared to all the genes in the pathway, the most affected pathway was NFKB, with 87.5% of differentially expressed genes (**Table 1**). The percentage of differentially expressed genes in the remaining pathways ranged from 7.7% (Mitogenic pathway) to 25% (WNT pathway). In addition to the nine analyzed signaling pathways, three genes relevant to the preimplantation process were also analyzed: homeobox A10 (*Hoxa10*), leukemia inhibitory factor (*Lif*), and prostaglandin-endoperoxide synthase 2 (*Ptgs2*). The transfer of embryos cultured in the presence of TNFα caused a statistically significant decrease in *Ptgs2* ($p < 0.05$) gene expression in the TNE group in comparison with the NE group (**Table 1**).

Clustering Analysis

Unsupervised clustering reveals clear separation of NE and TNE groups, which confirms that TNFα-treated embryos influence the expression of selected genes (genes are grouped in 3 groups: highly expressed, intermediate expression, and low expression). Results of clustering and separation of NE and TNE groups are presented on the heatmap (**Figure 3**).

Consensus partitioning revealed $K = 2$ as the most stable number of clusters with clear inclusion of NE and TNE groups into separate clusters. Consequently, the separation of NE and TNE groups confirmed that TNFα influences the expression of selected genes.

TABLE 2 | The developmental rate of embryos collected from mice at 1 dpc and cultured *in vitro* for 24 h in the presence or absence of TNFα (χ^2 test $p \geq 0.05$).

	2-cell embryos (arrested)	3-5-cell embryos	>5-cell embryos (morula)
Normal embryos $n = 60$	7 (11.66%)	38 (63.33%)	15 (25%)
TNFα-treated embryos $n = 60$	11 (18.33%)	39 (65%)	10 (16.66%)

TABLE 3 | The developmental rate of morulae obtained at 2 dpc after completed cultivation of embryos in the presence or absence of TNFα. Compacted morulae were selected, washed 10 times, and transferred to a fresh culture medium and then examined on three consecutive days (χ^2 test $p \geq 0.05$).

	2 dpc morula	3 dpc blastocyst	4 dpc hatched blastocyst
Normal embryos $n = 30$	30 (100%)	29 (96.66%)	19 (63.33%)
TNFα-treated embryos $n = 30$	30 (100%)	28 (93.33%)	18 (60.00%)

Differentially Expressed Proteins of Splenic CD4$^+$ T Lymphocytes in Pregnant Females After the Transfer of Normal and TNFα-Treated Embryos

Proteins isolated from CD4$^+$ T lymphocytes-and obtained from female mice after the transfer of TNFα-treated and normal embryos-were subjected to 2-DE with subsequent mass spectrometric identification of spots showing statistically significant changes. A representative 2-DE map of the experimental groups is presented in **Figure 4**. As a result of the detection images of 2-DE gels, we revealed the presence of 135–157 protein spots. The coefficient of variation (CV) of the replication ratio in different groups was as follows: for group TNE, 66.28%; for group NE, 67.44%. Thirteen protein spots in lymphocytes of recipients of TNFα-treated embryos were found (using bioinformatics software) significantly altered in comparison with the control group (**Table 4**).

Detailed properties and functions of the identified proteins according to the Swiss-Prot database are listed in **Table 4**. The adjustment for all the identified proteins was higher in splenocytes isolated from animals after the transfer of the embryos exposed to TNFα. Out of the 8 proteins (represented by 13 protein spots including isoforms of 3 proteins) of differential expression, 7 showed up-regulation [HSP70 (2.84-fold), TPM3 (1.39-fold), IL-24 (1.92-fold), GDIR2 (2.26-fold), PRDX2 (1.39-fold), ATP5H (1.24-fold), SEMA7A (2.42-fold)], and one was down-regulated (LSP1: 0.51-fold). Protein spots with differential expression are marked on the protein map (**Figure 4**). A graphic trend for spots with differential expression is shown in **Figure 5**.

DISCUSSION

The embryo-maternal dialogue during preimplantation pregnancy still involves many unresolved issues. The processes crucial for the maintenance of pregnancy such as genetic abnormal embryo selection, early immune recognition (34), induction of split tolerance (35), and epigenetic modification of embryo gene expression (36), are still not well-understood or are debated. However, it is known that the maternal organism needs to make a quick decision about the fate of pregnancy, because maintaining a pregnancy with a low development potential may result in a miscarriage or low birth weight (37). We showed that TNFα-treated embryos transferred into the uterus of the recipient female mice induce differential signals in mother tissues in comparison with untreated embryos. According to Fabian et al. (28) and Kawamura et al. (38), mouse embryos can produce TNFα and they express the receptors for this cytokine. However, other papers have shown that embryos are sensitive to the increased concentration of TNFα in their vicinity (28, 29). Embryos responded to higher levels of this cytokine by increased blastomeres' apoptosis and decreased proportion of implanted blastocyst. However, based on microscopical observation, such TNFα treatment did not compromise *in vitro* development of mice embryos until the blastocyst stage. On the other hand, an increased concentration of TNFα changed their metabolism by inducing a transient process of apoptosis. Thus, both metabolic changes and impaired implantation signals may influence the process of maternal recognition of TNFα-treated embryos despite the fact of natural production of TNFα by embryos *per se*. In this paper, we confirmed apoptosis induction and unchanged *in vitro* developmental potential of TNFα-treated embryos. Here, we utilize two different methodological approaches for the detection of early embryonic signals. The descriptive analysis showed us that both in local and peripheral compartment embryos of differential biological quality are differentially recognized.

To gain insight into the differences between the expression of genes regulated by all signal transduction pathways, data from all expressed genes in the uteri of NE and TNE groups were used in the cluster analysis. The obtained heatmap clearly suggests differential expression of examined genes between samples of two studied groups. Thus, at the preimplantation stage of pregnancy, a mother can distinguish the differential biological potential of developing embryos at the local level. Moreover, it is worth noting that the majority of examined genes were of low or moderate expression level. This confirms our previous observation on negative regulation of the expression of genes regulated by pathways of signal transduction in the murine uterus in preimplantation pregnancy (13). Similar observations were performed in bovine species where at the 6th and 13th day of normal pregnancy the majority of uterine genes with differential expression compared to non-pregnant females were down-regulated (20). On the other hand, in studies on the endometrial transcriptional activity at the 18th and 20th day of pregnancy, transferred cloned bovine embryos, which are characterized by limited biological potential, differently stimulated the transcriptional activity of genes in the uterus in compared to normal pregnancy. The majority of influenced genes are mainly involved in the immune response and metabolism (17, 39). Direct comparison with studies focusing on endometrial response cannot be considered, as here we

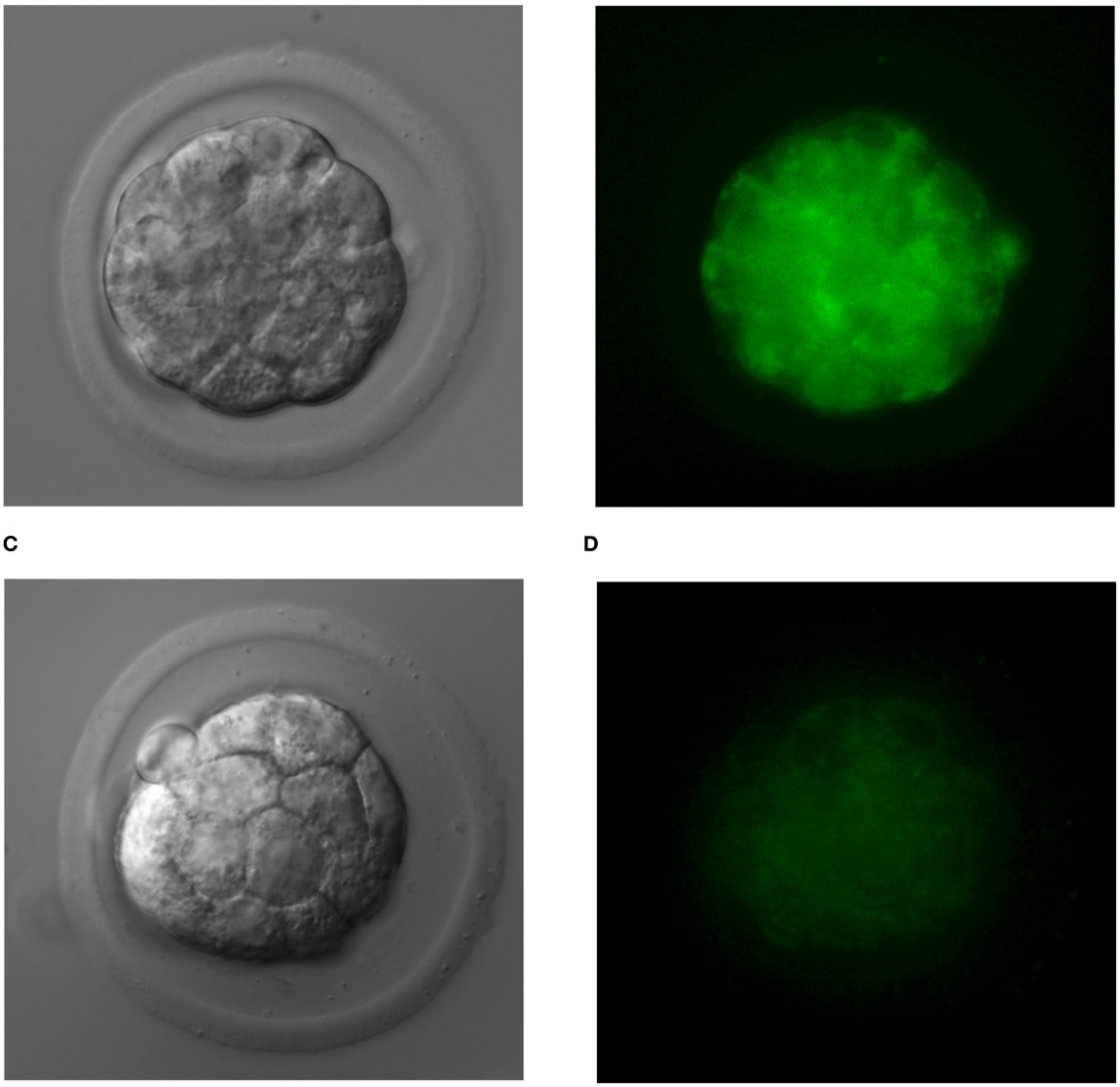

FIGURE 2 | The uniform pattern of phosphatidylserine expression in blastomeres of TNFα-treated embryos **(A,B)** and normal embryos **(C,D)**.

analyzed transcriptome from the whole uterus, which could be some limitation of our study. Future studies utilizing separated uterine layers would be beneficial to explore in which tissues gene expression alteration was mostly driven by the presence of TNFα-treated embryos.

Here, we have shown that among the nine analyzed signal transduction pathways, the NFKB pathway (with 87.5% of differentially expressed genes) was the most consistently down-regulated. The involvement of the NFKB pathway in the activity of uterine cells in the peri-implantation period of pregnancy is not well-explored. Nakamura et al. showed that in the pregnant uterus, the NF-kB DNA-binding activity is detectable at 1.5 dpc, and further strengthened and reached a peak at 6.5 dpc, when the implantation of the conceptus is completed (40). The NFKB pathway is regulated in various cells (epithelial, stromal, and immune cells) both by exogenous and endogenous ligands. This pathway could be activated in different manners: canonical, non-canonical, and atypical (41–43). Among the genes regulated by the canonical pathway, statistically, significant differences in expression of *Nfkbia* (Nucleus polypeptide gene enhancer in B cells inhibitor, α), *Myd88* (myeloid differentiation primary response gene 88), *Stat1* (transcript variant 2), and *Nos2* (nitric oxide synthase 2, inducible) were observed. Among the genes regulated by the non-canonical pathway: *Birc3* (baculoviral IAP repeat-containing 3), *Cxcl1* [chemokine (C-X-C motif) ligand 1], *Vcam1*, and *Nos2* showed differential expression between the examined groups. The increased expression of the *Myd88* gene in mice is evenly distributed in the uterine luminal epithelium

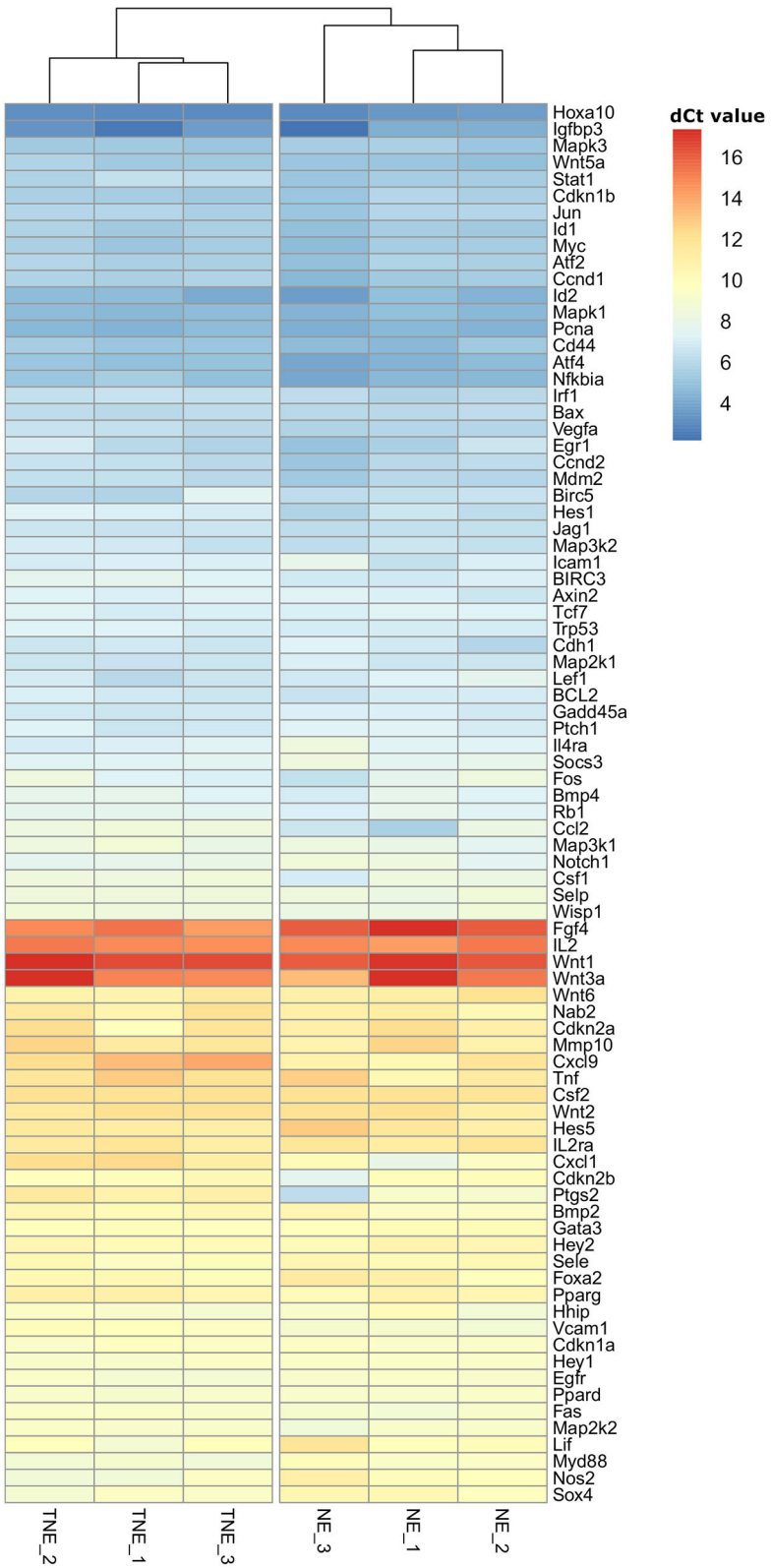

FIGURE 3 | Hierarchical clustering heatmap of mRNA transcripts of nine signal transduction pathways differentially expressed in recipients' uteri of normal (NE) and TNFα- (TNE) treated embryos. Gene expression level is color coded.

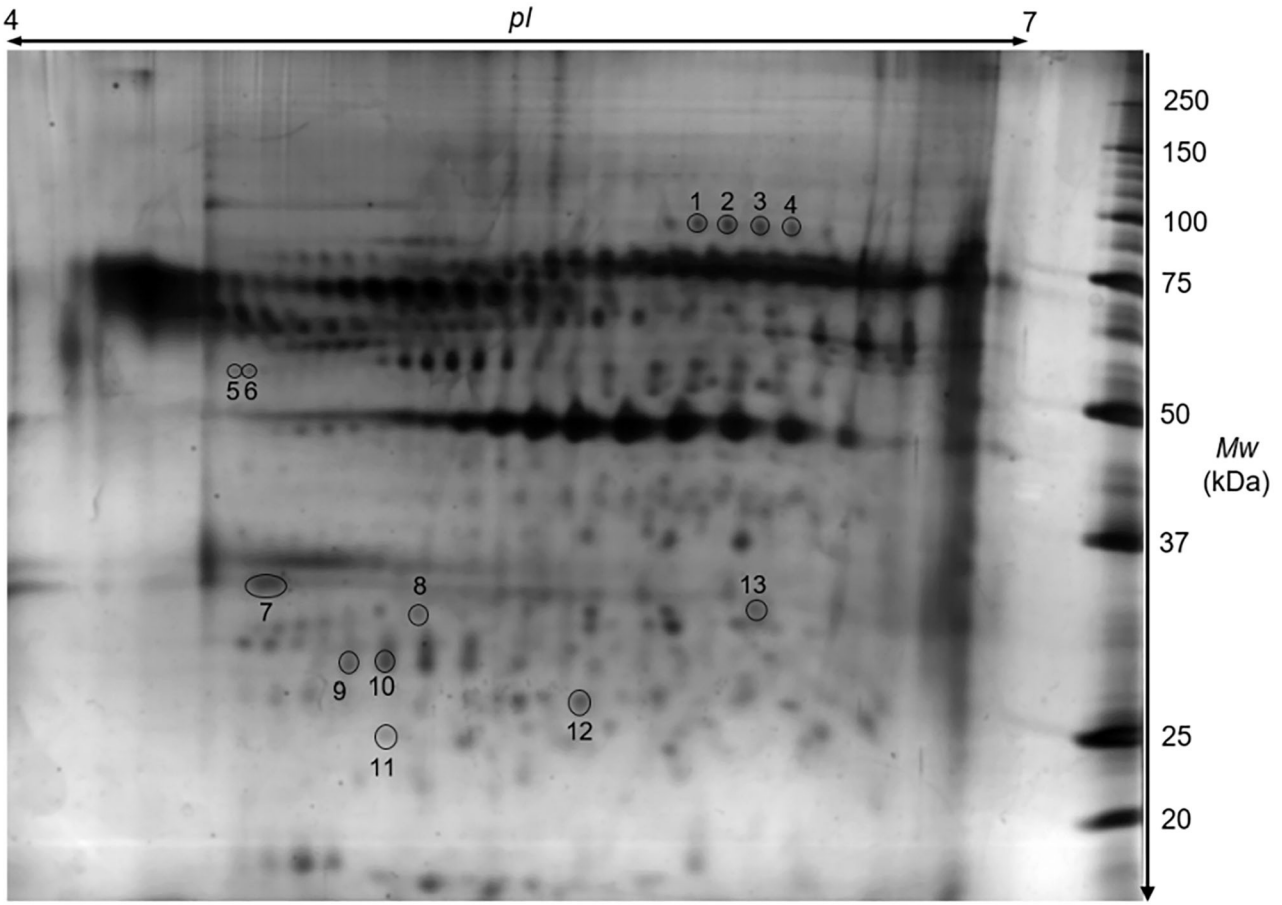

FIGURE 4 | A representative proteomic 2D map of splenic $CD4^+$ T cells. The 2-DE gel illustrates a Coomassie-stained protein pattern. Spot numbers correspond to the numbers in **Table 4**.

on day 4 of pregnancy, but its expression was not detected at 2 and 3 dpc (16). This result is consistent with our observation in a previous experiment in which uterine expression of *Myd88*, in natural pregnancy, at 3.5 dpc before implantation did not differ from that in pseudopregnant mice (13). In the present study, significantly increased expression of genes *Myd88* and *Nos2* and decreased expression of the *Nfkbia* pathway inhibitor suggests activation of the canonical pathway.

On the other hand, expression of genes mainly regulated by the non-canonical pathway was down-regulated in the uteri of mice after transplantation of TNFα-treated embryos. Decreased expression of genes of chemokine ligand *Cxcl1* and the *Vcam1* adhesion molecule suggests that the traffic of immune cells within the preimplantation pregnant uterus may be differentially regulated in recipients of normal and TNFα-treated embryos. Additionally, the NFKB pathway has control over the pregnancy implantation window, which is manifested by the regulation of recognition and maintenance factors like *Lif*, *Ptgs2*, and *Hoxa10*, which are essential for pregnancy (44). In our experiments, activation of the NFKB pathway did not correlate with the expression of genes *Lif* and *Hoxa-10*, although there was a correlation with diminished expression of *Ptgs2*. Prostaglandin 2 synthase (PTGS2, encoded by *Ptgs2*) expression is detectable during pregnancy in mice in the luminal epithelium and stroma at the time of blastocyst implantation (45), and even in the preimplantation period, i.e., 3.5 dpc (3). The blastocyst presence is a determinant of the induction of *Ptgs2* during pregnancy before implantation (46, 47). Thus, TNFα treated embryos may provoke differential regulation of gene expression of this importance, for the process of implantation, molecule. We believe that results of our study showing differential gene expression presumably influenced by the embryo biological potential, will bring new insight to the field of early embryo-maternal dialogue. Notwithstanding, due to the limitations resulting from the small sample number ($n = 3$ pooled uterine material), the results presented in **Table 1** should be considered as indicative and further in depth studies should be performed.

Similar to the aforementioned local response, the maternal peripheral immune system is sensitive to the presence of a developing embryo. Several previous results obtained in mice, humans and ruminants indicated that peripheral leukocytes changed their phenotype during preimplantation pregnancy. During *in vitro* experiments with human pregnancy, β-human chorionic gonadotropin exerts an immunomodulatory effect on

TABLE 4 | The list of differentially expressed proteins of splenic $CD4^+$ T cells between mice after the transfer of TNFα-treated embryos in comparison to mice after the transfer of biologically competent embryos (Student's *t*-test $p \leq 0.05$).

No	Protein name	Protein abbreviation	Fold change	Accession number	Peptides matched	Sequence coverage (%)/mascot score	Theoretical pI/Mr (pH/kDa)	Calculated pI/Mr (pH/kDa)	Subcellular localization
1	Heat shock cognate 71kDa protein	HSP70	2.84	Q3U9G0	14	32/109	5.37/71.05	6.1/97.8	Nucleus
2			3.10		11	26/80	5.37/71.05	6.2/97.8	Nucleus
3			3.35		29	49/203	5.37/71.05	6.3/96.2	Nucleus
4			2.63		10	24/73	5.37/71.05	6.4/95.4	Nucleus
5	Lymphocyte – specific protein 1	LSP1	0.51	Q8CD28	8	36/68	4.77/36.81	4.7/56.6	Nucleus
6			0.59		8	35/70	4.77/36.81	4.7/56.6	Nucleus
7	Tropomyosin alpha-3 chain	TPM3	1.39	P21107	11	33/99	4.75/29.02	4.8/34.1	Cytoskeleton
8	Interleukin – 24	IL24	1.92	Q925S4	5	27/61	9.22/20.97	5.2/31.9	Extracellular
9	Rho GDP – dissociation inhibitor 2	GDIR2	2.26	Q61599	7	54/70	4.97/22.89	5.0/28.8	Cytoplasm
10			1.88		6	83/54	4.97/22.89	5.1/29.0	Cytoplasm
11	Peroxiredoxin – 2	PRDX2	1.39	Q61171	5	42/61	5.2/21.94	5.1/25.0	Cytoplasm/ Mitochondrion
12	ATP synthase subunit d, mitochondrial	ATP5H	1.24	Q9DCX2	6	50/59	5.52/18.79	5.9/28.2	Mitochondrion
13	Semaphorin – 7A	SEMA7A	2.42	Q9QUR8	12	22/59	7.83/75.97	6.2/32.2	Extracellular

peripheral blood lymphocytes by decreasing production of IFN-gamma and IL-2 and by increasing production of IL-10 (48, 49). On the other hand, the last experiments performed by Pflitsch et al. showed that blood monocytes from pregnant women can be distinguished from monocytes from non-pregnant women based on their phenotype. Moreover, monocyte surface molecules' expression was correlated with serum β-hCG level (50). In ruminants the effect of an embryo-derived early pregnancy signal - IFN-tau is also observed at the periphery. In heifers, on the 18th day of pregnancy increased expression of interferon-stimulated genes in peripheral leukocytes is related to pregnancy outcome (51, 52).

Here, we demonstrated that in mice, the proteome of splenic $CD4^+$ T lymphocytes is different in female recipients of normal embryos in comparison with recipients of TNFα-treated embryos. Proteins with altered expression were classified as (1) proteins influenced by cell stress, (2) those involved in the regulation of cytoskeleton stabilization and lymphocyte motility, and (3) proteins of an immunomodulatory function. Two cell stress–sensing proteins, i.e., heat-shock protein (HSP) and its isoforms and peroxiredoxin 2 (PRDX2), were significantly up-regulated after the transfer of TNFα-treated embryos. It is known that an increased amount of heat shock protein 70 (HSP70) in the lymphocytes (53) and high concentrations of anti-HSP70 antibodies in the serum of pregnant women are considered prognostic factors of a birth outcome, in particular, delivery of new-borns with birth defects (54). Therefore, increased expression of HSP70 in peripheral lymphocytes of females bearing TNFα-treated embryos confirmed the indicator role of this protein for a risky pregnancy. On the other hand, the observed enhanced expression of peroxiredoxin II ($p < 0.05$) in splenic T lymphocytes of recipients transferred with TNFα-treated embryos is suggestive for the importance of protection from oxidative stress (55). Moreover, injection of an anti-PRDX2 neutralizing antibody increases NK-cell cytotoxicity and raises the fetal absorption rate in an abortion-prone mouse model (56). Thus, alteration of the levels of HSP70 and PRDX2 in T lymphocytes of the TNE group indicates that cells beyond the reproductive tract are sensitive to stress-inducing signaling from impaired embryos at the preimplantation stage of pregnancy.

Transplantation of TNFα-treated embryos also up-regulated the proteins with immunoregulatory properties in the lymphocytes of female recipients, i.e., interleukin 24 (IL-24) and semaphorin 7a (SEMA7A). To our knowledge, we are the first to report IL-24 presence in peripheral T lymphocytes at such early stages of pregnancy. In murine models, IL-24 has been shown to down-regulate Th1 responses and to up-regulate Th2 responses, indicating its possible positive role in early pregnancy outcomes (57). However, the exact role of IL-24 in pregnancy needs to be proven. In the TNE group, the increased level of SEMA7A, which plays a critical role in the negative regulation of T-cell activation and function, may also point to the engagement of $CD4^+$ T cells in the response to embryo signals. It is not clear how the altered expression of the two above-mentioned proteins participates in the modulation of an immune response during preimplantation pregnancy after transplantation of impaired embryos. Nevertheless, it may be assumed that the peripheral immune system can differentially respond to the presence of low-quality embryos. Another group of proteins that showed expression changes in mice after the transfer of TNFα-treated

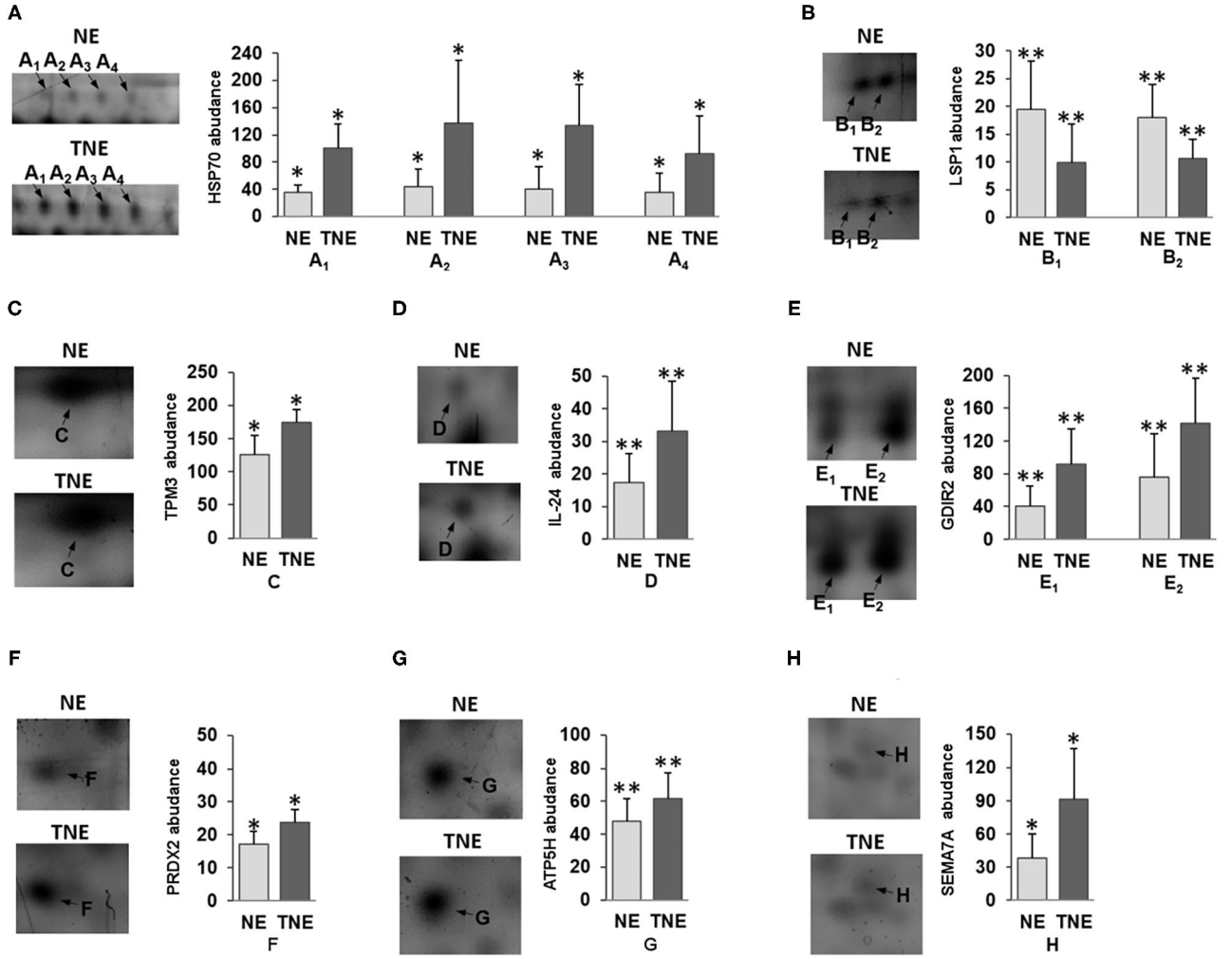

FIGURE 5 | The graphic trend for spots with a variable expression of **(A)** HSP70, **(B)** LSP1, **(C)** TPM3, **(D)** IL-24, **(E)** GDIR2, **(F)** PRDX2, **(G)** ATP5H and **(H)** SEMA7A proteins between TNE (dark gray bars) and NE group of mice (light gray bars). The data concerning the protein expression are given as arithmetic mean with SD (group $n = 6$). Student's t-test $^{*}p < 0.05$, $^{**}p < 0.01$.

embryos comprised: the α tropomyosin 3 chain (TPM3), dissociation inhibitor Rho-GDP 2 (GDIR2), ATP synthase d subunit (ATP5H), and protein specific for lymphocytes 1 (LSP1). As in our previous studies (26), we confirmed their differential expression in response to the presence of embryos of different quality. Therefore, the migration activity of splenic $CD4^+$ T lymphocytes may depend on the quality of the embryonic signal, especially during the development of the embryo under conditions of stress and the risk of pregnancy loss.

Taking into consideration all the aforementioned results, further studies should be performed to elucidate the influence of differential activation of proinflammatory signal transduction pathways locally in the uterus on the immunophenotype of peripheral lymphocytes and, most importantly, how it may influence on a maternal organism in deciding about the fate of pregnancy.

CONCLUSION

Our results suggest that the maternal organism can distinguish embryos with diverse developmental potentials already in the preimplantation period both in the local and peripheral compartment. Our study provides new insight into an embryo–maternal communication at the early stages of pregnancy. The nature of the signals capable of modulating cellular changes in distant compartments remains elusive, although it is tempting to speculate that these signals are generated differentially in response to normal and developmentally impaired embryos (58). We also suggest that peripheral lymphocytes in particular can serve as biological sensors of embryo quality upon implantation. Nevertheless, further detailed studies on the expression of activated proteins in signal transduction pathways, the significance of protein expression in $CD4^+$ lymphocytes

activity, and their mutual interactions during normal and compromised preimplantation pregnancy are needed.

DATA AVAILABILITY STATEMENT

The datasets presented in this study can be found in online repositories. The names of the repository/repositories and accession number(s) can be found here: Repository of the Wrocław University of Environmental and Life Sciences, Poland https://arche.upwr.edu.pl/index.php/s/OxfEzcZaMokEzdZ/download.

ETHICS STATEMENT

The animal study was reviewed and approved by Local Ethics Committee for Experiments on Animals at the Hirszfeld Institute of Immunology and Experimental Therapy in Wroclaw.

AUTHOR CONTRIBUTIONS

KB-M: conceptualization, methodology, investigation, and writing original draft. AK: methodology, visualization, investigation, and writing original draft. AL, AH, and MO: investigation and editing original draft. PK: visualization and writing-review and editing. AG, AS, and PD: methodology and writing-review and editing. DL: visualization and writing original draft. AC-S: conceptualization, resources, funding acquisition, and writing original draft. All authors have read and agreed to the published version of the manuscript.

FUNDING

This work was supported by the Polish National Research Centre (Grant No. NN311523940).

REFERENCES

1. Bazer FW, Wu G, Spencer TE, Johnson GA, Burghardt RC, Bayless K. Novel pathways for implantation and establishment and maintenance of pregnancy in mammals. *Mol Hum Reprod.* (2010) 16:135–52. doi: 10.1093/molehr/gap095
2. Wang H, Dey SK. Roadmap to embryo implantation: clues from mouse models. *Nat Rev Genet.* (2006) 7:185–99. doi: 10.1038/nrg1808
3. Forde N, Lonergan P. Transcriptomic analysis of the bovine endometrium: what is required to establish uterine receptivity to implantation in cattle? *J Reprod Dev.* (2012) 58:189–95. doi: 10.1262/jrd.2011-021
4. Saito S, Shima T, Nakashima A, Inada K, Yoshino O. Role of paternal antigen-specific treg cells in successful implantation. *Am J Reprod Immunol.* (2016) 75:310–6. doi: 10.1111/aji.12469
5. Ehrentraut S, Sauss K, Neumeister R, Luley L, Oettel A, Fettke F, et al. Human miscarriage is associated with dysregulations in peripheral blood-derived myeloid dendritic cell subsets. *Front Immunol.* (2019) 10:2440. doi: 10.3389/fimmu.2019.02440
6. Behura SK, Kelleher AM, Spencer TE. Regulation of uterine genes during the peri-implantation period, and its relationship to the maternal brain in gestating mice. *Mol Reprod Dev.* (2020) 87:482–92. doi: 10.1002/mrd.23338
7. Schiller M, Ben-Shaanan TL, Rolls A. Neuronal regulation of immunity: why, how and where? *Nat Rev Immunol.* (2021) 21:20–36. doi: 10.1038/s41577-020-0387-1
8. Clark DA, Rahmati M, Gohner C, Bensussan A, Markert UR, Chaouat G. Seminal plasma peptides may determine maternal immune response that alters success or failure of pregnancy in the abortion-prone CBAxDBA/2 model. *J Reprod Immunol.* (2013) 99:46–53. doi: 10.1016/j.jri.2013.03.006
9. Norwitz ER, Schust DJ, Fisher SJ. Implantation and the survival of early pregnancy. *N Engl J Med.* (2001) 345:1400–8. doi: 10.1056/NEJMra000763
10. Tayade C, Fang Y, Croy BA. A review of gene expression in porcine endometrial lymphocytes, endothelium and trophoblast during pregnancy success and failure. *J Reprod Dev.* (2007) 53:455–63. doi: 10.1262/jrd.18170
11. Reese ST, Franco GA, Poole RK, Hood R, Fernadez Montero L, Oliveira Filho RV, et al. Pregnancy loss in beef cattle: a meta-analysis. *Anim Reprod Sci.* (2020) 212:106251. doi: 10.1016/j.anireprosci.2019.106251
12. Teklenburg G, Salker M, Heijnen C, Macklon NS, Brosens JJ. The molecular basis of recurrent pregnancy loss: impaired natural embryo selection. *MHR Basic Sci Reprod Med.* (2010) 16:886–895. doi: 10.1093/molehr/gaq079
13. Buska K, Kedzierska AE, Slawek A, Chelmonska-Soyta A. Global decrease in the expression of signalling pathways' genes in murine uterus during preimplantation pregnancy. *Reprod Biol.* (2017) 17:89–96. doi: 10.1016/j.repbio.2017.01.003
14. Chen Y, Ni H, Ma X-H, Hu S-J, Luan L-M, Ren G, et al. Global analysis of differential luminal epithelial gene expression at mouse implantation sites. *J Mol Endocrinol.* (2006) 37:147–61. doi: 10.1677/jme.1.02009
15. Niklaus AL, Pollard JW. Mining the mouse transcriptome of receptive endometrium reveals distinct molecular signatures for the luminal and glandular epithelium. *Endocrinology.* (2006) 147:3375–90. doi: 10.1210/en.2005-1665
16. Pan H, Zhu L, Deng Y, Pollard JW. Microarray analysis of uterine epithelial gene expression during the implantation window in the mouse. *Endocrinology.* (2006) 147:4904–16. doi: 10.1210/en.2006-0140
17. Mansouri-Attia N, Sandra O, Aubert J, Degrelle S, Everts RE, Giraud-Delville C, et al. Endometrium as an early sensor of in vitro embryo manipulation technologies. *Proc Natl Acad Sci USA.* (2009) 106:5687–92. doi: 10.1073/pnas.0812722106
18. Walker CG, Meier S, Littlejohn MD, Lehnert K, Roche JR, Mitchell MD. Modulation of the maternal immune system by the pre-implantation embryo. *BMC Genomics.* (2010) 11:474. doi: 10.1186/1471-2164-11-474
19. Xiao S, Diao H, Zhao F, Li R, He N, Ye X. Differential gene expression profiling of mouse uterine luminal epithelium during periimplantation. *Reprod Sci.* (2014) 21:351–62. doi: 10.1177/1933719113497287
20. Binelli M, Scolari SC, Pugliesi G, Van Hoeck V, Gonella-Diaza AM, Andrade SCS, et al. The transcriptome signature of the receptive bovine uterus determined at early gestation. *PLoS ONE.* (2015) 10:e0122874. doi: 10.1371/journal.pone.0122874
21. Bauersachs S, Wolf E. Transcriptome analyses of bovine, porcine and equine endometrium during the pre-implantation phase. *Anim Reprod Sci.* (2012) 134:84–94. doi: 10.1016/j.anireprosci.2012.08.015
22. Tafuri A, Alferink J, Moller P, Hammerling GJ, Arnold B. T cell awareness of paternal alloantigens during pregnancy. *Science.* (1995) 270:630–3. doi: 10.1126/science.270.5236.630
23. Zenclussen ML, Thuere C, Ahmad N, Wafula PO, Fest S, Teles A, et al. The persistence of paternal antigens in the maternal body is involved in regulatory T-cell expansion and fetal-maternal tolerance in murine pregnancy. *Am J Reprod Immunol.* (2010) 63:200–8. doi: 10.1111/j.1600-0897.2009.00793.x
24. Slawek A, Maj T, Chelmonska-Soyta A. CD40, CD80, and CD86 costimulatory molecules are differentially expressed on murine splenic antigen-presenting cells during the pre-implantation period of pregnancy, and they modulate regulatory T-cell abundance, peripheral cytokine response, and pregnanc. *Am J Reprod Immunol.* (2013) 70:116–26. doi: 10.1111/aji.12108
25. Maj T, Slawek A, Chelmonska-Soyta A. CD80 and CD86 costimulatory molecules differentially regulate OT-II CD4(+) T lymphocyte proliferation and cytokine response in cocultures with antigen-presenting cells derived from pregnant and pseudopregnant mice. *Mediators Inflamm.* (2014) 2014:769239. doi: 10.1155/2014/769239

26. Chelmonska-Soyta A, Ozgo M, Lepczynski A, Herosimczyk A, Buska-Pisarek K, Kedzierska A, et al. Proteome of spleen CD4 lymphocytes in mouse preimplantation pregnancy. *J Physiol Pharmacol.* (2014) 65:719–31.
27. Thuere C, Zenclussen ML, Schumacher A, Langwisch S, Schulte-Wrede U, Teles A, et al. Kinetics of regulatory T cells during murine pregnancy. *Am J Reprod Immunol.* (2007) 58:514–23. doi: 10.1111/j.1600-0897.2007.00538.x
28. Fabian D, Juhas S, Il'kova G, Koppel J. Dose- and time-dependent effects of TNFalpha and actinomycin D on cell death incidence and embryo growth in mouse blastocysts. *Zygote.* (2007) 15:241–9. doi: 10.1017/S0967199407004200
29. Wuu YD, Pampfer S, Becquet P, Vanderheyden I, Lee KH, De Hertogh R. Tumor necrosis factor alpha decreases the viability of mouse blastocysts in vitro and in vivo. *Biol Reprod.* (1999) 60:479–83. doi: 10.1095/biolreprod60.2.479
30. Chelmońska-Soyta A, Majewska M, Buska K, Kurpisz M, Szczepańska P, Walczak R, et al. Tnf-α induced phosphatydilserine expression in mouse preimplantation embryos measured by a lab-on-chip method. *Reprod Domest Anim.* (2012) 47:18. doi: 10.1111/j.1439-0531.2012.01989.x
31. Buska K, Chełmońska-Soyta A, Nizański W. Non-surgical embryo transfer– a tool to study embryo-maternal interactions during pre-implantation period of pregnancy in mice. *Reprod Biol.* (2013) 13:13. doi: 10.1016/j.repbio.2012.11.103
32. Chevallet M, Luche S, Rabilloud T. Silver staining of proteins in polyacrylamide gels. *Nat Protoc.* (2006) 1:1852–8. doi: 10.1038/nprot.2006.288
33. Pink M, Verma N, Rettenmeier AW, Schmitz-Spanke S. CBB staining protocol with higher sensitivity and mass spectrometric compatibility. *Electrophoresis.* (2010) 31:593–8. doi: 10.1002/elps.200900481
34. Jauniaux E, Farquharson RG, Christiansen OB, Exalto N. Evidence-based guidelines for the investigation and medical treatment of recurrent miscarriage. *Hum Reprod.* (2006) 21:2216–22. doi: 10.1093/humrep/del150
35. de Mestre A, Noronha L, Wagner B, Antczak DF. Split immunological tolerance to trophoblast. *Int J Dev Biol.* (2010) 54:445–55. doi: 10.1387/ijdb.082795ad
36. Canovas S, Ivanova E, Romar R, García-Martínez S, Soriano-Úbeda C, García-Vázquez FA, et al. DNA methylation and gene expression changes derived from assisted reproductive technologies can be decreased by reproductive fluids. *Elife.* (2017) 6:e23670. doi: 10.7554/eLife.23670.027
37. Oron G, Son WY, Buckett W, Tulandi T, Holzer H. The association between embryo quality and perinatal outcome of singletons born after single embryo transfers: a pilot study. *Hum Reprod.* (2014) 29:1444–51. doi: 10.1093/humrep/deu079
38. Kawamura K, Kawamura N, Kumagai J, Fukuda J, Tanaka T. Tumor necrosis factor regulation of apoptosis in mouse preimplantation embryos and its antagonism by transforming growth factor alpha/phosphatidylionsitol 3-kinase signaling system. *Biol Reprod.* (2007) 76:611–8. doi: 10.1095/biolreprod.106.058008
39. Bauersachs S, Ulbrich SE, Zakhartchenko V, Minten M, Reichenbach M, Reichenbach H-D, et al. The endometrium responds differently to cloned versus fertilized embryos. *Proc Natl Acad Sci.* (2009) 106:5681–6. doi: 10.1073/pnas.0811841106
40. Nakamura H, Kimura T, Ogita K, Nakamura T, Takemura M, Shimoya K, et al. NF-kappaB activation at implantation window of the mouse uterus. *Am J Reprod Immunol.* (2004) 51:16–21. doi: 10.1046/j.8755-8920.2003.00116.x
41. Sun S-C. The non-canonical NF-kappaB pathway in immunity and inflammation. *Nat Rev Immunol.* (2017) 17:545–58. doi: 10.1038/nri.2017.52
42. Brown KD, Claudio E, Siebenlist U. The roles of the classical and alternative nuclear factor-kappaB pathways: potential implications for autoimmunity and rheumatoid arthritis. *Arthritis Res Ther.* (2008) 10:212. doi: 10.1186/ar2457
43. Kriete A, Mayo KL. Atypical pathways of NF-kappaB activation and aging. *Exp Gerontol.* (2009) 44:250–5. doi: 10.1016/j.exger.2008.12.005
44. Nakamura H, Kimura T, Ogita K, Koyama S, Tsujie T, Tsutsui T, et al. Alteration of the timing of implantation by in vivo gene transfer: delay of implantation by suppression of nuclear factor kappaB activity and partial rescue by leukemia inhibitory factor. *Biochem Biophys Res Commun.* (2004) 321:886–92. doi: 10.1016/j.bbrc.2004.07.045
45. Lim H, Dey SK. Prostaglandin E2 receptor subtype EP2 gene expression in the mouse uterus coincides with differentiation of the luminal epithelium for implantation. *Endocrinology.* (1997) 138:4599–606. doi: 10.1210/endo.138.11.5528
46. Chakraborty I, Das SK, Wang J, Dey SK. Developmental expression of the cyclo-oxygenase-1 and cyclo-oxygenase-2 genes in the peri-implantation mouse uterus and their differential regulation by the blastocyst and ovarian steroids. *J Mol Endocrinol.* (1996) 16:107–22. doi: 10.1677/jme.0.0160107
47. Paria BC, Huet-Hudson YM, Dey SK. Blastocyst's state of activity determines the "window" of implantation in the receptive mouse uterus. *Proc Natl Acad Sci USA.* (1993) 90:10159–62. doi: 10.1073/pnas.90.21.10159
48. Carbone F, Procaccini C, De Rosa V, Alviggi C, De Placido G, Kramer D, et al. Divergent immunomodulatory effects of recombinant and urinary-derived FSH, LH, and hCG on human CD4+ T cells. *J Reprod Immunol.* (2010) 85:172–9. doi: 10.1016/j.jri.2010.02.009
49. Komorowski J, Gradowski G, Stepień H. Effects of hCG and beta-hCG on IL-2 and sIL-2R secretion from human peripheral blood mononuclear cells: a dose-response study in vitro. *Immunol Lett.* (1997) 59:29–33. doi: 10.1016/S0165-2478(97)00096-5
50. Pflitsch C, Feldmann CN, Richert L, Hagen S, Diemert A, Goletzke J, et al. In-depth characterization of monocyte subsets during the course of healthy pregnancy. *J Reprod Immunol.* (2020) 141:103151. doi: 10.1016/j.jri.2020.103151
51. Oliveira JF, Henkes LE, Ashley RL, Purcell SH, Smirnova NP, Veeramachaneni DNR, et al. Expression of interferon (IFN)-stimulated genes in extrauterine tissues during early pregnancy in sheep is the consequence of endocrine IFN-tau release from the uterine vein. *Endocrinology.* (2008) 149:1252–9. doi: 10.1210/en.2007-0863
52. Green JC, Okamura CS, Poock SE, Lucy MC. Measurement of interferon-tau (IFN-tau) stimulated gene expression in blood leukocytes for pregnancy diagnosis within 18-20d after insemination in dairy cattle. *Anim Reprod Sci.* (2010) 121:24–33. doi: 10.1016/j.anireprosci.2010.05.010
53. Czopik AK, Bynoe MS, Palm N, Raine CS, Medzhitov R. Semaphorin 7A is a negative regulator of T cell responses. *Immunity.* (2006) 24:591–600. doi: 10.1016/j.immuni.2006.03.013
54. Child DF, Hudson PR, Hunter-Lavin C, Mukhergee S, China S, Williams CP, et al. Birth defects and anti–heat shock protein 70 antibodies in early pregnancy. *Cell Stress Chaperones.* (2006) 11:101–5. doi: 10.1379/CSC-130R1.1
55. Szabó KÉ, Line K, Eggleton P, Littlechild JA, Winyard PG. Structure and function of the human peroxiredoxin-based antioxidant system: the interplay between peroxiredoxins, thioredoxins, thioredoxin reductases, sulfiredoxins and sestrins. In: Jacob C Winyard PG editors. *Redox Signal Regul Biol Med*. (2009). doi: 10.1002/9783527627585.ch6
56. Yin G, Li C, Shan B, Wang W, Chen H, Zhong Y, et al. Insufficient peroxiredoxin-2 expression in uterine NK cells obtained from a murine model of abortion. *J Cell Biochem.* (2011) 112:773–81. doi: 10.1002/jcb.22893
57. Wang M, Liang P. Interleukin-24 and its receptors. *Immunology.* (2005) 114:1–70. doi: 10.1111/j.1365-2567.2005.02094.x
58. Pampfer S, Vanderheyden I, McCracken JE, Vesela J, De Hertogh R. Increased cell death in rat blastocysts exposed to maternal diabetes in utero and to high glucose or tumor necrosis factor-alpha in vitro. *Development.* (1997) 124:4827–36.

Conflict of Interest: The authors declare that the research was conducted in the absence of any commercial or financial relationships that could be construed as a potential conflict of interest.

frontiers in Veterinary Science

REVIEW
published: 15 April 2021
doi: 10.3389/fvets.2021.654064

Insights Into Extracellular Vesicle/Exosome and miRNA Mediated Bi-Directional Communication During Porcine Pregnancy

*Mallikarjun Bidarimath[1], Harshavardhan Lingegowda[2], Jessica E. Miller[2], Madhuri Koti[2,3] and Chandrakant Tayade[2]**

[1] Department of Pathobiological Sciences, School of Veterinary Medicine, Louisiana State University, Baton Rouge, LA, United States, [2] Department Biomedical and Molecular Sciences, Queen's University, Kingston, ON, Canada, [3] Department of Obstetrics and Gynecology, Queen's University, Kingston, ON, Canada

OPEN ACCESS

Edited by:
Dariusz Jan Skarzynski, Institute of Animal Reproduction and Food Research (PAS), Poland

Reviewed by:
Aneta Andronowska, Institute of Animal Reproduction and Food Research (PAS), Poland
Hakhyun Ka, Yonsei University, South Korea

***Correspondence:**
Chandrakant Tayade
tayadec@queensu.ca

Specialty section:
This article was submitted to Animal Reproduction - Theriogenology, a section of the journal Frontiers in Veterinary Science

Received: 15 January 2021
Accepted: 11 March 2021
Published: 15 April 2021

Citation:
Bidarimath M, Lingegowda H, Miller JE, Koti M and Tayade C (2021) Insights Into Extracellular Vesicle/Exosome and miRNA Mediated Bi-Directional Communication During Porcine Pregnancy. Front. Vet. Sci. 8:654064. doi: 10.3389/fvets.2021.654064

Spontaneous fetal loss is one of the most important challenges that commercial pig industry is still facing in North America. Research over the decade provided significant insights into some of the associated mechanisms including uterine capacity, placental efficiency, deficits in vasculature, and immune-inflammatory alterations at the maternal-fetal interface. Pigs have unique epitheliochorial placentation where maternal and fetal layers lay in opposition without any invasion. This has provided researchers opportunities to accurately tease out some of the mechanisms associated with maternal-fetal interface adaptations to the constantly evolving needs of a developing conceptus. Another unique feature of porcine pregnancy is the conceptus derived recruitment of immune cells during the window of conceptus attachment. These immune cells in turn participate in pregnancy associated vascular changes and contribute toward tolerance to the semi-allogeneic fetus. However, the precise mechanism of how maternal-fetal cells communicate during the critical times in gestation is not fully understood. Recently, it has been established that bi-directional communication between fetal trophoblasts and maternal cells/tissues is mediated by extracellular vesicles (EVs) including exosomes. These EVs are detected in a variety of tissues and body fluids and their role has been described in modulating several physiological and pathological processes including vascularization, immune-modulation, and homeostasis. Recent literature also suggests that these EVs (exosomes) carry cargo (nucleic acids, protein, and lipids) as unique signatures associated with some of the pregnancy associated pathologies. In this review, we provide overview of important mechanisms in porcine pregnancy success and failure and summarize current knowledge about the unique cargo containing biomolecules in EVs. We also discuss how EVs (including exosomes) transfer their contents into other cells and regulate important biological pathways critical for pregnancy success.

Keywords: angiogenesis, cytokines, exosomes, fetal loss, immune cells, inflammation, trophoblasts

INTRODUCTION

The pig industry around the world produces more than 100 million of pork annually and the value of U.S. and Canadian pork and pork products exports to the world reached a record $11 billion (1). Due to their high productive and reproductive efficiencies, the pigs contribute to the lower cost of pork production (2, 3). An average of 23.6 piglets per year can be produced by a single sow (4). Therefore, the litter size remains the prime contributing factor for greater yield of pork production. The litter size per gestation can be influenced by several entities such as ovulation rate, fertilization rate, and establishment of pregnancy and conceptus development and survival until the term. Pigs are highly prolific livestock species due to their certain reproductive characters such as higher ovulation rate (20−25 oocytes per cycle) (4) and fertilization rate (95%) (4–6). However, the litter size reduces to 10–13 piglets per sow, by the time they reach full term (7). The huge gap between these parameters is likely explained by a phenomenon called as spontaneous fetal loss, which occurs in two waves (8). A 20–30% of the conceptus are lost during the peri-attachment [gestation day (gd) 12–20] period (8) and an additional loss of 10–15% occurs during mid to late gestation, reviewed by (7, 9, 10). During early pregnancy, a delicate balance is absolutely critical between developing conceptus and the maternal immunomodulatory mechanisms (11). The porcine placentation is non-invasive, diffuse, epitheliochorial type, which is characterized by neither decidualization of the endometrium like in humans and mice nor invasion of fetal tissues into the endometrium, but instead both the compartments lie in close, yet firm adhesion (12, 13). Research over last decades has pointed out at several factors that are crucial to fetal development such as genetic makeup of the animal (14), nutrient intake (15), placental development and homeostasis (16), uterine capacity (14, 17), deficits in placental vasculature (18), disease outbreaks (19), immune mechanisms (20), and environment (21, 22) that specifically cause fetal loss. A variation in conceptus elongation rate and embryonic growth in early gestation especially around the peri-attachment period greatly alters the uterine environment, and thus negatively influencing the conceptus growth resulting in less developed conceptuses or even fetal demise (8). A similar variation in growth of littermates during the mid and late gestation leads to unequal space acquisition within the uterine lumen. The fetuses with comparatively higher growth rate exceed their uterine space, which pushes and compresses adjacent slow growing littermates resulting in stress/hypoxia induced conceptus arrest (8, 23, 24).

Successful porcine pregnancy is dependent on conceptus attachment and placental development, which requires a bidirectional communication between conceptus and endometrium. Previous studies have suggested many important factors that play a crucial role in pregnancy success. These factors include but not limited to conceptus-derived estrogen and growth factors (25), progesterone (26, 27), immune cells (18, 28–30), cytokines (18), chemokines (31, 32), miRNAs (29, 33), EVs including exosomes (34, 35), mRNA destabilizing factors (36), pro- and anti-angiogenic immune-related miRNAs (29, 34), and seminal fluid derived factors (37–41). However, most of these published studies only associate findings with fetal loss and a more comprehensive understanding of cause and effect relationship is required. In this review, we provide overview of important mechanisms associated with successful pregnancy or failure. We also summarize how contents from fetal and maternal derived EVs (including exosomes) contribute to pregnancy associated physiological adaptations.

IMMUNE MECHANISMS AT THE PORCINE MATERNAL-FETAL INTERFACE

Pleiotropic glycoprotein molecules such as cytokines are secreted by a variety of immune and non-immune cells in the uterine microdomain. Cytokines regulate several pregnancy related mechanisms including inflammation (42, 43), angiogenesis (18), innate and adaptive immune responses and cell death (44). These processes particularly influence the elongation and attachment of growing conceptus, endometrial adaptation to paternally derived antigens, successful conceptus attachment and overall development. Research over the past few years has characterized the role of members of the transforming growth factor beta superfamily, interferons (especially IFN-γ and IFN-δ), and interleukins (IL-1A, IL-1B, IL-1B2, IL-6) (44–46). During gd 9–10 and gd 15–18, there is dramatic change in the endometrial expression of TNFα, tumor necrosis factor alpha-inducible protein 6 (TNFAIP6), inter-α-trypsin inhibitor heavy chains (ITIH), and IL-6 that regulate the extracellular matrix expansion. IFN-γ is typically secreted around gd12 and dramatically increases around gd16 (47, 48). In our previous studies, the fetal loss during the peri-attachment period coincided with increased IFN-γ expression, while its expression was unaltered during a second wave of fetal loss around mid-pregnancy (gd50) (49). The transient increase in IFN-γ expression between gd12 and 15 influences the immune cell recruitment and differentiation at the maternal-fetal interface (50, 51). We observed increased expression of inflammatory cytokines such as TNF-α, IL-1B, and IL-1 receptor at the conceptus attachment sites associated with arresting/dying conceptus during the peri-attachment period (49). These studies suggest that these pro-inflammatory cytokines initiated acute inflammatory response that results in the conceptus loss and resorption. Although counter argument of immune cell infiltration and their functional products, cytokines, are released to clear dying/dead conceptus cannot be fully ruled out. This adds to the complexity of cause and effect question associated with fetal loss.

Immune cell recruitment to the maternal-fetal interface in porcine pregnancy is largely driven by conceptus derived signals and set of specific chemokines and growth factors (52–54). Secreted by several immune cell types, chemokines are small signaling molecules predominantly involved in the recruitment and activation of circulating leukocytes to the sites of inflammation (55). During early pregnancy, a remodeling in the uterine microdomain happens at the sites of conceptus attachment. Therefore, the chemokines secreted by uterine epithelial cells, fibroblasts as well as resident immune cells would act to influence an increased extravasation and chemotaxis along

the concentration gradient (54). However, a delicate balance is critical between a chemotaxis induced inflammatory processes and tissue homeostasis around the days of conceptus attachment and establishment of pregnancy.

Our previous research has explored these avenues by investigating the role of transcripts encoding decoy receptors, D6, duffy antigen receptor for chemokines (DARC) and chemocentryx decoy receptors (CCX-CKR). The mRNAs for decoy receptors (DARC and CCX-CKR) were dysregulated in the endometrium and chorioallantoic membrane; however, there was no difference in their expression at the protein level. A post-transcriptional and/or epigenetic modification of chemokines and their specific receptors, as well as action by proteolytic enzymes could explain these differences in expression during pregnancy (32). In another study, we investigated a distinct set of chemokines and their receptors that likely play a role in immune cell associated functions in laser microdissected endometrial lymphocytes, endometrium, and chorioallantoic membrane derived from both the arresting and healthy conceptus attachment sites. We demonstrated that lymphocytes residing in the arresting conceptus attachment sites had higher expression of *CXCR3* and *CCR5* mRNA, and there was greater expression of *CXCL10*, *CCL5*, *CCR5*, and *CXCR3* mRNA in the endometrium around peri-attachment period (gd20). Recently, Han and colleagues examined the expression of CXCL12 and CXCR4 at the maternal-conceptus interface during pregnancy in pigs. This study reported the highest expression of CXCL12 on day 15of pregnancy. Furthermore, CXCL12 protein expression was localized in endometrial epithelial cells, however, CXCR4 protein was detected in vascular endothelial cells, subepithelial stromal cells, and endometrial immune cells. CXCL12 increased the migration of cultured porcine trophectoderm cells and peripheral blood mononuclear cells as well as along with CXCR4 induced the migration of trophectoderm cells and T cells at the implantation in pigs. These experiments highlight role of CXCL12 in regulating trophoblast migration and T cell recruitment into the endometrium during implantation period in pigs (56). Recently, a study screened a broad range of chemokines (*CCL2*, *CCL4*, *CCL5*, *CCL8*, *CXCL2*, *CXCL8*, *CXCL10*, and *CXCL12*) and their receptors (CCR1, CCR2, CCR3, CCR5, CXCR2, CXCR3, and CXCR4) in luminal epithelial cells. This study suggests that CCL8 actively participates in embryo implantation and CXCL12 participates in endometrial receptivity and promotion of embryo attachment (57). Similarly, the same group screened the expression of same set of chemokines in endometrial stromal and endothelial cells and suggested that CCL2 modulates stromal cell function and CCL4 and CCL8 stimulate blood vessel development (58). These studies suggest that a further characterization of these chemokines and their specific receptors including decoy receptors may provide a better understanding of their role in immunomodulatory activity and overall function during conceptus attachment and subsequent development (31).

Previous studies in our laboratory and others have identified deficits in angiogenic stimuli that likely results in impaired vascular development at the maternal-fetal interface (18, 29, 49, 59). This is one of the important primary causes that leads to either stunted growth in surviving fetuses or fetal mortality during early stages of pregnancy. Various immune cell types have been evaluated for their crucial role during porcine pregnancy. Around the peri-attachment period (gd 12–15), the vascular remodeling of the endometrium coincides with infiltration of various innate and adaptive immune cells including natural killer cells, dendritic cells, macrophages, lymphocytes and plasma cells (60–62). The natural killer cells are generally detectable at gd 12 in pigs, which typically aggregate beneath the uterine luminal epithelium, around uterine glands, perivascular areas as well as randomly scattered throughout the uterine stroma (60, 61, 63).

It is important to note that the conceptus attachment to the endometrium is critical for the recruitment of uterine natural killer (uNK) cells in pigs as the decidualization is not induced in these species. However, in case of humans, mice and rats, where decidualization occurs, presence of conceptus is not critical for uNK cell recruitment (61, 64). T cells and uNK cell mobilization to the sites of blastocyst attachment and placentation typically noticed between gd 15–28 (65). However, their enrichment differs in various species. Compared to species with hemochorial placentation (human, mice), the uNK cell enrichment in the conceptus attachment sites of pigs is not pronounced, but only reaches about 3-fold. The immunological response at the maternal-fetal interface especially in mice and humans are characterized by intrauterine immune suppression, non-classical MHC molecule expression by trophectoderm and immune-protective molecules including Fas ligand (CD95) expression by the trophoblast (66–68). The porcine placental cells do not express MHC class I molecules (swine leukocyte antigens [SLAs]) (69), however, the stromal cells and luminal epithelial cells express classical and non-classical SLA class I molecules (SLA-1,−2,−3,−6,−7, and−8) as well as β2-microglobulin (70). Primarily involved in antigen presentation, MHC class II molecules (SLA DQA) demonstrate a greater expression in subepithelial stromal cells and endothelial cells of the endometrium in response to conceptus-derived IFN-γ during the window of conceptus attachment (71). The conceptus likely modulates SLA-DQA expression and hence indirectly influences the maternal immune system for its survival.

microRNAs INVOLVED IN REGULATION OF ANGIOGENESIS AND IMMUNE CELL DEVELOPMENT

The regulation of gene expression at the porcine maternal-fetal interface is controlled by several biomolecules at the genomic level. One of the most important implicated biomolecules are microRNAs (miRNAs), a class of small non-coding RNAs (∼18–22 nucleotide in length) that play a major role in RNA silencing and post-transcriptional gene regulation (72). MiRNAs negatively regulate translation either by deadenylating and destabilizing the mRNA or by repressing the translational machinery. miRNAs are primarily involved in regulating both physiological and pathological processes including but not limited to cellular proliferation and differentiation, homeostasis, inflammatory processes, and cell death (72, 73).

Most mammalian miRNAs are highly conserved among species (74, 75) and regulate at least 70% of all the genes in their specific genome (76). Each miRNA can repress the expression of multiple target mRNA, while each mRNA target is regulated by many miRNAs, suggesting that the regulation of gene expression is highly complex.

Because of their unique expression pattern in both physiological and pathological processes, miRNAs are projected as biomarkers of both healthy pregnancy and associated disorders. In one study, a set of 17 miRNAs were identified in the porcine placenta samples obtained from pigs at gd 30 and 90. Differentially expressed 8 miRNAs between the two time points, such as let-7i, miR-106a, miR-17, miR-24, miR-92b, miR-125b, miR-20, and miR-27a were validated by stem-loop RT-PCR. Further bioinformatic analysis of mRNA targets and potential biological pathways indicated that these miRNAs are involved in regulation of cell growth, trophoblast differentiation, maintenance of adherence junctions and angiogenesis (77). miRNAs appear to follow a pattern of expression depending on the overall dynamics of cellular processes, that are typical of porcine pregnancy. Based on the temporal expression patterns, a study had identified 65 miRNAs in the endometrium to capture crucial stages of pregnancy such as conceptus attachment (gd 15), placental development (gd 26), and mid-gestation (gd 50) (78). These miRNAs appear to regulate the processes associated with embryo attachment, placental development and overall homeostatic mechanisms associated with pregnancy. This study further characterized the binding sites of two miRNAs, miR-181a and miR-181c in the transcripts of genes such as ITGB3, ESR1, and SPP1, which are proven to play a crucial role in embryo implantation (78).

Studies over the past decade have characterized several miRNAs that regulate various porcine reproductive and pregnancy associated processes, including oocyte and conceptus development (35, 79, 80), implantation (35, 78), immune cell recruitment, and placental angiogenesis (29, 33), placental growth and function (77), and litter size (81–83). Specific examples include miRNA-29a that triggers the degradation of basement membrane and stromal matrix by interacting with *LAMC1* (encodes laminin subunit gamma 1), *COL1A2* (encodes collagen type 1 alpha, chain 2), and *COL3A1* (encodes collagen type 3 alpha, chain 1). Further, miR-200 family and miR-205 shown to control the trophoblast epithelial cell adherens junctions by interacting with *ZEB2* and *CDH1*. Similarly, miR-17-92 regulate trophoblast proliferation by interacting with *HBP1* and *ULK1* miRNAs (84). The miRNA synthesis and their transportation across the cellular compartments is also a highly regulated process. A set of 10 genes namely *DGCR8, AGO3*, *AGO4*, *XPO5, AGO1*, *AGO2*, *DICER1*, *DROSHA*, *TNRC6A*, and *TARBP2* that code for proteins involved in miRNA synthesis and transport have been investigated for their role in the endometrium of pigs. Using bioinformatics approach, this study identified target transcripts, VEGF, IL-6R, LIF, and PTGS2, that play a crucial role in maternal-fetal communication (35). Similarly, a distinct set of genes that regulate miRNA synthesis and transport (*DGCR8*, *TNRC6A*, *DROSHA*, *XPO5*, *DICER*, *AGO1 to−4*, and *TARBP2*) as well as miRNAs such as miR-140 were investigated in pregnant and cyclic endometria obtained on gd 12, 16, and 20 in pigs. The expression of *DROSHA*, *XPO5*, *DICER1*, *TARBP*, and *AGO1* was altered by the reproductive status of animals. Overall, these studies suggest that the interaction between miRNAs and genes involved in miRNA synthesis and transport likely involved in the regulation of estrous cycle and initial stages of embryo attachment (79).

Studies from our group evaluated the expression of 236 miRNAs in endometrial specimens and fetal trophoblasts derived from both the healthy and growth arrested conceptus attachment sites at gd 20. We reported significantly higher expression of miR-331-5p, 330-5p, 323, and 935, while miR-10a, 27a, 29c, and 374b-5p in the endometrial samples associated with healthy attachment site. These were one of the initial miRNA array-based studies to highlight the importance of miRNAs in the porcine pregnancy. Importantly, in this study, we found that the differentially expressed mRNAs indeed regulate many biological processes associated with pregnancy such as blood vessel development, nuclear transcription factor regulation, and extracellular matrix factors (85).

Due to the non-invasive superficial attachment, the epitheliochorial placentation in pigs enables us to easily isolate both maternal and fetal tissues to study molecular mechanisms without intermixing the compartments. Angiogenesis is one of the major mechanisms determines the success of implantation and growth of fetus. Therefore, our initial studies on immune-angiogenesis axis prompted us to explore miRNA regulation in recruited immune cells to the endometrium during pregnancy. Using laser capture microdissection, we isolated lymphocytes from the endometrium associated with both the arresting and healthy conceptus attachment sites and conducted targeted miRNA profiling on these immune cell subsets. Our major focus was to study miRNAs that are reported to be associated with immune cell development and overall pregnancy associated functions including angiogenesis. Interestingly, a distinct set of miRNAs such as miR-17P-5P, miR-18a, miR-19a, miR-150, and miR-296-5P were differentially expressed in the endometrial lymphocytes obtained from healthy conceptus attachment sites compared to their arresting counterparts. Further, there was significant differences in the expression of miR-17-5P, miR-20b, and miR-18a in the endometrium isolated during early pregnancy stages at gd20 (29). These studies provide concrete evidence into the role of miRNAs in the immune cell differentiation in the porcine endometrium and their expression levels changes depending on the pregnancy status. More importantly, this study also demonstrates that angiogenic miRNAs are enriched in the endometrial lymphocytes and can regulate immune cell promoted angiogenesis at the maternal-fetal interface to support developing conceptus (29).

BIOGENESIS AND SECRETORY MECHANISM OF EXTRACELLULAR VESICLES

Extracellular vesicles (EVs) is a general term used to describe membrane bound vesicles secreted by several cells for differing

functions. Although previously thought to be exclusively intended for the secretion and elimination of waste, EVs contain coding and non-coding nucleic acids, lipids, and proteins, which are highly relevant for intercellular communication, homeostatic processes and also contribute to pathologies including those at the maternal fetal interface (34, 86, 87). Although heterogeneric in size, composition, origin, and function, EVs are generally categorized into two groups: exosomes and microvesicles (MV). Exosomes range in size from 30 to 150 nm while MV range from 150 nm to 1 μm in diameter. In addition to size, morphology [described as round or saucer shaped (88)] and specific markers are used for categorization. Due to significant controversy surrounding the proper categorization of EVs together with a rise in scientific publications in recent years, the International Society for Extracellular Vesicles have proposed specific guidelines and protocols to direct the nomenclature, isolation of pure EV preparations and proper categorization of EVs (89). Briefly, isolation techniques of EVs include differential ultracentrifugation, density gradient centrifugation, filtration, and size exclusion chromatography. Characterization to confirm size, morphology, and marker presence is conducted by immunoblotting, flow cytometry, transmission electron microscopy, or nanoparticle tracking analysis. Although one marker does not exclusively identify EVs, proteins such as tetraspanins (including CD9, CD63, and CD82), as well as other sorting complex proteins are used to identify EVs (in both exosomes and MV).

Biogenesis and secretion of exosomes compared to MV is different. MV are released *via* budding of the plasma membrane and are thought to be released faster, as the cargoes targeted by these are situated at the plasma membrane. Whereas, exosomes are first formed as intralumenal vesicles (ILVs) within multivesicular endosomes (MVEs) of the cell and secretion requires sorting of cargoes through endosomal-sorting-complex-required-for-transport (ESCRT) dependent or independent pathways. Recent studies in the field have explored the possibility of sorting machineries, especially ESCRT complexes to be involved in decision making to target MVEs for either degradation or secretory pathway (90) through ALIX (ESCRT III associated complex) dependent mechanism (91). Similarly, another ESCRT complex associated protein (TSG101) has been studied by Villarroya-Beltri et al., where, a key posttranslational ubiquitin-like modification, ISGylation of TSG101 has been identified to be the probable signaling mechanisms that drives MVEs to fuse with lysosomes to induce degradation instead of secretion (92). Regardless of the outcomes, MVEs need to be transported continuously to either fuse with lysosomes or plasma membrane through general cellular transportation molecules such as actin, microtubule cytoskeleton, cortactin, RAB protein complexes and their effector molecules (93, 94). Studies in cancer cell lines have shown that actin cytoskeleton to be involved in the transportation and secretion of exosomes (94). Transportation of vesicles within the cells, including budding and fission of MVEs at the plasma membrane is tightly governed by GTPases-RAB protein family that consists of up to 60 members.

Even though the exact mechanism of action is not understood, members of RAB protein family such as RAB2B, RAB4, RAB5A, RAB7, RAB9A, RAB11, RAB27A, RAB27B, and RAB35 have been found to be involved specifically in endosome transport to plasma membrane and secretion of exosomes, as discussed elsewhere (95). Finally, fusion of MVEs to the plasma membrane is necessary to release ILVs as exosomes, which is thought to be primarily mediated by N-ethylmaleimide-sensitive factor attachment protein receptors (SNAREs). SNARE protein complexes are made up of three to four subunits forming helices that are conventionally involved in exocytosis of lysosomes (96, 97). Recent developments in the field has identified a few proteins of SNARE family members namely, vesicle-associated membrane protein 7 (VAMP7), Synaptobrevin Homolog YKT6, syntaxin 1A and syntaxin 5 to be crucial to facilitate the release of exosomes. Depending on the subtypes of MVEs, organism and cell type, diverse regulation of secretion by SNARE proteins have been identified in human embryonic kidney HEK293 cells (98), lung carcinoma A549 cells (99), *Drosophila* (98) (YKT6), and C. *elegnas* (syntaxin 1a and syntaxin 5) (100, 101). However, the exact stage where these molecules are recruited is yet to be identified. This limitation is mainly regarded to the technical approach as well as intracellular complexity of exosome release.

Interestingly, the release of EVs is an evolutionarily conserved process in both prokaryotes and eukaryotes and therefore EVs serve diverse biological functions, reviewed extensively here (102). As mentioned earlier, EVs including exosomes contain lipids, nucleic acids (mRNA, miRNA, DNA), enzymes, transcription factors and extracellular matrix proteins packaged by parental cells that exert drastic effects in the recipient cell (103). Conventional cell to cell communication occurs through surface protein interaction with neighboring cells, whereas hormones and cytokines are recruited to fulfill distant interactions (104). Considering the contents of exosome cargo, number of studies have centralized the approach toward understanding the molecular interactions between exosomes and recipient cells. Although the entire mechanism is not fully understood, it is known that exosomes are required to fuse with the plasma membrane, followed by signal transduction and internalization (endocytosis, phagocytosis, and micropinocytosis) with the target cells in order to deliver the cargo and establish intercellular communications. Known mechanism of action includes interaction with surface bound receptors, epigenetic modification *via* genetic material and activated receptor transfer to the target cell. Transmembrane proteins (integrins, tetraspanins) and extracellular matrices are primarily involved in binding exosomes to the target cells. Adhesion proteins such as intracellular adhesion molecules (ICAM) have been identified to interact during uptake with the integrins present on exosomes (105). Specific route of internalization is thought to be influenced by the content of molecules carried by exosomes. Studies in human pancreatic cancer cells have identified mutant KRAS gene to influence the exosomes to be internalized *via* micropinocytosis (106). Similarly, complexity of exosome action surrounding specific

cell targeting is believed to be determined based on the cargo carried by exosomes.

EXTRACELLULAR VESICLES IN PORCINE PREGNANCY

A successful conceptus attachment to the endometrium and subsequent maintenance of pregnancy requires a proper communication between endometrium and conceptus (11). There are already several well-understood mechanisms of cell-cell communication such as hormones, cytokines, and lipids that act in an autocrine and paracrine manner, intercellular nanotubules (107), direct adhesion between cell of origin and target cell, and membrane-bound microvesicles (108). Research over the past decade has provided critical evidence into intercellular communication *via* EVs (109). The EVs have been demonstrated to transfer information from the cell of origin to the recipient cells to regulate cellular activities (**Figure 1**). This information could be in the form of proteins, lipids, miRNAs, mRNAs, DNA and many other small molecules, and thus reflecting the physiological state of the originating cells (110, 111). However, the transfer of information could be two way, where the recipient cell can in turn stimulate/induce the originating cells in order to elicit the cellular signaling pathways (112, 113).

The bioactivity possessed by these EVs is distinct. Therefore, EVs have the ability to influence both physiological (110) and pathological processes (111). However, the precise mechanisms regulated by exosomes is difficult to understand, due to their complexity of cargo, abundance, cell of origin, biogenesis and secretory mechanisms, and extracellular environment as discussed in earlier section. Another important characteristic of the exosomes is their stability in the extracellular spaces due to their lipid bilayer containing cholesterol, ceramide, sphingomyelins and other detergent-resistant membrane molecules, which are likely derived from the originating cells (114). These unique features allow them to carry information without leaking into the extracellular spaces. Upon entering the recipient cell, the exosomes dissociate to release cargo, which may regulate gene expression and influence biological processes such as cell proliferation, differentiation, and migration. The exosomes have been demonstrated to be released by cells of the reproductive tissues such as endometrial (115), oviductal (116), and follicular cells (117) as well as bodily fluids such as saliva (118), blood plasma (119), milk (120), amniotic fluid (121), semen (122), urine (123), and uterine luminal fluid (35). The exosomes carried through different bodily fluids can selectively interact with target cells and deliver a diverse set of molecules to influence target cell activity suggesting that exosomes provide a highly regulated and complex mode of cellular communication.

Although there are many mechanisms of communication between conceptus and maternal endometrium, the documentary evidence is increasing exponentially about EVs/exosomes being the important mode of communication at the maternal-fetal interface. However, this is not a totally new concept as the discovery of small vesicles goes back to early 1990's, where multiple small vesicles have been shown at the porcine maternal-fetal interface on gd16 *via* electron microscopy (12). Research in recent years have shown that EVs including exosomes released by placental cells can cross into maternal endometrium to deliver cargo containing biomolecules to the recipient cells.

It already known that the exosomes have the ability to transfer many important biomolecules such as mRNA and miRNAs to their respective target cells, in which mRNA can be directed toward translating into protein and miRNA can be utilized to fine tune mRNA expression or repress translation (124, 125). Exosomes carrying these biomolecules can attach to the surface of target cell (126) and can be internalized by recipient cells (127, 128). Chromosome 19 miRNA cluster generates more than 50 miRNAs and this cluster appear to modulate immune response in pregnancy. The immunomodulatory mechanism is essential especially in early pregnancy to help recently attached conceptus to grow and favorably modulate maternal immune response to paternal antigen. Interestingly, one study demonstrated a viral resistance in recipient cells that received miRNAs that were packaged within the human trophoblast-derived exosomes (129).

Another interesting concept is that MV and exosomes can be released in a time dependent manner as well as based on the physiological status. For example, the secretome released from placenta during first trimester of human pregnancy predominantly consisted of exosomes (130), while during the second trimester, the composition of the secretome changed predominantly to microvesicles and also their number increased as the pregnancy advanced to term (131, 132). Similarly, the function regulated by these ever-changing components of microvesicles and exosomes also differs greatly depending on the stage of pregnancy. For example, the exosomes released during early human pregnancy contain HLA-G (MHC I G), that help in enabling maternal immune tolerance toward recently attached conceptus carrying paternal antigens (130). Furthermore, MV released by syncytiotrophoblasts induce pro-inflammatory activity, which is essential around the stages of pregnancy establishment (133). However, these dynamic variations in the components of secretome need to be investigated in pigs to understand how trophoblast derived EVs modulate maternal adaptions to pregnancy given the non-invasive type of placentation.

EVs have been shown to perform a variety of pregnancy associated functions that most often reflect the constituents of its cargo. Conceptus attachment sites in pigs undergo dramatic changes both during successful and abortive pregnancy. For example, conceptus attachment sites associated with arresting embryo undergo an acute inflammatory process to enable resorption without affecting the adjacent littermate. Apoptosis can also get elicited in the conceptuses to remove or replenish the unnecessary cells. This mechanism of programmed cell death has been reported in many reproductive tissues such as uterine epithelium (134). Human placenta derived exosomes have been shown to carry Fas ligand and TRAIL molecules and induce apoptosis in activated immune cells and thus providing maternal immune tolerance toward developing fetus (135). Similarly, a regulatory protein such as bcl-2-like protein 15 (BCL2L15) has

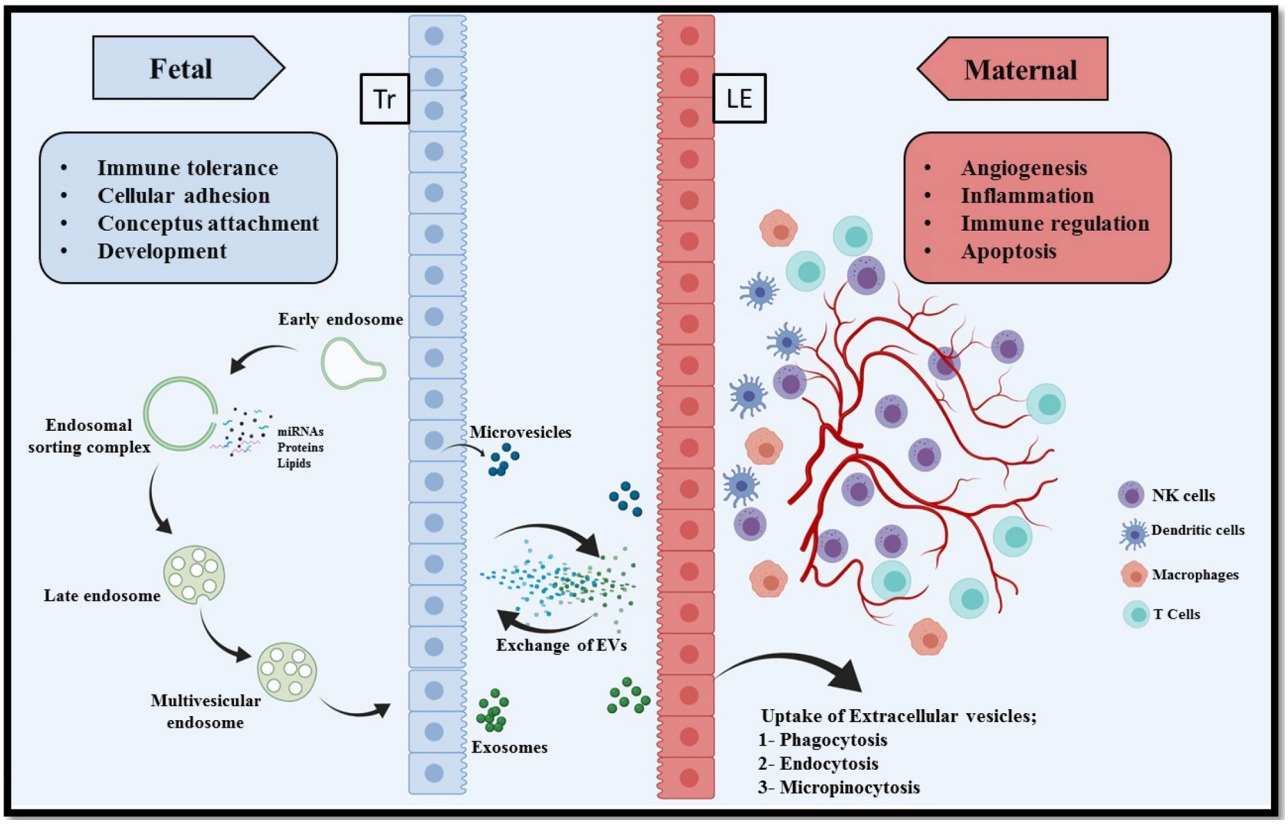

FIGURE 1 | Extracellular vesicle mediated bi-directional communication at the porcine maternal fetal interface. In epitheliochorial placentation in pigs, fetal trophoblasts (Tr) lay in simple apposition with maternal endometrial luminal epithelium (LE). Extracellular vesicles comprising microvesicles and exosomes are a heterogeneous group of cell-derived membranous structures originated from either endosomal system (microvesicles) or shed from the plasma membranes (exosomes). The unique cargo of these EVs contain biomolecules (nucleic acid, proteins, and lipids). These EVs can be internalized by multiple pathways including phagocytosis, endocytosis, pinocytosis, or can remain bound to the cell surface depending on the cell type. Interaction of EVs with recipient cells modulate several critical pregnancy associated processes, for example, conceptus attachment, development, immune tolerance on the fetal side and angiogenesis, inflammation, and apoptosis on the maternal side.

been reported in ovine uterine EVs during the periattachment period, gd17 (136). Another study in cows demonstrated that EVs obtained from gd17 induced greater expression of apoptotic-related genes, BAX, TNFA, TP53, and CASP3 in primary endometrial epithelial cells (137). These findings indicate a crucial role for EVs in apoptotic removal of immune cells (immunomodulation) and endometrial epithelial cells to help in uterine remodeling for conceptus attachment.

A recent study has isolated and characterized the EVs in porcine uterine flushing fluid collected on gd10, 13, and 18. Contents of these EVs especially small RNAs were comprehensively profiled through small RNA sequencing analysis. The cargo consisted of 152 known miRNAs, 43 novel miRNAs, 6248 known Piwi-interacting RNAs (piRNAs), and 110 novel piRNAs were identified. Subsequent bioinformatics analysis revealed that the miRNA enriched in the EVs involved in important pregnancy associated pathways such as immunomodulation, endometrial receptivity, implantation and embryo development. These studies add to the miRNA repository as well as serve as a resource to further investigate crosstalk at the maternal-fetal interface (138). As integrin family proteins play an important role in embryo implantation, previous study demonstrated that EVs in the bovine uterine flushings isolated on gd20 and 22 were able to upregulate VCAM1 expression in endometrial epithelial cells (139). Similarly, a study involving exosomes from estrogen or progesterone treated human endometrial epithelial cells contained several members of integrin family. The integrins are crucial for exosome docking to target cells and regulate trophoblast adhesion to the endometrium (140). EVs isolated from uterine lumen flushings on gd12, 14, and 16 reported to contain miR-26a and miR-125b and among these miRNAs, miR-125b directly regulated expression of genes that play role in attachment and embryo development in pigs (35). These studies support the notion that EVs can influence conceptus attachment and adhesion to the endometrium. However, given fundamental differences in the placentation between human, mice and pigs, a pig centric studies are warranted to investigate mechanisms by which the biomolecules packaged in EVS/exosomes regulate porcine pregnancy related functions.

Placental angiogenesis is an important pregnancy related processes crucial for conceptus development and remodeling of endometrium especially in early pregnancy to provide nutrients to the fetus. The placentation in pig typically initiates gd 15–20, which involves an abrupt change in endometrial microenvironment and associated biological processes including angiogenesis (141, 142). Studies from our laboratory have investigated angiogenesis at the porcine maternal-fetal interface and recently, we demonstrated that both the porcine trophectoderm cells, representing fetal tissues and endothelial cells, representing maternal tissues release EVs (34). Furthermore, these experiments demonstrate that EVs derived from porcine trophectoderm cells can stimulate endothelial cell proliferation, suggesting that EVs can stimulate angiogenesis. We have shown that EVs derived from porcine trophoectoderm cells (PTR2) contains several important proteins and miRNAs such as miR-126-5P, miR-296-5P, miR-16, and miR-17-5P that have been shown to play a major role in angiogenesis (34). miR-150 packaged within exosomes derived from porcine umbilical cord blood stimulated proliferation, migration, and tube formation of umbilical vein endothelial cells. These studies indicate that EVs especially those derived from fetal tissues have the ability to stimulate endometrial angiogenesis and thus, support the idea that an angiogenic deficit at the maternal-fetal interface can be therapeutically targeted by designer EVs and prevent subsequent conceptus loss.

The development of immunological tolerance against semi-allogeneic fetus is a crucial event in the pregnancy success. Since fetal allografts carry paternal antigens, the maternal immune system should reprogram itself to not to recognize fetal antigens and elicit an immune response. EVs have been reported to modulate maternal immune response toward the newly attaching conceptus (143). Depending on the nature of cargo and also type of receptors present on their membrane, EVs are able to modulate the immune response at the maternal-fetal interface. Bovine EVs obtained from gd20, were able to downregulate expression of immune-related genes in endometrial epithelial cells immediately after the conceptus attachment is initiated (144). Zhao et al. reported in bovine pregnancy that bta-miR-98 as a likely maternal immune system regulator based on the miRNA profiles of EVs combined with bioinformatic analysis. Similarly, miRNA-499 was reported to play a role in regulation of local inflammation at the bovine maternal-fetal interface by inhibiting NF-kB signaling. Further, disruption of miR-499 results in increased risk of pregnancy failure due to severe local inflammatory process, placental resorption in early pregnancy or even fetal growth restriction (87). These studies suggest that miRNA cargo present in the EVs can modulate immune response, ultimately, helping to achieve immune tolerance during early pregnancy. Although, our previous studies in pigs have pointed out a distinct set of miRNAs that may have immunomodulatory effect on the maternal immune system, more mechanistic *in vivo* evidence is needed to exploit the idea that miRNA loaded EVs can be used to potentially reduce spontaneous fetal loss in pigs in future.

EXTRACELLULAR VESICLES IN SELECTIVE REPRODUCTIVE DISORDERS IN PIGS

Extracellular vesicles in porcine pregnancy: Early pregnancy diagnosis or detecting early embryonic mortality could substantially improve reproductive efficiency in pigs and overall improve the economy of swine industry. Failure to conceive after insemination or undetected pregnancy at an early stage in pigs could result in severe economic loss. While there are many well-established techniques currently available, miRNAs and miRNAs packaged within the exosomes could be another important tool to be used as the earliest possible (before 25 days after fertilization) biomarkers of pregnancy (145). Zhou and colleagues profiled exosomes obtained from serum samples at days 9, 12, 15 from pregnant and non-pregnant pigs. They concluded that miR-92b-3p and miR-17-5p could be identified in the serum exosomes as earlier as day 9 of pregnancy and hence could be used as biomarkers of early pregnancy (145).

Interestingly, in one of our previous studies miR-17-5p was one of highly enriched miRNA present in the porcine trophectoderm cells, derived from day 12 of pregnancy, and porcine endothelial cells as well as exosomes released by these two cell types (34). miR-17-5p is involved in regulating many physiological and pathological processes including cell proliferation, apoptosis, and most importantly angiogenesis. In addition, the genes targeted by miR-17-5p are reported to be involved in important signaling pathways including MAPK, PI3K-Akt, and TGF-β. Similarly, a study involving cattle identified 27 circulating EV-derived miRNAs isolated from serum that were significantly increased on gd 17 embryonic mortality compared to pregnant cattle. Furthermore, a specific miRNAs such as miR-25, miR-16b, and miR3596 were differentially expressed on gestation days 17 and 24, reflecting the pregnancy status (146). In another study, a set of 27 miRNAs packaged within EVs from maternal blood were found to be in lower abundance in somatic cell nuclear transfer-derived bovine embryonic loss group that failed to reach term. Additionally, the predicted target genes of these 27 miRNAs were found to be associated with critical biological processes such as cell proliferation, apoptosis, and angiogenesis (147).

Role of extracellular vesicles in porcine reproductive and respiratory syndrome pathogenesis: EVs have been shown to play a role in diseases affecting reproductive organs in pigs. Porcine reproductive and respiratory syndrome (PRRS) is one of the important diseases affecting reproductive organs in pigs and causes a heavy economic loss to pork industry. It is characterized by reproductive failures in sows and respiratory syndrome in pigs of all ages (148). An emerging evidence indicates that exosomes released by cells infected by some viruses selectively package viral genetic material, viral proteins, or virions to transmit to neighboring healthy/uninfected cells (149). Purified exosomes isolated from PRRS virus infected cells contain viral genomic RNA and partial viral proteins. These exosomes loaded with viral components can deliver their contents to both PRRS virus susceptible and non-susceptible cells, indicating a viral

transmission *via* exosomes while evading the host immune response (150).

Exosomes can serve as small RNA transfer vehicles and act as effective therapeutic tools. Zhu and colleagues conducted a study to target two key receptors, Sialoadhesin (Sn) and CD163 for PRRS virus infection of porcine alveolar macrophages. They designed artificial miRNAs that can directly target Sn and CD163 as PRRS virus enters the target cells *via* receptor-mediated endocytosis. They generated two recombinant adenoviruses expressing the effective artificial miRNAs. It was observed that sequence-specific artificial miRNAs were expressed adequately and released from recombinant adenovirus transduced pig cells *via* exosomes. Overall, PRRSV infection of pulmonary alveolar macrophages was inhibited by transduction of two artificial miRNA expressing recombinant adenoviruses and or treatment with two artificial miRNAs packaged within the exosomes. This study suggest that exosomes can be utilized to effectively treat infectious diseases such as PRRS (151). Another study by the same group, used exosome mediated transfer of artificial miRNA targeting the 3' untranslated region of PRRSV. They generated a recombinant adenovirus expressing the artificial miRNA that can target 3' untranslated region of PRRSV and further concluded that exosomes derived from porcine cells can be utilized as miRNA cargo and miRNAs delivered *via* exosomes effectively elicited anti-viral effects against different PRRSV strains (152). Montaner-Tarbes et al. isolated serum-derived exosomes from naïve animals, from PRRSV viremic animals and from animals recovered from PRRSV infection and already free of viruses (non-viremic). Their experiments suggest that the serum-derived exosomes contain antigenic viral-proteins, which could be used as a novel vaccine strategy against PRRSV infection (149). Further this group conducted a targeted-pig trial on safety and immunogenicity of serum derived EVs containing viral proteins and concluded that this could be an effective vaccine strategy (153).

SUMMARY AND CONCLUSION

Co-ordinated interactions between maternal endometrium and fetal trophoblasts at the highly dynamic interface is critical to ensure pregnancy success. In epitheliochorial placentation seen in pigs, the fetal trophoblasts lie in simple opposition with luminal epithelial cells of the endometrium but there is no invasion. The significant alterations in the uterine stroma as seen in other species such as human and mice is also lacking in pigs except localized branching of new blood vessels to support the needs of a growing conceptus. We and others have shown that the conceptus mediates the recruitment of immune cells that adopt a specialized phenotype and these immune cells contribute to and regulate angiogenesis at the porcine maternal-fetal interface. It is important to recognize that because of the non-invasive placentation in pigs, trophoblasts do not physically interact with maternal-immune cells. In fact, trophoblasts in contact with luminal epithelium lacks SLA class I and II molecules and therefore avoid recognition by the maternal-immune cells. Maternal-immune cells predominantly NK cells and T cells are recruited around gd-12-15 at the maternal-fetal interface by conceptus mediated signals as well as specific sets of chemokines. The pro-inflammatory microenvironment and chemokine gradient is regulated by chemokine decoy receptors such as D6 and DARC. Recent evidence indicate that immune cell differentiation and function is also regulated by specific sets of miRNAs. Indeed, miRNAs are involved in modulating several physiological, homeostatic, and pathological processes including vascularization and inflammation. Several reports also indicate suitability of unique miRNA signatures in body fluids as predictors of health and disease.

The paradox of bi-directional communication between maternal and fetal compartments can be better explained by extracellular vesicle mediated inter-cellular cross talk, especially in species with epitheliochorial placentation where physical interactions between trophoblast and maternal immune cells is limited. The EV cargo containing genomic DNA fragments, RNAs, mRNAs, miRNAs, proteins, and lipids are specifically packaged and can be traced back to the cell of origin. The EV cargo contents are also influenced by the localized microenvironment cues and are involved in embryo implantation, placentation, pregnancy maintenance, and pregnancy associated disorders. With the advent of newer sequencing technologies and bioinformatics machine learning tools, the contents of EVs and their utility in understanding physiological changes in pregnancy and spontaneous fetal loss will be of immense value in future.

AUTHOR CONTRIBUTIONS

MB, MK, and CT conceived ideas and associated themes. HL and JM contributed sections of the manuscript. MB, HL, JM, MK, and CT wrote and edited manuscript. CT provided research funding and oversight. All authors contributed to the article and approved the submitted version.

FUNDING

This research was supported with funds from Natural Sciences and Engineering Research Council of Canada (Grant No. 388772).

REFERENCES

1. United states Department of Agriculture, Foreign Agriculture Service. *US Pork Hogs.* (2019). Available online at: https://www.fas.usda.gov/commodities/pork-and-hogs (accessed March 26, 2021).
2. Secco C, Luz LM da, Pinheiro E, de Francisco AC, Puglieri FN, Piekarski CM, et al. Circular economy in the pig farming chain: proposing a model for measurement. *J Clean Prod.* (2020) 260:1–10. doi: 10.1016/j.jclepro.2020.121003
3. McEwan K, Marchand L, Shang M, Bucknell D. Potential implications of COVID-19 on the Canadian pork industry. *Can J Agric Econ.* (2020) 68:201–6. doi: 10.1111/cjag.12236
4. Town SC, Patterson JL, Pereira CZ, Gourley G, Foxcroft GR. Embryonic and fetal development in a commercial dam-line genotype.

Anim Reprod Sci. (2005) 85:301–16. doi: 10.1016/j.anireprosci.2004.05.019
5. Youngs CR, Christenson LK, Ford SP. Investigations into the control of litter size in swine: III. A reciprocal embryo transfer study of early conceptus development. *J Anim Sci.* (1994) 72:725–31. doi: 10.2527/1994.723725x
6. Anderson LH, Christenson LK, Christenson RK, Ford SP. Investigations into the control of litter size in swine: II. Comparisons of morphological and functional embryonic diversity between Chinese and American breeds. *J Anim Sci.* (1993) 71:1566–71. doi: 10.2527/1993.7161566x
7. Geisert RD, Schmitt RaM. Early embryonic survival in the pig: can it be improved? *J Anim Sci.* (2002) 80:E54–65. doi: 10.2527/animalsci2002.0021881200800ES10009x
8. Pope WF. Uterine asynchrony: a cause of embryonic loss. *Biol Reprod.* (1988) 39:999–1003. doi: 10.1095/biolreprod39.5.999
9. Ross JW, Ashworth MD, Stein DR, Couture OP, Tuggle CK, Geisert RD. Identification of differential gene expression during porcine conceptus rapid trophoblastic elongation and attachment to uterine luminal epithelium. *Physiol Genom.* (2009) 36:140–8. doi: 10.1152/physiolgenomics.00022.2008
10. Stroband HW, Van der Lende T. Embryonic and uterine development during early pregnancy in pigs. *J Reprod Fertil.* (1990) 40:261–77.
11. Bazer FW, Johnson GA. Pig blastocyst-uterine interactions. *Differentiation.* (2014) 87:52–65. doi: 10.1016/j.diff.2013.11.005
12. Keys JL, King GJ. Microscopic examination of porcine conceptus-maternal interface between days 10 and 19 of pregnancy. *Am J Anat.* (1990) 188:221–38. doi: 10.1002/aja.1001880302
13. Enders AC, Blankenship TN. Comparative placental structure. *Adv Drug Deliv Rev.* (1999) 38:3–15. doi: 10.1016/S0169-409X(99)00003-4
14. Ford SP. Embryonic and fetal development in different genotypes in pigs. *J Reprod Fertil.* (1997) 52:165–76.
15. Foxcroft GR, Dixon WT, Dyck MK, Novak S, Harding JCS, Almeida FCRL. Prenatal programming of postnatal development in the pig. *Soc Reprod Fertil Suppl.* (2009) 66:213–31. doi: 10.1530/biosciprocs.18.0028
16. Miles JR, Freking BA, Blomberg LA, Vallet JL, Zuelke KA. Conceptus development during blastocyst elongation in lines of pigs selected for increased uterine capacity or ovulation rate. *J Anim Sci.* (2008) 86:2126–34. doi: 10.2527/jas.2008-1066
17. Freking BA, Leymaster KA, Vallet JL, Christenson RK. Number of fetuses and conceptus growth throughout gestation in lines of pigs selected for ovulation rate or uterine capacity. *J Anim Sci.* (2007) 85:2093–103. doi: 10.2527/jas.2006-766
18. Tayade C, Fang Y, Hilchie D, Croy BA. Lymphocyte contributions to altered endometrial angiogenesis during early and midgestation fetal loss. *J Leukoc Biol.* (2007) 82:877–86. doi: 10.1189/jlb.0507330
19. Pogranichniy RM, Schwartz KJ, Yoon KJ. Isolation of a novel viral agent associated with porcine reproductive and neurological syndrome and reproduction of the disease. *Vet Microbiol.* (2008) 131:35–46. doi: 10.1016/j.vetmic.2008.02.026
20. Linton NF, Wessels JM, Cnossen Sa, Croy BA, Tayade C. Immunological mechanisms affecting angiogenesis and their relation to porcine pregnancy success. *Immunol Invest.* (2008) 37:611–29. doi: 10.1080/08820130802191540
21. Hansen PJ. Effects of heat stress on mammalian reproduction. *Philos Trans R Soc B Biol Sci.* (2009) 364:3341–50. doi: 10.1098/rstb.2009.0131
22. Morrow-Tesch JL, McGlone JJ, Salak-Johnson JL. Heat and social stress effects on pig immune measures. *J Anim Sci.* (1994) 72:2599–609. doi: 10.2527/1994.72102599x
23. Wu MC, Hentzel MD, Dziuk PJ. Relationships between uterine length and number of fetuses and prenatal mortality in pigs. *J Anim Sci.* (1987) 65:762–70. doi: 10.2527/jas1987.653762x
24. Wilson ME, Biensen NJ, Ford SP. Novel insight into the control of litter size in pigs, using placental efficiency as a selection tool. *J Anim Sci.* (1999) 77:1654–8. doi: 10.2527/1999.7771654x
25. Bazer FW. Pregnancy recognition signaling mechanisms in ruminants and pigs. *J Anim Sci Biotechnol.* (2013) 4:23. doi: 10.1186/2049-1891-4-23
26. Spencer TE, Burghardt RC, Johnson GA, Bazer FW. Conceptus signals for establishment and maintenance of pregnancy. *Anim Reprod Sci.* (2004) 82–3:537–50. doi: 10.1016/j.anireprosci.2004.04.014
27. Spencer TE, Johnson GA, Burghardt RC, Bazer FW. Progesterone and placental hormone actions on the uterus: insights from domestic animals. *Biol Reprod.* (2004) 71:2–10. doi: 10.1095/biolreprod.103.024133
28. Croy BA, Wessels J, Linton N, Tayade C. Comparison of immune cell recruitment and function in endometrium during development of epitheliochorial (pig) and hemochorial (mouse and human) placentas. *Placenta.* (2009) 30(Suppl.A):26–31. doi: 10.1016/j.placenta.2008.09.019
29. Bidarimath M, Edwards AKAK, Wessels JMJM, Khalaj K, Kridli RTRT, Tayade C. Distinct microRNA expression in endometrial lymphocytes, endometrium, and trophoblast during spontaneous porcine fetal loss. *J Reprod Immunol.* (2015) 107:64–79. doi: 10.1016/j.jri.2014.11.004
30. Linton NF, Wessels JM, Cnossen Sa, van den Heuvel MJ, Croy BA, Tayade C. Angiogenic DC-SIGN(+) cells are present at the attachment sites of epitheliochorial placentae. *Immunol Cell Biol.* (2010) 88:63–71. doi: 10.1038/icb.2009.62
31. Bidarimath M, Khalaj K, Kridli RTRT, Wessels JMJM, Koti M, Tayade C. Altered expression of chemokines and their receptors at porcine maternal-fetal interface during early and mid-gestational fetal loss. *Cell Tissue Res.* (2016) 366:747–61. doi: 10.1007/s00441-016-2470-2
32. Wessels JM, Linton NF, van den Heuvel MJ, Cnossen Sa, Edwards AK, Croy BA, et al. Expression of chemokine decoy receptors and their ligands at the porcine maternal-fetal interface. *Immunol Cell Biol.* (2011) 89:304–13. doi: 10.1038/icb.2010.95
33. Bidarimath M, Khalaj K, Wessels JMJM, Tayade C. MicroRNAs, immune cells and pregnancy. *Cell Mol Immunol.* (2014) 11:538–47. doi: 10.1038/cmi.2014.45
34. Bidarimath M, Khalaj K, Kridli RTRT, Kan FWKFWK, Koti M, Tayade C. Extracellular vesicle mediated intercellular communication at the porcine maternal-fetal interface: a new paradigm for conceptus-endometrial cross-talk. *Sci Rep.* (2017) 7:40476. doi: 10.1038/srep40476
35. Krawczynski K, Najmula J, Bauersachs S, Kaczmarek MM. MicroRNAome of porcine conceptuses and trophoblasts: expression profile of microRNAs and their potential to regulate genes crucial for establishment of pregnancy. *Biol Reprod.* (2015) 92:21. doi: 10.1095/biolreprod.114.123588
36. Khalaj K, Wessels JMJM, Kridli RTRT, Bidarimath M, Lamarre J, Tayade C. mRNA destabilizing factors: tristetraprolin expression at the porcine maternal-fetal interface. *Am J Reprod Immunol.* (2015) 73:402–16. doi: 10.1111/aji.12347
37. Piehl LL, Fischman ML, Hellman U, Cisale H, Miranda PV. Boar seminal plasma exosomes: effect on sperm function and protein identification by sequencing. *Theriogenology.* (2013) 79:1071–82. doi: 10.1016/j.theriogenology.2013.01.028
38. Katila T. Post-mating inflammatory responses of the uterus. *Reprod Domest Anim.* (2012) 47:31–41. doi: 10.1111/j.1439-0531.2012.02120.x
39. Bischof RJ, Brandon MR, Lee C-S. Cellular immune responses in the pig uterus during pregnancy. *J Reprod Immunol.* (1995) 29:161–78. doi: 10.1016/0165-0378(95)00935-E
40. O'Leary S, Jasper MJ, Warnes GM, Armstrong DT, Robertson SA. Seminal plasma regulates endometrial cytokine expression, leukocyte recruitment and embryo development in the pig. *Reproduction.* (2004) 128:237–47. doi: 10.1530/rep.1.00160
41. Jalali BM, Kitewska A, Wasielak M, Bodek G, Bogacki M. Effects of seminal plasma and the presence of a conceptus on regulation of lymphocyte-cytokine network in porcine endometrium. *Mol Reprod Dev.* (2014) 81:270–81. doi: 10.1002/mrd.22297
42. Murphy SP, Tayade C, Ashkar AA, Hatta K, Zhang J, Croy BA. Interferon gamma in successful pregnancies. *Biol Reprod.* (2009) 80:848–59. doi: 10.1095/biolreprod.108.073353
43. Garlanda C, Maina V, Martinez de la Torre Y, Nebuloni M, Locati M. Inflammatory reaction and implantation: the new entries PTX3 and D6. *Placenta.* (2008) 29(Suppl.B):129–34. doi: 10.1016/j.placenta.2008.06.008
44. Geisert RD, Lucy MC, Whyte JJ, Ross JW, Mathew DJ. Cytokines from the pig conceptus: roles in conceptus development in pigs. *J Anim Sci Biotechnol.* (2014) 5:51. doi: 10.1186/2049-1891-5-51
45. Mathew DJ, Lucy MC, Geisert DR. Interleukins, interferons, and establishment of pregnancy in pigs. *Reproduction.* (2016) 151:R111–22. doi: 10.1530/REP-16-0047

46. Ross JW, Malayer JR, Ritchey JW, Geisert RD. Characterization of the interleukin-1beta system during porcine trophoblastic elongation and early placental attachment. *Biol Reprod.* (2003) 69:1251–9. doi: 10.1095/biolreprod.103.015842
47. Bazer FW, Burghardt RC, Johnson GA, Spencer TE, Wu G. Interferons and progesterone for establishment and maintenance of pregnancy: interactions among novel cell signaling pathways. *Reprod Biol.* (2008) 8:179–211. doi: 10.1016/S1642-431X(12)60012-6
48. Bazer FW, Song G, Kim J, Dunlap Ka, Satterfield M, Johnson Ga, et al. Uterine biology in pigs and sheep. *J Anim Sci Biotechnol.* (2012) 3:23. doi: 10.1186/2049-1891-3-23
49. Tayade C, Black GP, Fang Y, Croy BA. Differential gene expression in endometrium, endometrial lymphocytes, and trophoblasts during successful and abortive embryo implantation. *J Immunol.* (2006) 176:148–56. doi: 10.4049/jimmunol.176.1.148
50. Roberts RM, Chen Y, Ezashi T, Walker AM. Interferons and the maternal-conceptus dialog in mammals. *Semin Cell Dev Biol.* (2008) 19:170–7. doi: 10.1016/j.semcdb.2007.10.007
51. La Bonnardiere C, Martinat-Botte F, Terqui M, Lefevre F, Zouari K, Martal J, et al. Production of two species of interferon by Large White and Meishan pig conceptuses during the peri-attachment period. *J Reprod Fertil.* (1991) 91:469–78. doi: 10.1530/jrf.0.0910469
52. Wessels JM, Linton NF, Croy BA, Tayade C, Croy AB, Tayade C. A review of molecular contrasts between arresting and viable porcine attachment sites. *Am J Reprod Immunol.* (2007) 58:470–80. doi: 10.1111/j.1600-0897.2007.00534.x
53. Du M-R, Wang S-C, Li D-J. The integrative roles of chemokines at the maternal-fetal interface in early pregnancy. *Cell Mol Immunol.* (2014) 11:438–48. doi: 10.1038/cmi.2014.68
54. Nancy P, Erlebacher A. Epigenetic repression of chemokine expression at the maternal-fetal interface as a mechanism of feto-maternal tolerance. *Med Sci.* (2012) 28:1037–9. doi: 10.1051/medsci/20122812005
55. Zlotnik A, Yoshie O. The chemokine superfamily revisited. *Immunity.* (2012) 36:705–12. doi: 10.1016/j.immuni.2012.05.008
56. Han J, Jeong W, Gu MJ, Yoo I, Yun CH, Kim J, et al. Cysteine-X-cysteine motif chemokine ligand 12 and its receptor CXCR4: Expression, regulation, and possible function at the maternal-conceptus interface during early pregnancy in pigs. *Biol Reprod.* (2018) 99:1137–48. doi: 10.1093/biolre/ioy147
57. Złotkowska A, Andronowska A. Chemokines as the modulators of endometrial epithelial cells remodelling. *Sci Rep.* (2019) 9:14467. doi: 10.1038/s41598-019-49502-5
58. Złotkowska A, Andronowska A. Modulatory effect of chemokines on porcine endometrial stromal and endothelial cells. *Domest Anim Endocrinol.* (2020) 72:106475. doi: 10.1016/j.domaniend.2020.106475
59. Croy BA, Wessels JM, Linton NF, van den Heuvel M, Edwards AK, Tayade C. Cellular and molecular events in early and mid gestation porcine implantation sites: a review. *Soc Reprod Fertil Suppl.* (2009) 66:233–44. doi: 10.1530/biosciprocs.18.0029
60. Engelhardt H, Croy BA, King GJ. Role of uterine immune cells in early pregnancy in pigs. *J Reprod Fertil.* (1997) 52:115–31.
61. Engelhardt H, Croy BA, King GJ. Conceptus influences the distribution of uterine leukocytes during early porcine pregnancy. *Biol Reprod.* (2002) 66:1875–80. doi: 10.1095/biolreprod66.6.1875
62. Moffett A, Loke C. Immunology of placentation in eutherian mammals. *Nat Rev.* (2006) 6:584–94. doi: 10.1038/nri1897
63. Engelhardt H, Croy BA, King GJ. Evaluation of natural killer cell recruitment to embryonic attachment sites during early porcine pregnancy. *Biol Reprod.* (2002) 66:1185–92. doi: 10.1095/biolreprod66.4.1185
64. Croy BA, Waterfield A, Wood W, King GJ. Normal murine and porcine embryos recruit NK cells to the uterus. *Cell Immunol.* (1988) 115:471–80. doi: 10.1016/0008-8749(88)90199-2
65. Dimova T, Mihaylova A, Spassova P, Georgieva R. Superficial implantation in pigs is associated with decreased numbers and redistribution of endometrial NK-cell populations. *Am J Reprod Immunol.* (2008) 59:359–69. doi: 10.1111/j.1600-0897.2007.00579.x
66. Hunt JS, Vassmer D, Ferguson TA, Miller L. Fas ligand is positioned in mouse uterus and placenta to prevent trafficking of activated leukocytes between the mother and the conceptus. *J Immunol.* (1997) 158:4122–8.
67. Runic R, Lockwood CJ, LaChapelle L, Dipasquale B, Demopoulos RI, Kumar A, et al. Apoptosis and Fas expression in human fetal membranes. *J Clin Endocrinol Metab.* (1998) 83:660–6. doi: 10.1210/jc.83.2.660
68. Trowsdale J, Betz AG. Mother's little helpers: mechanisms of maternal-fetal tolerance. *Nat Immunol.* (2006) 7:241–6. doi: 10.1038/ni1317
69. Ramsoondar JJ, Christopherson RJ, Guilbert LJ, Dixon WT, Ghahary A, Ellis S, et al. Lack of class I major histocompatibility antigens on trophoblast of periimplantation blastocysts and term placenta in the pig. *Biol Reprod.* (1999) 60:387–97. doi: 10.1095/biolreprod60.2.387
70. Joyce MM, Burghardt JR, Burghardt RC, Hooper RN, Bazer FW, Johnson GA. Uterine MHC class I molecules and beta 2-microglobulin are regulated by progesterone and conceptus interferons during pig pregnancy. *J Immunol.* (2008) 181:2494–505. doi: 10.4049/jimmunol.181.4.2494
71. Kim M, Seo H, Choi Y, Shim J, Bazer FW, Ka H. Swine leukocyte antigen-DQ expression and its regulation by interferon-gamma at the maternal-fetal interface in pigs. *Biol Reprod.* (2012) 86:43. doi: 10.1095/biolreprod.111.094011
72. Baltimore D, Boldin MP, O'Connell RM, Rao DS, Taganov KD. MicroRNAs: new regulators of immune cell development and function. *Nat Immunol.* (2008) 9:839–45. doi: 10.1038/ni.f.209
73. Taganov KD, Boldin MP, Baltimore D. MicroRNAs and immunity: tiny players in a big field. *Immunity.* (2007) 26:133–7. doi: 10.1016/j.immuni.2007.02.005
74. Chen K, Rajewsky N. The evolution of gene regulation by transcription factors and microRNAs. *Nat Rev.* (2007) 8:93–103. doi: 10.1038/nrg1990
75. Winn VD, Haimov-Kochman R, Paquet AC, Yang YJ, Madhusudhan MS, Gormley M, et al. Gene expression profiling of the human maternal-fetal interface reveals dramatic changes between midgestation and term. *Endocrinology.* (2007) 148:1059–79. doi: 10.1210/en.2006-0683
76. Krol J, Loedige I, Filipowicz W. The widespread regulation of microRNA biogenesis, function and decay: abstract: nature reviews genetics. *Nat Rev Genet.* (2010) 11:597–610. doi: 10.1038/nrg2843
77. Su L, Zhao S, Zhu M, Yu M. Differential expression of microRNAs in porcine placentas on Days 30 and 90 of gestation. *Reprod Fertil Dev.* (2010) 22:1175–82. doi: 10.1071/RD10046
78. Su L, Liu R, Cheng W, Zhu M, Li X, Zhao S, et al. Expression patterns of microRNAs in porcine endometrium and their potential roles in embryo implantation and placentation. *PLoS ONE.* (2014) 9:e87867. doi: 10.1371/journal.pone.0087867
79. Krawczynski K, Bauersachs S, Reliszko ZP, Graf A, Kaczmarek MM. Expression of microRNAs and isomiRs in the porcine endometrium: implications for gene regulation at the maternal-conceptus interface. *BMC Genom.* (2015) 16:906. doi: 10.1186/s12864-015-2172-2
80. Stowe HM, Curry E, Calcatera SM, Krisher RL, Paczkowski M, Pratt SL. Cloning and expression of porcine Dicer and the impact of developmental stage and culture conditions on MicroRNA expression in porcine embryos. *Gene.* (2012) 501:198–205. doi: 10.1016/j.gene.2012.03.058
81. Córdoba S, Balcells I, Castelló A, Ovilo C, Noguera JL, Timoneda O, et al. Endometrial gene expression profile of pregnant sows with extreme phenotypes for reproductive efficiency. *Sci Rep.* (2015) 5:14416. doi: 10.1038/srep14416
82. Huang L, Yin ZJ, Feng YF, Zhang XD, Wu T, Ding YY, et al. Identification and differential expression of microRNAs in the ovaries of pigs (*Sus scrofa*) with high and low litter sizes. *Anim Genet.* (2016) 47:543–51. doi: 10.1111/age.12452
83. Lei B, Gao S, Luo LF, Xia XY, Jiang SW, Deng CY, et al. A SNP in the miR-27a gene is associated with litter size in pigs. *Mol Biol Rep.* (2011) 38:3725–9. doi: 10.1007/s11033-010-0487-2
84. Liu R, Wang M, Su L, Li X, Zhao S, Yu M. The expression pattern of microRNAs and the associated pathways involved in the development of porcine placental folds that contribute to the expansion of the exchange surface area. *Biol Reprod.* (2015) 93:62. doi: 10.1095/biolreprod.114.126540
85. Wessels JMJM, Edwards AKAK, Khalaj K, Kridli RTRT, Bidarimath M, Tayade C. The microRNAome of pregnancy: deciphering miRNA networks at the maternal-fetal interface. *PLoS ONE.* (2013) 8:e72264. doi: 10.1371/journal.pone.0072264

86. Van Niel G, D'Angelo G, Raposo G. Shedding light on the cell biology of extracellular vesicles. *Nat Rev Mol Cell Biol.* (2018) 19:213–28. doi: 10.1038/nrm.2017.125
87. Zhao G, Yang C, Yang J, Liu P, Jiang K, Shaukat A, et al. Placental exosome-mediated Bta-miR-499-Lin28B/let-7 axis regulates inflammatory bias during early pregnancy. *Cell Death Dis.* (2018) 9:704. doi: 10.1038/s41419-018-0713-8
88. Shao H, Chung J, Balaj L, Charest A, Bigner DD, Carter BS, et al. Protein typing of circulating microvesicles allows real-time monitoring of glioblastoma therapy. *Nat Med.* (2012) 18:1835–40. doi: 10.1038/nm.2994
89. Théry C, Witwer KW, Aikawa E, Alcaraz MJ, Anderson JD, Andriantsitohaina R, et al. Minimal information for studies of extracellular vesicles 2018 (MISEV2018): a position statement of the International Society for Extracellular Vesicles and update of the MISEV2014 guidelines. *J Extracell Vesicles.* (2018) 7:1535750. doi: 10.1080/20013078.2018.1461450
90. Willms E, Johansson HJ, Mäger I, Lee Y, Blomberg KEM, Sadik M, et al. Cells release subpopulations of exosomes with distinct molecular and biological properties. *Sci Rep.* (2016) 6:22519. doi: 10.1038/srep22519
91. Baietti MF, Zhang Z, Mortier E, Melchior A, Degeest G, Geeraerts A, et al. Syndecan-syntenin-ALIX regulates the biogenesis of exosomes. *Nat Cell Biol.* (2012) 14:677–85. doi: 10.1038/ncb2502
92. Villarroya-Beltri C, Baixauli F, Gutiérrez-Vázquez C, Sánchez-Madrid F, Mittelbrunn M. Sorting it out: regulation of exosome loading. *Semin Cancer Biol.* (2014) 28:3–13. doi: 10.1016/j.semcancer.2014.04.009
93. Villarroya-Beltri C, Baixauli F, Mittelbrunn M, Fernández-Delgado I, Torralba D, Moreno-Gonzalo O, et al. ISGylation controls exosome secretion by promoting lysosomal degradation of MVB proteins. *Nat Commun.* (2016) 7:13588. doi: 10.1038/ncomms13588
94. Hoshino D, Kirkbride KC, Costello K, Clark ES, Sinha S, Grega-Larson N, et al. Exosome secretion is enhanced by invadopodia and drives invasive behavior. *Cell Rep.* (2013) 5:1159–68. doi: 10.1016/j.celrep.2013.10.050
95. Hessvik NP, Llorente A. Current knowledge on exosome biogenesis and release. *Cell Mol Life Sci.* (2018) 75:193–208. doi: 10.1007/s00018-017-2595-9
96. Jahn R, Scheller RH. SNAREs - engines for membrane fusion. *Nat Rev Mol Cell Biol.* (2006) 7:631–43. doi: 10.1038/nrm2002
97. Pfeffer SR. Unsolved mysteries in membrane traffic. *Annu Rev Biochem.* (2007) 76:629–45. doi: 10.1146/annurev.biochem.76.061705.130002
98. Gross JC, Chaudhary V, Bartscherer K, Boutros M. Active Wnt proteins are secreted on exosomes. *Nat Cell Biol.* (2012) 14:1036–45. doi: 10.1038/ncb2574
99. Ruiz-Martinez M, Navarro A, Marrades RM, Viñolas N, Santasusagna S, Muñoz C, et al. YKT6 expression, exosome release, and survival in non-small cell lung cancer. *Oncotarget.* (2016) 7:51515–24. doi: 10.18632/oncotarget.9862
100. Koles K, Budnik V. Exosomes go with the Wnt. *Cell Logist.* (2012) 2:169–73. doi: 10.4161/cl.21981
101. Hyenne V, Apaydin A, Rodriguez D, Spiegelhalter C, Hoff-Yoessle S, Diem M, et al. RAL-1 controls multivesicular body biogenesis and exosome secretion. *J Cell Biol.* (2015) 211:27–37. doi: 10.1083/jcb.201504136
102. Yáñez-Mó M, Siljander PRM, Andreu Z, Zavec AB, Borràs FE, Buzas EI, et al. Biological properties of extracellular vesicles and their physiological functions. *J Extracell Vesicles.* (2015) 4:1–60. doi: 10.3402/jev.v4.27066
103. Mathivanan S, Ji H, Simpson RJ. Exosomes: extracellular organelles important in intercellular communication. *J Proteom.* (2010) 73:1907–20. doi: 10.1016/j.jprot.2010.06.006
104. Camussi G, Deregibus MC, Bruno S, Cantaluppi V, Biancone L. Exosomes/microvesicles as a mechanism of cell-to-cell communication. *Kidney Int.* (2010) 78:838–48. doi: 10.1038/ki.2010.278
105. Morelli AE, Larregina AT, Shufesky WJ, Sullivan MLG, Stolz DB, Papworth GD, et al. Endocytosis, intracellular sorting, and processing of exosomes by dendritic cells. *Blood.* (2004) 104:3257–66. doi: 10.1182/blood-2004-03-0824
106. Kamerkar S, Lebleu VS, Sugimoto H, Yang S, Ruivo CF, Melo SA, et al. Exosomes facilitate therapeutic targeting of oncogenic KRAS in pancreatic cancer. *Nature.* (2017) 546:498–503. doi: 10.1038/nature22341
107. Ratajczak J, Miekus K, Kucia M, Zhang J, Reca R, Dvorak P, et al. Embryonic stem cell-derived microvesicles reprogram hematopoietic progenitors: evidence for horizontal transfer of mRNA and protein delivery. *Leukemia.* (2006) 20:847–56. doi: 10.1038/sj.leu.2404132
108. Valadi H, Ekstrom K, Bossios A, Sjostrand M, Lee JJ, Lotvall JO, et al. Exosome-mediated transfer of mRNAs and microRNAs is a novel mechanism of genetic exchange between cells. *Nat Cell Biol.* (2007) 9:654–9. doi: 10.1038/ncb1596
109. Mittelbrunn M, Sánchez-Madrid F. Intercellular communication: diverse structures for exchange of genetic information. *Nat Rev Mol Cell Biol.* (2012) 13:328–35. doi: 10.1038/nrm3335
110. Scherjon S, Lashley L, van der Hoorn ML, Claas F. Fetus specific T cell modulation during fertilization, implantation and pregnancy. *Placenta.* (2011) 32(Suppl.4):S291–7. doi: 10.1016/j.placenta.2011.03.014
111. Mitchell MD, Peiris HN, Kobayashi M, Koh YQ, Duncombe G, Illanes SE, et al. Placental exosomes in normal and complicated pregnancy. *Am J Obstet Gynecol.* (2015) 213:S173–81. doi: 10.1016/j.ajog.2015.07.001
112. Luo S-SS, Ishibashi O, Ishikawa G, Ishikawa T, Katayama A, Mishima T, et al. Human villous trophoblasts express and secrete placenta-specific microRNAs into maternal circulation *via* exosomes. *Biol Reprod.* (2009) 81:717–29. doi: 10.1095/biolreprod.108.075481
113. Ng YH, Rome S, Jalabert A, Forterre A, Singh H, Hincks CL, et al. Endometrial exosomes/microvesicles in the uterine microenvironment: a new paradigm for embryo-endometrial cross talk at implantation. *PLoS ONE.* (2013) 8:e58502. doi: 10.1371/journal.pone.0058502
114. Sokolova V, Ludwig A-K, Hornung S, Rotan O, Horn PA, Epple M, et al. Characterisation of exosomes derived from human cells by nanoparticle tracking analysis and scanning electron microscopy. *Colloids Surf B Biointerfaces.* (2011) 87:146–50. doi: 10.1016/j.colsurfb.2011.05.013
115. Gurung S, Greening DW, Catt S, Salamonsen L, Evans J. Exosomes and soluble secretome from hormone-treated endometrial epithelial cells direct embryo implantation. *Mol Hum Reprod.* (2020) 26:510–20. doi: 10.1093/molehr/gaaa034
116. Alcântara-Neto AS, Fernandez-Rufete M, Corbin E, Tsikis G, Uzbekov R, Garanina AS, et al. Oviduct fluid extracellular vesicles regulate polyspermy during porcine *in vitro* fertilisation. *Reprod Fertil Dev.* (2019) 32:409–18. doi: 10.1071/RD19058
117. da Silveira JC, Veeramachaneni DNR, Winger QA, Carnevale EM, Bouma GJ. Cell-secreted vesicles in equine ovarian follicular fluid contain mirnas and proteins: a possible new form of cell communication within the ovarian follicle. *Biol Reprod.* (2012) 86:71. doi: 10.1095/biolreprod.111.093252
118. Ogawa Y, Miura Y, Harazono A, Kanai-Azuma M, Akimoto Y, Kawakami H, et al. Proteomic analysis of two types of exosomes in human whole saliva. *Biol Pharm Bull.* (2011) 34:13–23. doi: 10.1248/bpb.34.13
119. Caby M-P, Lankar D, Vincendeau-Scherrer C, Raposo G, Bonnerot C. Exosomal-like vesicles are present in human blood plasma. *Int Immunol.* (2005) 17:879–87. doi: 10.1093/intimm/dxh267
120. Chen T, Xi QY, Ye RS, Cheng X, Qi QE, Wang SB, et al. Exploration of microRNAs in porcine milk exosomes. *BMC Genom.* (2014) 15:100. doi: 10.1186/1471-2164-15-100
121. Keller S, Rupp C, Stoeck A, Runz S, Fogel M, Lugert S, et al. CD24 is a marker of exosomes secreted into urine and amniotic fluid. *Kidney Int.* (2007) 72:1095–102. doi: 10.1038/sj.ki.5002486
122. Barranco I, Padilla L, Parrilla I, Álvarez-Barrientos A, Pérez-Patiño C, Peña FJ, et al. Extracellular vesicles isolated from porcine seminal plasma exhibit different tetraspanin expression profiles. *Sci Rep.* (2019) 9:11584. doi: 10.1038/s41598-019-48095-3
123. Pisitkun T, Shen R-F, Knepper MA. Identification and proteomic profiling of exosomes in human urine. *Proc Natl Acad Sci USA.* (2004) 101:13368–73. doi: 10.1073/pnas.0403453101
124. Aliotta JM, Pereira M, Johnson KW, de Paz N, Dooner MS, Puente N, et al. Microvesicle entry into marrow cells mediates tissue-specific changes in mRNA by direct delivery of mRNA and induction of transcription. *Exp Hematol.* (2010) 38:233–45. doi: 10.1016/j.exphem.2010.01.002
125. Hergenreider E, Heydt S, Tréguer K, Boettger T, Horrevoets AJG, Zeiher AM, et al. Atheroprotective communication between endothelial cells and smooth muscle cells through miRNAs. *Nat Cell Biol.* (2012) 14:249–56. doi: 10.1038/ncb2441
126. Segura E, Guerin C, Hogg N, Amigorena S, Thery C, Guérin C, et al. CD8+ dendritic cells use LFA-1 to capture MHC-peptide complexes from exosomes *in vivo*. *J Immunol.* (2007) 179:1489–96. doi: 10.4049/jimmunol.179.3.1489

127. Mincheva-Nilsson L, Baranov V. The role of placental exosomes in reproduction. *Am J Reprod Immunol.* (2010) 63:520–33. doi: 10.1111/j.1600-0897.2010.00822.x
128. Salomon C, Torres MJ, Kobayashi M, Scholz-Romero K, Sobrevia L, Dobierzewska A, et al. A gestational profile of placental exosomes in maternal plasma and their effects on endothelial cell migration. *PLoS ONE.* (2014) 9:e98667. doi: 10.1371/journal.pone.0098667
129. Delorme-Axford E, Donker RB, Mouillet J-FF, Chu T, Bayer A, Ouyang Y, et al. Human placental trophoblasts confer viral resistance to recipient cells. *Proc Natl Acad Sci USA.* (2013) 110:12048–53. doi: 10.1073/pnas.1304718110
130. Kshirsagar SK, Alam SM, Jasti S, Hodes H, Nauser T, Gilliam M, et al. Immunomodulatory molecules are released from the first trimester and term placenta *via* exosomes. *Placenta.* (2012) 33:982–90. doi: 10.1016/j.placenta.2012.10.005
131. Clifton VL, Stark MJ, Osei-Kumah A, Hodyl NA. Review: the feto-placental unit, pregnancy pathology and impact on long term maternal health. *Placenta.* 5:S37–41. doi: 10.1016/j.placenta.2011.11.005
132. Germain SJ, Sacks GP, Sooranna SR, Soorana SR, Sargent IL, Redman CW. Systemic inflammatory priming in normal pregnancy and preeclampsia: the role of circulating syncytiotrophoblast microparticles. *J Immunol.* (2007) 178:5949–56. doi: 10.4049/jimmunol.178.9.5949
133. Southcombe J, Tannetta D, Redman C, Sargent I. The immunomodulatory role of syncytiotrophoblast microvesicles. *PLoS ONE.* (2011) 6:e20245. doi: 10.1371/journal.pone.0020245
134. Jacobson MD, Weil M, Raff MC. Programmed cell death in animal development. *Cell.* (1997) 88:347–54. doi: 10.1016/S0092-8674(00)81873-5
135. Stenqvist A-C, Nagaeva O, Baranov V, Mincheva-Nilsson L. Exosomes secreted by human placenta carry functional fas ligand and TRAIL molecules and convey apoptosis in activated immune cells, suggesting exosome-mediated immune privilege of the fetus. *J Immunol.* (2013) 191:5515–23. doi: 10.4049/jimmunol.1301885
136. Nakamura K, Kusama K, Bai R, Sakurai T, Isuzugawa K, Godkin JD, et al. Induction of IFNT-stimulated genes by conceptus-derived exosomes during the attachment period. *PLoS ONE.* (2016) 11:e0158278. doi: 10.1371/journal.pone.0158278
137. Kusama K, Nakamura K, Bai R, Nagaoka K, Sakurai T, Imakawa K. Intrauterine exosomes are required for bovine conceptus implantation. *Biochem Biophys Res Commun.* (2018) 495:1370–5. doi: 10.1016/j.bbrc.2017.11.176
138. Hua R, Wang Y, Lian W, Li W, Xi Y, Xue S, et al. Small RNA-seq analysis of extracellular vesicles from porcine uterine flushing fluids during peri-implantation. *Gene.* (2021) 766:145117. doi: 10.1016/j.gene.2020.145117
139. Bai R, Bai H, Kuse M, Ideta A, Aoyagi Y, Fujiwara H, et al. Involvement of VCAM1 in the bovine conceptus adhesion to the uterine endometrium. *Reproduction.* (2014) 148:119–27. doi: 10.1530/REP-13-0655
140. Greening DW, Nguyen HPTT, Elgass K, Simpson RJ, Salamonsen LA. Human endometrial exosomes contain hormone-specific cargo modulating trophoblast adhesive capacity: insights into endometrial-embryo interactions. *Biol Reprod.* (2016) 94:38. doi: 10.1095/biolreprod.115.134890
141. Dantzer V, Leiser R. Initial vascularisation in the pig placenta: I. Demonstration of nonglandular areas by histology and corrosion casts. *Anat Rec.* (1994) 238:177–90. doi: 10.1002/ar.1092380204
142. Leiser R, Dantzer V. Initial vascularisation in the pig placenta: II. Demonstration of gland and areola-gland subunits by histology and corrosion casts. *Anat Rec.* (1994) 238:326–34. doi: 10.1002/ar.1092380307
143. Giacomini E, Alleva E, Fornelli G, Quartucci A, Privitera L, Vanni VS, et al. Embryonic extracellular vesicles as informers to the immune cells at the maternal–fetal interface. *Clin Exp Immunol.* (2019) 198:15–23. doi: 10.1111/cei.13304
144. Nakamura K, Kusama K, Ideta A, Kimura K, Hori M, Imakawa K. Effects of miR-98 in intrauterine extracellular vesicles on maternal immune regulation during the peri-implantation period in cattle. *Sci Rep.* (2019) 9:20330. doi: 10.1038/s41598-019-56879-w
145. Zhou C, Cai G, Meng F, Xu Z, He Y, Hu Q, et al. Deep-sequencing identification of MicroRNA biomarkers in serum exosomes for early pig pregnancy. *Front Genet.* (2020) 11:536. doi: 10.3389/fgene.2020.00536
146. Pohler KG, Green JA, Moley LA, Gunewardena S, Hung WT, Payton RR, et al. Circulating microRNA as candidates for early embryonic viability in cattle. *Mol Reprod Dev.* (2017) 84:731–43. doi: 10.1002/mrd.22856
147. De Bem THC, Da Silveira JC, Sampaio RV, Sangalli JR, Oliveira MLF, Ferreira RM, et al. Low levels of exosomal-miRNAs in maternal blood are associated with early pregnancy loss in cloned cattle. *Sci Rep.* (2017) 7:14319. doi: 10.1038/s41598-017-14616-1
148. Done SH, Paton DJ. Porcine reproductive and respiratory syndrome: clinical disease, pathology and immunosuppression. *Vet Rec.* (1995)136:32–5. doi: 10.1136/vr.136.2.32
149. Montaner-Tarbes S, Borrás FE, Montoya M, Fraile L, Del Portillo HA. Serum-derived exosomes from non-viremic animals previously exposed to the porcine respiratory and reproductive virus contain antigenic viral proteins. *Vet Res.* (2016) 47:59. doi: 10.1186/s13567-016-0345-x
150. Wang T, Fang L, Zhao F, Wang D, Xiao S. Exosomes mediate intercellular transmission of porcine reproductive and respiratory syndrome virus (PRRSV). *J Virol.* (2017) 92:e01734–17. doi: 10.1128/JVI.01734-17
151. Zhu L, Song H, Zhang X, Xia X, Sun H. Inhibition of porcine reproductive and respiratory syndrome virus infection by recombinant adenovirus- and/or exosome-delivered the artificial microRNAs targeting sialoadhesin and CD163 receptors. *Virol J.* (2014) 11:225. doi: 10.1186/s12985-014-0225-9
152. Zhu L, Bao L, Zhang X, Xia X, Sun H. Inhibition of porcine reproductive and respiratory syndrome virus replication with exosome-transferred artificial microRNA targeting the 3' untranslated region. *J Virol Methods.* (2015) 223:61–8. doi: 10.1016/j.jviromet.2015.07.018
153. Montaner-Tarbes S, Novell E, Tarancón V, Borrás FE, Montoya M, Fraile L, et al. Targeted-pig trial on safety and immunogenicity of serum-derived extracellular vesicles enriched fractions obtained from Porcine Respiratory and Reproductive virus infections. *Sci Rep.* (2018) 8:17487. doi: 10.1038/s41598-018-36141-5

Conflict of Interest: The authors declare that the research was conducted in the absence of any commercial or financial relationships that could be construed as a potential conflict of interest.

frontiers in Veterinary Science

ORIGINAL RESEARCH
published: 26 April 2021
doi: 10.3389/fvets.2021.639249

Three-Dimensional Live Imaging of Bovine Preimplantation Embryos: A New Method for IVF Embryo Evaluation

*Yasumitsu Masuda[1], Ryo Hasebe[2], Yasushi Kuromi[2], Masayoshi Kobayashi[2], Kanako Urataki[3], Mitsugu Hishinuma[3], Tetsuya Ohbayashi[4] and Ryo Nishimura[3]**

[1] Department of Animal Science, Tottori Livestock Research Center, Tottori, Japan, [2] SCREEN Holdings Co., Ltd., Kyoto, Japan, [3] Laboratory of Theriogenology, Joint Department of Veterinary Medicine, Faculty of Agriculture, Tottori University, Tottori, Japan, [4] Organization for Research Initiative and Promotion, Tottori University, Tottori, Japan

OPEN ACCESS

Edited by:
Dariusz Jan Skarzynski, Institute of Animal Reproduction and Food Research (PAS), Poland

Reviewed by:
Zofia E. Madeja, Poznan University of Life Sciences, Poland
Ana Torres, University of Lisbon, Portugal

***Correspondence:**
Ryo Nishimura
ryon@tottori-u.ac.jp

Specialty section:
This article was submitted to Animal Reproduction - Theriogenology, a section of the journal Frontiers in Veterinary Science

Received: *08 December 2020*
Accepted: *11 March 2021*
Published: *26 April 2021*

Citation:
Masuda Y, Hasebe R, Kuromi Y, Kobayashi M, Urataki K, Hishinuma M, Ohbayashi T and Nishimura R (2021) Three-Dimensional Live Imaging of Bovine Preimplantation Embryos: A New Method for IVF Embryo Evaluation. Front. Vet. Sci. 8:639249. doi: 10.3389/fvets.2021.639249

Conception rates for transferred bovine embryos are lower than those for artificial insemination. Embryo transfer (ET) is widely used in cattle but many of the transferred embryos fail to develop, thus, a more effective method for selecting bovine embryos suitable for ET is required. To evaluate the developmental potential of bovine preimplantation embryos (2-cell stage embryos and blastocysts), we have used the non-invasive method of optical coherence tomography (OCT) to obtain live images. The images were used to evaluate 22 parameters of blastocysts, such as the volume of the inner cell mass and the thicknesses of the trophectoderm (TE). Bovine embryos were obtained by *in vitro* fertilization (IVF) of the cumulus-oocyte complexes aspirated by ovum pick-up from Japanese Black cattle. The quality of the blastocysts was examined under an inverted microscope and all were confirmed to be Code1 according to the International Embryo Transfer Society standards for embryo evaluation. The OCT images of embryos were taken at the 2-cell and blastocyst stages prior to the transfer. In OCT, the embryos were irradiated with near-infrared light for a few minutes to capture three-dimensional images. Nuclei of the 2-cell stage embryos were clearly observed by OCT, and polynuclear cells at the 2-cell stage were also clearly found. With OCT, we were able to observe embryos at the blastocyst stage and evaluate their parameters. The conception rate following OCT (15/30; 50%) is typical for ETs and no newborn calves showed neonatal overgrowth or died, indicating that the OCT did not adversely affect the ET. A principal components analysis was unable to identify the parameters associated with successful pregnancy, while by using hierarchical clustering analysis, TE volume has been suggested to be one of the parameters for the evaluation of bovine embryo. The present results show that OCT imaging can be used to investigate time-dependent changes of IVF embryos. With further improvements, it should be useful for selecting high-quality embryos for transfer.

Keywords: optical coherence tomography, embryo, 3D image, embryo transfer, quantification of embryo structures

INTRODUCTION

Bovine embryo transfer (ET) has been widely used to produce calf in combination with other reproductive technologies, such as *in vitro* fertilization (IVF). However, the conception rate of ET using IVF embryos (30–40%) is lower than that of using embryos produced *in vivo* (around 50%) (1–4). Embryos for transfer are usually selected by observation under a conventional optical microscope at the time of transfer, and embryo quality is subjectively assigned as one of the codes according to the International Embryo Technology Society (IETS) standards for embryo evaluation (5, 6).

In human artificial reproductive technology (ART), embryos are evaluated based on the Veeck and Gardner classification (7, 8) and time-lapse cinematography (TLC) with a visible light microscope, which has recently become a popular technology. Morphokinetic parameters, such as the number of pronuclei or nuclei, timing of cleavage, and the number of blastomeres, are used as potential indicators that may improve the success of ART (9). Furthermore, ART success rate has been improved by comprehensive chromosomal screening using techniques such as array comparative genomic hybridization, quantitative single nucleotide polymorphism arrays, and next-generation sequencing (10, 11). To evaluate *in vitro* developed bovine embryos, TLC has been used to determine the time of the first cleavage and the subsequent number of blastomeres, and the number of blastomeres at the onset of the lag-phase (4, 12–14). However, so far, live bovine embryos have not been evaluated based on their three-dimensional (3D) structure.

A morphological grading system in human ART was first described by Gardner and Schoolcraft (15). According to this system, three parameters (degree of blastocoel expansion, size and compactness of ICM, and the cohesiveness and number of TE) are graded. Based on these criteria, an additional consensus on embryo assessment was agreed including new references for each parameter (16, 17). In this consensus, ICM grade is suggested to be more important for determining the implantation potential of a blastocyst. To select the best blastocyst when performing ET on Day 5, several parameters have been suggested to contribute to the implantation potential of blastocyst. Some investigators have shown that the timing of blastocoel development and the grade of expansion are important parameters for implantation (18–20). Other investigators have suggested that the size and shape of ICM are related to implantation (21–23). Either a positive association or no association of TE cells with implantation has been reported (22, 24–26). Morphological grading, while common for human blastocysts, is difficult for bovine blastocyst because of their dark cytoplasm (27, 28).

Optical coherence tomography (OCT) has been developed for non-invasive, cross-sectional imaging in biological systems (29–31), and is presently used in ophthalmology, especially for funduscopic examination of the retina. OCT can be used to measure 3D images with high spatial resolution, because it can scan small biological structures, such as micro vessel structures during *in vitro* angiogenesis (31). Recently, OCT imaging of mouse (32–34) and porcine (34) early-stage embryo has been reported. In the mouse blastocysts, their nucleoli were also clearly visualized by OCT (34). In cattle, blastocysts have been imaged by OCT, and their cytoplasm movements that are potentially associated with viability were monitored, suggesting that OCT can be used for the measurement of the damage after cryopreservation (35). However, the quantification of the structures of bovine blastocysts for evaluating embryo quality has not been reported. We have recently developed a technique for the 3D imaging of bovine blastocysts and used it to evaluate 22 parameters including the volumes of the ICM, TE, zona pellucida (ZP) and blastocoel of an embryo (36). Here, we used this technique to compare the characteristics of embryos that did or did not develop to term in order to identify the parameters associated with successful ET. Furthermore, in the blastomere observation, the shape, size, cytoplasm color, even distribution of cytoplasm, and number of nucleus have been suggested to be related to the developmental potential of bovine embryos (4, 12–14). Because bovine and porcine early embryos contain much more lipid than human or mouse embryos, pronucleus formation in early embryos cannot be confirmed under a microscope, which made it difficult to evaluate their quality (27, 28, 37, 38). Thus, we have also tried to obtain 3D images of early-stage bovine embryos.

MATERIALS AND METHODS

Ethics Statement

Animal handling and experimental procedures were carried out following the Guidelines for Proper Conduct of Animal Experiments by the Science Council of Japan (http://www.scj.go.jp/ja/info/kohyo/pdf/kohyo-20-k16-2e.pdf).

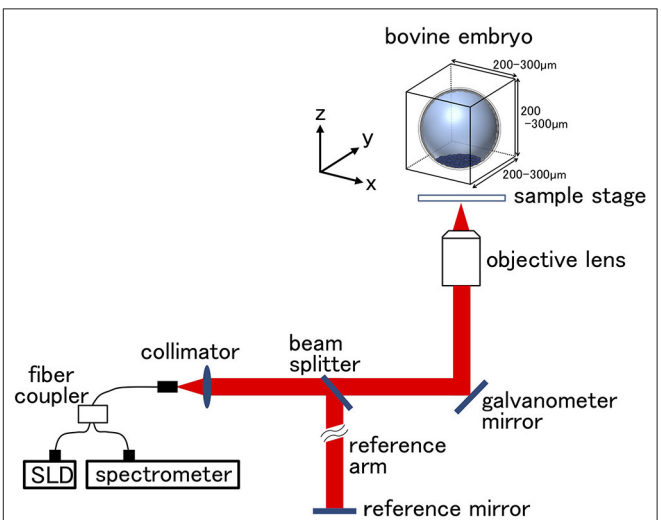

FIGURE 1 | Optical coherence tomography (OCT) setup. The super luminescent diode (SLD) output is coupled into a single mode fiber and split at the fiber coupler into the embryo sample and reference arms. Reflections from the two arms are combined at the coupler and detected by the spectrometer. Scanning scale for the bovine embryo was 200–300 μm in each direction. Longitudinal imaging was performed in the area of bovine embryo.

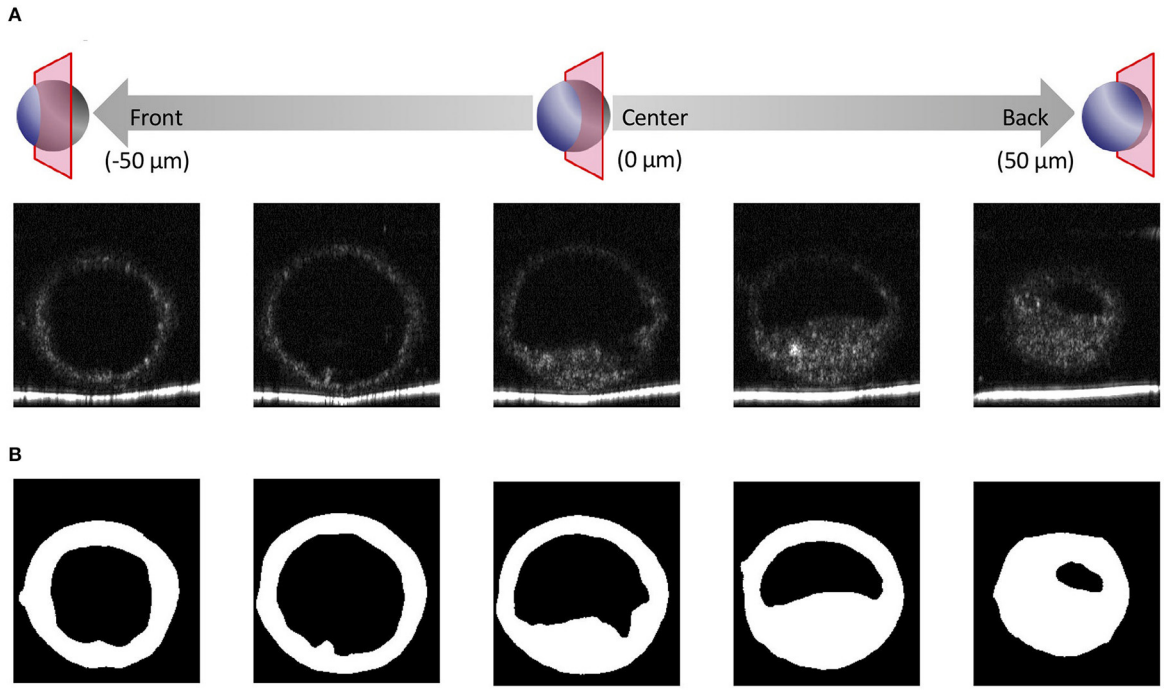

FIGURE 2 | Optical coherence tomography (OCT) images of the bovine embryo and each structure of an embryo. **(A)** Tomographic images obtained by OCT imaging. Panels are images shifted by 25 μm from the center of the embryo. **(B)** Based on the tomographic images, the structure of the embryo is visualized and binarized.

Production of Embryos Derived From Oocytes Collected by Ovum-Pick-Up (OPU) and *in vitro* Maturation (IVM)

As described previously (39), cumulus-oocyte complexes (COCs) were collected from Japanese Black cows ($n = 12$; 110.4 ± 34.3-month-old) by OPU using an ultrasound scanner (HS-2100; Honda Electronics, Toyohashi, Japan) and a 7.5-MHz convex array transducer (HCV-4710MV; Honda Electronics) with a 17-gauge stainless steel needle guide (242 COCs, in total). Follicles >2 mm in diameter were aspirated with a vacuum through a disposable aspiration needle (COVA Needle; Misawa Medical, Tokyo, Japan). The aspiration rate was 14 mL/min and the vacuum pressure was 100 mmHg. The IVM medium was 25 mM HEPES-buffered TCM199 (M199; Gibco, Paisley, Scotland, UK), supplemented with 10% newborn calf serum (NCS; 16010159, Gibco) and 0.01 AU/mL of follicle-stimulating hormone from porcine pituitary (Antorin-R10; Kyoritsu Seiyaku, Tokyo, Japan). COCs with two or more granulosa layers were washed three times with IVM medium. Recovered COCs were cultured in 4-well dishes (Non-Treated Multidishes; Nalge Nunc International, Roskilde, Denmark) in 600 μL of IVM medium, covered with mineral oil (M8414; Sigma-Aldrich, St. Louis, MO, USA), and incubated for 22 h at 38.5°C in 5% CO_2, 5% O_2, and 90% N_2 in humidified air. All cultures were maintained under these conditions.

IVF

Frozen semen of Japanese Black bulls stored in straws was thawed in water (37°C, 40 sec), and then centrifuged twice in IVF100 (Research Institute for the Functional Peptides, Yamagata, Japan; 600 × *g*, 5 min). After centrifugation, spermatozoa were removed from the pellet, and added to IVF100 to obtain a suspension with

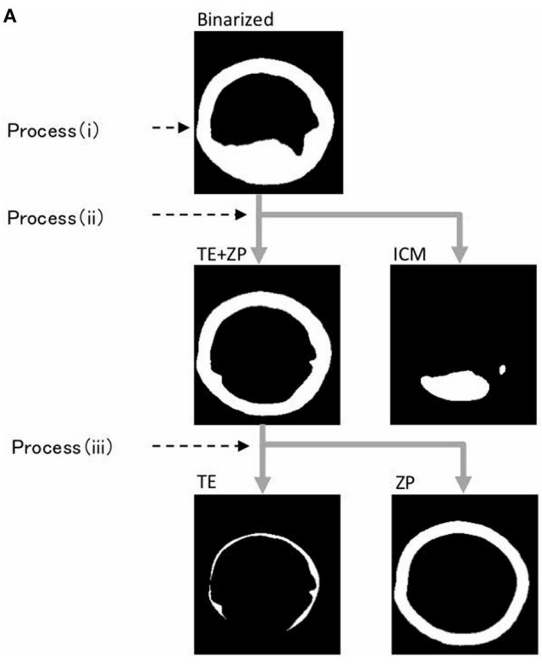

FIGURE 3 | Continued

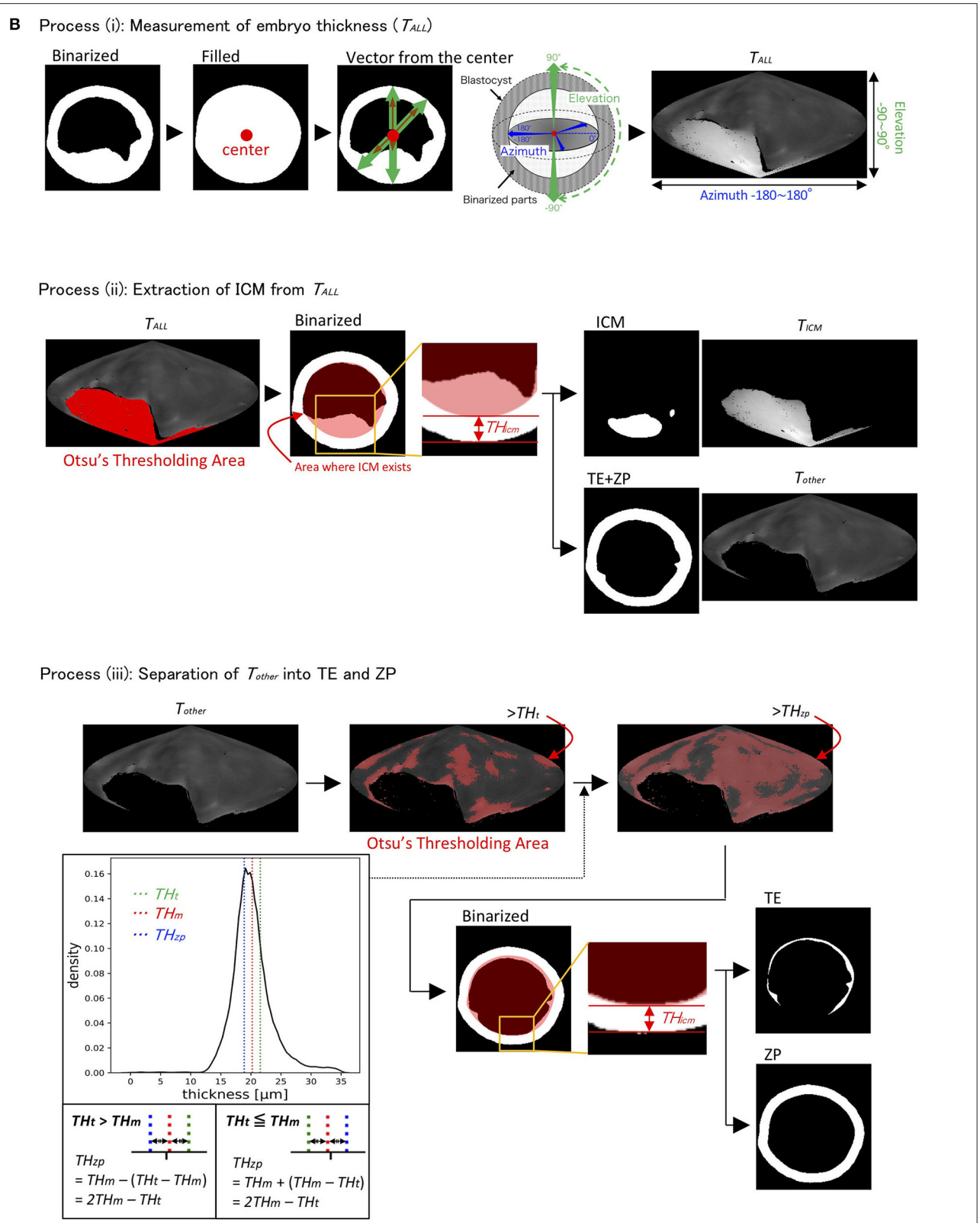

FIGURE 3 | The binarized image was separated into the inner cell mass (ICM), trophectoderm (TE), and zona pellucida (ZP) through processes (i)–(iii) **(A)**. **(B)** Process (i): Thickness of embryo (T_{ALL}) was measured by drawing vectors from the center to the outer and inner surfaces (the outermost of blastocoel) of the embryo.

(Continued)

FIGURE 3 | Process (ii): ICM parts were extracted from T_{ALL} by Otsu's thresholding method (41, 42). Process (iii): The parts, which remained after removing the ICM parts from T_{ALL}, were defined as T_{other}. T_{other} was separated into TE and ZP by calculating the average thickness of T_{other} (TH_m) and by using Otsu's thresholding method (41, 42). T_{All}, thicknesses of embryo along each vector; TH_{icm}, threshold of ICM; T_{ICM}, thickness of ICM; T_{other}, thickness of the areas other than ICM; TH_t, threshold of T_{other}; TH_m, average of THt; TH_{zp}, thickness of ZP (=2 TH_m-TH_t).

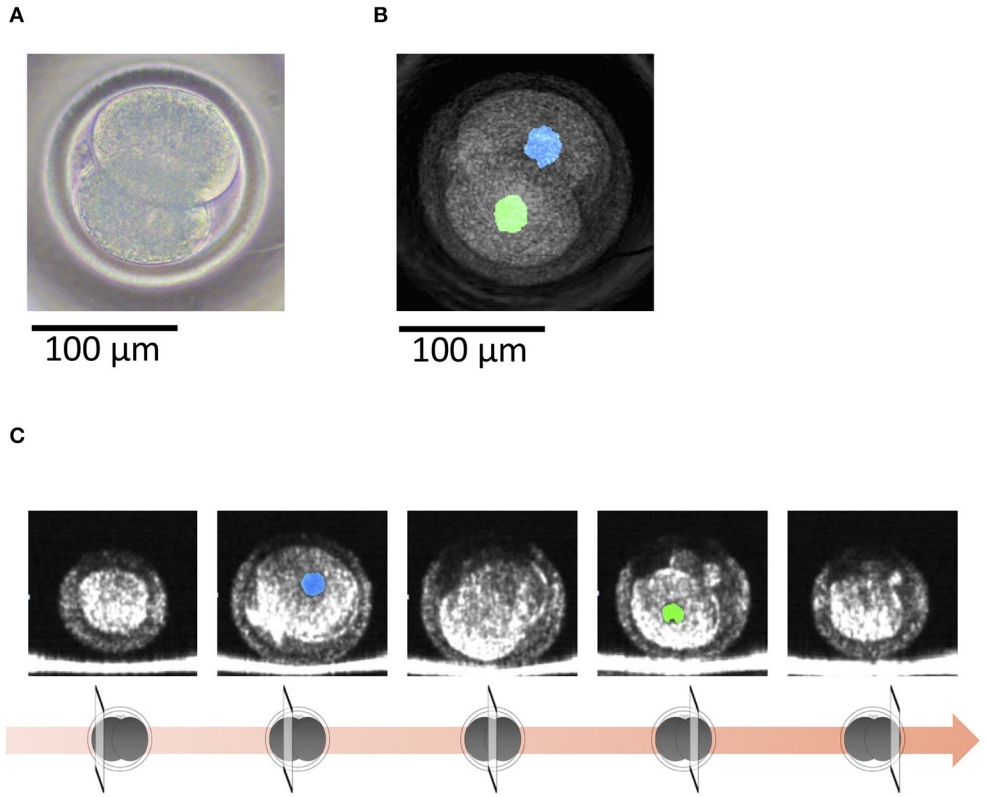

FIGURE 4 | (A) A bovine 2-cell embryo imaged by a microscope. **(B)** Optical coherence tomography (OCT) images of the bovine 2-cell embryo with visualization of the nucleus (blue and green) of the blastomere. **(C)** Tomographic images obtained by OCT imaging. Panels are images shifted by 25 µm from the center of the embryo with visualization of the nucleus (blue and green) of the blastomere.

a final sperm concentration of 1.0 × 10^7/mL. This suspension served as the IVF medium. After 22 h of IVM, the COCs were washed twice with IVF100. Up to 20 COCs were incubated in 100 µL droplets of IVF medium in 35 mm dishes (Falcon 351008; Corning, NY, USA) for 6 h.

In vitro Culture (IVC)

After insemination, oocytes were completely denuded from the cumulus cells and spermatozoa by pipetting with a glass pipette in IVC medium: potassium simplex optimized medium with amino acid (KSOMaa Evolve Bovine; Zenith Biotech, Bangkok, Thailand) supplemented with 5% NCS and 0.6 mg/mL of L-carnitine (C0158, Sigma-Aldrich). Subsequently, presumptive zygotes were washed three times with IVC medium and cultured in 100 µL droplets of IVC medium for 48 h. Each droplet contained approximately 20 presumptive zygotes. Average value of cleavage rate was 74.0% (179/242). At 48 h post-insemination (hpi), embryos with more than four cells were transferred from the 35 mm dishes to well-of-the-well (WOW) dishes (LinKID micro25, Dai Nippon Printing Co., Ltd., Tokyo, Japan) as described (12). WOW dishes, which have 25 microwells (5 columns × 5 rows) in a circular wall in the center of a 35 mm dish, can culture up to 25 embryos each with a single drop of medium and track individual embryos throughout the culture. IVC medium and mineral oil were pre-cultured for at least 12 h in glass bottles separately at 38.5°C in 5% CO_2, 5% O_2, and 90% N_2 in humidified air, and the pre-cultured IVC medium (100 µL) was placed within the circular wall and covered with the pre-cultured mineral oil. At 168 to 180 hpi, embryos that had developed to or beyond the blastocyst stage were observed under an inverted microscope. Finally, 123 embryos had developed to the blastocyst stage (50.8%), and 80 blastocysts had been cryopreserved.

OCT Observations

IVF embryos were cultured for seven days (by this time, they reached the expanded blastocyst stage) and examined under an inverted microscope at 27–31 hpi (at the 2-cell stage; $n = 15$)

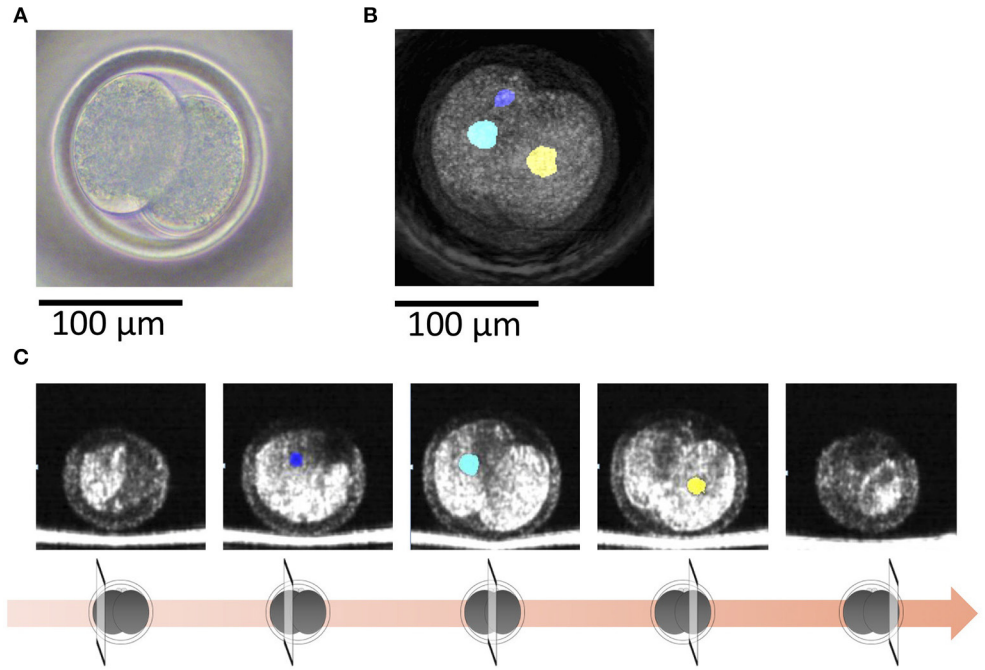

FIGURE 5 | (A) A bovine 2-cell embryo including a binuclear blastomere imaged by a microscope. **(B)** Optical coherence tomography (OCT) images of the bovine 2-cell embryo including a binuclear blastomere with visualization of the nucleus (blue, green, and yellow) of the blastomere. Blue and green nucleus are in a blastomere. **(C)** Tomographic images obtained by OCT imaging. Panels are images shifted by 25 µm from the center of the embryo with visualization of the nucleus (blue, green, and yellow) of the blastomere.

and at 168 to 180 hpi (at the blastocyst stage; $n = 30$). In blastocysts, only the embryos that were independently classified as Code1 according to the IETS standards by three skilled observers were used. OCT imaging was done as described previously (31, 36). Unstained live embryos were imaged by OCT using the Cell3iMager Estier (SCREEN Holdings Co., Ltd, Kyoto, Japan). The imaging system of Cell3iMager Estier is outlined in **Figure 1**. The system is equipped with a super luminescent diode (SLD; center wavelength: 890 nm, N.A. = 0.3). The SLD output is coupled to a single-mode optical fiber and split at an optical fiber coupler into the sample and reference arms. The reflections from the two arms are combined at the coupler and detected by the spectrometer. The 3D image data of the blastocysts were constructed from individual 2D ×-z cross-sectional images, which were obtained by a series of longitudinal scans obtained by laterally translating the optical beam position. The data acquisition window was 200–300 × 200–300 × 200–300 µm, and the voxel size was 1 × 1 × 1 µm. The OCT system scans light source positions in the x-axis direction while the shifting scanning line positions on the y-axis to obtain a signal on the x–y plane at a focus position on the z-axis. By repeating this scanning while shifting the z-axis focus positions, 3D images of the embryos were acquired. The lengths of the imaging range on the x-, y-, and z-axis were 300, 300, and 200 µm, respectively. The exposure time was 150 µs, and scanning an entire embryo was completed in a few minutes. OCT provided cross-sectional images with a slice thickness of 1 µm.

Cryopreservation

As described previously (40), blastocysts imaged by OCT were transferred to a cryoprotective solution [1.8 M of ethylene glycol and 0.1 M of sucrose in Dulbecco's PBS (D-PBS)], which was then placed in a 0.25-mL straw (IMV Technologies, L'Aigle, France) at room temperature. After the blastocysts were equilibrated at room temperature for 15 min, the straws were directly set in a programmable freezer (ET-1N; FUJIHIRA INDUSTRY CO., LTD, Tokyo, Japan) at −7°C where seeding was manually performed. Subsequently, the straws were cooled at a rate of 0.3°C/min to −30°C and then directly transferred to liquid nitrogen for storage until use. The straws were thawed in air for 10 s and then immersed in water (30°C, 20 s) for the ET. Because of the status of our farms, we have chosen a cryopreservation protocol rather than a verification protocol.

Image Analysis

We recently reported using OCT to image bovine embryos (36). After the 3D images were captured by OCT (**Figure 1**), the 3D images were analyzed in an automized way (**Figures 2**, **3**). Process (i) The 3D images of bovine embryos were binarized (**Figures 2**, **3**). For each image, vectors were drawn at equal angles in the elevation direction (−90–90°) and the azimuth direction (−180–180°) from the center of the embryo to the outer surface and the inner surface (the outermost of blastocoel). The thicknesses of the embryo along each vector (T_{All}) were then measured (**Figure 3**). Process (ii) To distinguish the ICM from T_{All}, an appropriate

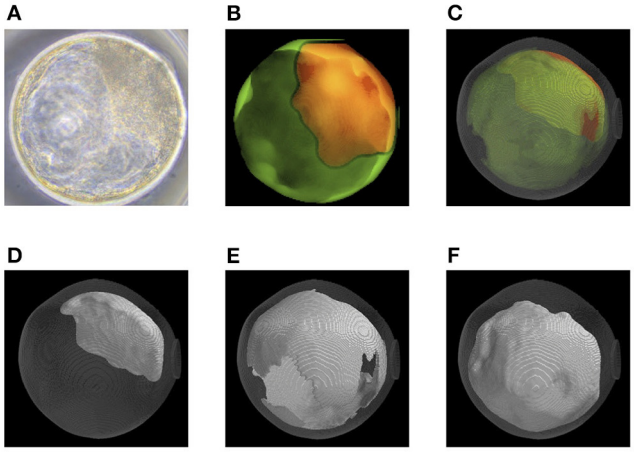

FIGURE 6 | Representative optical coherence tomography (OCT) images of a transferred bovine embryo that resulted in pregnancy. **(A)** A representative transferred embryo, determined as Code 1 according to the IETS standards, imaged by a microscope. **(B)** Sum of all pixel values in z-stack images of trophectoderm (TE; bright green) and inner cell mass (ICM; orange) part was extracted from the tomographic image and synthesized 2D image. **(C)** A 3D-visualization of structures of the embryo, including ICM (orange), TE (bright green), zona pellucida (ZP; gray), and blastocoel. **(D–F)** A 3D visualization of each structure of the embryo: ICM **(D)**, TE **(E)**, and blastocoel **(F)**. Colors in **(B–F)** are graphically added. See also **Supplementary Movies 1**–**4** for the 3D images of **(C–F)**, respectively.

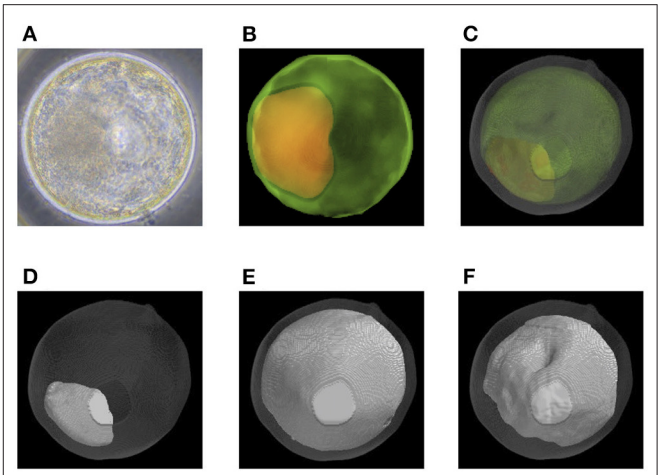

FIGURE 7 | Representative optical coherence tomography (OCT) images of a transferred bovine embryo that resulted in non-pregnancy. **(A)** A representative transferred embryo, determined as Code 1 according to the IETS standards, imaged by a microscope. **(B)** Sum of all pixel values in z-stack images of the trophectoderm (TE; bright green) and inner cell mass (ICM; orange) part was extracted from the tomographic image and synthesized 2D image. **(C)** A 3D-visualization of structures of the embryo, including ICM (orange), TE (bright green), zona pellucida (ZP; gray), and blastocoel. **(D–F)** A 3D visualization of each structure of the embryo: ICM **(D)**, TE **(E)**, and blastocoel **(F)**. Colors in **(B–F)** are graphically added. See also **Supplementary Movies 5**–**8** for the 3D images of **(C–F)**, respectively.

threshold (TH_{icm}; the cut-off value for distinguishing ICM from T_{All}) was set by Otsu's method (41, 42) (**Figure 3**). The parts where the thickness from the outer edge of the embryo region was lower than TH_{icm} were excluded from the binarized images. The largest object among the remaining objects after the exclusion was defined as ICM. T_{ALL} was separated into the thickness information of the area corresponding to ICM (T_{ICM}) and the thickness information areas other than ICM (T_{other}). Process (iii) Based on the T_{other} value, the average thickness (TH_m) was evaluated, and the threshold (TH_t) was set by Otsu's method (41, 42) (**Figure 3**). The threshold (TH_{zp}) that separates TE and ZP was set by TH_m–(TH_t-TH_m) (in case of $TH_t > TH_m$) or by $TH_m + (TH_m\text{-}TH_t)$ (in case of $TH_m \geqq TH_t$). The region where the thickness of T_{other} was lower than TH_{zp} was defined as ZP, and the remaining region after removing TH_{zp} from T_{other} was defined as TE. The unfulfilled region, surrounded by the embryo parts, such as ICM, ZP, and TE, in the binarized image was defined as the blastocoel. The volumes of the defined ICM, TE, ZP, and blastocoel were evaluated. The means, medians, standard deviations, minimum, maximum, and range of the thickness of ICM were evaluated from T_{ICM}. The thickness of TE was evaluated from the thickness information, which was obtained by subtracting TH_{zp} from T_{other}. Summary statistics related to the thickness of ZP was set by TH_{zp}.

ET and Pregnancy Diagnosis

The OCT-imaged embryos were transferred to 30 recipient cows [47.5 ± 25.5-month-old Holstein (18 lactating cows) and Japanese Black cows (10 cows; two cows received ET twice)] from March 2018 to February 2019 at the farms in Tottori prefecture, Japan. The cows were clinically normal with body condition scores (BCS) between 2.75 and 3.0 (BCS scale goes from 1 to 5 with 0.25 increments). Before ET, recipients were estrus-synchronized by the administration of a CIDR device (CIDR 1900; Zoetis Japan, Tokyo, Japan) for 9 days and a treatment with cloprostenol (Dalmazin 150 μg [i.m.]; Kyoritsu Seiyaku Corporation, Tokyo, Japan) 2 days before the CIDR removal. Estrus of recipient cows was monitored, and embryos were transferred seven days after estrus with the confirmation of the presence of corpus luteum (CL; diameter ≧20 mm). The recipients were examined for pregnancy 23 days after ET using ultrasonography (HS101V; Honda Electronics). Pregnancy was confirmed in nine Holstein cows and six Japanese Black cows by observation of a CL ≧ 20 mm in diameter and an embryo with a detectable heartbeat in the intraluminal uterine fluid and an embryonic membrane. Ages of pregnant and non-pregnant cows were 42.3 ± 19.9 and 52.7 ± 29.5-months-old, respectively. Cows with BCS of 2.75 and 3.0 were included equally in both pregnant and non-pregnant cows.

Data Analysis

Hierarchical clustering analysis was performed using 13 blastocoel-related and ZP-related parameters of bovine blastocysts. Metrics and linkage criteria for hierarchical clustering were Pearson's correlation and unweighted average linkage. The data was normalized so that the $average = 0$ and

TABLE 1 | Quantification of 22 parameters in bovine embryo (Pregnancy: $n = 15$, Non-pregnancy: $n = 15$).

		Pregnancy			Non-pregnancy			*p*-value	$p < 0.05$
		Median	**Min**	**Max**	**Median**	**Min**	**Max**		
Structural thickness (μm)									
	Mean	56.2	22.1	77.8	55.4	32.5	90.7	0.7	n.s.
ICM	Median	57.1	20.4	78.1	56.4	28.9	90.4	0.8	n.s.
	SD	7.1	3.3	10.8	7.3	4.8	12.0	1.0	n.s.
	Mean	4.3	2.3	6.2	3.8	2.8	7.2	0.8	n.s.
TE	Median	3.1	2.4	4.8	2.9	1.9	5.4	0.9	n.s.
	SD	4.1	1.5	6.2	3.1	1.8	6.1	0.8	n.s.
	Mean	14.9	10.3	20.2	13.9	7.8	21.9	1.0	n.s.
ZP	Median	15.4	11.1	21.0	15.0	8.1	23.1	1.0	n.s.
	SD	2.6	1.9	3.4	2.7	1.5	4.5	0.9	n.s.
	Mean	19.6	13.1	25.1	19.4	10.8	28.4	1.0	n.s.
TE + ZP	Median	19.1	13.1	24.0	19.2	10.2	27.0	0.8	n.s.
	SD	4.8	3.1	6.7	4.3	3.3	7.7	0.4	n.s.
Volume ($\times 10^5$ μm^3)									
ICM		3.6	2.4	6.7	3.6	2.0	6.8	1.0	n.s.
TE		1.9	0.6	2.9	1.9	0.6	4.2	1.0	n.s.
ZP		15.1	13.5	23.0	15.3	9.1	26.6	0.5	n.s.
TE+ZP		18.1	15.4	25.0	17.5	11.2	32.3	0.5	n.s.
ICM+TE+ZP		21.7	17.7	27.7	20.0	13.4	38.5	0.4	n.s.
Blastocoel		14.4	2.6	21.6	12.5	3.3	21.2	0.9	n.s.
Whole embryo		37.4	22.9	49.3	33.0	24.4	50.9	0.6	n.s.
Diameter of blastocoel (μm)									
Mean		54.3	31.6	62.8	52.3	39.5	62.0	0.8	n.s.
Median		56.7	32.1	65.8	54.2	39.3	65.2	0.8	n.s.
SD		15.1	9.8	16.5	14.8	11.9	17.4	0.8	n.s.

ICM, inner cell mass; TE, trophectoderm; ZP, zona pellucida.

$SD = 1$ for each of the parameter. Hierarchical clustering analysis was performed using the SciPy (ver.1.3.0) package in Python (ver.3.6.5). Statistical significance was analyzed using the Mann-Whitney U test. A value of $p < 0.05$ was considered statistically significant. Mann-Whitney U test was performed using the SciPy (ver.1.3.0) package in Python (ver.3.6.5). Principal component analysis (PCA) was performed using 22 parameters of bovine blastocysts. The data was normalized so that the $average = 0$ and $SD = 1$ for each of the parameter. PCA was performed using the scikit-learn (ver.0.23.2) package in Python (ver.3.6.5).

RESULTS

3D Imaging of Bovine IVF Embryos at the 2-Cell Stage

With OCT, it was possible to non-invasively obtain live 3D images of a 2-cell embryo. OCT images also showed the nuclei (**Figures 4B,C**), which made it easy to find binuclear blastomeres (blue and green in **Figures 5B,C**). Of the 15 embryos examined by OCT, two were binuclear and were not used for transfer.

Quantification of Bovine Embryo Morphology at the Blastocyst Stage and ET Success Rate

Before transfer, we obtained images of an embryo with a microscope (**Figures 6A**, **7A**) and with OCT. OCT images of the trophectoderm (TE) and inner cell mass (ICM) of representative embryos resulting in pregnancy (P embryos) and non-pregnancy (NP embryos) are shown in **Figures 6B**, **7B**, respectively. In these figures, TE and ICM were artificially colored green and orange, respectively. The structure of a whole embryo, including ICM (orange), TE (green), and zona pellucida (ZP; gray) were also 3D-visualized (**Figures 6C**, **7C**; **Supplementary Movies 1, 5**). Each part of the embryo, the ICM (**Figures 6D**, **7D**; **Supplementary Movies 2, 6**), TE (**Figures 6E**, **7E**; **Supplementary Movies 3, 7**), and blastocoel (**Figures 6F**, **7F**; **Supplementary Movies 4, 8**), was also 3D-visualized individually.

Twenty-two parameters were measured for each of the 30 embryos (**Table 1**). For the embryos that were subjected to ET ($n = 30$), the average thicknesses of ICM, TE, ZP, and TE + ZP were 55.1 ± 14.1, 4.2 ± 1.2, 15.2 ± 3.4, and 19.5 ± 3.8 μm, respectively (mean ± SD). The average volumes of ICM, TE, ZP, TE + ZP, ICM + TE + ZP, blastocoel, and whole embryo were

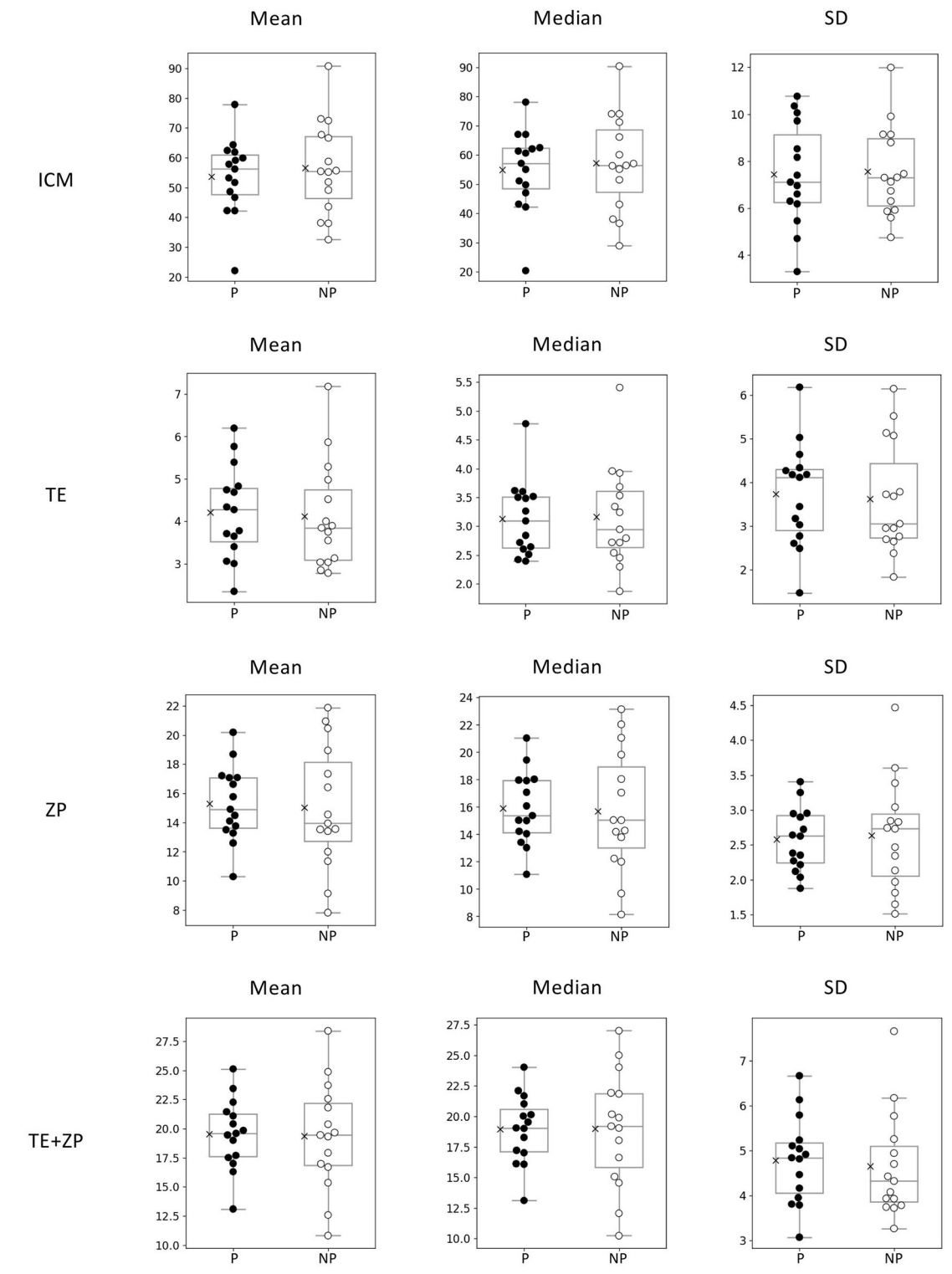

FIGURE 8 | Continued

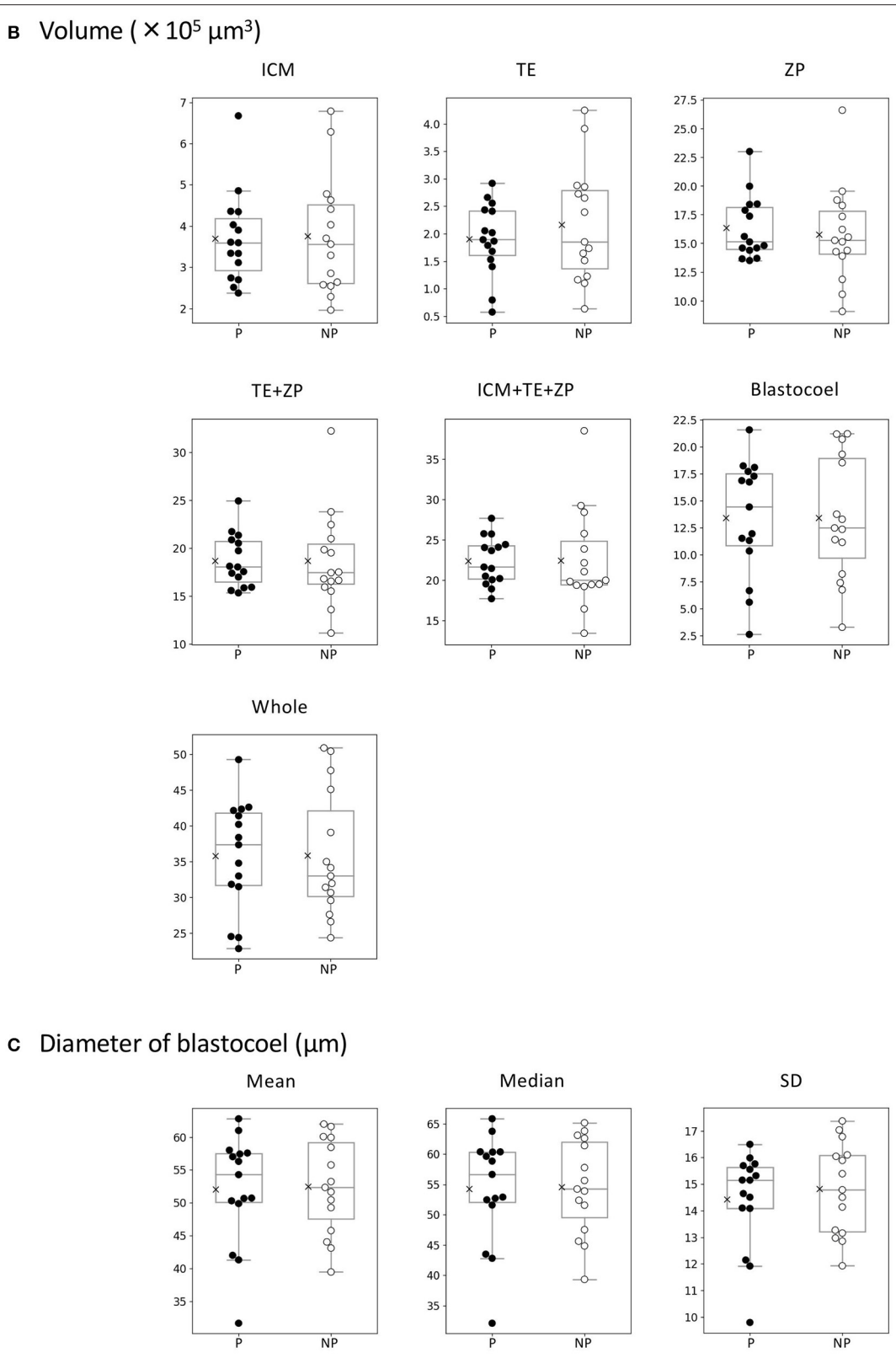

FIGURE 8 | Comparison of 22 morphological parameters of bovine blastocysts between pregnancy (P: $n = 15$) and non-pregnancy (NP: $n = 15$). **(A)** Parameters related to structural thickness including mean, median, and standard deviation (SD) of inner cell mass (ICM), trophectoderm (TE), zona pellucida (ZP), and TE + ZP.

(Continued)

FIGURE 8 | (B) Parameters related to the volume of each part of blastocyst (ICM, TE, ZP, TE + ZP, ICM + TE + ZP, blastocoel, and whole embryo). **(C)** Parameters related toblastocoel diameter (mean, median, and SD). Statistical significance was analyzed using the Mann-Whitney *U* test. A value of $p < 0.05$ was considered statistically significant.

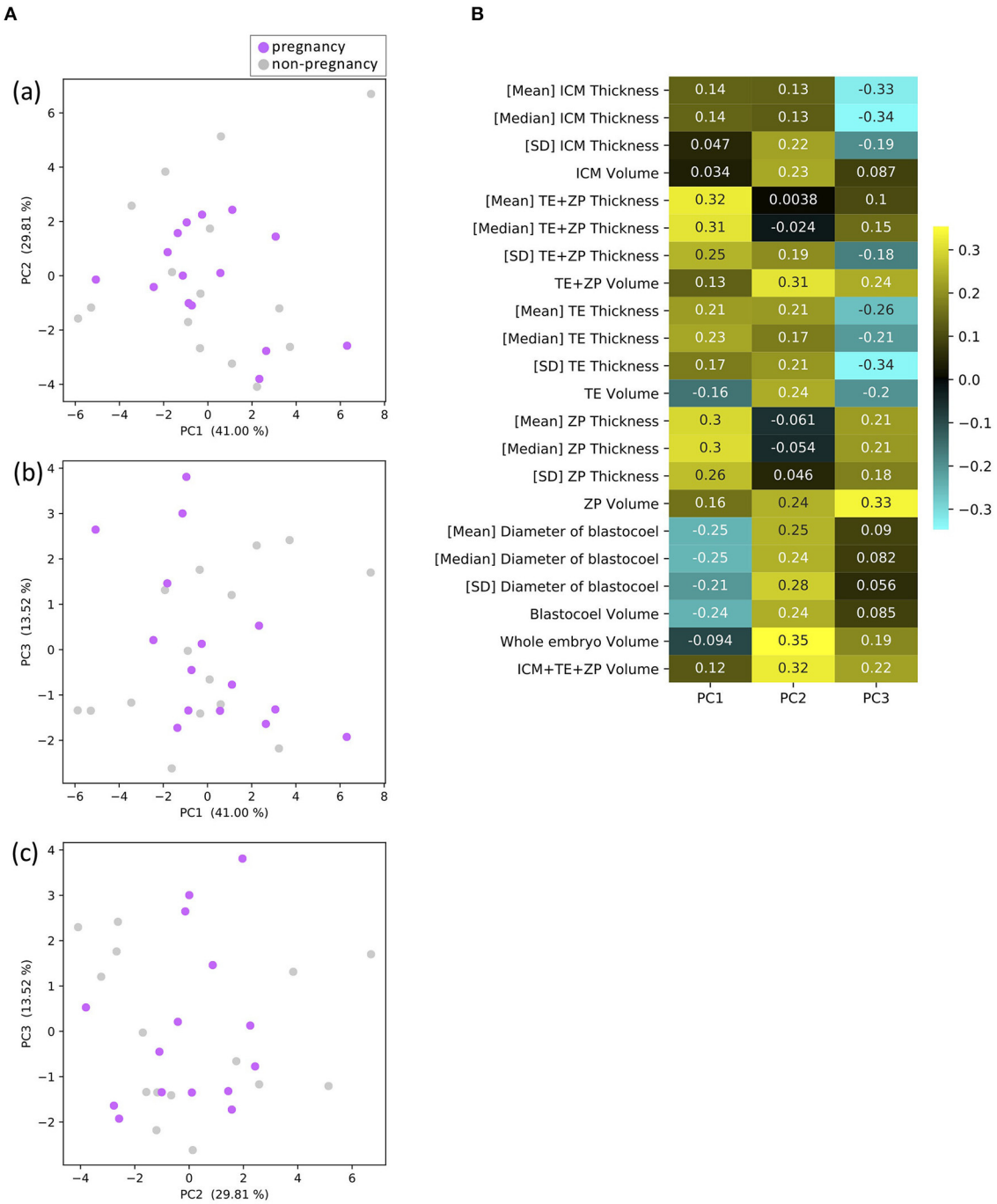

FIGURE 9 | Results of principal component analysis (PCA) based on the 22 morphological parameters of bovine blastocysts (pregnancy: $n = 15$, non-pregnancy: $n = 15$). **(A)** Two-dimensional PCA plots [**(a)** PC1–PC2, **(b)** PC1–PC3, **(c)** PC3–PC2] profiled based on the morphological parameters evaluated from the OCT-scanned 3D images of bovine blastocysts. Each purple and gray dot represents blastocyst resulting in pregnancy and non-pregnancy, respectively. **(B)** Eigenvectors for PC1, 2, and 3.

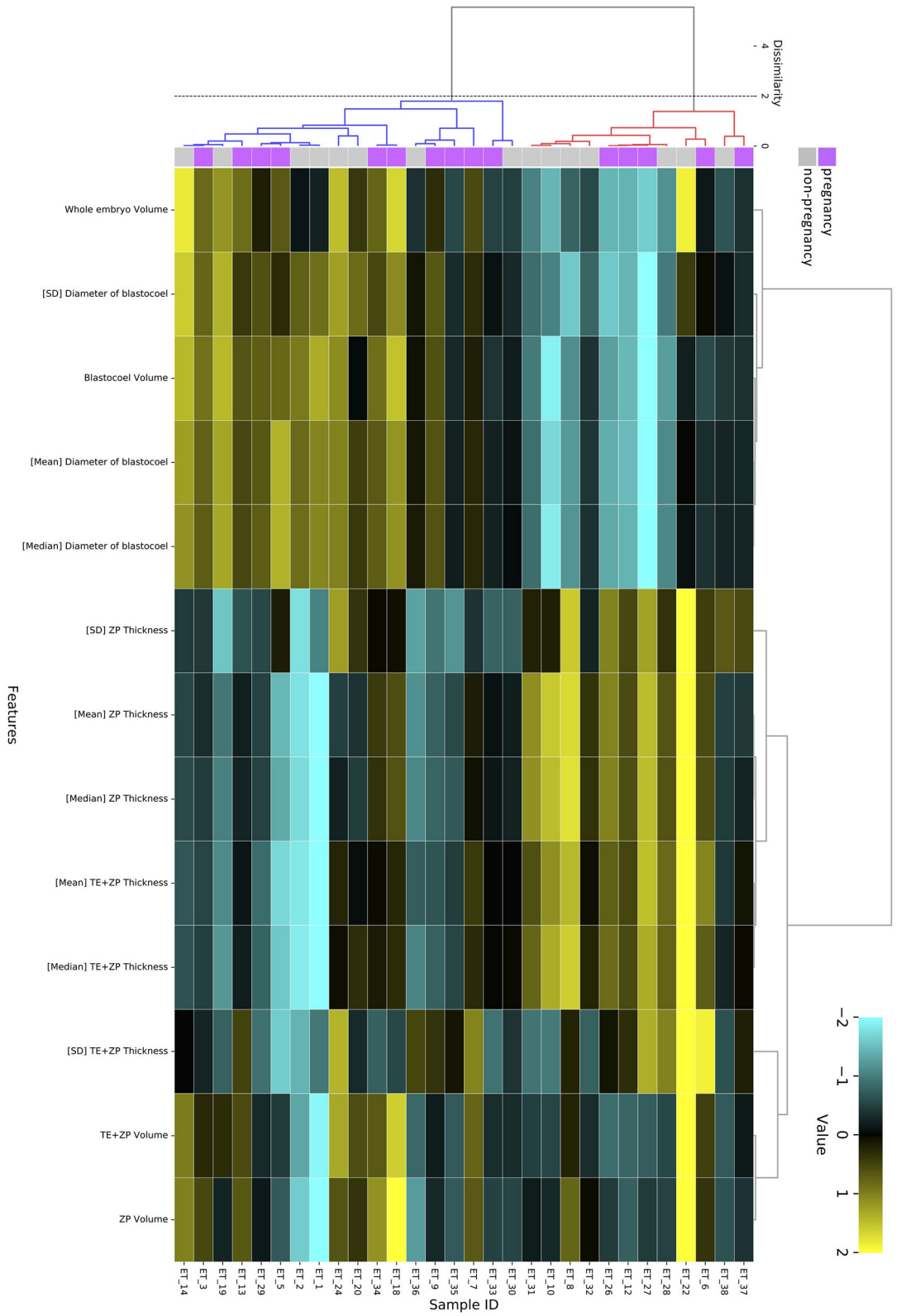

FIGURE 10 | Hierarchical clustering analysis performed using 13 blastocoel-related and ZP-related parameters obtained from 30 blastocysts applied for transfer [pregnancy (purple): $n = 15$, non-pregnancy (gray): $n = 15$]. Embryos displaying similar patterns for these 13 parameters were grouped together on closely connected

(Continued)

FIGURE 10 | branches of the dendrogram with the same color. The color map indicates normalized values that were based on the average value of each parameter (*average = 0* and *SD = 1*). Yellow represents a high value; black represents approximately an equal to average value; and sky blue represents a low value. Metrics and linkage criteria for hierarchical clustering were Pearson's correlation and unweighted average linkage. Two clusters marked with red and blue were obtained with a threshold of *Dissimilarity = 2.0*.

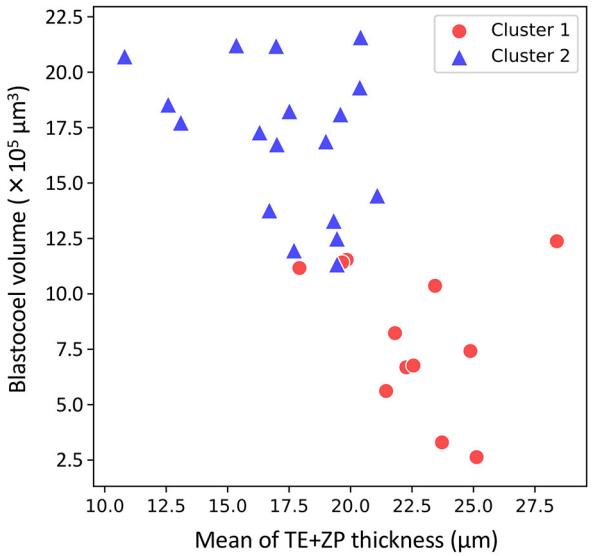

FIGURE 11 | Two-dimensional plots profiled based on the mean of trophectoderm (TE) + zona pellucida (ZP) thickness and blastocoel volume evaluated from the optical coherence tomography (OCT)-scanned 3D images of bovine blastocysts (Cluster 1: red circle, Cluster 2: blue triangle; pregnancy: $n = 15$, non-pregnancy: $n = 15$).

3.7 ± 1.3, 2.0 ± 0.9, 16.1 ± 3.5, 18.7 ± 4.0, 22.4 ± 4.7, 13.4 ± 5.5, and $35.8 \pm 8.1 \times 10^5$ μm^3, respectively (mean ± SD), and the blastocoel diameters were 52.3 ± 7.7 μm (mean ± SD). Fifteen of the 30 recipients became pregnant. None of the parameters were significantly different between the embryos that did (P) or did not (NP) lead to pregnancy (**Table 1**; **Figure 8**). Twelve of the 15 pregnant cows gave birth (six males and six females), and the remaining three cows experienced a late embryonic death. Newborn calves had typical weights (male: 40.2 kg; female: 35.5 kg, in average), and did not show any congenital defects, neonatal overgrowth, and death.

PCA of 22 Morphological Parameters of Bovine Blastocysts

A PCA identified three principal components, PC1, PC2, and PC3. PC1 was related to the thickness of ZP and TE, which accounted for 41.00% of the variance; PC2 was related to the volumes of parts, which accounted for 29.81% of the variance; and PC3 was related to the thickness of ICM and TE, which accounted for 13.52% of the variance (**Figure 9B**). **Figure 9A** shows plots of PC1 vs. PC2 (a), PC1 vs. PC3 (b), and PC3 vs. PC2 (c). None of the plots clearly separated the P and NP embryos.

Hierarchical Clustering Analysis of the Morphological Parameters of Bovine Blastocysts

The hierarchical clustering analysis based on the blastocoel-related and ZP-related parameters (**Figure 10**) showed two clusters with a threshold of *Dissimilarity = 2.0*, and these clusters were also found separated into low (Cluster 1) and high (Cluster 2) blastocoel volume clusters on blastocoel volume-TE + ZP thickness plane (**Figure 11**). In Cluster 1, no significant difference was found in any of the 22 parameters between the P and NP embryos (**Figure 12**), while in Cluster 2, TE volume was significantly lower in the P embryos ($p < 0.05$) (**Figure 12**, **13**). No difference between the P and NP embryos in any of the 22 parameters was common to both clusters (**Figures 12**, **13**).

DISCUSSION

The present study describes the 3D images of bovine embryos at the 2-cell and blastocyst stages obtained by OCT. Blastomere nuclei at the 2-cell stage were also clearly visualized by the same system. At the blastocyst stage, 22 morphological parameters were evaluated based on the 3D OCT images. The transfer of 30 bovine embryos after being imaged by OCT resulted in 15 pregnancies (pregnancy rate: 50%) and 12 births (birth rate: 40%), which was typical for the ET attempts (1–4). Bovine blastocysts appeared healthy after a long-term (over 18 h) capture by OCT for monitoring their micro-scale movements (35). These results indicate that OCT can be used to evaluate embryos before ET. As described previously, OCT can capture the inside structure of mammalian embryos (32–36). In addition, the present study has made it possible to quantify several parts of bovine blastocysts including its inside structure, such as the blastocoel, which could not be visualized by conventional microscopy.

A PCA of the measured parameters was unable to find the critical parameters associated with pregnancy. To find the critical parameters for pregnancy, a greater number of transfers of OCT-imaged embryos is needed. As bovine embryos expand into blastocysts, the thickness of the ZP decreases (5). In addition, we detected the blastocoel-related parameters (volume and diameter), which were originally quantified in our recent study by OCT (36). Thus, we conducted a hierarchical clustering analysis based on the blastocoel-related and ZP-related parameters. The hierarchical clustering analysis (**Figure 10**) shows two clusters with a threshold of *Dissimilarity = 2.0*, and these clusters were also found separated into two clusters with low (Cluster 1) or high (Cluster 2) blastocoel volumes on a blastocoel volume-TE + ZP thickness plane. While no difference common to both clusters were found in any of the 22 parameters between the P and NP embryos, TE volume in Cluster 2 was significantly lower

FIGURE 12 | *P*-values in the comparison of 22 parameters evaluated from the optical coherence tomography (OCT)-scanned 3D images of bovine blastocysts between pregnancy and non-pregnancy in each cluster (pregnancy: $n = 15$, non-pregnancy: $n = 15$). Statistical significance was analyzed using the Mann-Whitney *U* test. A value of $p < 0.05$ was considered statistically significant.

in the P embryos than in the NP embryos. In Cluster 2, blastocoel volumes were relatively high and the TE + ZP thicknesses were relatively low (**Figure 11**), suggesting that embryos in Cluster 2 were well-expanded. These results imply that a low TE volume could be one of the parameters for selecting embryo for ET especially in well-expanded blastocysts. However, since in Cluster 1, there was no significant difference in TE volume between the P and NP embryos, more precise methods for the quantification of TE-related parameters and/or a combination of parameters based on the increased number of OCT images are needed to find the critical parameters for the evaluation of bovine embryos for ET. Furthermore, embryo evaluation is more effective if the OCT measurements are done in parallel with time lapse imaging to evaluate other developmental landmarks, such as the timing of embryo cleavage, timing of each developmental stage, and evaluating cell number.

The present study imaged blastomere nuclei at the 2-cell stage. Karnowski et al. (34) reported that OCT could visualize not only nuclei but also pronuclei and nucleoli in mouse early embryos and blastocysts. They also used OCT to show time dependent changes in these nuclear architectures (34). In cattle, TLC analysis has revealed that the time-dependent changes, such as the time of the first cleavage and the subsequent number of blastomeres, and the number of blastomeres at the onset of the lag-phase are useful for selecting embryos with a development potential (4, 12–14). Since we also visualized binuclear cells in a blastomere at the 2-cell stage, which is known as a negative indicator for development (43), OCT should also be useful for weeding out poor quality embryos. Previous reports also indicate that morphological indices also help to select high quality bovine embryos (4, 13, 43). Furthermore, the structure of bovine blastocyst has been precisely quantified in the present study. Together, the above findings suggest that detecting time-dependent structural changes of early-stage bovine embryo by OCT could improve evaluations at the blastocyst stage.

The present study reports the first normal deliveries of calves following the transfer of OCT-analyzed bovine embryos.

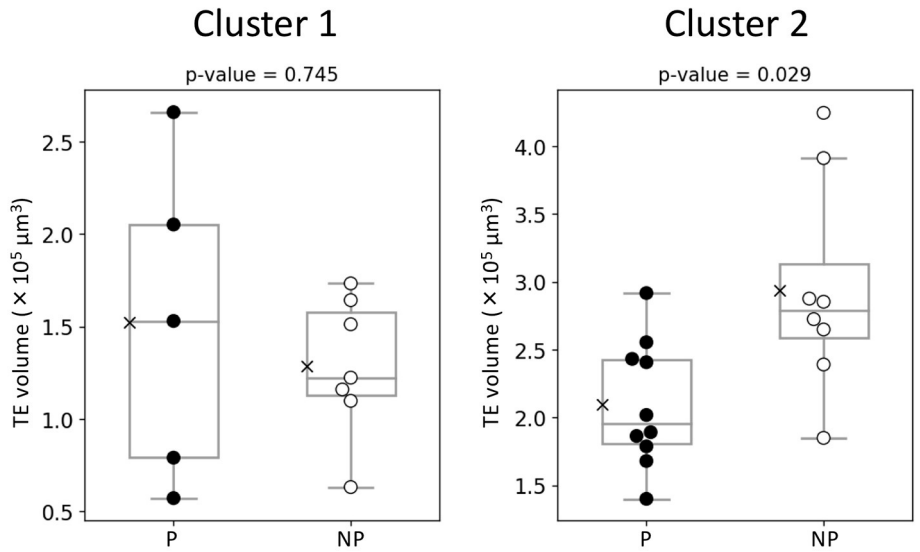

FIGURE 13 | Comparison of TE volume evaluated from the optical coherence tomography (OCT)-scanned 3D images of bovine blastocysts between pregnancy (P) and non-pregnancy (NP) in each cluster (pregnancy: $n = 15$, non-pregnancy: $n = 15$). Statistical significance was analyzed using the Mann-Whitney *U* test. A value of $p < 0.05$ was considered statistically significant.

The present conception rate (50%) and the birth rate (40%) following OCT are typical for ETs, indicating that OCT did not adversely affect ET. Although a PCA was unable to identify the parameters associated with pregnancy, TE-related parameters may be useful for evaluating bovine embryos. At present, OCT imaging should be useful for investigating the time-dependent changes of IVF embryos, and with further improvements, be useful for the selection of high-quality embryos for transfer.

DATA AVAILABILITY STATEMENT

The original contributions presented in the study are included in the article/**Supplementary Material**, further inquiries can be directed to the corresponding author/s.

ETHICS STATEMENT

Ethical review and approval was not required for the animal study because the presented results were based on the bovine blastocyst images captured in culture conditions, so that the present experiments did not have any stress to animals. Animal handling and experimental procedures in farms were carried out following the Guidelines for Proper Conduct of Animal Experiments by Science Council of Japan (http://www.scj.go.jp/ja/info/kohyo/pdf/kohyo-20-k16-2e.pdf). Written informed consent was obtained from the owners for the participation of their animals in this study.

AUTHOR CONTRIBUTIONS

RN: conceptualization, resources, data curation, supervision, project administration, and writing—review and editing. YM: methodology, investigation, and writing—original draft preparation. RH, YK, MK, and KU: methodology, investigation, and writing—review and editing. MH and TO: writing—review and editing. All authors have read and agreed with the manuscript for publication.

ACKNOWLEDGMENTS

We thank the owners and crews of the farms in Tottori prefecture (Field Science Center, Faculty of Agriculture, Tottori University, Tottori; Tottori Livestock Research Center, Tohaku; Takemoto Farm, Kurayoshi) for their outstanding cooperation and for donor cow feeding management.

SUPPLEMENTARY MATERIAL

The Supplementary Material for this article can be found online at: https://www.frontiersin.org/articles/10.3389/fvets.2021.639249/full#supplementary-material

REFERENCES

1. Rizos D, Clemente M, Bermejo-Alvarez P, de La Fuente J, Lonergan P, Gutiérrez-Adán A. Consequences of *in vitro* culture conditions on embryo development and quality. *Reprod Domest Anim.* (2008) 43 (Suppl. 4):44–50. doi: 10.1111/j.1439-0531.2008.01230.x
2. Lim KT, Jang G, Ko KH, Lee WW, Park HJ, Kim JJ, et al. Improved cryopreservation of bovine preimplantation embryos

cultured in chemically defined medium. *Anim Reprod Sci.* (2008) 103:239–48. doi: 10.1016/j.anireprosci.2006.12.020
3. Ferraz PA, Burnley C, Karanja J, Viera-Neto A, Santos JE, Chebel RC, et al. Factors affecting the success of a large embryo transfer program in Holstein cattle in a commercial herd in the southeast region of the United States. *Theriogenology.* (2016) 86:1834–41. doi: 10.1016/j.theriogenology.2016.05.032
4. Sugimura S, Akai T, Imai K. Selection of viable *in vitro*-fertilized bovine embryos using time-lapse monitoring in microwell culture dishes. *J Reprod Dev.* (2017) 63:353–7. doi: 10.1262/jrd.2017-041
5. Stringfellow DA, Givens MD, International Embryo Transfer S. Manual of the International Embryo Transfer Society: a procedural guide and general information for the use of embryo transfer technology emphasizing sanitary procedures. In: *Savory, Ill.: International Embryo Transfer Society*. Champaign, IL (2010).
6. Bo GA, Mapletoft RJ. Evaluation and classification of bovine embryos. *Anim Reprod.* (2013) 10:344–8.
7. Veeck LL. Oocyte assessment and biological performance. *Ann NY Acad Sci.* (1988) 541:259–74. doi: 10.1111/j.1749-6632.1988.tb22263.x
8. Gardner DK, Schoolcraft WB, Wagley L, Schlenker T, Stevens J, Hesla J. A prospective randomized trial of blastocyst culture and transfer in in-vitro fertilization. *Hum Reprod.* (1998) 13:3434–40. doi: 10.1093/humrep/13.12.3434
9. Gardner DK, Meseguer M, Rubio C, Treff NR. Diagnosis of human preimplantation embryo viability. *Hum Reprod Update.* (2015) 21:727–47. doi: 10.1093/humupd/dmu064
10. Yao GD, Xu JW, Xin ZM, Niu WB, Shi SL, Jin HX, et al. Developmental potential of clinically discarded human embryos and associated chromosomal analysis. *Sci Rep.* (2016) 6:23995. doi: 10.1038/srep23995
11. Tsuiko O, Catteeuw M, Esteki MZ, Destouni A, Pascottini OB, Besenfelder U, et al. Genome stability of bovine *in vivo*-conceived cleavage-stage embryos is higher compared to *in vitro*-produced embryos. *Hum Reprod.* (2017) 32:2348–57. doi: 10.1093/humrep/dex286
12. Sugimura S, Akai T, Hashiyada Y, Aikawa Y, Ohtake M, Matsuda H, et al. Effect of embryo density on *in vitro* development and gene expression in bovine *in vitro*-fertilized embryos cultured in a microwell system. *J Reprod Dev.* (2013) 59:115–22. doi: 10.1262/jrd.2012-113
13. Sugimura S, Akai T, Hashiyada Y, Somfai T, Inaba Y, Hirayama M, et al. Promising system for selecting healthy *in vitro*-fertilized embryos in cattle. *PLoS ONE.* (2012) 7:e36627. doi: 10.1371/journal.pone.0036627
14. Sugimura S, Akai T, Somfai T, Hirayama M, Aikawa Y, Ohtake M, et al. Time-lapse cinematography-compatible polystyrene-based microwell culture system: a novel tool for tracking the development of individual bovine embryos. *Biol Reprod.* (2010) 83:970–8. doi: 10.1095/biolreprod.110.085522
15. Gardner DK, Schoolcraft WB. *In vitro* culture of human blastocyst. In: Janson R, Mortimer D, editors. *Towards Reproductive Certainty: Infertility and Genetics Beyond.* Carnforth: Parthenon Press (1999). p. 378–88.
16. Alpha Scientists In Reproductive M, ESHRE Special Interest Group E. The Istanbul consensus workshop on embryo assessment: proceedings of an expert meeting. *Hum Reprod.* (2011) 26:1270-83.
17. Alpha Scientists In Reproductive M, ESHRE Special Interest Group E. Istanbul consensus workshop on embryo assessment: proceedings of an expert meeting. *Reprod Biomed Online.* (2011) 22:632–46. doi: 10.1016/j.rbmo.2011.02.001
18. Dokras A, Sargent IL, Barlow DH. Human blastocyst grading: an indicator of developmental potential? *Hum Reprod.* (1993) 8:2119–27. doi: 10.1093/oxfordjournals.humrep.a137993
19. Shapiro BS, Harris DC, Richter KS. Predictive value of 72-hour blastomere cell number on blastocyst development and success of subsequent transfer based on the degree of blastocyst development. *Fertil Steril.* (2000) 73:582–6. doi: 10.1016/S0015-0282(99)00586-5
20. Yoon HJ, Yoon SH, Son WY, Im KS, Lim JH. High implantation and pregnancy rates with transfer of human hatching day 6 blastocysts. *Fertil Steril.* (2001) 75:832–3. doi: 10.1016/S0015-0282(00)01797-0
21. Balaban B, Urman B, Sertac A, Alatas C, Aksoy S, Mercan R. Blastocyst quality affects the success of blastocyst-stage embryo transfer. *Fertil Steril.* (2000) 74:282–7. doi: 10.1016/S0015-0282(00)00645-2
22. Richter KS, Harris DC, Daneshmand ST, Shapiro BS. Quantitative grading of a human blastocyst: optimal inner cell mass size and shape. *Fertil Steril.* (2001) 76:1157–67. doi: 10.1016/S0015-0282(01)02870-9
23. Shapiro BS, Richter KS, Harris DC, Daneshmand ST. A comparison of day 5 and day 6 blastocyst transfers. *Fertil Steril.* (2001) 75:1126–30. doi: 10.1016/S0015-0282(01)01771-X
24. Gardner DK, Lane M, Stevens J, Schlenker T, Schoolcraft WB. Blastocyst score affects implantation and pregnancy outcome: towards a single blastocyst transfer. *Fertil Steril.* (2000) 73:1155–8. doi: 10.1016/S0015-0282(00)00518-5
25. Zaninovic N, Berrios R, Clarke RN, Bodine R, Ye Z, Veeck LL. Blastocyst expansion, inner cell mass (ICM) formation, and trophectoderm (TM) quality: is one more important for implantation? *Fertil Steril.* (2001) 76:S8. doi: 10.1016/S0015-0282(01)02038-6
26. Ahlström A, Westin C, Reismer E, Wikland M, Hardarson T. Trophectoderm morphology: an important parameter for predicting live birth after single blastocyst transfer. *Hum Reprod.* (2011) 26:3289–96. doi: 10.1093/humrep/der325
27. Nagano M, Takahashi Y, Katagiri S. *In vitro* fertilization and cortical granule distribution of bovine oocytes having heterogeneous ooplasm with dark clusters. *J Vet Med Sci.* (1999) 61:531–5. doi: 10.1292/jvms.61.531
28. Jeong WJ, Cho SJ, Lee HS, Deb GK, Lee YS, Kwon TH, et al. Effect of cytoplasmic lipid content on *in vitro* developmental efficiency of bovine IVP embryos. *Theriogenology.* (2009) 72:584–9. doi: 10.1016/j.theriogenology.2009.04.015
29. Lee E, Takahashi H, Pauty J, Kobayashi M, Kato K, Kabara M, et al. A 3D *in vitro* pericyte-supported microvessel model: visualisation and quantitative characterisation of multistep angiogenesis. *J Mater Chem B.* (2018) 6:1085–94. doi: 10.1039/C7TB03239K
30. Pauty J, Usuba R, Cheng IG, Hespel L, Takahashi H, Kato K, et al. A vascular endothelial growth factor-dependent sprouting angiogenesis assay based on an *in vitro* human blood vessel model for the study of anti-angiogenic drugs. *Ebiomedicine.* (2018) 27:225–36. doi: 10.1016/j.ebiom.2017.12.014
31. Takahashi H, Kato K, Ueyama K, Kobayashi M, Baik G, Yukawa Y, et al. Visualizing dynamics of angiogenic sprouting from a three-dimensional microvasculature model using stage-top optical coherence tomography. *Sci Rep.* (2017) 7:42426. doi: 10.1038/srep42426
32. Zheng JG, Lu DY, Chen TY, Wang CM, Tian N, Zhao FY, et al. Label-free subcellular 3D live imaging of preimplantation mouse embryos with full-field optical coherence tomography. *J Biomed Opt.* (2012) 17.7.070503. doi: 10.1117/1.JBO.17.7.070503
33. Zheng JG, Huo TC, Chen TY, Wang CM, Zhang N, Tian N, et al. Understanding three-dimensional spatial relationship between the mouse second polar body and first cleavage plane with full-field optical coherence tomography. *J Biomed Opt.* (2013) 18.1.010503. doi: 10.1117/1.JBO.18.1.010503
34. Karnowski K, Ajduk A, Wieloch B, Tamborski S, Krawiec K, Wojtkowski M, et al. Optical coherence microscopy as a novel, non-invasive method for the 4D live imaging of early mammalian embryos. *Sci Rep.* (2017) 7:4165. doi: 10.1038/s41598-017-04220-8
35. Caujolle S, Cernat R, Silvestri G, Marques MJ, Bradu A, Feuchter T, et al. Speckle variance OCT for depth resolved assessment of the viability of bovine embryos. *Biomed Opt Express.* (2017) 8:5139–50. doi: 10.1364/BOE.8.005139
36. Masuda Y, Hasebe R, Kuromi Y, Kobayashi M, Iwamoto M, Hishinuma M et al. Three-dimensional live imaging of bovine embryos by optical coherence tomography. *J Reprod Dev.* (2021) 67:149–54. doi: 10.1262/jrd.2020-151
37. Kikuchi K, Ekwall H, Tienthai P, Kawai Y, Noguchi J, Kaneko H, et al. Morphological features of lipid droplet transition during porcine oocyte fertilisation and early embryonic development to blastocyst *in vivo* and *in vitro*. *Zygote.* (2002) 10:355–66. doi: 10.1017/S0967199402004100
38. Romek M, Gajda B, Krzysztofowicz E, Kepczyn ski M, Smorag Z. Lipid content in pig blastocysts cultured in the presence or absence of protein and vitamin E or phenazine ethosulfate. *Folia Biol.* (2011) 59:45–52. doi: 10.3409/fb59_1-2.45-52
39. Hidaka T, Fukumoto Y, Yamamoto S, Ogata Y, Horiuchi T. Variations in bovine embryo production between individual donors for OPU-IVF are closely related to glutathione concentrations

in oocytes during *in vitro* maturation. *Theriogenology*. (2018) 113:176–82. doi: 10.1016/j.theriogenology.2018.03.002
40. Dochi O. Direct transfer of frozen-thawed bovine embryos and its application in cattle reproduction management. *J Reprod Dev*. (2019) 65:389–96. doi: 10.1262/jrd.2019-025
41. Otsu N. Threshold selection method from gray-level histograms. *IEEE Trans Syst Man Cybern*. (1979) 9:62–6. doi: 10.1109/TSMC.1979.4310076
42. Xue JH, Zhang YJ. Ridler and Calvard's, Kittler and Illingworth's and Otsu's methods for image thresholding. *Pattern Recognit Lett*. (2012) 33:793–7. doi: 10.1016/j.patrec.2012.01.002
43. Yao T, Suzuki R, Furuta N, Suzuki Y, Kabe K, Tokoro M, et al. Live-cell imaging of nuclear-chromosomal dynamics in bovine *in vitro* fertilised embryos. *Sci Rep*. (2018) 8:7460. doi: 10.1038/s41598-018-25698-w

Conflict of Interest: RH, YK, and MK were employed by SCREEN Holdings Co., Ltd.

The remaining authors declare that the research was conducted in the absence of any commercial or financial relationships that could be construed as a potential conflict of interest.

frontiers in Veterinary Science

ORIGINAL RESEARCH
published: 10 May 2021
doi: 10.3389/fvets.2021.650291

Short Term Safety, Immunogenicity, and Reproductive Effects of Combined Vaccination With Anti-GnRH (Gonacon) and Rabies Vaccines in Female Feral Cats

*Shiri Novak[1], Boris Yakobson[2], Shir Sorek[1], Liat Morgan[1], Smadar Tal[1], Ran Nivy[1], Roni King[3], Lauren Jaebker[4], Douglas C. Eckery[4] and Tal Raz[1]**

[1] Koret School of Veterinary Medicine, The Robert H. Smith Faculty of Agricultural, Food, and Environment, The Hebrew University of Jerusalem, Rehovot, Israel, [2] Kimron Veterinary Institute, Ministry of Agriculture, Rishon Lezion, Israel, [3] Israel Nature and Parks Authority, Jerusalem, Israel, [4] National Wildlife Research Center, United States Department of Agriculture Animal and Plant Health Inspection Service Wildlife Services, Fort Collins, CO, United States

OPEN ACCESS

Edited by:
Dariusz Jan Skarzynski, Institute of Animal Reproduction and Food Research (PAS), Poland

Reviewed by:
Martin G. Maquivar, Washington State University, United States
Stefano Romagnoli, University of Florence, Italy

***Correspondence:**
Tal Raz
tal.raz@mail.huji.ac.il

Specialty section:
This article was submitted to Animal Reproduction - Theriogenology, a section of the journal Frontiers in Veterinary Science

Received: *06 January 2021*
Accepted: *07 April 2021*
Published: *10 May 2021*

Citation:
Novak S, Yakobson B, Sorek S, Morgan L, Tal S, Nivy R, King R, Jaebker L, Eckery DC and Raz T (2021) Short Term Safety, Immunogenicity, and Reproductive Effects of Combined Vaccination With Anti-GnRH (Gonacon) and Rabies Vaccines in Female Feral Cats. Front. Vet. Sci. 8:650291. doi: 10.3389/fvets.2021.650291

Overpopulation of free-roaming cats is a major problem leading to negative impacts on animal health and welfare, public nuisance, transmission of zoonotic diseases, and well-documented harm to wildlife. Surgical sterilization had failed to provide a practical solution to free-roaming cats' overpopulation under field conditions; therefore, efficient and safe non-surgical immunocontraception methods are aspired. Rabies is a deadly virus that may infect people and animals. However, the safety and efficacy of combined vaccination with anti-GnRH and rabies vaccines in feral cats, which often suffer from disrupted health conditions and experienced high stress level, has never been studied. Therefore, our objective was to examine the short-term safety and efficacy of anti-GnRH vaccine (Gonacon), in combination with rabies vaccine in female feral cats. Mature feral female cats were captured and divided into the following groups: (I) GonaconX1-Rabies: queens vaccinated with both Gonacon and rabies ($n = 5$); (II) GonaconX2-Rabies: queens vaccinated twice with Gonacon (3 weeks apart) and with Rabies ($n = 4$); (III) OVx-Rabies: queens ovariohysterectomized and vaccinated with rabies ($n = 4$); (IV) Intact-Rabies: queens vaccinated against rabies and remained intact ($n = 3$). Comprehensive veterinary examinations and blood tests were performed every 2 weeks for 14 weeks. Data were analyzed by Repeated-Measures-ANOVA or Fisher-Exact-Test. There were neither systemic nor local adverse reactions at the vaccination sites. Blood count (PCV, TS, RBC, HGB, HCT, WBC) and chemistry (Total protein, Total globulin, Albumin, Urea, Creatinine, Creatine kinase, Bilirubin, GGT, ALT, AST) analyses revealed no differences among groups. There were no differences in serum rabies antibodies titers among groups, and queens kept a protective titer (>0.5 IU/mL) starting at 2–4 weeks after vaccination. Anti-GnRH antibodies were detected in all Gonacon-vaccinated queens, excluding one queen (GonaconX2-Rabies group). Anti-müllerian hormone serum concentrations reduced significantly after ovariohysterectomy, as well as gradually following vaccination with Gonacon, but it remained high in intact queens.

Evaluation of vaginal cytology and ovarian histology suggested that reproductive cyclicity was suppressed in Gonacon-vaccinated queens. Our results support the conclusion that in the short term, the combined vaccination with Gonacon and rabies is safe and effective in female feral cats. However, further long-term studies are warranted to test this immunologic regimen in feral cats.

Keywords: feral cats, anti-GnRH vaccine, Gonacon, non-surgical contraception, contraception, sterilization, rabies

INTRODUCTION

Overpopulation of free-roaming cats is a global problem in both urban and rural societies (1). It negatively impacts the cats' welfare and health (starvation, diseases, run over by cars, etc.), as well as causing public health risks due to the transmission of zoonotic diseases to humans (e.g., toxoplasmosis, rabies, cat scratch disease, leptospirosis, Q fever, toxocariasis, flea-borne typhus, etc.); some of these are reported to cause important health issues including abortion, blindness, pruritic skin rashes and other various symptoms, as well as mortality (2–6). Free-roaming abandoned and feral cats are non-native predators; they cause substantial wildlife destruction and ecosystem disruption, including the deaths of millions of birds, small mammals, reptiles, amphibians, and fish (7). Furthermore, disease transmission from cats to livestock and wild animals, attacks on humans, traffic accidents, and nuisance behavior, are just part of many concerns involved with this matter (6, 8, 9). Currently, surgical sterilization (ovariohysterectomy; orchiectomy) is the most common practice to control free-roaming cat reproduction, mainly *via* "Trap-Neutering-Return" (TNR) programs. It provides a permanent solution, should be done only once, and may positively affect the health and welfare of individual feral cats (10). However, the surgical approach is expensive, and requires surgical and anesthetic materials, equipment, as well as skilled veterinarians. Furthermore, it may cause significant stress to the animals (9, 11, 12). Therefore, the surgical approach practically failed to provide a solution for the millions of free-roaming cats that are confined and euthanized annually (9, 13–15). An efficient non-surgical sterilization/contraception method could have a significant impact on the control of cat overpopulation. However, to the best of our knowledge, despite significant efforts over the several last decades, there are currently no efficient commercial products that can be used for mass non-surgical sterilization/contraception of free-roaming cat populations (15, 16).

Rabies is a deadly, vaccine-preventable, zoonotic, viral disease, which may infect people and animals (17). According to the World Health Organization report (updated in April 2020), most human cases worldwide are due to disease transmission from domestic dogs. However, mandatory dog vaccination programs have halted the natural spread of rabies among domestic dogs in many countries. According to the information from the USA Centers for Disease Control and Prevention (CDC; updated on April 2020), as well as from other reports (4, 18, 19), in the USA, cats have become the companion animal species most commonly reported as rabid. Accordingly, in many endemic countries, including Israel and the USA, combined animal reproduction control and rabies vaccination programs are aspired.

Reproduction in the domestic queens is affected by photoperiod, as this species is considered as seasonal, polyestrous, long day breeder, with multiple ovulations induced following vaginal stimulation during mating (20, 21). Gonadotropin-Releasing Hormone (GnRH), which is released from the hypothalamus, is the master hormone of reproduction; it controls steroidogenesis and gametogenesis by stimulating the release of the pituitary gonadotropins, luteinizing hormone (LH) and follicle-stimulating hormone (FSH), triggering a cascade of endocrine effects that lead to sperm production in males and follicular development and ovulation in females. Gonacon is an anti-GnRH vaccine, developed by the National Wildlife Research Center, USDA APHIS Wildlife Services, USA. This immunocontraceptive vaccine was designed to trigger the production of antibodies that neutralize GnRH. It has been tested in many species, including white-tail deer (22), elk (23), horses (24, 25), cattle (26), ferrets (27), domestic, and wild pigs (28), as well as to a limited extent in dogs (29) and cats (30–33). However, none of the four previous studies conducted on cats included measurements of rabies antibodies in Gonacon-vaccinated cats, even in the studies in which cats were vaccinated with both vaccines (32, 33). Furthermore, in previous Gonacon studies conducted on cats, animals were not feral cats; they were either specific-pathogen-free (SPF) laboratory cats (30, 31), cats from research colony (32), or well-maintained friendly cats obtained from animal control agencies or from private individuals who posted cats for rehoming (33). All cats were kept in excellent health and body conditions, and were accustomed to human interactions. However, many previous reports documented that feral cats often suffer from high rates of morbidity and pre-mature mortality due to infectious (e.g., FIV, FeLV, parasites) and non-infectious diseases, malnutrition, poor body condition, traumas, etc. (9, 10, 34–36). Furthermore, most of these cats are typically too fearful and too wild to be handled awake, as they are not accustomed to close interactions with people. Therefore, feral cats, which are the main target population for non-surgical contraception/sterilization, often suffer from acute and chronic

Abbreviations: AMH, Anti-müllerian hormone; LH, Luteinizing hormone; FSH, follicle-stimulating hormone; GnRH, Gonadotropin-releasing hormone; PCV, Packed cell volume; RBC, red blood cell count; MCV, mean corpuscular hemoglobin; MCH, mean corpuscular hemoglobin concentration; MCHC, mean corpuscular hemoglobin concentration; CHCM, cell hemoglobin concentration mean; CH, cellular hemoglobin; RDW, red cell distribution width; HDW, hemoglobin distribution width; WBC, white blood cells count; LUC, large unstained cells; ALT, alanine aminotransferase; GGT, gamma-glutamyl transpeptidase; AST, aspartate aminotransferase.

health problems and are under chronic stress due to their lifestyle and environment (5, 9, 10, 34–36). Potentially, these suboptimal conditions might weaken the immune response and antibody production following vaccination, such as to Gonacon and rabies vaccines, as has been documented for other vaccines and species (37–42). As recently reviewed by Zimmermann and Curtis (41), several factor might affect the immune respond and antibody production of individuals following vaccination; these include age, sex, genetics, comorbidities, infections, parasites, microbiota, pre-existing immunity, acute and choric stress, body condition, nutritional status, micronutrients (vitamins A, D, and E and zinc), as well as environmental factors, and vaccine factors (vaccine type, product, strain, and batch; vaccination route; combinations of vaccines, cet.). For example, some studies indicated poorer humoral response to influenza vaccine in humans with chronic diseases (37); Chronic inflammatory processes like rheumatoid arthritis alter the immune system and antibody formation (43); furthermore, depression and dementia as well as psychological stress are associated with poor antibody response and a higher range of inflammation markers (44). Thus, vaccines should optimally be tested in the typical target population and conditions.

Therefore, the objective of the current study was to examine the short-term safety and efficacy of the anti-GnRH vaccine (Gonacon), given either as a single dose, or two doses 3 weeks apart, in combination with rabies vaccine, in mature feral female cats. Our main hypotheses were that: (1) in the short term (14 weeks), the combined vaccination with Gonacon and rabies will not be harmful and will not have adverse side effects; (2) antibody titers against GnRH and rabies will increase following the combined vaccination; (3) as compared to a single dose Gonacon vaccination, two doses of Gonacon given 3 weeks apart (booster) will induce higher anti-GnRH titer, but anti-rabies antibodies titer will not differ; (4) development of anti-GnRH antibodies will be associated with suppression of the ovarian function; and (5) antibody titers against rabies will not be negatively influenced by the simultaneous vaccination approach and will remain protective during the study period.

MATERIALS AND METHODS

Cats, Housing, and Handling

The study was conducted according to the ethical approval of the Hebrew University's Institutional Animal Care and Use Committee (IACUC MD-17-14613-2). As part of the trap-neuter-return (TNR) program in a large city in Israel (Be'er-Sheva), free-roaming feral domestic short-hair (DSH) queens were captured by professional trappers using commercial traps, and were transported to the cats' housing facility located at the municipal veterinary department. Mature intact queens ($n = 16$; estimated age ranged from 1 to 3 years), with no severe injuries, were randomly selected for the study, which was conducted during the natural breeding season of cats in Israel (July to September). During the 14-weeks study, queens were housed individually in cages in the same ventilated room and maintained at ambient temperature and light. They could see and smell each other, without direct contact. Food and water were available *ad libitum,* and environmental enrichment was provided in each cage.

Queens were observed by professional veterinarians and staff, at least twice every day during the 14-weeks study period. The attitude, appetite, and alertness of the queens were evaluated while the cats were in their cages. However, these queens could not be handled safely while awake, as they were not friendly and not used to any human contact (typical for most free-roaming cats in Israel). Therefore, full physical examinations, treatments, and sampling (blood and vaginal smears) were performed under heavy sedation. Every 2 weeks, starting at the vaccination day, the queens were sedated using a combination of Medetomidine (0.02–0.04 mg/kg; Orion Pharma, Finland), Butorphanol (0.2–0.4 mg/kg; intramuscular injection; Richter Pharma AG, Austria), and Midazolam (0.1–0.25 mg/kg intramuscular injection; Rafa laboratories, Israel). At the end of the procedure, Medetomidine was reversed by subcutaneous administration of atipamezole (0.05–0.10 mg/kg; Orion Pharma, Finland). After the study was completed, cats that had relatively calm temperaments were acclimated, and thereafter were adopted. Others were released back to the exact location in which they were initially trapped, in compliance with the Israeli Feral Cat Low. All queens were in good health and body condition at the time of adoption or release.

Treatments and Study Design

At study initiation, queens were allocated into one of the following groups: (I) GonaconX1-Rabies: queens were vaccinated with both Gonacon and rabies vaccines ($n = 5$); (II) GonaconX2-Rabies: queens were vaccinated twice with Gonacon (at study initiation, and again 3 weeks later) and once with rabies vaccine, at study initiation ($n = 4$); (III) OVx-Rabies: queens underwent surgical ovariohysterectomy and vaccinated against rabies at study initiation ($n = 4$); (IV) Intact-Rabies: queens vaccinated against rabies and remained intact ($n = 3$). Vaccination against rabies was performed at study initiation in all queens by subcutaneous administration of a commercial rabies vaccine (Rabisin, Merial, France) at the left thigh. Vaccination with Gonacon was performed by intramuscular administration of vaccines provided by USDA-APHIS NWRC (Fort Collins, CO, USA). The Gonacon vaccine was injected into the right quadriceps muscle group. Before the administration of the vaccines, the fur was clipped, and the injection sites were cleaned with 70% isopropyl alcohol.

Monitoring and Sampling

Throughout the study, queens were monitored daily for their attitude, appetite, and alertness. Every 2 weeks, for a total period of 14 weeks, full physical examinations were performed by a certified veterinarian, including also evaluation of body condition on a 5-point scale (45), examinations of the injection sites, as well as collections of vaginal smears. Furthermore, blood samples were collected by jugular venipuncture every 2 weeks into potassium-EDTA tubes, as well as into plain tubes containing no anticoagulant. Blood samples in potassium-EDTA tubes were stored at 4°C and used for complete blood count (CBC) analysis within 4 h. Blood in plain tubes was allowed to clot, centrifuged,

and serum samples were stored at −80°C until analyses at study completion, which included serum chemistry, anti-GnRH and anti-rabies antibody titer, serology for FIV and FeLV, as well as analysis of serum Anti Müllerian Hormone (AMH) concentration. At study termination, all queens underwent surgical ovariohysterectomy, except the cats in the OVx-Rabies group, in which ovariohysterectomy was performed at study initiation. The removed reproductive tracts from all queens were kept and processed for histological evaluation, as detailed below.

Complete Blood Count and Blood Chemistry Analyses

Blood samples collected in potassium-EDTA tubes on weeks 0, 2, 4, 6, 8, 10, 12, and 14 were used for complete blood count (CBC; Advia 2120, Siemens, Erfurt, Germany). Packed cell volume (PCV) was measured routinely, using a hematocrit tube sealed with clay that was centrifuged for ∼3 min; plasma total solids was measured by placing the plasma directly onto a refractometer (Clinical Refractometer RHC-200 ATC, Cmall, Medent, Israel). Blood smears were prepared and stained by automatic slide Stainer with a modified Wright's staining solution (Modified Wright's Stain, Bayer Hematek 2000 Slide Stainer, Siemens, Elkhart, IN, USA), and used for microscopic evaluation of blood cells. Neutrophil cytoplasmic toxicity was evaluated microscopically as previously described (46), by an experienced observer who was blinded to the identity of the queens and treatments (Dr. Nivi, DVM, Dip.ECVIM-CA).

Serum samples collected on weeks 0, 2, 8, and 14 were used for chemistry analysis (Cobas Integra 400 Plus; Roche, Mannheim, Germany, at 37°C). The analysis included the following parameters: Urea, Creatinine, Albumin, Alanine Amino-Transferase (ALT), Aspartate Amino-Transferase (AST), Gamma-Glutamyl Transpeptidase (GGT), Bilirubin, Creatine Kinase (CK), Globulins, and Total protein (TP).

Detection of GnRH Antibodies

Serum samples were sent frozen to USDA-APHIS NWRC and were analyzed for GnRH antibodies using an Enzyme-Linked Immunosorbent Assay, as previously described (31). Serum samples were diluted in two-fold series from 1:8,000 to 1:64,000 in phosphate-buffered saline (PBS) and run in duplicate. A positive control sample was also run in duplicate on each plate. The cutoff values for each plate were generated from the pre-vaccination samples from all animals at each dilution as the mean + 3SD. The %CV for the positive control samples at each dilution was low, demonstrating little inter-plate variability (1:8,000, 7.3%; 1:16,000, 5.9%; 1:32,000, 8.2%, 1:64,000, 11.2%).

Detection of Anti-Rabies Antibodies

Serum samples collected on weeks 0, 2, 4, 6, 8, 10, 12, and 14 were analyzed for anti-Rabies antibodies concentrations using Rapid Fluorescent Focus Inhibition Test (RFFIT), as previously described (47), in the OIE-accredited laboratory of Dr. Boris Yakobson at the Kimron Veterinary Institute (Veterinary Services and Animal Health, Israel). The RFFIT assay has been shown to have a sensitivity and specificity of 100 and 89%, respectively, and is considered as the gold standard by the World Health Organization (47, 48). Briefly, titers were recorded as serial dilutions with positive and negative control samples. All serum dilutions were added with an equal volume of virus and incubated at 37°C in a controlled humidity carbon dioxide 0.5% chamber for 90 min. Then, a suspension of 1×10^5 cells (MNA-Mouse neuroblastoma, CDC USA, Wistar Institute, Philadelphia, USA) in 0.2 mL of growth medium (MEM EAGLE, with fetal bovine serum, vitamin solution concentrated, L-Glutamine, Sodium Bicarbonate, Penicillin G, Streptomycin and Amphotericin B; Biological Industries, Israel) was added to each well, and the chamber was returned to incubation for 20 h. Thereafter, the growth medium was removed, the chambers were rinsed in phosphate-buffered saline (PBS), and the cells were fixed with cold acetone (−20°C) at room temperature for 10 min. FITC anti-rabies conjugate (Fujirebio, USA) was added, and the chamber was incubated for 30 min in a humidity incubator (37°C), and finally washed with PBS. The slides were examined with a microscope (Olympus BX40, 470 excitation wavelength, ×200 magnification). Each well was divided into 20 fields, and the number of fields containing fluorescent cells was tabulated (49). Serological titers were converted to international units per mL (IU/mL). A titer value of >0.5 IU/mL was considered as a protective antibody level (47).

Serum Anti Müllerian Hormone Analysis

Serum anti-Müllerian hormone (AMH) concentrations were analyzed in samples from weeks 0, 8, and 14 using an Enzyme-Linked Immunosorbent Assay kit (AMH Gen II ELISA; Beckman coulter, Inc. Brea, CA, USA) according to the manufacturer's instructions and as previously described and validated for cats (50). Briefly, 300 μL of AMH Gen II Assay Buffer were mixed with 60 μL of calibrator, control, or sample, and 120 μL from the mix were pipetted into the wells in the plate, in duplicates. After incubation and washing, 100 μL of anti-AMH biotin conjugate was added to each well. After a second incubation and washing, 100 μL of the streptavidin-enzyme conjugate were added. Following a third incubation and washing step, 100 μL of TMB chromogen solution were added, followed by the final addition of 100 μL of an acidic stopping solution. The degree of enzymatic turnover of the substrate was determined by using a microplate reader (SpectraMax Paradigm Multi-mode detection platform, Molecular Devices, Austria) using dual-wavelength absorbance measurement at 450 and 620 nm. The inter- and intra- coefficient of variations (%CV) were 5.4 and 4.2%, respectively.

Vaginal Cytology

A fine cotton swab was used to obtain cells from the cranial vagina, which were spread on glass slides, as previously described (51). Slides were stained with Diff-Quick, and were evaluated microscopically (1,000× magnification. Primo Star, Carl Zeiss, Germany) by a single experienced observer, who was blinded to the origin of the slides and the status of the queens. For each Diff-Quick stained slide, >200 epithelial vaginal cells were classified as parabasal, intermediate or superficial (nucleate and anucleate) cells (52). If >60% of the vaginal cells were superficial cells, the queen was considered to be in proestrus/estrus.

Ovarian and Uterine Histology

Ovaries and uterine tissues collected during ovariohysterectomies were fixed immediately after collection in Bouin's solution for 24 h at 4°C, and then were moved to 70% ethanol. Tissues were embedded in paraffin, sectioned (4 μm thickness), and stained with hematoxylin and eosin (H&E; Sigma-Aldrich, Israel). Histological evaluation of these sections was performed using a light microscope (Axio Imager M1, AxioCam HRc camera; Carl Zeiss, Germany). In the ovary, we subjectively assessed the general morphology and presence of primordial follicles, antral follicles, corpora lutea, and oocytes; in the uterus, we assessed the general structural layers, as well as the competence of the luminal epithelium, and morphology of the endometrial glands within the endometrium.

FIV/FeLV Serology

As part of the evaluation of the cats' health, serum samples collected prior to vaccination (week 0) were analyzed to detect antibodies for Feline immunodeficiency virus (FIV) and Feline leukemia virus (FeLV), using FIV/FeLV antibody commercial test kit (SNAP* Combo plus, IDEXX, USA), according to the manufacturer's instructions.

Statistical Analysis

Statistical analyses were performed using Statistix 8 software (Analytical Software, Tallahassee, FL USA); plots were produced by Prism 5.01 (GraphPad Software; San-Diego, CA, USA). Continuous data were analyzed by Repeated-Measures-ANOVA, to evaluate the effects of Group (between-subject factor), Time (within-subject factor), and Group-by-Time interactions,

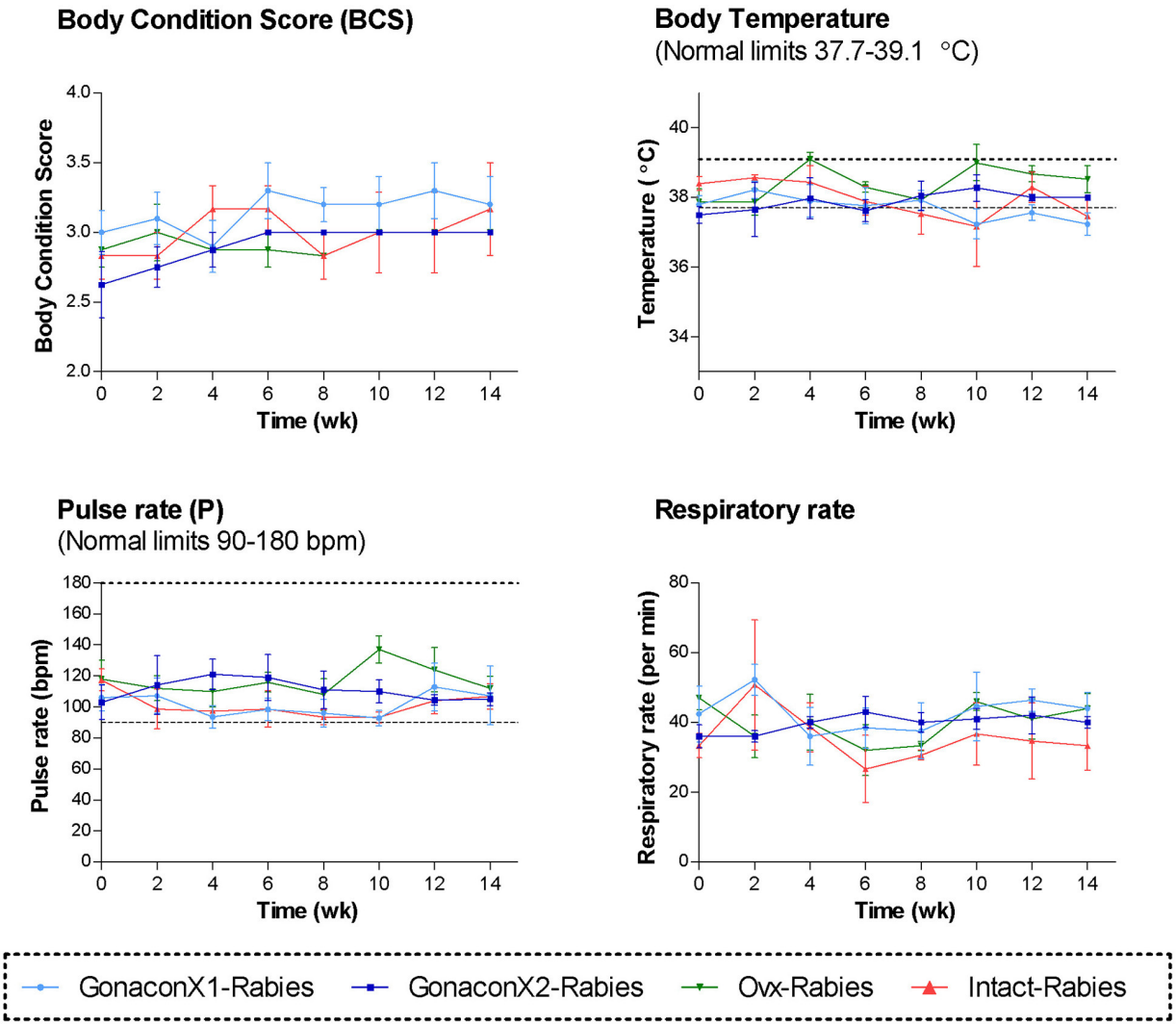

FIGURE 1 | Body condition score and the vital signs of cats in the research groups. Mean ± SEM of temperature, pulse, respiratory rate, and body condition score are presented for each group: GonaconX1-Rabies: cats vaccinated with both Gonacon and Rabies ($n = 5$); GonaconX2-Rabies: cats vaccinated twice with Gonacon (3 weeks apart) and with rabies ($n = 4$); OVx-Rabies: cats ovariohysterectomized and vaccinated with rabies ($n = 4$); Intact-Rabies: cats vaccinated against rabies and remained intact ($n = 3$). Parameters were collected every 2 weeks for a total of 14 weeks, while cats were under heavy sedation. Dotted lines indicate normal limits.

followed by Tukey HSD All-Pairwise Comparisons Test. When was applicable, two groups were compared by Wilcoxon Rank Sum Test. Fisher-Exact-Test was used to compare proportional data. Differences were considered significant at $P < 0.05$. Unless otherwise noted, results are presented as mean ± SEM.

RESULTS

Physical Examinations, Complete Blood Count, and Blood Chemistry Analyses

During the course of the study, no swelling, signs of inflammation, or tenderness were detected at the injection sites, in any of the queens. All queens were in fair to good physical condition, and had a normal attitude and appetite. Vital signs (TPR; Temperature, Pulse, and Respiratory rates) remained within normal ranges, with no significant differences among the groups or over time (**Figure 1**). Body condition score (BCS) did not differ among the groups, but overall, it improved over the study period ($p = 0.0281$); BCS of individual cats stayed the same or increased by up to one point in a 5-point BCS scale (45).

Complete blood count (CBC) was completed for all the samples (8 samples for each cat). There were no significant differences among the groups in all the CBC parameters (**Figures 2**, **3**). However, in some individuals, some of the parameters were abnormal at study initiation, mainly indicating mild anemia or inflammatory condition, but they improved over the study period, and were within normal limits later on. Accordingly, there were significant differences along time (Repeated Measure ANOVA; $p < 0.05$) in the following parameters; PCV, TS, RBC, Hemoglobin, HCT, MCH, MCV, HDW, CH, WBC, Neutrophils, Lymphocytes, and Large unstained cells (LUC, which are activated lymphocytes and peroxidase-negative cells). In addition, overall, signs of neutrophil toxicity were common at study initiation, but were absent at study completion (6/16, 38% vs. 0/16, 0%; $p = 0.0177$).

Analyses of blood chemistry parameters were conducted on blood samples from weeks 0, 2, 8, and 14, to overall estimate the function of internal organs, such as liver and kidney, after vaccination. As illustrated in **Figure 4**, there were no significant differences among the groups at the chemistry parameters, except for a few parameters, at study initiation, before the queens were vaccinated; mean AST and CK concentrations were significantly high at the GonaconX1 group, and ALT was high in both GonaconX1-Rabies and Intact-Rabies groups ($p < 0.05$). However, all parameters improved over the study period, and were within normal limits later on, excluding albumin and total proteins, which were relatively low throughout the study.

None of the queens in the study had positive serology for FeLV; however, one queen in the GonaconX1-Rabies group was positive for FIV.

GnRH Antibodies

There were significant effects of the group, the time, and the group X time interaction on the anti-GnRH antibody titer ($p \leq 0.0003$; **Figure 5**). As expected, anti-GnRH antibodies were not detected in any the control queens (OVx-Rabies and Intact-Rabies groups). However, following vaccination with Gonacon, anti-GnRH antibodies titer increased in all vaccinated queens (GonaconX1-Rabies and GonaconX2-Rabies groups), except for one queen (cat #9) from the GonaconX2-Rabies group, in which no anti-GnRH antibodies could not be detected in any of its serum samples (**Figure 6**). There was no significant difference between the GonaconX1-Rabies and GonaconX2-Rabies groups ($p = 0.4943$). In all responder queens, positive anti-GnRH antibody titers were detected, typically within 2 or 4 weeks, and remained high during the study period; except for one queen from the GonaconX1-Rabies group (cat #4), in which antibodies decreased in the last two samples. This queen was identified later on as FIV positive.

Rabies Antibodies

There were no significant differences in the anti-rabies antibodies among groups ($p = 0.3169$), or group X time interaction ($p = 0.7220$); however, time was a significant factor ($p < 0.0001$; **Figure 7**). Following vaccination with rabies, all queens from all the groups produced antibodies against rabies, which remained above 0.5 IU/mL throughout the study, a titer that is considered protective. Typically, the anti-rabies antibodies titer peaked at 4–8 weeks following vaccination, and then gradually reduced and appeared to be stabilized.

Anti-müllerian Hormone Serum Concentrations

As illustrated in **Figure 8**, AMH serum concentrations reduced significantly after ovariohysterectomy ($p = 0.0023$), but it remained high in intact queens ($p = 0.4174$). In queens vaccinated with Gonacon, the reduction in AMH concentration was gradual ($p = 0.0006$). In all Gonacon-vaccinated queens, AMH serum concentrations were lower at study completion, as compared to study initiation, except in the non-responder queen in the GonaconX2-Rabies, who kept relatively stable AMH concentrations. In the GonaconX1-Rabies group, mean AMH concentration was significantly lower at study completion, as compared to study initiation ($p = 0.0081$). In the GonaconX2-Rabies group, mean AMH concentration was not statistically different at study completion ($p = 0.1257$); however, when the data of the non-responder queen was excluded from the analysis, the difference in AMH concentrations between study initiation and study completion was significant also in that group ($p = 0.0178$).

Vaginal Cytology

The analysis of the percentage of superficial cells in vaginal cytology smears by Repeated Measure ANOVA revealed no significant effect of the group ($p = 0.6286$), time ($p = 0.4027$), and group X time interaction ($p = 0.4804$). None of the queens in the Ovx-Rabies group had cytological signs of estrus/proestrus (i.e., >60% superficial cells) after ovariohysterectomy, while in the intact-Rabies group, two out of three queens showed such cytological signs. Interestingly, none of the Gonacon-vaccinated queens had signs of proestrus/estrus in the last 2 weeks of the study, excluding the non-responder queen in the GonaconX2-Rabies group. Furthermore, overall, among the cytology slides

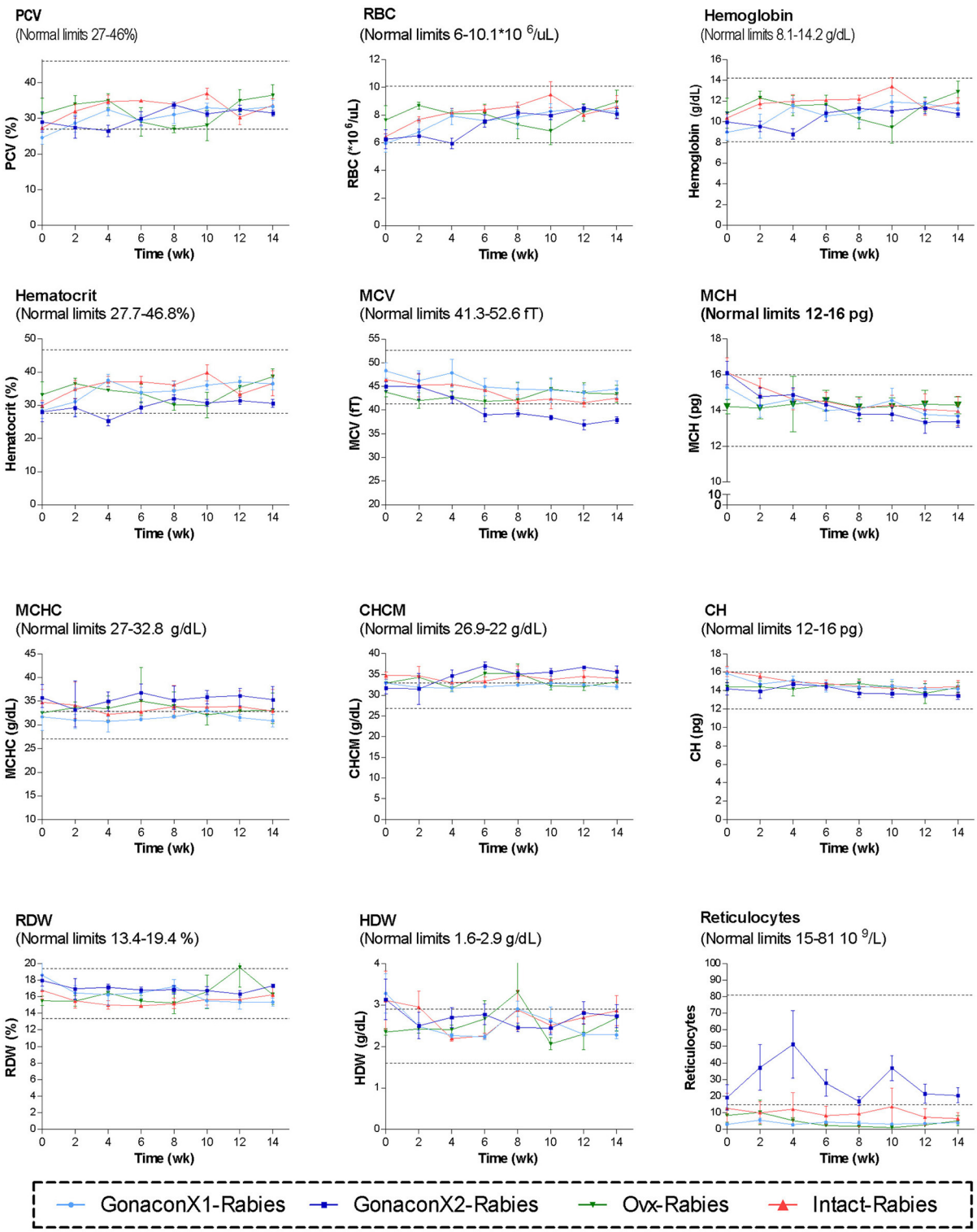

FIGURE 2 | Red blood cells parameters of cats in the research groups. Mean ± SEM of red blood cells parameters are presented for each group: GonaconX1-Rabies: cats vaccinated with both Gonacon and rabies ($n = 5$); GonaconX2-Rabies: cats vaccinated twice with Gonacon (3 weeks apart) and with rabies ($n = 4$); OVx-Rabies: cats ovariohysterectomized and vaccinated with rabies ($n = 4$); Intact-Rabies: cats vaccinated against rabies and remained intact ($n = 3$). Blood samples were collected every 2 weeks for a total of 14 weeks. Dotted lines indicate normal limits. PCV, packed cell volume; RBC, red blood cell count; MCV, mean corpuscular hemoglobin; MCH, mean corpuscular hemoglobin concentration; MCHC, mean corpuscular hemoglobin concentration; CHCM, cell hemoglobin concentration mean; CH, cellular hemoglobin; RDW, red cell distribution width; HDW, hemoglobin distribution width.

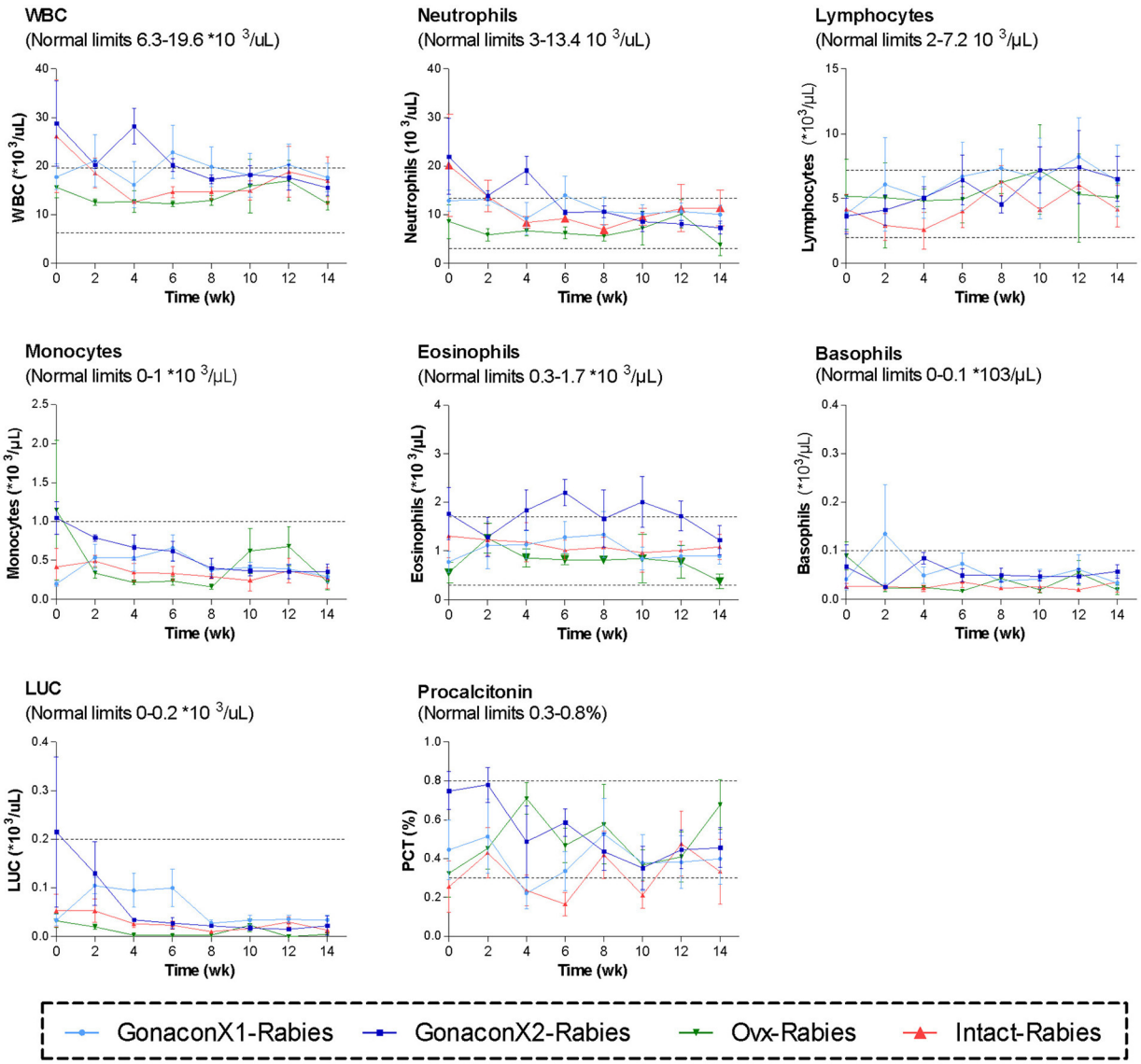

FIGURE 3 | White blood cells parameters of cats in the research groups. Mean ± SEM of white blood cells parameters are presented for each group: GonaconX1-Rabies: cats vaccinated with both Gonacon and rabies ($n = 5$); GonaconX2-Rabies: cats vaccinated twice with Gonacon (3 weeks apart) and with rabies ($n = 4$); OVx-Rabies: cats ovariohysterectomized and vaccinated with rabies ($n = 4$); Intact-Rabies: cats vaccinated against rabies and remained intact ($n = 3$). Blood samples were collected every 2 weeks for a total of 14 weeks. Dotted lines indicate normal limits. WBC, white blood cells count; LUC, large unstained cells.

obtained from Gonacon-vaccinated cats, the percentage of superficial cells in the smear was significantly lower when the anti-GnRH titer was high (titer 0, 43.7 ± 8.7%, vs. titer 1:64, 10 ± 1.9%; $p = 0.0135$).

Histology of the Reproductive Tract

Histologic evaluation of the ovaries collected from Gonacon-vaccinated cats demonstrated many degenerative oocytes, and no to only a few very small antral follicles (**Figure 9**). In contrast, ovaries of cats that were not vaccinated with Gonacon had normal histology, with various follicles (primary, secondary, and antral follicle), and very few degenerative oocytes. The ovaries of the non-responder cat from the GonaconX2-Rabies were similar to that of non-Gonacon- vaccinated controls cats, with obvious large antral follicles, compatible with estrus. There were no apparent differences between Gonacon-vaccinated cats to controls in the shape, morphology, or amount of the crowded primordial follicles under the ovary's tunica albuginea, at the ovarian cortex. Furthermore, no obvious difference could be observed in the endometrium of Gonacon-vaccinated cats vs. controls (data not shown).

DISCUSSION

The rationale of this study was to examine the short-term safety and efficacy of combined vaccination with anti-GnRH (Gonacon) and rabies vaccines, specifically in female feral cats, which often

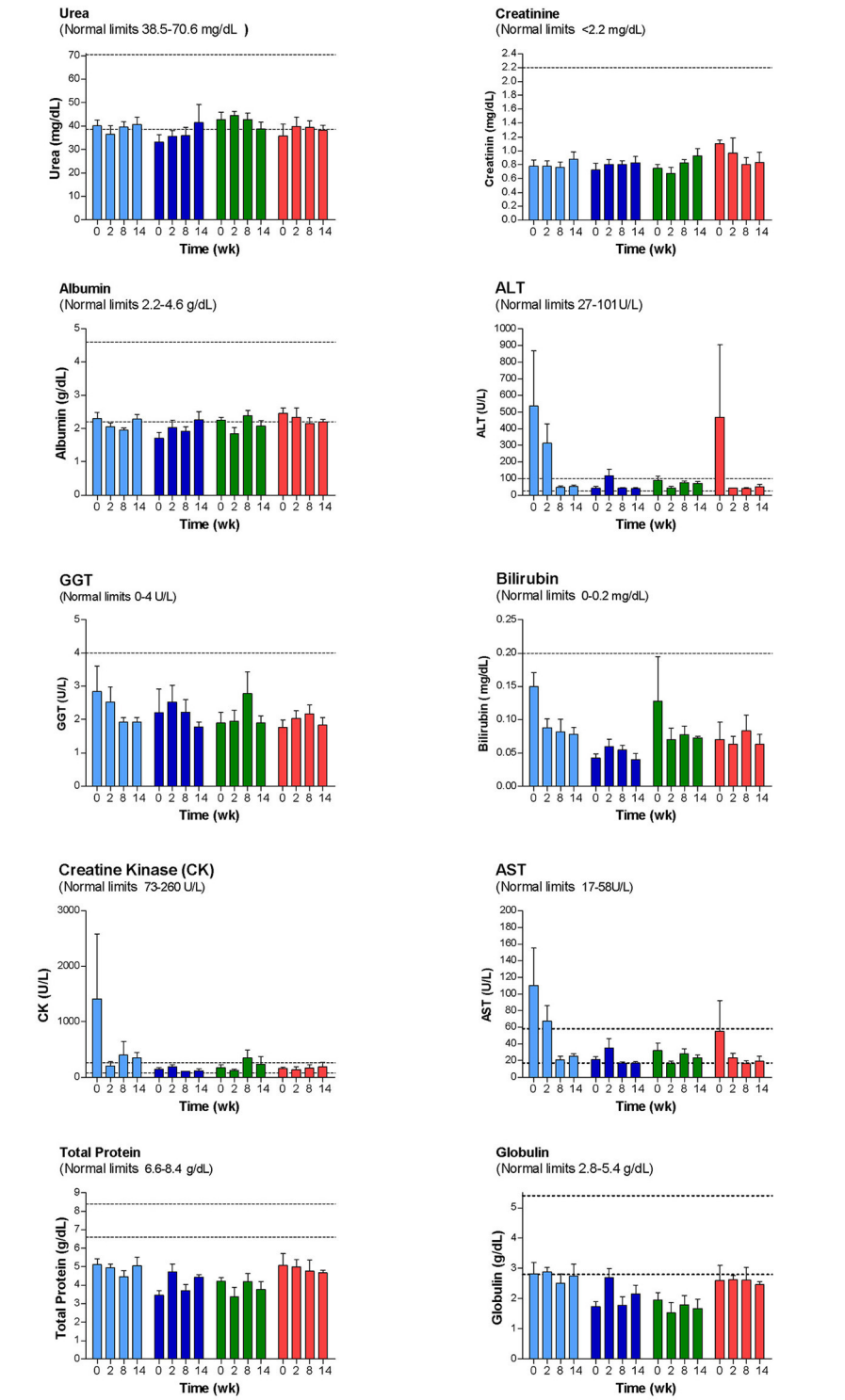

FIGURE 4 | Blood chemistry parameters of cats in the research groups. Mean ± SEM of blood chemistry parameters are presented for each group: GonaconX1-Rabies: cats vaccinated with both Gonacon and rabies ($n = 5$); GonaconX2-Rabies: cats vaccinated twice with Gonacon (3 weeks apart) and with rabies ($n = 4$); OVx-Rabies: cats ovariohysterectomized and vaccinated with rabies ($n = 4$); Intact-Rabies: cats vaccinated against rabies and remained intact ($n = 3$). Analyses were performed on blood samples collected at 0, 2, 8, and 14 weeks after the initial vaccination. Dotted lines indicate normal limits. ALT, alanine aminotransferase; GGT, gamma-glutamyl transpeptidase; AST, aspartate aminotransferase.

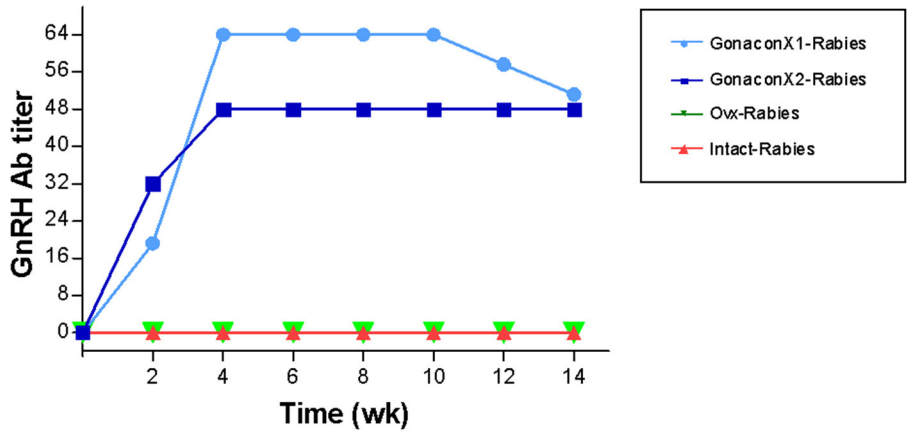

FIGURE 5 | Serum GnRH antibodies titer of cats in the research groups. Mean ± SEM GnRH titers are presented for each group: GonaconX1-Rabies: cats vaccinated with both Gonacon and rabies ($n = 5$); GonaconX2-Rabies: cats vaccinated twice with Gonacon (3 weeks apart) and with rabies ($n = 4$); OVx-Rabies: cats ovariohysterectomized and vaccinated with rabies ($n = 4$); Intact-Rabies: cats vaccinated against rabies and remained intact ($n = 3$). Blood samples were collected every 2 weeks for a total of 14 weeks. There were significant effects of the group, the time, and the group X time interaction on the anti-GnRH antibodies titer (Repeated measure ANOVA, $p \leq 0.0003$). Variability within each group was extremely small, and therefore the SEM are unnoticeable.

suffer from disrupted health conditions and experience high-stress levels, which potentially may alter vaccination efficacy. Our study indicated that in the short term, the combined vaccination with Gonacon and rabies is safe and effective in female feral cats, with no apparent benefits for two Gonacon vaccinations as compared to a single dose. Over the study period, no local or systemic adverse health concerns were detected, in accordance with our hypothesis. There were no differences in serum rabies antibody titers among groups, and queens kept a protective titer throughout the study. Anti-GnRH antibodies were detected in all Gonacon-vaccinated queens, excluding one queen (GonaconX2-Rabies group). Furthermore, evaluation of serum AMH concentrations, vaginal cytology, and ovarian histology suggested that reproductive cyclicity was indeed suppressed in Gonacon-vaccinated queens, as hypothesized.

Different from previous studies in which researchers examined the effects of Gonacon in experimental cats or pets cats from colonies, in the current study we utilized feral cats. In previous Gonacon studies (30–33), animals were domestic short hair cats kept in excellent health and body conditions, and were accustomed to human interactions. In the studies of Levy et al. (30, 31), specific-pathogen-free (SPF) males and females, respectively, were acquired from a commercial vendor and housed in climate-controlled indoor spaces with controlled light cycles (30, 31). Vansandt et al. (32) used ovariohysterectomized cats from a research colony at the Cincinnati Zoo and Botanical Garden's Center for Conservation and Research of Endangered Wildlife. In the study conducted by Fischer et al. (33), well-maintained friendly cats were obtained from animal control agencies, or from private individuals who posted cats for rehoming on a classified advertisement website; all cats were in excellent body condition and health. However, it is well-documented that feral cats often suffer from high rates of pre-mature mortality and morbidity due to infectious and non-infectious diseases, internal and external parasites, starvation and poor body condition, weather extremes, trauma, etc. (9, 10, 34–36). Furthermore, most of these cats are not accustomed to contact with people and are typically too fearful and too wild to be handled. Therefore, feral cats often suffer from health issues and are under chronic stress conditions, which might weaken the immune response to vaccination (41), such as to the combined vaccination with Gonacon and rabies vaccines. Therefore, although some adjustments were needed in order to perform a study with feral cats as compared to well-maintained friendly cats (in regards to capturing, management, handling, cet.), the study was designed to examine the short term safety and efficacy of our combined vaccination approach specifically in feral queens, as they are the main target population for non-surgical contraception/sterilization.

Accordingly, in our study, the feral queens were captured by traps, and were maintained under ambient summer temperature and light. The study was conducted during the Israeli summer to avoid suppressing effects of the photoperiod or climate conditions on the reproductive system (8, 21, 53, 54). Furthermore, queens were vaccinated 24–72 h after they were captured, while their health condition was still typical to that of feral cats. Indeed, our physical examination and blood tests performed at study initiation, just prior to vaccination, indicated that many of the queens were in suboptimal body condition, and some had signs of anemia, inflammation, or muscle injuries. Furthermore, many cats had a high eosinophilic count in their blood, suggesting high infestation of gastrointestinal or other parasites. Despite the suboptimal health condition of the feral cats in the current study, the combined vaccination with Gonacon and rabies was safe and effective in the short term. None of the animals showed any local or systemic adverse reactions. In the study of Levy et al. (31), late-onset (2 years post-treatment) granulomatous injection-site masses developed

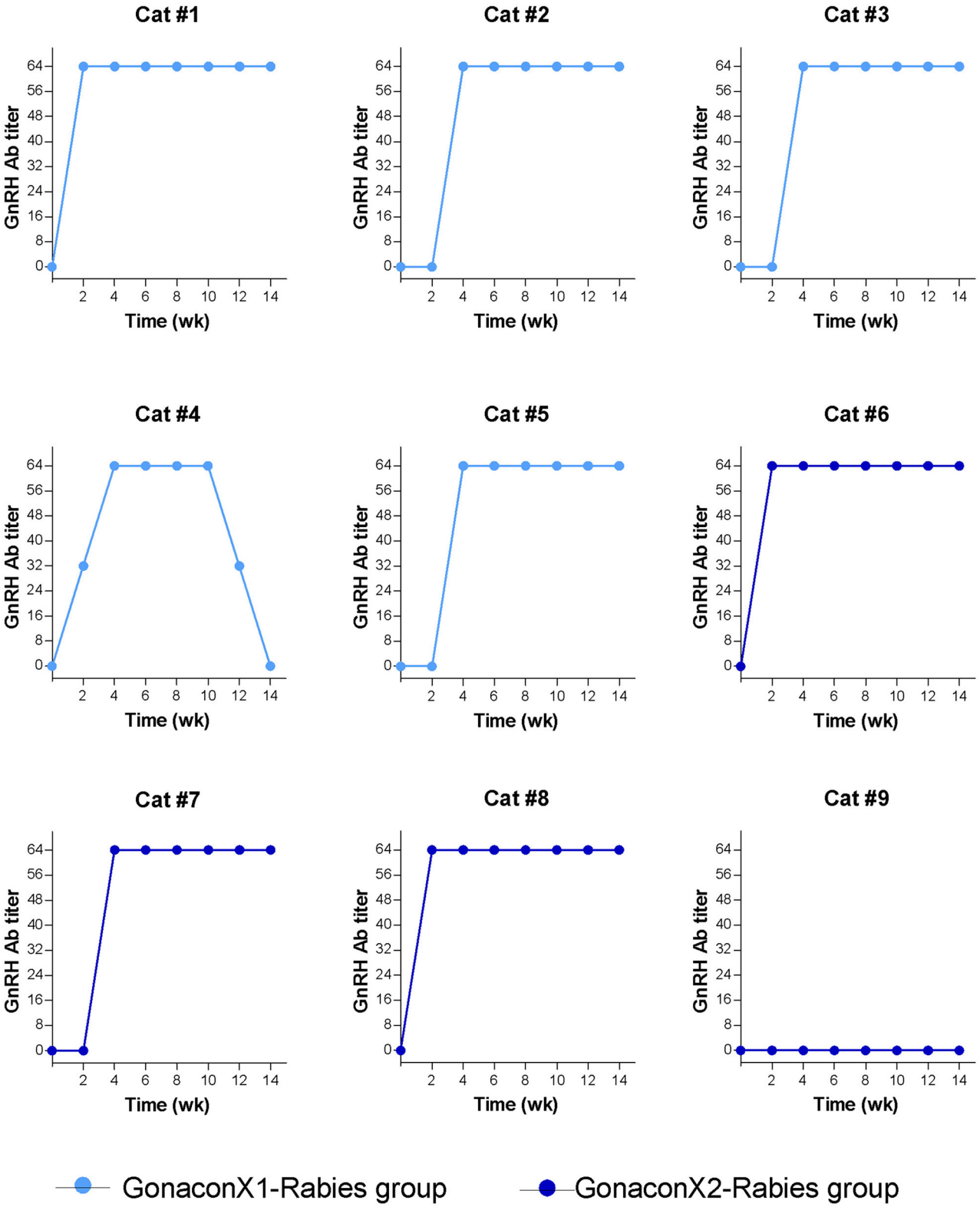

FIGURE 6 | Serum GnRH antibodies titer of individual cats vaccinated with Gonacon. Each graph represents data of a single cat. GonaconX1-Rabies group: cats vaccinated once with both Gonacon and rabies ($n = 5$; light blue); GonaconX2-Rabies group: cats vaccinated twice with Gonacon (3 weeks apart) and once with rabies ($n = 4$; dark blue); Blood samples were collected every 2 weeks for a total of 14 weeks. Note the reduction of antibodies in cat#4 at weeks 12 and 14, as well as the non-responder cats (#9) in the GonaconX2-Rabies group.

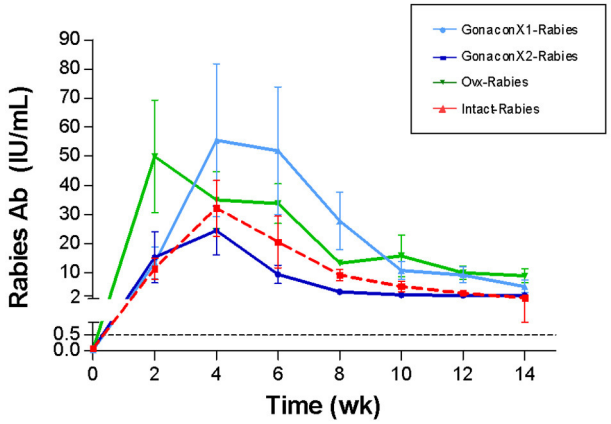

FIGURE 7 | Serum rabies antibodies of cats in the research groups. Mean ± SEM rabies antibodies concentrations are presented for each group: GonaconX1-Rabies: cats vaccinated with both Gonacon and rabies ($n = 5$); GonaconX2-Rabies: cats vaccinated twice with Gonacon (3 weeks apart) and with rabies ($n = 4$); OVx-Rabies: cats ovariohysterectomized and vaccinated with rabies ($n = 4$); Intact-Rabies: cats vaccinated against rabies and remained intact ($n = 3$). Blood samples were collected every 2 weeks for a total of 14 weeks. There were no significant differences in the rabies antibodies among the groups ($p = 0.3169$), or group X time interaction ($p = 0.7220$); however, the time was a significant factor (Repeated measure ANOVA, $p < 0.0001$). Dotted lines indicate protective titer (>0.5 IU/mL).

in 5/15 (33%) of the Gonacon-vaccinated female cats. However, in another study conducted by the same group, no injection site masses were detected in male cats at a period of 6 months post-injection (30). In the study conducted by Vansandt et al. (32), four cats developed a sterile, painless, self-limiting mass at the site of Gonacon injection, after only few weeks. Fisher et al. (33) reported injection-site reactions ranging from swelling to transient granulomatous masses in 45% ($n = 9/20$) of vaccinated cats, beginning at least 1 month after treatment. Furthermore, in another study conducted in our laboratory (Novak and Raz, unpublished data), we also documented injection-site masses 3 to 12 months post-Gonacon vaccination in 7/44 (16%) owner-owned cats. Therefore, it is possible that in the current study, masses were not detected at all as the monitoring period of 14 weeks was relatively short; furthermore, we cannot rule out the possibility of local reactions later on, after the queens were released back to their environment or adopted. Regarding the systemic health conditions of the queens, although it was initially suboptimal for many of the animals, as typical for feral cats in Israel and other places, it improved over the study period. This improvement in the cats' health is probably due to the housing conditions during the study which allow the queens to recover; i.e., good availability of food, water, and shelter; reduced risks of infectious diseases and injuries; as well as reduced stress due to the acclimation of the cats to their environment.

Despite the initial suboptimal health condition of the feral cats in the current study, the combined vaccination with Gonacon and rabies was effective in the short term. Following vaccination with rabies, all queens from all the groups produced antibodies against rabies, which remained above the level considered protective. Bender et al. (29) vaccinated dogs with both Gonacon and a commercial rabies vaccine (Defensor 3, Pfizer, Inc., New York, NY, USA), and reported no adverse effects of simultaneous vaccination on rabies virus neutralizing antibody production. None of the previous studies measured rabies antibodies in Gonacon-vaccinated cats, even if cats were vaccinated with both vaccines (32, 33). Nevertheless, our results support our hypothesis that antibody titers against rabies will not be negatively influenced by the simultaneous vaccination approach and will remain protective during the study period.

Following vaccination with Gonacon, anti-GnRH antibodies titer increased in all vaccinated queens within 2–4 weeks, except for one non-responder queen from the GonaconX2-Rabies group. In all responder queens, anti-GnRH titer remained high during the study period, except for one queen from the GonaconX1-Rabies group, in which it reduced in the last two examinations. This queen was identified as FIV positive, which could have affected the immunogenicity of the Gonacon vaccine; however, the production of anti-rabies antibodies did not appear to be negatively affected in this queen. Nevertheless, the possibility of immunogenicity alteration of any immunocontraception vaccine due to FIV infection is interesting and warrants further investigation, as FIV might be quite prevalent among free-roaming cat populations (35, 55–57). There was no significant difference in GnRH antibodies between the GonaconX1-Rabies and GonaconX2-Rabies groups. However, as our study focused on the short-term effects, we cannot rule out the possibility that repeated Gonacon vaccinations would extend the effective period, and potentially provide extended contraception. Furthermore, as our assay was limited to series dilutions from 1:8,000 to 1:64,000, it is possible that the double Gonacon vaccination could have shown positive results in higher dilutions than 1:64,000. Previous studies showed that some cats did not respond to the Gonacon vaccine (i.e., no anti-GnRH antibodies), while others responded to the vaccine with anti-GnRH antibodies detected for various periods after injection. The only other study which compared a single to double Gonacon vaccination could not detect differences in the anti-GnRH antibody at 1:1,024 dilution at 4-month post-vaccination of ovariectomized queens (3 cats in each group) (32). Nevertheless, our hypothesis that two doses of Gonacon would induce higher anti-GnRH titer, as compared to a single vaccination, require further long-term study.

There are several relevant approaches to evaluate the function of the reproductive system following the administration of an immunocontraceptive agent, but it is clear that breeding provides the most definitive results. However, breeding trials, particularly in overpopulated species like cats, are practically challenging, require time and resources, as well as carry some ethical dilemmas, as to the destiny of the newborn offspring (or performing ovariohysterectomy of pregnant animals). Therefore, in the current study, we were looking for other alternatives. Accordingly, we evaluated the effects of Gonacon vaccination on the reproductive system by a combination of serum AMH concentrations measurements, vaginal cytology, and ovarian histology; which all suggested that the reproductive cyclicity was indeed suppressed in

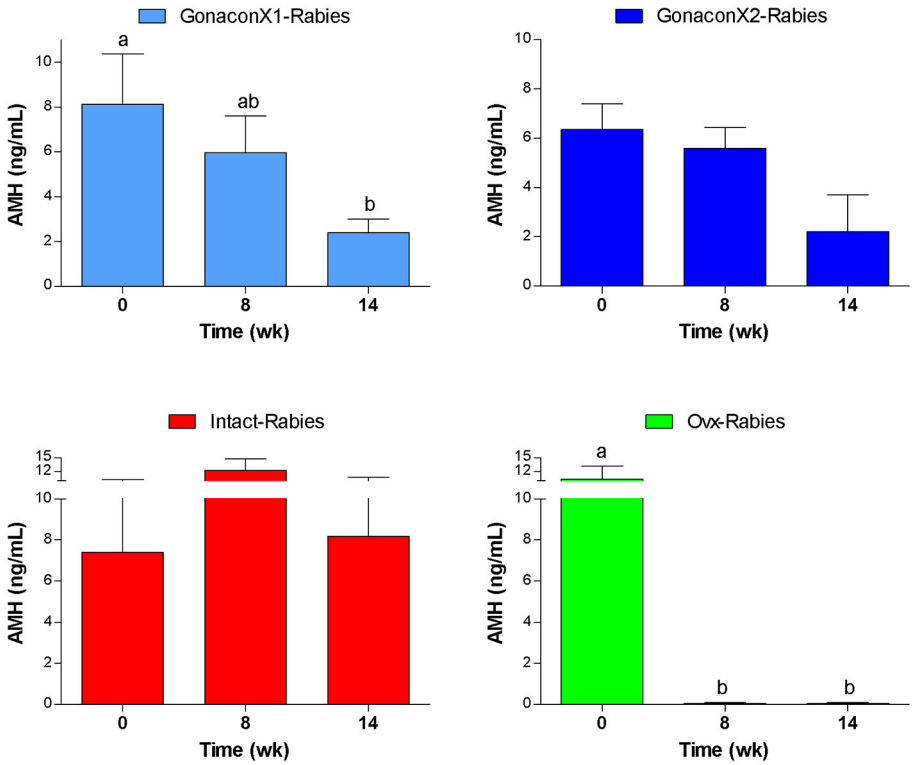

FIGURE 8 | Serum concentrations of anti-müllerian hormone of cats in the research groups. Serum concentrations of anti-müllerian hormone (Mean ± SEM) are presented for each group: GonaconX1-Rabies: cats vaccinated with both Gonacon and rabies ($n = 5$); GonaconX2-Rabies: cats vaccinated twice with Gonacon (3 weeks apart) and with rabies ($n = 4$); OVx-Rabies: cats ovariohysterectomized and vaccinated with rabies ($n = 4$); Intact-Rabies: cats vaccinated against rabies and remained intact ($n = 3$). Analyses were performed on blood samples collected at 0, 8, and 14 weeks after the initial vaccination. [a,b]Different letters above bars represent significant differences ($p < 0.0.5$).

Gonacon-vaccinated queens. In females, AMH is a hormone produced in the ovaries by small and developing follicles, and has a pivotal role in the regulation of ovarian follicle reserve and folliculogenesis. Studies in other species have shown that there is a correlation between the number of developing follicles in the ovary and serum AMH concentration (58). It has also been found that when a queen is spayed, AMH serum concentration drops abruptly (50, 59). Accordingly, we initially hypothesized that AMH serum concentrations would be reduced following ovariohysterectomy, as well as following vaccination with Gonacon, due to the vaccine potential suppression effect on gonadotropins and folliculogenesis. Indeed, in the current study, AMH serum concentration was extremely low following ovariohysterectomies, but it remained high in intact queens, in agreement with previous studies in cats and other species (50, 59, 60). Interestingly, in queens vaccinated with Gonacon, the reduction in AMH concentration was gradual. Eventually, at study completion, AMH serum concentrations were lower in all Gonacon-vaccinated queens, as compared to study initiation, except in the non-responder queen from the GonaconX2-Rabies group, in which AMH concentrations remained stable throughout the study. Furthermore, statistical analysis of all serum samples obtained from Gonacon-vaccinated queen revealed that AMH concentrations were significantly lower in serum samples with high anti-GnRH titers (titer 0, 6.7 ± 1.1 ng/mL, vs. titer 1:64, 3.9 ± 0.7 ng/mL; $p = 0.0429$). Overall, these findings suggest, for the first time to the best of our knowledge, that measuring AMH serum concentration is a valuable method for evaluating the efficacy of immunocontraception.

Evaluation of vaginal cytology smears and histology of the ovaries at study completion indicated that none of the Gonacon-vaccinated queens was in estrus, except the non-responder queen. However, the assessment of these results, particularly those of the vaginal cytology, could have been clearer if other analyses could have done, such as measurements of other sexual hormones (e.g., estrogen, LH, and FSH), and ultrasonography of the reproductive tract. Nevertheless, the typical histological finding in the ovaries of Gonacon-vaccinated queens was the presence of a high number of degenerated oocytes, and lack of antral follicles, alongside a low percentage of superficial cells in vaginal smears. In contrast, in intact animals (samples of the Ovx-Rabies group just before spaying; and samples of Intact-Rabies at study completion), ovaries had normal histology, with various follicles (primary, secondary, and antral follicle), and very few degenerative oocytes. Interestingly, the ovaries of the non-responder queen from the GonaconX2-Rabies group were histologically similar to those of the controls, and the

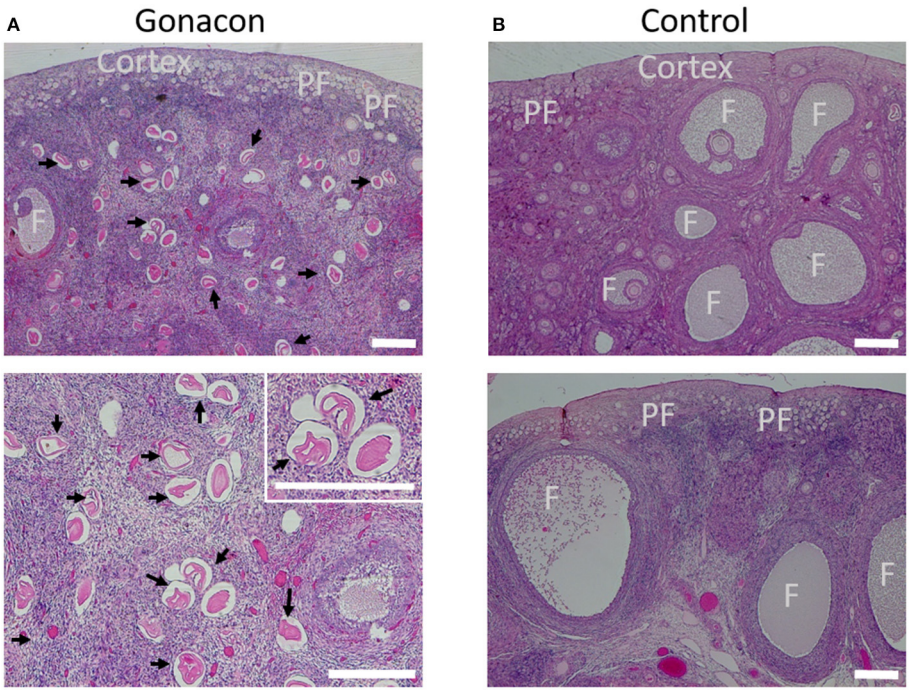

FIGURE 9 | Histology of ovaries of Gonacon-vaccinated cats. Representative ovaries of Gonacon-vaccinated cats **(A)** are shown, as compared to ovaries of non-vaccinated cats **(B)**. Note the large number of degenerative oocytes (black arrows) in the ovaries of Gonacon-vaccinated cats. PF, crowded primordial follicles under the ovary's tunica albuginea, at the ovarian cortex; F, antral follicles. H&E staining. Scale bars in all images are 30 μm.

vaginal cytology smear had a high number of superficial cells (∼90%) indicated that this female was in estrus. In our histologic evaluation, we were not able to detect apparent differences in the primordial follicle reserve in the ovaries, nor differences in the endometrium. Future studies should consider exploring the possible short and long-term effects of immunocontraceptive agents on the primordial follicle reserve, as the reduction or elimination of this pool would be beneficial for long-term contraception/sterilization.

Out of the three previous publications regarding Gonacon vaccination in female cats, two studies examined the contraceptive effect. In the long-term study conducted by Levy et al. (31), 15 queens were vaccinated with the early generation Gonacon vaccine, and were exposed to intact males. Gonacon-vaccinated queens re-gained fertility at a later time, as compared to controls; of the 15 vaccinated queens, 93% were infertile for at least 1 year, 73% for 2 years, 53% for 3 years, and 40% for 4 years; 27% were still infertile at the conclusion of the 5-year study. In the study conducted by Vansandt et al. (32), ovariectomized queens were used, and therefore, the possible effects of Gonacon vaccination on the reproductive system could not be determined. Later on, Fischer et al. (33) reported poor contraceptive efficacy of the Gonacon vaccine in colony cats. In their study, queens were exposed to intact males 4 months after vaccination with the newer Gonacon version. All control queens ($n = 10/10$) and 60% ($n = 12/20$) of Gonacon-vaccinated queens became pregnant within 4 months of the introduction of males. Two additional vaccinated queens became pregnant (70%; $n = 14/20$) within 1 year of treatment. Overall, vaccinated queens had a significantly longer ($P = 0.0120$) median time to conception (212 days), and lower fetal counts. Nevertheless, the results of their study were disappointing. In the current study, which utilized the same Gonacon formulation as in the study of Fischer et al. (33) but of different batch, our approach indicated that ovarian cyclicity was suppressed in all queens who respond to the Gonacon vaccine, as detailed above. The differences among studies could be due to variability in the vaccine itself [overtime differences in formulas, as reviewed by Benka et al. (15); different batches]; differences between cats (laboratory vs. free-roaming vs. stray cats); environmental conditions; as well as individual variability.

There are several limitations to our study. It is possible that due to the small number of cats in each of the groups, as well as the short duration of the study, we were not able to detect uncommon adverse reactions, or other safety issues, that could have been detected in a large group of vaccinated cats or at a later stage. Also, the validity of the vaccines' immunogenicity and the assessment of the proportion of non-responder cats (i.e., no antibody formation), as well as the assessment of reproductive effects, based on a small number of vaccinated cats examined over a short period, is limited. In regards to the assessment of the cats' health before and after vaccination, future studies should consider performing additional lab tests, such as urinalysis and fecal examination for the detection of intestinal parasites, which were not performed in our study, and could have provided a better understanding of the cat health

status at vaccination. In regards to reproductive effects, other methods, such as assessment of other sexual hormones (e.g., estrogen, LH, FSH), ultrasonography of the reproductive tract, and breeding, should be considered and combined. In addition, during our study period, the queens were housed in individual cages, in conditions that were not similar to that of feral cats in an urban environment. Our study emphasizes the need to explore the safety and efficacy of the Gonacon vaccine in several target populations, and we therefore believe that further long-term studies are warranted, including in populations of stray cats in their natural environment, as well as in pet indoor vs. outdoor cats.

In summary, to the best of our knowledge, this is the first study that examined the short-term safety and efficacy of combined vaccination approach, which included anti-GnRH vaccine (Gonacon), given either as a single dose, or as two doses 3 weeks apart, in parallel with rabies vaccine, specifically in female feral cats. Overall, our results indicate that in the short term, the combined vaccination with Gonacon and rabies is safe and effective in female feral cats, with no apparent benefits for two Gonacon vaccinations as compared to a single dose. Following the combined vaccination, anti-GnRH and rabies antibodies were detected, despite the suboptimal health condition of the queens. Furthermore, evaluation of serum AMH concentrations, vaginal cytology, and ovarian histology suggested that reproductive cyclicity was indeed suppressed in Gonacon-vaccinated queens for at least 3 months. However, future studies should examine the long-term effects of contraceptive agents in free-roaming cats in their natural environment.

DATA AVAILABILITY STATEMENT

The original contributions presented in the study are included in the article/supplementary material, further inquiries can be directed to the corresponding author/s.

ETHICS STATEMENT

The animal study was reviewed and approved by The Hebrew University's Institutional Animal Care and Use Committee.

AUTHOR CONTRIBUTIONS

SN: investigation, data analysis and interpretation, methodology, and writing—original draft. BY: conceptualization, investigation, data curation, writing—review, and editing. SS: investigation, data curation, writing—review, and editing. LM, ST, RN, and LJ: investigation, writing—review, and editing. RK: conceptualization, writing—review, and editing. DE: providing Gonacon vaccines, investigation, data analysis and interpretation, writing—review, and editing. TR: conceptualization, supervision, data curation, formal analysis, funding acquisition, project administration, investigation, methodology, validation, visualization, writing—review, and editing. All authors: contributed to the article and approved the submitted version.

FUNDING

This study was funded by the Israel Chief Scientist, Ministry of Agriculture and Rural Development (12-11-0009).

ACKNOWLEDGMENTS

We are grateful to Dr. Roman Zinger and Dr. Dmitry Altshuler for allowing us to conduct the study at the cat veterinary municipal facility of the city Be'er-Sheva, as well as for their team for providing valuable technical help throughout the study. Thanks to Daria Tarhov from the Koret School of Veterinary Medicine for technical help.

REFERENCES

1. Massei G, Miller LA. Nonsurgical fertility control for managing free-roaming dog populations: a review of products and criteria for field applications. *Theriogenology.* (2013) 80:829–38. doi: 10.1016/j.theriogenology.2013.07.016
2. Day MJ. One health: the importance of companion animal vector-borne diseases. *Parasit Vectors.* (2011) 4:49. doi: 10.1186/1756-3305-4-49
3. Deplazes P, Van Knapen F, Schweiger A, Overgaauw PA. Role of pet dogs and cats in the transmission of helminthic zoonoses in Europe, with a focus on echinococcosis and toxocarosis. *Vet Parasitol.* (2011) 182:41–53. doi: 10.1016/j.vetpar.2011.07.014
4. Gerhold RW, Jessup DA. Zoonotic diseases associated with free-roaming cats. *Zoonoses Public Health.* (2013) 60:189–95. doi: 10.1111/j.1863-2378.2012.01522.x
5. Mcmanus CM, Levy JK, Andersen LA, Mcgorray SP, Leutenegger CM, Gray LK, et al. Prevalence of upper respiratory pathogens in four management models for unowned cats in the Southeast United States. *Vet J.* (2014) 201:196–201. doi: 10.1016/j.tvjl.2014.05.015
6. Wareth G, Melzer F, El-Diasty M, Schmoock G, Elbauomy E, Abdel-Hamid N, et al. Isolation of *Brucella abortus* from a dog and a cat confirms their biological role in re-emergence and dissemination of bovine brucellosis on dairy farms. *Transbound Emerg Dis.* (2017) 64:e27–30. doi: 10.1111/tbed.12535
7. Trouwborst A, Mccormack PC, Martínez Camacho E. Domestic cats and their impacts on biodiversity: a blind spot in the application of nature conservation law. *People Nat.* (2020) 2:235–50. doi: 10.1002/pan3.10073
8. Gunther I, Raz T, Berke O, Klement E. Nuisances and welfare of free-roaming cats in urban settings and their association with cat reproduction. *Prev Vet Med.* (2015) 119:203–10. doi: 10.1016/j.prevetmed.2015.02.012
9. Crawford HM, Calver MC, Fleming PA. A case of letting the cat out of the bag-why trap-neuter-return is not an ethical solution for stray cat (*Felis catus*) management. *Animals (Basel).* (2019) 9:171. doi: 10.3390/ani9040171
10. Gunther I, Raz T, Klement E. Association of neutering with health and welfare of urban free-roaming cat population in Israel, during 2012-2014. *Prev Vet Med.* (2018) 157:26–33. doi: 10.1016/j.prevetmed.2018.05.018
11. Glerum LE, Egger CM, Allen SW, Haag M. Analgesic effect of the transdermal fentanyl patch during and after feline ovariohysterectomy. *Vet Surg.* (2001) 30:351–8. doi: 10.1053/jvet.2001.24387
12. Pankratz KE, Ferris KK, Griffith EH, Sherman BL. Use of single-dose oral gabapentin to attenuate fear responses in cage-trap confined community cats: a double-blind, placebo-controlled field trial. *J Feline Med Surg.* (2018) 20:535–43. doi: 10.1177/1098612X17719399

13. Root Kustritz MV. Effects of surgical sterilization on canine and feline health and on society. *Reprod Domest Anim 47 Suppl.* (2012) 4:214–22. doi: 10.1111/j.1439-0531.2012.02078.x
14. Roebling AD, Johnson D, Blanton JD, Levin M, Slate D, Fenwick G, et al. Rabies prevention and management of cats in the context of trap-neuter-vaccinate-release programmes. *Zoonoses Public Health.* (2014) 61:290–6. doi: 10.1111/zph.12070
15. Benka VA, Levy JK. Vaccines for feline contraception: GonaCon GnRH-hemocyanin conjugate immunocontraceptive. *J Feline Med Surg.* (2015) 17:758–65. doi: 10.1177/1098612X15594989
16. Kutzler M, Wood A. Non-surgical methods of contraception and sterilization. *Theriogenology.* (2006) 66:514–25. doi: 10.1016/j.theriogenology.2006.04.014
17. Carrada-Bravo T. Rabies as a public health problem. *Bol Med Hosp Infant Mex.* (1989) 46:432–43.
18. Fogelman V, Fischman HR, Horman JT, Grigor JK. Epidemiologic and clinical characteristics of rabies in cats. *J Am Vet Med Assoc.* (1993) 202:1829–33.
19. Campagnolo ER, Lind LR, Long JM, Moll ME, Rankin JT, Martin KF, et al. Human exposure to rabid free-ranging cats: a continuing public health concern in Pennsylvania. *Zoonoses Public Health.* (2014) 61:346–55. doi: 10.1111/zph.12077
20. Axner E. Updates on reproductive physiology, genital diseases and artificial insemination in the domestic cat. *Reprod Domest Anim 43 Suppl.* (2008) 2:144–9. doi: 10.1111/j.1439-0531.2008.01154.x
21. Faya M, Carranza A, Priotto M, Abeya M, Diaz JD, Gobello C. Domestic queens under natural temperate photoperiod do not manifest seasonal anestrus. *Anim Reprod Sci.* (2011) 129:78–81. doi: 10.1016/j.anireprosci.2011.10.007
22. Miller LA, Gionfriddo JP, Fagerstone KA, Rhyan JC, Killian GJ. The single-shot GnRH immunocontraceptive vaccine (GonaCon) in white-tailed deer: comparison of several GnRH preparations. *Am J Reprod Immunol.* (2008) 60:214–23. doi: 10.1111/j.1600-0897.2008.00616.x
23. Killian G, Kreeger TJ, Rhyan J, Fagerstone K, Miller L. Observations on the use of GonaCon in captive female elk (Cervus elaphus). *J Wildl Dis.* (2009) 45:184–8. doi: 10.7589/0090-3558-45.1.184
24. Killian G, Thain D, Diehl NK, Rhyan J, Miller L. Four-year contraception rates of mares treated with single-injection porcine zona pellucida and GnRH vaccines and intrauterine devices. *Wildlife Res.* (2008) 35:531–9. doi: 10.1071/WR07134
25. Baker DL, Powers JG, Ransom JI, Mccann BE, Oehler MW, Bruemmer JE, et al. Reimmunization increases contraceptive effectiveness of gonadotropin-releasing hormone vaccine (GonaCon-Equine) in free-ranging horses (*Equus caballus*): limitations and side effects. *PLoS ONE.* (2018) 13:0201570. doi: 10.1371/journal.pone.0201570
26. Massei G, Koon KK, Law SI, Gomm M, Mora DSO, Callaby R, et al. Fertility control for managing free-roaming feral cattle in Hong Kong. *Vaccine.* (2018) 36:7393–8. doi: 10.1016/j.vaccine.2018.09.071
27. Miller LA, Fagerstone KA, Wagner RA, Finkler M. Use of a GnRH vaccine, GonaCon, for prevention and treatment of adrenocortical disease (ACD) in domestic ferrets. *Vaccine.* (2013) 31:4619–23. doi: 10.1016/j.vaccine.2013.07.035
28. Killian G, Miller L, Rhyan J, Doten H. Immunocontraception of Florida feral swine with a single-dose GnRH vaccine. *Am J Reprod Immunol.* (2006) 55:378–84. doi: 10.1111/j.1600-0897.2006.00379.x
29. Bender SC, Bergman DL, Wenning KM, Miller LA, Slate D, Jackson FR, et al. No adverse effects of simultaneous vaccination with the immunocontraceptive GonaCon (TM) and a commercial rabies vaccine on rabies virus neutralizing antibody production in dogs. *Vaccine.* (2009) 27:7210–3. doi: 10.1016/j.vaccine.2009.09.026
30. Levy JK, Miller LA, Cynda Crawford P, Ritchey JW, Ross MK, Fagerstone KA. GnRH immunocontraception of male cats. *Theriogenology.* (2004) 62:1116–30. doi: 10.1016/j.theriogenology.2003.12.025
31. Levy JK, Friary JA, Miller LA, Tucker SJ, Fagerstone KA. Long-term fertility control in female cats with GonaCon (TM), a GnRH immunocontraceptive. *Theriogenology.* (2011) 76:1517–25. doi: 10.1016/j.theriogenology.2011.06.022
32. Vansandt LM, Kutzler MA, Fischer AE, Morris KN, Swanson WF. Safety and effectiveness of a single and repeat intramuscular injection of a GnRH vaccine (GonaCon) in adult female domestic cats. *Reprod Domest Anim.* (2017) 52:348–53. doi: 10.1111/rda.12853
33. Fischer A, Benka VA, Briggs JR, Driancourt MA, Maki J, Mora DS, et al. Effectiveness of GonaCon as an immunocontraceptive in colony-housed cats. *J Feline Med Surg.* (2018) 20:786–92. doi: 10.1177/1098612X18758549
34. Slater MR. The welfare of feral cats. In: I. Rochlitz, editor. *The Welfare Of Cats*. Dordrecht: Springer Netherlands (2007). p. 141–75.
35. Stojanovic V, Foley P. Infectious disease prevalence in a feral cat population on Prince Edward Island, Canada. *Can Vet J.* (2011) 52:979–982.
36. Rioja-Lang F, Bacon H, Connor M, Dwyer CM. Determining priority welfare issues for cats in the United Kingdom using expert consensus. *Vet Rec Open.* (2019) 6:e000365. doi: 10.1136/vetreco-2019-000365
37. Brydak LB, Machala M. Humoral immune response to influenza vaccination in patients from high risk groups. *Drugs.* (2000) 60:35–53. doi: 10.2165/00003495-200060010-00004
38. Meeusen EN, Walker J, Peters A, Pastoret PP, Jungersen G. Current status of veterinary vaccines. *Clin Microbiol Rev.* (2007) 20:489–510, table of contents. doi: 10.1128/CMR.00005-07
39. Hogenesch H, Thompson S. Effect of ageing on the immune response of dogs to vaccines. *J Comp Pathol 142 Suppl.* (2010) 1:S74–7. doi: 10.1016/j.jcpa.2009.09.006
40. Jamieson AM. Influence of the microbiome on response to vaccination. *Hum Vaccin Immunother.* (2015) 11:2329–31. doi: 10.1080/21645515.2015.1022699
41. Zimmermann P, Curtis N. Factors that influence the immune response to vaccination. *Clin Microbiol Rev.* (2019) 32:18. doi: 10.1128/CMR.00084-18
42. Tizard IR. Chapter 14—Feline vaccines. In: Tizard IR, editor. *Vaccines for Veterinarians*. Amsterdam: Elsevier (2021). p. 167–78.e161.
43. Kwetkat A, Heppner HJ. Comorbidities in the elderly and their possible influence on vaccine response. *Interdiscip Top Gerontol Geriatr.* (2020) 43:73–85. doi: 10.1159/000504491
44. Segerstrom SC, Miller GE. Psychological stress and the human immune system: a meta-analytic study of 30 years of inquiry. *Psychol Bull.* (2004) 130:601–30. doi: 10.1037/0033-2909.130.4.601
45. Baldwin K, Bartges J, Buffington T, Freeman LM, Grabow M, Legred J, et al. AAHA nutritional assessment guidelines for dogs and cats. *J Am Anim Hosp Assoc.* (2010) 46:285–96. doi: 10.5326/0460285
46. Segev G, Klement E, Aroch I. Toxic neutrophils in cats: clinical and clinicopathologic features, and disease prevalence and outcome–a retrospective case control study. *J Vet Intern Med.* (2006) 20:20–31. doi: 10.1111/j.1939-1676.2006.tb02819.x
47. Yakobson B, Taylor N, Dveres N, Rozenblut S, Tov BE, Markos M, et al. Cattle rabies vaccination—a longitudinal study of rabies antibody titres in an Israeli dairy herd. *Prev Vet Med.* (2015) 121:170–5. doi: 10.1016/j.prevetmed.2015.05.004
48. Bahloul C, Taieb D, Kaabi B, Diouani MF, Ben Hadjahmed S, Chtourou Y, et al. Comparative evaluation of specific ELISA and RFFIT antibody assays in the assessment of dog immunity against rabies. *Epidemiol Infect.* (2005) 133:749–57. doi: 10.1017/S095026880500381X
49. Smith JS, Yager PA, Baer GM. A rapid reproducible test for determining rabies neutralizing antibody. *Bull World Health Organ.* (1973) 48:535–41.
50. Axner E, Strom Holst B. Concentrations of anti-Mullerian hormone in the domestic cat. Relation with spay or neuter status and serum estradiol. *Theriogenology.* (2015) 83:817–21. doi: 10.1016/j.theriogenology.2014.11.016
51. Edens MSD, Heath AM. Chapter 2—Breeding Management in the Bitch and Queen. In: Root Kustritz MV, Messonnier SP. *Small Animal Theriogenology*. Saint Louis: Butterworth-Heinemann (2003). p. 33–4.
52. Mills JN, Valli VE, Lumsden JH. Cyclical changes of vaginal cytology in the cat. *Can Vet J.* (1979) 20:95–101.
53. Gunther I, Finkler H, Terkel J. Demographic differences between urban feeding groups of neutered and sexually intact free-roaming cats following a trap-neuter-return procedure. *J Am Vet Med Assoc.* (2011) 238:1134–40. doi: 10.2460/javma.238.9.1134
54. Finkler H, Terkel J. The contribution of cat owners' attitudes and behaviours to the free-roaming cat overpopulation in Tel Aviv, Israel. *Prev Vet Med.* (2012) 104:125–35. doi: 10.1016/j.prevetmed.2011.11.006
55. Malik R, Kendall K, Cridland J, Coulston S, Stuart AJ, Snow D, et al. Prevalences of feline leukaemia virus and feline immunodeficiency virus infections in cats in Sydney. *Aust Vet J.* (1997) 75:323–7. doi: 10.1111/j.1751-0813.1997.tb15701.x

56. Bande F, Arshad SS, Hassan L, Zakaria Z, Sapian NA, Rahman NA, et al. Prevalence and risk factors of feline leukaemia virus and feline immunodeficiency virus in peninsular Malaysia. *BMC Vet Res.* (2012) 8:33. doi: 10.1186/1746-6148-8-33
57. Szilasi A, Denes L, Kriko E, Heenemann K, Ertl R, Mandoki M, et al. Prevalence of feline immunodeficiency virus and feline leukaemia virus in domestic cats in Hungary. *JFMS Open Rep.* (2019) 5:2055116919892094. doi: 10.1177/2055116919892094
58. Monniaux D, Drouilhet L, Rico C, Estienne A, Jarrier P, Touze JL, et al. Regulation of anti-Mullerian hormone production in domestic animals. *Reprod Fertil Dev.* (2012) 25:1–16. doi: 10.1071/RD12270
59. Place NJ, Hansen BS, Cheraskin JL, Cudney SE, Flanders JA, Newmark AD, et al. Measurement of serum anti-Mullerian hormone concentration in female dogs and cats before and after ovariohysterectomy. *J Vet Diagn Invest.* (2011) 23:524–7. doi: 10.1177/1040638711403428
60. La Marca A, De Leo V, Giulini S, Orvieto R, Malmusi S, Giannella L, et al. Anti-Mullerian hormone in premenopausal women and after spontaneous or surgically induced menopause. *J Soc Gynecol Investig.* (2005) 12:545–8. doi: 10.1016/j.jsgi.2005.06.001

Conflict of Interest: The authors declare that the research was conducted in the absence of any commercial or financial relationships that could be construed as a potential conflict of interest.

frontiers in Veterinary Science

ORIGINAL RESEARCH
published: 25 May 2021
doi: 10.3389/fvets.2021.647153

Integrating miRNA and mRNA Profiling to Assess the Potential miRNA–mRNA Modules Linked With Testicular Immune Homeostasis in Sheep

Taotao Li[1,2], *Xia Wang*[1], *Ruirui Luo*[1], *Xuejiao An*[1], *Yong Zhang*[3], *Xingxu Zhao*[3] *and Youji Ma*[1,2]*

[1] College of Animal Science and Technology, Gansu Agricultural University, Lanzhou, China, [2] Sheep Breeding Biotechnology Engineering Laboratory of Gansu Province, Minqin, China, [3] College of Veterinary Medicine, Gansu Agricultural University, Lanzhou, China

Beyond its well-known role in spermatogenesis and androgen production, mammalian testes are increasingly recognized as an immune-privileged organ for protecting autoantigenic germ cells, especially meiotic and postmeiotic germ cells, from systemic immune responses. Despite its importance, the molecular mechanisms underlying this regulation in mammals, including sheep, are far from known. In this study, we searched for the genes associated with testicular immune privilege and assessed their possible modulating mechanisms by analyzing systematic profiling of mRNAs and miRNAs on testicular tissues derived from prepubertal and postpubertal Tibetan sheep acquired by RNA sequencing. We identified 1,118 differentially expressed (DE) mRNAs associated with immunity (245 increased mRNAs and 873 decreased mRNAs) and 715 DE miRNAs (561 increased miRNAs and 154 decreased miRNAs) in postpubertal testes compared with prepuberty. qPCR validations for 20 DE mRNAs and 16 miRNAs showed that the RNA-seq results are reliable. By using Western blot, the postpubertal testes exhibited decreased protein abundance of CD19 and TGFBR2 (two proteins encoded by DE mRNAs) when compared with prepuberty, consistent with mRNA levels. The subsequent immunofluorescent staining showed that the positive signals for the CD19 protein were observed mainly in Sertoli cells and the basement membrane of pre- and postpubertal testes, as well as the prepubertal testicular vascular endothelium. The TGFBR2 protein was found mostly in interstitial cells and germ cells of pre- and postpubertal testes. Functional enrichment analysis indicated that DE mRNAs were mainly enriched in biological processes or pathways strongly associated with the blood–testis barrier (BTB) function. Many decreased mRNAs with low expression abundance were significantly enriched in pathways related to immune response. Also, multiple key miRNA-target negative correlation regulatory networks were subsequently established. Furthermore, we verified the target associations between either oar-miR-29b or oar-miR-1185-3p and ITGB1 by dual-luciferase reporter assay. Finally, a putative schematic model of the miRNA-mRNA-pathway network mediated by immune homeostasis-related genes was

OPEN ACCESS

Edited by:
Juan G. Maldonado-Estrada, University of Antioquia, Colombia

Reviewed by:
Sigrid Lehnert, Commonwealth Scientific and Industrial Research Organisation (CSIRO), Australia
Nelida Rodriguez-Osorio, Universidad de la República, Uruguay

***Correspondence:**
Youji Ma
yjma@gsau.edu.cn

Specialty section:
This article was submitted to Animal Reproduction - Theriogenology, a section of the journal Frontiers in Veterinary Science

Received: *29 December 2020*
Accepted: *07 April 2021*
Published: *25 May 2021*

Citation:
Li T, Wang X, Luo R, An X, Zhang Y, Zhao X and Ma Y (2021) Integrating miRNA and mRNA Profiling to Assess the Potential miRNA–mRNA Modules Linked With Testicular Immune Homeostasis in Sheep. Front. Vet. Sci. 8:647153. doi: 10.3389/fvets.2021.647153

proposed to show their potential regulatory roles in sheep testicular privilege. Taken together, we conclude that many immune-related genes identified in this study are negatively regulated by potential miRNAs to participate in the homeostatic regulation of testicular immune privilege of sheep by sustaining BTB function and inhibiting immune responses under normal physiological conditions. This work offers the first global view of the expression profiles of miRNAs/mRNAs involved in sheep testicular immune privilege and how the genes potentially contribute to immune-homeostatic maintenance.

Keywords: Tibetan sheep, testis, immune privilege, blood-testis barrier, RNA-seq, miRNA

INTRODUCTION

Tibetan sheep (*Ovis aries*) provide food and livelihood to the inhabitants of Tibet (1) and play an important role in the functions of the Tibetan ecosystem (2). However, this breed of sheep is slow to mature. Thus, insight into the gonad development (including homeostasis of the internal environment) of Tibetan sheep is of great practical importance to the reproductive biology of sheep and other domestic animals.

The testes are an extremely important reproductive organ that determines male fertility. They contain spermatogenic cells that can maintain the production of male gametes. Immunologically, the testes are also perceived as an immune-privileged organ (3). Protection of the immunogenic spermatogenic cells (especially meiotic and postmeiotic cells) from the host immune response is fundamental to guarantee continuous spermatogenesis and male fertility. This process has been increasingly reported to rely on this privilege (4, 5). Except germ cells (GCs), almost all testicular cell types including Sertoli cells (SCs) (6), myoid cells (7), Leydig cells, and immune cell populations, such as macrophages, lymphocytes (mainly T cells), dendritic cells (DCs), and mast cells (3, 8), are regarded as possessing immunoregulatory properties, collectively participating in the formation of testicular immune privilege. On the one hand, testicular immune privilege prevents immunogenic GCs from autoimmune responses, while on the other hand, it protects GCs against inflammatory responses and microbial infections (3). Previous studies have documented that testicular immune privilege is tightly regulated by numerous genes, such as tight junction protein catenins (CTNNs), occludins (OCLNs), and claudins (CLDNs) (9–11), and transforming growth factor β (TGFB) family members (3, 12). Nevertheless, the genes that control testicular immune privilege in sheep and their expression modulation are poorly known.

MicroRNAs (miRNAs), a class of endogenous short non-coding small RNAs (sRNAs), can modulate the expression patterns of genes at the transcriptional and posttranscriptional levels. miRNAs participate in almost all essential biological and physiological processes, including reproductive process (13) and development of the immune system (14). Additionally, current research on miRNAs involved in reproductive immunity has mainly focused on the female reproductive tract (15, 16) and is highly limited in terms of the testes (17), especially sheep testes.

RNA sequencing (mRNA-seq and sRNA-seq) has emerged as a powerful tool to identify and characterize the genes and miRNAs expressed in mammalian testes (18, 19). RNA sequencing is of great significance for further filtering the immune-related mRNAs–miRNAs in testes and understanding the complex processes that modulate the maintenance of the testes' immune privilege. Based on this background, we hypothesized that genes participating in the regulation of immune privilege maintenance in ram testes could be identified on the background of gene expression changes due to other cellular processes involved in sexual maturation of testis tissue. By filtering genes with differential expression between prepubertal and sexually mature ram testes according to their proposed involvement in immune-related processes, we are attempting to focus on the biological mechanisms involved in immune privilege development. We further hypothesized that specific miRNAs with potential involvement in regulating these genes could be identified in parallel. This study was therefore conducted by RNA-seq analysis combined with molecular biological experiments to screen and mine the immune-related genes that show differential abundance in prepubertal and postpubertal ram testes. Besides, we explore if the genes that participate in testicular immune privilege are regulated by miRNAs, thus, contributing to understanding the complex processes that modulate the maintenance of testis immune privilege.

MATERIALS AND METHODS

Experimental Animals and Sampling

A total of 16 healthy male Tibetan sheep derived from the same ram was selected based on their birth records and divided into two age groups: sexual immaturity (3-month old; $n = 8$) and sexual maturity (1-year old; $n = 8$). All animals were purchased from the Ganjia Tibetan Sheep Breeding Cooperative (Xiahe, Gansu, China). Following sacrifice, the right testicular tissues were obtained from all the sheep of the two age groups (testes from 3-month-old sheep, T3M; testes from 1-year-old sheep, T1Y) and then divided in the following two parts: one part was stored at −80°C used for RNA and protein extraction, and the other was fixed in 4% paraformaldehyde for at least 24 h, embedded in paraffin, and sectioned in 5-μm paraffin sections.

RNA Extraction

Total RNA of each testis sample was extracted using Trizol reagent (Invitrogen, Carlsbad, CA, USA) according to the kit's operation manual. RNA quality was evaluated first by 1.0% agarose electrophoresis, then determined on an Agilent 2100

Bioanalyzer (Agilent Technologies, Palo Alto, CA, USA). All samples had an RNA integrity number (RIN) >7.5. Of the RNA samples from eight rams for each age group, four were randomly selected and used to construct cDNA libraries for mRNA and sRNA sequencing, and all eight RNA samples from each group were used for qPCR validation.

Library Preparation for mRNA-seq and Data Processing

The 470- to 500-bp size ligation products were enriched to generate a strand-specific cDNA library for mRNA-seq. Construction of the mRNA libraries was performed as described earlier (20). A total of eight prepared cDNA libraries from two age groups were sequenced on Illumina HiSeq^{TM} 4000 by Gene Denovo Biotechnology Co., Ltd. (Guangzhou, China). The high-quality clean reads were screened from the raw reads by trimming and filtering reads with adaptors, more than 10% of unknown nucleotides (N), and low-quality reads with more than 50% of low-quality (q-value ≤20) bases. The clean reads of each sample were first filtered for ribosomal RNAs and then mapped to the *Ovis aries* reference genome (Oar_v4.0) by TopHat2 (version 2.1.1) using default parameters (21).

Library Preparation for sRNA Sequencing and Data Processing

The 140- to 160-bp size ligation products were enriched to generate a cDNA library for sRNA sequencing. A total of eight cDNA libraries from two age groups were sequenced on the Illumina HiSeq^{TM} 2500 platform by Gene Denovo Biotechnology Co., Ltd. (Guangzhou, China). The clean tags were obtained from the raw reads by filtering out the low-quality reads with more than one low quality (q-value ≤20) base or containing unknown nucleotides (N), and reads without 3′ adapters, reads containing 5′ adapters, 3′ and 5′ adapters but no small RNA fragment between them, polyA in small RNA fragment, and reads with lengths shorter than 18 nt (not including adapters). All of the clean tags were aligned with small RNAs in the GenBank database (http://blast.ncbi.nlm.nih.gov) and Rfam database (http://sanger.ac.uk/software/Rfam) to identify and discard the cellular structural RNAs (rRNA, snRNA, snoRNA, and tRNA).

Identification of Known and Novel miRNAs

All of the clean tags were mapped to the miRBase 21.0 database (http://www.mirbase.org/) to identify known ovine miRNAs. The remaining clean tags that were not mapped to the sheep miRBase were then mapped to the other animal species included in the miRBase database to identify the known miRNAs. For all of the other unannotated tags aligned with the reference genome using Bowtie (v1.1.2), the novel miRNAs were predicted by software Mireap_v0.2 and identified according to their genome positions and hairpin structures. The default parameters were used in all software.

Screening of Differentially Expressed mRNAs and miRNAs

mRNA abundances were quantified via the software RSEM (22), and their expression levels in each sample were normalized by using the FPKM method (23). The miRNA expression level from each sample was calculated and normalized to TPM (TPM = actual miRNA count/total count of clean reads $\times$ 10^6). Differentially expressed (DE) mRNAs and miRNA analyses between the two age groups were performed using the edgeR package (http://www.bioconductor.org/packages/release/bioc/html/edgeR.html). We identified DE mRNAs with an absolute fold change >2 and FDR < 0.05, and DE miRNAs with an absolute fold change >2 and p-value < 0.05.

Functional Enrichment of Differentially Expressed mRNAs and Screening of Immune-Related Differentially Expressed Genes

Gene Ontology (GO) annotation and Kyoto Encyclopedia of Genes and Genomes (KEGG) enrichment analysis for all DE mRNAs were performed with the GO database (http://www.geneontology.org/) and KEGG database (http://www.genome.jp/kegg/pathway.html), respectively. GO terms and pathways with a q-value < 0.05 were considered significantly enriched by DE mRNAs. To explore the potential function of some genes implicated in the maintenance of testicular immune privilege, the immune-related DE mRNAs were filtered based on the results from the above GO and KEGG analysis, and again mapped to GO terms in the GO database and pathways in the KEGG database.

Target Prediction of Differentially Expressed miRNAs and Integrative Analysis of Immune-Related miRNA–mRNA Pairs

The candidate target genes of DE miRNAs were predicted by using the RNAhybrid (v2.1.2) + svm_light (v6.01), Miranda (v3.3a), and TargetScan (v 7.0) software. The intersection of the results from three software packages were selected as predicted miRNA target genes. Expression correlation between miRNA and its predicted target was assessed by Pearson correlation coefficient (PCC). Subsequently, the negatively coexpressed immune-related miRNA–mRNA pairs with PCC < −0.7 and p-value < 0.05 were screened to construct miRNA–mRNA networks.

Validation of Differentially Expressed mRNAs and miRNAs Using Quantitative Real-Time PCR

Total RNA was extracted from all 16 testis samples of two age groups using Trizol reagent (TransGen, Beijing, China). The first-strand cDNA for mRNAs was synthesized from 500 ng of each total RNA sample using a TransScript II All-in-One First-Strand cDNA Synthesis SuperMix (TransGen Biotech, Beijing, China) following the manufacturer′s recommendations. cDNA synthesis for miRNAs was performed from 500 ng of each total

RNA sample using a Mir-X™ miRNA FirstStrand Synthesis Kit (Takara, Shiga, Japan) according to the kit instructions. The qPCR was carried out using a TB Green™ Fast qPCR Mix (Takara, Shiga, Japan) on a LightCycler 96 Real-Time System (Roche, Switzerland). The specific primers used in qPCR were designed and synthesized by the Qingke Biological Company (Xi'an, China). Primer sequences are provided in **Supplementary Table 1**. Eight independent biological replicates were included in qPCR analysis. β-actin and U6 were used as internal control genes for expression normalization of mRNAs and miRNAs, respectively. The relative expression levels of mRNAs and miRNAs were calculated using the $2^{-\Delta\Delta Ct}$ method (24).

Western Blot

Total protein was extracted from all 16 testis samples in two age groups, and its concentration was detected using a BCA protein assay reagent (Beyotime, Shanghai, China). Western blot assay was performed, as described in a previous report (25). β-actin was used as a protein-loading control. Briefly, a total of 20 μg of protein from each sample was separated by 12% SDS-PAGE gradient gels and electrotransferred onto PVDF membranes. Membranes were incubated with rabbit polyclonal anti-CD19 antibody (Bioss, Beijing, China; 1:500 dilution), rabbit polyclonal anti-TGF beta receptor II antibody (Bioss, Beijing, China; 1:500 dilution), or rabbit polyclonal anti-beta-actin antibody (Bioss, Beijing, China; 1:1,500 dilution) and the secondary antibody goat anti-rabbit IgG conjugated with HRP (Bioss, Beijing, China; 1:5,000 dilution). Protein bands were visualized using an ECL kit (NCM Biotech, Suzhou, China) and quantified using AlphaEaseFC software (Protein Simple, Santa Clara, CA, USA).

Immunofluorescence

Paraffin sections were deparaffinized, hydrated, and subjected to antigen retrieval. An immunofluorescence assay was carried out as described previously (25). In brief, sections were blocked with 5% bovine serum albumin (BSA) for 1 h and incubated with rabbit polyclonal anti-CD19 antibody (Bioss, Beijing, China; 1:150 dilution) or rabbit polyclonal anti-TGF beta receptor II antibody (Bioss, Beijing, China; 1:200 dilution). After being washed in PBST (PBS with 0.5% Tween-20), the sections were incubated with the secondary antibody goat anti-rabbit IgG conjugated with Cy3 or FITC. Nuclei were visualized using DAPI (Servicebio, Wuhan, China). Sections were visualized under a fluorescence microscope (Nikon, Eclipse C1, Tokyo, Japan), and images were acquired using CaseViewer software (3DHISTECH, Budapest, Hungary). For negative controls, the primary antibody was replaced with 5% BSA.

Dual-Luciferase Reporter

The wild-type ITGB1 3′UTR fragment containing the putative miR-29b or miR-1185-3p binding site and their corresponding mutant-type fragments were designed and synthesized (GENEWIZ, Suzhou, China), and then cloned into the pmirGLO plasmid (Promega, Madison, USA) between the XhoI and SalI multicloning sites, named as ITGB1-29-3′UTR WT, ITGB1-1185-3′UTR WT, ITGB1-29-3′UTR MUT, and ITGB1-1185-3′UTR MUT, respectively. The miR-29b mimic (5′-UAGCACCAUUUGAAAUCAGUGU-3′, 5′-ACUGAUUUCAAAUGGUGCUAUU-3′), miR-1185-3p mimic (5′-AUAUACAGAGGGAGACUCUUAU-3′, 5′-AAGAGUCUCCCUCUGUAUAUUU-3′), and mimic negative control (5′-UUCUCCGAACGUGUCACGUTT-3′, 5′-ACGUGACACGUUCGGAGAATT-3′) were bought from GenePharma (Shanghai, China). The reporter plasmids were cotransfected with either the corresponding mimic or mimic NC into HEK293T cells (Beina Biology, Beijing, China) using the Lipofectamine 2000 vehicle (Invitrogen, Carlsbad, USA) as per the vendor's recommendations. Both firefly luciferase and Renilla luciferase activities were monitored at 48 h following transfection, using a dual-luciferase reporter assay system (Promega, USA). Data are shown as relative luciferase activity generated by dividing the firefly luciferase values with those of the Renilla luciferase.

Statistical Analysis

At least three independent repeats were undertaken for each of the experiments. Comparisons between two groups were made using independent-samples *t*-tests or one-way ANOVAs in SPSS 21.0 (SPSS, Inc., Chicago, IL, USA). The results were expressed as mean ± SD. Significant differences between the two groups were considered in terms of the associated *p*-value relative to $p < 0.05$ and $p < 0.01$.

RESULTS

Identification and Functional Classification of Differentially Expressed mRNAs

We carried out mRNA-seq analysis and obtained an average of 85, 301, 018 (99.04% of raw reads) and 78, 331, 884 high-quality clean reads (98.27% of raw reads) from T3M and T1Y, respectively, after removal of rRNA and low-quality reads. Of the high-quality clean reads, on average, 77.17% of the reads were uniquely mapped to the ovine reference genome. The detailed statistics for each library are listed in **Supplementary Table 2**. The hierarchical clustering results showed that the samples from T3M and T1Y groups separated into two distinct clusters (**Figure 1A**). The sample correlation heat map from the mRNA expression profiles indicated that four replicate samples from each group had good repeatability (**Figure 1B**). Here, we identified 26,084 DE mRNAs (17,472 genes), of which 10,247 were more abundant, while 15,837 were less abundant in the T1Y group ($|\text{fold change}| > 2$, FDR < 0.05). GO and KEGG enrichment analysis showed that most DE genes were mainly involved in the biological processes and pathways related to cell growth, reproduction, immunity, and metabolism (**Figures 1C,D**).

Screening of Differentially Expressed mRNAs Related to Immunity

To explore the potential functions of genes involved in maintaining testis' immune privilege during development, we further screened the immune-related DE mRNAs. Herein, we identified 1,118 DE mRNAs that were associated with immunity.

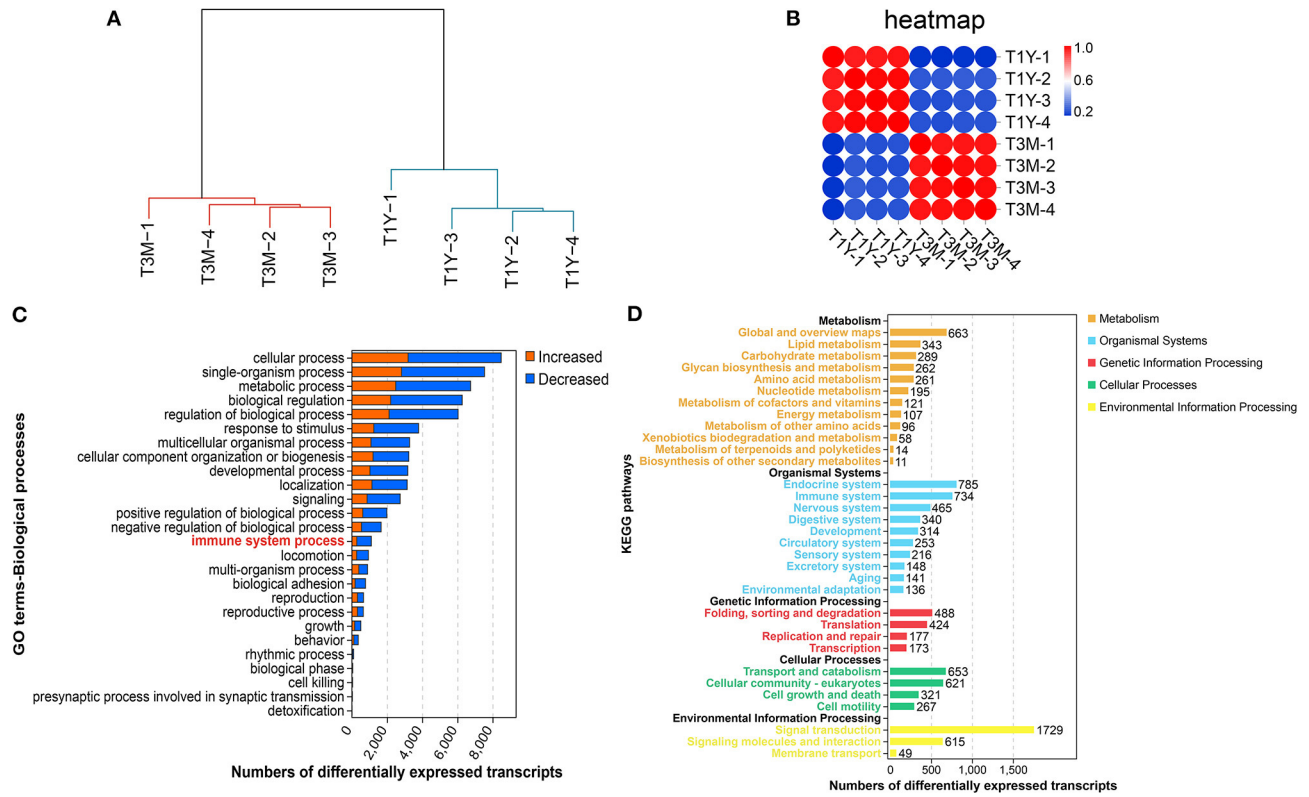

FIGURE 1 | Differential gene expression analysis between T3M and T1Y. **(A)** Hierarchical clustering dendrograms of the biological duplicates. **(B)** Sample correlation heatmap. **(C)** Biological processes mediated by DE mRNAs based on Gene Ontology (GO) annotation results. **(D)** Kyoto Encyclopedia of Genes and Genomes (KEGG) enrichment analysis for DE mRNAs. T3M, testes from 3-month-old sheep; T1Y, testes from 1-year-old sheep; DE, differentially expressed.

Of these, 245 mRNAs exhibited increased abundance in the T1Y group relative to the T3M group, with the remaining 873 mRNAs exhibiting decreased abundance (**Figures 2A,B**). Clustering heatmap analysis for these mRNAs showed excellent repeatability and gene expression profiles for the different age groups (**Figure 2C**). For a detailed list of all these mRNAs and their expression levels, see **Supplementary Table 3**.

Functional Annotation of Immune-Related Genes

GO analysis showed that these immune-related genes, in the category of biological process, were mainly involved in immune system processes, cell adhesion/junction, responding to stimulus and immune responses; in the category of cell component, they were mainly implicated in the cell junction, extracellular matrix (ECM), membrane region, cell part, and receptor complexes; and in the category of molecular function, they were mainly associated with protein binding, receptor binding, receptor regulator activity, and cytokine receptor activity (**Figure 3A** and **Supplementary Table 4**). KEGG enrichment results revealed that most of these genes were significantly enriched in pathways associated with the immune system, such as the chemokine signaling pathway, T- and B-cell receptor pathways, leukocyte trans endothelial migration, NF-κB signaling, and focal adhesion (**Figure 3B** and **Supplementary Table 5**). There were 17 DE mRNAs (corresponding to 14 DE genes) associated with four functions: immune response, presence at the cell junction, ECM remodeling, and cell adhesion (**Figure 3C**).

Identification and Analysis of DE miRNAs

After removing low-quality reads and adapter sequences, an average of 12, 737, 654 (95.45% of raw reads) and 10, 898, 503 (79.13% of raw reads) clean tags were obtained from the four samples of the T3M group and four samples of the T1Y, respectively. Of the clean tags, 81.70% of the tags from the T3M and 73.25% of the tags from the T1Y were mapped to the reference sequence. The detailed statistics for each library are given in **Supplementary Table 6**. A total of 715 DE miRNAs, including 561 increased and 154 decreased miRNAs, were obtained in the T1Y group compared with the T3M group (**Figures 4A,B**), in which 443 known miRNAs and 272 novel miRNAs were identified (**Figure 4A**). Among these DE miRNAs, 19 miRNAs were specifically expressed in the testes from the T3M group, 260 miRNAs were specifically expressed in the testes from the T1Y group, and 436 miRNAs were expressed in both (**Figure 4C**). Detailed information on miRNA expression is given in **Supplementary Table 7**.

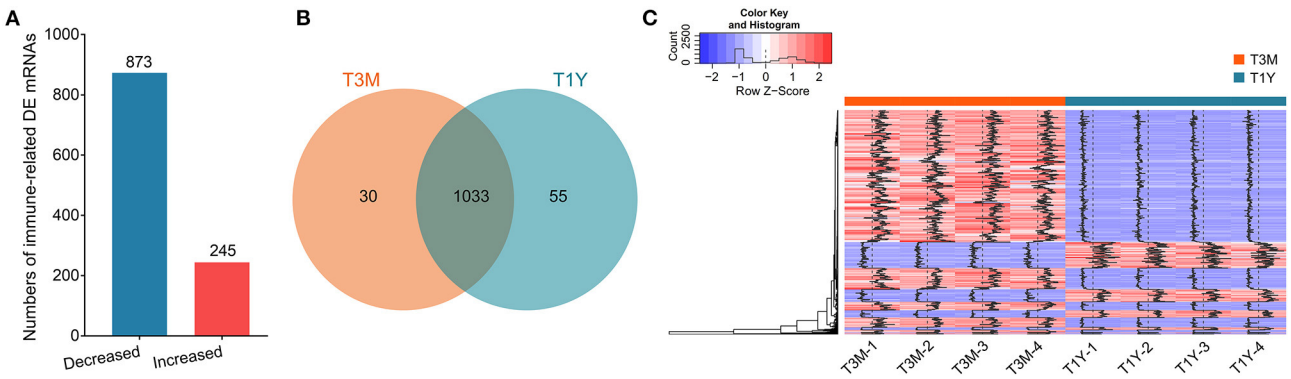

FIGURE 2 | Filtering of DE mRNAs related to immunity. **(A)** The histogram shows the numbers of the immune-related DE mRNAs. Red and blue represent increased and decreased mRNA abundance in T1Y, respectively. **(B)** Venn diagram of the immune-related DE mRNAs in two age groups. **(C)** The clustering heatmap for the immune-related DE mRNAs. T3M, testes from 3-month-old sheep; T1Y, testes from 1-year-old sheep; DE, differentially expressed.

Interaction Network of miRNAs and Target mRNAs Associated With Immunity

To explore potential miRNA target transcripts involved in the homeostatic regulation of testicular immune privilege, the expression profiles of DE miRNAs and immune-related DE mRNAs were combined for further correlation analysis. In total, we obtained 554 DE mRNAs, corresponding to 471 DE genes as putative targets for 714 DE miRNAs (442 known and 272 novel miRNAs) through integrated analysis, presenting a negatively correlated expression pattern (**Supplementary Table 8**). DE mRNAs (564) were not found to have potential target miRNAs. The resulting key potential regulatory networks of miRNA-target genes associated with testicular immune privilege were visualized with the Cytoscape software (version 3.7.1). For instance, a total of 24 known miRNAs were potentially targeted for CD19, a gene implicated in immune response (**Figure 5A**). Three BTB maintenance-related genes (CLDN11, ITGA6, and ITGB1) were potentially targeted by 87 known miRNAs, of which ITGA6 and ITGB1 were shared by 10 miRNAs (**Figure 5B**). Four genes associated with testicular immune homeostasis (TGFB1, TGFBR2, TGFBR3, and FASLG) were potentially regulated by 117 known miRNAs, in which FASLG and TGFBR3 were coregulated by 17 miRNAs (**Figure 5C**). miR-146-5p (an immune homeostasis maintenance-related miRNA) was identified as potentially involved in regulating the expression of 51 DE mRNAs (**Figure 5D**).

qPCR Validation of DE mRNAs and DE miRNAs

To verify the results of mRNA-seq and miRNA-seq, 20 DE mRNAs and 16 DE miRNAs were randomly selected for qPCR analysis. The results showed that the expression of all the selected mRNAs and miRNAs except for miR-486-5p was significantly different between the two age groups ($p < 0.01$) (**Figures 6A,B**). Overall, the expression trends of mRNA and miRNA upregulation or downregulation revealed by the qPCR data were consistent with those derived from RNA sequencing data (**Figures 6C,D**), which indicates that our transcriptome data were credible for identification of the differentially expressed mRNAs and miRNAs.

Expression and Localization Patterns of Proteins Encoded by Immune-Related Genes

To determine gene expression status at the protein level, Western blot analysis was performed for two immune-related genes (CD19 and TGFBR2). The results showed that CD19 and TGFBR2 proteins were downregulated in the T1Y group compared with the T3M group (**Figures 7A,B**), which exhibited a similar trend to those at the mRNA level. To explore the potential roles of CD19 and TGFBR2 in developmental sheep testes, and their localization patterns in sexual immaturity (T3M) and maturity (T1Y), testes were assayed by immunofluorescence. As shown in **Figure 7C**, stronger positive signals for the CD19 protein were observed in vascular endothelium from the T3M group as well as SCs and the basement membranes from the T3M and T1Y groups, and weak positive signals were observed in interstitial cells from the T3M group. For the TGFBR2 protein, strong positive signals were distributed in the interstitial cells of both T3M and T1Y, and moderate positive signals were also observed in gonocytes and spermatogonia from T3M, as well as spermatogonia, spermatocytes, and spermatids from T1Y.

Validation of Targeting Relations Between Either miR-29b or miR-1185-3p and ITGB1

ITGB1, a well-known cell adhesion-associated molecule that is implicated in the function of the blood–testis barrier (26), was discovered to be potentially regulated by 40 known miRNAs based on miRNA–mRNA coexpression network analysis. Among these, high abundance miR-29b and low abundance miR-1185-3p were randomly chosen to verify the targeting relationships between them and ITGB1. First, Pearson correlations revealed that ITGB1 expression exhibited a strong negative correlation with either miR-29b or miR-1185-3p (**Figure 8A**). Validation by qPCR confirmed a significant increase in miR-29b or miR-1185-3p and a significant decrease in ITGB1 mRNA observed in

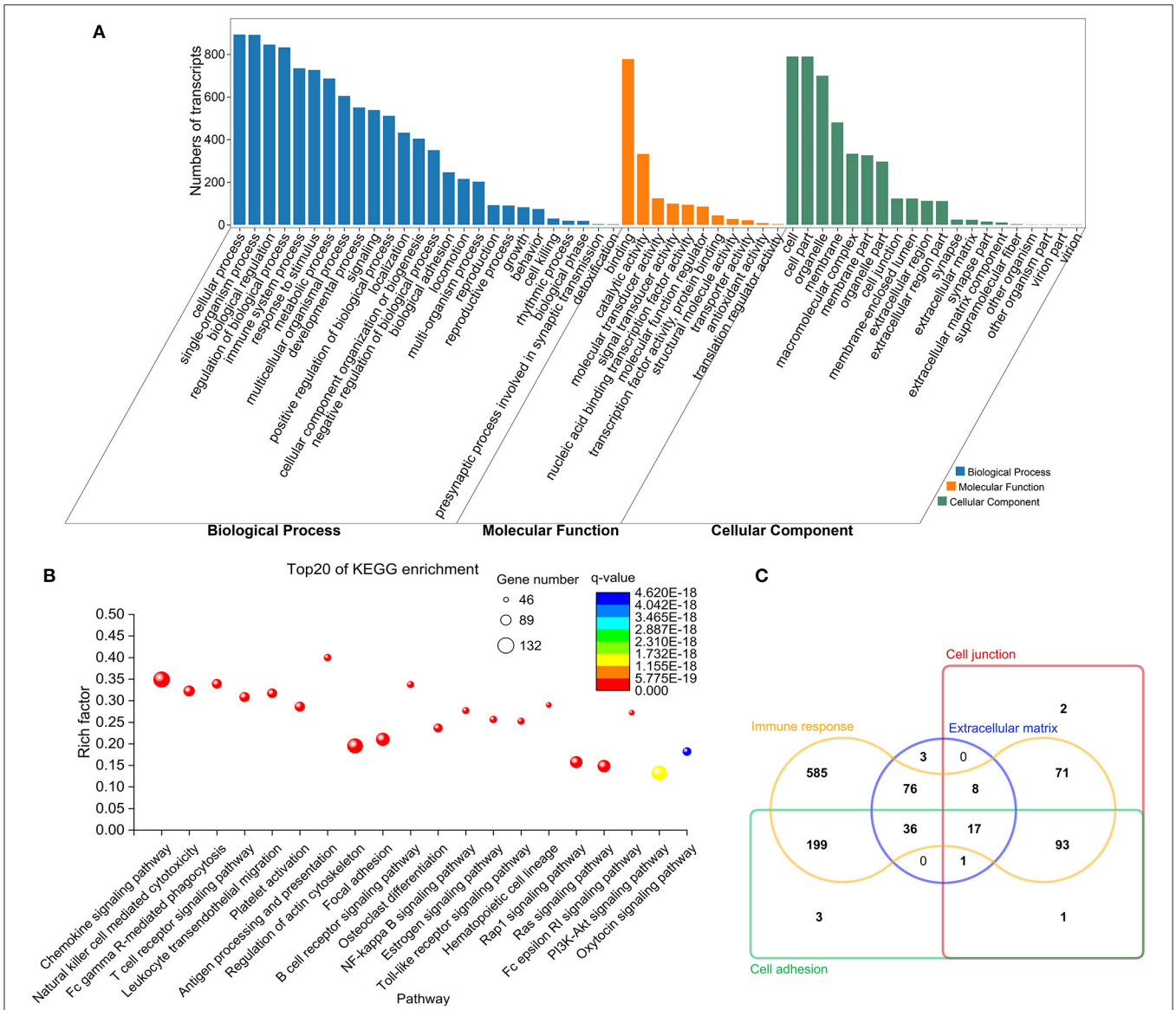

FIGURE 3 | Functional annotation and enrichment analysis for immune-related DE mRNAs. **(A)** GO annotation results. **(B)** Top 20 KEGG pathways enriched by immune-related mRNAs. Y-axis denotes the enrichment factor, which was calculated by dividing the number of enriched genes (mRNAs) in the KEGG pathway by the number of annotated genes in this pathway. **(C)** Venn diagram of DE mRNAs related to extracellular matrix remodeling, cell junction, cell adhesion, and immune response.

the RNA-seq analysis (**Figure 8B**). To validate whether ITGB1 is a genuine miR-29b and miR-1185-3p target, we employed a luciferase reporter assay by constructing the 3′UTR of ITGB1 containing the putative miR-29b or miR-1185-3p binding sites into XhoI and SalI sites of the pmirGLO dual-luciferase miRNA target expression vector (**Figure 8C**). As demonstrated in **Figure 8D**, the luciferase reporter activity for wild-type ITGB1 3′UTR (ITGB1-29-3′UTR WT and ITGB1-1185-3′UTR WT) rather than the mutant ones, was significantly reduced following transfection with either miR-29b or miR-1185-3p (**Figure 8D**). Together, these data initially corroborated that ITGB1 is a common target of miR-29b and miR-1185-3p.

DISCUSSION

To identify the potential genes involved in sheep testes' immune privilege, mRNA-seq was carried out for testis tissues derived from T3M (pre-puberty) and T1Y (post-puberty) individuals. We identified a total of 1,118 immune-related DE mRNAs corresponding to 208 genes with increased abundance and 725 genes with decreased abundance in the T1Y group compared with the T3M group. Functional bioinformatics analysis based on the GO and KEGG database showed that these genes were mainly involved in various biological processes or pathways related to immune response, tight junction, cell

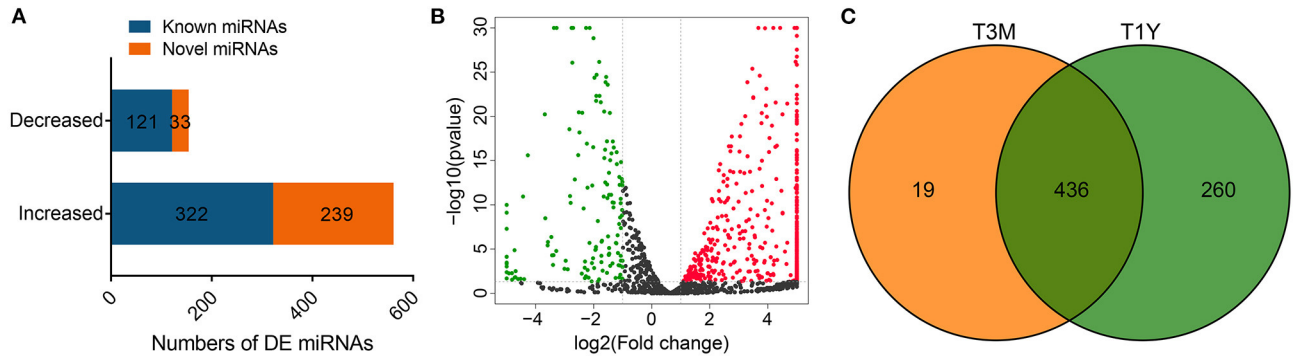

FIGURE 4 | Analysis of DE miRNAs. **(A)** Numbers of DE miRNAs. **(B)** Volcano plot of DE miRNAs. Red represents increased miRNA abundance, and green represents decreased miRNA abundance in T1Y relative to T3M. **(C)** Venn diagram representation of the common and group-specific DE miRNAs. T3M, testes from 3-month-old sheep; T1Y, testes from 1-year-old sheep; DE, differentially expressed.

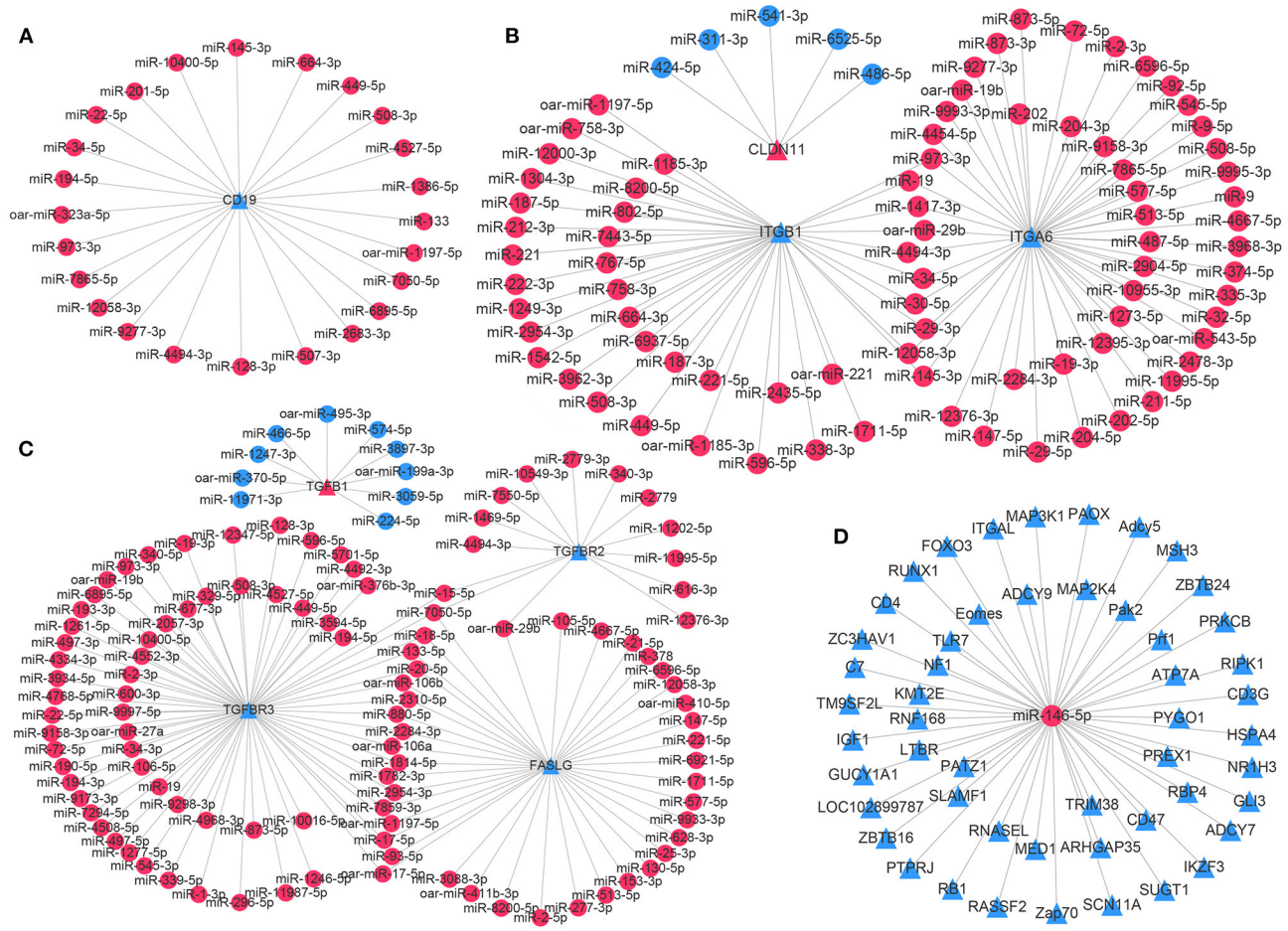

FIGURE 5 | Integrated miRNA-target negative correlation regulatory networks. **(A)** Immune-related gene CD19 was potentially regulated by 24 known miRNAs. **(B)** Three genes related to the blood–testis barrier function, namely, CLDN11, ITGA6, and ITGB1, were potentially regulated by 87 known miRNAs. **(C)** Four genes that have been reported as testicular immune homeostasis-related genes, including TGFB1, TGFBR2, TGFBR3, and FASLG, were potentially regulated by 117 known miRNAs. **(D)** Fifty-one DE genes were potentially regulated by miR-146-5p, an miRNA related to immune homeostasis maintenance. The circle nodes represent miRNAs; the triangle nodes suggest target genes. The differentially expressed miRNAs/target genes are highlighted in red and blue, describing higher and lower expression in the T1Y group compared with the T3M group, respectively. T3M, testes from 3-month-old sheep; T1Y, testes from 1-year-old sheep.

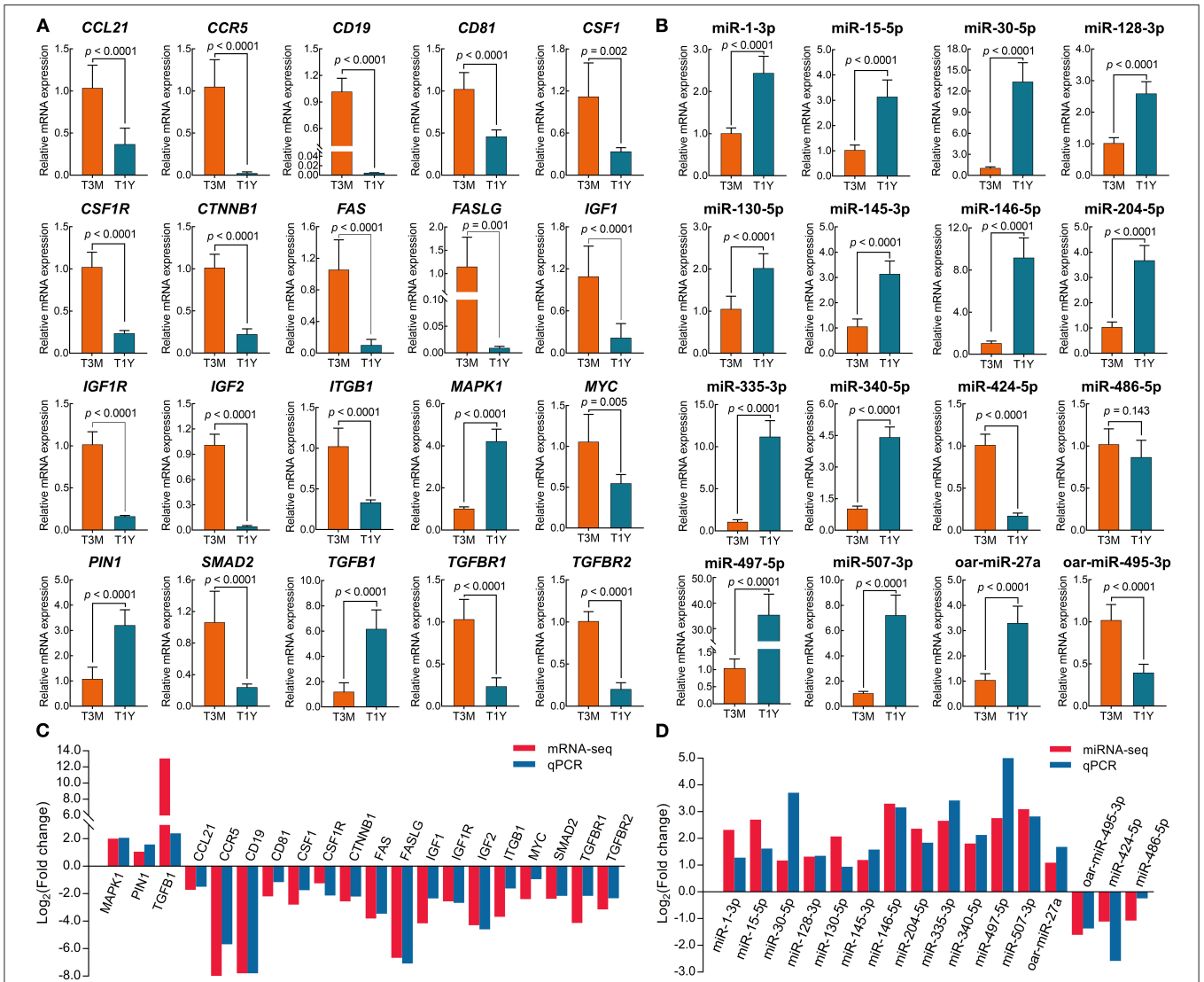

FIGURE 6 | Verification of DE mRNAs and DE miRNAs by qPCR. **(A)** qPCR analysis for 20 randomly selected mRNAs. Data represent the mean ± SD. **(B)** qPCR analysis for 16 randomly selected miRNAs. Data represent the mean ± SD. **(C)** The comparison of mRNA expression in terms of Log_2 (fold change) as assessed by mRNA sequencing and qPCR. **(D)** The comparison of mRNA expression in terms of the Log_2 (fold change) as assessed by miRNA sequencing and qPCR. T3M, testes from 3-month-old sheep; T1Y, testes from 1-year-old sheep; DE, differentially expressed.

adhesion, and ECM organization. To understand the possible modulating mechanisms of the genes implicated in testicular immune privilege, the subsequent miRNA-seq was carried out, and miRNA–mRNA regulatory networks were constructed by merging miRNA–mRNA pairs with strong negative correlations and putative miRNA binding sites. Here, we identified a total of 37,950 potential miRNA–mRNA target pairs that involved 714 DE miRNAs. It should be noted that, of course, not all genes were potentially regulated by miRNAs. Among these immune-related DE genes, none of the 460 genes corresponding to 564 mRNAs have yet been identified as regulated by miRNAs.

The testes' immune privilege involves almost every aspect of immunological regulation, including BTB with an immunoprotective role conferred by SCs, local immunosuppression, antigen-specific immune response, and immune tolerance (6). As one of the tightest tissue barriers existing in the body of mammals, BTB is mainly formed by the junctional complex at adjacent SCs, SCs-GCs, or SCs-ECM, such as tight junctions, gap junctions, and apical ectoplasmic specializations (apical ES, a testis-specific type of adhesion junction) (27, 28). Based on KEGG pathway analysis, in the present study, we found that 39, 36, and 37 DE genes were significantly enriched in tight junctions, gap junctions, and adhesion junctions, respectively. Gow et al. (29) reported that the junctional protein CLDN11 deletion leads to a lack of tight junction strands between SCs. As analyzed by mRNA-seq and qPCR, our results showed that CLDN11 expression was increased in T1Y and was potentially regulated by five known

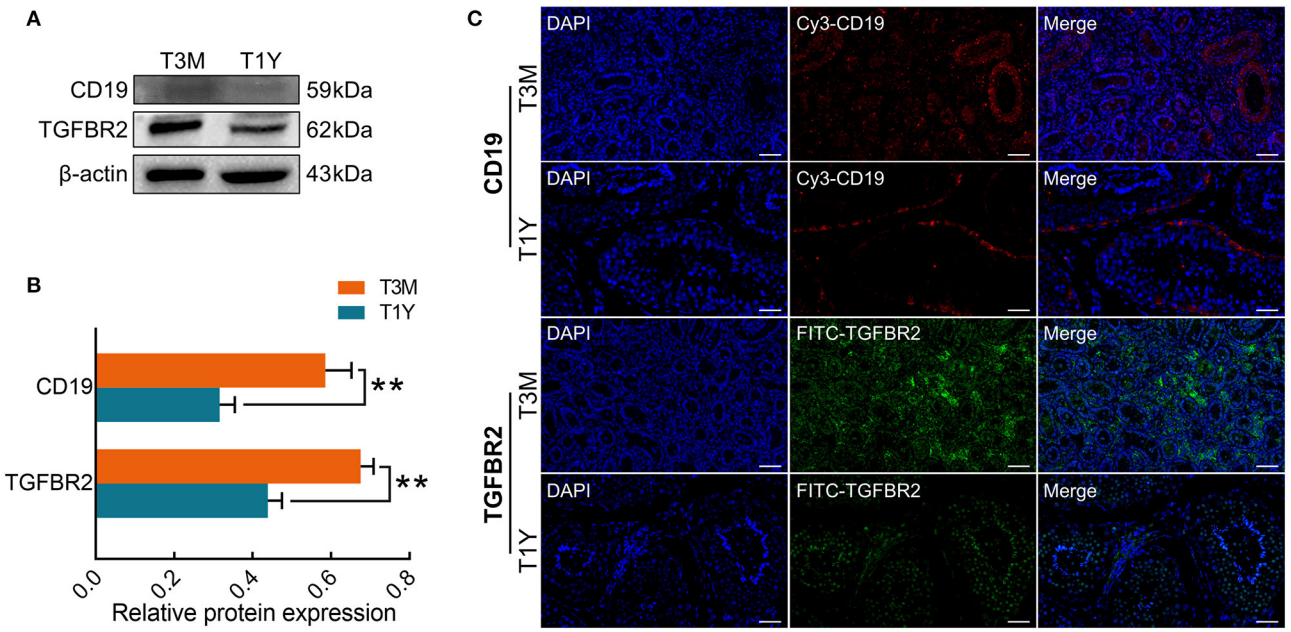

FIGURE 7 | Expression and localization patterns of CD19 and TGFBR2 proteins. **(A)** Western blot analysis. **(B)** Relative protein expression. Data represent the mean ± SD. **(C)** Immunofluorescence staining. Blue, DAPI; red/CY3, CD19; green/FITC, TGFBR2. Scale bar, 50 μm. T3M, testes from 3-month-old sheep; T1Y, testes from 1-year-old sheep; DE, differentially expressed. $^{**}P < 0.01$.

miRNAs (miR-311-3p, miR-424-5p, miR-486-5p, miR-541-3p, and miR-6525-5p).

Furthermore, we found 11 integrin molecules (i.e., ITGA2-A6, A9, B1, B2, B7, AL, and AX), the expression of which was reduced in T1Y. Cell adhesion mediated by integrins (e.g., ITGA4, A6, A7, A9, B1) has a critical role in self-renewal and differentiation of stem cells (including spermatogonial stem cells, SSCs) within the niche through direct interaction with the molecules expressed in ECM or the ECM-rich basal membranes (30). This finding would suggest that these integrins, and particularly their significant expression in T3M, may function in maintaining an optimal microenvironment for the early spermatogenesis, especially self-renewal and differentiation of SSCs, in pre-pubertal sheep testis. Of these integrins, ITGA6 and ITGB1 have been identified as the main components of hemidesmosome, which is a special junction between SCs and ECM interfaces in the basement membrane and participates in coordinating the cellular events of spermiation and BTB restructuring during spermatogenesis via the apical ES–BTB–hemidesmosome functional axis (26). We, thus, speculate that a significant decrease in expression of ITGA6 and ITGB1, as well as their homologous genes in postpubertal sheep testes, may be mainly attributed to the disassembly of this junction and subsequent BTB restructuring, with the release of mature sperm into the lumen. In addition, the integrated analysis of miRNA–mRNA showed that the expression of ITGA6 and ITGB1 was potentially regulated by 52 and 40 known miRNAs, respectively, with elevated abundance in the T1Y group. The subsequent dual-luciferase reporter assay partially confirmed that both miR-29b and miR-1185-3p targeted ITGB1. Collectively, the results illustrate that these junction-related genes may facilitate the restructuring events involving extensive cell junctions in the seminiferous epithelium, as well as contributing to the immunological barrier function of the BTB. PIN1, one of the three known prolyl-isomerase types, was reported to play a key role in adult mice spermatogenesis. The genetic deletion of PIN1 may lead to testicular atrophy and a consequent reduction in fertility (31). Recent studies showed that PIN1 participates in the maintenance of BTB function and integrity by regulating the expression of junction proteins between SCs: connexin43 (Cx43; gap junction) and N-cadherin (CDH2; adhesion junction), and its deficiency results in the destruction of BTB integrity (32, 33). In the present study, PIN1 was identified as having a significantly increased abundance in postpubertal testes, a finding suggestive of an active role for the PIN1 gene in BTB function during sheep spermatogenesis. Nevertheless, the specific mechanism requires further clarification via experiments.

In addition to BTB, active immunosuppression is another important feature of testicular immune privilege. TGFB1, a known immunosuppressive cytokine secreted mainly by SCs, is reportedly involved in maintaining testicular immune privilege by directly or indirectly suppressing immune cell activation (3, 34). In this study, a significantly increased TGFB1 was discovered in T1Y by RNA-seq and qPCR, suggesting a potential function of TGFB1 in immunosuppressive properties in postnatal sheep testes, notably postpubertal testes, as confirmed by previous studies. Additionally, we found that its three receptors (TGFBR1-3) showed significantly decreased expression in T1Y. For TGFBR2, Western blot also confirmed that its

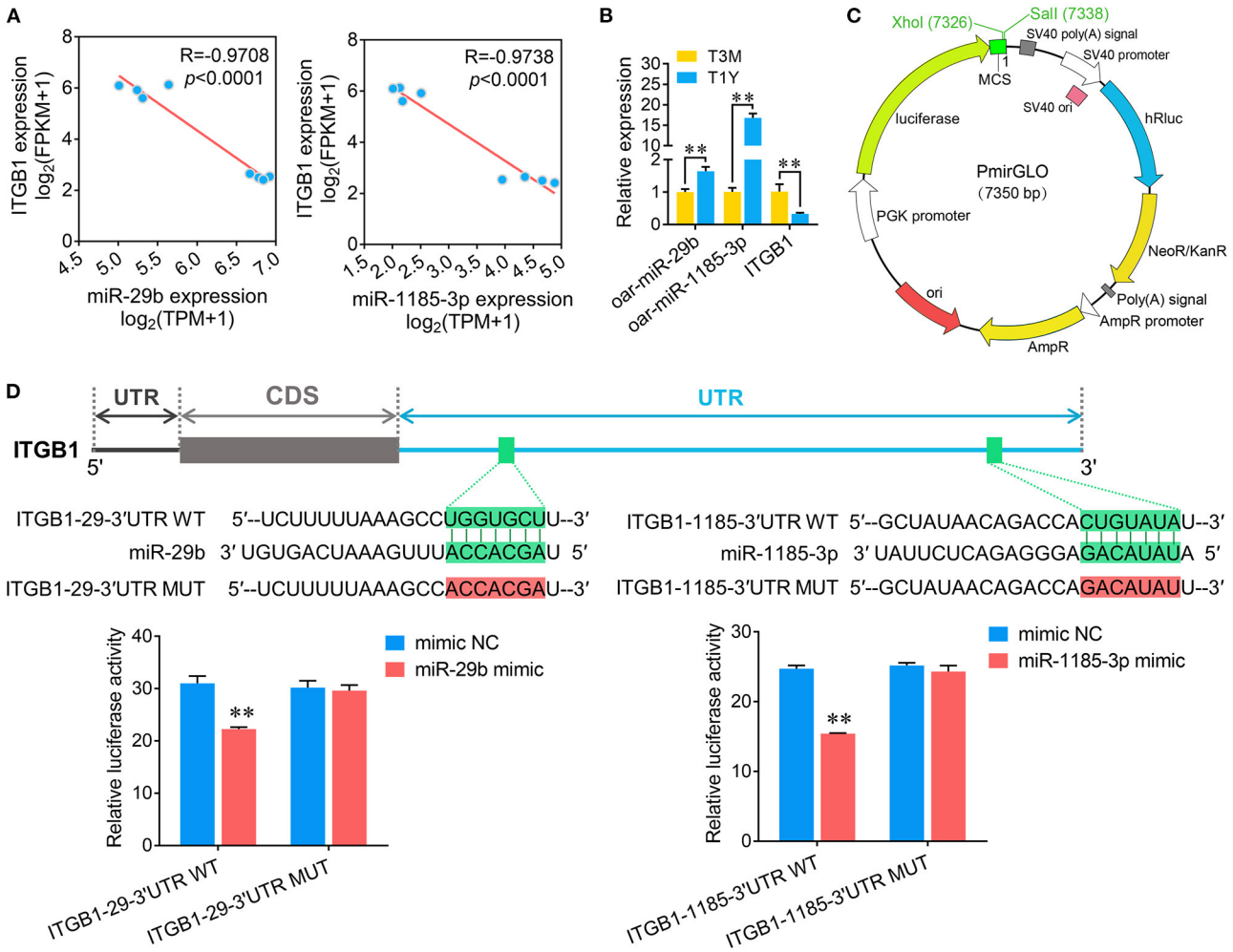

FIGURE 8 | Validation of targeted associations between either miR-29b or miR-1185-3p and ITGB1. **(A)** Pearson correlation assessment between oar-miR-29b/oar-miR-1185-3p and ITGB1 expression. **(B)** Quantitative real-time PCR (qPCR) detection for oar-miR-29b, oar-miR-1185-3p, and ITGB1 expression. **(C)** Schematic presentation of the pmirGLO dual-luciferase miRNA target expression vector used for constructing ITGB1-3′UTR. **(D)** A dual-luciferase reporter assay verified the interaction between miR-29b/miR-1185-3p and ITGB1. (Upper panel) The binding sites on ITGB1 3′-UTR and the seed region of miR-29b or miR-1185-3p. (Lower panel) Relative luciferase activity was measured by a dual-luciferase reporter assay. Data represent the mean ± SD. T3M, testes from 3-month-old sheep; T1Y, testes from 1-year-old sheep. $^{**}P < 0.01$.

protein abundance was significantly reduced. The subsequent immunofluorescence analysis showed high levels of TGFBR2 protein in interstitial cells in T3M and T1Y, as well as moderate expression in gonocytes and spermatogonia of T3M, and spermatogonia, spermatocytes, and spermatids of T1Y. Similarly, TGFBR2 has been expressed in spermatogonia, spermatocytes, and spermatids in human testis (35). In murine testes, TGFBR2 has been reported to exist in gonocytes and Leydig cells during fetal development (36). A previous study demonstrated that TGFBR2 expression in epididymal DCs is crucial for immunotolerance to sperm in mice epididymis, the absence of which exhibits an immune response against sperm resulting in severe epididymal leukocytosis (37). Considering these previous findings, we speculate that TGFBR2 in sheep testes may be implicated in maintaining testicular immune homeostasis, along with being involved in the regulation of the development of GCs. Moreover, our results showed that TGFB1 and its two receptors TGFBR2 and TGFBR3, are predicted to be targeted by 10, 23, and 113 putative DE miRNAs, respectively, in which TGFBR2 and TGFBR3 are coregulated by miR-15-5p and miR-7050-5p.

As macrophages are the largest immune cell population in testes, their importance for testicular immune privilege is reflected by their tolerance to the autoantigenic germ cells and the local innate immune responses against microbial infections (38). In our study, we identified CD68, a macrophage marker, expressed in Tibetan sheep testes and significantly decreased in T1Y. This indicates that macrophages also exist in sheep testes and shows a possible decrease in cell number in postpubertal testes. Accumulated evidence suggests that

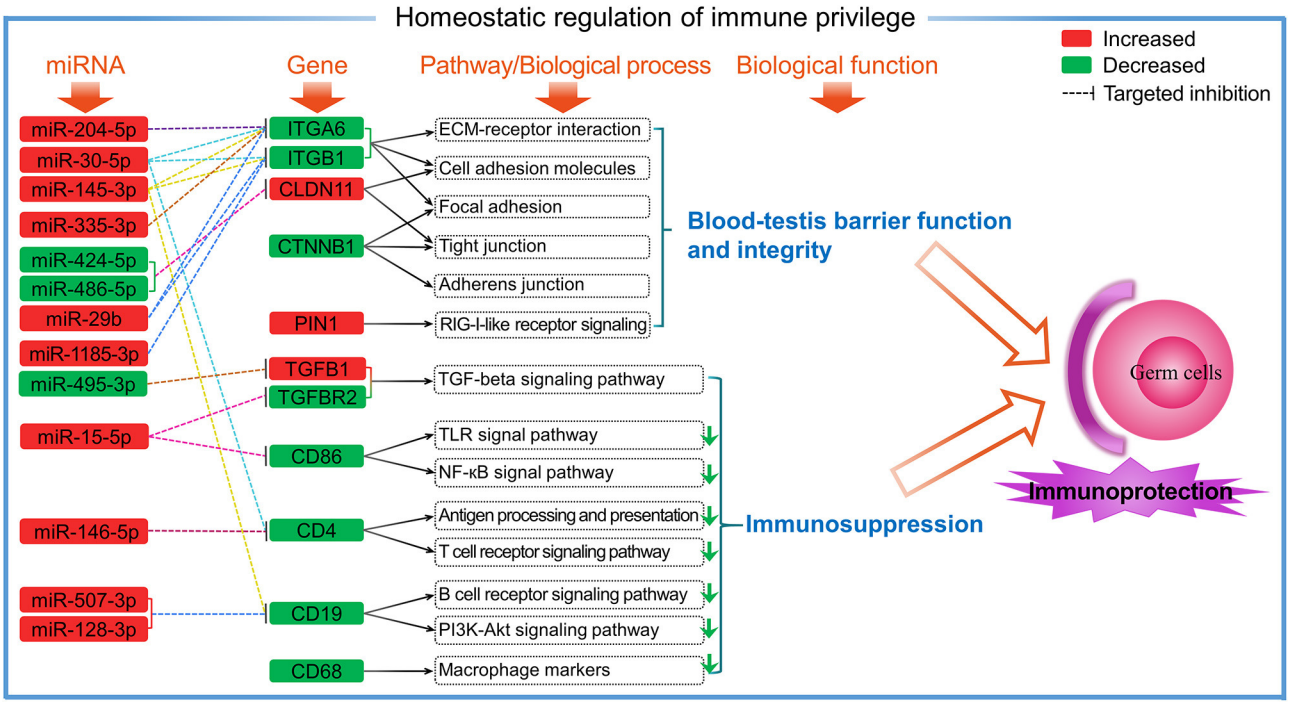

FIGURE 9 | A proposed putative model showing the involvement of DE genes and miRNAs in testicular immune homeostasis through related pathways.

testicular macrophages can secrete high anti-inflammatory cytokines and express low levels of TLR signaling pathway genes, along with simultaneous inhibition of pro-inflammatory signaling pathways, such as the NF-κB pathway (39). Similarly, our results showed that 48 (e.g., TRAF6, IRAK1, IRF3, TLR4, and TLR7) and 47 DE genes (e.g., IKBKBC, CCL19, CCL21, and NFKB1) were significantly enriched in TLR and NF-κB signaling pathway, respectively. Among these genes, the vast majority were expressed at low levels (FPKM $<$ 10) in testes at two age groups and exhibited a reduced expression in the T1Y group. By miRNA–mRNA integrated analysis, miR-146-5p was potentially targeted to six genes involved in the TLR or NF-κB pathway (TLR7, LTBR, MAP2K4, PRKCB, RIPK1, and Zap70). Fifty-one target genes potentially regulated by miR-146-5p participated in biological processes or pathways with immune responses as well, such as adaptive immune responses, leukocyte transendothelial migration, antigen processing and presentation, and the TCR signaling pathway. The miR-146 family has been widely reported to have a role in maintaining immune tolerance, including pregnancy tolerance and sperm-borne immunomodulation (16). Also, miR-146 is involved in regulating the functional tolerance of immune cell subtypes, including T cells, DCs, and macrophages (16). For example, miR-146 inhibits the maturation of DCs by reducing the expression of its surface markers. In normal testes, DCs are phenotypically immature and immunologically tolerogenic (34). Consistent with these findings, in our study, a decreased CD86 gene (a surface marker for mature DCs; FPKM $<$ 2.5) with lower abundance was identified, suggesting that DCs exist in normal sheep testis in an inactive immature state.

It has been reported that immature DCs can suppress the activation and proliferation of T cells that allow spermatogenic cells to avoid being directly recognized by the activated T cells (34). In this study, we found low CD4 expression (FPKM $<$ 3.5 per independent sample) in both T3M and T1Y, and was decreased in T1Y. These findings suggest that the number of CD4+ T cells is kept at a very low level as well as in a quiescent state in normal sheep testes, especially in postpubertal testes, thereby preventing the potential DC-induced antigen-specific immune response. Furthermore, the present study showed that the mRNA expression and protein abundance of CD19 significantly decreased in T1Y compared with T3M. By using immunofluorescence, weak CD19 protein signals were found in interstitial cells in T3M. Interestingly, CD19 protein signals were also observed in vascular endothelium in T3M and SCs and the basement membrane in T3M and T1Y. CD19 is a known B-cell marker, but its expression is not limited to B cells, as demonstrated by the expression of CD19 in human SSCs and granulosa cells (39). Considering that CD19 is also found in the main components of BTB (SCs, basement membrane, and vascular endothelium) suggests a possible role of CD19 in the maintenance of BTB function and immune homeostasis in sheep testes. Still, the detailed mechanisms remain to be further verified. Based on the current results, a hypothetical model is proposed to reveal the potential roles of DE genes and miRNAs in the homeostatic regulation of immune privilege in sheep testes (**Figure 9**).

CONCLUSION

To the best of our knowledge, this is the first systematic report investigating the expression patterns of miRNAs and target mRNAs related to immunity in developmental testes of sheep. Here, most of the miRNAs exhibited increased abundance, whereas most genes enriched in immune-related pathways/biological processes showed decreased abundance in postpubertal testis compared with prepubertal testis. CD19 and TGFBR2 were revealed to both exhibit reduced mRNA and protein expression. The CD19 protein was localized mainly on prepubertal testicular vascular endothelium and throughout developmental Sertoli cells and the basement membrane, whereas the TGFBR2 protein was localized primarily in interstitial cells and germ cells throughout development. Integrated analysis of miRNAs and mRNAs demonstrate that these genes, most of which may be regulated by miRNAs, participate in the homeostatic regulation of testicular immune privilege both through maintenance of the blood–testis barrier and through inhibition of the immune response and interstitial immune cell activity. Furthermore, oar-miR-29b and miR-1185-3p were confirmed to directly interact with ITGB1. These findings provide further insights into the mechanism underlying testicular immune privilege in sheep and other mammals.

DATA AVAILABILITY STATEMENT

The datasets presented in this study can be found in online repositories. The names of the repository/repositories and accession number(s) can be found in the article/**Supplementary Material**.

ETHICS STATEMENT

The animal study was reviewed and approved by Laboratory Animal Welfare and Ethics Committee of Gansu Agricultural University.

AUTHOR CONTRIBUTIONS

TL and YM conceived and designed the study. XW, RL, and XA collected the samples. TL, XW, and RL performed the experiments and analyzed the data. TL wrote the paper. YZ, XZ, and YM contributed to revisions of the manuscript. All authors read and approved the manuscript.

FUNDING

This research work was supported by the National Natural Science Foundation of China (31960662), the Fostering Foundation for the Excellent Ph.D. Dissertation of Gansu Agricultural University (YB2018001), and the National Key R&D Program of China (2018YFD0502100).

ACKNOWLEDGMENTS

We thank the Guangzhou Genedenovo Biotechnology Co., Ltd. for assisting in RNA sequencing.

SUPPLEMENTARY MATERIAL

The Supplementary Material for this article can be found online at: https://www.frontiersin.org/articles/10.3389/fvets.2021.647153/full#supplementary-material

REFERENCES

1. Wang X, Li T, Liu N, Zhang H, Zhao X, Ma Y. Characterization of GLOD4 in Leydig cells of Tibetan sheep during different stages of maturity. *Genes.* (2019) 10:796. doi: 10.3390/genes10100796
2. Jing X, Wang W, Degen A, Guo Y, Kang J, Liu P, et al. Tibetan sheep have a high capacity to absorb and to regulate metabolism of SCFA in the rumen epithelium to adapt to low energy intake. *Br J Nutr.* (2020) 123:721736. doi: 10.1017/S0007114519003222
3. Zhao S, Zhu W, Xue S, Han D. Testicular defense systems: immune privilege and innate immunity. *Cell Mol Immunol.* (2014) 11:428–37. doi: 10.1038/cmi.2014.38
4. Meng J, Greenlee A, Taub C, Braun R. Sertoli cell-specific deletion of the androgen receptor compromises testicular immune privilege in mice. *Biol Reprod.* (2011) 85:254–60. doi: 10.1095/biolreprod.110.090621
5. Smith B, Braun R. Germ cell migration across Sertoli cell tight junctions. *Science.* (2012) 338:798–802. doi: 10.1126/science.1219969
6. Meinhardt A, Hedger M. Immunological, paracrine and endocrine aspects of testicular immune privilege. *Mol Cell Endocrinol.* (2011) 335:60–8. doi: 10.1016/j.mce.2010.03.022
7. Rokade S, Madan T. Testicular expression of SP-A, SP-D and MBL-A is positively regulated by testosterone and modulated by lipopolysaccharide. *Immunobiology.* (2016) 221:975–85. doi: 10.1016/j.imbio.2016.05.005
8. Kaur G, Thompson L, Dufour J. Sertoli cells-immunological sentinels of spermatogenesis. *Semin Cell Dev Biol.* (2014) 30:36–44. doi: 10.1016/j.semcdb.2014.02.011
9. Pérez C, Theas M, Jacobo P, Jarazo-Dietrich S, Guazzone V, Lustig L. Dual role of immune cells in the testis: protective or pathogenic for germ cells? *Spermatogenesis.* (2013) 3:e23870. doi: 10.4161/spmg.23870
10. Qu N, Itoh M, Sakabe K. Effects of chemotherapy and radiotherapy on spermatogenesis: the role of testicular immunology. *Int J Mol Sci.* (2019) 20:957. doi: 10.3390/ijms20040957
11. Mital P, Hinton B, Dufour J. The blood-testis and blood-epididymis barriers are more than just their tight junctions. *Biol Reprod.* (2011) 84:851–8. doi: 10.1095/biolreprod.110.087452
12. Qu N, Ogawa Y, Kuramasu M, Nagahori K, Sakabe K, Itoh M. Immunological microenvironment in the testis. *Reprod Med Biol.* (2020) 19:24–31. doi: 10.1002/rmb2.12293
13. Reza A, Choi Y, Han S, Song H, Park C, Hong K, et al. Roles of microRNAs in mammalian reproduction: from the commitment of germ cells to peri-implantation embryos. *Biol Rev Camb Philos Soc.* (2019) 94:415–38. doi: 10.1111/brv.12459
14. Bronevetsky Y, Ansel K. Regulation of miRNA biogenesis and turnover in the immune system. *Immunol Rev.* (2013) 253:304–16. doi: 10.1111/imr.12059
15. Schjenken J, Zhang B, Chan H, Sharkey D, Fullston T, Robertson S. miRNA regulation of immune tolerance in early pregnancy. *Am J Reprod Immunol.* (2016) 75:272–80. doi: 10.1111/aji.12490
16. Robertson S, Zhang B, Chan H, Sharkey D, Barry S, Fullston T, et al. MicroRNA regulation of immune events at conception. *Mol Reprod Dev.* (2017) 84:914–25. doi: 10.1002/mrd.22823

17. Parker M, Palladino M. MicroRNAs downregulated following immune activation of rat testis. *Am J Reprod Immunol.* (2017) 77:e12673. doi: 10.1111/aji.12673
18. Zhang Q, Wang Q, Zhang Y, Cheng S, Hu J, Ma Y, et al. Comprehensive analysis of microrna-messenger RNA from white yak testis reveals the differentially expressed molecules involved in development and reproduction. *Int J Mol Sci.* (2018) 19:3083. doi: 10.3390/ijms19103083
19. Bai M, Sun L, Jia C, Li J, Han Y, Liu H, et al. Integrated analysis of miRNA and mRNA expression profiles reveals functional miRNA-Targets in development testes of Small Tail Han Sheep. *G3.* (2019) 9:523–33. doi: 10.1534/g3.118.200947
20. Ye C, Rasheed H, Ran Y, Yang X, Xing L, Su X. Transcriptome changes reveal the genetic mechanisms of the reproductive plasticity of workers in lower termites. *BMC Genomics.* (2019) 20:702. doi: 10.1186/s12864-019-6037-y
21. Kim D, Pertea G, Trapnell C, Pimentel H, Kelley R, Salzberg S. TopHat2: accurate alignment of transcriptomes in the presence of insertions, deletions and gene fusions. *Genome Biol.* (2013) 14:R36. doi: 10.1186/gb-2013-14-4-r36
22. Li B, Dewey C. RSEM: accurate transcript quantification from RNA-Seq data with or without a reference genome. *BMC Bioinformatics.* (2011) 12:323. doi: 10.1186/1471-2105-12-323
23. Trapnell C, Roberts A, Goff L, Pertea G, Kim D, Kelley D, et al. Differential gene and transcript expression analysis of RNA-seq experiments with TopHat and Cufflinks. *Nat Protoc.* (2012) 7:562–78. doi: 10.1038/nprot.2012.016
24. Livak KJ, Schmittgen TD. Analysis of relative gene expression data using real-time quantitative PCR and the $2^{-\Delta\Delta CT}$ method. *Methods.* (2001) 25:402–8. doi: 10.1006/meth.2001.1262
25. Li T, Zhang H, Wang X, Yin E, Chen N, Kang L, et al. Cloning, molecular characterization and expression patterns of DMRTC2 implicated in germ cell development of male Tibetan sheep. *Int J Mol Sci.* (2020) 21:2448. doi: 10.3390/ijms21072448
26. Yan H, Mruk D, Wong E, Lee W, Cheng C. An autocrine axis in the testis that coordinates spermiation and blood-testis barrier restructuring during spermatogenesis. *Proc Natl Acad Sci USA.* (2008) 105:8950–5. doi: 10.1073/pnas.0711264105
27. Mruk D, Cheng C. The mammalian blood-testis barrier: its biology and regulation. *Endocr Rev.* (2015) 36:564591. doi: 10.1210/er.2014-1101
28. Cheng C, Mruk D. A local autocrine axis in the testes that regulates spermatogenesis. *Nat Rev Endocrinol.* (2010) 6:380–95. doi: 10.1038/nrendo.2010.71
29. Gow A, Southwood C, Li J, Pariali M, Riordan G, Brodie S, et al. CNS myelin and sertoli cell tight junction strands are absent in Osp/claudin-11 null mice. *Cell.* (1999) 99:649–59. doi: 10.1016/S0092-8674(00)81553-6
30. Chen S, Lewallen M, Xie T. Adhesion in the stem cell niche: biological roles and regulation. *Development.* (2013) 140:255–65. doi: 10.1242/dev.083139
31. Liou Y, Ryo A, Huang H, Lu P, Bronson R, Fujimori F, et al. Loss of Pin1 function in the mouse causes phenotypes resembling cyclin D1-null phenotypes. *Proc Natl Acad Sci USA.* (2002) 99:1335–40. doi: 10.1073/pnas.032404099
32. Islam R, Yoon H, Kim B, Bae H, Shin H, Kim W, et al. Blood-testis barrier integrity depends on Pin1 expression in Sertoli cells. *Sci Rep.* (2017) 7:6977. doi: 10.1038/s41598-017-07229-1
33. Kim W, Kim B, Kim H, Cho Y, Shin H, Yoon H, et al. Intratesticular peptidyl prolyl isomerase 1 protein delivery using cationic lipid-coated fibroin nanoparticle complexes rescues male infertility in mice. *ACS Nano.* (2020) 14:13217–31. doi: 10.1021/acsnano.0c04936
34. Gao J, Wang X, Wang Y, Han F, Cai W, Zhao B, et al. Murine Sertoli cells promote the development of tolerogenic dendritic cells: a pivotal role of galectin-1. *Immunology.* (2016) 148:253–65. doi: 10.1111/imm.12598
35. Zhang Y, He X, Zhang J, Wang R, Zhou J, Xu R. Stage-specific localization of transforming growth factor beta1 and beta3 and their receptors during spermatogenesis in men. *Asian J Androl.* (2004) 6:105–9.
36. Moreno S, Attali M, Allemand I, Messiaen S, Fouchet P, Coffigny H, et al. TGFbeta signaling in male germ cells regulates gonocyte quiescence and fertility in mice. *Dev Biol.* (2010) 342:74–84. doi: 10.1016/j.ydbio.2010.03.007
37. Pierucci-Alves F, Midura-Kiela M, Fleming S, Schultz B, Kiela P. Transforming growth factor beta signaling in dendritic cells is required for immunotolerance to sperm in the epididymis. *Front Immunol.* (2018) 9:1882. doi: 10.3389/fimmu.2018.01882
38. Bhushan S, Meinhardt A. The macrophages in testis function. *J Reprod Immunol.* (2017) 119:107–12. doi: 10.1016/j.jri.2016.06.008
39. Maleki M, Ghanbarvand F, Reza Behvarz M, Ejtemaei M, Ghadirkhomi E. Comparison of mesenchymal stem cell markers in multiple human adult stem cells. *Int J Stem Cells.* (2014) 7:118–26. doi: 10.15283/ijsc.2014.7.2.118

Conflict of Interest: The authors declare that the research was conducted in the absence of any commercial or financial relationships that could be construed as a potential conflict of interest.

frontiers in Veterinary Science

ORIGINAL RESEARCH
published: 16 August 2021
doi: 10.3389/fvets.2021.650687

Inhibition of the C-X-C Motif Chemokine 12 (CXCL12) and Its Receptor CXCR4 Reduces Utero-Placental Expression of the VEGF System and Increases Utero-Placental Autophagy

Ryan L. Ashley, Cheyenne L. Runyan†, Marlie M. Maestas, Elisa Trigo and Gail Silver*

Department of Animal and Range Sciences, New Mexico State University, Las Cruces, NM, United States

OPEN ACCESS

Edited by:
Fuller Warren Bazer, Texas A&M University, United States

Reviewed by:
Bouchra El Amiri, Institut National de la Recherche Agronomique de Settat, Morocco
Lawrence P. Reynolds, North Dakota State University, United States

***Correspondence:**
Ryan L. Ashley
ryashley@nmsu.edu

†Present address:
Cheyenne L. Runyan, Department of Animal Science and Veterinary Technology, Tarleton State University, Stephenville, TX, United States

Specialty section:
This article was submitted to Animal Reproduction-Theriogenology, a section of the journal Frontiers in Veterinary Science

Received: *07 January 2021*
Accepted: *15 July 2021*
Published: *16 August 2021*

Citation:
Ashley RL, Runyan CL, Maestas MM, Trigo E and Silver G (2021) Inhibition of the C-X-C Motif Chemokine 12 (CXCL12) and Its Receptor CXCR4 Reduces Utero-Placental Expression of the VEGF System and Increases Utero-Placental Autophagy. Front. Vet. Sci. 8:650687. doi: 10.3389/fvets.2021.650687

The placenta, a unique organ that only develops during pregnancy, is essential for nutrient, oxygen, and waste exchange between offspring and mother. Yet, despite its importance, the placenta remains one of the least understood organs and knowledge of early placental formation is particularly limited. Abnormalities in placental development result in placental dysfunction or insufficiency whereby normal placental physiology is impaired. Placental dysfunction is a frequent source of pregnancy loss in livestock, inflicting serious economic impact to producers. Though the underlying causes of placental dysfunction are not well-characterized, initiation of disease is thought to occur during establishment of functional fetal and placental circulation. A comprehensive understanding of the mechanisms controlling placental growth and vascularization is necessary to improve reproductive success in livestock. We propose chemokine C-X-C motif ligand 12 (CXCL12) signaling through its receptor CXCR4 functions as a chief coordinator of vascularization through direct actions on fetal trophoblast and maternal endometrial and immune cells. To investigate CXCL12–CXCR4 signaling on uteroplacental vascular remodeling at the fetal–maternal interface, we utilized a CXCR4 antagonist (AMD3100). On day 12 post-breeding in sheep, osmotic pumps were surgically installed and delivered either AMD3100 or saline into the uterine lumen ipsilateral to the corpus luteum for 14 days. On day 35 of ovine pregnancy, fetal/placental and endometrial tissues were collected, snap-frozen in liquid nitrogen, and uterine horn cross sections were preserved for immunofluorescent analysis. Suppressing CXCL12–CXCR4 at the fetal–maternal interface during initial placental vascularization resulted in diminished abundance of select angiogenic factors in fetal and maternal placenta on day 35. Compared to control, less vascular endothelial growth factor (VEGF) and VEFG receptor 2 (KDR) were observed in endometrium when CXCL12–CXCR4 was diminished. Less VEGF was also evident in fetal placenta (cotyledons) in ewes receiving AMD3100 infusion compared to control. Suppressing CXCL12–CXCR4 at the fetal–maternal interface also resulted in greater autophagy induction in fetal and maternal

placenta compared to control, suggestive of CXCL12–CXCR4 impacting cell survival. CXCL12–CXCR4 signaling may govern placental homeostasis by serving as a critical upstream mediator of vascularization and cell viability, thereby ensuring appropriate placental development.

Keywords: CXCL12, CXCR4, CXCR7, angiogenesis, placenta, MAPK, fetal/maternal crosstalk, autophagy

INTRODUCTION

Reproductive losses due to embryonic and fetal deaths result in crucial economic constraints to livestock and dairy production systems and also manifest in loss of genetically important animals. Many pregnancy losses occur due to complications that arise when the embryo attaches to maternal endometrium (implantation) and subsequent formation of the placenta (placentation). The placenta, a unique organ that only develops during pregnancy, is essential for nutrient, oxygen, and waste exchange between offspring and mother. Abnormalities in placental development result in placental dysfunction or insufficiency whereby normal placental physiology is impaired. Placental insufficiency is a frequent source of pregnancy loss in livestock, inflicting serious economic impact to producers (1, 2), but the underlying causes of impaired placental function are not well-characterized. Placental dysfunction is at the root of numerous pregnancy complications such as pre-eclampsia and intrauterine growth restriction (IUGR). These pregnancy complications are the leading cause of maternal, fetal, and neonatal morbidity and mortality worldwide in humans. Impaired placental function pre-disposes offspring to cardiovascular disease, type 2 diabetes, insulin resistance, obesity, hypertension, and stroke during adulthood (3–8). Though less studied in livestock, these same health problems occur in farm animals, negatively affecting livestock production (9). A comprehensive understanding of the mechanisms controlling placental growth and vascularization are necessary to improve reproductive success in livestock and dairy systems.

Despite its importance, the placenta remains one of the least understood organs and knowledge of early placental formation is particularly limited. Placental development requires intricately coordinated communication between fetal trophoblast and maternal endometrial and immune cells at the fetal–maternal interface during a defined window early in gestation. Numerous factors including chemokines, cytokines, and growth factors contribute to the dialog at the fetal–maternal interface to direct placental development (10, 11). Among these, the unique chemokine network, more known for immune system-specific functions, has emerged as a critical player in regulating implantation and placentation. Chemokines constitute a family of small (8–14 kDa) structurally similar peptides that elicit actions by binding and activating various G protein-coupled receptors. Chemokine ligand 12 (CXCL12) also known as stromal cell-derived factor (SDF-1) is involved in several processes that are also central to placentation including stimulation of cell proliferation and migration, vascularization, immune cell recruitment, and cytokine production through direct actions on fetal trophoblast and maternal endometrial and immune cells (12). As CXCL12 acts directly upon fetal trophoblast and maternal endometrial and immune cells, all of which coordinate placentation, it has great potential to generate a supportive placental microenvironment, thereby directing placental formation. However, the precise roles that CXCL12 plays in livestock placental development are limited.

Using an *in vivo* sheep model in combination with *in vitro* methods, we have gained insight into CXCL12-induced actions during conceptus attachment and initial placentation. Suppressing CXCL12/CXCR4 signaling during the small window of conceptus implantation diminishes placental vascularization, induces autophagy, and dampens the inflammatory placental environment (13–16). Moreover, we recently published evidence demonstrating that suppressing CXCL12-induced actions at the fetal–maternal interface reduces trophoblast invasion into maternal endometrium and delays uterine remodeling (13). Notably, several observed outcomes in our studies mirror those of placental dysfunction, suggesting that an imbalance in CXCL12-mediated signaling may be causative. Building on these studies, we hypothesized that the reduced vascularization, diminished trophoblast invasion, and altered uterine receptivity observed upon suppressing CXCL12–CXCR4 during attachment would manifest in compromised placentation later in gestation. To test, we investigated impact to placental vascularization, cell survival, and relevant signaling pathways in the placenta on d35 of gestation after suppressing CXCL12–CXCR4 signaling at the fetal–maternal during implantation. Day 35 of pregnancy was selected to represent a time when the conceptus should be firmly attached, and uteroplacental vascular remodeling is rampant (17–19). We suggest that CXCL12 signaling through its receptor CXCR4 functions as a chief coordinator of placentation through direct actions on fetal trophoblast and maternal endometrial cells. The goal is to increase understanding of CXCL12-induced actions on controlling placental growth and vascularization to improve reproductive success and fetal health in livestock and dairy production systems.

MATERIALS AND METHODS

Animals

All procedures involving animals were conducted with approval by the New Mexico State University Institutional Animal Care and Use Committee. Fifteen Western white face ewes (primarily Rambouillet, Targhee, and Columbia), similar in age (3–5 years) and weight, received intravaginal controlled internal drug release (CIDR) inserts for 5 days to synchronize estrus, and upon removal, two injections of dinoprost tromethamine (5 mg intramuscular; Lutalyse; Pfizer, New York, NY) were

administered 4 h apart (14). Ewes were mated by a fertile ram and randomly placed into experimental groups of either control (PBS; $n = 7$) or treatment (CXCR4 inhibitor; AMD3100; $n = 8$). On day 12 of gestation, ewes were anesthetized (5 mg xylazine and 100 mg ketamine, 1 ml intravenous) and maintained on isoflurane. Mini-osmotic pumps developed for 14-day delivery (2 ml reservoir volume and pumping rate of 5 μl/h; Alzet 2ML1, Cupertino, CA, USA) were pre-loaded with AMD3100 (2,060 ng; Selleckchem, Houston, TX, USA) or PBS. The AMD3100 dose is based on the pharmacokinetic profiling of AMD3100 and median values reported in circulation (20). The catheter attached to the pump was inserted into the lumen of the uterus ipsilateral to the corpus luteum, thus dispensing treatments into the uterine lumen. The pump and catheter were anchored to the uterus with cyanoacrylate glue (super glue, Ontario, CA) and secured with suture (MWI Vet Supply, Boise, ID. USA).

Tissue Collections

On day 35 of gestation, ewes were anesthetized with sodium pentobarbital (20 mg/kg, intravenous) and reproductive tract was removed using a mid-ventral laparotomy. Endometrial (caruncle and intercaruncle) and cotyledon tissues were collected, snap-frozen in liquid nitrogen, and stored at −80°C for subsequent protein isolation. Using a sterile razor blade, frontal sections (0.5 cm thick) of the ipsilateral uterine horn were also collected and immersed in 4% paraformaldehyde for 24 h. Uterine horn cross sections were embedded in paraffin, sectioned at 5 μm, and mounted onto glass slides using standard procedures (AML Laboratories). Ewes that did not have fetal membrane or embryos present at time of tissue collection were designated as non-pregnant. Ewes were euthanized by exsanguination while under anesthesia.

Protein Isolation and Immunoblot

Protein was isolated from endometrial and cotyledon tissues of all pregnant ewes by homogenizing 100 mg of tissue in 1 ml of RIPA buffer supplemented with phosphatase and protease inhibitor tablets. Protein samples were placed on ice for 15 min and centrifuged at 12,000 × g for 10 min at 4°C before supernatant was removed and lysates were stored at −80°C until further analysis. Protein lysate concentrations were quantified using BCA protein assay (Thermo Fisher Scientific). Equal amounts of protein lysate were separated using SDS-PAGE followed by transfer to methanol-activated polyvinyl difluoride (PVDF) membranes for immunoblotting. All washes and dilutions were made in TBS supplemented with 0.10% TWEEN 20, unless otherwise noted. Membranes were blocked in either 5% non-fat milk or 5% BSA for 1 h at room temperature, followed by incubation with primary antibody diluted in either 5% non-fat milk or 5% BSA overnight at 4°C. Antibody specifications are as follows: vascular endothelial growth factor (VEGF; 1:500; sc-152; Santa Cruz Biotechnology), C-X-C chemokine receptor type 7 (CXCR7; 1:500; NBP2024779, Novus Biologicals), kinase insert domain receptor/VEGF Receptor 2 (KDR; 1:1,000; NB100-627, Novus Biologicals), microtubule-associated proteins 1A/1B light chain 3B (LC3B-II; 1:1000; PA1-46286; Thermo Fisher Scientific), phosphorylated extracellular signal-regulated kinase 1/2 (pERK; 1:1,000, sc93, Santa Cruz Biotechnology), extracellular signal-regulated kinase 1/2 (ERK; 1:1,000; sc7383; Santa Cruz Biotechnology), phosphorylated c-Jun N-terminal Kinase (pJNK; 1:1,000; cst 9252; Cell Signaling Technology), c-Jun N-terminal Kinase (JNK; 1:1,000; cst 9251; Cell Signaling Technology), phosphorylated p38 MAP kinase (p-p38; 1:1,000; cst 4511; Cell Signaling Technology), and p38 MAP kinase (p38; 1:1,000; cst 9212; Cell Signaling Technology). After three 10-min washes, membranes were incubated with appropriate horseradish peroxidase (HRP)-conjugated secondary antibody at room temperature for 1 h, followed by two final 10-min washes and subsequent incubation with chemiluminescent HRP substrate (34076; Thermo Fisher Scientific). Proteins of interest were visualized using the ChemiDoc XRS System and Image Lab Software (version 3, Bio-Rad Laboratories), and optical densitometry values of each band were recorded. Equal loading of all protein samples was validated using an antibody specific to glyceraldehyde phosphate dehydrogenase (GAPDH).

Immunofluorescence

Paraffin-embedded tissues were sectioned at 5 μm, mounted onto glass slides, and de-paraffinized using a histologic clearing agent (Histo-clear, National Diagnostics, Atlanta, GA) followed by a series of rehydration ethanol washes (100, 95, 70, and 50% ethanol, respectively). Antigen retrieval was performed by boiling samples in 10 mM sodium citrate buffer, pH 6, in a microwave for 10 min, and each slide was rinsed twice in TBS with 0.025% Triton X-100. To prevent non-specific binding of antibodies, each slide was treated for 1 h with blocking buffer (TBS + 1% BSA + 10% normal goat serum). Tissue sections were incubated with a specific primary antibody specific to von Willebrand factor (vWF; cat no. ab6994; Abcam). Slides were rinsed 2 × 5 min in TBS-T and incubated for 1 h at room temperature with Alexa 568-labeled goat anti-rabbit secondary antibody. Each slide was mounted with Fluoromount (Sigma-Aldrich) with 4,6-diamidion-2-phenylindole (Life Technologies, Grand Island, NY) to counterstain nuclei. Control sections were incubated with dilution buffer (TBS + 1% BSA).

Microscopy Image Analysis

For each tissue section, photomicrographs were taken at 10× at the same exposure time with Zeiss Axio Scope and AxioCam MRm camera for immunofluorescence (Carl Zeiss Microscopy, LLC, Thornwood, NY). Using this method, we obtained images of placental and gravid uterus vasculature that can be quantified. Blood vessel abundance was analyzed as previously described (21). Each level was scanned for blood vessels and imaged. Within each level, endothelial cell marker, vWF expression, blood vessel number, and blood vessel circumference were analyzed.

Statistical Analysis

Significant differences in immunoblot data were determined by performing an unpaired, two-tailed Student's *t*-test analysis using Prism (version 9, GraphPad Software, Inc.). Chemiluminescent signals for Western blots were quantified using the Image Lab software program; the mean intensity value was obtained for each band of interest and normalized by dividing that of the

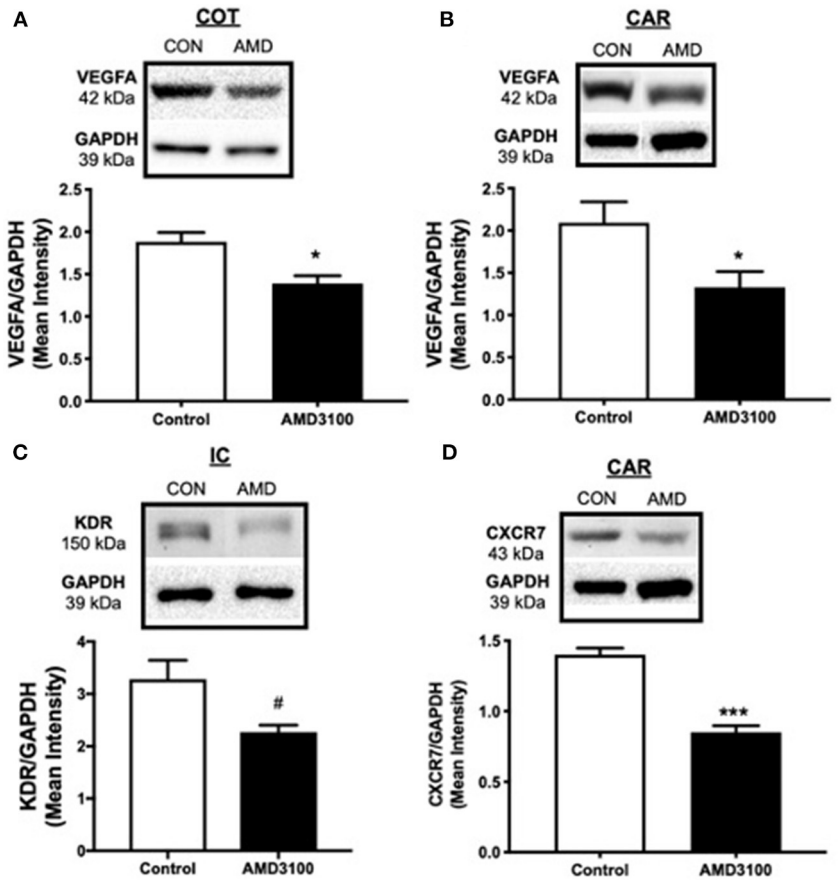

FIGURE 1 | Impact to placental vascularization after suppressing the CXCL12–CXCR4 network. Protein abundance and representative immunoblots of VEGFA in ovine fetal cotyledon (COT) placenta **(A)** and maternal caruncle (CAR) placenta **(B)**, the VEGFA receptor KDR in intercaruncle (IC) tissue **(C)**, and CXCR7 in caruncle placenta **(D)** following intrauterine saline (CON) or AMD3100 (AMD) infusion. Data are presented as the mean ± SEM, and significance is denoted with an asterisk (*) when $p < 0.05$, or (***) when $p < 0.0001$. $^{\#}p = 0.08$.

corresponding band for GAPDH. Immunofluorescent signals from uterine cross sections were quantified using the ImageJ software program; the mean integrated density values were obtained and averaged. Tissue autofluorescence was accounted for by measuring the integrated density of the background, averaging the values from each image, and subtracting from the average integrated density of that animal. Values were quantified using ImageJ, and the average integrated density value, area circumference, and blood vessel number were analyzed using the unpaired Student's *t*-test.

RESULTS

To evaluate placental vascularization on day 35 of gestation, angiogenic and growth factors central to placentation were assayed using Western blot. Fibroblast growth factor 2 (FGF2), VEGFA, VEGFB, angiopoietin 1 (ANG1), KDR, fms-like tyrosine kinase-1 (FLT1/VEGFR1), Hypoxia inducible factor alpha (HIF1A), CXCL12, CXCR4, and CXCR7 were detected in cotyledon and caruncle placental tissue on day 35 of gestation but only significant changes in protein amounts are included. Suppressing CXCL12–CXCR4 signaling at the fetal–maternal interface from days 12 to 26 of gestation resulted in less angiogenic factors in the placenta on day 35, 9 days post-treatment (**Figure 1**). Using immunoblot analysis, protein abundance for VEGFA in both fetal cotyledon (COT) and maternal caruncle (CAR) placenta was diminished ($p < 0.05$) upon suppressing CXCR4 signaling during conceptus attachment (**Figures 1A,B**). Receptors for VEGF were also assayed and while levels of FLT1 were similar between control and AMD3100-treated ewes in fetal and maternal placenta (data not shown), quelling CXCL12–CXCR4 actions tended ($p < 0.1$) to reduce KDR amounts in intercaruncle (IC) tissue (**Figure 1C**). Protein expression for CXCR4 did not differ in placenta on day 35 regardless of treatments (data not shown), but protein abundance for the other CXCL12 receptor, CXCR7, was diminished in caruncle placenta when ewes received CXCR4 inhibitor in utero (**Figure 1D**).

To further determine if vascularization is impacted when CXCL12–CXCR4 signaling is suppressed at the fetal–maternal interface, the expression of vWF was assayed in the placenta

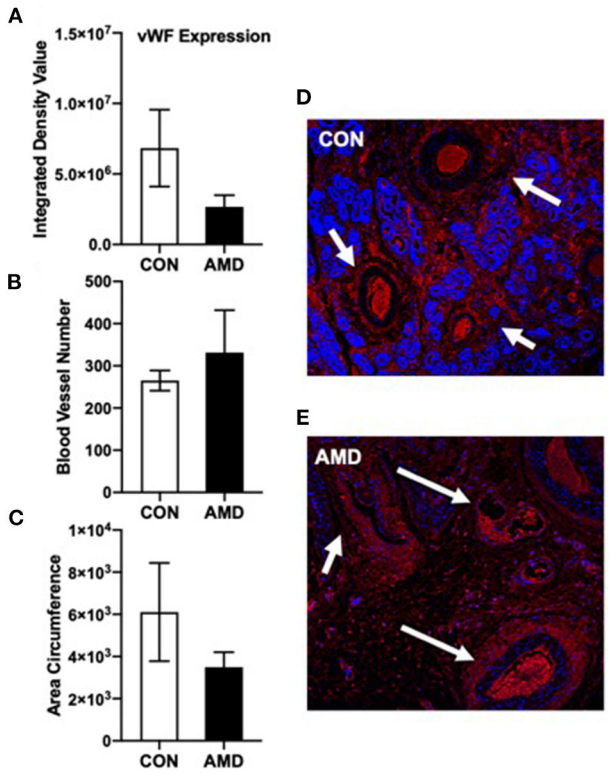

FIGURE 2 | Immunoreactive vWF cells (endothelial cell marker) in ovine uterine cross sections on day 35 of gestation. vWF red fluorescence expression **(A)** was similar ($p > 0.05$) and the number of blood vessels **(B)** and blood vessel circumference **(C)** did not change ($p > 0.05$) between CON and AMD. Representative 10× magnification (100 μm) images of vWF (red) with DAPI (blue) as nuclear stain in ovine uterine horn cross sections following intrauterine treatment with control (CON) phosphate buffer saline **(D)** or CXCR4 inhibitor (AMD) **(E)**. White arrows denote developing blood vessels.

using immunofluorescent imaging (**Figure 2**). Our objectives were to determine immunohistochemical expression of vWF and to evaluate blood vessel number (BVN) and blood vessel circumference (BVC) of the uterine horn on day 35 of gestation. Representative immunofluorescent images of vWF in uterine cross sections from control (CON) and AMD3100-treated (AMD) ewes are shown in **Figures 2D,E**, respectively. The expression of vWF was similar between control and AMD3100-treated ewes (**Figure 2A**). Similarly, the number of blood vessels (**Figure 2B**) and respective circumferences (**Figure 2C**) did not differ between control and AMD3100-treated ewes on day 35.

Induction of autophagy, a cell survival mechanism, was investigated by quantifying protein abundance for LC3B-II, a classic marker of autophagy induction using immunoblot. Compared to control ewes, greater amounts of LC3B-II were evident in both cotyledon (**Figure 3A**) and caruncle (**Figure 3B**) placenta from ewes receiving CXCR4 inhibitor during conceptus attachment and beginning stages of placental vascularization.

Compared to control ewes receiving saline, all three major MAPKs were altered in placenta 9 days after receiving CXCR4 inhibitor at the fetal–maternal interface (**Figure 4**). In COT placenta, suppressing CXCL12–CXCR4 resulted in a tendency ($p = 0.08$) for increased ERK activation compared to control as evidenced by the phosphorylated 42- and 44-kDa bands (**Figure 4A**). The pJNK signaling pathway, however, was diminished ($p < 0.05$) in COT placenta after suppressing CXCR4 at the fetal–maternal interface with less phosphorylated JNK at 46 and 54 kDa (**Figure 4B**). In maternal placenta (CAR), greater ($p < 0.05$) activation of the p38 pathway was evident after inhibiting CXCL12–CXCR4 during implantation and initial placentation (**Figure 4C**).

DISCUSSION

Embryonic and fetal survival is a major factor affecting production and economic efficiency in livestock meat and milk production (22–25) with the majority of losses occurring during implantation and initial placental vascularization (23, 26–30). Placental vascularization is a critical period of early gestation supporting not only embryonic survival but also subsequent fetal growth and development. Diminished placental vascularization can result in placental dysfunction, a fundamental cause of fetal growth abnormalities, pre-eclampsia, and early pregnancy loss (1, 2). The importance of placental circulation to successful pregnancy is recognized and exemplified by the close relationships among fetal weight, placental size, and uterine and umbilical blood flows during normal pregnancies (31–33). Establishment of functional fetal and placental circulations is one of the earliest events during embryonic development (34). The large increase in transplacental exchange, supporting the exponential increase in fetal growth during the last half of gestation, depends primarily on the dramatic growth of placental vascular beds and large increases in uterine and umbilical blood flows early in pregnancy (31–33, 35–39).

Despite clear evidence that placental formation and angiogenesis during early pregnancy are critical for normal fetal growth and development, the underlying molecular mechanisms driving placental vascularization are not well-characterized. Factors influencing placental vascular development drastically impact fetal health, and thus neonatal survival and growth (39–41), whereas compromised fetal growth significantly impacts life-long health and productivity (40, 42, 43). The predominant angiogenic factor driving placental growth and vascularization is vascular endothelial growth factor (VEGFA) signaling through its receptors VEGFA receptor-1 (FLT1) and VEGFA receptor-2 (KDR) (32), yet illuminating central upstream master regulators of the VEGFA angiogenic axis is key to increasing our understanding of placental development.

The CXCL12–CXCR4 chemokine axis has a special relationship with VEGFA and stimulates VEGF production and secretion, which, in turn, drives CXCL12 and CXCR4 synthesis, thereby creating a powerful proangiogenic feed-forward loop (44–47). This angiogenic connection between CXCL12–CXCR4 and VEGFA signaling may be one of the primary pathways promoting early placental vascularization and angiogenesis. Synthesis of CXCL12 and CXCR4 increase in fetal membranes and endometrium prior to VEGFA and VEGFA

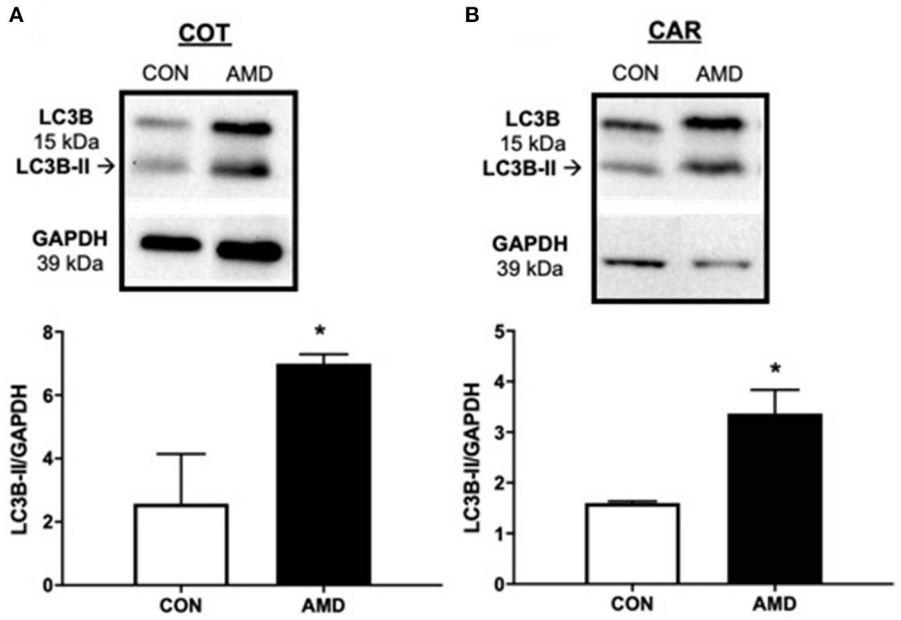

FIGURE 3 | Evidence of placental autophagy induction after suppressing the CXCL12–CXCR4 network. Protein abundance of cellular autophagy marker LC3B-II and representative immunoblots in ovine fetal cotyledon (COT) placenta **(A)** and maternal caruncle (CAR) placenta **(B)** following intrauterine saline (CON) or AMD3100 (AMD) infusion. Data are presented as the mean ± SEM, and significance is denoted with an asterisk when $p < 0.05$ (*).

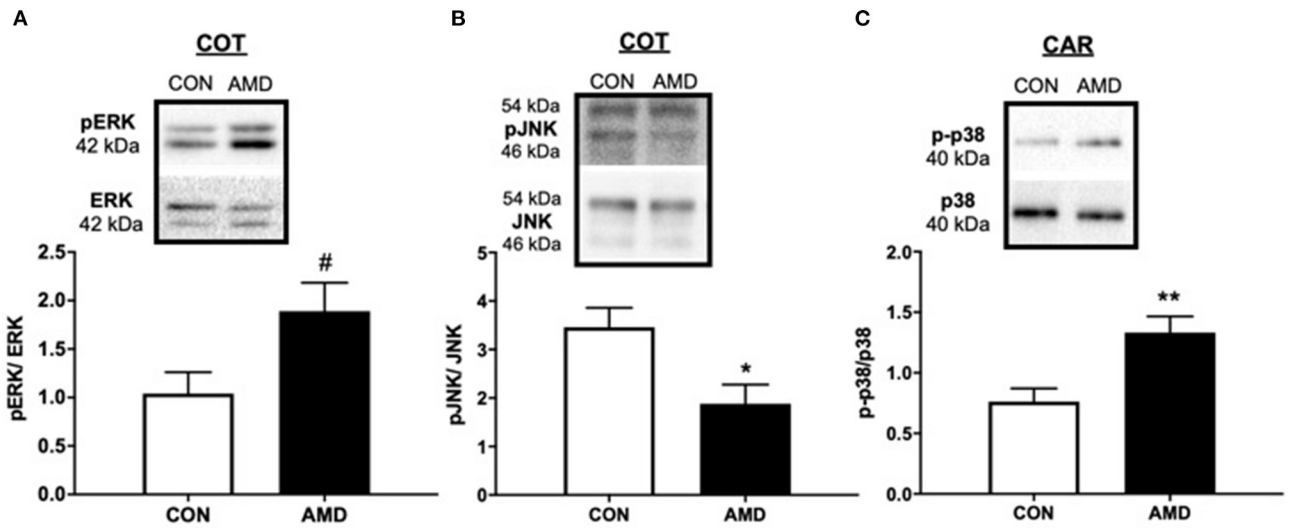

FIGURE 4 | The MAPK-signaling pathways mediated by ERK, JNK, and p38 protein kinases are activated after suppressing the CXCL12–CXCR4 network. Tendency for ERK activation **(A)**, suppression of JNK **(B)** in ovine fetal cotyledon (COT) placenta, and activation of p38 **(C)** in maternal caruncle (CAR) placenta following intrauterine saline (CON) or AMD3100 (AMD) infusion. Phosphoprotein data are shown with corresponding representative immunoblots. Statistical comparisons were made using Student's *t*-test; significance is denoted with an asterisk (*) when $p < 0.05$ or (**) when $p < 0.01$. $^{\#}p = 0.08$.

receptors and the amplified CXCL12–CXCR4 signaling at the fetal–maternal interface may be a central regulator activating the VEGFA angiogenic axis (17, 18, 45, 48). As early as day 18 of pregnancy in sheep, the fetal extraembryonic membranes begin to form blood vessels (31) that coincidently correlates with increased CXCL12 and CXCR4 endometrial expression (45). To determine if CXCL12–CXCR4 signaling is critical to placental production of VEGFA and overall placental vascularization, we developed an *in vivo* model to suppress CXCL12–CXCR4 at the fetal–maternal interface with the CXCR4 antagonist,

AMD3100. Suppressing CXCL12–CXCR4 signaling negatively impacts placental vascularization in endometrium as early as day 20 of pregnancy (16) with deleterious impact to placental vascularization still evident 3 days later (15). These data imply that the detrimental impact to placental vascularization when CXCL12–CXCR4 is suppressed may persist, resulting in compromised placental development and negative impact to fetal growth and health later in gestation.

To determine if diminished CXCL12–CXCR4 signaling at the fetal–maternal interface during implantation and initial placental vascularization results in long-term detrimental effects to the placenta, we suppressed CXCL12–CXCR4 at the fetal–maternal interface for 14 days starting on day 12 of gestation (days 12–26) and then collected placental tissues on day 35 of gestation, 9 days after treatment delivery to uterus had stopped. Placental growth, vascularization, cell survival, and relevant signaling pathways were evaluated in fetal and maternal placenta on day 35 of gestation. Similar to previous reports, the negative impact to placental vascularization early in gestation when CXCR4 is antagonized remains evident in placenta several days after treatments subsided. VEGFA abundance was diminished in fetal (COT) and maternal (CAR) placenta on day 35, but unlike our previous studies, FLT1 levels did not differ (15, 16). Instead, production of the other VEGFA receptor, KDR, tended to decrease in maternal placenta after suppressing CXCL12–CXCR4. The current study suppressed CXCL12–CXCR4 signaling at the fetal–maternal interface for 14 days whereas previous studies antagonized CXCR4 for 7 days, which may account for the differences in the production of the different VEGF receptors in the studies. Taken together, it appears that CXCL12–CXCR4 signaling regulates many components of the VEGFA pathway at the fetal–maternal interface including VEGFA and both receptors (15, 16) and thus may be a key upstream regulator of the placental VEGFA angiogenic axis in the placenta.

In an attempt to further quantify placental angiogenesis, we evaluated expression of vWF, as previously used in sheep (49). A large glycoprotein, vWF is produced by endothelial cells and megakaryocytes (50). It is often used as a marker of blood vessels due to its selective endothelial expression and has been used to quantify angiogenesis in a variety of tumors (51–53). Our objectives were to determine immunohistochemical expression of vWF, and to evaluate blood vessel number (BVN) and blood vessel circumference (BVC) of placenta on d35 of gestation. A reduction in vWF was expected because of the reduced VEGFA and associated signaling in placenta in concert with the knowledge that vWF synthesis is upregulated by VEGFA (54). Despite reduced levels of VEGFA in fetal and maternal placenta, vWF remained similar between control and AMD3100-treated ewes. Though not significant, observing vWF immunolocalization, control ewes appeared to have more uniform distribution of vWF and greater vessel circumference compared to AMD3100-treated ewes, which appeared disorganized. It is possible that evaluating vWF on day 35 of gestation is too soon to observe significant changes to placental angiogenesis. Similar to placental dysfunction and pre-eclampsia, the negative impact to placental growth and vascularization may manifest much later in gestation (mid-gestation and onward) after insults during early pregnancy.

The impaired placental vascularization observed on day 35 suggests a stressful placental environment. To determine if overall placental homeostasis was affected, the autophagy pathway was investigated. In addition to degrading cellular components under stress to survive, autophagy also participates in tissue remodeling, growth control, and cellular immunity (55–58), all of which are crucial to proper placental development (59, 60). In the current study, suppressing CXCL12–CXCR4 during implantation and initial placental vascularization resulted in greater abundance of the autophagy marker LC3B-II in fetal and maternal placenta on day 35, consistent with our previous studies (13, 16). However, this is our first observation of autophagy still evident 9 days after treatments had stopped. Whether the main purpose of autophagy induction is survival, tissue remodeling, growth control, or all the above remains to be determined.

To gain a better understanding of the molecular signaling at the fetal–maternal interface upon inhibiting CXCR4, we quantified the MAPK-signaling pathways mediated by ERK, JNK, and p38 protein kinases, which are central to placental growth, survival, and vascularization. The downregulation of p-JNK signaling in fetal (COT) placenta in the current study may indicate a suppression of apoptosis. Given the corresponding rise in autophagy induction observed in the same tissue suggests that these cells are attempting to survive and continue placental development. Moreover, p-ERK tended to increase in COT, which may signify activation of pro-survival and growth signaling mechanisms. Likewise, activation of the p-p38 pathway would indicate that the maternal (CAR) placenta is reacting to a stressful situation and trying to survive. While further studies are needed to determine the downstream consequences to placental development, it is interesting that suppressing a single chemokine receptor, CXCR4 for a brief period results in global changes to several MAPK proteins in the placenta numerous days later in gestation.

CXCR7 is another receptor for CXCL12, though it was only recently demonstrated to elicit intracellular signaling upon CXCL12 binding (61, 62). A study of both receptors at the fetal–maternal interface is needed to illuminate CXCL12-induced actions mediating placental vascularization. While CXCR4 abundance did not change on day 35 after ADM3100 treatment (data not shown), CXCR7 abundance decreased in maternal placenta (CAR) when CXCR4 was inhibited. This is in contrast to our previous studies antagonizing CXCR4 at the fetal–maternal interface where CXCR4 expression is typically altered and CXCR7 remains stable after antagonizing CXCR4 signaling (15, 16). A change to receptor levels suggests possible alterations to CXCL12-induced actions during placental development. The manifestation to placental growth and function later in gestation because of these alterations to CXCL12 receptors during early pregnancy remains to be seen but advocates for further research deciphering roles of CXCR4 and CXCR7 during implantation and placentation.

In conclusion, we demonstrated the impact a short interruption in CXCL12–CXCR4 signaling during implantation

has on placental development in sheep. The fact that we can manipulate this chemokine axis during a defined window of early pregnancy with great potential to impact placental development and thus offspring health is exciting and widely applicable to livestock and human health. CXCL12 is a highly conserved chemokine across livestock species and stimulates several biological processes essential to placental development through direct actions on trophoblast, endometrial, and immune cells. As CXCL12 acts upon all cell types responsible for placental formation across eutherian mammals, we propose that modulating CXCL12-induced actions is a novel approach to manipulating the fetal–maternal environment during the window when most pregnancy losses occur, and impaired placental development transpires. Increasing our understanding of CXCL12-induced actions controlling placental growth and vascularization will hopefully reveal methods to improve reproductive success and fetal health in livestock and dairy production systems.

DATA AVAILABILITY STATEMENT

The raw data supporting the conclusions of this article will be made available by the authors, without undue reservation.

ETHICS STATEMENT

All procedures involving animals were conducted with approval by the New Mexico State University Institutional Animal Care and Use Committee.

AUTHOR CONTRIBUTIONS

RA oversaw all of the experimental design, and performed surgical procedures, integrated comments from co-authors, and finalized the manuscript. CR, ET, GS, and MM conducted analyses of protein abundance and provided drafts of manuscript. All authors read and approved the final manuscript.

FUNDING

This work was supported by the USDA National Institute of Food and Agriculture (Hatch project #1025423) and the New Mexico Agricultural Experiment Station (AES).

SUPPLEMENTARY MATERIAL

The Supplementary Material for this article can be found online at: https://www.frontiersin.org/articles/10.3389/fvets.2021.650687/full#supplementary-material

REFERENCES

1. Redmer DA, Aitken RP, Milne JS, Reynolds LP, Wallace JM. Influence of maternal nutrition on messenger RNA expression of placental angiogenic factors and their receptors at midgestation in adolescent sheep. *Biol Reprod.* (2005) 72:1004–9. doi: 10.1095/biolreprod.104.037234
2. Reynolds LP, Grazul-Bilska AT, Redmer DA. Angiogenesis in the female reproductive organs: pathological implications. *Int J Exp Pathol.* (2002) 83:151–63. doi: 10.1046/j.1365-2613.2002.00277.x
3. Barker DJ, Fall CH. Fetal and infant origins of cardiovascular disease. *Arch Dis Child.* (1993) 68:797–9. doi: 10.1136/adc.68.6.797
4. Barker DJ, Hales CN, Fall CH, Osmond C, Phipps K, Clark PM. Type 2 (non-insulin-dependent) diabetes mellitus, hypertension and hyperlipidaemia (syndrome X): relation to reduced fetal growth. *Diabetologia.* (1993) 36:62–7. doi: 10.1007/BF00399095
5. Brar HS, Rutherford SE. Classification of intrauterine growth retardation. *Semin Perinatol.* (1988) 12:2–10.
6. Ghidini A. Idiopathic fetal growth restriction: a pathophysiologic approach. *Obstet Gynecol Surv.* (1996) 51:376–82. doi: 10.1097/00006254-199606000-00023
7. Hales CN, Barker DJ, Clark PM, Cox LJ, Fall C, Osmond C, et al. Fetal and infant growth and impaired glucose tolerance at age 64. *BMJ.* (1991) 303:1019–22. doi: 10.1136/bmj.303.6809.1019
8. Pollack RN, Divon MY. Intrauterine growth retardation: definition, classification, and etiology. *Clin Obstet Gynecol.* (1992) 35:99–107. doi: 10.1097/00003081-199203000-00015
9. Wu G, Bazer FW, Wallace JM, Spencer TE. Board-invited review: intrauterine growth retardation: implications for the animal sciences. *J Anim Sci.* (2006) 84:2316–37. doi: 10.2527/jas.2006-156
10. Bairagi S, Quinn KE, Crane AR, Ashley RL, Borowicz PP, Caton JS, et al. Maternal environment and placental vascularization in small ruminants. *Theriogenology.* (2016) 86:288–305. doi: 10.1016/j.theriogenology.2016.04.042
11. Seo H, Bazer FW, Burghardt RC, Johnson GA. Immunohistochemical examination of trophoblast syncytialization during early placentation in sheep. *Int J Mol Sci.* (2019) 20:4530. doi: 10.3390/ijms20184530
12. Wang L, Li X, Zhao Y, Fang C, Lian Y, Gou W, et al. Insights into the mechanism of CXCL12-mediated signaling in trophoblast functions and placental angiogenesis. *Acta Biochim Biophys Sin (Shanghai).* (2015) 47:663–72. doi: 10.1093/abbs/gmv064
13. McIntosh SZ, Maestas MM, Dobson JR, Quinn KE, Runyan CL, Ashley RL. CXCR4 signaling at the fetal-maternal interface may drive inflammation and syncytia formation during ovine pregnancydagger. *Biol Reprod.* (2021) 104:468–78. doi: 10.1093/biolre/ioaa203
14. McIntosh SZ, Maxam CJ, Maestas MM, Quinn KE, Ashley RL. Intrauterine inhibition of chemokine receptor 4 signaling modulates local and systemic inflammation in ovine pregnancy. *Am J Reprod Immunol.* (2019) 82:e13181. doi: 10.1111/aji.13181
15. Quinn KE, Prosser SZ, Kane KK, Ashley RL. Inhibition of chemokine (C-X-C motif) receptor four (CXCR4) at the fetal-maternal interface during early gestation in sheep: alterations in expression of chemokines, angiogenic factors and their receptors. *J Anim Sci.* (2017) 95:1144–11153. doi: 10.2527/jas2016.1271
16. Runyan CL, McIntosh SZ, Maestas MM, Quinn KE, Boren BP, Ashley RL. CXCR4 signaling at the ovine fetal-maternal interface regulates vascularization, CD34+ cell presence, and autophagy in the endometrium. *Biol Reprod.* (2019) 101:102–11. doi: 10.1093/biolre/ioz073
17. Grazul-Bilska AT, Borowicz PP, Johnson ML, Minten MA, Bilski JJ, Wroblewski R, et al. Placental development during early pregnancy in sheep: vascular growth and expression of angiogenic factors in maternal placenta. *Reproduction.* (2010) 140:165–74. doi: 10.1530/REP-09-0548
18. Grazul-Bilska AT, Johnson ML, Borowicz PP, Minten M, Bilski JJ, Wroblewski R, et al. Placental development during early pregnancy in sheep: cell proliferation, global methylation and angiogenesis in

the fetal placenta. *Reproduction.* (2011) 141:529–40. doi: 10.1530/REP-10-0505
19. Reynolds LP, Redmer DA. Growth and microvascular development of the uterus during early pregnancy in ewes. *Biol Reprod.* (1992) 47:698–708. doi: 10.1095/biolreprod47.5.698
20. Hendrix CW, Flexner C, MacFarland RT, Giandomenico C, Fuchs EJ, Redpath E, et al. Pharmacokinetics and safety of AMD-3100, a novel antagonist of the CXCR-4 chemokine receptor, in human volunteers. *Antimicrob Agents Chemother.* (2000) 44:1667–73. doi: 10.1128/AAC.44.6.1667-1673.2000
21. Braun T, Li S, Moss TJ, Newnham JP, Challis JR, Gluckman PD, et al. Maternal betamethasone administration reduces binucleate cell number and placental lactogen in sheep. *J Endocrinol.* (2007) 194:337–47. doi: 10.1677/JOE-07-0123
22. Diskin MG, Morris DG. Embryonic and early foetal losses in cattle and other ruminants. *Reprod Domest Anim.* (2008) 43(Suppl. 2):260–7. doi: 10.1111/j.1439-0531.2008.01171.x
23. Diskin MG, Murphy JJ, Sreenan JM. Embryo survival in dairy cows managed under pastoral conditions. *Anim Reprod Sci.* (2006) 96:297–311. doi: 10.1016/j.anireprosci.2006.08.008
24. Hansen PJ, Block J. Towards an embryocentric world: the current and potential uses of embryo technologies in dairy production. *Reprod Fertil Dev.* (2004) 16:1–14. doi: 10.1071/RD03073
25. Santos JE, Thatcher WW, Chebel RC, Cerri RL, Galvao KN. The effect of embryonic death rates in cattle on the efficacy of estrus synchronization programs. *Anim Reprod Sci.* (2004) 82–83:513–35. doi: 10.1016/j.anireprosci.2004.04.015
26. Berg DK, Van Leeuwen J, Beaumont S, Berg M, Pfeffer PL. Embryo loss in cattle between days 7 and 16 of pregnancy. *Theriogenology.* (2010) 73:250–60. doi: 10.1016/j.theriogenology.2009.09.005
27. Diskin MG, Sreenan JM. Fertilization and embryonic mortality rates in beef heifers after artificial insemination. *J Reprod Fertil.* (1980) 59:463–8. doi: 10.1530/jrf.0.0590463
28. Roche JF, Bolandl MP, McGeady TA. Reproductive wastage following artificial insemination of heifers. *Vet Rec.* (1981) 109:401–4. doi: 10.1136/vr.109.18.401
29. Diskin MG, Parr MH, Morris DG. Embryo death in cattle: an update. *Reprod Fertil Dev.* (2011) 24:244–51. doi: 10.1071/RD11914
30. Chebel RC, Santos JE, Reynolds JP, Cerri RL, Juchem SO, Overton M. Factors affecting conception rate after artificial insemination and pregnancy loss in lactating dairy cows. *Anim Reprod Sci.* (2004) 84:239–55. doi: 10.1016/j.anireprosci.2003.12.012
31. Reynolds LP, Borowicz PP, Caton JS, Vonnahme KA, Luther JS, Buchanan DS, et al. Uteroplacental vascular development and placental function: an update. *Int J Dev Biol.* (2010) 54:355–66. doi: 10.1387/ijdb.082799lr
32. Reynolds LP, Borowicz PP, Vonnahme KA, Johnson ML, Grazul-Bilska AT, Wallace JM, et al. Animal models of placental angiogenesis. *Placenta.* (2005) 26:689–708. doi: 10.1016/j.placenta.2004.11.010
33. Reynolds LP, Caton JS, Redmer DA, Grazul-Bilska AT, Vonnahme KA, Borowicz PP, et al. Evidence for altered placental blood flow and vascularity in compromised pregnancies. *J Physiol.* (2006) 572:51–8. doi: 10.1113/jphysiol.2005.104430
34. Charnock-Jones DS, Kaufmann P, Mayhew TM. Aspects of human fetoplacental vasculogenesis and angiogenesis. *I Mol Regul Placenta.* (2004) 25:103–13. doi: 10.1016/j.placenta.2003.10.004
35. Kaufmann P, Mayhew TM, Charnock-Jones DS. Aspects of human fetoplacental vasculogenesis and angiogenesis. *II Changes During Normal Preg Placenta.* (2004) 25:114–26. doi: 10.1016/j.placenta.2003.10.009
36. Magness RR. *Maternal Cardiovascular and Other Physiological Responses to the Endocrinology of Pregnancy*. Totowa, NJ: Humana Press (1998).
37. Mayhew TM, Wijesekara J, Baker PN, Ong SS. Morphometric evidence that villous development and fetoplacental angiogenesis are compromised by intrauterine growth restriction but not by pre-eclampsia. *Placenta.* (2004) 25:829–33. doi: 10.1016/j.placenta.2004.04.011
38. Reynolds LP, Killilea SD, Redmer DA. Angiogenesis in the female reproductive system. *FASEB J.* (1992) 6:886–92. doi: 10.1096/fasebj.6.3.1371260
39. Reynolds LP, Redmer DA. Utero-placental vascular development and placental function. *J Anim Sci.* (1995) 73:1839–51. doi: 10.2527/1995.7361839x
40. Reynolds LP, Borowicz PP, Caton JS, Vonnahme KA, Luther JS, Hammer CJ, et al. Developmental programming: the concept, large animal models, and the key role of uteroplacental vascular development. *J Anim Sci.* (2010) 88(Suppl. 13):E61–72. doi: 10.2527/jas.2009-2359
41. Reynolds LP, Borowicz PP, Vonnahme KA, Johnson ML, Grazul-Bilska AT, Redmer DA, et al. Placental angiogenesis in sheep models of compromised pregnancy. *J Physiol.* (2005) 565:43–58. doi: 10.1113/jphysiol.2004.081745
42. Barker DJ, Clark PM. Fetal undernutrition and disease in later life. *Rev Reprod.* (1997) 2:105–12. doi: 10.1530/ror.0.0020105
43. Breier BH, Vickers MH, Ikenasio BA, Chan KY, Wong WP. Fetal programming of appetite and obesity. *Mol Cell Endocrinol.* (2001) 185:73–9. doi: 10.1016/S0303-7207(01)00634-7
44. Mirshahi F, Pourtau J, Li H, Muraine M, Trochon V, Legrand E, et al. SDF-1 activity on microvascular endothelial cells: consequences on angiogenesis in *in vitro* and *in vivo* models. *Thromb Res.* (2000) 99:587–94. doi: 10.1016/S0049-3848(00)00292-9
45. Quinn KE, Ashley AK, Reynolds LP, Grazul-Bilska AT, Ashley RL. Activation of the CXCL12/CXCR4 signaling axis may drive vascularization of the ovine placenta. *Domest Anim Endocrinol.* (2014) 47:11–21. doi: 10.1016/j.domaniend.2013.12.004
46. Salcedo R, Oppenheim JJ. Role of chemokines in angiogenesis: CXCL12/SDF-1 and CXCR4 interaction, a key regulator of endothelial cell responses. *Microcirculation.* (2003) 10:359–70. doi: 10.1080/mic.10.3-4.359.370
47. Salcedo R, Wasserman K, Young HA, Grimm MC, Howard OM, Anver MR, et al. Vascular endothelial growth factor and basic fibroblast growth factor induce expression of CXCR4 on human endothelial cells: In vivo neovascularization induced by stromal-derived factor-1alpha. *Am J Pathol.* (1999) 154:1125–35. doi: 10.1016/S0002-9440(10)65365-5
48. Ashley RL, Antoniazzi AQ, Anthony RV, Hansen TR. The chemokine receptor CXCR4 and its ligand CXCL12 are activated during implantation and placentation in sheep. *Reprod Biol Endocrinol.* (2011) 9:148. doi: 10.1186/1477-7827-9-148
49. Palmieri C, Loi P, Reynolds LP, Ptak G, Della Salda L. Placental abnormalities in ovine somatic cell clones at term: a light and electron microscopic investigation. *Placenta.* (2007) 28:577–84. doi: 10.1016/j.placenta.2006.08.003
50. Randi AM, Laffan MA, Starke RD. Von Willebrand factor, angiodysplasia and angiogenesis. *Mediterr J Hematol Infect Dis.* (2013) 5:e2013060. doi: 10.4084/mjhid.2013.060
51. Hoyer LW, De los Santos RP, Hoyer JR. Antihemophilic factor antigen Localization in endothelial cells by immunofluorescent microscopy. *J Clin Invest.* (1973) 52:2737–44. doi: 10.1172/JCI107469
52. Ito TK, Ishii G, Chiba H, Ochiai A. The VEGF angiogenic switch of fibroblasts is regulated by MMP-7 from cancer cells. *Oncogene.* (2007) 26:7194–203. doi: 10.1038/sj.onc.1210535
53. Vermeulen PB, Gasparini G, Fox SB, Toi M, Martin L, McCulloch P, et al. Quantification of angiogenesis in solid human tumours: an international consensus on the methodology and criteria of evaluation. *Eur J Cancer.* (1996) 32A:2474–84. doi: 10.1016/S0959-8049(96)00379-6
54. Zanetta L, Marcus SG, Vasile J, Dobryansky M, Cohen H, Eng K, et al. Expression of Von Willebrand factor, an endothelial cell marker, is up-regulated by angiogenesis factors: a potential method for objective assessment of tumor angiogenesis. *Int J Cancer.* (2000) 85:281–8. doi: 10.1002/(SICI)1097-0215(20000115)85:2%3C281::AID-IJC21%3E3.0.CO;2-3
55. Cuervo AM. Autophagy: in sickness and in health. *Trends Cell Biol.* (2004) 14:70–7. doi: 10.1016/j.tcb.2003.12.002
56. Levine B, Klionsky DJ. Development by self-digestion: molecular mechanisms and biological functions of autophagy. *Dev Cell.* (2004) 6:463–77. doi: 10.1016/S1534-5807(04)00099-1
57. Mizushima N. Autophagy: process and function. *Genes Dev.* (2007) 21:2861–73. doi: 10.1101/gad.1599207

58. Yoshimori T. Autophagy: a regulated bulk degradation process inside cells. *Biochem Biophys Res Commun.* (2004) 313:453–8. doi: 10.1016/j.bbrc.2003.07.023
59. Gong JS, Kim GJ. The role of autophagy in the placenta as a regulator of cell death. *Clin Exp Reprod Med.* (2014) 41:97–107. doi: 10.5653/cerm.2014.41.3.97
60. Toschi P, Czernik M, Zacchini F, Fidanza A, Loi P, Ptak GE. Evidence of placental autophagy during early pregnancy after transfer of *in vitro* produced (IVP) sheep embryos. *PLoS ONE.* (2016) 11:e0157594. doi: 10.1371/journal.pone.0157594
61. Hernandez L, Magalhaes MA, Coniglio SJ, Condeelis JS, Segall JE. Opposing roles of CXCR4 and CXCR7 in breast cancer metastasis. *Breast Cancer Res.* (2011) 13:R128. doi: 10.1186/bcr3074
62. Wani N, Nasser MW, Ahirwar DK, Zhao H, Miao Z, Shilo K, et al. C-X-C motif chemokine 12/C-X-C chemokine receptor type 7 signaling regulates breast cancer growth and metastasis by modulating the tumor microenvironment. *Breast Cancer Res.* (2014) 16:R54. doi: 10.1186/bcr3665

Conflict of Interest: The authors declare that the research was conducted in the absence of any commercial or financial relationships that could be construed as a potential conflict of interest.

Publisher's Note: All claims expressed in this article are solely those of the authors and do not necessarily represent those of their affiliated organizations, or those of the publisher, the editors and the reviewers. Any product that may be evaluated in this article, or claim that may be made by its manufacturer, is not guaranteed or endorsed by the publisher.

Advantages of publishing in Frontiers

OPEN ACCESS
Articles are free to read for greatest visibility and readership

FAST PUBLICATION
Around 90 days from submission to decision

HIGH QUALITY PEER-REVIEW
Rigorous, collaborative, and constructive peer-review

TRANSPARENT PEER-REVIEW
Editors and reviewers acknowledged by name on published articles

Frontiers
Avenue du Tribunal-Fédéral 34
1005 Lausanne | Switzerland

Visit us: www.frontiersin.org
Contact us: frontiersin.org/about/contact

REPRODUCIBILITY OF RESEARCH
Support open data and methods to enhance research reproducibility

DIGITAL PUBLISHING
Articles designed for optimal readership across devices

FOLLOW US
@frontiersin

IMPACT METRICS
Advanced article metrics track visibility across digital media

EXTENSIVE PROMOTION
Marketing and promotion of impactful research

LOOP RESEARCH NETWORK
Our network increases your article's readership